Joana Raquel Correia Faria

"Functional characterization of *Leishmania infantum* asparagine synthetase A and ribose 5-phosphate isomerase B as potential drug targets"

Tese do 3º Ciclo de Estudos Conducente ao

Grau de Doutoramento em Ciências Farmacêuticas –

Microbiologia

Trabalho realizado sob a orientação de:

Professora Doutora Anabela Cordeiro-da-Silva (Professora Associada com Agregação da Faculdade de Farmácia da Universidade do Porto, Porto, Portugal)

Doutora Joana Tavares (Investigadora do Instituto de Biologia Molecular e Celular da Universidade do Porto, Porto, Portugal)

Doutor Lucio Holanda Freitas Junior (Investigador no Laboratório Nacional de Biociências, Campinas, Brasil)

Janeiro, 2016

This work was performed at the Parasite Disease Group of the Institute for Molecular and Cell Biology (IBMC, Porto, Portugal), now part of Institute of Investigation and Innovation in Health (I3S, Porto, Portugal) in collaboration with the Protein Crystallography Group of IBMC, now part of I3S, and the Centre of Neglected Diseases 3 (CND3) of Institut Pasteur Korea (IPK, Seoul, South Korea). The author has received financial support through an individual doctoral fellowship credited by the Foundation for Science and Technology (FCT, Portugal) with the reference SFRH/BD/79712/2011. The experimental research performed in this work has received financial support from FEDER funds through the Operational Competitiveness Program – COMPETE and National Funds through FCT under the project Pest-C/SAU/LA0002/2011. The research leading to these results has also received funding from the European Community's Seventh Framework Programme under grant agreement No.602773 (Project KINDRED; Kinetoplastid Drug Development: strengthening the preclinical pipeline; HEALTH-F3-2013-602773). The COST Actions CM0801 "New drugs for neglected diseases" and CM1307 "Targeted chemotherapy towards diseases caused by endoparasites" and TRICONT project under ERA-NET New INDIGO have also contributed for this work.

Author's declaration

Under the terms of the "Decreto-lei nº 216/92, de 13 de Outubro", is hereby declared that the author afforded a major contribution to the conceptual design and technical execution of the work, interpretation of the results and manuscript preparation of the published articles included in this dissertation.

Under the terms of the "Decreto-lei nº 216/92, de 13 de Outubro", is hereby declared that the following original articles/communications were prepared in the scope of this dissertation.

SCIENTIFIC PUBLICATIONS

Articles in international peer-reviewed journals

In the scope of this dissertation

Faria J, Loureiro I, Santarem N, Cecílio P, Macedo-Ribeiro S, Tavares J*, Cordeiro-da-Silva A* (2015) Disclosing ribose-5-phosphate isomerase B essentiality in Trypanosomatids. (*submitted*);

Faria J, Loureiro I, Santarem N, Macedo-Ribeiro S, Tavares J, Cordeiro-da-Silva A (2015) *Leishmania infantum* asparagine synthetase A is dispensable for parasites survival and infectivity. *PLoS Neglected Tropical Diseases* (*in press*) doi: 10.1371/journal.pntd.0004365;

Loureiro I, **Faria J**, Clayton C, Macedo-Ribeiro S, Santarém N, Roy N, Cordeiro-da-Silva A*, Tavares J* (2015) Ribose-5-phosphate isomerase B knockdown compromises *Trypanosoma brucei* bloodstream form infectivity. *PLoS Neglected Tropical Diseases*, **9(1):** e3430. doi: 10.1371/journal.pntd.0003430;

Loureiro I, **Faria J**, Clayton C, Macedo-Ribeiro S, Roy N, Santarém N, Tavares J*, Cordeiro-da-Silva A* (2015) Knockdown of asparagine synthetase A renders *Trypanosoma brucei* auxotrophic to asparagine. *PLoS Neglected Tropical Diseases*, **7(12):** e2578. doi: 10.1371/journal.pntd.0002578.

Publications outside the scope of the thesis

Faria J*, Moraes CB*, Song R, Pascoalino BS, Lee N, Siqueira-Neto JL, Cruz DJ, Parkinson T, Loset JR, Cordeiro-da-Silva A, Freitas-Junior LH (2015) Drug discovery for human African trypanosomiasis: identification of novel scaffolds by the newly developed HTS/Sybr Green assay for *Trypanosoma brucei*. *Journal of Biomolecular Screening*, **20(1):** 70-81. doi: 10.1177/1087057114556236.

*The authors contributed equally to the work

COMMUNICATIONS

Oral Communications

"Searching for novel drug targets in *Leishmania*: a tale of two proteins" in I3S seminars, 11/11/15, at I3S (Porto);

"Enzyme-based assays for drug discovery in Trypanosomatids" 27/07/12, at Institut Pasteur Korea (Seoul, South Korea).

Poster Communications

Faria J, Loureiro I, Santarem N, Cecílio P, Macedo-Ribeiro S, Tavares J, Cordeiro-da-Silva A. "Disclosing ribose-5-phosphate isomerase B essentiality for *Leishmania infantum* survival and infectivity" presented in Molecular Parasitology Meeting 2015, 20-24th September of 2015, at the Marine Biological Laboratory in Woods Hole, Boston, MA, USA;

Faria J, Loureiro I, Tavares J, Santarem N, Macedo-Ribeiro S, Cordeiro-da-Silva A. "*Leishmania infantum* asparagine synthetase A is dispensable for parasites *in vivo* infectivity" presented in the British Society for Parasitology Spring Meeting 2015, 16-18th April of 2015, at the BT Convention Centre, in Liverpool, UK;

Loureiro I, Costa D, Gaspar L, Graça N, Baptista C, Ribeiro H, **Faria J**, Tavares J & Cordeiro-da-Silva A. "Evaluation of the *in vivo* efficacy of bisnaphtalimidopropyl derivative

compound against *Trypanosoma brucei*" presented in the 16th Drug Design & Development Seminar (DDDS), 16-17th March of 2015, at Robert Koch Institut, in Berlin, Germany;

Loureiro I, **Faria J**, Clayton C, Macedo-Ribeiro S, Roy N, Tavares J & Cordeiro-da-Silva A "Ribose-5-phosphate isomerase B knockdown compromises *Trypanosoma brucei* bloodstream form infectivity" presented in I3S Annual Meeting, 30-31st October of 2014, at Hotel Axis Vermar, Póvoa do Varzim;

Loureiro I, **Faria J**, Clayton C, Macedo-Ribeiro S, Roy N, Tavares J & Cordeiro-da-Silva A "Ribose-5-phosphate isomerase B knockdown compromises *Trypanosoma brucei* bloodstream form infectivity" presented in British Society of Parasitology Spring Meeting, 6-9th April of 2014, at Cambridge University, UK;

Loureiro I, **Faria J**, Clayton C, Macedo-Ribeiro S, Roy N, Santarém N, Tavares J & Cordeiro-da-Silva A "Functional characterization of asparagine synthetase A in Trypanosomes" presented in EMBO YOUNG SCIENTISTS FORUM 2013, 15-16th July at IMM, Lisbon;

Loureiro I, **Faria J**, Clayton C, Macedo-Ribeiro S, Roy N, Santarém N, Tavares J & Cordeiro-da-Silva A "Knockdown of asparagine synthetase A renders *Trypanosoma brucei* auxotrophic to asparagine" presented in British Society for Parasitology Spring Meeting 2013, 8-11th April of 2013, at Bristol University, UK;

Loureiro I, **Faria J**, Tavares J, Roy N, Cordeiro-da-Silva A "Ribose-5-phosphate isomerase B in Trypanosomatids" presented in I3S Scientific Retreat, 10-11th May of 2012, at Hotel Axis Vermar, Póvoa do Varzim;

Acknowledgements

And this is it… It is still hard to believe I have finished this journey. I have not revolutionized anything really but I certainly grew up as a scientist, and as a person in ways I could not even imagine when I first started. In the last four years I had the pleasure, and in some cases the privilege, of meeting people who have given a contribution (scientific and emotional) beyond measure in this challenging yet gratifying journey.

Firstly, I must acknowledge my supervisors, Prof. Anabela Cordeiro-da-Silva, Dr. Joana Tavares and Dr. Lucio Freitas-Junior.

To Prof. Anabela, I must thank you for the opportunity to join your research group and give my first steps in Molecular Parasitology under your supervision. I would like to thank you for your guidance, encouragement, and more importantly, support and trust. My words are of sincere gratitude, I will not forget. To Dr. Lucio, I would like to acknowledge the opportunity to work at Institut Pasteur Korea, where I had a different perspective on Science. The whole Korea experience was extremely enriching at a professional and personal level. Thank you for your trust and encouragement.

To my supervisor and mentor Joana Tavares, my most sincere thank you. Essentially, there are two things that fuel my scientific performance: 1) passion and 2) people that inspire me. I look up at you as an example of the researcher I would like to become. No matter how busy, how overwhelmed with work and preoccupations, you cannot walk away and leave one in need. There was not a single episode you did not have time for a discussion (even at 10 pm on a Friday!). You question anything, and more importantly, you raise the right questions: the ones that made me search papers overnight looking for an answer, or at least a theory (eventually almost killing me with anxiety every now and then! :P). You are an example of passion, hard work and determination, and ultimately, of sincerity and kindness.

It is with unimaginable joy I dedicate a few words to my partner in crime and friend Inês, although they will probably fail to express my profound gratitude and admiration. Thank you for all the things you taught me, for all the encouragement and critical discussions. And of course, thank you for all the nights we spent working together, in which there was no room for demotivation or exhaustion, those gave place to laughs and funny situations instead. I was fortunate to have such a companion, an example of perseverance, hard work, determination and humility. I just hope to witness all the success you will certainly achieve, for you deserve no less. Thank you.

To Nuno Santarém (“O chefe”), what can I say? You know. Thank you for all the support, talking to you always spiralled out into a sea of possibilities and theories, but it has stimulated me into thinking and more importantly thinking differently. You always have an

opinion on EVERYTHING, isn't it? Thank you for your mentoring and for the friendship. Thank you also for your humanity, for there are words that can make a difference, and some really did.

I must thank you, Ricardo Silvestre, for being someone I always looked up to, since the time I was still your student. Your enthusiasm, your talks, your contribution in the lab meetings have been missed, as well as your sense of humour and your general sympathy towards everyone around. Thanks for being part of this journey, you know how much you have positively influenced me as a researcher to be. Besides our passion for Science, there was also our passion for Music (*Music expresses that which cannot be said and on which it is impossible to be silent.* Victor Hugo).

And of course, I would like to thank all past and present members of Parasite Disease. Diana, Renata, Tânia, Pedro and Vasco, you know you own a special place in my heart. Diana, I will miss our late hours' geekiness! And Metabolism is really the key, they will listen one day! I would also like to thank all the members of CND3 and of other groups at Institut Pasteur Korea. A special acknowledgement to Jair Siqueira-Neto, Carol Borsoi Moraes, Jean-Robert Loset, Eric Chatelain and Tanya Parkinson.

I would also like to thank Prof. Sandra Macedo-Ribeiro, Prof. Pedro Pereira and Dr. Frederico Silva for all you have taught me, thank you for the patience, guidance and support. I would like to thank Dr. Ali Quaissi for the critical discussion and the kind encouraging words. Also, to Dr. Paula Magalhães, my words are of sincere gratitude for all the support and friendship I could find in CCGen.

Aos meus amigos, os quais não sei como ainda preservo, tantas ausências, tantos momentos em que o trabalho veio primeiro, e sempre com um sorriso encontrei em vós compreensão, apoio e incentivo. Cá ou fora, pessoalmente ou por skype, sempre pude contar com todos vós. Não preciso nomear-vos, apenas um profundo "obrigada" por fazerem parte da minha vida.

E por fim, e não menos importante, a minha família. Os meus pais, o meu querido irmão, os meus padrinhos (verdadeiramente os meus segundos pais), os meus primos (Mafalda, Jorge, Miguel e Paulo), ao senhor Aníbal e em memória da D. Leopoldina, obrigada por fazerem de mim quem sou hoje, é por vós e por tudo o que me ensinaram e me proporcionaram que me tornei uma boa parte do que sou. Deram-me lições que a vida académica não ensina, e que não são menos importantes.

Dedico esta tese à minha mãe, mais do que mãe uma amiga, a quem nunca poderei agradecer o suficiente todos os esforços e sacrifícios. É graças ao teu amor, ao teu apoio incondicional, à força e valores que me transmitiste que aqui cheguei.

Thank you for letting me carry a little bit of each one of you in me.

Abstract

Leishmaniasis is a neglected tropical disease caused by *Leishmania* parasites associated with an important burden worldwide. Visceral leishmaniasis (VL) is the most severe form of the disease, and it is fatal if left untreated. Disease control relies mostly on chemotherapy, which is frequently associated to safety issues, drug resistance, among other disadvantages that hinder disease eradication in endemic areas. Therefore, the search for new drugs and novel drug targets becomes imperative.

In order to identify new potential molecular targets, an *in silico* comparative genomic analysis has been performed. Asparagine synthetase A (AS-A) and ribose-5-phosphate isomerase B (RPIB), which lack human homologues, have been selected as promising candidates. This thesis presents the first functional characterization of these two proteins in *Leishmania infantum* and *Trypanosoma brucei*, including both biochemical and genetic studies.

Asparagine synthase (AS) is responsible for the conversion of aspartate into asparagine (Asn) in an ATP-dependent manner, using ammonia or glutamine as a nitrogen source. There are two structurally distinct AS: the strictly ammonia dependent, type A, and the type B, which preferably uses glutamine. Interestingly, we found that AS-A enzymes from trypanosomatids can use both ammonia and glutamine as nitrogen donors. Moreover, we have successfully generated *ASA* null mutants by targeted gene replacement in *L. infantum* and these parasites do not exhibit significant growth or infectivity defects. Indeed, a severe impairment of *in vitro* growth was only observed when null mutants were cultured in Asn limiting conditions. Our results demonstrate that despite being important upon Asn deprivation, *Li*AS-A is not essential for parasite survival, growth or infectivity in normal *in vitro* and *in vivo* conditions. The same pattern was observed in the related parasite *T. brucei*, using RNAi studies. Therefore, we exclude AS-A as a suitable drug target against trypanosomatids.

Ribose-5-phosphate isomerase belongs to the non-oxidative branch of the pentose phosphate pathway, catalysing the interconversion of D-ribose-5-phosphate (R5P) and D-ribulose-5-phosphate (Ru5P). Trypanosomatids encode a type B RPI, whereas humans have a structurally unrelated type A. RPIB from trypanosomatids preferentially converts Ru5P into R5P. We demonstrated that its knockdown in *T. brucei* dramatically impairs parasites infectivity. Moreover, null mutants generation in *L. infantum* was only possible when an episomal copy of *RPIB* gene was provided, and the latter was preserved both *in vitro* and *in vivo*, even in the absence of drug pressure for a long period indicating the gene is essential for survival. *In vitro*, sKO promastigotes exhibited no defect in growth, metacyclogenesis or macrophages infection, however, an impairment in intracellular

amastigotes' replication was observed. Additionally, mice infected with *Lis*KO mutants presented a reduced parasite burden in the liver, rescued by *RPIB* complementation. To gain further insights whether RPIB essentiality is due to its isomerase function, sKO mutants were complemented with an episomal copy of *RPIB* carrying a mutation on Cys69 that abrogates isomerase function. In this case, the inability to remove the second allele of *RPIB* gene suggests the essentiality is due to the annotated metabolic function. Moreover, *T. brucei* is reluctant to complete *RPIB* removal, and mice experienced an extended survival upon infection with sKO mutants.

In summary, our results genetically validate RPIB as a novel drug target candidate in trypanosomatids.

Keywords: *L. infantum*; *T. brucei*; asparagine synthetase A; ribose-5-phosphate isomerase B; genetic validation; biochemical analysis

Resumo

A leishmaniose é uma doença tropical negligenciada causada por parasitas do género *Leishmania*, com grande impacto na saúde pública mundial. A leishmaniose visceral é a forma mais severa da doença, sendo fatal caso não seja tratada. O seu controlo singe-se principalmente à quimioterapia, a qual está frequentemente associada a toxicidade, resistência, entre outras limitações que comprometem a erradicação da doença nos países endémicos. Deste modo, a descoberta de novos fármacos e novos alvos terapêutico é uma prioridade.

Com o objectivo de identificar potenciais alvos moleculares no parasita que não apresentam homólogos em humanos foi realizada uma análise genómica comparativa. De entre os vários genes candidatos selecionamos a asparagina sintetase A (AS-A) e a ribose-5-fosfato isomerase B (RPIB) para estudos funcionais. Nesta dissertação encontra-se a primeira caracterização bioquímica e genética destas duas proteínas em *Leishmania infantum* e *Trypanosoma brucei.*

A AS é responsável pela conversão de aspartato em asparagina (Asn), consumindo ATP, e utilizando a amónia ou a glutamina como fonte de azoto. Na natureza, existem dois tipos de AS, que são estruturalmente distintos: o tipo A, caracterizado como estritamente dependente de amónia, e o tipo B, que utiliza preferencialmente glutamina. Curiosamente, as AS-A dos tripanossomatídeos demonstraram ser capazes de utilizar quer amónia, quer glutamina como fontes de azoto. Adicionalmente, foram gerados parasitas trangénicos, *knockout* para o gene que codifica a AS-A. Estes parasitas não apresentam qualquer defeito no que diz respeito quer ao seu crescimento, quer à sua infectividade. Aliás, apenas em condições limitantes de Asn é que o seu crescimento *in vitro* é substancialmente afectado. Apesar de ser importante na ausência de Asn, em condições normais, a AS-A é dispensável para a sobrevivência do parasita, para o seu crescimento e infectividade quer *in vitro*, quer *in vivo*. Um comportamento semelhante foi observado num parasita da mesma família, *T. brucei*, utilizando a tecnologia de RNA de interferência. Como tal, a AS-A não parece ser uma alvo terapêutico apropriado em tripanossomatídeos.

Relativamente à RPIB, esta proteína está envolvida no ramo não-oxidativo da via das pentoses fosfato, catalisando a interconversão da D-ribose-5-fosfato (R5P) em D-ribulose-5-fosfato (Ru5P). Os tripanossomatídeos codificam uma RPI do tipo B, enquanto o hospedeiro humano possui uma RPIB estruturalmente distinta e designada como do tipo A. A RPIB dos tripanssomatídeos converte preferencialmente a Ru5P em R5P. O *knockdown* da RPIB no *T. brucei* compromete dramaticamente a sua infectividade. Por sua vez, em *L. infantum*, a obtenção de mutantes *knockout* para o gene que codifica a RPIB foi apenas conseguida na presença de episoma contendo o gene, que foi preservado quer *in*

vitro quer *in vivo* na ausência de composto de selecção por um longo período de tempo. Este cenário indica que o gene é essencial para a sobrevivência do parasita. *In vitro*, os mutantes *single knockout* (sKO) no estadio promastigota não manifestaram qualquer comprometimento no seu crescimento, metaciclogénese, infecção de macrófagos ou diferenciação, mas sim na replicação da forma amastigota. É igualmente importante salientar que ratinhos infectados com os mutantes sKO apresentaram uma diminuição da carga parasitária no fígado, sendo este defeito revertido quando estes parasitas são complementados com um episoma contendo o gene que codifica para a RPIB. Adicionalmente, para clarificar se a essencialidade da RPIB para o parasita era devida à sua função enzimática, os mutantes sKO foram complementados com um episoma contendo uma forma mutada do gene que gera uma proteína sem actividade isomerase. Neste caso, não foi possível remover o segundo alelo do gene sugerindo que a essencialidade é devida à função isomerase. Foi também impossível inactivar o gene em *T. brucei* após várias tentativas, e os mutantes sKO que foram obtidos apresentaram uma menor infectividade, prolongando a sobrevivência de ratinhos infectados com estes parasitas.

Em conclusão , os resultados apresentados nesta dissertação validam geneticamente a RPIB como um novo candidato a alvo terapêutico em tripanossomatídeos.

Palavras-chave: *L. infantum*; *T. brucei*; asparagina sintetase A; ribose-5-fosfato isomerase B; validação genética; análise bioquímica

Table of contents

Index of figures

Index of tables

Abbreviations list

4-PEH	4-Phospho-D-erythronohydroxamic acid
4E-BP1	Eukaryotic initiation factor 4F binding protein
6PGDH	6-Phosphogluconate dehydrogenase
6PGL	6-Phosphogluconolactonase
AAT	Amino acid transporters
ABC	ATP-binding cassette
ACP	Acyl carrier protein
AdoMet	S-adenosylmethionine
AdoMetDC	S-adenosylmethionine decarboxylase
AdoMetT1	S-adenosylmethionine transporter
AGO1	Argonaute
ALD	Fructose-1,6-bisphosphate aldolase
ALX	LipoXin A4 receptor
AmphB	Amphotericin B
AMPK	AMP activated protein kinase
APA	3-Aminooxy-1-aminopropane
APC	Anaphase promoting complex
AQP	Aquaglyceroporin
ARG	Arginase
AS	Asparagine synthetase
AS-A	Asparagine synthetase A
AS-B	Asparagine synthetase B
Asn	Asparagine
AsnRS	Asparaginyl-tRNA synthetase
ATF4	Activating transcription factor 4
ATP	Adenosine triphosphate
BMMØ	Bone marrow derived macrophages
BLEO	*Streptoalloteichus hindustanus* bleomycin resistance protein
BSD	Blasticidin S deaminase
CDK	Cyclin dependent kinase
CL	Cutaneous leishmaniasis
CP	Cysteine protease
CR	Complement receptor
CRIPSR	Clustered regularly interspaced palindromic short repeat

dAdoMet	Decarboxylated S-adenosylmethionine
DC	Dendritic cell
DCL1	Dicer-like enzyme 1
DCL2	Dicer-like enzyme 2
DDL1	Delta-like ligand 1 for Notch 3
DDT	Dichlorodiphenyltrichloroethane
DHEA	Dehydroepiandrosterone
DHFR-TS	Dihydrofolate reductase - thymidylate synthase
DNA	Deoxyribonucleic acid
DSB	Double-strand DNA breaks
dsRNA	Double strand RNA
dTMP	Deoxythymidine-monophosphate
dUMP	Deoxyuridine-monophosphate
E4P	Erythrose-4-phosphate
EA	Epiandrosterone
eIF2α	Eukaryotic initiation factor 2α
eIF4F	Eukaryotic initiation factor 4F
ELISA	Enzyme-linked immunosorbent assay
ELO	Elongase
ENO	Enolase
EPC	Ethanolamine phosphorylceramide
F6P	Fructose-6-phosphate
FAE	Fatty acid elongation
FASII	Fatty acid synthesis type II
FBPase	Fructose-1, 6-biphosphatase
Fcγ	Fragment crystallizable
FKBP	FK506 binding protein
FnRs	Fibronectin receptors
FT	Folate transporter
G3P	Glyceraldehyde-3-phosphate
G6P	Glucose-6-phosphate
G6PDH	Glucose-6-phosphate dehydrogenase
GAPDH	Glyceraldehyde-3-phosphate dehydrogenase
GAS	Group A *Streptococcus*

GCN2	General control nonderepressible kinase 2
GFP	Green fluorescent protein
GILP	Glycosylinositolphospholipid
GOI	Gene of interest
GP	Glutathione peroxidase
GR	Glutathione reductase
GSH	Glutathione
gRNA	Guide RNA
H2F	Dihydrofolate
H4F	Tetrahydrofolate
HAT	Human African trypanosomiasis
HCS	High content screening
HDR	Homology-directed repair
HIV	Human immunodeficiency virus
HK	Hexokinase
HRI	Heme regulator eIF2α kinase
HSP	Heat shock protein
HTS	High throughput screening
HYG	Hygromycin B phosphotransferase
IFNγ	Interferon gamma
IL	Interleukine
IPC	Inositol phosphorylceramide
IV	Intravenous
iNOS	Inducible nitric oxide synthetase
JAK	Janus kinase
kDNA	Kinetoplast DNA
KKT	Kinetoplastid kinetochore protein
LAMP1	Lysosome-associated membrane protein 1
LCF	*Leishmania* chemotactic factor
LFR	*Leishmania* ferric ion reductase
LHR1	*Leishmania* heme receptor 1
LIT1	*Leishmania* ferrous iron transporter 1
LKB1	Liver kinase B1
LPG	Lipophosphoglycan

LRO	Lysosome-related organelles
LRV	*Leishmania* RNA virus
MØ	Macrophage
MAPK	Mitogen-activated protein kinase
MARK	Myristoylated alanine-rich C kinase
MDR1	Multi-drug resistance protein 1
MKP	Mitogen-activated protein kinase phosphatase
MMEJ	Micro-homology mediated end joining
ML	Mucocutaneous leishmaniasis
MR	Manose receptor
mRNA	Messenger RNA
mTOR	Mammalian target of rapamycin
mTORC1	mTOR complex 1
$NADP^+$	Nicotinamide adenine dinucleotide phosphate
NEO	Neomycin phosphotransferase
NHEJ	Non-homologous end joining
NMR	Nuclear magnetic resonance
NO	Nitric oxide
NRAMP1	Natural resistance-associated macrophage protein 1
ODC	Ornithine decarboxylase
PAC	Puromycin N-acetyl transferase
PAO	Polyamine oxidase
PC	Phosphatidylcholine
PCR	Polymerase chain reaction
PE	Phosphatidylethanolamine
PERK	Protein kinase RNA- like endoplasmic reticulum kinase
PFK	Phosphofrutokinase
PG	Phosphatidylglycerol
PGAM	Phosphoglycerate mutase
PGC	Polycistronic gene cluster
PI	Phosphatidylinositol
PKC	Protein kinase C
PKDL	Post kala-azar dermal leishmaniasis
PKR	Protein kinase R

PM	Peritrophic membrane
PMN	Polymorphonuclear cells
Poly P	Polyphosphate
POT1	Polyamine transporter 1
PPG	Proteophosphoglycan
PPi	Pyrophosphate
PPP	Pentose phosphate pathway
PS	Phosphatidylserine
PSG	Promastigote secretory gel
PTP	Protein tyrosine phosphatase
PTR1	Pteridine reductase 1
PTS	Peroxisomal targeting sequence
PUFA	Polyunsaturated fatty acids
PV	Parasitophorous vacuole
PYK	Phosphoglycerate kinase
QDPR	Quinonoid dihydropteridine reductase
R5P	Ribose-5-phosphate
RdRp	RNA-dependent RNA polymerase
RFLP	Restriction fragment length polymorphism
rK39	Recombinant K39
RISC	RNAi silencing complex
RNA	Ribonucleic acid
RNAi	RNA interference
RNase	Ribonuclease
ROS	Reactive oxygen species
RPI	Ribose-5-phosphate isomerase
RPIA	Ribose-5-phosphate isomerase A
RPIB	Ribose-5-phosphate isomerase B
rRNA	Ribossomal RNA
Ru5P	Ribulose-5-phosphate
S7P	Sedoheptulose-7-phosphate
SAP	Secreted acid phosphatases
SAT	Spermidine/spermidine N1-acetyltransferase
SIRT1	NAD-dependent protein deacetylase sirtuin-1

SL	Spliced leader
SM	Sphingomyelin
Spd	Spermidine
Spm	Spermine
SpdS	Spermidine synthase
SpmS	Spermine synthase
STAT1	Signal transducer and activator of transcription 1
TAL	Transaldolase
TCA	Tricarboxylic acid
tet	Tetracycline
TDR1	Thiol-dependent reductase 1
TfR	Transferrin receptor
TGF-β	Transforming growth factor beta
Th	T helper lymphocyte
TKT	Transketolase
TLR	Toll-like receptor
TPI	Triosephosphate isomerase
tRNA	Transfer RNA
TrxR	Thioredoxin reductase
TryR	Trypanothione reductase
TryS	Trypanothione synthetase
TXNPx	Tryparedoxin peroxidase
UPS	Unfolded protein stress
UTR	Unstranslated region
VL	Visceral leishmaniasis
VSG	Variant surface glycoprotein
WHO	World Health Organization
WT	Wild type
X5P	Xylulose-5-phosphate
XO	Xanthine oxidase

Chapter I

Leishmania spp. and leishmaniasis

1. History, taxonomy and evolution

In India 1885, Cunningham described the *Leishmania* parasite for the first time, from a sore designated Delhi boil, which at the time was thought to have fungal origin. Thirteen years later, Borovsky has reported the agent to be a protozoan and described its morphology (Bari, 2006).

However, William Leishman and Charles Donovan were the first to relate the agent to the disease, after independently discovering the parasite in the spleens of patients with kala azar, today known as visceral leishmaniasis (VL). In 1904, the agent responsible for this infection received the taxonomic designation of *Leishmania donovani* (Bari, 2006).

In 1924, it was proposed that the sand fly was the vector of *L. donovani* by John Sinton. This was further supported by others, like Robert Knowles, who provided evidences to support that theory. Nevertheless, only in 1931 Short *et al.* provided the first unequivocal experiment showing the transmission of *L. donovani* by the bite of the sand fly (Sacks & Kamhawi, 2001).

Leishmania parasites belong the subkingdom Protozoa, order Kinetoplastida, family Trypanosomatidae, and genus *Leishmania* (Stevens et al, 2001). In the last quarter of the 20th century, the evaluation of antigenic features (Anthony et al, 1985; de Ibarra et al, 1982) or polymorphism patterns in the kinetoplast DNA (Rodriguez-Gonzalez et al, 2007) allowed the identification of a total of 31 *Leishmania* species, 20 of which thought to be pathogenic to humans.

The modern phylogenetic studies have helped elucidating the taxonomy of the *Leishmania* genus and clearly suggest the existence of two major divergent lineages, *Euleishmania* and *Paraleishmania* (Cupolillo et al, 2000). The latter includes several species that infect sloths or rodents such as porcupines and squirrels, collectively known as *L. hertigi* complex. Additionally, some members of *Endotrypanum*, a *Leishmania* close related genus, also belong to *Paraleishmania* lineage (Cupolillo et al, 2000). On the other hand, the *Euleishmania* division comprises all the species that are pathogenic to humans and is subdivided into the *Viannia* and *Leishmania* subgenera (Cupolillo et al, 2000). The latter encompasses three species complexes with a worldwide distribution, *L. mexicana*, *L. donovani* and *L. tropica*, which cause cutaneous, visceral and cutaneous leishmaniasis, respectively (Pont-Sucre et al, 2013), as illustrated on figure 1. The lizard infecting group, designated as *Sauroleishmania* seems closely related to *Leishmania* subgenera (Croan et al, 1997). The *Viannia* subgenera, in its turn, includes species of the *L. braziliensis* complex, responsible for cutaneous (CL) and mucocutaneous (ML) leishmaniasis (Stevens et al, 2001).

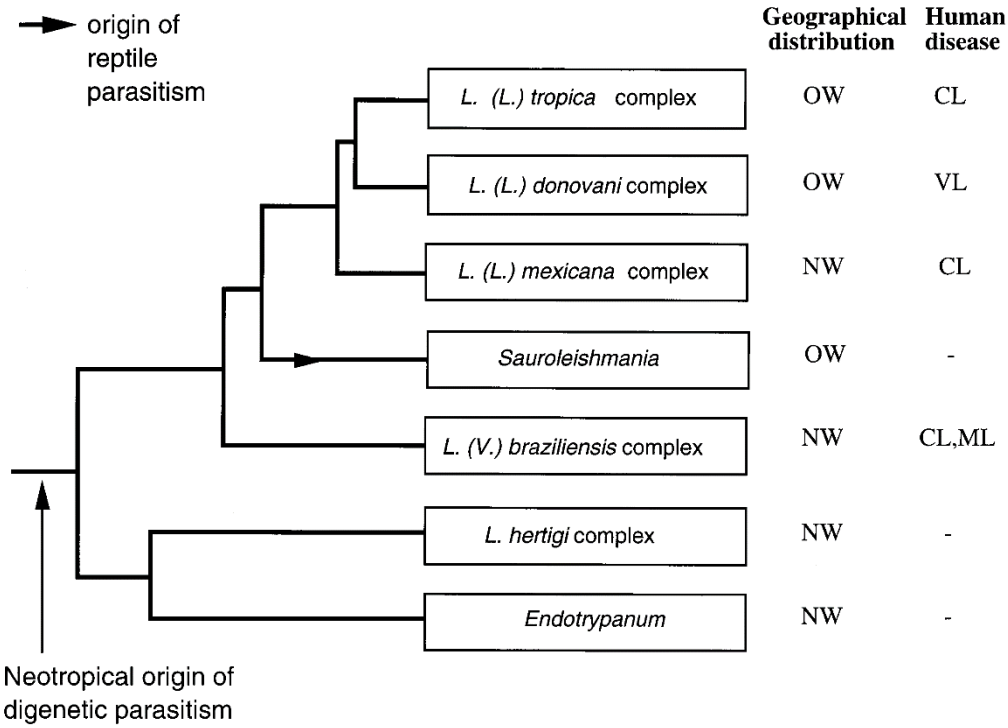

Figure 1. Phylogenetic tree illustrating the *Leishmania/Endotrypanum* subtree of the Kinetoplastida. An indication of the geographical distribution (OW, Old World; NW, New World), common disease pathology (CL, cutaneous; VL, visceral; MC, mucocutaneous) or subgenera (*Leishmania* (*L.*) or *Viannia* (*V.*)) are represented. Adapted from Croan et al, 1997).

The family Trypanosomatidae also includes the genus *Trypanosoma*, which contains the human parasites *Trypanosoma brucei* and *Trypanosoma cruzi*, responsible for the sleeping sickness and Chagas disease, respectively. *T. brucei*, *T. cruzi* and *Leishmania* spp. have different patterns of evolution and the divergence between the *Leishmania* and *Trypanosoma* lineages is also ancient (Stevens et al, 2001).

2. Life cycle

Leishmania is a digenetic protozoan that requires a vertebrate host and an insect vector to complete its complex life cycle. It alternates between two major forms: the promastigote form that parasitizes the sand fly vector, and the amastigote form that proliferates inside the phagolysosome of the mammalian host macrophages (MØs) (Kaye & Scott 2011; Sacks & Noben-Trauth, 2002).

Leishmania promastigotes, which are motile flagellated forms, colonize the digestive tract of *Phlebotomus* spp. and *Lutzomyia* spp. female sand flies. Within the vector midgut promastigotes undergo several transformations (Kaye & Scott 2011; Sacks & Noben-Trauth, 2002). Indeed, promastigotes attach to the midgut wall, and while migrating to the

anterior part differentiate into non-replicative infectious metacyclic promastigotes (Kaye & Scott 2011; Sacks & Noben-Trauth, 2002). The infection of the mammalian host is initiated through the bite of the sand fly that inoculates metacyclic promastigotes in the skin, which can be directly or indirectly phagocytosed by MØs (Kaye & Scott 2011; Van Zandbergen et al, 2004). It is unanimously accepted MØs are the predominantly infected cells by *Leishmania* in the vertebrate host, nonetheless, they are not the first or the only ones to be recruited (Kaye & Scott 2011; Van Zandbergen et al, 2004). For instance, neutrophils rapidly arrive to the inoculation site, internalize *Leishmania* promastigotes, and after infection, dying neutrophils secrete chemotactic factors for MØs (Van Zandbergen et al, 2004). Both MØs and dendritic cells (DCs) are able to remove neutrophil apoptotic bodies containing *Leishmania* promastigotes (Van Zandbergen et al, 2004). The internalized parasites are delivered to the phagolysosome, where they eventually differentiate into amastigotes. This intracellular form has no external flagellum, is replicative, periodically escape the host cell to rapidly reinfect other cells, exploring a mechanism poorly characterized to the date (Kaye & Scott 2011). Among the possibly infected cells are phagocytic (MØs and DCs) and non-phagocytic cells (fibroblasts). Interestingly, the latter have been implicated in the establishment of chronic latent infections (Antoine et al, 2004; Bogdan et al, 2000). The cycle is completed when the sand fly takes another blood meal, taking free amastigotes or infected cells. These infected cells are disrupted in the insect midgut releasing the amastigotes, which rapidly transform into replicative non-infectious promastigotes and the cycle is then perpetuated (Kaye & Scott 2011; Sacks & Noben-Trauth, 2002).

A simplified version of *Leishmania* life cycle is illustrated in figure 2.

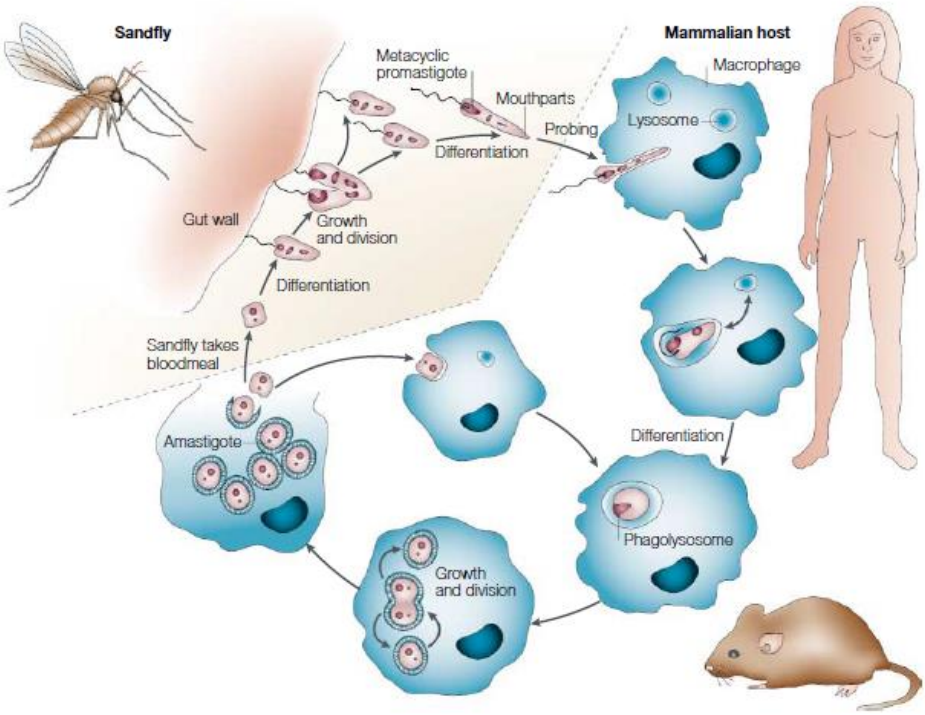

Figure 2. *Leishmania* spp. life cycle. *Leishmania* promastigotes are transmitted to the mammalian host through the bite of an infected female sand fly. These forms once inoculated in the dermis are phagocytosed by MØs and inside the phagolysosome differentiate into replicative amastigotes. Infected MØs are taken by the sand fly vector during the blood meal, releasing in the insect midgut amastigotes that rapidly transform into replicative non-infectious promastigotes. These latter forms attach to the posterior midgut wall, and differentiation into metacyclic promastigotes is accompanied by anterior migration. This non-replicative infectious form can be transmitted to the vertebrate host in the following blood meal, completing the cycle. Adapted from Sacks & Noben-Trauth, 2002.

3. Leishmaniasis

3.1. Disease burden and geographic distribution

Leishmania parasites have successfully evolved to survive and proliferate inside the mammalian host, ultimately causing disease. However, only a small fraction of those infected by *Leishmania* parasites will eventually develop the disease (WHO, 2015)**.** Leishmaniasis is classically divided in three major medical conditions: cutaneous, mucocutaneous and visceral. Usually, a species of *Leishmania* is implicated in a clinical form of the disease, but not necessarily exclusively (Murray et al, 2005). Considering all forms of the disease, leishmaniasis is prevalent in 98 countries, distributed in five different continents, rendering approximately 350 million of people at risk of contracting the infection (WHO, 2015). Only in 33 of these 98 countries reporting is mandatory, thus the real burden is probably much higher than the actual estimation of 1.3 millions of new cases per year (Alvar et al, 2012; WHO, 2015). Among all infectious diseases, leishmaniasis accounts for

the ninth largest disease burden, and among parasitic infections in particular, the 20,000 to 30,000 annual deaths are only surpassed by malaria (Alvar et al, 2012; WHO, 2015).

3.2. Cutaneous leishmaniasis

CL is the most common form, causing skin lesions on exposed parts of the body, mainly ulcers, which can cause serious disability. CL has a worldwide distribution, but most cases (~95%) occur in America, the Mediterranean basin, the Middle East and Central Asia (Fig. 3). CL is endemic in 70 countries, but strikingly, more than two thirds of CL cases take place in 6 countries: Afghanistan, Algeria, Brazil, Colombia, Iran and the Syrian Arab Republic. Estimates point to 0.7 to 1.3 million new cases worldwide annually WHO, 2015).

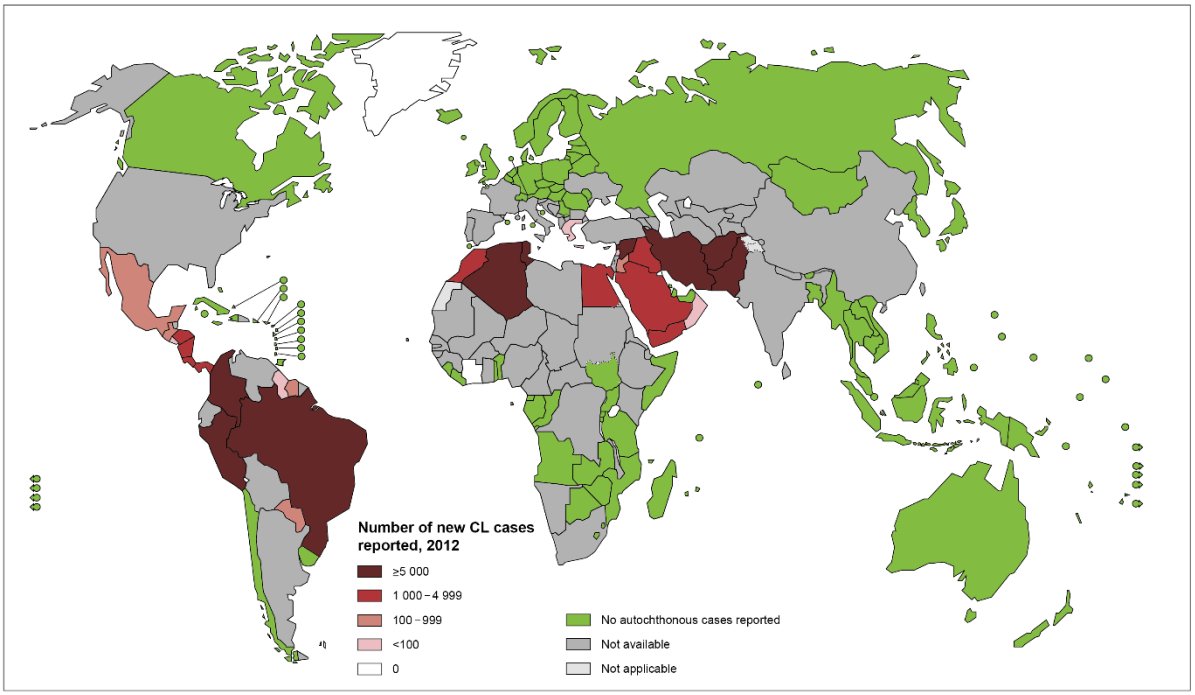

Figure 3. Worldwide distribution of cutaneous leishmaniasis (WHO, 2012).

Several species of *Leishmania* can be responsible for CL. In the Old World, *L. tropica*, *L. major* and *L. aethiopica* are the main causative agents. On the other hand, in the New World, CL can result from infection by species of both the *Leishmania* and *Viannia* subgenera, such as *L. amazonensis* and *L. braziliensis*, respectively (Alvar et al, 2012; WHO, 2015). Nevertheless, some species usually associated with visceral ailment may also cause cutaneous lesions, like *L. infantum*, which is the most frequent cause of CL in Europe (Alvar et al, 2012; WHO, 2015). CL is mainly a zoonotic disease, although humans may serve as *L. tropica* reservoirs.

Typically, an erythema appears at the site of the sandfly bite, which further develops into a slow growing papule or nodule that normally takes weeks to reach its final size. Following, a crust is formed and eventually falls off, exposing the ulcerated lesion. Ulcers progressively heal over months or even years, but often leave life-long scars (Alvar et al, 2012; David & Craft, 2009). The high diversity of CL causative species, as well as the variability of the host status underlie the encountered differences in the clinical manifestations of the disease, regarding in particular, ulcers formation, inflammation level or required time for lesions to self-heal (Alvar et al, 2012; David & Craft, 2009).

3.3. Mucocutaneous leishmaniasis

ML leads to a partial or total destruction of mucous membranes of the nose, mouth and throat and almost 90% of the cases occur in South America, particularly in Bolivia, Brazil and Peru (WHO, 2015). It is caused by species of the *Viannia* subgenera, namely *L. braziliensis*, *L. panamensis* and *L. guyanensis*.

Posteriorly to the resolution of a primary cutaneous lesion, *Leishmania* species responsible for ML are able to metastasize, via blood or lymph, to the mucosal tissues surrounding the mouth or the upper respiratory tract (Alvar et al, 2012; David & Craft, 2009). The mucocutaneous lesions appear only in 5 to 10% of the patients, with a latency period ranging from a few months to many years. Usually in the beginning, the appearance of an erythema and ulceration of the nares take place and the appearance of nodules in the nasal septum follows. Subsequently, the septum is perforated and eventually collapses, broadening the nose. In several patients, pharynx, larynx and trachea can also be affected (Alvar et al, 2012; David & Craft, 2009). Importantly, spontaneous healing in ML is very seldom, and it is potentially fatal, normally due to opportunistic bacterial infections (David & Craft, 2009). Moreover, another preoccupying aspect, not always emphasized, is that the ML driven facial disfigurement profoundly burdens the patients as they are likely doomed to lifelong social stigma.

Typically in ML, there is a massive tissue destruction accompanied by immune cell infiltration and inflammation, in an uncontrollable fashion, and curiously, few parasites are found in the lesions (Ronet et al, 2011). Taken all together, these evidences pointed to a major contribution of the host genetic background in the outcome of the disease, and inclusively, polymorphisms in genes encoding for mediators of the inflammatory response have been implicated (Ronet et al, 2011). Actually, the current view is now that the occurrence of ML is determined by the host genetic background, but the severity of the pathology may be exacerbated by parasite-driven factors (Hartley et al, 2012). One of these

factors is the presence of *Leishmania* RNA Virus (LRV), a double-stranded RNA virus that parasites some *Leishmania* species (Zangger et al, 2013).

3.4. Visceral leishmaniasis

VL, also known as kala-azar, is fatal if left untreated. Inclusively, all the mortality associated to leishmaniasis results mainly from visceral disease with 20,000 to 30,000 annual deaths (WHO, 2015). The asymptomatic period of VL varies from a few weeks to one year (or more). The disease usually progresses gradually over several months. The main signs and symptoms include irregular rounds of fever, weight loss, augmentation of the spleen and liver and anaemia (Alvar et al, 2012).

As depicted in figure 4, it is particularly endemic in the Indian subcontinent (India, Bangladesh, Nepal) and East Africa (Sudan, Ethiopia and Somalia). Annually, estimates point to 200,000 to 400,000 new cases of VL worldwide, but mostly (more than 90%) occur in Bangladesh, Brazil, Ethiopia, India, South Sudan and Sudan (WHO, 2015). However, the degree of under-reporting is much accentuated.

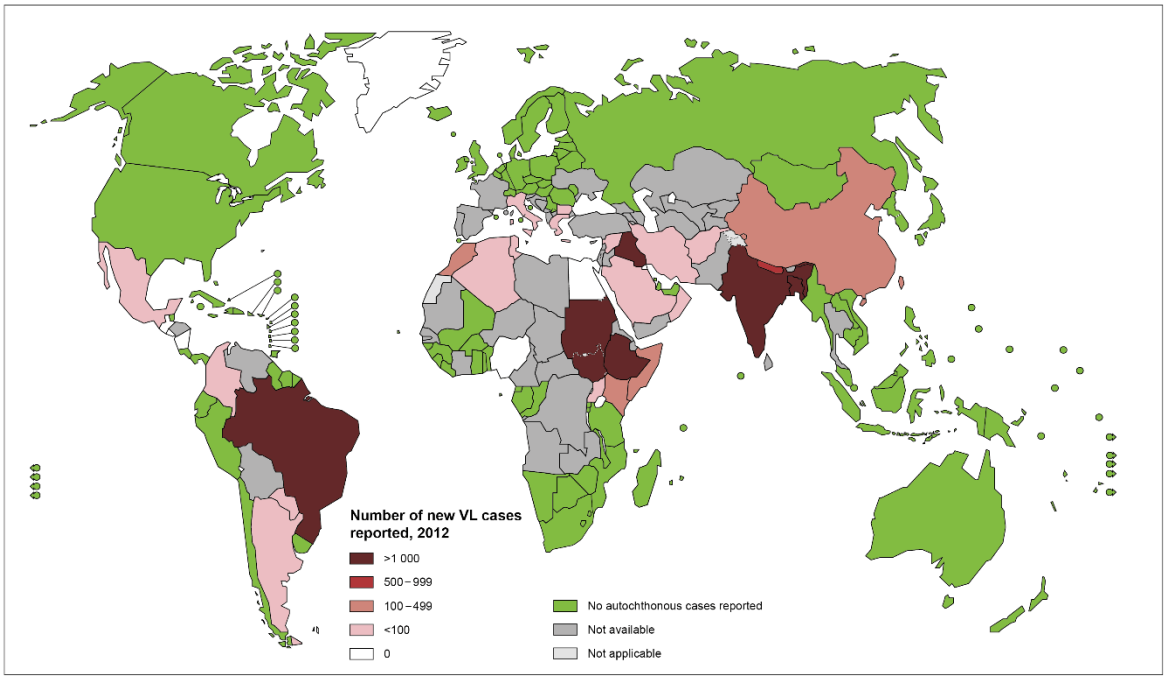

Figure 4. Worldwide distribution of visceral leishmaniasis (WHO, 2012).

L. donovani is the causative agent of VL in Asia and East Africa, whereas *L. infantum* equally leads to visceral compromise but in the Mediterranean Basin and South America (Murray et al, 2005). Differently, while dogs are the most important reservoirs of VL caused by *L. infantum*, in the case of *L. donovani*, the disease is mostly anthroponotic (Chappuis et al, 2007). Another striking difference is that *L. donovani* is capable of causing disease in

people of all ages, although children and young adults are the most affected. In the case of *L. infantum*, small children used to be the main age group, however, as HIV (Human Immunodeficiency Virus)/*L. infantum* co-infections emerged, nowadays adults actually represent almost half of VL cases in Europe (Chappuis et al, 2007; WHO, 2015).

The disease manifestation always include splenomegaly, not always accompanied by hepatomegaly. For instance, lymphadenopathy is not as frequent and occurs mainly in Sudan (Van Griensven & Diro, 2012). Spleen, liver, bone marrow and lymph nodes' phagocytes are extremely parasitized, albeit lymphocyte infiltration is scarce. In the spleen, the disruption of the lymphoid architecture is common and plasma cells are abundant and probably related to the polyclonal hypergammaglobulinemia (Van Griensven & Diro, 2012). The observed anaemia is likely a result of splenic sequestration and suppression of bone marrow function, but additionally, complement activation also seems to make a contribution. The first two also lead to thrombocytopenia and neutropenia (Van Griensven & Diro, 2012). The latter is probably responsible for an increased susceptibility to secondary infections, like tuberculosis or pneumonia, which are frequent causes of death (Van Griensven & Diro, 2012). The presence of immune complexes can sometimes lead to nephritis, proteinuria and hematuria. Liver function may be altered (Chappuis et al, 2007; Murray et al, 2005; Van Griensven & Diro, 2012; WHO, 2015). Inclusively, prothrombin depletion can lead to mucosal haemorrhage at advanced stages, when jaundice and ascite can also occur.

Importantly, in *L. donovani* endemic regions, 10 to 60% of the patients experience the so called post kala-azar dermal leishmaniasis (PKDL), which is a skin rash that appears within 6 months to one year after VL resolution (Ramesh et al, 2007). Nevertheless, there are also cases of PKDL described in patients not previously diagnosed with or treated for VL. PKDL typically appears with the formation of erythematous macules and papules, which can eventually evolve to nodules. Any part of the body may be affected, but the most frequently affected sites are the face, the trunk and the extremities (Ramesh et al, 2007). Although the responsible parasite species is the same, comparing PKDL in India or Sudan leads to important differences, namely in the percentage of people that experience PKDL after treatment for VL, the timeframe between both presentations and the disease characteristics (Ramesh et al, 2007).

The cause, risk factors and pathogenesis of PKDL are largely unknown, although several host factors (Ramesh et al, 2007) and the possibility that PKDL is a drug related phenomenon (Croft, 2008) have been broadly considered. Traditionally, PKDL has been proposed to be a relevant *L. donovani* reservoir during intra-epidemic periods of VL (Addy & Nandy, 1992) Inclusively, research aiming detailed disclosure of the transmissibility of different morphologies of PKDL remains a priority (Ramesh et al, 2007; WHO, 2012).

3.5. Visceralization determinants

Leishmaniasis is associated with a wide spectrum of clinical manifestations, ranging from cutaneous to visceral forms of the disease, as described above. Actually, one of the oldest and most important questions in *Leishmania* research is precisely why some species are confined to the skin whereas others find their way to the viscera, and therefore which are the determinants of the visceralization process. Genetic, immunologic and animal models have begun to provide some insights on the process, however, overall it is still modestly comprehended (McCall et al, 2013). Generally vector, host and pathogen related factors are important mediators. Moreover, the knowledge of this process is deeply appealing to understand the disease evolution, as well as the survival mechanisms in the targeted organs (McCall et al, 2013).

Experimental animal models using different infection routes have highlighted interesting features. When using a subcutaneous needle infection, *L .major* not only generates skin lesions but also disseminates to the visceral organs in BALB/c mice, contrasting with C57BL/6 mice, in which visceralization is not observed (Laskay et al, 1995). This *per se* evidences the importance of the host immune response in the process. Using the same injection route, *L. donovani* for instance causes a minimal swelling at the site of the injection but also fails to visceralize (Melby et al, 1998), emphasizing that subcutaneous injection does not mimic the observed disease onset in humans. Animal models of VL based on intradermal infection have been established in both mice (Ahmed et al, 2003) and hamsters (Gomes et al, 2008), displaying parasite clearance in the skin coupled with dissemination to internal organs. Although the initial inoculum is much higher than the one of the sand fly, they are still the models that more closely mimic the “natural” infection and therefore more valuable to gain hints on the cells and pathways involved in the visceralization process (McCall et al, 2013).

Animal models based on intravenous infection in their turn do not mimic at all the natural course of the infection, although they are commonly adopted to study VL using BALB/c mice (McCall et al, 2013). As the normal requirement for the parasite to migrate from the skin to the visceral organs is bypassed, these models ultimately focus on the ability of the parasites to survive and proliferate in the organs. However, at least they have led to some important conclusions. For instance, intravenous injection of *L. major* causes a very limited parasite burden in the spleen and in the liver, in opposition to *L. donovani* or *L. infantum* (Zhang & Matlashewski, 2001), suggesting that independently of the mechanisms to exit the skin, overall, visceral species are better adapted to survive in the viscera (McCall et al, 2013).

Several factors have been reported to play a role in the permissiveness of the host to VL. Actually, considering that only a small percentage of the people infected with a visceral species of *Leishmania* develops disease (Badaró et al, 1986), this already points to an important contribution of the host genetic and immunological background. Regarding the host genetics, several polymorphisms in genes encoding for cytokines and their receptors (Bucheton et al, 2007; Frade et al, 2011; Karplus et al, 2002; Mehrotra et al, 2011; Mohamed et al, 2003), as well as in natural resistance-associated MØ protein 1 (NRAMP1, Bucheton et al, 2003), mannan-binding lectin (Alonso et al, 2007) and the delta-like 1 ligand for Notch 3 (DDL1, Mehrotra et al, 2012) have been implicated. Apart from genetic factors, some acquired factors can also play an important contribution, such as HIV infection (Desjeux & Alvar, 2003), malnutrition (Maciel et al, 2008) or youth (Muller et al, 2008), which increase the risk to develop symptomatic VL due to compromised immune responses. Inclusively, in HIV co-infected patients, VL can be caused by *Leishmania* species that normally are associated with cutaneous disease (Gramiccia, 2003). These observations indicate that an effective Th1 cellular response is indispensable to control the disease, although not sufficient *per se* (McCall et al, 2013).

Additionally, there are also vector related factors that seem to play a role in visceralization. The level of vasodilatation upon the sand fly bite was proposed to be one of them, as the higher it was, better access to visceral organs would be provided, and therefore vector species might influence the disease progression (McCall et al, 2013). For instance, *L. chagasi* transmitted by *Lutzomyia longipalpis* sand flies can cause CL or VL in South America, and the saliva of flies from cutaneous regions induced lower vasodilatation (Warburg et al, 1994). However, this might not be as straight forward as it seems, as sequence analysis of the salivary proteins from a *Phlebotomus* species associated with *L. infantum*-driven cutaneous infections in the Old World demonstrated that those proteins were actually more closely related to those of vectors transmitting visceral *L. donovani* or *L. infantum* than the ones transmitting cutaneous *L. major* and *L. tropica* (Rohousova et al, 2012). Another vector related factor that seems to be important is the number of the inoculated parasites, as a higher dose may elicit a more intense local immune response that can restrain the parasite dissemination to the visceral organs (Maia et al, 2011). Moreover, protection against VL has been achieved using sand fly salivary proteins in hamsters (Gomes et al, 2008), in a nonhuman primate model (Oliveira et al, 2015) and the same may also apply to humans (Vinhas et al, 2007; Aquino et al, 2010). Consequently, the role of the sand fly in pathology experiences a growing interest.

Notwithstanding, although vector and host factors influence the appearance of symptomatic VL, parasite-driven factors seem to be the most important visceralization

determinants. A very indicative observation is that intravenous infection of inbred mice with *L. infantum* strains recovered from patients with CL were unable to establish VL in opposition to strains recovered from patients with the visceral form (Sulahian et al, 1997). Overall, differences in species or even subspecies-specific genes, genetic polymorphisms, pseudogenes and expression of virulence and stress response genes can be crucial for the pathology (McCall et al, 2013).

In this context, it is imperative to mention the A2 gene family, as it represents a gene family that is clearly required for visceralization. It is expressed in visceral species such as *L. donovani* and *L. infantum*, while it corresponds to pseudogenes in cutaneous species such as *L. major* and *L. tropica* (Charest & Matlashewski, 1994; Ghedin et al, 1997). A2 genes are arranged in tandem on chromosome 22 and are made almost entirely of 40 to 90 copies of the same repetitive ten amino acid sequence (Zhang et al, 1996). Their expression is triggered by promastigote differentiation into amastigotes (Charest & Matlashewski, 1994), as well as stressful conditions such as heat shock (McCall & Matlashewski, 2010), unfolded protein stress (UPS, Gosline et al, 2011) and misfolded protein stress (Barak et al, 2005). Partial knockout of these genes led to a decrease in the parasite burden in the liver of BALB/c mice (Zhang & Matlashewski, 2001), and in opposition, their insertion in *L. major* led to an increase in parasite survival in the viscera (Zhang et al, 2003). Another evidence of the key role of A2 genes for parasite survival in visceral organs is that their expression is downregulated in PKDL (Sharma et al, 2010). Visceral *Leishmania* species are more resistant to higher temperatures than cutaneous species, and the promastigotes of the latter are also more susceptible to heat shock (Callahan et al, 1996; McCall & Matlashewski, 2010). Additionally, the fever found in VL increases oxidants production by phagocytic cells (Beachy & Repasky, 2011), but visceral *Leishmania* species are also more resistant to these reactive species (Sarkar et al, 2012). A2 may be an important player in these characteristics of viscerotropic species as it does protect against heat shock (McCall & Matlashewski, 2010) and oxidative stress (McCall & Matlashewski, 2012). Actually, A2 is a candidate for a VL vaccine in dogs, and potentially in humans (Fernandes et al, 2012).

Out of over 8,000 genes, only 19 turned to be *L. donovani* specific, being absent or pseudogenes in cutaneous species (Peacock et al, 2007). Some of these genes were investigated and ectopically expressed in *L. major* to see whether it would induce visceralization (Zhang & Matlashewski, 2010). Apart from A2 family genes, a cytosolic protein of unknown function, a nucleotide sugar transporter localized in the Golgi and a cytosolic glyceraldehyde-3-phosphate dehydrogenase (GAPDH), which is a key glycolytic enzyme (Zhang & Matlashewski, 2010) were identified as potential visceralization factors. With the exception of the first protein, the last two are also present in *L. mexicana* and

besides promoting visceralization when ectopically expressed in *L. major*, they also increase the skin lesions, suggesting they are virulence, rather than visceralization determinant factors (Zhang & Matlashewski, 2010). Ectopic expression in *L. major* did increase the survival rate in visceral organs, but never in an extent comparable to *L. donovani* (Zhang & Matlashewski, 2010). These results also suggest that *L. donovani* gene specific combinations, along with gene amplifications, polymorphisms and post-transcriptional regulation may play an important role in the whole process (Zhang & Matlashewski, 2010).

Moreover, it is important to highlight the MØ population targeted by *Leishmania* differs, as cutaneous species infect monocyte-derived MØ (De Trez et al, 2009), whereas visceral species infect Kupffer cells, spleen MØ and bone marrow derived MØ (BMMØ) (McCall et al, 2013). These MØ populations differ at several levels, namely in the expression of surface markers and cytokine production (Taylor et al, 2005). Cutaneous and visceral species have adapted to these different cellular environments, although the susceptibility and microbicidal potential of these different MØ populations in the context of *Leishmania* infection have not been specifically addressed (McCall et al, 2013).

Overall, there are still many questions in the visceralization process, regarding the mechanism (free parasites or infected cells; *via* blood or lymph; same mechanism or not for the different organs; chronology; etc) and the identification of novel visceralization factors (for instance, factors that allow *L. donovani* to switch from visceral (VL) to cutaneous (PKDL)). Additionally, in an evolutionary perspective, was visceralization a newly acquired characteristic? What is the importance of the reservoir?

4. *Leishmania* Cell biology

Trypanosomatids (among which, *Leishmania* spp, Trypanosomes) are kinetoplastids, corresponding to a large group of flagellated parasitic protozoans that have several singular and remarkable features. Apart from the impact of some of them on public health, they represent a fascinating model to study several cellular functions and mechanisms. These parasites are equipped with several specific and unique cellular organelles. One of the most notable is the kinetoplast, which corresponds to a special part of their single mitochondrion containing a complex DNA structure. Another striking characteristic is the presence of glycosomes, peroxisome-related microbodies that contain most of the glycolytic pathway, among others. Moreover, the genomic organization and plasticity, *trans*-splicing, RNA editing mechanisms and eukaryotic polycistronic transcription of protein-coding genes never cease to impress.

4.1. Specific cellular organelles

Two distinctive characteristics of trypanosomatids are the presence of a flagella (Fig. 5) and a flagellar pocket (Fig. 5), which corresponds to an invagination of the plasma membrane (Landfear & Ignatushchenko, 2001). Actually, the membrane of these organisms has been divided in three morphologically different domains: the pellicular plasma membrane, the flagellar pocket, and the flagellar membrane (Balber, 1990). Although they are physically contiguous and part of the plasma membrane, they have unique protein compositions and specialized functions (Landfear & Ignatushchenko, 2001). The pellicular plasma membrane involves the cell body and is attached to a dense and stable arrangement of microtubules. It contains many classical nutrient transporters, it confers cell body shape , and in some cases, it can be heavily coated with proteins or glycolipids (Landfear & Ignatushchenko, 2001), which can for instance play a role in immune evasion, as the variant surface glycoproteins (VSGs) in *T. brucei* (Van der Ploeg, 1990) or lipophosphoglycan (LPG) in *Leishmania* spp (Turco & Descoteaux, 1992).

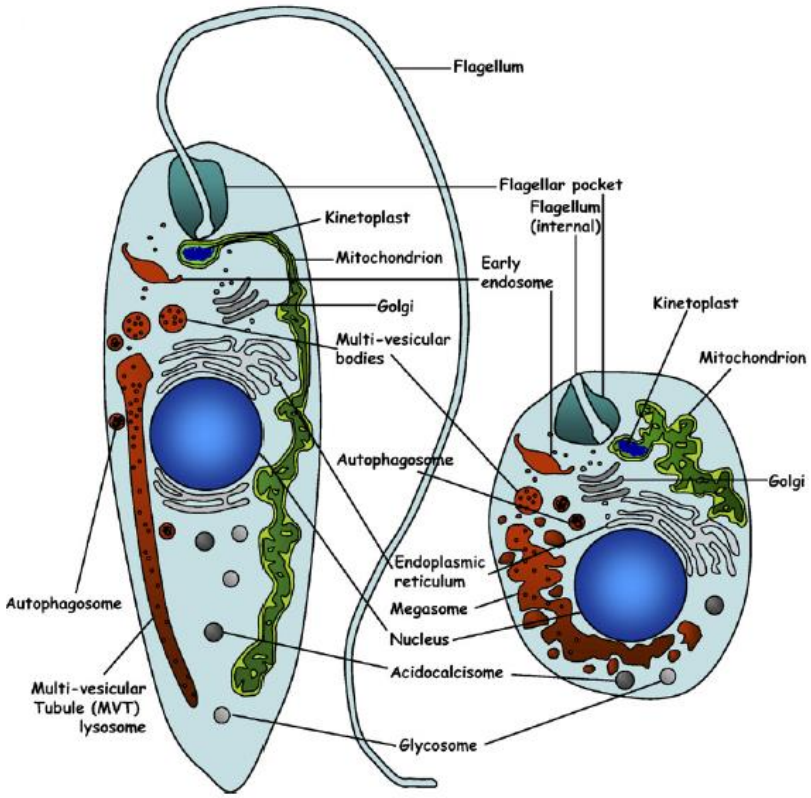

Figure 5. Developmental stages of *Leishmania* parasites. Scheme depicting the main structural features and intracellular organelles from *Leishmania* promastigote (left) and amastigote (right) forms. Adapted from Besteiro et al, 2007.

The flagellar pocket, particularly, is responsible for larger nutrients uptake by receptor-mediated endocytosis, integration of proteins in the cell surface and protein secretion (Field & Carrington, 2009; Landfear & Ignatushchenko, 2001).

The flagellum is a classical motility organelle but can be involved in additional biological activities, such as parasite attachment to the insect host epithelium (da Cunha e Silva et al, 1989). In the particular case of *Leishmania* promastigotes' flagellum, its axoneme is organized in a canonical fashion, displaying a "9+2" microtubule arrangement (da Cunha e Silva *et al*., 1989; Landfear & Ignatushchenko, 2001). On the other hand, amastigotes are often and inaccurately described as "aflagellated", as they do present a short flagellum, which is likely to be important for sensorial purposes (Gluenz et al, 2010). The central pair of microtubules is absent in these forms, but is occupied by one or more of the peripheral pairs, which is considered a 9*v* (variable) arrangement (Gluenz et al, 2010).

Other of their most remarkable possessions is the kinetoplast (Fig. 5), unique to the single mitochondrion of parasites belonging to Kinetoplastida order. It is noteworthy the kinetoplast not only possesses an incredibly complex and singular network structure but also hosts a novel RNA editing mechanism (Lukes et al, 2002).

The glycocomes are another singular organelle of these parasites once more emphasizing their uniqueness. Glycosomes (Fig. 5) are specialized peroxisomes that harbour most part of the glycolysis, the pentose phosphate pathway (PPP), β-oxidation of fatty acids, gluconeogenesis, purine salvage and biosynthesis of pyrimidines, ether lipids and squalenes (Parsons et al, 2001; Szoor et al, 2014). The compartmentalization of these metabolic pathways is thought to prevent accumulation of toxic intermediates as well as to facilitate a rapid response to environmental stimuli (Besteiro et al, 2007; Kaye & Scott, 2011). The glycosome number as well as the qualitative and quantitative enzymatic content differs among trypanosomatids, in a species and life cycle stage dependent manner (Parsons et al, 2001; Szoor et al, 2014).

Moreover, trypanosomatids also possess acidocalcisomes (Fig. 5), which are acidic organelles whose function might be related to cations and phosphorus storage, calcium homeostasis, pH maintenance and osmoregulation, among others (Docampo et al, 1995; Moreno & Docampo, 2009). Their membranes present a great number of pumps (Ca^{2+}-ATPase, V-H^+-ATPase, H^+-PPase), exchangers (Na^+/H^+, Ca^{2+}/H^+) and channels (aquaporins). Great amounts of phosphorus can be found in their matrix, present as pyrophosphate (PPi) and polyphosphate (poly P), complexed with calcium and other cations, as well as enzymes involved in their metabolism (Moreno & Docampo, 2009). Acidocalcisomes resemble lysosome-related organelles (LRO) from mammalian cells in many aspects. Moreover, in some microorganisms like *Toxoplasma gondii* and *T. cruzi*,

they also interact with other organelles, namely vacuoles, which reinforces their association with the endosomal/lysosomal pathway (Moreno & Docampo, 2009).

4.2. Cell division

Studies on *L. mexicana* have revealed that cell division in *Leishmania* is generically similar to other trypanosomatids. However, if the regulation of some cellular processes is common, others may be specifically adapted to the biology of each species (Wheeler et al, 2011). *L. mexicana* exponentially growing promastigotes progress through the cell cycle in an asynchronous manner. Impressively, these promastigotes display several different morphologies that reflect different stages of a single proliferative cycle (Wheeler et al, 2011). Typically, trypanosomatids possess one nucleus (N), one kinetoplast (K) and one flagellum (F), and each replicates once during a cell cycle. In *Leishmania*, the flagellum growth initiates first, followed by mitosis, and only after the onset of nuclear anaphase, kinetoplast division takes place (Fig. 6). The following morphologies are then subsequently present 1K1N1F, 1K1N2F, 1K2N2F, 2K2N2F and 2x (1K1N1F). Interestingly, these events are concentrated in the remaining 20% of the cell cycle (Wheeler et al, 2011).

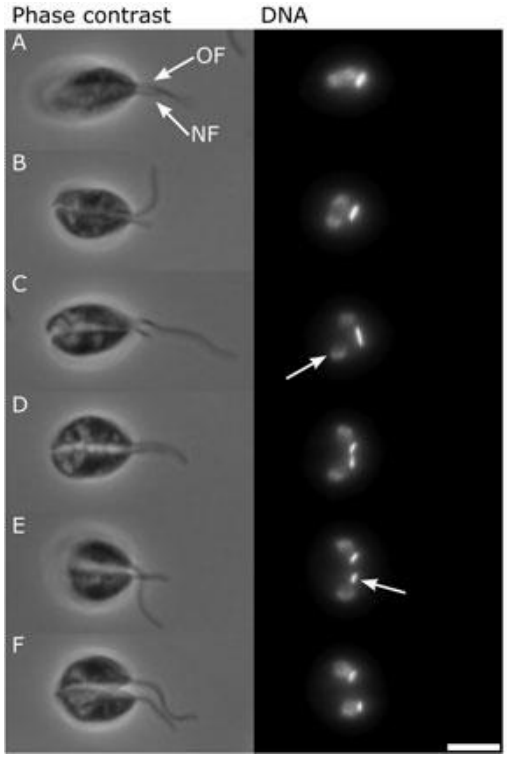

Figure 6. ***L. mexicana*** **promastigotes' cell division.** A-F correspond to phase-contrast image, displayed in order of the cell cycle progress and correspond to a single z-stack. The kinetoplast (K) and the nucleus (N) are DAPI stained. At the end of S phase, the new flagellum (NF) emerges from the flagellar pocket, and is considerably shorter than the old flagellum (OF). K and N enter division on the OF side of the cell (A). During the mitosis, one N is repositioned to the NF side of the cell (C). K segregation occurs only after nuclear

anaphase, eventually, one daughter K is positioned in the NF side of the cell (E). The scale bar corresponds to 5 µm. Adapted from Wheeler et al, 2011.

L. mexicana nuclear and kinetoplast S phase are synchronous and correspond to 40% of the overall cycle. Its nuclear S phase is rather long when comparing to trypanosomes (Elias et al, 2007; Woodward & Gull, 1990), and it does not correlate to the genome size. This can instead reflect differences in chromosome number, genome architecture or in DNA replication machinery processing (Wheeler et al, 2011). The kinetoplast S phase is more similar to other trypanosomatids, though. However, unlike *T. brucei* (Woodward *et al*., 1990), *Leishmania* undergoes mitosis before kinetoplast segregation is complete (Wheeler et al, 2011).

In both *Leishmania* and *T. brucei* basal body duplication pattern is similar and the changes in the cell shape during cytokinesis seem symmetrical, contrasting with mitosis and kinetoplast division, which are asymmetrical (Fig. 6). This suggests that the regulation of these events in the two organisms may rely on common mechanisms (Wheeler et al, 2011). On the other hand, concerning the flagellum growth regulation, *Leishmania* sharply contrasts with *T. brucei*, suggesting that different regulatory mechanisms may be involved (Wheeler et al, 2011).

The *Leishmania* flagellum starts growing in G1, remains constant during S phase, and the new flagellum eventually emerges from the flagellar pocket at the end of S phase (Wheeler et al, 2011). At division, in contrast to *T. brucei* (Farr & Gull, 2009), the two daughter cells have flagella of unequal length (the new flagellum is usually considerably shorter). One of the most notorious aspects in *Leishmania* is that flagellum length apparently keeps growing over several consecutive cycles (Wheeler et al, 2011).

Curiously, during *L. mexicana* cell division, abscission may not occur after cytokinesis, generating doublets, meaning two cells connected by a cytoplasmatic bridge in their posterior ends, which correspond to 10% of the total population (Wheeler et al, 2011). Doublets go through the cell cycle normally and in a synchronous manner. The *in vivo* relevance of these forms is debatable as they may actually be an *in vitro* culture artefact or alternatively, in the sand fly gut, they may be advantageous to the daughter cell, facilitating its attachment to the epithelium (Wheeler et al, 2011).

Another important question is the fact these parasites have different life cycle stages, and these differentiation events may involve a specialized division in which one of the daughter cells has a modified morphology and/or biochemistry (Wheeler et al, 2011). Recently, an asymmetric cell division was characterized in *T. cruzi*, showing how it discards the flagellum during the remodelling of the trypomastigote form into oval amastigotes that possess no external flagellum (Kurup & Tarleton, 2014).

Concerning the cell division machinery, kinetoplastids display an amazing feature that even challenges the long lasting issue of the eukaryotic tree of life root position (Akiyoshi & Gull, 2014). They do possess the CDK/cyclin system, aurora B, anaphase promoting complex (APC) and proteasomes, suggesting that the basic cell cycle machinery is conserved (Akiyoshi & Gull, 2013). However, in comparison to all the remaining sequenced eukaryotes, they lack any conventional kinetochore protein homologue. This challenged the assumption of kinetochore universality and recently, 19 novel kinetochore proteins (KKT1-19) were identified in *T. brucei*, the majority of them appear conserved among kinetoplastids (Akiyoshi & Gull, 2014). Furthermore, these parasites build these protein macrocomplexes that orient chromosome segregation, using a different set of proteins, which display a variety of features not found in conventional kinetochores (Akiyoshi & Gull, 2014).

4.3. Genome organization and gene expression

One of the biggest revolutions in the field was the genome sequencing of several *Leishmania* spp. The availability of the nuclear genome provided new insights on parasite evolution, immune evasion strategies and many unusual aspects of the biology of these eukaryotes. In 2005, the first *Leishmania* genome became available, the genome of *L. major* (Ivens et al, 2005). In 2007, the genomes of *L. infantum* and *L. braziliensis* were also sequenced, and ever since, others have progressively followed (Peacock et al, 2007; Raymond et al, 2011; Rogers et al, 2011).

The comparison of the genome of different *Leishmania* spp., associated with distinct disease presentations, showed that among the 8300 predicted genes, surprisingly only 78 were actually species specific. This was also extremely important to screen for potential parasite related visceralization determinants (Peacock et al, 2007). Interestingly, even *L. tarentolae*, which is not a human pathogen, presents 90% conservation, and only lacks 250 genes in comparison to the core of *Leishmania* spp. genome (Raymond et al, 2011). Additionally, when comparing both gene content and genomic architecture with *T. brucei* (Fig. 7) and *T. cruzi*, a core of approximately 6200 genes is conserved in large syntenic polycistronic gene clusters (El-Sayed et al, 2005). This impressive conservation once more reinforces that a massively diverse genetic background does not underlie the distinct life cycles and disease outcomes in trypanosomatids.

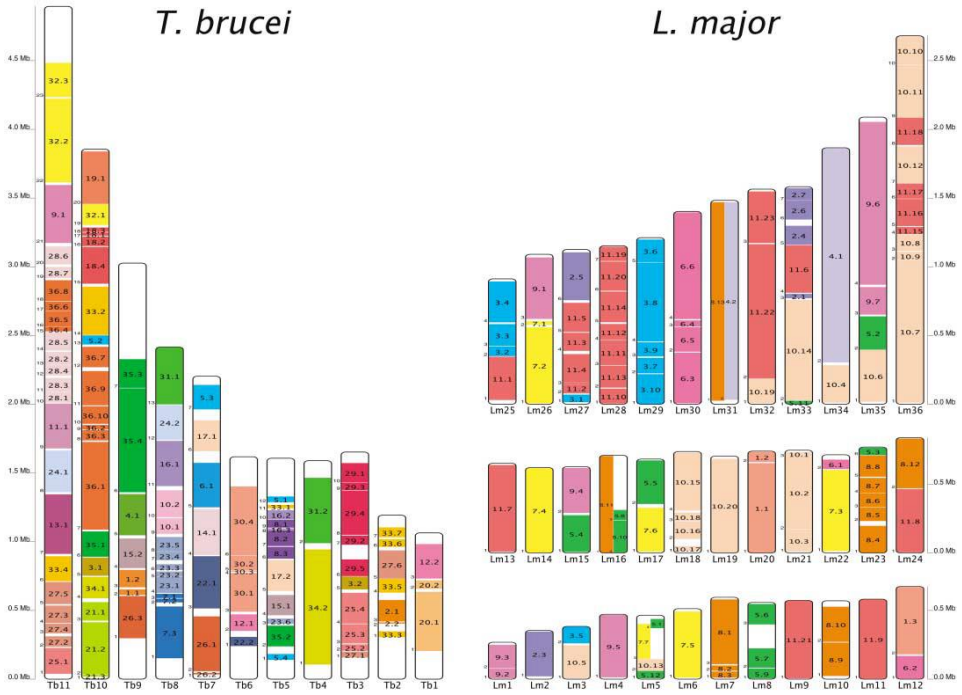

Figure 7. *L. major* and *T. brucei* genomes comparison: synteny maps. The 36 different colours in the *T. brucei* (left) panel represent the location of the indicated synteny blocks in the 36 chromosomes of *L. major*, and the 11 colours in the *L. major* (right) panel illustrate the locations of the indicated synteny blocks in the 11 chromosomes in *T. brucei*. Adapted from El-Sayed et al, 2005.

Kinetoplastids possess, like all other eukaryotes, two genomes: nuclear and mitochondrial (kinetoplast). The nuclear genome is around 34 Mb, with inter-species variations, and each chromosome has between 0.3 and 2.8 Mb (Bastien et al, 1992; Wincker et al, 1996). The karyotype is variable in number, as Old World and New World species present 36 and 34 or 35 chromosomes, respectively (Wincker et al, 1996; Britto et al, 1998).

Leishmania nuclear genome is renowned for the extensive plasticity (Bastien et al, 1992), which ultimately may allow a rapid and appropriate adaptation to environmental changes, but often drives genetic manipulation quite challenging. As the core genome of *Leishmania* is relatively conserved, this plasticity may have a significant contribution to virulence or drug resistance differences, observed in different clinical isolates (Sterkers et al, 2011; Ubeda et al, 2008). From high spontaneous chromosomal polymorphisms (Sterkers et al, 2011) to spontaneous or stress-driven genetic amplification (Grondin et al, 1996; Olmo et al, 1995; Navarro et al, 1994; Segovia, 1994; Ubeda et al, 2008; Ubeda et al, 2014), several mechanisms have been described.

A few years ago, the possibility of genetic exchange between parasites was a controversial subject, as it was generally accepted that *Leishmania* multiplies by binary

fission (Banuls et al, 2007). However, there were several independent reports of interspecies hybrids (Chargui et al, 2009; Odiwuor et al, 2011; Ravel et al, 2006) over time. In 2009, a study clearly demonstrated the formation of hybrids in the sand fly (Akopyants et al, 2009), using *L. major*, and later in 2011, using *L. donovani* (Sadlova et al, 2011). Recently, a cross-species genetic exchange between cutaneous and visceral strains in the vector was reported (Romano et al, 2014), as well as the rate of sexual and asexual reproduction in vector-isolated parasites (Rogers et al, 2014).

As for the mitochondrial genome, the kinetoplast DNA (kDNA) corresponds to a huge network of thousands of catenated circular DNAs, being the most structurally complex known mitochondrial DNA structure. It is formed by maxicircles (20 to 40 kb) and minicircles (0.5 to 10 kb), present in a few dozen identical copies per network or thousands of copies per network similar in size but heterogeneous in sequence, respectively (Estévez & Simpson, 1999; Gott & Emeson, 2000; Lukes et al, 2002). Maxicircles encode for classical mitochondrial gene products, as rRNA or subunits of the respiratory chain, but impressively, some of the protein-coding genes are encrypted. The transcripts of these encrypted genes must undergo post-translational modifications, through a novel RNA editing mechanism that comprises deletion and insertion of uridine residues in specific sites of the transcripts, to ultimately generate a functional mRNA (Estévez & Simpson, 1999; Gott & Emeson, 2000; Lukes et al, 2002). This editing process requires guide RNAs (gRNA), which are mainly encoded by minicircles, and only a few of them by maxicircles. Actually, the only known function of the minicircles DNA is encoding and providing enough gRNAs for the RNA editing process (Estévez & Simpson, 1999; Gott & Emeson, 2000; Lukes et al, 2002).

Apart from the above described genomic plasticity and RNA editing mechanism, the transcription initiation in *Leishmania*, as well as in all kinetoplastids, remarkably differs from the remaining eukaryotes. One of the most notorious differences concerning gene expression is the almost complete absence of RNA polymerase II promoters (Alsford et al, 2012; Clayton, 2002; Requena, 2011). It is generally accepted that in these organisms, RNA polymerase II mediated transcription is initiated upstream of most 5' genes of each cluster, generating polycistronic transcripts, which will be then processed by *trans*-splicing at the 5' end (Martinez-Calvillo et al, 2003), as depicted on figure 8. *Trans*-splicing replaces the capping system, found in the majority of eukaryotes, and basically requires a common 39 nucleotide methylated mini-exon sequence or spliced leader (SL), which is *trans*-spliced upstream the start codon of the mRNA (Sturm et al, 1999; Clayton, 2002). The SL gene in *Leishmania* is present in a 150 copies tandem array that corresponds to 0.1% of the parasite genome (Lamontagne & Papadopoulou, 1999). In striking contrast to the majority of protein encoding genes in trypanosomatids, the SL gene has an identifiable promoter with a short

consensus initiator element (Luo et al, 1999) and it is transcribed by RNA polymerase II (Gilinger & Bellofatto, 2001).

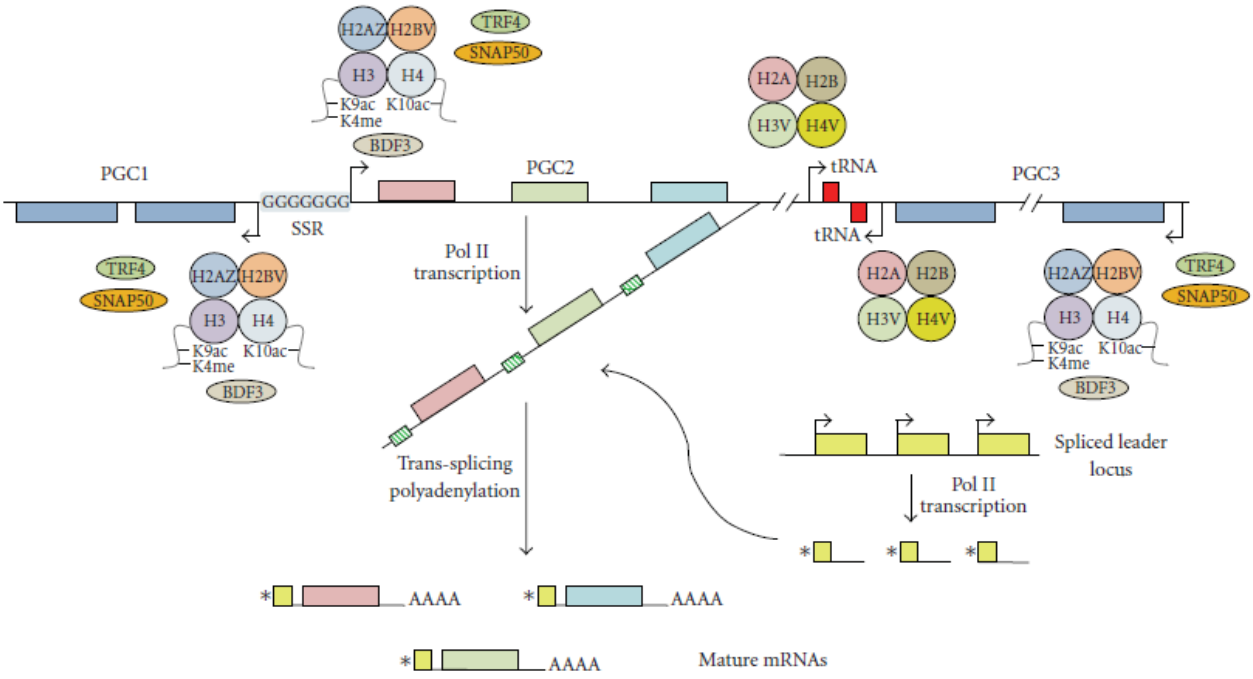

Figure 8. Transcription and processing of mRNA in trypanosomatids. On top, there is a hypothetical chromosome with three different polycistronic gene clusters (PGC1-3). RNA polymerase II mediated transcription begins upstream of the first gene of the PGCs (arrows). The G-run is normally present at divergent strand-switch regions (SSR). Nucleosomes close to the transcription initiation regions include histone variants H2AZ and H2BV. The N-terminal of histone H3 is acetylated at K9/K14 (K9ac) and tri-methylated at K4 (K4me). The N-terminal of histone H4 is acetylated at K10 (K10ac) and at K5/K8/K12/K16 (not shown in the figure). The bromodomain factor 3 (BDF3) and transcription factors TRF4 and SNAP50 also bind at the transcription initiation regions. RNA polymerase II mediated transcription of some PGCs stops close to tRNA genes in DNA regions that contain nucleosomes with H3V and H4V histone variants. The PGCs primary transcripts (shown only for PGC2 in the figure) are processed by *trans*-splicing and polyadenylation to ultimately generate a mature mRNA. By *trans*-splicing, a capped SL RNA (yellow box) is added to the 5' end of every single mRNA. The cap in the SL RNA is indicated by an asterisk at the 5' end of the RNA. The polycistronic primary transcript contains pyrimidine enriched regions (striped box in the intergenic regions) that are necessary for both *trans*-splicing and polyadenylation. The four As at the 3' end of the mature mRNAs depict the polyA tail. Adapted from Martinez-Calvillo et al, 2010.

Due to this near absence of RNA polymerase II promoters, there is a great loss in terms of transcriptional regulation of gene expression in these parasites. Instead, it seems they have adopted and explored post-transcriptional mechanisms (Alsford et al, 2012; Clayton, 2002; Requena, 2011). *Leishmania* ability to post-transcriptionally regulate gene

expression can rely on modulation of both mRNA stability (Brittingham et al, 2001; Muller et al, 2010a; Muller et al, 2010b) and protein translation rate (Boucher et al, 2002; Zeiner et al, 2003).

The combination of genomic and proteomic approaches demonstrated that an almost constitutive expression of *Leishmania* genome occurs in both promastigotes and amastigotes (Leifso et al, 2007; McNicoll et al, 2006), with few examples of stage specific proteins, like amastin family, specifically expressed in amastigotes (Moore et al, 1996; Nourbakhsh et al, 1996; Souza et al, 1992; Wu et al, 2000). However, quantitative proteomics has revealed a great variability in protein expression levels in both stages (Leifso et al, 2007; McNicoll et al, 2006; Rosenzweig et al, 2008), which shows how efficient these post-transcriptional mechanisms are.

4.3.1. Genetic manipulation of trypanosomatids

Up until the 1990s, studying gene specific functions within trypanosomatids was much harder. With the advents of complete genomes sequencing and DNA transfection systems, gene knockout and overexpression became possible, leading to significant advances in the study of the biology and pathology of these parasites (Clayton, 2002).

Transient or stable transfection of DNA can be achieved. The transcription of the latter is driven by endogenous RNA polymerases, whenever is integrated in a chromosome or, in the case of *Leishmania* for instance, by “trapping” on circular episomes (Beverley, 2003). There are several positive and negative selectable markers available. Regarding the positive selection, some of the most common used markers are *HYG* (hygromycin B phosphotransferase), *PAC* (puromycin N-acetyl-transferase), *BLEO* (*Streptoalloteichus hindustanus* bleomycin resistance protein), *BSD* (blasticidin S deaminase) or *NEO* (neomycin phosphotranferase). As for the negative selection, the most used are *TK* (thymidine kinase) or *CDA* (cytidine deaminase) (Beverley, 2003).

Successful integration of protein tags, for protein localization studies for instance, or integration of reporter genes like green fluorescent protein (GFP) or luciferase, for *in vitro* drug screening assays or *in vivo* imaging among other applications, have been extensively explored over the years (Clayton, 2002; Beverley, 2003).

Concerning the study of gene function, different techniques can be used, which induce either gain or loss of function.

To abolish gene function, some of the most common available approaches include gene knockdown and gene knockout. The first is broadly used in *T. brucei*, after the discovery of a functional RNAi pathway (Djikeng et al, 2001; Durand-Dubief & Bastin, 2003; Ngô et al, 1998; Patrick et al, 2009; Shi et al, 2004; Shi et al, 2006). In metazoans, RNAi

plays a role in mRNA levels and translation regulation, DNA arrangements, genome surveillance, anti-viral response, among others. The phylogenetic distribution of key required genes, encoding for proteins like Dicer or Argonaute, suggests that this pathway has been present in the common eukaryotic ancestor (Lye et al, 2010). However, in eukaryotic microorganisms, the scenario is complex, as some retained active RNAi pathways, whereas others did not (Kolev et al, 2011; Lye et al, 2010). RNAi deficiency in eukaryotes has arisen independently a number of times through the eukaryotic lineage, in trypanosomatids in particular, it happened twice, first with *T. cruzi*, and a second time after the divergence of the *Viannia* subgenus from other *Leishmania* species. *T. cruzi* and all *Leishmania* species, with exception of *Viannia* subgenus, do not present a functional RNAi pathway (Kolev et al, 2011; Lye et al, 2010).

In *T. brucei* (Fig. 9), the type III RNase known as Dicer-like enzymes, DLC1 and DLC2, process long dsRNA molecules that derive from sense and antisense transcripts from retroposons and repeats into small interference RNAs (siRNAs) in the cytoplasm and the nucleus, respectively (Kang & Hong, 2008; Kolev et al, 2011; Owino et al, 2008). During RNAi silencing complex (RISC) assembly, Argonaute (AGO1) directly binds the siRNAs cleaving them into sense and antisense oligonucleotides. The latter remain associated to RISC. After RISC assembly, the antisense strand directs this complex to the target mRNA, which is cleaved in a single site in the centre of the double strand region between the guide siRNA and the mRNA (Kang & Hong, 2008; Kolev et al, 2011; Owino et al, 2008).

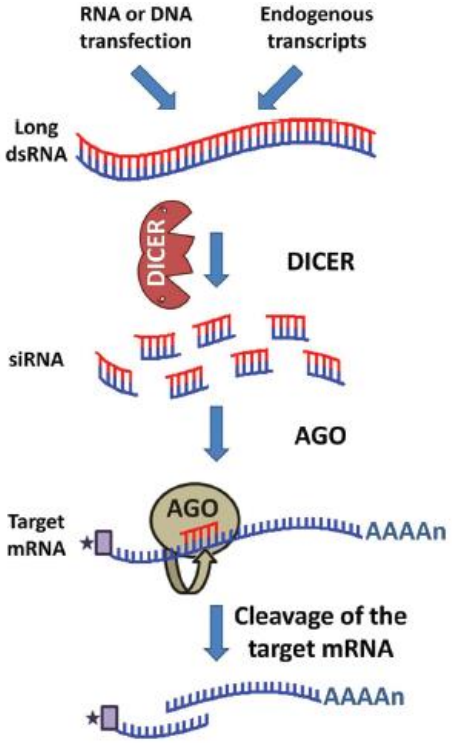

Figure 9. Schematic representation of the mechanism of RNAi in *T. brucei*. dsRNA endogenously produced or transfected is processed by a RNase III enzymes known as Dicer (DCL1 and DCL2) into small siRNA molecules. These molecules associate with AGO1, which corresponds to the catalytic core of RISC, with the siRNA sense strand being released and the antisense remain bound to RISC complex, directing it to the target mRNA. The latter is cleaved at a single site. Adapted from Teixeira et al, 2012.

Although deletion of RNAi genes in *T. brucei* causes a transient chromosome miss-segregation and defective mitosis, accompanied by an increase in retroposon transcripts, parasites lacking the RNAi are capable of completing a life cycle, therefore the biological role of this pathway is not clear (Janzen et al, 2006).

The first study in *T. brucei* demonstrated that a dsRNA transfection elicited a significant downregulation of the target mRNA, however, the effect was transient and lasted about one cell cycle (Ngô et al, 1998). This indicated there was no amplification of the response to dsRNA, which in other organisms is linked to the activity of RNA-dependent RNA polymerase (RdRp). Proficient trypanosomatids do not seem to harbour a potential gene encoding this enzyme (Kolev et al, 2011). In order to overcome this transient effect and develop a methodology that would enable functional studies upon gene downregulation, a tetracycline (tet)-regulated expression of dsRNA was engineered (Kolev et al, 2011).

The RNAi tool rapidly became the method of choice to downregulate genes in *T. brucei*, The further emergency of the RNAi based genome wide screens was a break

through, providing numerous “hits” that can be then individually studied and validated, allowing a massive contribution in the dissection of several aspects of the parasite biology, drug target validation and drug resistance mechanisms (Alsford et al, 2011; Alsford et al, 2012; Erben et al, 2014; Glover et al, 2015; Mony et al, 2014; Preubert et al, 2014). Disappointingly, due to the number of missing elements of the RNAi pathway in *T. cruzi* and most of *Leishmania* species (Kolev et al, 2011), engineer it in these organisms would not be feasible.

RNAi studies have some disadvantages, including the possibility of off target effects, and even though, few complementation studies can be found in the literature (Loureiro et al, 2015; Sienkiewicz et al, 2010). Another is the fact that the knockdown can be more or less efficient, and sometimes, even low protein levels may suffice to ensure normal cellular function (Kang & Hong, 2008; Kolev et al, 2011; Owino et al, 2008). Knockdown can also be performed at the protein level, like the HaloTag based system (Neklesa et al, 2011). In Apicomplexa parasites for instance, several systems in which the knockdown is achieved by the induction of protein degradation have been successfully used, as the auxin-based (Philip & Water, 2015) or the FK506 binding protein (FKBP) based (Zhang et al, 2014c) systems, among others. For trypanosomatids, none has been successfully engineered so far.

Another common strategy to abrogate gene function is gene knockout. If the gene is not essential, it can be removed by homologous recombination, using untranslated regions (UTR), upstream and downstream the gene of interest (GOI), 5’ and 3’ UTR, respectively, on either side of a selectable marker (Clayton, 2002). Because trypanosomatids are diploid, a complete knockout requires two rounds of transfection, using two different selectable markers (Clayton, 2002). It is also possible to achieve gene ablation by deleting just part of the coding region, designated gene disruption (Dumas et al, 1997; Mottram et al, 1996). This can lead to deceptive results if the parasite is still able to express fragments of the protein (Clayton, 2002) that can be toxic or simply preserve the activity of the full length protein. The phenotypes observed for mutant parasites must be interpreted carefully as prolonged *in vitro* culture or cloning can lead to modifications in biological properties *per se*. For this reason, it is imperative to re-transfect null mutants with the gene that has been deleted in order to evaluate whether the phenotype can be rescued (Clayton, 2002).

In the case of an essential gene, usually the first allelic copy is successfully removed, but not the second, leading to a lethal phenotype with no transfectants survival in *T. brucei* or double resistant mutants in *Leishmania* that still possess a copy of the GOI, though. Along with chromosome aneuploidy, DNA amplification by gene rearrangement, which is a

highly dynamic and stochastic process, is one of the strategies *Leishmania* successfully explores in order to respond to environmental changes, such as drug pressure (Genest et al, 2005; Ouellette et al, 1991; Papadopoulou et al, 1994; Ubeda et al, 2014). Several mechanisms to defend essential genes have been reported over the years in *Leishmania*, such as whole genome amplification (Cruz et al, 1993), single chromosome amplification (Cruz et al, 1993) or intrachromosomal tandem duplication (Mukherjee et al, 2011).

Consecutive inability to generate viable transfectants and aneuploidy generation in *T. brucei* and *Leishmania*, respectively, are then suggestive of gene essentiality. In *Leishmania*, the classical strategy to approach this, broadly used for drug target validation for instance, consists in providing an ectopic copy of the gene (episomal or integrated), and under such circumstances the second allele removal must be successful, ultimately generating the so-called facilitated null mutants (Mukherjee et al, 2009; Wang et al, 2005; Wiese, 1998). However, whether this approach is the ultimate proof of essentiality is quite debatable, as a transgene expression may simply facilitate parasite survival during genetic manipulation and selection (Dacher et al, 2014). As *Leishmania* tends to lose episomal vectors in the absence of drug pressure, their preservation in such conditions has been used as an additional readout of essentiality (Mukherjee et al, 2009), but again, this can merely mean that the transgene provides an advantage for *in vitro* or *in vivo* growth (Dacher et al, 2014). This classical approach does not allow to decipher the biological implications of the gene loss and limits structure/function analysis based on mutagenesis or genetic complementation, for instance (Dacher et al, 2014). An elegant manner in attempt to overcome some of these issues is to use an episomal vector, like pXNG, containing *TK* marker that allows for negative selection by bioactivating ganciclovir, which then becomes toxic (Dacher et al, 2014; Murta et al, 2009). The vector carries a GOI copy, and in case of gene essentiality, *Leishmania* should preserve the vector even when exposed to the selection drug. Moreover, this type of vector also allows plasmid shuffle studies, as the original plasmid can be switched for others carrying mutated or truncated versions of the GOI, which ultimately provide structural/biological insights on the protein (Dacher et al, 2014).

In the case of *T. brucei*, a conditional system is available to study essential genes (Fig. 10). Basically, a tet-regulatable copy of the GOI is inserted in an rDNA intergenic locus prior to the removal of the two allelic copies of the gene or after the removal of the first one by homologous recombination. Upon tet removal, which represses transcription of the regulatable allele in null mutants, if the parasites die, the gene is proved essential (Merritt & Stuart, 2013; Wyllie et al, 2009). Another elegant addition to this scheme is the generation of an exclusive expressor cell line, which constitutively expresses a WT or mutated allele, through its insertion in the β-tubulin locus of a conditional null mutant (Fig. 10). Upon tet withdrawal, this allele will be expressed and can be used for functional complementation purposes (Merritt & Stuart, 2013). One of the applications is to test the rescue from loss of gene function upon tet removal in conditional null mutants.

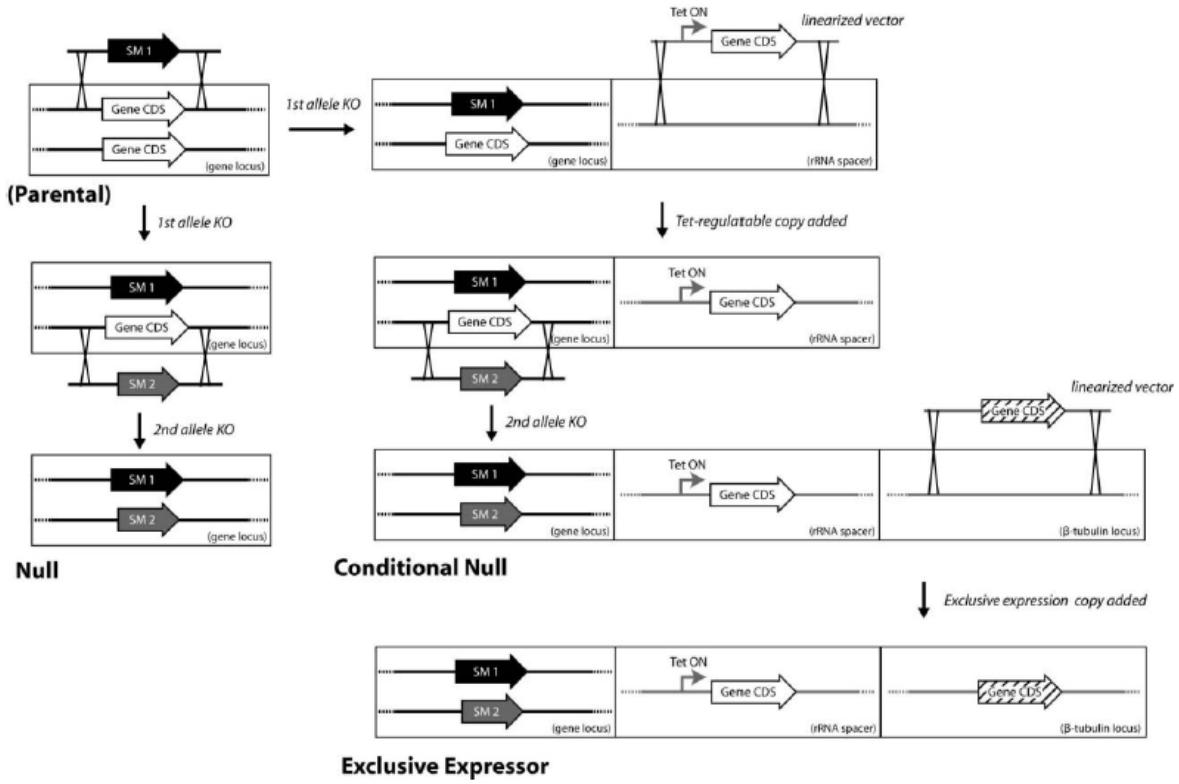

Figure 10. Transfection scheme to generate null, conditional null and exclusive expressor mutants in *T. brucei*. Replacement cassettes that contain the selectable marker (SM) flanked by the 5' and 3' UTRs of the target gene are transfected into *T. brucei* parasites to sequentially knock-out each allele by homologous recombination. This is possible for non-essential genes. For essential genes, conditional null mutants are generated by transfecting a tet-regulatable allele into an rRNA intergenic region in cells prior to both alleles removal or after the removal of the first allele. In these cells, the alleles removal occurs in the presence of tet, as in its absence, there is a repression of the transcription of the regulatable allele and whether this is lethal or nor not for the parasites, the gene is essential or not, respectively. The transfection of an additional allele into the

tubulin locus generates exclusive expressor cell lines, which express constitutively the allele, even upon tet-removal. Adapted from Merritt & Stuart, 2013.

The generation of this type of conditional mutants in *Leishmania* has been hindered by the absence of inducible expression systems (Dacher et al, 2014), as only recently, one has been described in *L. mexicana* (Kraeva et al, 2014).

In *T. brucei*, there is an additional knock-out strategy available using Cre recombinase and loxP sites, allowing both null and conditional null mutants generation (Scahill et al, 2008; Kim et al, 2013). This approach is especially advantageous when multiple simultaneous gene knock-outs are intended, as once using the conventional techniques, not only there is a limited number of selection markers available, as it would definitely be more laborious and time-consuming (Scahill et al, 2008; Kim et al, 2013). Cre recombinase removes the GOI in a complete and instantaneous fashion, upon recognition of loxP sequences in the orientation that permits gene deletion over inversion or translocation (Scahill et al, 2008; Kim et al, 2013). A constitutive expression of the recombinase can induce genotoxicity, therefore it can be either stably incorporated into an rDNA spacer with tet-inducible expression or transiently transfected (Scahill et al, 2008). The latter relies on the short term incorporation of episomal vectors in *T. brucei*. In *Leishmania*, the only option would be inducible expression, which then again has only recently been described. The null or conditional null mutants are at last obtained by negative selection, using the previously referred *TK* marker (Scahill et al, 2008; Kim et al, 2013).

In the recent years, the discovery of CRIPSR (clustered regularly interspaced short palindromic repeat)/Cas9 gene editing has emerged as a promising break-through for gene therapy, but also, it has been brought to the spotlight as a valuable tool for genetic manipulation in basic research (Dow et al, 2015; Hsu et al, 2014; O'Connell et al, 2014; Shalem et al, 2014; Wang et al, 2014). These days, there is a boom of CRISPR/Cas9 technology everywhere, and fortunately, molecular parasitology is taking the first steps exploring its potential (Lander et al, 2015; Peng et al, 2014; Sidik et al, 2014; Sollelis et al, 2015; Zhang et al, 2014a; Zhang et al, 2015). For people working in *T. brucei* it may not be as exciting due to the diverse and valuable tools already available, but for *Leishmania* and *T. cruzi* genetic manipulation, this can be definitely revolutionary. Actually, despite generally *T. cruzi* is more difficult to manipulate than *Leishmania*, it seems in the case of CRISPR/Cas9 technology, the efficiency is superior in the first (Zhang et al, 2015).

The CRISPR/Cas9 is a prokaryotic immune system, consisting of an RNA-guided endonuclease that facilitates site-specific DNA cleavage in a wide range of microorganisms. The gRNA directs the Cas9 to its target DNA, and this nuclease induces double-strand DNA breaks (DSBs). Those can be repaired by homologous recombination or non-homologous

end joining (NHEJ) pathway in mammalian cells, but in *L. donovani*, the repair relies on homology-directed repair (HDR) and micro-homology mediated end joining (MMEJ) (Zhang et al, 2015). This is in agreement with previous *in silico* studies, which suggested NHEJ was absent in trypanosomatids. So far *in Leishmania*, the introduction of mutations, antibiotic selection markers, protein tags (like GFP) and gene deletion have been achieved using CRISPR/Cas9-mediated gene editing (Sollelis et al, 2015; Zhang et al, 2015). For gene deletion in particular, previously characterized non-essential genes were knockedout as proof of concept, and off target effects discarded by whole genome sequencing (Sollelis et al, 2015). The development of an inducible version would be great for essential genes studies. Moreover, the improvement of the system efficiency would be also important in order to enable a future genome-scale knockout screening in *Leishmania* (Zhang et al, 2015). Such screenings have already been carried out in human cells, for instance (Shalem et al, 2014; Wang et al, 2014).

As for the gain of function studies, overexpression has been extensively used and depending on the available tools for each organism, episomes or integrated cassettes can be used, with constitutive or inducible expression (Clayton, 2002).

In summary, forward genetics has been challenged by diploidy and the lack or difficulty of sexual crossing, but several methods, as genetic rescue, transposon tagging or RNAi-based mutant screens, among other, have been developed, complementing the ability to perform reverse genetic manipulations (Beverley, 2003; Damasceno et al, 2015). Currently, several novel molecular genetic tools are now allowing a rapid progress in the field.

5. Host-parasite interaction

5.1. Interaction with the vector

Sand flies (order Diptera, family Psychodidae, subfamily Phlebotominae) are the natural vectors of *Leishmania* spp. However on rare occasions, the vector requirement can be bypassed, such as in transplacental transmission, laboratory accidents or needle sharing (Murray, 2005). About 70 species have been proved to be *Leishmania* vectors, belonging to *Lutzomyia* or *Phlebotomus* genus in the New or Old World, respectively (Bates, 2008). Only female sand flies can transmit the parasite as they need periodic blood meals in order to get the required nutrients for egg development. They can be permissive or specific vectors, whether they allow the development of one or several *Leishmani*a species, respectively (Bates, 2008; Volf & Myskova, 2007).

The development of the parasites in the vector midgut is initiated when the sand fly takes a blood meal, taking free amastigotes or infected cells. Both blood components and

parasites become involved by a type I peritrophic membrane (PM), which is secreted by the epithelial cells and composed by an arrangement of proteins and glycoproteins held together by chitinous microfibrils (Secundino et al, 2005). PM is semipermeable enabling the diffusion of digestive enzymes that will catabolize the ingested contents (Secundino et al, 2005). Amastigotes differentiation into procyclic promastigotes is triggered by the temperature decrease and pH increase when compared to the mammalian host, occurring within 6 to 12 hours post feeding (Dostalova & Volf, 2012).

Procyclic promastigotes are small, ovoid, with a short flagellum, highly replicative and have great amounts of proteophosphoglycan (PPG) at their surface membrane. This glycoconjugate functions as a shield against proteolytic damage by digestive enzymes (Secundino et al, 2010). Procyclic forms undergo several developmental stages in the vector (Sacks & Noben-Trauth, 2002; Kaye & Scott, 2011). Two days after the blood meal, they differentiate into nectomonad forms that correspond to longer and highly motile parasites, which eventually escape the PM, as it starts to dismember, in order to avoid excretion. Parasites migrate anteriorly, oriented by chemotactic gradients of molecules like sugars, and insert their flagella in the thoracic gut epithelia to effectively avoid defecation (Bates, 2007; Bates, 2008). This attachment is mediated by promastigotes' LPG and lectins expressed by epithelial cells (Sacks et al, 1995). LPG is extremely polymorphic and is one of the most determinant factors for species-specific vectors (Bates, 2007; Bates, 2008). As soon as the midgut empties, nectomonads differentiate into shorter and replicative leptomonads that synthesize a secretory form of the PPG, one of the major components of the promastigote secretory gel (PSG). Interestingly, the continuous production of PSG leads to the generation of a PSG plug that occupies the thoracic midgut in a great extent (Bates, 2007). Some leptomonads differentiate into leaf-shaped haptomonads that attach to the stomodeal valve and corrupt its structure and function through the secretion of a chitinase, which is important for both vector colonization and transmission (Rogers et al, 2008).

Around day 5, the midgut has already emptied all the reminiscences from the blood meal and the PSG occupies a considerable area of the anterior part of the midgut. During the production of the PSG, many leptomonads undergo metacyclogenesis, a process that leads to the differentiation into metacyclic promastigotes, the final stage of the parasite in the sand fly. Metacyclics are smaller than nectomonads, displaying a flagellum that is longer than the cell body (Bates, 2007). An active autophagic pathway is critical for metacyclogenesis, mostly to enable parasite survival under starvation, considering nutrients are probably limited at this point (Besteiro et al, 2006, Bates, 2008). Figure 11 illustrates *Leishmania* development in the sand fly vector from procyclic promastigote to metacyclic promastigote forms.

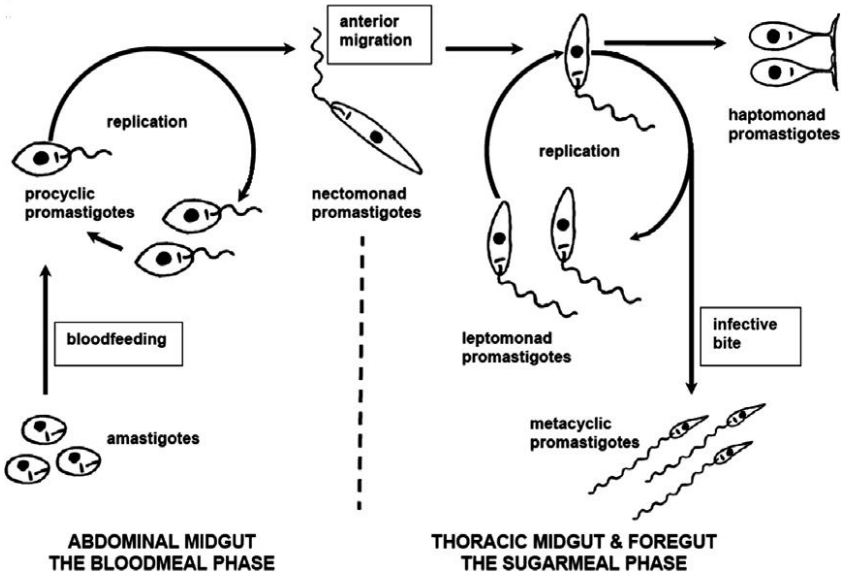

Figure 11. *Leishmania* development in the sand fly vector. The developmental sequence of the five major promastigote forms: procyclic, nectomonad, leptomonad, haptomonad and metacyclic promastigotes. Adapted from Bates, 2007.

Sand flies feed on the emerging blood from wounded superficial vessels and keep it fluid by continuously secreting saliva (Bates, 2007, Bates, 2008). They ingest the blood through the proboscis and the most accepted hypothesis is that the parasites transmitted to the mammalian host are regurgitated (Fig. 12). When an infected fly tries to feed, the presence of the PSG plug blocks the blood entrance in the midgut, therefore, the fly must first regurgitate part of that plug to allow the blood flow passage (Rogers et al, 2004).

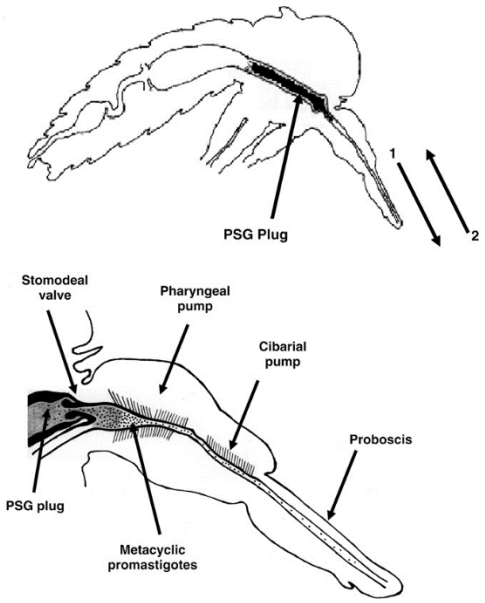

Figure 12. Sagital section of *Leishmania* infected female sand fly. The upper panel depicts the position of the PSG plug within the anterior midgut and foregut. The plug must be partially regurgitated **(1)** before the blood feeding can occur **(2)**, and consequently

injecting metacyclic promastigotes and the PSG in the skin of the host. The lower panel displays at detail of the anterior midgut and the foregut: the PSG plug exerts pressure on the stomodeal valve, extending into the pharynx region. Metacyclic promastigotes are concentrated in the anterior pole of the plug, but can be found along the foregut in both the cibarium and the proboscis. Adapted from Bates, 2007.

The damage to the stomodeal valve induced by the parasite secreted chitinase also plays a contribution, as this valve remains open, promoting the reflux of the parasites from the midgut to the mouth (Rogers et al, 2008). The formation of the PSG plug and the regurgitation look like an efficient mechanism the parasite has evolved in order to condition the fly and facilitate transmission.

5.2. Interaction with the mammalian host

Leishmania parasites have evolved different strategies in order to manipulate and subvert the cellular machinery. From the silent entry in the host cells to the interference with signalling pathways that trigger the immune response or from hijacking the host cell metabolism to the manipulation of apoptotic and autophagic pathways, are among the arms of this successful parasite.

5.2.1. Host cell invasion and the establishment of infection

During *Leishmania* transmission, apart from virulent metacyclic promastigotes, dead parasites and PPGs are also inoculated in the skin of the mammalian host during the blood meal (Van Zandbergen et al, 2006). Neutrophils and MØs are rapidly recruited to the site of the sand fly bite (Kaye & Scott, 2011; Peters et al, 2008; Van Zandbergen et al, 2004), inclusively, the inoculated PPGs are strong stimulators of MØ recruitment (Rogers et al, 2009; Rogers et al, 2010). On the other hand, dead parasites seem to be required for an efficient infection, as they expose phosphatidylserine (PS) in the outer leaflet of the plasma membrane, allowing a silent entry in neutrophils (Peters et al, 2008; Van Zandbergen et al, 2006). This silent invasion triggers the production of anti-inflammatory cytokines like TGF-β (Fadok et al, 1998). *Leishmania* parasites release *Leishmania* chemotactic factor (LCF) that attracts neutrophils and interacts with lipoxin A4 receptors (ALX), deactivating their oxidative burst (Van Zandbergen et al, 2002; Wenzel & Van Zandbergen, 2009). *Leishmania* also produces an inhibitor of the neutral elastase, one of the most important proteases involved in the neutrophils' microbicidal response (Faria et al, 2011). However, promastigotes do not differentiate into amastigotes inside these phagocytes. Therefore, neutrophil infection is transient and following apoptosis, both MØs and DCs remove their apoptotic bodies, which contain *Leishmania* parasites (Peters et al, 2008; Van Zandbergen

et al, 2004). Overall, MØs are indeed the most important cells regarding infection establishment and persistence (Kaye & Scott, 2011; Van Zandbergen et al, 2004), and this way parasites manage to reach their primary host cell in disguise, using the so-called "Trojan Horse" strategy (Afonso et al, 2008).

The very first interaction of the promastigotes with the MØ is flagellum-mediated, as this may induce the release of survival factors by the parasite in order to modulate the phagocytic process (Forestier et al, 2011; Rotureau et al, 2009). As depicted in figure 13, there are several MØ receptors involved in *Leishmania* recognition and uptake, including complement (CRs), mannose (MRs), fibronectin (FnRs) and Fcγ receptors (FcγRs) (Podinovskaia & Descoteaux, 2015; Ueno & Wilson, 2012; Walker et al, 2014). It is noteworthy that different receptors may be involved in promastigotes or amastigotes recognition and uptake.

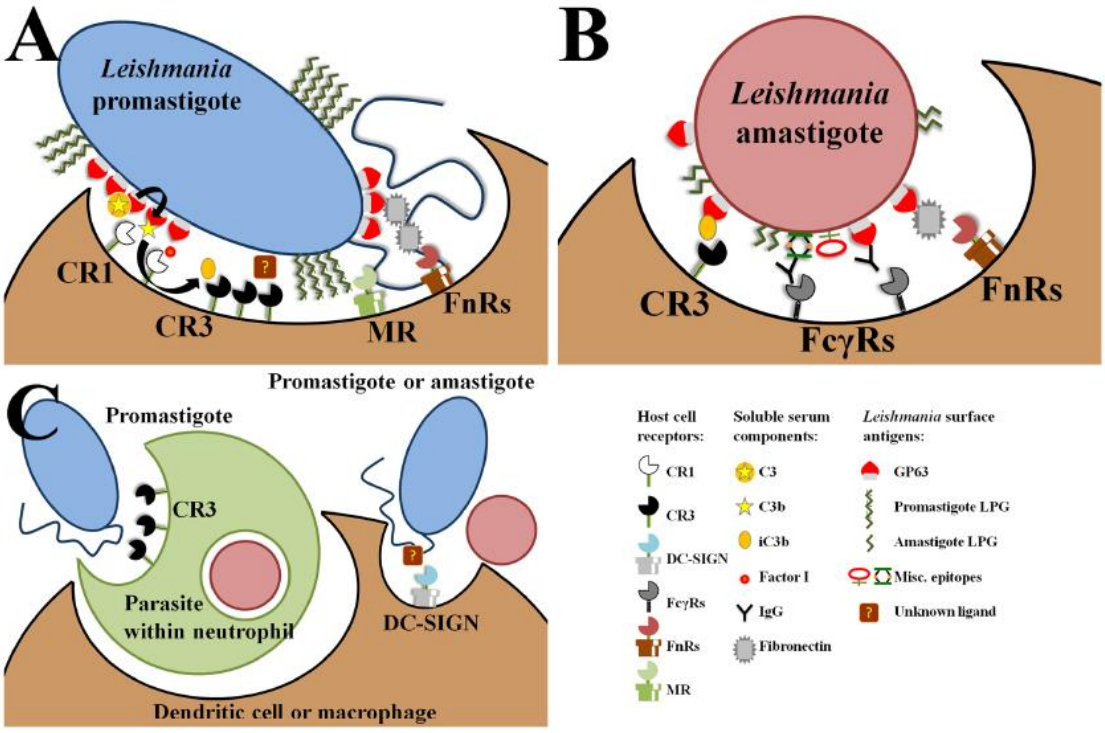

Figure 13. *Leishmania* recognition and uptake by host cell receptors. Promastigotes are represented in blue, amastigotes in red, MØ in brown and PMN in green. **A)** GP63, a metalloprotease highly expressed in promastigotes, cleaves C3 opsonins into C3b that binds CR1. CR1 and factor I cleave C3b into iC3b that binds CR3. CR3 may directly bind a yet unknown antigen present in the promastigote surface. LPG terminal sugars may be recognised by MRs, although not formally proven. GP63 also binds fibronectin, which bridges the binding to FnRs. **B)** GP63 is scarcely expressed in amastigotes, but so is LPG, allowing GP63 access to C3 and subsequently to CR3. Additionally, antibody and fibronectin binding to amastigotes allow their internalization *via* FcγRs and FnRs, respectively. **C)** At the inoculation site, after the sand fly bite, promastigotes enter predominantly in PMNs, like neutrophils, via CR3, and posteriorly enter MØ and DCs. Both

promastigotes and amastigotes may directly enter DCs via DC-SIGN, through a so far unidentified ligand. Adapted from Ueno & Wilson, 2012.

Interestingly, different receptors may have a different impact on the infection course. For instance, CR-mediated uptake, *via* CR3 or CR1, inhibits inflammation, superoxide burst and lysosome markers accumulation, like cathepsin D or lysosome-associated membrane protein 1 (LAMP1), creating more favourable conditions for the parasite establishment (Ueno & Wilson, 2012). In contrast, *Leishmania* uptake mediated by any of the other three receptors can trigger more inflammatory conditions, which can result in parasite clearance (Ueno & Wilson, 2012). *Leishmania* attachment to the MØs is rather fast (10-20 minutes) (Forestier et al, 2011), however, the downstream events regarding the phagolysosome assembly depend on the host receptors involved in parasite recognition and uptake. If the phagolysosome biogenesis as well as parasite survival/clearance seem to be affected by receptor choice, parasite uptake does not (Podinovskaia & Descoteaux, 2015; Polando et al, 2013).

Upon recognition at the host cell surface, promastigotes are internalized *via* calveolae composed of cholesterol-rich membrane lipid microdomains, contrasting with amastigotes in which phagocytosis seems to occur independently of such domains (Chattopadhyay & Jafurulla, 2012; Rodriguez et al, 2011; Roy et al, 2014). Interestingly, the disruption of lipid microdomains, through cholesterol depletion, compromises *Leishmania* promastigotes uptake *via* nonopsonic pathways, however, opsonized parasites are internalized normally (Chattopadhyay & Jafurulla, 2012). Actually, *Leishmania* promastigotes promote lipid microdomain formation, by activating the host acid sphingomyelinase that produces ceramide, an important component (Majumder et al, 2012). *Leishmania* also depends on actin-mediated uptake, thus the integrity of the host actin cytoskeleton is necessary (Roy et al, 2014).

Several human pathogens infect, survive and proliferate inside MØs, however, the great majority of them subverts or escapes the phagocytic pathway (McConville et al, 2007). But not *Leishmania*. Interestingly, *Leishmania* parasites manage to counteract the hostile environment of the phagolysosome, successfully surviving and proliferating in this compartment (McConville et al, 2007).

Leishmania LPG is inserted into the above described cholesterol-rich lipid microdomains of the phagosome, excluding the exocytosis regulator synaptogamin V and subsequently preventing the incorporation of cathepsin D and H^+-ATPases (Vinet et al, 2009). These *Leishmania*-containing vacuoles poorly interact with endosomes and lysosomes, and the recruitment of late endosomal/lysosomal proteins such as LAMP1 and Rab7 occurs with a delayed kinetics (Scianimanico et al, 1999). Moreover, LPG scavenges

reactive oxygen species (ROS) and prevents their generation by inhibiting NADPH-dependent oxidases (NOX) recruitment to the phagosome membrane (Lodge et al, 2006; Spaeth et al, 2003). These mechanisms temporarily preclude acidification as well as activation of the microbicidal machinery, providing sufficient time for promastigotes to differentiate into amastigotes (Vinet et al, 2009; Walker et al, 2014). Eventually, some lysosomes may fuse with the parasitophorous vacuole (PV) leading to a pH decrease, which is accompanied by LAMP1, Rab7 and lysosomal hydrolases acquisition (Antoine et al, 1998; Forestier et al, 2011).

Promastigotes differentiation into amastigotes is thought to be mainly triggered by the increase in the temperature and the decrease in pH, and it has been suggested the first prevails over acidification (Alcolea et al, 2010).

5.2.2. Playing with the host metabolism and signalling cascades: the path to intracellular survival and immune evasion

Once *Leishmania* parasites reach their definitive host cell, MØs, they apply great efforts in order to protect their niche, and one of them is to increase the life span of the host cell through apoptosis inhibition. This buys promastigotes time to differentiate into amastigotes that are then fully adapted to the life in the phagolysosome (Cecílio et al, 2014; Moore & Matlashewski, 1994). However, it is important to mention parasites can delay MØs death but cannot avoid it. Some studies also point to *Leishmania*-mediated induction of host cell autophagy, which has been suggested to have an impact on the outcome of the infection (Cyrino et al, 2012; Pinheiro et al., 2009).

Amastigotes survive and multiply in the phagolysosome using a wide range of strategies. To begin with, *Leishmania* parasites are well equipped with a vast antioxidant machinery, from which trypanothione synthetase (TryS) and trypanothione reductase (TryR) must be highlighted (Tovar et al, 1998). Apart from that, they also manage to deactivate ROS generation machinery (Lodge & Descoteaux, 2006), as well as nitric oxide (NO) production, in the case of the latter, the expression of the inducible nitric oxide synthetase (iNOS) can be suppressed by glycosylinositolphospholipid (GILP), a component of the amastigotes' glycocalyx (Proudfoot et al, 1996). Additionally, these parasites profoundly rely on heat shock proteins (HSPs) as they alleviate thermal, acidic and oxidative stress (Bifeld & Clos, 2015; Hübel et al, 1995).

Leishmania amastigotes seem to have more complex nutritional requirements than those of the majority of prokaryotes and fungal pathogens. However, the phagolysosome must somehow be a permissive niche (McConville et al, 2007).

Iron acquisition is a classic example of how *Leishmania* is able to subvert the host cell metabolism in its favor, in a fashion we can designate as metabolic virulence (Fig. 14). Iron uptake in *Leishmania* is mediated by three major proteins: ferric iron reductase (LFR), ferrous iron transporter (LIT1) and heme transporter (LHR1). The host is able to reduce iron availability in the phagolysosome by expressing NRAMP1, and in response, *Leishmania* produces tryparedoxin peroxidase (TXNPx) that inhibits this iron efflux pump, and also upregulates LIT1 (Arango-Duque & Descoteaux, 2015; Podinovskaia & Descoteaux, 2015). The inhibition of NRAMP1-mediated iron efflux leads to intracellular iron depletion that triggers an upregulation of transferrin receptors (TfRs), and therefore iron uptake through the endocytic network. By an unknown mechanism, *Leishmania* infected cells also express higher levels of hepcidin, which leads to the degradation of the iron exporter ferroportin (Arango-Duque & Descoteaux, 2015; Podinovskaia & Descoteaux, 2015), contributing to iron retention inside MØs.

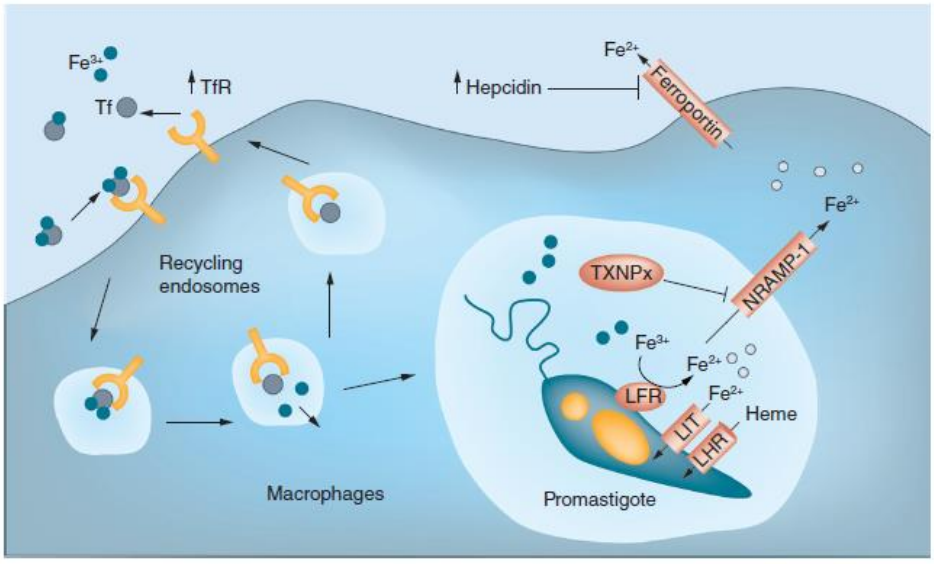

Figure 14. Iron acquisition by *Leishmania* in macrophages. Iron uptake inside the phagolysosome by *Leishmania* parasites is mediated by a heme transporter (LHR1) and an ion transporter (LIT1) in the heme and ferrous ion form, respectively. Additionally, *Leishmania* ferric reductase, LFR1, converts ferric iron to ferrous iron, and the latter is transported by LIT1. *Leishmania* expresses TXNPx that inhibits the host iron efflux pump NRAMP1, expressed in the phagolysosome, increasing iron reserves inside this compartment and depleting the cytosolic ones. The depletion of intracellular iron triggers the upregulation of TfRs enhancing iron uptake by receptor-mediated endocytosis. *Leishmania* infected macrophages also express higher levels of hepcidin that induces iron exporter ferroportin degradation, reinforcing iron retention inside these phagocytes. Adapted from Podinovskaia & Descoteaux, 2015.

It has also been reported that *L. infantum* is able to subvert MØ metabolism by modulating important energetic sensors, such as the SIRT1-LKB1-AMPK axis, ultimately

triggering the switch from an early aerobic glycolysis to a later mitochondrial metabolism in the host, which has a crucial impact on parasite survival (Moreira et al, 2015). It has also been shown that GP63 released by *L. donovani* in the liver cleaves Dicer preventing mir-122 maturation, which is involved in lipid metabolism, leading to a decrease in cholesterol levels in the serum, ultimately promoting parasite growth (Descoteaux et al, 2013).

Moreover, this successful parasite also employs numerous strategies to efficiently evade the immune system. The Th1/Th2 paradigm is the hallmark of the immune response to *Leishmania* parasites. The production of IL-12 by MØs and DCs induces naïve $CD4^+$ T cells towards an IFN-γ producing Th1 phenotype, which leads to MØ M1 activation and parasite clearance (Diaz-Gandarilla et al, 2013). Th2 cytokines, such as IL-4 or IL-10 and TGF-β in the case of CL or VL, respectively, induce an M2 MØ phenotype, related with disease susceptibility and progression (Gautam et al, 2011). Therefore, *Leishmania* parasites appear to modulate the immune response towards a Th2 phenotype, although this strict polarization seems confined to murine models, as in humans this is not completely applicable (McMahon-Pratt & Alexander, 2004; Nylen & Gautam, 2010). *Leishmani*a is able to interfere with normal cytokine production, modulate toll-like receptor (TLR) signalling (Fig. 15) or impair the cellular function, by compromising antigen presentation or inducing cellular anergy or exhaustion (Cecílio et al, 2014).

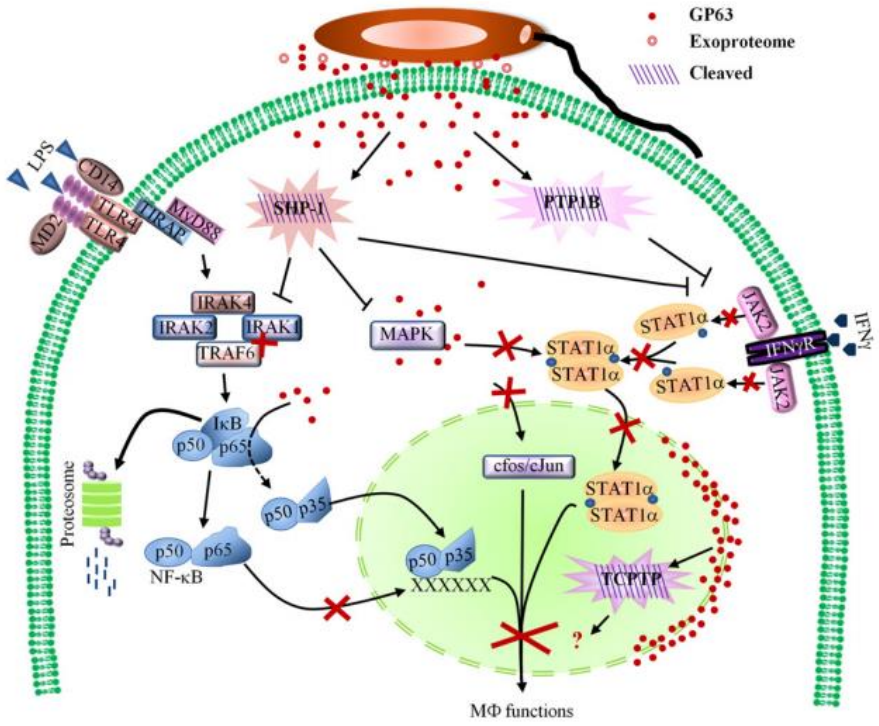

Figure 15. *Leishmania* compromises TLR and cytokine signalling pathways. In the picture, GP63 is highlighted. GP-63 cleaves and activates the host protein tyrosine phosphatases (PTPs), such as SHP-1, PTP1B and TCPTP. For instance, SHP-1 is involved

in the downregulation of IRAK-1, MAPK and JAK/STAT signalling pathways and PTP1B inactivates JAK2. Arrows indicate activation; red crosses indicate signalling alteration or inhibition; abrogated lines indicate downregulation of specific kinases. Adapted from Olivier et al, 2012.

Regarding the interference with cytokine production, *Leishmania* can modulate several cellular signalling pathways (Figs. 15 and 16). For instance, it can attenuate protein kinase C (PKC) activity (Bhattacharyya et al, 2001; Olivier et al, 1992; Fig. 16) or activate mitogen-activated protein kinase (MAPK) phosphatases (MKPs), MKP-1 and MKP-3, interfering with extracellular signal-regulated kinases (ERK), ERK1 and ERK2, and p38 MAPK signalling, which regulate IL-10 and IL-12 production by infected MØs (Mathur et al, 2004). As for the impairment on antigen presentation, one of the mechanisms *Leishmania* employs for the purpose is the induction of ceramide *de novo* synthesis, which in abundance eventually displaces cholesterol, disrupting the membrane lipid microdomains' architecture (Majumder et al, 2012). *Leishmania* can also drive cells unresponsive to molecules such as interferon-γ (IFNγ), for instance by dysregulating Janus kinase (JAK)/signal transducer and activator of transcription 1 (STAT1) pathway, through membrane cholesterol depletion (Sen et al, 2011; Fig. 15). Moreover, the metalloprotease GP63 may cleave the mammalian target of rapamycin (mTOR), inhibiting mTOR complex 1 (mTORC1) formation. Consequently, the translational repressor 4E-BP1 will not be inactivated by mTORC1-mediated phosphorylation, and will inhibit the eukaryotic initiation factor 4F (eIF4F), leading to an overall translation repression, including interferon response-related proteins (Jaramillo et al, 2011; Fig. 16).

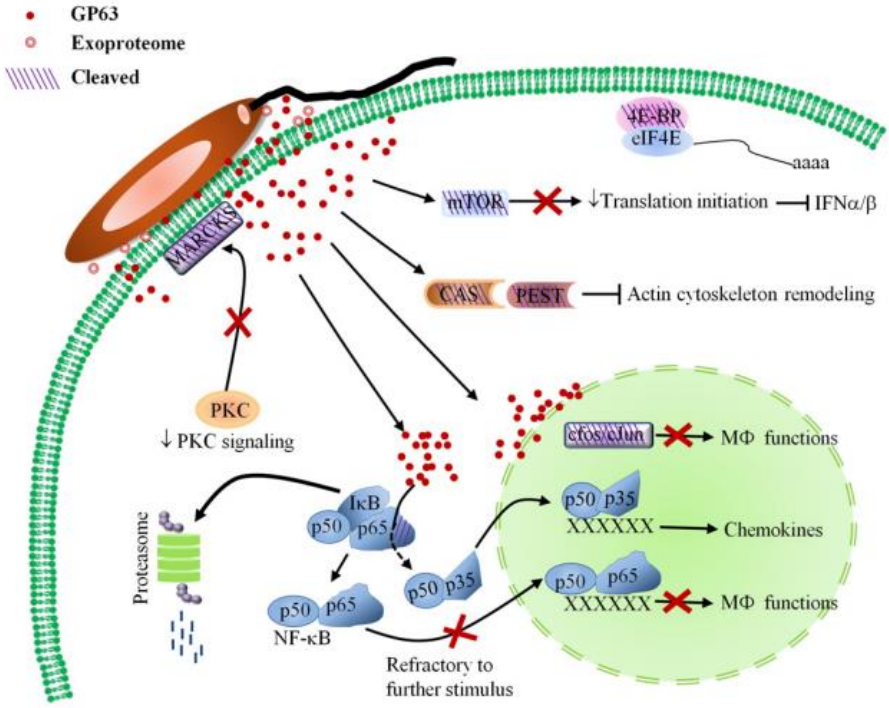

Figure 16. *Leishmania* GP63 mediated impact on host cell signalling and functions. GP63 can cleave several important proteins: the myristoylated alanine-rich C kinase (MARKs), which is a critical substrate to PKC-dependent signalling; the adaptor molecules p130CAS and PEST, involved in the actin cytoskeleton remodelling; mTOR, affecting translation initiation and consequently type I IFN production, as well as transcription factors such as NF-kB and AP-1. Arrows indicate GP63 targets that are involved in signalling pathways; red crosses indicate signalling cascade alteration; abrogates lines indicate functional inhibition. Adapted from Olivier et al, 2012.

Recently, a study even described parasite-driven changes in the MØ methylome. Infection with *L. donovani* modifies the host DNA methylation status, shutting down genes that play an important role on antimicrobial responses, thus facilitating parasite survival and persistence (Marr et al, 2014). One of the hypothesis is that parasites export DNA methyltransferases or methylation inhibitors, potentially *via* exosomes (Marr et al, 2014).

Figure 17 illustrates some of the most important *Leishmania* virulence factors.

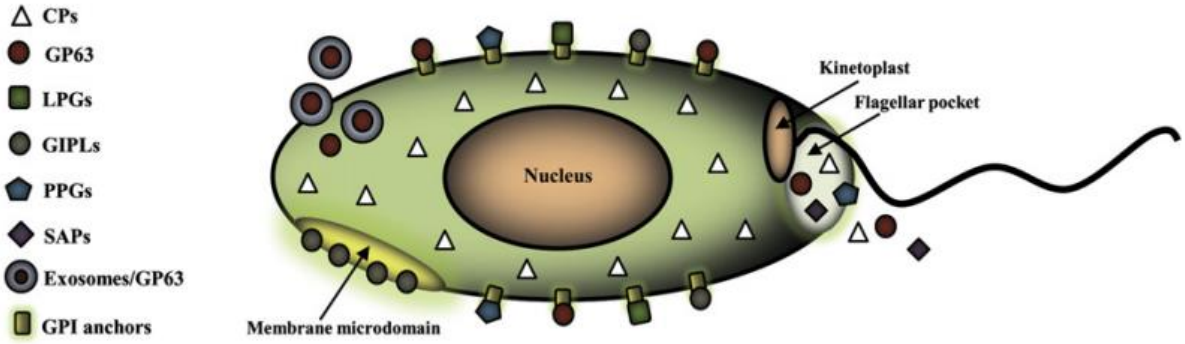

Figure 17. *Leishmania* virulence factors. The image depicts GPI-anchored surface molecules, such as GP63, LPGs, PPGs and GILPs, which are mainly associated to membrane microdomains. Some virulence factors that are not anchored to the membrane can be released via exosomes (GP63) or via classical secretion through the flagellar pocket (GP63, PPGs, secreted acid phosphatases (SAPs) and cysteine proteases (CPs)). Adapted from Olivier et al, 2012.

In summary, *Leishmania* is a well-adapted and successful parasite that has evolved many clever and elegant mechanisms to enter, survive and proliferate inside the host cells. These parasites are masters of disguise, experts in deceiving the host immune system and exploiting the cellular machinery and resources to their best benefit.

6. Leishmaniasis diagnosis

As previously described, leishmaniasis can lead to a broad spectrum of clinical manifestations, however, most of the symptoms associated with the disease are not specific. Actually, it can mimic other pathologies, rendering the clinical diagnosis harder. In order to achieve a differential diagnosis, which is critical to confirm a clinical suspicion, different methods can be employed (Herwaldt, 1999). Those include direct parasite observation in infected tissues, immunological detection of *Leishmania* antigens or anti-*Leishmania* antibodies and parasite DNA or RNA detection in tissues samples.

The direct observation of amastigotes in clinical samples is the gold standard for leishmaniasis diagnostic, and naturally, the sensitivity will depend on the parasite number and their dispersion in the sample (Herwaldt, 1999; Murray et al, 2005). The biological specimens that are more commonly analysed are skin biopsies, in the case of CL and ML, or spleen, bone marrow and lymph nodes aspirates, in the case of VL. Some of the major disadvantages of this method are the frequent requirement of invasive procedures for sample recovery as well as the impossibility of implementation outside a hospital/laboratory (Murray et al, 2005).

Classic serological diagnosis of leishmaniasis relies mostly on enzyme-linked immunosorbent assay (ELISA) based techniques. Due to their high sensitivity and specificity, as well as requirement for low technological expertise (*eg*. immunochromatography-based tests), some of these methods have become reference (Chappuis et al, 2006). In particular, when the purpose is the detection of anti-*Leishmania* antibodies, two important considerations must be made. Firstly, in some cases, *Leishmania*-specific antibodies may persist after cure, therefore these methods do not allow the distinction between resolved and active infections, leading to false positive results (Santarém et al, 2005). On the other hand, in immunocompromised patients, false negative results may arise merely due to immunosuppression. Obviously, the sensitivity and specificity of these methods deeply depend on the antigen used. The recombinant K39 (rK39) protein is the one of the most important antigens used for VL and PKDL diagnosis, inclusively an rK39-based dipstick test is commercially available (Sundar et al, 2002). Of course, serological methods are indirect approaches that can raise problems in endemic areas where the presence of antibodies or parasite material may simply indicate contact with the parasite and not necessarily disease (Santarém et al, 2005).

Another direct method is based on the use of molecular biology techniques, by detecting *Leishmania* unique DNA or RNA sequences (*eg*. mitochondrial minicircles, rRNA genes), which confers a high sensitivity and specificity (Reithinger & Dujardin, 2007). Assays based on polymerase chain reaction (PCR) are the major molecular diagnostic approach in developed countries and are able to detect *Leishmania* nucleic acids only a few weeks after the symptoms appearance, especially appropriate for samples with low parasite loads (*eg*. blood), displaying high specificity (~100%) and high predictive power (Reithinger & Dujardin, 2007). Inclusively, a positive PCR is usually required for the differential diagnosis that precedes therapy initiation (Reithinger & Dujardin, 2007), and later to confirm a successful treatment in the case of VL (Maurya et al, 2005). PCR-based diagnosis is also particularly important in the case of *Leishmania*/HIV co-infected patients (De Doncker et al, 2005). The combination of PCR with restriction fragment length polymorphism (RFLP) sequencing further allows *Leishmania* spp. identification. Of course, one of the biggest disadvantages is that PCR-based techniques are restricted to laboratory use.

Overall, in non-endemic countries, molecular approaches prevail over microscopic analysis, contrasting with the endemic regions, where the opposite is observed (Reithinger & Dujardin, 2007).

7. Leishmaniasis control

In order to accomplish a direct control of the disease, WHO prioritizes the use of efficient diagnosis tools, appropriate therapeutical options and compulsory report of all cases of leishmaniasis. Due to the absence of human vaccines, leishmaniasis control relies mainly on chemotherapy and vector/reservoir control (Kedzierski, 2010).

7.1. Control of vectors and reservoirs

There are different indirect strategies to control disease transmission, through the control of the vector and the reservoirs, or the adoption of personal protection measures.

Sand flies rest in dark moist places, typically only a few hundred meters apart from their breeding site. Following urbanization in the periphery of cities, sometimes there is an invasion of the vector breeding grounds, leading to an increase in the disease incidence. Feasible measures to control the sand fly vector include deforestation near urbanized grounds as well as the use of insecticides. Focusing on the latter, the use of dichlorodiphenyltrichloroethane (DDT) had a massive impact on the vector control in endemic areas, with a particular highlight to India, where a dramatic reduction in the number of VL cases was observed in some regions (Vanlerberghe et al, 2007). DDT has nefarious effects on the environment and human health and has been extensively replaced by synthetic pyrethroids (*eg*. Deltamethrin or cyhalotrin), which have been proven equally effective (Davies et al, 2000).

The control of the reservoirs is also extremely important for both CL and VL. In the case of zoonotic VL, we must highlight the importance of the canine reservoir, in which measures must be taken in order to both protect the dogs and restrict the availability of parasite reservoir. For this purpose, several measures can be adopted such as euthanasia of infected dogs, which showed a limited impact, use of insecticide-based devices, like deltamethrin-impregnated collars (Gramiccia & Gradoni, 2005) and dog vaccination (Gradoni, 2015). Currently, only two vaccines that consist of parasite purified fractions with saponin derivatives as adjuvants conferred a significant protection, and have been registered as canine vaccines: FML-QuilA (Leishmune®) in Brazil, and LiESP/QA-21 (CaniLeish®) in Europe (Gradoni, 2015). Of course, these measures will have a reduced impact if they are not adopted for the whole canine population and/or if there is still an unknown sylvatic reservoir that maintains a sufficient number of infected animals to perpetuate the infectious cycle (Gramiccia & Gradoni, 2005).

Finally, WHO also advises the adoption of personal preventive measures such as the use of mechanical barriers, like insecticide-impregnated bednets, avoidance of outdoor

activities during the periods when sand flies are more active (twilight to morning fall), wearing protective clothing or use of insect repellents (Gramiccia & Gradoni, 2005).

7.2. Chemotherapy: the search for new drugs urges

In the last seven decades, the chemotherapy against this disease has relied mostly on pentavalent antimonium-based (SbV) drugs, and the commercially available formulations include stibogluconate (Pentostam®) and meglumine antimoniate (Glucantime®) (Croft & Olliaro, 2011). It is generally accepted that SbV is a prodrug, bioactivated through reduction to SbIII. This bioactivation can occur inside the phagolysosome or inside the parasite (Frezard et al, 2009). Glutathione (GSH), present mainly in the MØs cytosol, and cysteine or cysteinylglycine thiols, found mostly inside the lysosomes, can actively reduce SbV (Ferreira Cdos et al, 2003). The entry of SbIII in the parasite is mediated by aquaglyceroporin AQP1 (Gourbal et al, 2004). Inside *Leishmania* parasites, the most abundant thiol is trypanothione, a glutathionespermidine conjugate, which is able to reduce SbV as well (Ferreira Cdos et al, 2003). Additionally, *Leishmania* enzymes such as thiol dependent reductase 1 (TDR1) and antimoniate reductase have also been implicated in SbV bioactivation (Denton et al, 2004). The mechanism of action of these drugs is not fully disclosed, but it is known that SbIII is the active species that ultimately leads to parasite death, and DNA fragmentation suggests a role for apoptosis (Sudhandiran & Shaha, 2003). There are some evidences supporting trypanothione reductase or zincfinger proteins as possible molecular targets (Cunningham & Fairlamb, 1995; Demicheli et al, 2008). Some studies also suggest antimonials compromise vital metabolic processes like fatty acid oxidation or glycolysis (Chakravarty & Sundar, 2010). Moreover, SbV is capable of forming complexes with ribonucleosides, which can inhibit purine transporters or directly interfere with purine salvage pathway in *Leishmania* (dos Santos Ferreira et al, 2006).

These drugs require repeated parenteral administration during long periods of time, unleash several adverse effects (including cardiotoxicity and pancreatitis) and have been stroked by the emergence of resistances over usage (Ashutosh et al, 2007; Croft & Olliaro, 2011). Actually, antimonial resistance is a severe issue in endemic areas, and several resistance mechanisms have been described over the years, including loss of AQP1 activity (Gourbal et al, 2004), extrusion of trypanothione/SbIII complexes by ATP-binding cassette (ABC) transporters, sequestration of SbIII in vacuoles (Legare et al, 2001) or downregulation of MAPK1 that is a negative regulator of P-glycoprotein type efflux pumps (Garg & Goyal, 2015). These drugs are still highly effective in areas where resistance has not emerged yet (Vanlerberghe et al, 2007). Moreover, the combination of antimonial drugs

with allopurinol, a xanthine oxidase (XO) inhibitor, and the antibiotic paromomycin have much improved the curative efficiency (Gutiérrez et al, 2015).

Pentamidine, an aromatic diamine, is commonly used as second line drug against leishmaniasis and is also used in the treatment of sleeping sickness (first stage). It has been suggested it enters *Leishmania* promastigotes *via* arginine and polyamine transporters (Kandpal & Tekwani, 1997). In the case of *T. brucei*, this task is on P2 adenosine transporter charge, although at least other two transporters can uptake the drug, as AQP2 (Baker et al, 2012; De Koning, 2001**)**. Although its mechanism of action remains unclear, some evidences support the inhibition of polyamine biosynthesis, DNA minor groove binding and effect on mitochondrial inner membrane potential (Bray et al, 2003; Croft et al, 2006). Resistance to pentamidine has been described for trypanosomes and several *Leishmania* species. In the case of *Leishmania*, ABC transporters have been implicated in the resistance (Coelho et al, 2007). In *T. brucei*, the resistance mechanisms have been more broadly dissected, in particular, AQP2 has been extensively studied (Alsford et al, 2012; Baker et al, 2015; Graf et al, 2015; Munday et al, 2014). The latter is a determinant of melarsoprol-pentamidine cross-resistance in lab strains and recently the chimerization at the AQP2-AQP3 tandem locus was found responsible for this cross-resistance in clinical isolates (Graf et al, 2015). The use of pentamidine in the treatment of VL is hindered by the higher toxicity it inflicts in the patients when compared to antimonials (Jha, 1983). However, it is still a good alternative for CL, as it provides high cure rates with short periods of treatment an even performs better than antimonials for some CL species (Berman, 1997).

Amphotericin B (amphB), a macrolide antifugal, which can be formulated as a deoxycholate salt or even better, delivered by liposomes (AmBisome), is extremely efficient against VL and a very attractive alternative in areas of antimonial resistance (Thakur et al, 1993). It was developed as a systemic antifugal drug that targets ergosterol-like sterols, and ergosterol happens to be the more abundant sterol in *Leishmania* membranes (Berman et al, 1986; Bern et al, 2006). Besides amphB direct effect on the parasites through formation of aqueous pores in the plasma membrane, AmBisome seems to interact with the membrane sterols of MØs, preventing *Leishmania* entry as well (Paila et al, 2010; Ramos et al, 1996). In spite of its high efficacy, amphB has severe adverse effects, including a pronounced nephrotoxicity. The use of the liposomal formulations has helped reducing the toxicity and extend the plasma half-life of this compound, however, it is not an affordable alternative in developing endemic countries and therefore not a first line therapy on those (Bern et al, 2006). In the treatment of VL caused by *L. infantum* in Southern Europe, AmBisome is the first line treatment (Vanlerberghe et al, 2007). Few cases of resistance have been reported and the underlying mechanisms are poorly understood (Brotherton et

al, 2014). Laboratory acquired resistance has been associated to ergosterol deficiency in the parasite membrane or the enzyme S-adenosyl methionine transferase, which is involved in the ergosterol synthesis (Mbongo et al, 1998; Pourshafie et al, 2004). Recently a large scale proteomic study identified several proteins that were differentially expressed in amphB resistant parasites, among them enzymes involved in metabolic pathways (glycolysis, TCA), in transcription and translation, in ROS scavenging and also HSPs (Brotherton et al, 2014).

Paromomycin, an aminoglycoside antibiotic, has a similar efficacy to amphB, with less side effects, a shorter treatment and has been approved for the treatment of VL in India (Gutiérrez et al, 2015; Musa et al, 2010). It also requires parenteral administration. It has also shown some interesting results for CL treatment (Ben Salah et al, 2009). The mechanism of action is not completely clear, but it seems to interfere with mitochondrial function and protein translation, in the case of the latter through direct interference with the ribosomes (Jhingran et al, 2009). Aminoglycosides have strong potential for the development of resistances: a decrease in the uptake, coupled with drug efflux have been implicated in laboratory-induced resistance (Bhandari et al, 2014; Jhingran et al, 2009). Moreover, the combination of antimonial drugs with paromomycin results in a highly efficacious regimen accompanied by a reduction of the side effects of both drugs (Berman, 1997).

One of the great efforts in drug discovery against leishmaniasis was to find an efficacious oral drug. The first oral compound used against leishmaniasis was ketoconazole, an imidazole derivative that inhibit ergosterol biosynthesis. This compound, as well as itraconazole and fluconazole, which are also imidazole derivatives, present variable success rates against different causative species of CL and in general not very promising in monotherapy against VL (Navin et al, 1992; Rashid et al, 1994). They may have some interest in the context of a combination therapy against VL (Shakya et al, 2011). Allopurinol, a hypoxanthine analogue and xanthine oxidase (XO) inhibitor, inhibits purine anabolism in *Leishmania* (LaFon et al, 1985). Similarly to the imidazole derivatives, it is not valuable in monotherapy, in combination it displays some success in CL but not as promising in VL (Momeni et al, 2002; Ramesh et al, 2010).

Miltefosine is the only oral drug prescribed against VL, and it was a major accomplishment in the field. It was originally developed as an anti-cancer drug and it has been proven highly efficacious for the treatment of CL, ML and VL (Bhattacharya et al, 2007; Tappe et al, 2010). It can be safely used in children and treats patients who were refractory to antimonials (Berman, 2008). Nevertheless, miltefosine displays an adverse effect that constitutes a great limitation to its use in women of reproductive age – its teratogenicity (Berman, 2008). Its mechanism of action remains unknown but it seems one of the

requirements is the intracellular accumulation of the drug, which is mediated by two transporters, ultimately leading to the development of an apoptosis-like death (Paris et al, 2004). Moreover, some studies indicate it may be related to a disturbance in phospholipids synthesis (Rakotomanga et al, 2007; Zufferey & Mamoun, 2012). Additionally, regarding two particular characteristics of miltefosine, it is indeed much prone for resistance emergence. One is that as an oral drug, the treatment may often be unsupervised and non-compliance of the treatment can lead to subtherapeutical doses in the patients. The second concerns the long half-life of this drug, as it can still be detected in the blood 5 months after the treatment (Berman, 2008).

Laboratory-induced resistant strains unravelled some of the potential resistance mechanisms, namely mutations in miltefosine transporters and drug efflux (*eg* overexpression of glycoprotein MDR1) (Perez-Victoria et al, 2003). In a recent study, a transcriptomic analysis of resistant *versus* susceptible strains to miltefosine revealed differential expression of genes related to DNA repair/replication machinery, protein translation and folding, lipid metabolism, antioxidant defense and transporters activity (Kulshrestha et al, 2014). Miltefosine is certainly the most cost-effective option to treat leishmaniasis in the areas of antimonial resistance, however, its use as first line therapy is inevitably limited by its teratogenicity and high potential for resistance development (Vanlerberghe et al, 2007).

Sitamaquine (8-aminoquinoline) was specifically developed for VL treatment, actually in CL the results were disappointing. In high concentrations it affects parasite motility, morphology and growth, however, its mechanism of action is not clear. It seems to be inserted in biological membranes through electrostatic interactions and accumulates in acidocalcisomes (Lopez-Martin et al, 2008). More studies are still required to further disclose its mode of action, adverse effects, resistance-associated mechanisms in order to become or not a reasonable alternative to the already established VL treatments (Loiseau et al, 2011).

Tables 1 and 2 summarize the treatment details and complications and the advantages /disadvantages, respectively, for the most commonly used drugs against leishmaniasis.

Table 1. Summary of the most important drugs used in the treatment of leishmaniasis. Modified from De Menezes et al, 2015

Drugs	Administration route	Dosage	Efficacy	Toxicity
Pentavalent antimonials	IM, IV, or IL	20mg/kg/day (28–30 days)	35–95% (depending on area)	Severe cardiotoxicity, pancreatitis, nephrotoxicity, hepatotoxicity
Amphotericin B	IV	0.75–1mg/kg/day (15-20 days, daily or alternately)	>90%	Severe nephrotoxicity, infusion-related reactions, hypokalemia, high fever
Liposomal amphotericin B	IV	10–30mg/kg total dose (single dose 3-5mg/kg/dose)	>97%	Mild rigors and chills during infusion Mild nephrotoxicity (infrequent and mild)
Miltefosine	Oral	100–150mg/day (28 days)	Asia: 94% (India); Africa: 60%–93%	Vomiting and diarrhoea, nephrotoxicity, hepatotoxicity, teratogenicity
Paromomycin	IM (VL) or topic (CL)	15mg/day (21 days) or 20mg/kg (17 days)	94% (India) 46–85% (Africa)	Severe nephrotoxicity, ototoxicity, hepatotoxicity
Pentamidine	IM	3mg/kg/day IM every other day for 4 injections	35–96% (depending on *Leishmania* species)	High rate of hyperglycemia, as a result of pancreatic damage; hypotension, tachycardia, and electrocardiographic changes

IV: intravenous administration; IM: intramuscular administration; IL: intralymphatic administration.

Table 2. Advantages and disadvantages of the most important drugs used in the treatment of leishmaniasis. Modified from De Menezes et al, 2015

Drugs	Advantages	Disadvantages	Resistance	Price	Comment
Pentavalent antimonials	Easily availability and low cost	Quality control; length of treatment; painful injection; toxicity; resistance in India	Common (>65% in Bihar, India)	$50–198	First line drugs but with high incidences of resistance; variable response in different species that cause CL
Amphotericin B	Primary resistance is unknown	Need for slow intravenous infusion; dose-limiting nephrotoxicity; heat instability	Laboratory strains	~$21–100	Severe toxicity; need for prolonged hospitalization; first-line drug for VL in India, where there is antimonial resistance
Liposomal amphotericin B	Highly effective; low toxicity	Price; need for slow intravenous infusion; heat stability (needs to be stored below 25∘C)	Not documented	$280–3000	High cost
Miltefosine	Effective and safe	Price; possibly teratogenic; potential for resistance (half-life); poor patient compliance	Laboratory strains	$70–150	Effective orally but its long half-life may encourage emergence of resistance on prolonged use; effective for VL and against some species that cause CL; contraindicated in pregnancy as found to be teratogenic in rats
Paromomycin	Effective, well tolerated, and relatively cheap	Efficacy varies between and within regions; potential for resistance	Laboratory strains	$10–15	Low cost; lack of efficacy in East Africa; topical formulation available for CL
Pentamidine	Short-time course	Efficacy varies between *Leishmania* species	Not documented	—	For specific forms of CL in South America only; first line of treatment of CL in French Guiana

It is also important to highlight the particular case of *Leishmania*/HIV co-infection. A successful therapy counts on a competent immune system, thus for instance in the case of this co-infection much will depend on the immune status of the patient. Actually, these patients tend to have lower cure rates, higher toxicity/fatality rates and predisposal for relapses with complicated parasitological contours (Alvar et al, 2008). The latter makes

secondary prophylaxis a reasonable measure (Lopez-Velez et al, 2004). The lack of uniform clinical data hinders the establishment of optimal treatment regimes (Alvar et al, 2008).

As final remark on this subject, leishmaniasis is certainly one of the most neglected infectious diseases when it comes to drug development (Modabber et al, 2007). Although there are many treatment options available, they present several preoccupying limitations concerning toxicity, cost, administration route and importantly, resistance emergence, rendering the search for new drugs and novel targets a priority (Guerra et al, 2011).

Chapter II

Exploring *Leishmania* metabolic pathways

The general metabolism is relatively conserved in eukaryotic cells, however, trypanosomatids display distinctive features concerning particular enzymes and pathways, compartments as well as sensing and regulatory mechanisms. This uniqueness can be explored in order to dissect novel and specific molecular targets, ultimately allowing rational design of anti-parasitic drugs.

1. Searching for new drugs and novel drug targets

In the beginning of the nineteenth century, drug discovery field was revolutionized as it became possible to isolate the active molecules responsible for the observed pharmacological effects (Terstappen et al, 2007). In the 1990s, following the advances in molecular biology and biochemistry, testing molecules in complex systems was abandoned, in favour of a target based approach (Fig. 18). This approach, more rational and efficient in theory, was further supported by the rise of a post-genomic era, with the sequencing of the human and several pathogens genomes (Terstappen et al, 2007). However, currently this target based strategy, not as successful as initially expected, has been progressively replaced by a phenotypic-based strategy (Fig. 18).

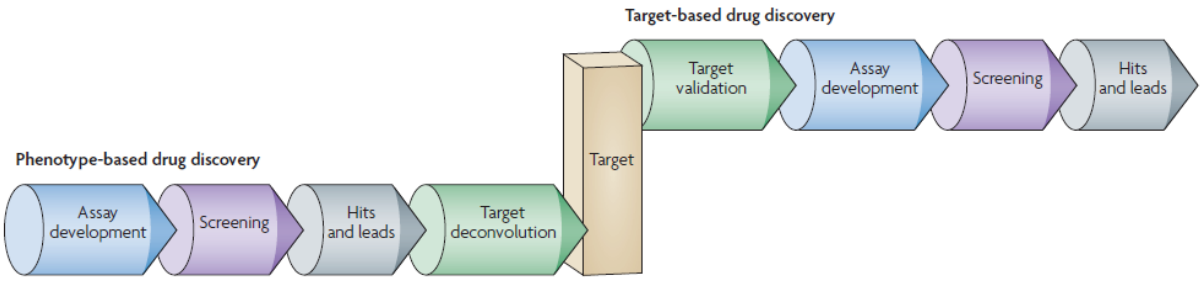

Figure 18. Drug discovery approaches: phenotype based versus target based. In the phenotype based approach, lead compounds are firstly obtained, followed by target deconvolution, whereas in the target based approach, firstly the molecular targets are validated, and only then screened to identify lead molecules. Adapted from Terstappen et al, 2007.

Therefore, there is a renaissance of a more holistic approach, in which compounds are tested in living cells or model organisms, such as nematodes or zebrafish. The most common is the use of cells in culture that are more compatible with high throughput screening (HTS) with a phenotypic readout. Moreover, cell lines can be genetically engineered to mimic aspects of the disease biology or to monitor the activation/inhibition of pathways that may be relevant for the process (Terstappen et al, 2007). HTS campaigns may comprise viability assays, making use of commercial reagents or reporter genes, such as fluorescent proteins or luciferase. Reporter genes can also be used to measure the

activation/inhibition of a certain pathway, for instance. In addition, phenotypic alterations like morphological changes can be measured using image based high content screening (HCS) systems, which use sophisticated algorithms for automated image acquisition and analysis (Terstappen et al, 2007).

Focusing on neglected tropical diseases drug discovery, in the target based approach, screenings are designed in order to inhibit proteins that are essential for parasite survival and/or infectivity and absent or sufficiently different from the host at a structural level (Reguera et al, 2014). Over the years, many efforts have been made to identify essential genes in trypanosomatids, and the availability of genomic data on these parasites has been crucial for this purpose. Further, *in silico* HTS virtual screenings and docking procedures using 3D X-ray structured atomic coordinates or homology models enable structure-based design of new anti-parasitic drugs (Reguera et al, 2014).

Nevertheless, target-based approach also has its drawbacks. For instance, in the case of *Leishmania*, a desired drug must be able to pass across several membranes and remain stable at acidic pH, considering amastigotes dwell in the phagolysosome. Moreover, the desired drug must not be metabolized to inactive molecules by host or parasite enzymes. It has also been observed that many compounds designed against specific targets often display a low selectivity (Reguera et al, 2014).

Consequently, nowadays phenotype-based strategies comprising HTS of compound libraries using whole cell assays is a well-established approach for early drug discovery programs in neglected diseases (Faria et al, 2015c). This type of assay normally results in a simple readout, precluding the need for a validated target, which can be difficult to achieve. In contrast to a biochemical target based assay, the active compounds are discovered under physiologically relevant conditions (Faria et al, 2015c). Additionally, whole cell based assays have been quite successful in resulting in approved drugs for infectious diseases in general (Keller et al, 2011; Pink et al, 2005).

In the case of trypanosomatids, several HTS assays have been developed (Faria et al, 2015c; Mackey et al, 2006; Moon et al, 2014; Siqueira-Neto et al, 2012; Sykes & Avery, 2009a; Sykes & Avery, 2009b). For intracellular parasites, at least in the clinical relevant form, such as *Leishmania* or *T. cruzi*, these assays tend to be HCS based, and host cell and parasite segmentation may be achieved only by performing nucleic acid staining (Moon et al, 2014; Siqueira-Neto et al, 2012) or using transgenic parasites expressing reporter genes (Aulner et al, 2013; Sadeghi et al, 2015). In the case of extracellular parasites, as *T. brucei*, viability assays can be used, based on resazurin (Sykes & Avery, 2009b), sybr green (Faria et al, 2015c) or ATP levels measurement (Sykes & Avery, 2009a) assays.

Many different molecular or biochemical technologies may be used afterwards to identify the molecular targets of a compound. Importantly, there is a common aspect to all of them: at one stage the affinity between the compound and its putative target is exploited (Terstappen et al, 2007). Among the available technologies are affinity chromatography based methods, yeast and mammalian three-hybrid systems (Fig. 19), phage or RNA display-based methods or protein microarrays (Terstappen et al, 2007).

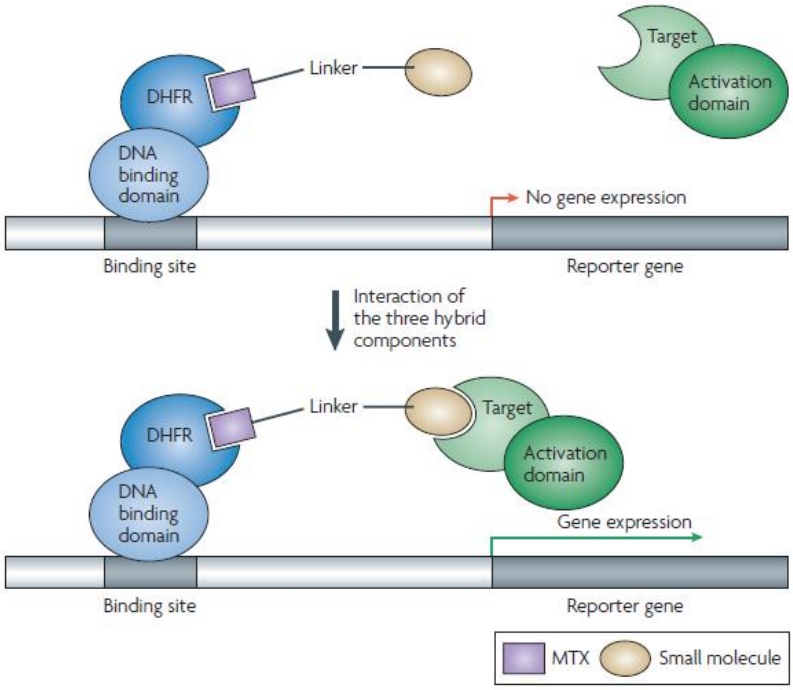

Figure 19. Three hybrid systems for target deconvolution. The components are a DNAbinding domain fused to a ligand binding domain (DHFR), a ligand molecule (MTX) linked to the compound of interest and a component that consists of a transcriptional activation domain fused to a protein from a cDNA library. The binding of the compound to its target protein will allow the three components interaction, enabling the activation of a reporter gene expression. DHFR, dihydrofolate reductase; MTX, methotrexate. Adapted from Terstappen et al, 2007.

The lead compounds, generated by either target or phenotype based approaches, must be tested in *in vivo* models of the diseases as part of their preclinical development. In neglected tropical diseases, the adoption of *in vivo* real time imaging systems, in which fluorescent or bioluminescent parasites are used is a great step forward (Calvo-Álvarez et al, 2015; Lewis et al, 2015; McLatchie et al, 2013; Mehta et al, 2008; Millington et al, 2010; Pulido et al, 2012). These techniques allow the reduction of the number of animals per experiment, as well as the collection of a lot of qualitative and quantitative information concerning the infection (Reguera et al, 2014). Not only can the parasite burden be extrapolated but also its distribution in the body, for instance in internal organs. In the

particular case of visceral models, bioluminescence performs better than fluorescence due to the poor penetration of the excitation light and tissue autofluorescence. However, in the case of CL and ML models, fluorescence would be more appropriate as it would not require the injection of a light-emitting substrate (Reguera et al, 2014). A good alternative is the use of infrared fluorescent proteins as the emission/excitation wavelengths penetrate well the tissues, minimizing the absorbance by haemoglobin, water, lipids as well as the light scattering (Calvo-Álvarez et al, 2015).

In summary, public and private initiatives are supporting the drug discovery process in neglected tropical diseases. The primary goal is to find molecules with high selectivity indexes in the first drug-screening phase, which also present good results in a preclinical model of the disease. Often promising hit compounds selected in target-based screenings ultimately fail due to poor permeability, enzymatic inactivation, among others. More recently, target free HTS has emerged as the most promising strategy, however, for this purpose it is imperative to find a unanimous screening model. Such a model must comprise the interaction of the parasite forms with the definitive host cells, and ideally resemble the pathophysiological environment of infected spleens and lymph nodes, combined with cutting edge bioimaging devices. This could become a promising *ex vivo* system to screen small molecules against *Leishmania*.

1.1. Target validation

As previously stated, on target based approaches for drug discovery in neglected tropical diseases, molecular targets correspond to proteins that are essential for parasite survival and/or infectivity and absent or sufficiently different from the host (Reguera et al, 2014). The availability of genomic data on trypanosomatids has been indispensable for this process and several tools have allowed the genetic validation of several drug targets. In the case of *T. brucei*, with the advents of RNAi mediated protein knockdown, much more studies concerning target validation can be found in the literature. In most of species of *Leishmania*, the inability to perform RNAi mediated knockdown renders gene knockout the only option. Genetic manipulation of trypanosomatids has been extensively addressed on chapter I (4.3.1).

Over the years, many efforts have been made to identify essential genes in trypanosomatids. Inclusively, the Special Programme for Research and Training in Tropical Diseases (TDR) database, hosted by WHO, is a deposit of potential drug targets obtained from biochemical, genetic and pharmacological data of several pathogens (Reguera et al, 2014). Several enzymes have been validated in *Leishmania*, such as TryR, a crucial component of the anti-oxidant machinery of these parasites (Eberle et al, 2011);

dihydrofolate reductase, involved in the purine biosynthesis; cysteine protease B, a virulence factor secreted by the amastigotes into the phagolysosome (Caffrey et al, 2011); DNA topoisomerases, involved in DNA replication, transcription and recombination, and drastically different from the ones in the host (Prada et al, 2013); as well as several kinases (Palmeri et al, 2011). In the case of *T. brucei*, many different pathways have been explored such as polyamine biosynthesis, energy, purine, pyrimidine, pteridine or lipid metabolism, cell cycle kinases, phosphodiesterases, among others (extensively reviewed by Jacobs et al, 2011).

The validation of a drug target further leads to the need of setting up enzymatic assays that allow the screening of inhibitory molecules. For this purpose, the expression and purification of a considerable amount of recombinant proteins in native form are required. *Escherichia coli* is the most widely used organism to produce recombinant proteins (Khow & Suntrarachun, 2012). Recombinant proteins are coupled with fusion tags, which are crucial for protein purification, often by affinity chromatography in a first step (Arnau et al, 2006). Affinity tags correspond to exogenous residues that tightly bind a chemical ligand or an antibody, enabling a high degree of purification of the target protein (Arnau et al, 2006). When the protein cannot be expressed in native conditions, denaturing purification has to be used, further limiting activity assays.

After setting up an *in vitro* enzymatic assay for the molecular target, kinetic studies can be undertaken (Sidoli et al, 2006), in order to determine the catalytic constants conveyed by Michaelis-Menten (K_m, v_{max}, k_{cat}) (Cleland, 1967). Inclusively, the kinetic parameters determination in the presence or absence of several concentrations of an inhibitory molecule disclose whether there is competitive, non competitive or uncompetitive like inhibition (Robertson, 2005). In the context of enzymatic inhibition, the determination of the inhibition constant (K_i) and the compound concentration that leads to a 50% drop on the enzymatic activity (IC_{50}) are also crucial (Robertson, 2005).

Following the *in vitro* inhibitory activity, the compounds must be tested in whole cell assays to confirm its anti-parasitic activity, and further in mammalian cells to evaluate their selectivity. In order to improve potency and selectivity, it is important to understand how and where the compound binds its molecular target, allowing structure based lead optimization. Currently, there are several methods available to identify the inhibitor binding site: X-ray crystallography (Hassell et al, 2007), nuclear magnetic resonance (NMR) spectroscopy (Pellecchia *et al*., 2008), computational docking (Mobley & Dill, 2009) and photo crosslinking (Robinette et al, 2006). Frequently, site directed mutagenesis is used to validate the referred methods (Claustre et al, 2002).

2. Metabolic pathways with distinct features

In order to identify novel drug targets, great efforts have been made to explore the particularities of trypanosomatids metabolism when compared to the host. The following sections address some of the most explored metabolic pathways in these parasites.

2.1. Polyamines

Polyamines, simple aliphatic compounds found in all tissues and microorganisms, play detrimental roles on cell proliferation and differentiation, as well as protein, nucleic acids and trypanothione synthesis, being the latter crucial for anti-oxidant defences in these parasites (Colotti & Ilari, 2011). L-ornithine is the polyamine precursor, obtained from L-arginine by arginase (ARG). Following, ornithine decarboxylase (ODC) catalyses the first and rate limiting step of polyamine biosynthesis, by converting L-ornithine into putrescine (Colotti & Ilari, 2011; Heby et al, 2007). Putrescine is further used as a substrate for the constitutive spermidine synthase (SpdS) that adds the aminopropyl group provided by the decarboxylated S-adenosylmethionine (dAdoMet), the latter resulting from S-adenosylmethionine decarboxylase (AdoMetDC) activity. Ultimately, spermine synthase (SpmS) performs a similar reaction on spermidine (Spd), generating spermine (Spm), by adding another aminopropyl group (Fig. 20) (Colotti & Ilari, 2011; Heby et al, 2007).

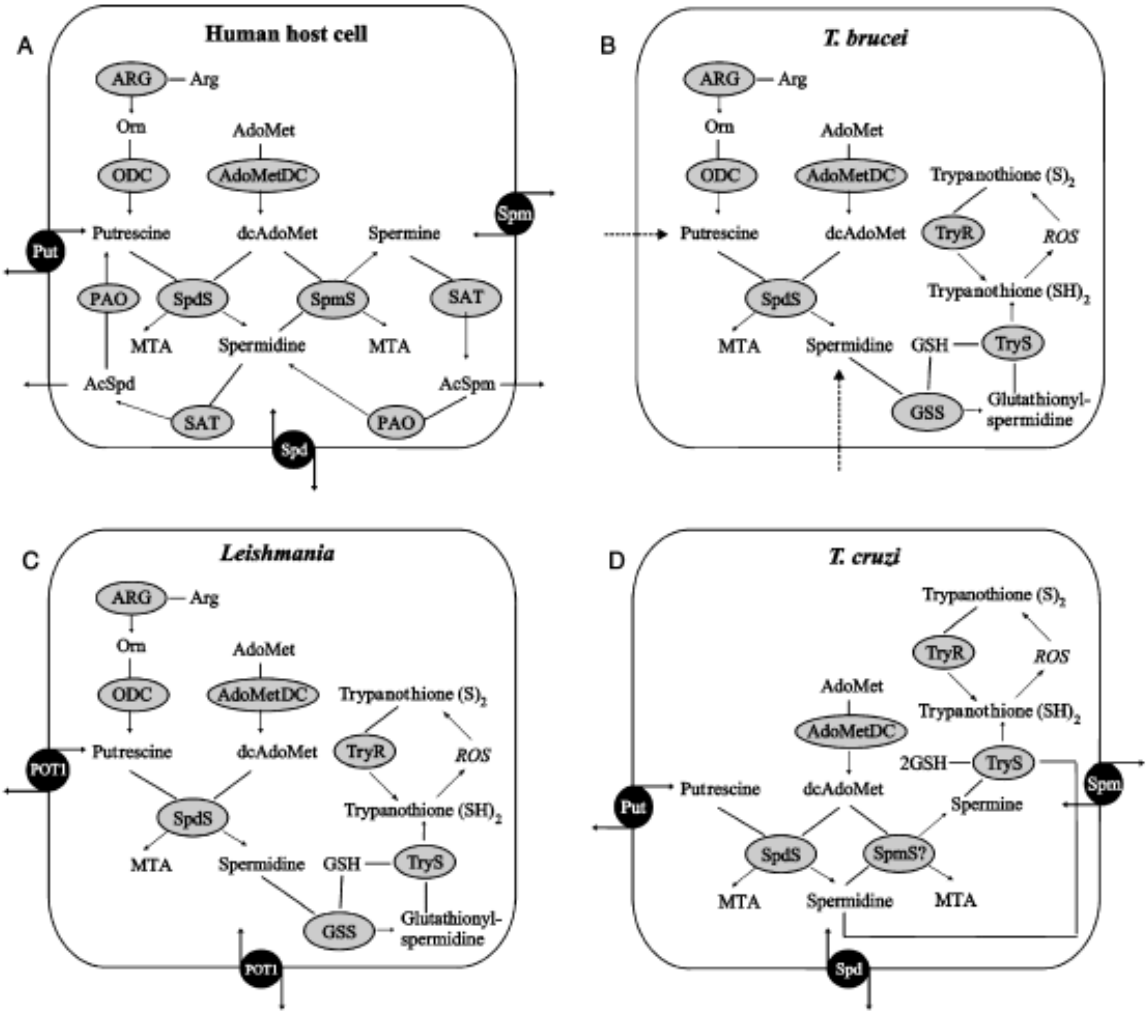

Figure 20. Polyamine metabolism in trypanosomatids and mammalian cells. ARG is crucial for L-ornithine production, the polyamine precursor, in most cell types but not in *T. cruzi*. **A)** In human cells, the decarboxylases (ODC and AdoMetDC) have extremely short half lives, whereas the synthases (SpdS and SpmS) are constitutively expressed. SAT and PAO enable a back conversion from spermine to spermidine and finally to putrescine via acetylated intermediates (AcSpm and AcSpd). Importantly, polyamine transporters (black circles) allow polyamine uptake from extracellular medium, and are crucial for the regulation of their intracellular levels. **B)** In *T. brucei*, ODC and AdoMetDC have long half lives, and SpmS is absent. Spd and glutathione (GSH) are conjugated by two enzymes (GSS and TryS) in order to generate trypanothione, a key molecule for anti-oxidant defence. **C)** In *L. donovani*, polyamine biosynthesis occurs in a similar fashion to *T. brucei*, but *Leishmania* has a more efficient polyamine transporter (POT1). **D)** *T. cruzi* does not have ODC, but has AdoMetDC and two aminopropyltransferases. One may be a SpmS, as these parasites have Spm, which can also be conjugated with GSH by TryS. The latter has a wide polyamine substrate specificity, generating trypanothione and several analogues. *T. cruzi*, is dependent on putescine uptake from the extracellular medium and has a high-affinity transporter for the purpose. AcSpd, acetylated spermidine; AcSpm, acetylated spermine; AdoMet, S-adenosylmethionine; AdoMetDC, S-adenosylmethionine decarboxylase; ARG, arginase; dcAdoMet, decarboxylated S-adenosylmethionine; GHS, glutathione; GSS, glutathionylspermidine synthase; MTA, 50-deoxy-50-methylthioadenosine; ODC, ornithine decarboxylase; PAO, polyamine oxidase; Put, putrescine; ROS, reactive oxygen species;

SAT, spermidine/spermidine N1-acetyltransferase; Spd, spermidine; Spm, spermine; TryR, trypanothione reductase; TryS, trypanothione synthetase. Adapted from Heby et al, 2007.

Interestingly, polyamine metabolism in trypanosomatids has some distinct features when compared to mammals. Firstly, in human cells, ODC and AdoMetDC, both decarboxylases, are extensively regulated and present short half lives, whereas SpdS and SpmS are constitutively expressed. ODC and AdoMetDC in *T. brucei* and *Leishmania* have a considerably higher half-life (Heby et al, 2007). Secondly, human cells have two enzymes that catalyse back-conversion from spermine to spermidine to putrescine via acetylated intermediates, namely spermidine/spermidine N1-acetyltransferase (SAT) polyamine oxidase (PAO), which are absent in trypanosomatids (Heby et al, 2007). Thirdly, human cells have the ability to uptake polyamines *via* specific high affinity transporters, allowing a regulation of the intracellular levels of these molecules. *T. brucei* exhibits negligible uptake capacity, but on the contrary, *Leishmania* has a more efficient high affinity polyamine transporter (POT1) for both putrescine and spermidine (Fig. 20C). *T. cruzi*, for instance, lacks ARG and ODC, deeply relying on extracellular putrescine uptake, which inclusively is 10-50 fold higher than in *L. mexicana*, in epimastigotes (Carrillo et al, 2006; González et al, 1992; Hasne & Ullman, 2005). Finally, the most important thiol in human cells is GSH, whereas in trypanosomatids is trypanothione. The latter is synthesized by TryS, which has a wide polyamine substrate specificity, generating not only trypanothione, but also several trypanothione analogues (Colotti & Ilari, 2011; Heby et al, 2007). For instance, besides spermidine, *T. cruzi* also has spermine, which can also be conjugated with GSH by TryS. Thus, *T. cruzi*, in opposition to *Leishmania* and *T. brucei*, also has an additional aminopropyltransferase, namely SpmS, which produces the so called spermine (Fig. 20) (Heby *et al*., 2007; Colotti *et al*., 2011).

L-arginine is an essential amino acid for *Leishmania* growth, only semi-essential to mammalian cells. *L. donovani* can transport this amino acid via LdAAP3 transporter, which localises to the surface membrane and has a high affinity for L-arginine, in opposition to the human transporter that equally binds L-lysine and L-ornithine. *L. donovani* may have the ability to sense L-arginine cellular concentration and adjust LdAAP3 expression and activity in accordance (Darlyuk et al, 2009).

Contrarily to human cells, *L. mexicana* promastigotes express a single ARG, which catalyses a detrimental function for the parasite, namely the production of L-ornithine, the precursor of polyamines. ARG null mutants become auxotrophic for L-ornithine or polyamines (Roberts et al, 2004).

In their turn, ODC null mutants could not grow in polyamine deficient medium, which was overcome by adding putrescine and spermidine, but not spermine. This has also shown

that *L. donovani* lacks polyamine back conversion that is present in human cells (Fig. 20A) (Jiang et al, 1999). In *T. brucei*, ODC knockout cell lines also require exogenous putrescine for proliferation, and when those were injected in mice, the parasites were unable to multiply and were quickly cleared from the bloodstream (Li et al, 1998). Actually, ODC is currently a drug target against human African trypanosomiasis (HAT), and it is irreversibly inhibited by eflornithine, a reference drug for the neurological stage of *T. b. gambiense* infection (Poulin et al, 1992). This drug is ineffective against American trypanosomes as those lack its molecular target, and rely instead on putrescine uptake, as referred above (Heby et al, 2007). In *T. brucei*, this drug is quite successful for several reasons: 1) the parasite ODC is stable and has a lower turnover in comparison to the human one; 2) the negligible ability of the parasite to uptake polyamines from extracellular environment; 3) the depletion of spermidine compromises trypanothione synthesis; 4) the absence of putrescine and spermidine leads to a general decrease in macromolecules synthesis, such as VSG; 5) the depletion of putrescine leads to an accumulation of AdoMet and dAdoMet, which ultimately lead to aberrant methylation in the parasite; 6) the depletion of polyamines leads to parasite differentiation into non replicative forms (stumpy forms), which present a lower life span (Heby et al, 2007). In the case of *Leishmania*, 3-aminooxy-1-aminopropane (APA), an ODC inhibitor, with potent anti-parasitic activity in both promastigote and amastigote forms of *L. donovani* (Singh et al, 2007) may not be a suitable drug, especially in India, where resistance to pentavalent antimonials is a major problem. This relates to the fact that several clinical isolates displaying antimonial resistance overexpressed ODC (Singh et al, 2007).

Recently, a high affinity AdoMet transporter (AdoMetT1) has been identified in *L. major* (Dridi et al, 2010). In the case of *L. donovani* AdoMetDC and SpdS, null mutants to these genes cannot grow unless upon spermidine supplementation, but not putrescine (Roberts et al, 2002). The stability of *L. donovani* AdoMetDC contrasting with the fast turnover in human cells suggests that irreversible inhibition of this enzyme may have a leishmanicidal effect. MDL 73811 (aka AbeAdo) is a specific irreversible inhibitor of AdoMetDC, and a structural analogue of dAdoMet (Roberts et al, 2007), and CGP 40215A is a competitive inhibitor of AdoMetDC, with a strong leishmanicidal activity (Mukhopadhyay et al, 1996). However, in the case of SpdS, it is equally stable in the parasites and the host cells, therefore, inhibitors would likely interfere with both, unless structural differences are explored in order to design selective molecules (Roberts et al, 2001). In *T. brucei* bloodstream forms, RNAi mediated knockdown of these two enzymes has led to decreased levels of spermidine and parasite death or growth arrest in the first and the second, respectively (Willert & Phillips, 2008; Xiao et al, 2009). Actually, AdoMetDC inhibitors have shown to display a potent trypanocidal activity (Bacchi et al, 1996).

The above described results show that polyamine metabolism is extremely attractive in a drug discovery regard. Structural differences between the parasites' enzymes and their human equivalents may be explored for selective inhibitors design, precluding adverse effects on the mammalian hosts (Colotti & Ilari, 2011; Heby et al, 2007).

2.2. Thiols

Mammals make use of GSH reductase (GR)/GSH peroxidase (GP) system in order to regulate the intracellular levels of thiols and ultimately redox metabolism. Trypanosomatids lack genes encoding GR, selenocysteine-containing GSH peroxidases, thioredoxin reductase (TrxR) and catalase (Berriman et al, 2005; Colotti & Ilari, 2011; El-Sayed et al, 2005; Ivens et al, 2005). Instead, their redox metabolism is based on trypanothione ($T(SH)_2$), a low molecular weight dithiol, maintained in its reduced form by TryR (Fig. 21).

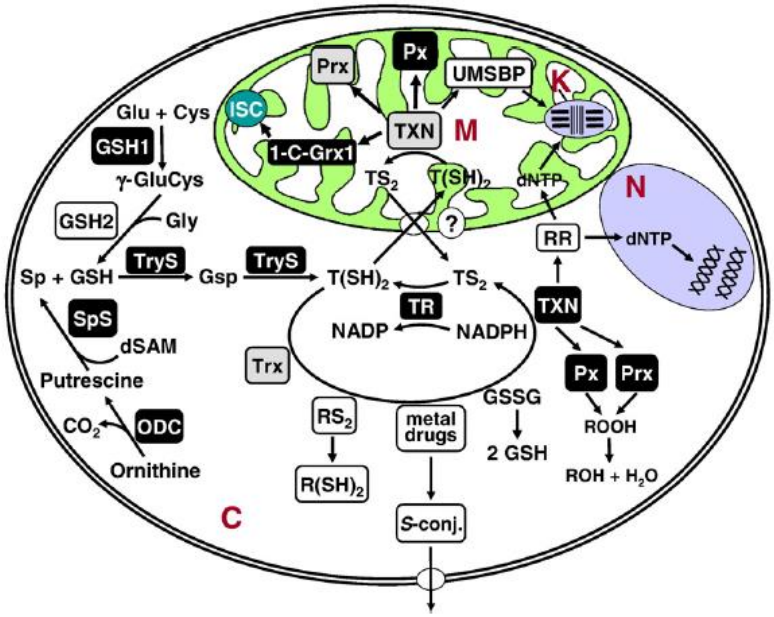

Figure 21. Trypanothione-based thiol metabolism in *T. brucei*. Trypanothione ($T(SH)_2$) is synthesized from GSH and Spd. GSH is produced by GSH1 and GSH2 and formed by glutamate, cysteine and glycine. TryS conjugates two molecules of GSH with a single molecule of Sp, generating trypanothione. Trypanothione disulfide (TS2) is back to the active dithiol upon reduction by TryR in a NADPH dependent manner. Trypanothione can be conjugated to metal containing drugs, which can be sequestered inside the cell or extruded by a specific transporter. TryR and TryS are not detectable in the mitochondria, it remains to be disclosed whether the parasite possesses a redox shuttle mechanism between this organelle and the cytosol. Proteins that have been reported as essential or dispensable for *T. brucei* are represented in black or light grey, respectively. 1-C-Grx1, monothiol glitaredoxin; C, cytosol; dSAM, decarboxylated S.adenosyl-L-methionine; GSH1, γ-glutamylcysteine synthetase 1; GSH2, GSH synthetase 2; ISC, iron sulphur clusters; K, kinetoplast; M, mitochondrion; N, nucleus; ODC, ornithine decarboxylase; Prx, 2-cys-

peroxiredoxins; Px, GSH-peroxidase-type enzymes; RR, ribonucleotide reductase; Sp, spermidine; SpS, spermidine synthase; Trx, thioredoxin; TryR, trypanothione reductase; TryS, trypanothione synthetase; TXN, tryparedoxin; UMSBP, universal minicircle sequence binding protein. Adapted from Krauth-Siegel & Comini, 2008.

In trypanosomatids, TryS is bifunctional, catalysing the synthesis and hydrolysis of GSH-Spd adduct – $T(SH)_2$ (Fig. 21). This enzyme displays two catalytic domains, the N-terminal corresponds to a papain-like cysteine protease domain, and the C-terminal corresponds to an ATP dependent synthetase domain (Fyfe et al, 2008). In the C-terminal, two molecules of GSH are conjugated with a single molecule of Spd, *via* glutathionylspermidine intermediate, with two molecules of ATP spent. The N-terminal domain is able to hydrolyse the just referred reactional intermediate (Fyfe et al, 2008). TryS is important in *T. brucei*, as corroborated by RNAi mediated knockdown and further by gene knockout. RNAi experiments demonstrated a loss of proliferation and viability, associated with increased susceptibility to oxidative stress (Comini et al, 2004; Wyllie et al, 2009). This enzyme has additionally been chemically validated using inhibitors obtained from a HTS campaign (Torrie et al, 2009). TryS is unlikely to raise resistance issues because trypanosomatids only have a single copy of the gene and there is no bypass mechanism, and it is equally unlikely to raise safety issues as there is no human homologue (Colotti & Ilari, 2011). In *L. infantum*, genetic and chemical analyses have demonstrated that TryS, but not glutathionylspermidine synthetase, is essential for the parasite survival (Sousa et al, 2014).

As previously stated, trypanothione is reduced by TryR, which is a FAD-dependent NADPH oxidoreductase (Fig. 21). *L. infantum* and *T. cruzi* TryR have been crystallized (Baiocco et al, 2009; Colotti & Ilari, 2011). This protein occurs as a dimer and each monomer has three different domains, a FAD binding domain, a NADPH binding domain and an interface domain (Baiocco et al, 2009). It is essential for *L. donovani* survival, validating it as promising drug target. On the other hand, in the case of *T. brucei*, conditional gene knockout demonstrated that parasites survive up to 90% reduction of TryR activity, suggesting that low levels of this enzyme suffice the cellular needs. However, TryR depleted parasites display reduced infectivity in mice (Krieger et al, 2000; Tovar et al, 1998).

Moreover, TryR inhibitors were identified and did not affect the closest mammalian homologue, GR (Spinks et al, 2009). Nonetheless, *in vivo* efficacy in a *T. brucei* infection model was quite disappointing, as redox metabolism was not affected at all, unless TryR was titrated down to less than 5% of normal (Krieger et al, 2000). Recent efforts focus on the generation of TryR irreversible inhibitors, as competitive ones fail to provide the sustained inhibition that is required (Flohe, 2012). It is also noteworthy that TryR inhibition

has been widely used in the treatment of the late stage *T. b. rhodesiense* infection, through the use of melarsoprol (Fairlamb et al, 1989). Equally remarkable is the fact that antimonials, one of the main drugs used to treat leishmaniasis, interfere with trypanothione metabolism, actually, they bind and inhibit TryR (Cunningham & Fairlamb, 1995).

In summary, the lack of a functional redundancy between the parasite thiol system and the mammalian, along with the sensitivity of these parasites to oxidative stress, renders the enzymatic components of this metabolism promising drug target candidates (Colotti & Ilari, 2011).

2.3. Energy metabolism

Trypanosomatids have unique organelles in order to respond to their specific lifestyle needs. Among those are glycosomes, peroxisome related organelles which comprise enzymes of important metabolic pathways such as glycolysis, PPP, β-oxidation, gluconeogenesis, purine salvage and biosynthesis of pyrimidines, ether lipids and squalenes (Michels et al, 2006). This compartmentalisation of metabolic pathways can prevent the accumulation of toxic intermediates (Haanstra et al, 2008) or enable a fast metabolic adaptation to environmental changes (Michels et al, 2006).

Briefly, most organisms have operational negative feedback mechanisms on glycolysis in order to prevent the autocatalytic pathway from losing control (*eg.* inhibition of hexokinase (HK) by glucose-6-phosphate (Newsholme et al, 1967) or phosphofrutokinase (PFK) by phosphoenolpyruvate (Blangy et al, 1968)). However, trypanosomatids lack this sort of regulation, therefore, in *T. brucei* it has inclusively been demonstrated that without this confinement, ATP produced in later glycolytic steps would be accessible in the first reactions. This would cause a turbo explosion within the pathway, and the accumulation of toxic intermediates would ultimately lead to death (Haanstra et al, 2008).

The glycosome number (average: 10-100 glycosomes per cell) as well as the qualitative and quantitative enzymatic content differ among trypanosomatids, reflecting the metabolic adaptions of the different parasite species and life cycle stages to the environment (Parsons et al, 2001; Szoor et al, 2014). Regarding number for instance, *T. brucei* bloodstream forms have around 65 glycosomes with an average diameter of 0.27 µm, and *Leishmania* promastigotes only around 50, followed by amastigotes with 5-10 times less glycosomes (Szoor et al, 2014). Due to their uniqueness, these organelles provide potential drug targets at several levels: 1) in the enzymes they contain; 2) in the metabolic communication between their matrix and the cytosol *via* transporters and channels; 3) their biogenesis and degradation (Cull et al, 2015; Gualdrón-López et al, 2013; Michels et al, 2006).

Focusing on metabolic pathways and particularly on hexose metabolism, substantial differences can be encountered when comparing *Leishmania* and *T. brucei*, or even the different developmental stages of each one of these parasites. *Leishmania* promastigotes preferentially catabolise sugars *via* glycolysis, whose first seven enzymes localise to the glycosomes (Opperdoes & Coombs, 2007). Inclusively, in replicative promastigotes a high glucose uptake and glycolytic flux can be observed. The ATP and NAD that are consumed in the early glycolytic steps are at least partially regenerated by fermentation of phosphoenolpyruvate to succinate. Following, glycolysis and succinate fermentation end products can be further catabolised in a canonical tricarboxylic acid (TCA) cycle (Saunders et al, 2011). A noteworthy feature of promastigote metabolism is the apparent lack of feedback regulation of glycolytic fluxes, and subsequently, glucose uptake usually exceeds mitochondrial capacity to oxidise glucose, which leads to the secretion of partially catabolised metabolites, such as succinate, acetate or alanine (Saunders et al, 2010). Interestingly, amastigotes enter a glucose sparing program, characterized by a reduction in glucose consumption and a negligible secretion of metabolic end products (Saunders et al, 2014). This growth limiting state, which will be further discussed in this dissertation, has been proposed to facilitate amastigote survival in the nutrient limited environment of the phagolysosome (Saunders et al, 2014). For instance in the case of *T. brucei* bloodstream forms, glycolysis of host glucose provides the sole source of carbon for ATP production (Michels et al, 2006), in contrast to procyclic forms, which contain an extended glycolytic pathway catalysing the aerobic fermentation of glucose to succinate (Coustou et al, 2003). In bloodstream forms, the exclusive dependency on glycolysis-mediated ATP production, due to an insufficient mitochondrial function, coupled with the structural differences found between their glycolytic enzymes and the human counterparts, point these enzymes as interesting drug target candidates (Coley et al, 2011).

Indeed in *T. brucei*, the genetic validation of glycolytic enzymes as drug targets has been obtained by RNAi-mediated knockdown and conditional knockout experiments. The glycosomal enzymes include HK (Albert et al, 2005), PFK (Albert et al, 2005), fructose-1,6-bisphosphate aldolase (ALD) (Caceres et al, 2010), triosephosphate isomerase (TPI) (Helfert *et al.*, 2001) and GAPDH (Caceres et al, 2010), while the cytosolic enzymes include phosphoglycerate mutase (PGAM), enolase (ENO) and phosphoglycerate kinase (PYK) (Albert et al, 2005). Some of them have also been chemically validated, namely HK1 (Sharlow et al, 2010), PFK (Brimacombe et al, 2014), ALD (Azema et al, 2006), GAPDH (Aronov et al, 1999), PYK (Drew et al, 2003) and ENO (de A S Navarro et al, 2007). In *Leishmania*, HK is the only glycolytic enzyme that has been formally validated, as well as a gluconeogenic enzyme, fructose-1, 6-biphosphatase (FBPase) (Gualdrón-López et al,

2013). In the case of the latter, *L. major* null mutants cannot replicate inside the phagolysosome as amastigotes and fail to generate normal lesions (Naderer et al, 2006).

Moreover, a plasma membrane glucose transporter has been chemically validated as a drug target in *T. brucei* (Bakker et al, 1999), and in *Leishmania*, a hexose transporter null mutant cannot survive as amastigote in MØ (Rodríguez-Contreras & Landfear, 2006).

Apart from sugar metabolism, enzymes involved in other glycosomal pathways have been validated as drug targets in *Leishmania* and/or *T. brucei*, namely in sterol synthesis, purine salvage and sugar nucleotide pathways, as well as PPP (Gualdrón-López et al, 2013). The latter will be extensively characterized later in this chapter.

2.4. Lipids

Lipid metabolism has a major importance for pathogens. Lipids serve as cellular building blocks, signalling molecules, energy reserves, post-translational modifiers, and virulence factors. Therefore, parasites must rely on a complex system of uptake and synthesis mechanisms to satisfy their demands (Ramakrishnana et al, 2013). The energy amount that is required for fatty acid synthesis is much higher than the one implicated in uptake, thus the latter is likely preferred over fatty acid synthesis pathway. However, when the host fatty acid supply is not sufficient, parasites must rely on intracellular synthesis (Lee et al, 2006).

Trypanosomatids encode for enzymes of two distinct pathways to synthesize fatty acids, a fatty acid synthesis type II (FASII) pathway and a fatty acid elongation (FAE) pathway (Ramakrishnana et al, 2013) (Fig. 22). Both have been characterized in *T. brucei* using genetic and biochemical approaches. The relevance of the FASII pathway in other kinetoplastids has not been addressed yet. In *T. cruzi* and *L. major*, these parasites encode for homologues of the enzymes involved in these pathways, suggesting that their fatty acid metabolism may be similar to that of *T. brucei* (Ramakrishnana et al, 2013). Inclusively, it has been demonstrated that expression of *L. major* dehydratase and ketoacyl reductase rescues the respiration defect of yeast mutants for the corresponding enzymes (Pillai et al, 2003). Moreover, *in silico* studies indicate the presence of additional FASII components in both *L. major* and *T. cruzi*, and all candidates are predicted to localize to the mitochondria, as they present an N-terminal signal peptide for this compartment (Ramakrishnana et al,

2013). Taken all together, these data suggest that the FASII pathway is likely conserved among trypanosomatids.

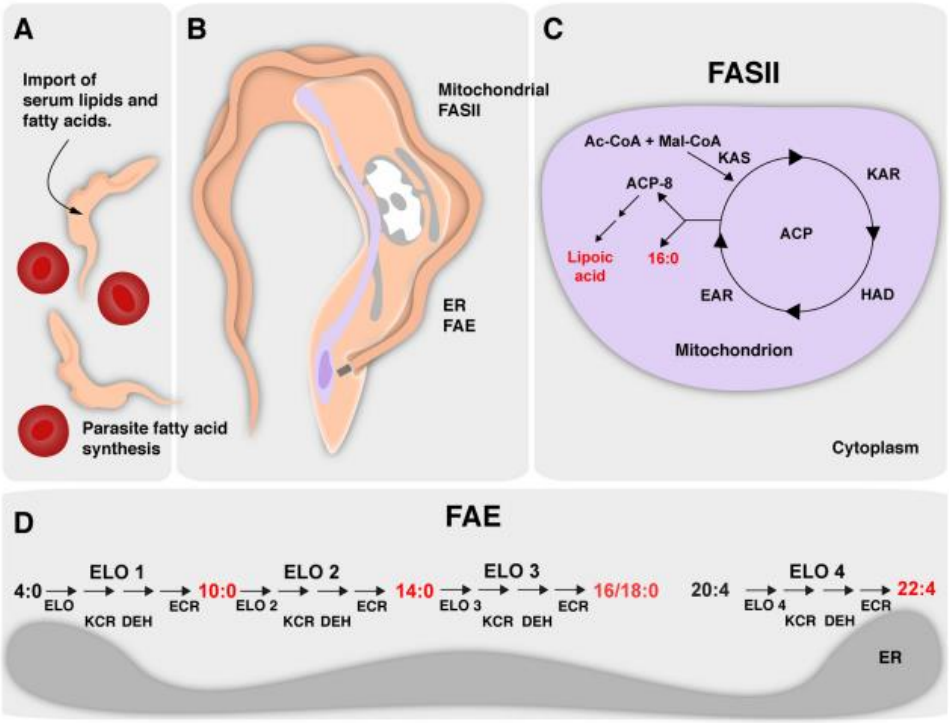

Figure 22. Fatty acid synthesis in kinetoplastids. A) *T. brucei* parasites are depicted representing kinetoplastids in general, as most of the studies were undertaken in this organism. These parasites replicate extracellularly in the bloodstream of the mammalian host, red blood cells are also shown (red). **B)** Additionally, parasites harbour two distinct pathways for fatty acid synthesis that are localized in two different organelles. **C)** FASII pathway localizes to the mitochondrion (light violet), generating lipoic acid and palmitic acid. **D)** Kinetoplastids also harbour an elongase-based pathway that localises to the endoplasmic reticulum. Unlike all other organisms, kinetoplastid FAE is used for *de novo* synthesis of fatty acids. In this pathway, butyrate and malonate are used as substrates to generate myristate/stearate and adrenate. Major products are highlighted in red. Ac-CoA, acetyl-CoA; Ac, acetate; ACP, acyl carrier protein; DEH, acyl-CoA dehydratase; EAR, enoyl-ACP reductase; ELO, elongase; ER, endoplasmic reticulum; FASII, fatty acid synthesis type II; FAE, fatty acid elongation; HAD, hydroxyacyl-ACP dehydratase; KAR, ketoacylACP reductase; KAS, ketoacyl-ACP synthase; KCR, ketoacyl-CoA reductase; Mal, malonate; Mal-CoA, malonyl-CoA. Adapted from Ramakrishnana et al, 2013.

The FASII pathway in trypanosomatids (Fig.22) is overall similar to the FASII pathway from other organisms. An acyl carrier protein (ACP) holds the growing acyl chain while the chain is modified by a synthase, dehydratase and two reductases (Ramakrishnana et al, 2013). The major difference for instance between apicomplexan and kinetoplastid parasites is that FASII pathway localises to the apicoplast or the mitochondrion, respectively (Stephens et al, 2007).

The *Tb*FASII pathway has palmitate as its final product and displays only a moderate activity, overall contributing only about 10% of total parasite fatty acid synthesis (Stephens et al, 2007). Therefore, an alternative pathway, FAE pathway that localises to the endoplasmic reticulum, serves as the major pathway for fatty acid synthesis in these parasites (Lee et al, 2006). The ablation of FASII pathway in *T. brucei* blocks lipoic acid production, pointing that the second and probably more important role of this pathway is being the major source of octanoic acid for lipoic acid synthesis (Stephens et al, 2007; Fig. 22). Thiolactomycin, which is thought to be a more specific FAS II inhibitor, and several derivatives were found to inhibit growth of *T. cruzi*, *T. brucei*, and *L. donovani* (Jones et al, 2004; Jones et al, 2005).

On the other hand, as mentioned above, trypanosomatids rely mostly on FAE pathway for fatty acids *de novo* synthesis. This pathway localises to the endoplasmic reticulum membrane and includes several elongases, dehydratases and reductases (Fig. 22). The best-characterized components are the four elongase enzymes of *T. brucei* (ELO1-4), whose functions are remarkably different from other eukaryotes (Lee *et al*., 2006). In the *Tb*FAE pathway, ELO1-3 act on saturated fatty acids, whereas ELO4 is specific for polyunsaturated fatty acids (PUFAs). *Tb*ELO1 starts the chain elongation using butyryl-CoA to generate decanoyl-CoA, which is further extended by *Tb*ELO2 to myristoyl-CoA (Lee et al, 2006). Until the discovery and characterization of FAE pathway, and due to the low abundance of myristic acid in the serum of the mammalian host, it was quite intriguing how the parasites would satisfy their great need for this fatty acid. *T. brucei* GPI anchors are composed exclusively of myristic acid, which is unique, requiring a complex fatty acid remodelling process to ensure this exclusivity (Ferguson & Cross, 1984; Masterson et al, 1990). Inclusively, *T. brucei* bloodstream forms are heavily coated by VSG, anchored to the membrane by GPI structures, in order to evade the immune system through antigenic variation (Ferguson et al, 1988; Van der Ploeg, 1990). For instance, those were the first fully characterized GPI structures in eukaryotes (Ferguson et al, 1988). Interestingly and unexpectedly, *T. brucei* bloodstream forms lacking FAE pathway did not display any growth or infectivity defect (Lee et al, 2006). However, in contrast, FAE appears to be essential for growth in procyclic forms. Overall, FAE pathway impact on parasite survival may depend on both the life cycle stage and the availability of fatty acids in the host environment (Ramakrishnana et al, 2013). Importantly, N-myristoyltransferase, the enzyme responsible for the attachment of myristate to the GPI anchor, showed to be essential for parasite viability based on RNAi-mediated knockdown (Price et al, 2003). Several inhibitors of this enzyme have been obtained by rational drug design displaying anti-parasitic activity (Frearson et al, 2010; Sheng et al, 2009).

Additionally, FAE pathway components have also been detected in *T. cruzi* and *L. major*, but while *T. brucei* encodes four elongase genes, *T. cruzi* seems to contain five and *L. major* fourteen. None of these candidate enzymes have been experimentally studied (Ramakrishnana et al, 2013). *L. major* and *T. cruzi* present GPI anchors composed of longer fatty acids (Ferguson, 1997), and this is probably the reason for the presence of additional elongases. *Leishmania* anchors several virulence factors to the membrane *via* GPI, namely GP63, LPG, PPG or GILP (Olivier et al, 2012), whose role has been explored in the first chapter of this dissertation. LPG is composed of very long (24 and 26 carbon) alkyl chains, probably derived from very long fatty acids (Ferguson, 1997).

Concerning phospholipids, *T. brucei* has a glycerophospholipid composition similar to other eukaryotic cells, with phosphatidylcholine (PC) and phosphatidylethanolamine (PE) representing the most abundant, followed by phosphatidylinositol (PI), PS, cardiolipin and phosphatidylglycerol (PG) (Ramakrishnana et al, 2013). Similarly, in *Leishmania*, PC is the most abundant glycerophospholipid, followed by PE and PI, but for instance cardiolipin and PG are present in trace amounts (Wassef et al, 1985; Zheng et al, 2010).

PI can be used to generate different phosphorylated forms of this phospholipid, several of them are important signalling molecules in eukaryotes (Michell, 2008). Besides, PI also represents the precursor for GPI anchors (Wichroski & Ward, 2003). Several enzymes involved in PI and GPI synthesis were already validated as targets in *T. brucei* (Martin & Smith, 2006; Smith et al, 2001). *T. cruzi* and *Leishmania* present orthologue genes for myo-inositol–3-phosphate synthase and PI synthase, suggesting that *de novo* synthesis of myo-inositol occurs in all kinetoplastids. Moreover, myo-inositol uptake has been reported in several *Leishmania* species, in which orthologues of the *T. brucei* myoinositol transporter have been found (Drew et al, 1995; Gonzalez-Salgado et al, 2012).

Still on glycerophospholipid metabolism, for instance miltefosine, the only oral drug available to treat leishmaniasis, may interfere with phospholipid biosynthesis. Among the possible modes of action are the inhibition of PE N-methyltransferase and CDP-phosphocholine cytidylyltransferase (Rakotomanga et al, 2007) as well as inhibition of extracellular choline uptake (Zufferey & Mamoun, 2002), resulting in changes in parasite PC and PE contents.

As for the sphingophospholipid classes, sphingomyelin (SM), inositol phosphorylceramide (IPC) and ethanolamine phosphorylceramide (EPC) constitute 10–15% of total lipid phosphorus in *T. brucei* (Sutterwala et al, 2008). The enzymes involved in their synthesis are developmentally regulated, so relative amounts of each one of them differ between procyclic and bloodstream forms (Sutterwala et al, 2008). In *Leishmania*, IPC corresponds to the major sphingophospholipid, unusually composed by long chain bases,

suggesting that the parasite preferentially uses myristoyl-CoA for ceramide synthesis, instead of palmitoyl-CoA as in *T. brucei* (Sutterwala et al, 2008), *T. cruzi* (Bertello et al, 1995), mammalian cells and yeast (Pinto et al, 1992; Williams et al, 1984). A key enzyme of sphingolipid biosynthesis pathway is sphingolipid synthase, which has been implicated in *T. brucei* survival, using RNAi and chemical inhibition (Mina et al, 2009; Sheng et al, 2009). On the other hand, neutral sphingomyelinase, responsible for the intracellular degradation of SM in *T. brucei*, is detrimental for growth, survival and proper VSG traffic (Young & Smith, 2010). Unlike trypanosomes, *Leishmania* parasites do not synthesize SM (Kaneshiro et al, 1986).

Moreover, protein prenylation is an important regulatory mechanism for signal transduction. This is enzymatically achieved through the attachment of farnesyl to proteins, mediated by farnesyltransferase, which was genetically and chemically shown to be a good target in *T. brucei* (Ali et al, 1999; Eastman et al, 2006).

In summary, the uniqueness of parasites lipid metabolism makes it a source of potential drug targets, inclusively, several enzymes have already been validated (Lee et al, 2007).

2.5. Folates

Folate is a crucial cofactor on DNA and amino acids biosynthesis, therefore the inhibition of its metabolism leads to profound alterations on cell replication and function (Vickers *et al*., 2011).

Trypanosomatids do not have a *de novo* pathway for the synthesis of pteridines (folate and biopterins) and rely on salvage from the host. Indeed, they salvage folates and unconjugated pteridines from their mammalian hosts and insect vectors through multiple transporters. They also harbour a limited set of folate-dependent metabolic reactions. In these parasites, a bifunctional dihydrofolate reductase (DHFR) - thymidylate synthase (TS) and a novel pteridine reductase 1 (PTR1) reduce folates or both folates and unconjugated pteridines, respectively. Therefore, PTR1 can be a metabolic bypass of DHFR (Vickers & Beverley, 2011).

The extent to which *Leishmania* can interconvert unconjugated pteridines into folates is debatable. These parasites usually grow upon biopterin supplementation alone. Nevertheless, it is hard to conclude whether *Leishmania* uses biopterin to synthesize folate, as trace levels of folate from serum or other medium components cannot be disregarded, along with *Leishmania*'s high-affinity folate transporters (FTs) (Petrillo-Peixoto & Beverley, 1987). Regardless, it is clear *T. brucei* and *Leishmania* have distinct biopterin and folate requirements (Vickers & Beverley, 2011).

In higher plants and protozoa, such as trypanosomatids, the DHFR and TS occur as a fusion protein (DHFR-TS). TS performs the reductive methylation of deoxyuridine-monophosphate (dUMP) to deoxythymidine-monophosphate (dTMP), the latter used for DNA biosynthesis (Gamarro et al, 1995). DHFR, in its turn, restores the tetrahydrofolate (H4F) pool, by reducing dihydrofolate (H2F) in a NADPH dependent manner (Gamarro et al, 1995). DHFR-TS has been chemically and genetically validated as a key drug target in *T. brucei* (Sienkiewicz et al, 2008). In *L. major*, DHFR-TS null mutants, obtained from an avirulent strain, survive for less than two months in the animal host, suggesting that reduced folates and thymidylate salvage does not suffice the parasites' needs, rendering them unable to cause disease. Inclusively, a null DHFR-TS mutant has been used to induce immune protection (Cruz & Beverley, 1990; Titus et al, 1995). However, it has proven impossible to ablate DHFR-TS in fully virulent *L. major* (Cruz et al, 1993).

PTR1 catalyses the reduction of both folate and biopterin, and belongs to the family of short-chain dehydrogenases/reductases (Robello et al, 1997). In *T. brucei*, its knockdown resulted in loss of viability and virulence (Sienkiewicz et al, 2010). Several scaffolds were identified as PTR1 selective inhibitors but displayed a reduced *in vitro* anti-parasitic activity (Mpamhanga et al, 2009; Tulloch et al, 2010). In *Leishmania*, similarly to DHFR-TS, PTR1 is not essential in attenuated laboratory-adapted strains (Bello et al, 1994; Papadopoulou et al, 1994) nor required for animal virulence (Cunningham et al, 2001) but it has been proven difficult to ablate PTR1 in virulent *L. major* (Vickers & Beverley, 2011). The differences found between *Leishmania* and *T. brucei* concerning the dependency on PTR1 may arise from the fact that trypanosomes lack quinonoid dihydropteridine reductase (QDPR) genes (Vickers & Beverley, 2011).

Overall, the PTR1 bypass of DHFR much contributes for the low success rate of antifolates against trypanosomatids. One of the strategies that has been employed to overcome the current limitations is the identification of agents able to simultaneously inhibit both DHFR and PTR1 (Cavazzuti et al, 2008). This is a daunting task, regarding the enzymes' structural divergence. A second approach consists in targeting the two activities with two separate inhibitors (Cavazzuti et al, 2008). It is noteworthy that the essentiality of PTR1 in trypanosomes suggests that PTR1-selective inhibitors *per se* may be successful, whereas in *Leishmania* joint inhibition may be necessary, due to the preservation of QDPR. Great efforts have been and are still employed in order to develop molecules that could target these QDPR in *Leishmania* (Cavazzuti et al, 2008; Gourley et al, 2001; Vickers & Beverley, 2011).

Folate metabolism is a source of promising drug targets, with strong potential for "drug repurposing", making use of compounds originally designed to treat human cancers

or other infectious agents (Vickers & Beverley, 2011). Currently, research encompasses the role of specific folate-pathway enzymes in metabolism, in virulence, in resistance to anti-folates and their characterization as drug targets.

3. Living in the phagolysosome

Many clinically relevant microorganisms are able to survive and replicate inside macrophages (MØ). Most of them have evolved mechanisms to divert or escape the phagocytic pathway, ultimately evading the microbicidal responses of these cells. *Leishmania* protozoans, in particular, somehow manage to counteract the phagolysosome hostile environment, living and proliferating inside this compartment.

Remarkably, *Leishmania* promastigotes preferentially catabolise sugars *via* glycolysis, inclusively, a high glucose uptake and glycolytic flux can be observed in replicative forms (Opperdoes & Coombs, 2007). However, in contrast, *Leishmania* amastigotes have complex nutritional demands, and this has probably precluded these parasites from establishing themselves in compartments such as early endosomal or non-hydrolytic vacuoles of MØ (McConville et al, 2007). The latter compartments are enriched in lipids, but lack sustainable levels of sugars or amino acids (Lorenz et al, 2004; Muñoz-Elías & McKinney, 2005), and *Leishmania* is not able to use fatty acids as its primary energy source (McConville et al, 2007). Actually, the variable nutritional composition of the host cell phagolysosome might be one of the reasons why *Leishmania* promastigotes cannot replicate or differentiate into amastigotes in neutrophils (Van Zandbergen et al, 2004). Some of the metabolites *Leishmania* amastigotes can successfully uptake include hexoses, amino acids, polyamines, purines, vitamins, sphingolipids, heme, Fe^{2+} and Mg^{2+} cations, among others (Podinovskaia & Descoteaux, 2015).

Despite the phagolysosome seems like an inhospitable environment, *Leishmania* amastigotes somehow manage to survive and proliferate long-term inside the mature phagolysosome of mammalian MØs (Saunders et al, 2014). Actually, considering many *Leishmania* auxotrophs do not display any loss of virulence or manage to persist for long terms in animal hosts, this suggests that the phagolysosome may be somehow a permissive niche (McConville et al, 2007).

Amastigotes undergo a glucose-sparing state, characterized by a sharp decrease in glucose uptake and a negligible secretion of metabolic end-products. This phenotype can be classified as a “stringent metabolic response” (Saunders et al, 2014). However, importantly, the general decrease in glucose uptake is not associated to an increase in amino acid metabolism and only in a small extent to an increase in fatty acid β-oxidation. Thus, this unique metabolic state is related to a more efficient energy metabolism, coupled

with a decrease in protein and lipid biosynthesis, processes that occur at a great energy expense. There is inclusively a carbon redirection into intracellular carbohydrate reserves (Saunders et al, 2014). However, these parasites become much dependent on mitochondrial metabolism for glutamate and glutamine biosynthesis, which apparently they are unable to salvage in the required extent from the phagolysosome (Saunders et al, 2014). The infectivity defects found for glucose transporter knockout (Rodríguez-Contreras et al, 2006) and gluconeogenic enzyme FBPase knockout (Naderer et al, 2006) mutants highlight the importance of carbohydrates in amastigotes, demonstrating that glucose transporters and gluconeogenesis are required for viability.

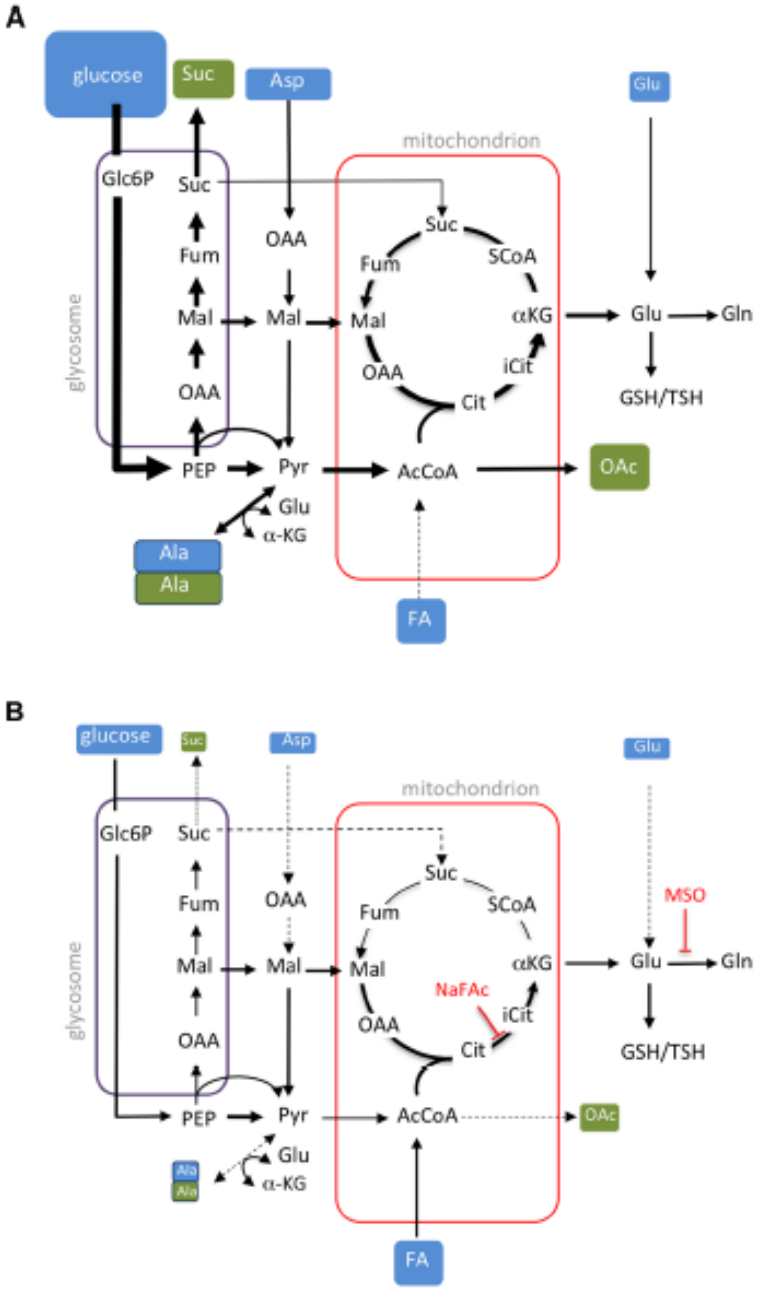

Figure 23. Rearrangement of *L. mexicana* carbon metabolism in different developmental stages. The image depicts key pathways of carbon utilization in

promastigotes **(A)** and amastigotes **(B)**. Major carbon sources (blue box) and overflow metabolites (open box). Fluxes through dotted pathways are down-regulated relative to the other stage. Steps inhibited by NaFAc and MSO are illustrated. aKG, a-ketoglutarate; AcCoA, acetyl-CoA; Ala, alanine; Asp, aspartate; Cit, citrate; Fum, fumarate; FA, fatty acids; G6P, glucose-6-phosphate; G3P, glyceraldehyde 3-phosphate; Gln, glutamine; Glu, glutamate; Mal, malate; OAA, oxaloacetate; OAc, acetate; PEP, phosphoenolpyruvate; PPP, pentose phosphate pathway; Pro, proline; Pyr, pyruvate; SCoA, succinyl-CoA; Suc, succinate; TCA, tricarboxylic acid cycle. Adapted from Saunders et al, 2014.

It has been proposed that this stringent metabolic state may facilitate a long-term amastigote survival in the nutrient-limited environment of the phagolysosome, but simultaneously and paradoxically increasing the dependency on carbohydrates uptake and metabolism (Saunders et al, 2014).

4. Targeting the pentose phosphate pathway

Apart from glycolysis, glucose is metabolized by PPP, whose role on protozoa and their interaction with their hosts has become very attractive.

It is a key metabolic pathway that relies on the use of glucose and is classically divided in two branches: an oxidative branch and a non-oxidative branch, the latter is responsible for the interconvertion of phosphorylated saccharides (Fig. 24). The resulting products (ribose-5-phosphate - R5P), intermediates (glyceraldehyde-3-phosphate - G3P, fructose-6-phosphate - F6P) and cofactors (NADPH) are used to synthesize nucleic acids and lipids, as well as to maintain redox homeostasis (Stryer, 1999). PPP does not necessarily act as a cycle, as the enzymatic reactions can be adjusted according to the cell demands (Stryer, 1999). In most organisms, this pathway localises to the cytosol, but in trypanosomatids it localises between the glycosomes and the cytosol (Hannaert et al, 2003).

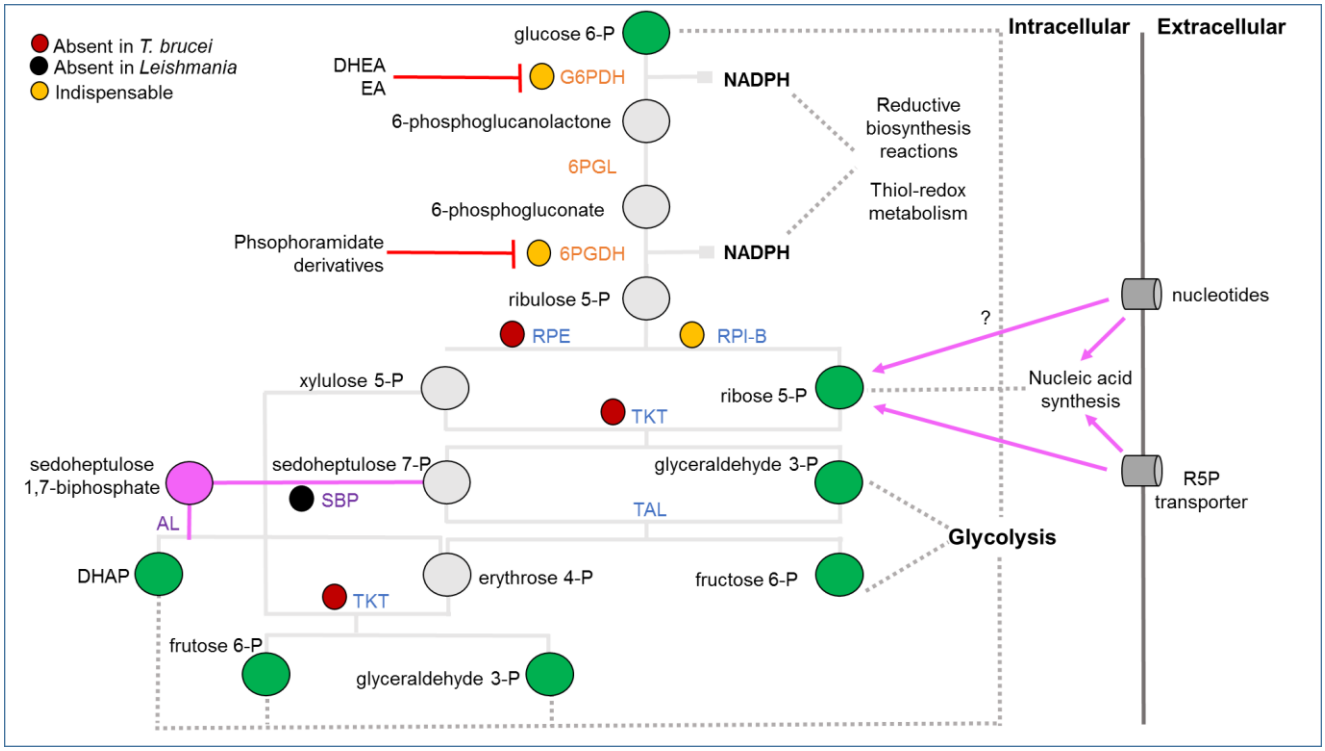

Figure 24. Pentose phosphate pathway in trypanosomatids. The green dots represent substrates and products that are shared with other pathways. The enzymes of the oxidative and non-oxidative branch are depicted in orange and light blue, respectively: G6PDH, glucose-6-phosphate dehydrogenase; 6PGL, 6-phosphogluconolactonase; G6PDH, 6-phosphogluconate dehydrogenase; RPIB, ribose-5-phosphate isomerase B; RPE, ribose-5-phosphate epimerase; TKT, transketolase; TAL, transaldolase; AL, aldolase. The figure also illustrates 1) membrane transporters of R5P and/or nucleotides; 2) the phosphorylation of ribose by ribokinase (question mark); 3) the riboneogenesis pathway that accounts on aldolase (AL), sedoheptulose biphosphatase (SBP) and tansketolase (TKT). DHAP, dihydroxyacetone phosphate. Essential enzymes are marked in yellow, and enzymes absent in *Leishmania* and *T. brucei* are marked in black and red, respectively. Adapted from Comini et al, 2013.

On a drug development perspective, some PPP enzymes seem worthy to explore due to several crucial aspects: 1) detrimental for parasite survival or infectivity and/or substantial divergence to the mammalian counterparts; 2) ease of producing recombinant proteins in native conditions as well as ease of performing *in vitro* activity assays; 3) availability of structural data (Comini et al, 2013).

4.1. The oxidative branch

The oxidative branch includes three steps, resulting in two NADPH molecules for each glucose-6-phosphate (G6P) molecule that is consumed, finally generating ribulose-5-phopshate (Ru5P) (Barrett, 1997).

Glucose-6-phosphate dehydrogenase (G6PDH; Fig. 24) is the first enzyme of the oxidative branch of PPP, catalysing the oxidation of G6P to 6-phosphogluconolactone as $NADP^+$ is reduced to NADPH. This enzyme shares approximately 50% identity to the human orthologue (Comini et al, 2013). It localises mostly to the cytosol, although there is a small fraction compartimentalized in the glycosomes, although a typical peroxisomal targeting sequence (PTS) is absent (Duffieux et al, 2000; Opperdoes & Szikora, 2006). *T. brucei* and *L. mexicana* have a single copy sequence, whereas *T. cruzi* has five copies, two of them being pseudogenes. This enzyme has been validated as a drug target in *T. brucei*, using RNAi, probably due to the depletion of nucleotide and NADPH pools (Cordeiro et al, 2009). The steroids dehydroepiandrosterone (DHEA) and epiandrosterone (EA) inhibit the *T. brucei* enzyme, and exhibit *in vitro* anti-parasitic activity against bloodstream forms (Cordeiro et al, 2009). A critical role in anti-oxidant defence has been demonstrated for G6PDH in *T. cruzi* and *Leishmania* (Ghosh *et al*., 2015; Gupta *et al*., 2011).

The second step of this pathway is catalysed by 6-phosphogluconolactonase (6PGL; Fig. 24), which hydrolyses 6-phospogluconolactone into 6-phosphogluconate (Duffieux et al, 2000). In *T. brucei*, it localises mostly in the cytosol, but around 15% localises to the glycosomes, and a PTS-1 signal peptide can be found (Duclert-Savatier et al, 2009; Opperdoes & Szikora, 2006). It has only 20% identity to the human orthologue and the structure has been recently solved. Although its substrate, 6-phospogluconolactone, can spontaneously hydrolyse, in conditions of high NADPH demand, it may accumulate especially inside the glycosomes. Due to its electrophilic character, it may irreversibly inactivate key metabolic enzymes. Therefore, 6PGL may have a detrimental role to prevent the accumulation of this PPP intermediate. However, its essentiality has not been addressed in any trypanosomatid (Comini et al, 2013).

The last step is catalysed by 6-phosphogluconate dehydrogenase (6PGDH; Fig. 24), which is responsible for the oxidation and decarboxylation of 6-phosphogluconate to Ru5P, while again reducing $NADP^+$ to NADPH (Dickens & Glock, 1951). It has only around 35% homology to the human counterpart, however there is a high conservation of the residues involved in the substrate and coenzyme binding, challenging the design of selective inhibitors (Barrett, 1997; Comini et al, 2013). Similarly to the first two enzymes of the pathway, it localises predominantly to the cytosol, and in a less extent to the glycosomes (Heise & Opperdoes, 1999). In *T. brucei*, deletion of 6PGDH leads to the accumulation of 6-phosphogluconate, which inhibits phosphoglucose isomerase and consequently glycolysis. This is probably exacerbated *in vivo* with the increase of G6P flow through the PPP. Moreover, it remains to be investigated whether a decrease in R5P production also plays a role in the observed defect (Comini et al, 2013). Some analogues of the high energy

intermediate (hydroxamate derivatives of D-erythronic acid) were found to be potent and selective inhibitors of *Tb*6PGDH (Dardonville et al, 2004), however the best compounds did not have trypanocidal activity due to its poor membrane permeability. Therefore, phosphate prodrugs have been developed to overcome this limitation. In particular, aryl phosphoramidate prodrugs of 2,3-*o*-isopropylidene-4-erythrono hydroxamate displayed a high *in vitro* antiparasitic activity (Ruda et al, 2010). 6PGDH essentiality has not been addressed so far in *Leishmania* and *T. cruzi*.

In summary, the oxidative branch is therefore crucial, as it supplies not only Ru5P, a precursor of the non-oxidative branch, but also NADPH, an essential molecule for lipid synthesis, defence against oxidative stress by regenerating GSH, among other important cellular processes (Comini et al, 2013).

4.2. The non-oxidative branch

The non-oxidative branch generates important metabolites that can be then used for nucleic acids or amino acids synthesis. It starts with the conversion of Ru5P generated in the last step of the oxidative branch into R5P or xylulose-5-phosphate (X5P). Immediately downstream there two enzymes, transketolase (TKT) and transaldolase (TAL), which catalyse interconversion reactions between R5P/ X5P and glycolytic intermediates G3P/F6P (Stryer, 1999).

Ribose-5-phosphate isomerase (RPI; Fig. 24) is responsible for the interconversion of R5P in Ru5P. Two types of RPI enzymes can be found. Type A RPI (RPIA) is represented in all life kingdoms, contrasting with the type B (RPIB), restricted to some bacteria and protozoans (Sorensen & Hove-Jensen, 1996). An adverse phenotype was observed in *E. coli* (Sorensen & Hove-Jensen, 1996) and also humans (Huck et al, 2004) upon RPI deficiency, suggesting a critical conserved role through evolution. Trypanosomatids possess a type B RPI with no mammalian homologue (Al-Mulla Hummadi et al, 2006; Cronin et al, 1989; Kaur et al, 2012; Loureiro et al, 2015; Stern et al, 2007; Stern et al, 2011). RPIB has been previously proposed as a drug target in *Leishmania* and *T. cruzi*, awaiting genetic validation (Kaur et al, 2012; Stern et al, 2011). Moreover, an analogue of the isomerization intermediate, 4-phospho-D-erythronohydroxamic acid (4-PEH), has been proven to inhibit *Tc*RPIB (Stern et al, 2007). However, it also inhibits RPIA (Roos et al, 2005) and its anti-parasitic has not been tested yet.

Another player of the PPP non-oxidative branch is ribose-5-phosphate epimerase (RPE; Fig. 24), which interconverts Ru5P and X5P. In *T. brucei* RPE activity was detected in procyclics, but not in parasites isolated from mice (Cronin et al, 1989). In *T. cruzi*, the enzyme is expressed in all developmental stages (Comini et al, 2013). *Leishmania* encodes

for two isoenzymes that differ in the presence and absence of a PTS (Opperdoes & Coombs, 2007), and the first has been recently detected in *L. donovani* glycosomes (Jamdhade et al, 2015). Inclusively, its activity has been detected in *L. mexicana* promastigotes and was 3 fold higher than its competitor enzyme, RPIB (Maugeri et al, 2003).

TKT (Fig. 24) can catalyse two different reversible reactions, using thiamine diphosphate as a cofactor. The first converts X5P to R5P, producing G3P and sedoheptulose-7-phosphate (S7P). The second converts X5P to erythrose-4-phosphate (E4P), generating G3P and F6P (Stryer, 1999). In trypanosomatids, at least two residues involved in the substrate and cofactor binding are not conserved when comparing to the human counterpart (Comini et al, 2013). TKT is expressed in all developmental stages of *T. cruzi* and its activity has been reported in several *Leishmania* species (Comini et al, 2013). In particular, in *L. mexicana* it displays dual localization (cytosol and glycosomes) (Veitch et al, 2004). TKT activity has not been detected in *T. brucei* parasites recovered from the mice (Cronin et al, 1989), very similarly to RPE. Therefore, these two enzymes do not qualify as drug targets against African trypanosomes. Apparently a great extent of the non-oxidative branch of PPP appears dispensable for *T. brucei* bloodstream forms contrarily to insect stage (Comini et al, 2013; Creek et al, 2015). This metabolic adaptation may be employed in order to channel sugar metabolization exclusively into R5P and NADPH generation, to support the high proliferation rate of the bloodstream forms (Comini et al, 2013; Creek et al, 2015). Since *T. cruzi* and *Leishmania* present a fully operative PPP, the role of TKT in these parasites still awaits to be unravelled. This enzyme may prevent the accumulation of toxic metabolites or modulate NADPH production by redirecting sugar phosphates towards the oxidative branch of the pathway (Comini et al, 2013).

Another enzyme is TAL (Fig. 24), which transfers a three-carbon fragment, dihydroaxyacetone, from S7P to G3P, producing F6P and E4P. It also catalyses the inverse reaction (Comini et al, 2013). TAL activity has been detected in *Leishmania* and trypanosomes (Comini et al, 2013). In *T. brucei*, due to its defective PPP non-oxidative branch, this enzyme can be disregarded as a drug target. However, in *Leishmania* and *T. cruzi* further studies should be undertaken in order to draw any conclusions.

It is also noteworthy that organisms, like yeast, have an alternative pathway for R5P synthesis, designated riboneogenesis pathway, which is NADP-independent. This pathway transforms glycolytic intermediates into sedoheptulose-1, 7-biphosphate, by a combined action of TKL and ALD. Sedoheptulose-1, 7-biphosphate, through the action of sedoheptulose-1, 7-biphosphatase (Fig. 24), is converted into S7P, which can be a substrate of TKL to ultimately generate R5P (Clasquin et al, 2011). Genes encoding a

putative sedoheptulose-1, 7-biphosphatase are present in the genomes of *T. brucei* and *T. cruzi*, but absent in *Leishmania* (Opperdoes & Coombs, 2007). Importantly, it has not been formally demonstrated that this pathways operates in trypanosomes.

Overall the components of the non-oxidative branch of PPP are more heterogeneous, comprising members that do not possess a mammalian homologue (RPIB) and others that are developmentally regulated and specifies-specific dispensable (RPE and TKT) (Comini et al, 2013). Furthermore, this branch deserves more attention in the context of drug target validation.

5. Targeting asparagine metabolism

Asparagine (Asn) metabolism has become very attractive in the recent years. Apart from cancer cells, in some pathogenic microorganisms, it has been surprisingly associated to survival, invasion and/or virulence (Baruch et al, 2014; Gesbert et al, 2014; Gouzy et al, 2014; Hofreuter et al, 2008; Kullas et al, 2012; Leduc et al, 2010; Scotti et al, 2010; Shibayama et al, 2011).

Asn is the last nonessential amino acid synthesised from glucose metabolism. This means it can be synthesized from central metabolic pathway intermediates and therefore is not required from the diet (Zhang et al, 2014b). Asn displays a high nitrogen/carbon ration, being associated to nitrogen homeostasis as well. For a long time, in contrast with the other nineteen common amino acids, it seemed Asn was not involved in any other pathway but protein synthesis in mammalian cells (Ubuka & Meister, 1971; Zhang et al, 2014b). However, recent studies suggest Asn somehow coordinates cell responses with metabolic reserves, ultimately regulating cell fate (Zhang et al, 2014b).

In the context of basic cell biology, Asn (N)-linked glycosylation of proteins is one of the most important post-translational modifications, in which there is the covalent attachment of an oligosaccharide into an Asn residue of polypeptide chains. This protein modification is found both in eukaryotes and in prokaryotes and classically takes place in the endoplasmic reticulum (Schwarz & Aebi, 2011).

There are two major pathways involved in Asn metabolism – tRNA-dependent and tRNA-independent pathways. Additionally, cells also uptake Asn from the extracellular environment (Min et al, 2002). Different environmental and physiological conditions challenge organisms to adjust their Asn intracellular production and uptake (Zheng & Haselkorn, 1996). Some cells, genetically manipulated or leukemic cells, may actually rely mostly on Asn uptake. Some mutants become auxotrophic to Asn and require exogenous supplementation in order to grow (Qian et al, 2013). Leukemic cells, for instance, have low

levels of Asn and therefore become especially sensitive to its extracellular depletion, which has been explored in a therapeutic perspective (Avramis, 2012).

Across trypanosomatids' species and life cycle stages, the amino acid transporters (AAT) repertoire has a high interspecific variation, regarding number, affinity, specificity and capacity (Jackson, 2007). However, few information is available regarding Asn transport. In *T. brucei*, a protein presenting putative orthologues in *Leishmania* (Aurrecoechea et al, 2010; El-Sayed et al, 2005; Ivens et al, 2005) was characterized as a transporter of several neutral amino acids, among which Asn (*Tb*AATP1) (Ebikeme, 2007). For instance, Asn transporter inactivation in *Francisella tularensis* does not compromise phagosomal escape but it is critical for bacterial multiplication in the cytosol of the host (Gesbert et al, 2014). Nonetheless, the redundancy in AATs suggests that targeting them would be pointless (Ebikeme, 2007).

5.1. tRNA dependent reactions

Aminoacyl-tRNA synthetases are key enzymes in protein translation, as they synthesize the tRNAs required for the process, in an ATP dependent manner. They perform a reaction that comprises two steps: 1) generation of an aminoacyladenylate, as ATP and an amino acid enter the catalytic site; 2) esterification of the amino acid to the tRNA, ultimately generating the final 'charged' aminoacyl-tRNA (Pham et al, 2014).

The synthesis of Asn-tRNA^{Asn} can be catalysed by two independent aminoacyl-tRNA synthetases, a discriminating and a non-discriminating enzyme. In the presence of the first, a classical aminoacylation occurs resulting in Asn-tRNA^{Asn} (Min et al, 2002). Interestingly, a great part of prokaryotes, bacteria and archaea, uses a undiscriminating aspartyl-tRNA synthetase (Blaise et al, 2011). The latter generates a misacylated Asp-tRNA^{Asn} molecule that suffers an amidation catalysed by Asp-tRNA^{Asn} amidotransferase, ultimately generating Asn-tRNA^{Asn} (Blaise et al, 2011). The presence of undiscriminating aspartyl-tRNA synthetases normally occur in organisms that lack the asparaginyl-tRNA synthetase (AsnRS), with few exceptions of organisms that can simultaneously use both (Curnow et al, 1998; Roy et al, 2003).

For a long time, aminoacyl-tRNA synthetases have been pursued as drug targets in bacteria and fungi, and more recently in protozoa. Actually drug repurposing of inhibitors, firstly designed to inhibit the bacterial counterparts, is a very prominent strategy to obtain new anti-parasitic drugs (Pham et al, 2014). However, the major issue is selectivity, because humans encode for 36 aminoacyl-tRNA synthetases that have eukaryotic and bacterial origins. As several crystal structures for parasite enzymes have been solved, this may enable rational drug design (Pham et al, 2014). For the purpose, structures that diverge

from the human homologue or parasite specific modifications must be explored to achieve the desired selective inhibition (Bour et al, 2009; Gowri et al, 2012). Several aminoacyl-tRNA synthetases appear to be promising drug targets against several parasites such as *Plasmodium*, *Brugia* (causative agent of lymphatic filariasis), trypanosomes and *Leishmania* (Pham et al, 2014).

The cytoplasmic AsnRS has been a longstanding drug target in *Brugia malayi* (Pham et al, 2014), and recently, in *T. brucei* bloodstream forms, its knockdown led to a severe growth impairment (Kalidas et al, 2014).

5.2. tRNA independent reactions

Within the t-RNA independent pathway for Asn synthesis, asparagine synthetase (AS) is a crucial player. It catalyses Asn formation from aspartate in an ATP dependent manner using ammonia or glutamine as nitrogen donors. The reaction mechanism comprises two crucial steps: 1) the formation of β-aspartylAMP, in which β-carboxylate group of aspartate is activated by ATP; 2) nucleophilic attack by an ammonium ion. This mechanism mirrors the close evolutionary relation to aminoacyl-tRNA synthetase enzymes (Nakatsu et al, 1998). There are two structurally distinct types of AS: A and B (Sugiyama et al, 1992).

Type B (AS-B) uses preferably glutamine over ammonia, with exception of the human enzyme that uses both in the same extent. It can be found in prokaryotes and eukaryotes (mammalian cells, yeasts, *Chlamydomonas reinhardtii*, higher plants) (Andrulis et al, 1987; Andrulis et al, 1989; Ciustea et al, 2005; Humbert & Simoni, 1980; Merchant et al, 2007; Ramos & Wiame, 1980; Scofield et al, 1990). In the N-terminal there is a glutaminase domain that hydrolyses glutamine, releasing ammonia, which travels through an intramolecular channel till the C-terminal where the synthetase domain is assembled. The released ammonia performs the nucleophilic attack to the β-aspartylAMP, generating Asn and releasing AMP (Boehlein et al, 1994; Boehlein et al, 1998). It has been proposed that AS-B results from the fusion of an ancestral glutamine amidotransferase gene with an ancestral ammonia dependent *AS* gene homologous to *ASA* (Gaufichon et al, 2013). As previously stated, leukemic cells display low levels of Asn due to the lack of constitutive expression of AS-B, becoming particularly sensitive to Asn extracellular depletion, and for this reason L-asparaginase has been successfully employed in the treatment of acute lymphoblastic leukemia (Avramis, 2012). Resistance to this treatment has been associated to AS-B and therefore a combination therapy comprising L-asparaginase and AS-B inhibitors has been pursued (Stams et al, 2005). AS-B *per se* has been regarded as a potential drug target in some forms of solid cancer as well (Dufour et al, 2012; Yang et al,

2014). Importantly, in mammalian cells, AS-B is a transcriptional target of the well characterized GCN2/eIF2α/ATF4 axis (Fig. 25), in response to amino acid starvation. The phosphorylation of eIF2 leads to a repression of general protein synthesis, as well as an activation of gene-specific translation (Horiguchi et al, 2012; Ye et al, 2010).

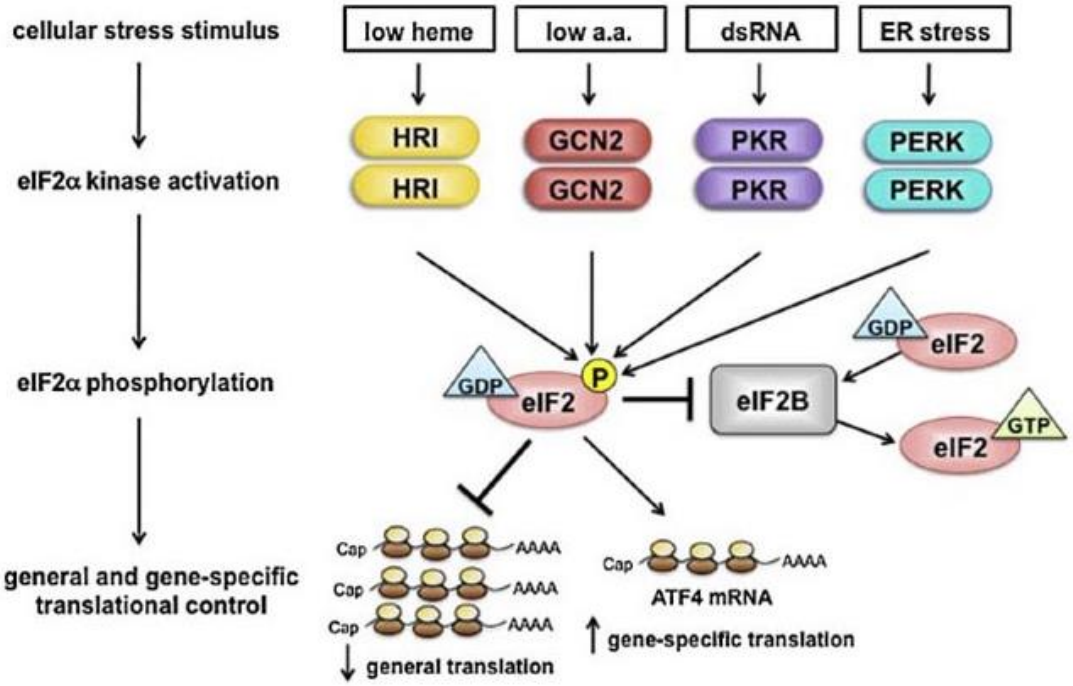

Figure 25. Translational control by eIF2 kinases in mammalian cells. Mammals that possess four eIF2 kinases: GCN2, HRI, PKR and PEK/PERK, which are activated under different stressful conditions, such as amino acid, glucose or purine deprivation, among others. The phosphorylation of eIF2 leads to a repression of general protein synthesis, as well as an activation of gene specific translation. In the case of GCN2 mediated eIF2 phosphorylation, upon activation of ATF4, there is an increase in *ASB* transcription. ATF4, activating transcription factor 4; eIF2α, eukaryotic initiation factor 2α**;** GCN2, general control nonderepressible kinase 2; HRI, heme regulator eIF2α kinase; PERK, protein kinase RNA-like endoplasmic reticulum kinase; PKR, protein kinase R. Adapted from Trinh & Klann, 2013.

On the other hand, type A enzymes (AS-A) are found mainly in prokaryotes (*E. coli* and *Klebsiella aerogenes*) or in archaea (*Pyrococcus abyssi*) and initially described as strictly ammonia dependent (Blaise et al, 2011; Nakamura et al, 1981; Reitzer & Magasanik, 1982). It has been proposed that AS-A descends from an aspartyl-tRNA synthetase ancestor, which first lost the anticodon binding domain, followed by a rearrangement of the catalytic site in order to acquire the ability to activate the β-carboxylate of aspartate (Blaise et al, 2011).

Several roles have been attributed to bacterial AS. For instance, in *Pasteurella multocida*, AS-A is substantially upregulated during host infection, in *Mycobacterium*

smegmatis AS-B is involved in natural resistance to antibiotics and in *Mycobacterium tuberculosis*, AS-B was reported to be required for *in vitro* growth (Boyce et al, 2002; Griffin et al, 2011; Ren & Liu, 2006; Sassetti et al, 2003).

Surprisingly, kinetoplastids and other protozoans, despite being eukaryotes, possess not only a putative AS-B but also a bacterial type AS-A (Gowri et al, 2012; Manhas et al, 2014). *L. donovani* AS-A was reported to be essential for parasite survival, and due to its absence in the human host, emerged as a novel drug target candidate (Manhas et al, 2014).

Another important player in t-RNA-independent pathway of Asn metabolism are asparaginases. These enzymes hydrolyse Asn into aspartate and ammonium ion. This reaction is performed in two subsequent steps: 1) generation an acyl-enzyme intermediate, as the nucleophilic threonine attacks the carbonyl group of the amide substrate, releasing ammonia; 2) aspartate production, as water attacks the acyl-enzyme intermediate (Michalska & Jaskolski, 2006). Asparaginases have been implicated in the virulence of several pathogens, and some striking examples include *Helicobacter pylori*, *Campylobacter jejuni*, *Salmonella typhimurium* and *M. tuberculosis*. *H. pylori*, *C. jejuni*, *S. typhimurium* secrete asparaginase into the periplasm, which is thought to contribute to Asn depletion and starvation mediated immune cell exhaustion, allowing the colonization of the host (Gesbert et al, 2014; Hofreuter et al, 2008; Kullas et al, 2012; Leduc et al, 2010; Scotti et al, 2010; Shibayama et al, 2011). In *M. tuberculosis* (Fig. 26), for instance, secretion of asparaginase into the phagosome is important for nitrogen and aspartate assimilation and allows mycobacterial growth in acidic conditions through ammonia release and pH buffering (Gouzy et al, 2014).

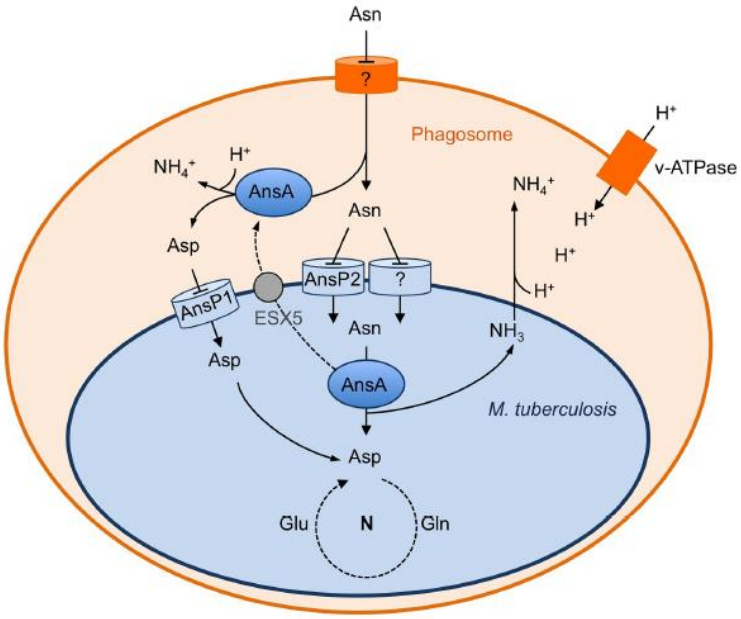

Figure 26. The role of asparagine catabolism in *M. tuberculosis* intracellular survival. In macrophages, Asn enters *M. tuberculosis* phagosome by an unknown mechanism. Asn is uptaken by the bacteria through AnsP2 and one or more additional transporter(s) yet to be identified. Further, it is hydrolysed by cytosolic AnsA resulting in nitrogen assimilation into glutamine and glutamate and release of ammonia. AnsA is also secreted in the phagosome and hydrolyses Asn, producing aspartate and ammonia. Aspartate is imported by AnsP1. The released ammonia neutralises the protons and allows pH buffering. AnsA, asparaginase; AnsP1/AnsP2, amino acid transporters; Asn, asparagine. Adapted from Gouzy et al, 2014.

Another noteworthy example of the relevance of Asn metabolism in the context of infection is the extracellular pathogenic bacterium group A *Streptococcus* (GAS). The bacteria is able to elegantly modulate the host metabolism in order to regulate its own sensing and proliferation. Adhering GAS delivers streptolysins O and S to host cells triggering endoplasmatic reticulum stress and AS-B upregulation. Subsequent increased levels of Asn are sensed by GAS inducing the transcription of, among others, genes responsible for bacterial proliferation. Bacteremia without a defined focus is a hallmark of highly invasive GAS, and treatment with asparaginase successfully arrested GAS growth in an *in vivo* model of infection (Baruch et al, 2014). Considering that *Staphylococcus aureus*, *Listeria monocytogenes* and *Clostridium botulinium* also possess the same streptolysins, eventually, they may be able to manipulate host cell metabolism in their favour in a similar fashion, and therefore, treatment with asparaginase could be successful in a broad range of human pathogens (Baruch et al, 2014).

In *T. brucei*, asparaginase does not seems to be present (Ginger et al, 2007). In contrast, *L. donovani* has genes encoding for putative asparaginase enzymes, however,

this has not been experimentally demonstrated, nor its role on parasite survival and development (Singh et al, 2015).

Chapter III

Objectives and results

1. Scope of the thesis

Leishmaniasis has a significant impact on public health worldwide. VL is the most severe form of the disease, and its control relies mainly on chemotherapy and vector control, both presenting several limitations that hinder disease eradication in endemic areas (Kedzierski, 2010). Traditional chemotherapy is often associated with high cost, toxicity, complex administration regimes and resistances (Maltezou, 2010). This preoccupying scenario renders the search for new drugs and novel drug targets a priority.

Exploring the availability of genome sequence and *in silico* prediction tools, we have performed a comparative genomic analysis to identify potential molecular targets in trypanosomatids. *L. infantum* and *L. major* genomes have been considered representatives of VL and CL causative agents, respectively (Ivens et al, 2005; Peacock et al, 2007; Rogers et al, 2011). Additionally, the genomes of *T. brucei* and *T. cruzi*, which cause sleeping sickness and Chagas disease respectively, have also been screened (Berriman et al, 2005; El-Sayed et al, 2005). African and American trypanosomiasis are also neglected tropical diseases associated with a great world burden, whose chemotherapy has been facing similar challenges to leishmaniasis. Starting with a total of 5791 orthologue genes, the application of several consecutive filters led to seven hits: 1) crucial for survival; 2) absence of a human homologue; 3) involvement in several metabolic pathways; 4) previously validated as a drug target in other microorganism. AS-A and RPIB were selected among the seven last hits based on the following criteria: 1) gene copy number; 2) “workable” size of the gene and protein; 3) availability of homologous 3D structures; 4) availability of theoretical inhibitors.

However, *in silico* selection demands a chemical or genetic validation. Indeed, one of the main purposes of this thesis was to evaluate the impact of AS-A and RPIB on *L. infantum* and *T. brucei* survival and infectivity. Furthermore, proteins expression levels throughout parasite development as well as their cellular localization were also investigated. Moreover, recombinant proteins were expressed and *in vitro* enzymatic assays were established allowing their biochemical characterization.

The functional characterization of AS-A and RPIB candidate targets comprised the following specific objectives:

i. *In silico* analysis of the theoretical 3D structures;
ii. Expression, purification and biochemical characterization of the recombinant proteins;
iii. Analysis of protein expression level in different parasite developmental stages;

iv. Protein subcellular localization studies;

v. *In vitro* and *in vivo* phenotypic analysis of RNAi or gene knockout transgenic parasites.

2. Results

2.1. Asparagine synthetase A

2.1.1. Knockdown of asparagine synthetase A renders *Trypanosoma brucei* auxotrophic to asparagine

Asparagine synthetase (AS) catalyzes the ATP-dependent conversion of aspartate into asparagine using ammonia or glutamine as nitrogen source. There are two distinct types of AS, asparagine synthetase A (AS-A), known as strictly ammonia-dependent, and asparagine synthetase B (AS-B), which can use either ammonia or glutamine. The absence of ASA in humans, and its presence in trypanosomes, suggested AS-A as a potential drug target that deserved further investigation. We report the presence of functional AS-A in *Trypanosoma cruzi* (*Tc*AS-A) and *Trypanosoma brucei* (*Tb*AS-A): the purified enzymes convert L-aspartate into L-asparagine in the presence of ATP, ammonia and Mg2+. *Tc*AS-A and *Tb*AS-A use preferentially ammonia as a nitrogen donor, but surprisingly, can also use glutamine, a characteristic so far never described for any AS-A. TbAS-A knockdown by RNAi didn't affect *in vitro* growth of bloodstream forms of the parasite. However, growth was significantly impaired when *Tb*AS-A knockdown parasites were cultured in medium with reduced levels of asparagine. As expected, mice infections with induced and non-induced *T. brucei* RNAi clones were similar to those from wild-type parasites. However, when induced *T. brucei* RNAi clones were injected in mice undergoing asparaginase treatment, which depletes blood asparagine, the mice exhibited lower parasitemia and a prolonged survival in comparison to similarly-treated mice infected with control parasites. Our results show that *Tb*AS-A can be important under *in vivo* conditions when asparagine is limiting, but is unlikely to be suitable as a drug target.

Reprinted from PLoS Neglected Tropical Diseases 2013 Dec 5; 7(12): e2578. doi: 10.1371/journal.pntd.0002578

OPEN ACCESS Freely available online

PLOS | NEGLECTED TROPICAL DISEASES

Knockdown of Asparagine Synthetase A Renders *Trypanosoma brucei* Auxotrophic to Asparagine

Inês Loureiro[1], Joana Faria[1], Christine Clayton[2], Sandra Macedo Ribeiro[3], Nilanjan Roy[4], Nuno Santarém[1], Joana Tavares[1☯*], Anabela Cordeiro-da-Silva[1,5☯*]

1 Parasite Disease Group, Instituto de Biologia Molecular e Celular da Universidade do Porto, Porto, Portugal, **2** Zentrum für Molekulare Biologie der Universität Heidelberg, DKFZ-ZMBH Alliance, Heidelberg, Germany, **3** Protein Crystallography Group, Instituto de Biologia Molecular e Celular da Universidade do Porto, Porto, Portugal, **4** Ashok and Rita Patel Institute of Integrated Study and Research in Biotechnology and Allied Sciences, New Vallabh Vidyanagar, Gujarat, India, **5** Departamento de Ciências Biológicas, Faculdade de Farmácia da Universidade do Porto, Porto, Portugal

Abstract

Asparagine synthetase (AS) catalyzes the ATP-dependent conversion of aspartate into asparagine using ammonia or glutamine as nitrogen source. There are two distinct types of AS, asparagine synthetase A (AS-A), known as strictly ammonia-dependent, and asparagine synthetase B (AS-B), which can use either ammonia or glutamine. The absence of AS-A in humans, and its presence in trypanosomes, suggested AS-A as a potential drug target that deserved further investigation. We report the presence of functional AS-A in *Trypanosoma cruzi* (*Tc*AS-A) and *Trypanosoma brucei* (*Tb*AS-A): the purified enzymes convert L-aspartate into L-asparagine in the presence of ATP, ammonia and Mg^{2+}. *Tc*AS-A and *Tb*AS-A use preferentially ammonia as a nitrogen donor, but surprisingly, can also use glutamine, a characteristic so far never described for any AS-A. *Tb*AS-A knockdown by RNAi didn't affect *in vitro* growth of bloodstream forms of the parasite. However, growth was significantly impaired when *Tb*AS-A knockdown parasites were cultured in medium with reduced levels of asparagine. As expected, mice infections with induced and non-induced *T. brucei* RNAi clones were similar to those from wild-type parasites. However, when induced *T. brucei* RNAi clones were injected in mice undergoing asparaginase treatment, which depletes blood asparagine, the mice exhibited lower parasitemia and a prolonged survival in comparison to similarly-treated mice infected with control parasites. Our results show that *Tb*AS-A can be important under *in vivo* conditions when asparagine is limiting, but is unlikely to be suitable as a drug target.

Citation: Loureiro I, Faria J, Clayton C, Ribeiro SM, Roy N, et al. (2013) Knockdown of Asparagine Synthetase A Renders *Trypanosoma brucei* Auxotrophic to Asparagine. PLoS Negl Trop Dis 7(12): e2578. doi:10.1371/journal.pntd.0002578

Editor: Alejandro Buschiazzo, Institut Pasteur de Montevideo, Uruguay

Received August 1, 2013; **Accepted** October 25, 2013; **Published** December 5, 2013

Funding: The authors received no specific funding for this study.

Competing Interests: The authors have declared that no competing interests exist.

* E-mail: jtavares@ibmc.up.pt (JT); cordeiro@ibmc.up.pt (ACdS)

☯ These authors contributed equally to this work.

Introduction

Asparagine is a naturally occurring non-essential amino acid found in many proteins. Due to its high nitrogen/carbon ratio, asparagine is likely to be linked to nitrogen homeostasis and protein biosynthesis [1]. AS is the protein involved in asparagine biosynthesis. There are two distinct types of AS, AS-A and AS-B, encoded by *asnA* and *asnB* genes, respectively. AS-A encoding genes have been reported in archaea [2,3], prokaryotes [4–7], and in the protozoan parasite *Leishmania* [8]. The AS-B encoding gene is present in prokaryotes [5,9] and also in eukaryotes, including mammalian cells [10,11], yeasts [12], algae [13], and higher plants [14]. Both types catalyze the ATP-dependent conversion of aspartate into asparagine. While AS-B can use both ammonia and glutamine (reaction B) as amide nitrogen donors [5,15–20], *Escherichia coli* (*E. coli*) AS-A was reported to be dependent strictly on ammonia (reaction A) [21,22].

A) ATP + L-aspartate + $NH4^+$ => AMP + diphosphate + L-asparagine

B) ATP + L-aspartate + L-glutamine [or $NH4^+$] => AMP + diphosphate + L-asparagine + L-glutamate

AS-A and AS-B share no sequence or structural similarities. Their three-dimensional structures provided important information concerning their distinct catalytic mechanisms [2,23–25]. AS-A exists as a dimer where each monomer has a core of eight β-strands flanked by α-helices, resembling the catalytic domain of class II aminoacyl-tRNA synthetases such as aspartyl-tRNA synthetase [24]. AS-A synthesizes asparagine in two steps: the β-carboxylate group of aspartate is first activated by ATP to form an aminoacyl-AMP, followed by amidation by a nucleophilic attack with an ammonium ion [2]. The AS-B enzyme also forms a dimer, but each monomer contains two distinct domains, each of which contains a catalytic site. The N-terminal site catalyzes the conversion of glutamine into glutamic acid and ammonia, while aspartate reacts with ATP in the C-terminal site, generating the intermediate β-aspartyl-AMP [26,27]. Similarly to other glutamine dependent amidotransferases, ammonia released in the N-terminal domain of the enzyme travels through an intramolecular tunnel connecting the active sites, and reacts with the reactive acyladenylate intermediate to produce asparagine [28].

An open reading frame encoding a putative AS-A is present in the genome of the protozoan parasites, *Trypanosoma cruzi* (*T. cruzi*) and *Trypanosoma brucei* (*T. brucei*) [29–31]. *T. cruzi* and *T. brucei* are

Author Summary

The amino acid asparagine is important not only for protein biosynthesis, but also for nitrogen homeostasis. Asparagine synthetase catalyzes the synthesis of this amino acid. There are two forms of asparagine synthetase, A and B. The presence of type A in trypanosomes, and its absence in humans, makes this protein a potential drug target. Trypanosomes are responsible for serious parasitic diseases that rely on limited drug therapeutic options for control. In our study we present a functional characterization of trypanosomes asparagine synthetase A. We describe that *Trypanosoma brucei* and *Trypanosoma cruzi* type A enzymes are able to use either ammonia or glutamine as a nitrogen donor, within the conversion of aspartate into asparagine. Furthermore, we show that asparagine synthetase A knockdown renders *Trypanosoma brucei* auxotrophic to asparagine. Overall, this study demonstrates that interfering with asparagine metabolism represents a way to control parasite growth and infectivity.

transmitted to a mammalian host through an invertebrate vector, and are responsible for Chagas disease and African sleeping sickness, respectively. Disease control is dependent on drug therapy, but treatment options are limited, both by high toxicity and recent emergence of drug resistance [32–34]. Vaccines for *T. brucei* infections are unlikely to be developed not only because of extensive antigenic variation [35], but also because infections compromise host humoral immune competence [36].

Trypanosome AS-A might be a drug target due to the absence of a homologue in humans [8]. AS-A is important in other microorganisms. For example, *asnA* is an essential gene in *Haemophilus influenzae* (DEG10050178) [37], and is strongly up-regulated in *Pasteurella multocida* during host infection [38], and when *Klebsiella aerogenes* is grown in an amino acid-limited but ammonia rich environment [5]. We therefore undertook biochemical and genetic studies of AS-A in trypanosomes to ascertain its biological role and evaluate its potentiality as drug target.

Materials and Methods

Ethics statement

All experiments involving animals were carried out in accordance with the IBMC.INEB Animal Ethics Committees and the Portuguese National Authorities for Animal Health guidelines, according to the statements on the directive 2010/63/EU of the European Parliament and of the Council. IL, JT and ACS have an accreditation for animal research given by the Portuguese Veterinary Direction (Ministerial Directive 1005/92).

Parasite culture

Procyclic and bloodstream forms of *Trypanosoma brucei brucei* Lister 427 were used. Procyclic forms were grown in MEM-Pros medium supplemented with 7.5 μg/ml hemin, 10% fetal calf serum (FCS) and 100 IU/mL of penicillin/streptomycin at 27°C, with cell densities between 5×10^5 cells/ml to $1–2\times10^7$ cells/ml. Bloodstream forms were grown in complete HMI-9 medium (supplemented with 10% FCS and 100 IU/mL of penicillin/streptomycin) [39] in vented tissue culture flasks; these cultures were diluted when cultures reached the cell density of 2×10^6/ml and incubated in a humidified atmosphere of 5% CO2, at 37°C. Bloodstream RNAi cell cultures were supplemented with 7.5 μg/ml hygromycin and 0.2 μg/ml phleomycin.

Cloning of *T. brucei* and *T. cruzi ASA* genes

T. brucei asparagine synthetase A (*TbASA*) and *T. cruzi* asparagine synthetase (*TcASA*) genes were obtained by performing PCR on genomic DNA from *Trypanosoma brucei brucei* TREU927 and *Trypanosoma cruzi* CL Brener Non-Esmeraldo-like. Fragments of the open reading frames of *TbASA* (Tb927.7.1110; chromosome Tb927_07_v4; 28861 to 289067) and *TcASA* (Tc00.1047053503625.10; chromosome TcChr29-P; 687159–688206) were PCR-amplified using a Taq DNA polymerase with proofreading activity (Roche). The sequences of the primers were as follows: sense primer 5′ - CTAATTACATATGGGCGACGACGGTTATTC - 3′ and antisense primer 5′ - CCCAAGCGAATTCTTACAACA-AATTGTGC - 3′, sense primer 5′ - CAAT TTGCATATGACA-TCGGGAGATCC - 3′ and antisense primer 5′ - CCCAAGCA-AGCTTTCACAGCAAGGG - 3′, respectively. PCR conditions were as follows: initial denaturation (2 min at 94°C), 35 cycles of denaturation (30 s at 94°C), annealing (30 s at 45°C) and elongation (2 min at 68°C) for *Tb*AS-A, and annealing (30 s at 50°C) and elongation (2 min at 68°C) for *Tc*AS-A, and a final extension step (10 min at 68°C). The PCR products were isolated from a 1% agarose gel, purified by the Qiaex II protocol (Qiagen), and cloned into a pGEM-T Easy vector (Promega) and sent to Eurofins MWG (Germany) for sequencing.

Expression and purification of poly-His-tagged recombinant *Tb*AS-A and *Tc*AS-A

The *TbASA* and *TcASA* genes were subcloned into pET28a(+) expression vector (Novagen). The recombinant 6-His-tagged proteins were expressed in *E. coli* BL21DE3 by induction of log-phase cultures with 0.5 mM IPTG (NZYTech) for 3 h at 37°C (*Tc*AS-A) and at 18°C, overnight (O/N) (*Tb*AS-A). Bacteria were harvested and resuspended in buffer A [0.5 M NaCl (Sigma), 20 mM Tris.HCl (Sigma), pH 7.6]. The sample was sonicated and centrifuged to obtain the bacterial crude extract. The recombinant proteins were purified using Ni^{2+} resin (ProBond) and washing and elution with increasing levels (25 mM to 1 M) of imidazole (Sigma). The presence and purity of the recombinant protein in the several fractions was determined by SDS-PAGE and Coomassie staining. Dialysis was performed against PBS [137 mM NaCl (Sigma), 2.7 mM KCl (Sigma), 10 mM $Na_2HPO_4.2H_2O$ (Riedel-de Haën), 2 mM KH_2PO_4 (Riedel-de Haën) pH 7.4].

To generate rat and rabbit polyclonal antibodies against *Tb*AS-A, each animal was first immunized with 150 μg of recombinant *Tb*AS-A protein. After 2 weeks, 4 boosts with 100 μg of recombinant *Tb*AS-A were given weekly. The collected blood samples were centrifuged to obtain the serum.

Protein extracts and western blot analysis

Extracts were obtained in RIPA buffer [(20 mM Tris-HCl (Sigma) (pH 7.5), 150 mM NaCl (Sigma), 1 mM Na_2EDTA (Sigma), 1 mM EGTA (Sigma), 1% Nonidet P-40 (Sigma), 1% sodium deoxycholate (Sigma), 2.5 mM sodium pyrophosphate (Sigma), 1 mM β-glycerophosphate (Sigma), 1 mM Na_3VO_4 (Sigma)], with freshly-added complete protease inhibitor cocktail (Roche Applied Science). The total protein amount was quantified using Biorad Commercial Kit (Reagents A, B and S) and the samples were then kept at −80°C. For analysis of parasites from mice, trypanosomes were purified from mouse blood using a DE-52 (Whatman) column [40].

For Western blotting, 2 μg of recombinant *Tb*AS-A and *Tc*AS-A proteins, 10 μg of total soluble cell extract, or 1×10^7 parasites, were resolved in SDS/PAGE and transferred on to a nitrocellulose

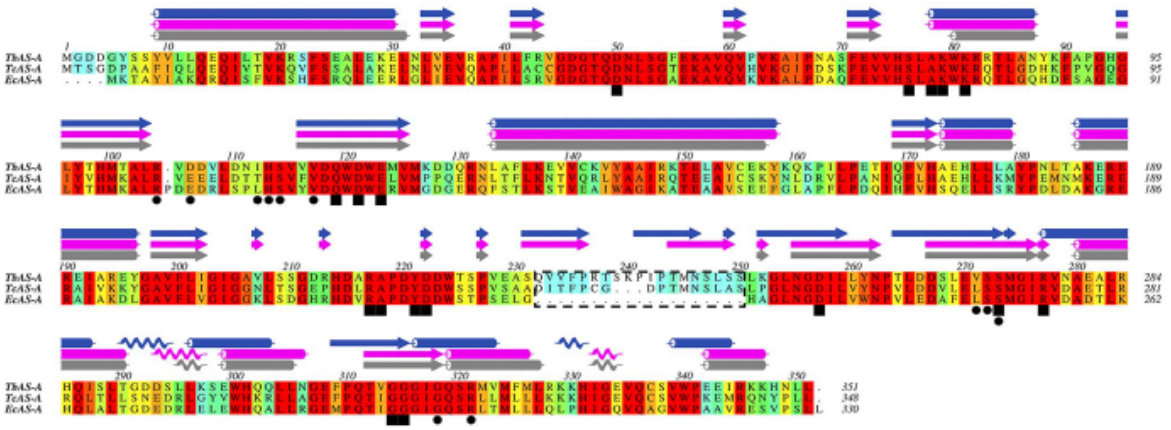

Figure 1. Multiple-sequence alignment of AS-A protein. Alignment of type A asparagine synthetase from *T. brucei* (NCBI-GeneID:3658321/Tb927.7.1110), *T. cruzi* (NCBI-GeneID:3534325/Tc00.1047053503625.10) and *E. coli* (NCBI-GeneID:948258/pdb:12AS). The residues are colored according to ALSCRIPT Calcons (Aline version 011208) using a predefined colour scheme (red: identical residues; orange to blue: scale of conservation of amino acid properties in each alignment column; white: dissimilar residues). Secondary structure elements of *Ec*AS-A crystal structure (grey) and of *Tc*AS-A (purple) and of *Tb*AS-A (blue) homology models are depicted above the alignment. In all protein sequences, asparagine (squares) and AMP binding residues (circles) were identified. The dashed box indicates a structurally divergent region.
doi:10.1371/journal.pntd.0002578.g001

Hy-bond ECL membrane (Amersham Biosciences). The membrane was blocked in 5% (w/v) non-fat dried skimmed milk in PBS/0.1% Tween-20 (blocking solution), followed by incubation with an anti-His-tag rabbit antibody (MicroMol-413) (1:5000) or a combination of an anti-*Tb*AS-A rabbit antibody (1:1000) with an anti-aldolase rabbit antibody (1:5000) in blocking solution at 4°C O/N, respectively. Blots were washed with PBS/0.1% Tween-20 (3×15 min). Horseradish peroxidase-conjugated goat anti-rabbit IgG (Amersham) (1:5000 for 1 h, at room temperature) in blocking buffer was used as the secondary antibody. The membranes were developed using SuperSignal WestPico Chemiluminescent Substrate (Pierce). ImageJ software (version 1.43u) was used for protein bands semi-quantification.

Enzyme assays

AS activity was assessed by quantification of asparagine formation [41]. The reactions were performed in a total of 150 µl of enzyme assay mixture in 85 mM Tris-HCl (Sigma) containing aspartate (Sigma), ammonia (Sigma), ATP (Sigma) and 8.4 mM Mg^{2+} (Sigma). Following incubation for set times at 37°C, enzymatic reactions were terminated by boiling 4 min, and then centrifuged at maximum speed for 30 s. 100 µl of the reaction mixture supernatant was added to 900 µl of ninhydrin 0.05% in ethanol. The resulting mixtures were boiled at 100°C for 5 min, then centrifuged for 30 s and maintained on ice. 300 µl of clear supernatant fluids were transferred to 96-well plates, and the absorbance at 340 nm determined [41]. Based on reaction linearity studies, 7.5 µg of enzyme and 15 min incubation at 37°C were selected as final conditions. To determine K_ms, the concentrations of substrates were varied in the following ranges: 1.25–20 mM (aspartate), 0.78–50 mM (ammonia) and 0.62–10 mM (ATP), while the remaining substrates concentrations were in excess ([aspartate] >20 mM, [ATP] >10 mM, and [ammonia] >50 mM). K_m for glutamine was determined using a concentration range of 1.5625–25 mM, while ATP and aspartate were maintained in excess. Measurements were performed in triplicate, and the initial rate was analyzed to obtain values of V_{max} and K_m by curve fitting using GraphPad Prism (5.0 version).

Using a query based on L-cysteine-S-sulfinic acid inhibitor [42], the ZINC database was screened using the program ROCS (version 2.3.1) to find compounds that have good shape similarity (measured by 3D Tanimoto) and similar functional group overlap to the query molecule. L-cysteine-S-sulfate (Sigma; PubChem Substance ID 24892471) was used under the following conditions: 2.5 mM aspartate, 1.25 mM ATP, 12.5 mM ammonia, and 8.4 mM Mg^{2+}. The characterization of the mechanism of inhibition consisted in the determination of K_m and V_{max} for each substrate, in the presence of four inhibitor concentrations (0.025, 0.050, 0.1 and 0.2 mM). The following substrate concentration ranges 1.25–10 and 1.25–50 mM were used for aspartate and ammonia, respectively, while to determine K_m for ATP, a range from 0.625 to 10 mM (*Tb*AS-A) or from 0.3125 to 5 mM (*Tc*AS-A) was assayed. K_i was determined by "$K_{m\ app}$ Method"[43].

AS-A protein alignments and *Tb*AS-A/*Tc*AS-A homology models

*Ec*AS-A, *Tb*AS-A and *Tc*AS-A protein alignments were performed using ClustalW [44]. Aline, Version 011208 [45], was used for editing protein sequence alignments and preparing Fig. 1. *Tb*AS-A and *Tc*AS-A homology models were obtained with SWISS-MODEL, using *Ec*AS-A crystal structure (Protein Data Bank (PDB) accession code 12AS [24]) as a template (percentage of sequence identity of 56% and 57%, respectively) [46–48]. The 3D structures were rendered in PyMOL (The PyMOL Molecular Graphics System, Version 1.3, Schrödinger, LLC).

Generation of *Tb*AS-A RNAi cell lines

The "stuffer strategy" was used to generate RNAi-mediated AS-A depletion. First, the *TbASA* fragment (amplified with a sense oligo with a BglII – SphI linker 5′ - GAGAAGATCTGCA-TGCGCGACGACGGTTATTCGTCATAC - 3′, and an anti-sense oligo with a EcoRI – SalI 5′ – CGGAATTCGTCGA-CACTCCGTTTTTCGGATTGCGGC – 3′) was cloned twice in opposite direction on either sides of a 'stuffer' fragment of the pHD1144 vector (also digested with SphI and SalI) (Fig. S1A). The

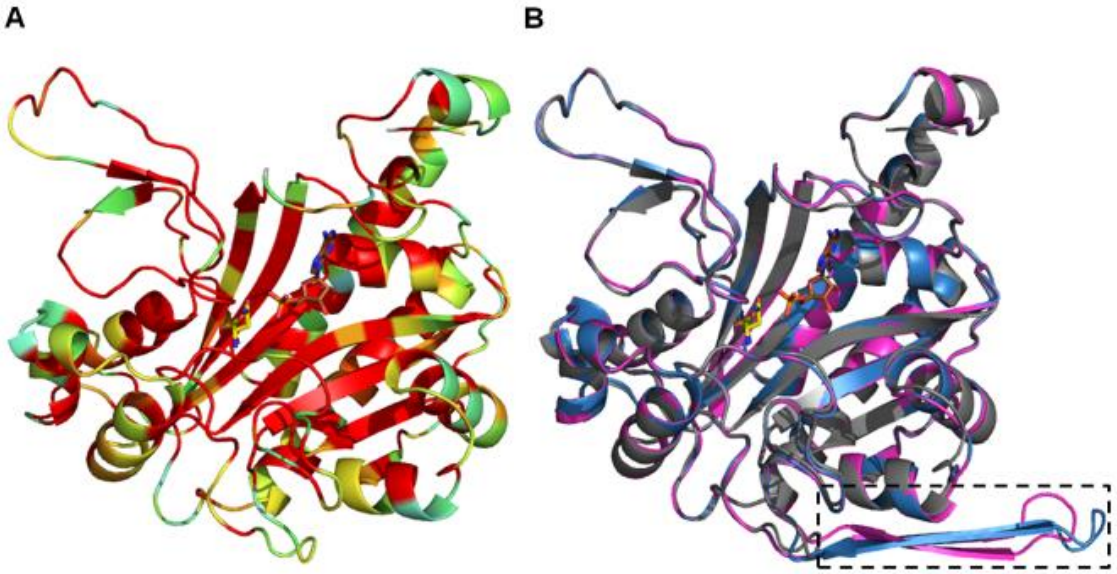

Figure 2. Homology models of AS-A from trypanosomes. (A) Ribbon representation of *Ec*AS-A colored according to the sequence similarity with *Tb*AS-A and *Tc*AS-A as shown in Fig. 1. (B) Superposition of *Ec*AS-A structure (grey) (PDB accession code 12AS), with *Tb*AS-A (blue) and *Tc*AS-A (purple) homology models (obtained from the SWISS-MODEL server, using PDB 12AS as a template). A small structurally divergent region is marked by a dashed rectangle. Ligand color schemes: asparagine is shown in yellow (oxygen, red; nitrogen blue) and AMP is shown in brown (oxygen, red; nitrogen blue; phosphorous orange).
doi:10.1371/journal.pntd.0002578.g002

resulting [(target)-stuffer-(reverse-complement target)] construct obtained through HindIII and BglII digestion, which generates a stem-loop RNA, was cloned into pHD1145 (also digested with HindIII and BglII) (Fig. S1B). The final construct was linearized with NotI and 10 µg of DNA was transfected into 2×10^7/ml bloodstream form cell line carrying pHD1313 plasmid (contains two copies of the tet repressor and a phleomycin resistance cassette) by electroporation using Amaxa Basic Parasite Nucleofector Kit (Lonza). Transcription occurs on induction with tetracycline (100 ng/ml), hence producing mRNA homologs to the target the gene. Stable individual clones were selected 5 to 7 days after transfection with 7.5 µg/ml of hygromycin.

In vitro analysis of *Tb*AS-A RNAi

To analyse growth, *T. brucei* RNAi cell line and cells expressing the tet repressor only (wt), were seeded at 2×10^5 cells/ml of complete HMI9 medium, in the presence and absence of tetracycline. Cell growth was monitored microscopically on a haemocytometer (Marienfeld) and the culture diluted back to 2×10^5 cells/ml daily. The same protocol was repeated in complete HMI9 medium with basal IMDM without asparagine, complete HMI9 medium with basal IMDM without asparagine supplemented with 6.7×10^4 nM of asparagine (levels found in human plasma [49]), and complete HMI9 medium with basal IMDM without asparagine supplemented with 1.67×10^5 nM of asparagine (levels found in normal medium).

In vivo analysis of *Tb*AS-A RNAi

Wild-type and transgenic bloodstream *T. brucei* parasites were cultured in the absence of selecting drugs (hygromycin and phleomycin) for 24 h, then tetracycline was added. After a further 48 h, parasites were inoculated in mice. For each experiment, 4 groups of BALB/c mice (6–8 weeks old, n = 4) (Harlan Laboratories, United Kingdom) were infected by intraperitoneal injection of 10^4 *T. brucei* bloodstream forms. 2 groups were injected with wt strain (with or without tetracycline) and the other 2 groups were injected with RNAi cell line (with or without tetracycline). 48 h prior infection the 2 RNAi induced groups were given doxycycline (treated with 1 mg/ml doxycycline hyclate and 5% sucrose containing water). The 2 non-induced groups were given standard water. To evaluate the virulence of RNAi induced parasites in mice with reduced plasmatic levels of asparagine, animals were treated with 50 IU of *E. coli* L- asparaginase (ProSpec-Tany TechnoGene) 48 h before injection and every 48 h. According to the literature, L-asparagine could not be detected in the blood 48 h following an intravenous injection of *E. coli* L-asparaginase, at a dose of 50 IU/mouse [50]. Mice were monitored every day for general appearance and behaviour. Parasitemia was monitored daily from the fifth day post-infection, using tail-vein blood, in a haematocytometer under a microscope. Animals with a parasitemia greater than 10^8 parasites/ml were euthanized, as previous studies had established that these levels were consistently lethal within the next 24 h.

Immunofluorescence

T. brucei bloodstream forms from log-phase cultures, with or without RNAi, were fixed in µ-Chamber 12 well (Ibidi) for 15 min, at room temperature, in PBS containing 3% p-formaldehyde, washed twice with PBS, and then permeabilized in PBS containing 0.1% of Triton X-100. Fixed cells were incubated for 60 min in PBS containing 10% FCS at room temperature (RT), in a humidified atmosphere, then washed twice with PBS/2% FCS. Cells were then incubated with primary rat or rabbit polyclonal antibody against *Tb*AS-A (1:100 and 1:5000 respectively, both

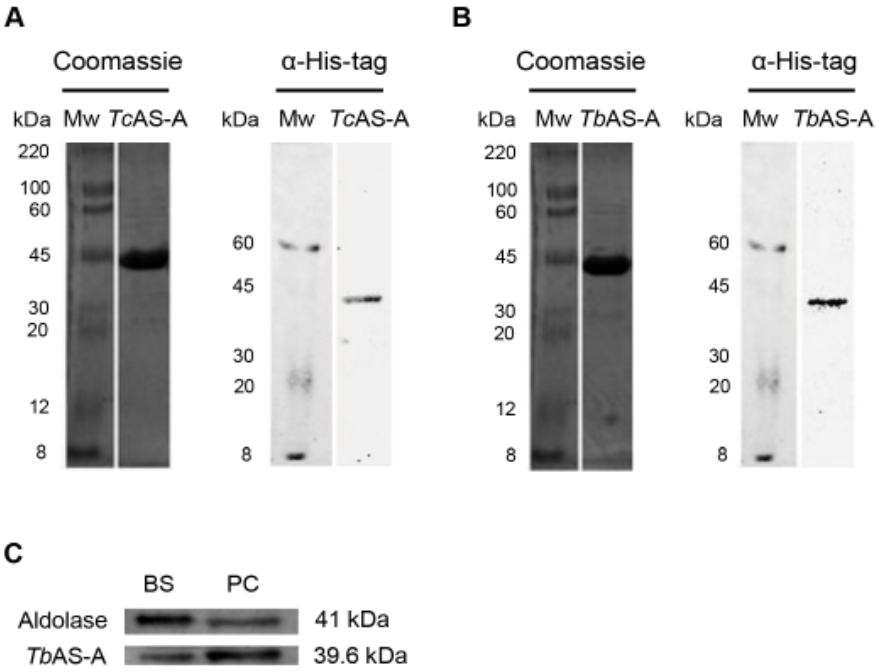

Figure 3. Analysis of purified recombinant *Tc*AS-A/*Tb*AS-A and of AS-A expression within *T. brucei* life cycle stages. Purified *Tc*AS-A (A) and *Tb*AS-A (B) recombinant proteins were analyzed using 12% SDS-PAGE and visualized using Coomassie blue staining. MW, molecular weight marker. Rabbit anti-histidine monoclonal antibody (1:1000) was used in immunoblotting assays with the *Tc*AS-A (A) and *Tb*AS-A (B) purified recombinant proteins. (C) AS-A expression within *T. brucei* life-cycle stages: 10 µg of protein from BS (bloodstream forms) and PC (procyclic forms) lysates were analysed by Western blot. Aldolase was used as a loading control. Rabbit anti-*Tb*AS-A and anti-aldolase polyclonal antibodies were used for protein detection. The results are representative of three independent experiments.
doi:10.1371/journal.pntd.0002578.g003

diluted in blocking solution) overnight at 4°C, followed by two washes with PBS/2% FCS. Subsequently, cells were incubated with Alexa Fluor 647 conjugated goat anti-rat or Alexa Fluor 488 conjugated goat anti-rabbit secondary antibodies (Molecular probes from Life technologies) (1:500 diluted in blocking solution) for 1 h at RT in an humidified atmosphere, then washed twice with PBS. Next, the slides were stained and mounted with Vectashield-DAPI (Vector Laboratories, Inc.). Images were captured using fluorescence microscope AxioImager Z1 and software Axiovision 4.7 (Carl Zeiss, Germany). Pseudo-coloring of images was carried out using ImageJ software (version 1.43u).

In case of *Tb*AS-A immunolocalization, *T. brucei* wt bloodstream forms cells were co-stained using rat anti-*Tb*AS-A antibody (1:100 diluted in blocking solution), rabbit anti-aldolase antibody (1:5000 diluted in blocking solution), anti-BiP antibody (kindly provided by Dr. Jay Bangs, 1:500 diluted in blocking solution), anti-enolase antibody (kindly provided by Dr. Paul Michels, 1:5000 diluted in blocking solution) or anti-GRASP antibody (kindly provided by Dr. Graham Warren, 1:200 diluted in blocking solution). Alexa Fluor 647 conjugated goat anti-rat (1:500) and Alexa Fluor 488 conjugated goat anti-rabbit (1:500) were used as secondary antibodies. Staining with MitoTracker Orange (Invitrogen) followed by Alexa Fluor 488 conjugated goat anti-rabbit (1:500),

Table 1. *Tb*AS-A and *Tc*AS-A kinetic parameters for aspartate, ATP and ammonia.

Species	Substrate	K_m (mM)	$V_{max} \times 10^{-3}$ (mM.s^{-1})	k_{cat} (s^{-1})	k_{cat}/K_m (M^{-1}.s^{-1})
T. brucei	Aspartate	5.39±0.31	6.72±0.14	5.31±0.11	9.85×10^{2}
	ATP	1.80±0.32	7.88±0.48	6.22±0.38	3.46×10^{3}
	Ammonia	5.55±0.41	7.21±0.16	5.69±0.13	1.03×10^{3}
T. cruzi	Aspartate	6.45±2.05	3.09±0.40	2.41±0.32	3.74×10^{2}
	ATP	0.72±0.01	4.42±0.02	3.45±0.02	4.79×10^{3}
	Ammonia	7.75±1.55	3.14±0.21	2.45±0.17	3.16×10^{2}

The values are the means ± standard deviation obtained from 3 independent experiments.
doi:10.1371/journal.pntd.0002578.t001

Table 2. *Tb*AS-A and *Tc*AS-A kinetic parameters for glutamine.

Species	K_m(mM)	$V_{max} \times 10^{-3}$ (mM.s^{-1})	k_{cat}(s^{-1})	k_{cat}/K_m (M^{-1}.s^{-1})
T. brucei	8.20±1.70	7.06±0.61	5.58±0.48	6.80×10^2
T. cruzi	15.33±3.66	4.33±0.53	3.38±0.41	2.20×10^2

The values are the means ± standard deviation obtained from 3 independent experiments.
doi:10.1371/journal.pntd.0002578.t002

as a secondary antibody. The labelling of parasites with MitoTracker was done by adding 250 nM to the cell culture medium (without FCS) for 30 minutes, prior to washing, fixing and staining using the protocol described above. Images were captured using the confocal microscope Leica TCS SP5II and LAS 2.6 software (Leica Microsystems, Germany). Again, image analysis was done using ImageJ version 1.43U software.

Digitonin permeabilization

For each sample condition, 1.0×10^7 bloodstream cells were washed once with cold trypanosome homogenization buffer (THB), containing 25 mM Tris (Sigma), 1 mM EDTA (Sigma) and 10% sucrose (Sigma), pH = 7.8. Just before cell lysis, leupeptin (Sigma) (final concentration of 2 µg/ml) and different digitonin (Calbiochem) quantities (final concentrations of 5, 12.5, 25, 50, 100, 150 and 200 ug/ml) were added to 500 µl of cold THB, for cell pellet resuspension. Untreated cells (0 µg/ml of digitonin) and those completely permeabilized (total release, the result of incubation in 0.5% Triton X-100) were used as controls. Each sample was incubated 60 min on ice, and then centrifuged at 2000 rpm, 4°C, for 10 min. Supernatants were transferred to new chilled tubes and 500 µl of cold THB was added to each pellet and then mixed. All fractions were analysed through Western blot as described above.

Cell cycle analysis

T. brucei bloodstream forms were analyzed by flow cytometry for DNA content following RNAi induction. Cells were collected by centrifugation and washed twice with PBS containing 2% FCS. Each 2×10^6 cells were resuspended in 1 mL of PBS/2% FCS and 3 mL of cold absolute ethanol was added while vortexing. Cells were fixed for 1 hour at 4°C and then washed twice in PBS. 1 mL of staining solution [3.8 mM sodium citrate dehydrate (Sigma), 50 µg/mL propidium iodide (Sigma), 0.5 µg/µL RNAse A (Sigma) in PBS] was added to the cell pellets and vortex. Samples were analysed by FACS (Becton Dickinson) after a incubation at 4°C for 30 min. Data was analyzed by FlowJo software (Ashland, OR).

Statistical analysis

One-way ANOVA and two-tailed Student's test were used for statistical analysis. Statistical analysis was performed using GraphPad Prism Software (version 5.0), and p values≤0.01 were considered to be statistically significant. Asterisks indicate statistically significant differences (*** $p\leq0.001$, ** $p\leq0.01$).

Results

Conservation of AS-A in trypanosomes

One open reading frame that code for a putative AS-A is present in the genomes of *T. cruzi* CL Brener Non-Esmeraldo-like and *T. brucei* TREU927 (http://tritrypdb.org) [29–31]. A protein multiple sequence alignment, performed using ClustalW [44], of AS-A from *T. brucei* (Tb927.7.1110, NCBI-GeneID:3658321), *T. cruzi* (Tc00.1047053503625.10, NCBI-GeneID:3534325) and *E. coli* (NCBI-GeneID:948258) is shown in Figure 1. The amino acid residues known to be involved in the active-site formation in *E. coli* [24] are highly conserved within the three sequences (Fig. 1). Protein alignments demonstrated 58% similarity for *Ec*AS-A *versus* *Tb*AS-A, 60% for *Ec*AS-A *versus* *Tc*AS-A, and 63% for *Tb*AS-A *versus* *Tc*AS-A.

Like *Ec*AS-A, *Tb*AS-A and *Tc*AS are predicted to be dimeric, as seen from superimposed homology models with the *Ec*AS-A crystal structure [24] (Fig. 2A). The only structurally divergent region (area marked by dashed rectangle) (Fig. 1, 2B), is present in both *Tb*AS-A (from residues Q232 to S250) and *Tc*AS-A (from residues D232 to S247), but absent in *Ec*AS-A. This region is distant from the enzyme active site and the dimer interface and its functional and structural significance are unknown. The amino acids involved in asparagine binding are all strictly conserved, while in the AMP binding pocket, the majority of the residues are conserved, except for three residues (Fig. 1). In *Ec*AS-A, E103 (D106 and E106 in *Tb*AS-A and *Tc*AS-A, respectively) and L109 (I112 and T112 in *Tb*AS-A and *Tc*AS-A, respectively) (Fig. 1) are not directly involved in polar interactions with the nucleotide base, but form part of the outer wall of the binding site [24]. The main chain of L249 in *Ec*AS-A (V271 and L268 in *Tb*AS-A and *Tc*AS-A, respectively) is directly involved in hydrogen bonds with ribose from AMP, however the different side chains of leucine and valine do not affect the shape of AMP binding site.

Trypanosome AS-A catalyze asparagine synthesis using either ammonia or glutamine as nitrogen donors

*Tb*AS-A and *Tc*AS-A coding sequences were cloned into the bacterial expression vector pET28a. Histidine-tagged fusion proteins were purified under non-denaturing conditions (Fig. 3A, B). As expected, the recombinant proteins were recognized by anti-His Tag monoclonal antibody (Fig. 3A, B). Rabbit polyclonal antibodies produced against recombinant *Tb*AS-A recognized the protein in total extracts from two different parasite developmental stages, bloodstream forms (mammalian host parasite stage) and procyclic forms (insect vector parasite stage) (Fig. 3C).

The capacities of *Tb*AS-A and *Tc*AS-A to produce asparagine from aspartate in the presence of ATP, ammonia and Mg^{2+} were determined using a specific quantitative colorimetric assay for L-asparagine [41]. The pH optimum was 7.6, with detectable activity from 6.0 to 9.0 (data not shown). Mg^{2+} was an essential co-factor for *Tb*AS-A and *Tc*AS-A (data not shown), as previously described for *Ec*AS-A [22]. We included 8.4 mM Mg^{2+} in the final reaction mixture. Lower concentrations (2, 4 and 6 mM) gave lower activity while increased concentrations (up to 16 mM) resulted in no substantial activity improvement (data not shown). *Tb*AS-A and *Tc*AS-A showed similar K_ms for aspartate and ammonia ($p>0.01$), while *Tc*AS-A showed higher K_m for ATP than *Tb*AS-A ($p=0.0042$) (Table 1). ATP is the substrate required for the generation of the β-aspartyl adenylate intermediate, which reacts with ammonia, releasing asparagine. In its absence, the reaction did not occur (data not shown). To our surprise, both *Tb*AS-A and *Tc*AS-A could also use glutamine as a nitrogen donor (Table 2). *Tb*AS-A showed higher K_m for this nitrogen donor than *Tc*AS-A, however not statistically significant ($p>0.01$). Both enzymes present higher K_m values for ammonia than for glutamine, but these differences were not statistically significant ($p>0.01$) (Table 1 and 2). *Tb*AS-A had a higher V_{max} than *Tc*AS-A, for both ammonia ($p<0.0001$) and glutamine ($p=0.0043$) dependent-activities (Table 1 and 2). *Tb*AS-A had similar catalytic

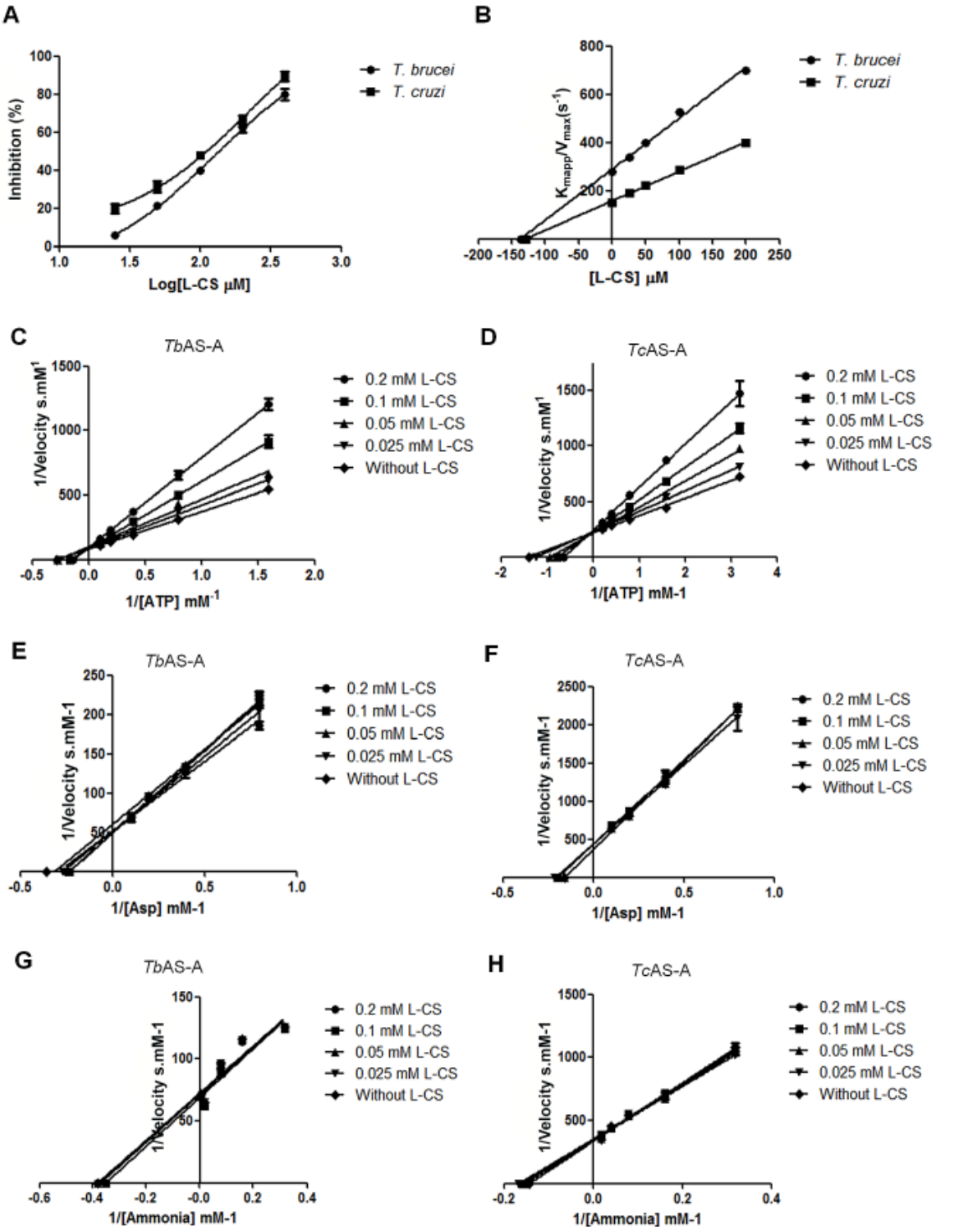
A
Inhibition (%)
Log[L-CS µM]
T. brucei
T. cruzi
B
$K_{mapp}/V_{max}(s^{-1})$
[L-CS] µM
T. brucei
T. cruzi
C
TbAS-A
1/Velocity s.mM-1
1/[ATP] mM-1
0.2 mM L-CS
0.1 mM L-CS
0.05 mM L-CS
0.025 mM L-CS
Without L-CS
D
TcAS-A
1/Velocity s.mM-1
1/[ATP] mM-1
0.2 mM L-CS
0.1 mM L-CS
0.05 mM L-CS
0.025 mM L-CS
Without L-CS
E
TbAS-A
1/Velocity s.mM-1
1/[Asp] mM-1
0.2 mM L-CS
0.1 mM L-CS
0.05 mM L-CS
0.025 mM L-CS
Without L-CS
F
TcAS-A
1/Velocity s.mM-1
1/[Asp] mM-1
0.2 mM L-CS
0.1 mM L-CS
0.05 mM L-CS
0.025 mM L-CS
Without L-CS
G
TbAS-A
1/Velocity s.mM-1
1/[Ammonia] mM-1
0.2 mM L-CS
0.1 mM L-CS
0.05 mM L-CS
0.025 mM L-CS
Without L-CS
H
TcAS-A
1/Velocity s.mM-1
1/[Ammonia] mM-1
0.2 mM L-CS
0.1 mM L-CS
0.05 mM L-CS
0.025 mM L-CS
Without L-CS

Figure 4. ***T. brucei*** **and** ***T. cruzi*** **AS-A** ***in vitro*** **inhibition.** (A) Inhibition (%) of *T. brucei* and *T.cruzi* AS-A activity by L-cysteine-S-sulfate (L-CS). (B) Plot of K_{mapp}/V_{max} *versus* L-CS concentration was established; K_i corresponds to the symmetric value of the X-axis intersection. (C-H) Plots showing the effect of different L-CS concentrations on the inverse of the initial velocity *versus* the inverse of several concentrations of ATP, aspartate or ammonia for *Tb*AS-A (C, E and G, respectively) and *Tc*AS-A (D, F and H, respectively) enzymes. Error bars indicate standard deviation of the means of two replicates and data shown are representative of three independent experiments.
doi:10.1371/journal.pntd.0002578.g004

rates for both glutamine and ammonia-dependent activities ($p>0.01$), whereas *Tc*AS-A presented a slightly higher, but not statistically significant, rate for glutamine-dependent activity ($p>0.01$) (Table 1 and 2). The high conservation of the active sites and the small amino acid differences identified in the homology models do not allow an accurate structural interpretation of the small differences observed. Indeed, these might have been due to slight differences in the proportion of protein that was correctly folded.

L-cysteine-S-sulfate, considered a putative AS-A inhibitor from a virtual screening, inhibited both enzymes, with IC_{50}s of 126 and 100 µM for *Tb*AS-A and *Tc*AS-A, respectively (Fig. 4A). For both enzymes, the kinetic characteristics suggested competition with ATP binding (Fig. 4C, D). No changes in the K_ms and V_{max}s for aspartate and ammonia were observed ($p>0.01$) (Fig. 4E, F, G, H), suggesting the inhibition is exclusively due to ATP binding interference ($p\leq0.01$) . K_i values of 137 and 128.9 µM were determined for *Tb*AS-A and *Tc*AS-A, respectively (Fig. 4B).

AS-A localizes in the cytosol of *T. brucei* bloodstream forms

The subcellular localization of *Tb*AS-A was determined by immunofluorescence and digitonin fractionation in bloodstream forms. As expected, induction of RNAi resulted in a decrease in the fluorescence intensity (Fig. S2A, B, C). *Tb*AS-A is in the cytosol, as revealed by colocalization with the cytosolic enzyme enolase [51] (Fig. 5A) and no colocalization with aldolase, BiP, GRASP or mitotracker (Fig. S3), markers for glycosomes [52],

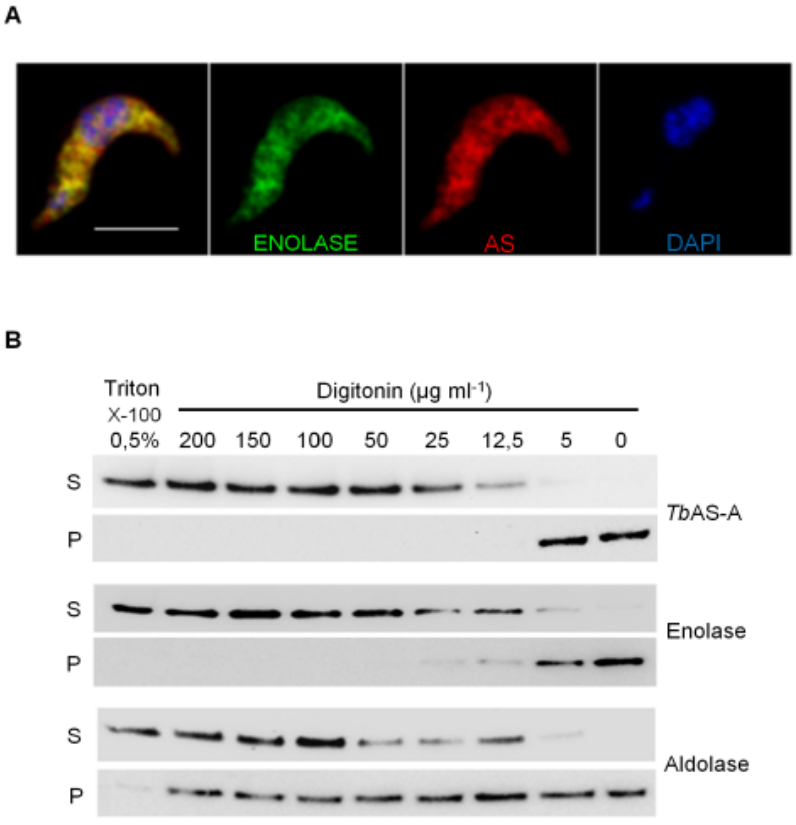

Figure 5. AS-A subcellular localization in ***T. brucei*** **bloodstream forms.** (A) Immunofluorescence analysis by confocal microscopy of *Tb*AS-A (red) and enolase (green) in bloodstream forms. DAPI locate nuclear and kinetoplast mitochondrial DNA (blue). Bar, 5 µm. Images are maximal Z-projections of 50 contiguous stacks separated by 0.1 µm. (B) For digitonin permeabilization, selected supernatant (S) and pellet (P) fractions obtained at different digitonin concentrations were subjected to Western-blot analysis and probed with rabbit antisera raised against *Tb*AS-A, enolase (cytoplasmic marker) and aldolase (glycosome marker). Data shown is representative of two independent experiments. Untreated cells (0 µg/ml of digitonin) and those completely permeabilized in Triton X-100 0.5% were used as controls.
doi:10.1371/journal.pntd.0002578.g005

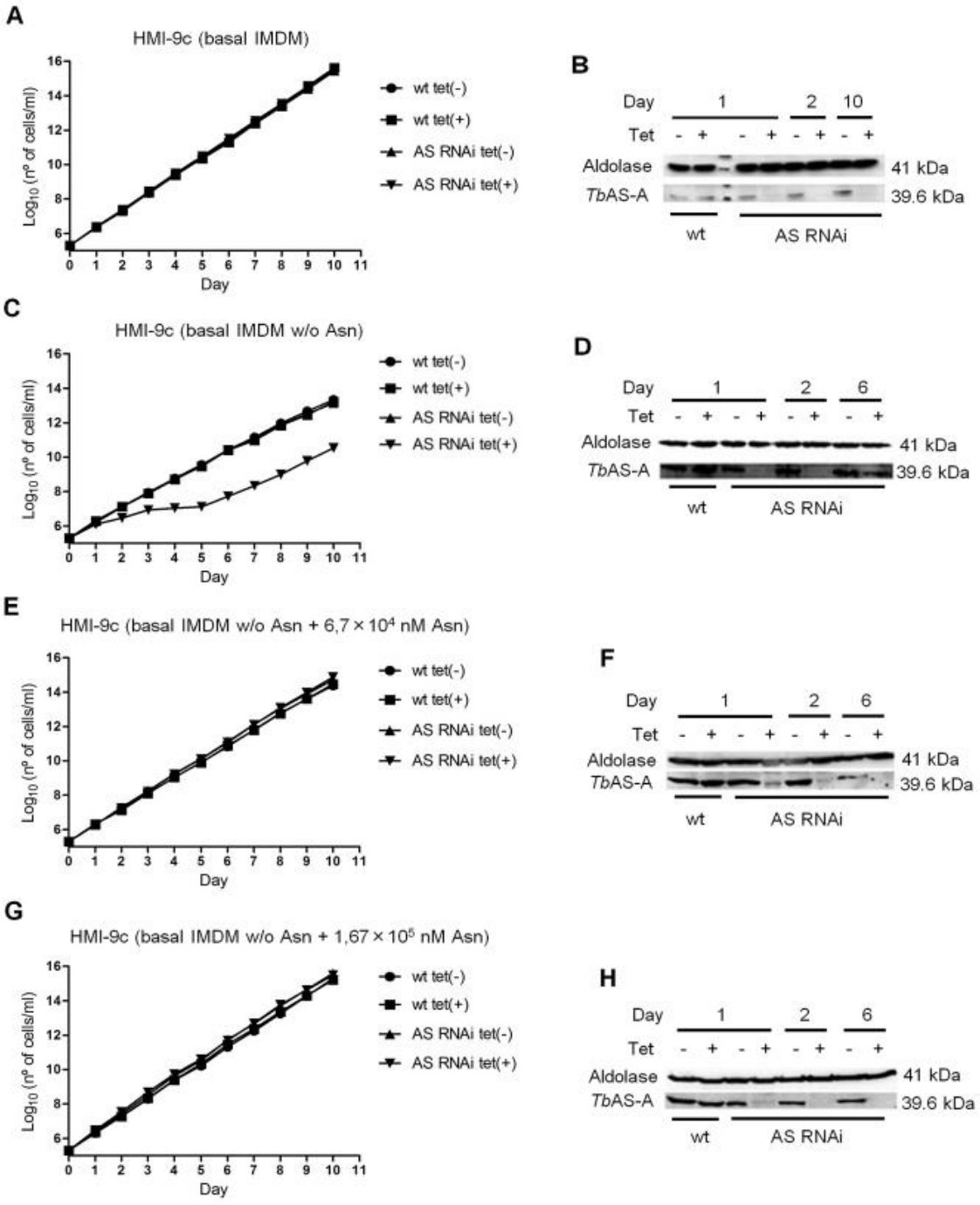

Figure 6. ***In vitro*** **effect of RNAi-mediated AS-A down-regulation in** ***T. brucei*** **bloodstream forms.** Growth curve of a wt *versus* a representative AS RNAi cell line were performed in unmodified medium [complete HMI-9 (HMI-9c) with basal IMDM] (A), modified medium [HMI-9c with basal medium without asparagine - HMI-9c (basal IMDM w/o Asn)] (C), modified medium supplemented with 6.7×10^4 nM of asparagine [HMI-9c (basal IMDM w/o Asn + 6.7×10^4 nM Asn)] (E), modified medium supplemented with 1.67×10^5 nM of asparagine [HMI-9c (basal IMDM w/o Asn + 1.67×10^5 nM Asn)] (G). Circles and squares represent wild-type growth in the absence or presence of tetracycline, respectively, while up triangles and down triangles represent clones growth in the absence or presence of tetracycline, respectively. Cumulative cell numbers are plotted as the product

of cell number and total dilution. Error bars indicate standard deviation. The effect of RNAi on the AS-A protein levels was analyzed by Western blots with extracts of noninduced tet(−), and RNAi-induced tet(+) cells, isolated from unmodified medium (B), modified medium (complete HMI-9 medium with basal IMDM without asparagine) (D), modified medium supplemented with 6.7×10^4 nM of asparagine (F), modified medium supplemented with 1.67×10^5 nM of asparagine (H). Cells were collected at day 1, 2, 6 and 10 of RNAi induction. Results are representative of three independent experiments.
doi:10.1371/journal.pntd.0002578.g006

endoplasmic reticulum [53], Golgi and mitochondria compartments [54], respectively. Controls performed with rat or rabbit pre-immune sera and secondary antibody alone, showed no detectable signal (data not shown). Digitonin fractionation also resulted in similar profiles for AS-A and enolase (cytosolic marker) and no similarity to aldolase (glycosomes marker) (Fig. 5B).

AS-A knockdown makes *T. brucei* bloodstream forms dependent on extracellular asparagine

To study the biological role of AS-A in *T. brucei* bloodstream forms, cells were stably transfected with an RNA interference plasmid construct. RNAi against asparagine synthetase A was induced in normal medium (complete HMI-9) by adding tetracycline. No difference was observed in cell proliferation between induced and non-induced cells (Fig. 6A), although AS-A protein was reduced to ≈13% of the normal level within 48 hours (Fig. 6B). When, however, the AS-A-depleted cells were grown in HMI-9 medium with only the asparagine from the fetal calf serum, growth was impaired, with an increase in the proportion of cells in G0/G1 (Fig. 6C and 7B, C). Presumably the asparagine from the serum allowed this slower growth. Levels of asparagine usually found in human serum (6.7×10^4 nM) [49], which are somewhat lower than in normal medium (1.67×10^5 nM; IMDM - Iscove's modified Dulbecco's basal medium from Gibco Invitrogen), were sufficient to overcome this defect (Fig. 6E, G). In complete HMI-9 medium, with only asparagine from the fetal calf serum, the growth defects of induced RNAi clones are abrogated at day 5 post-induction (Fig. 6C, 7D), and the percentage of cells in GO/G1 and S phases of the cell cycle return to the ones found in non-induced cells (Fig. 7A), suggesting the appearance of RNAi revertants, as is also visible on the Western blot (Fig. 6D). Similar reversion to evade lethal RNAi in trypanosomes has been seen many times before [55]. In the presence of asparagine, low AS-A levels were maintained (Fig. 6B, F and H).

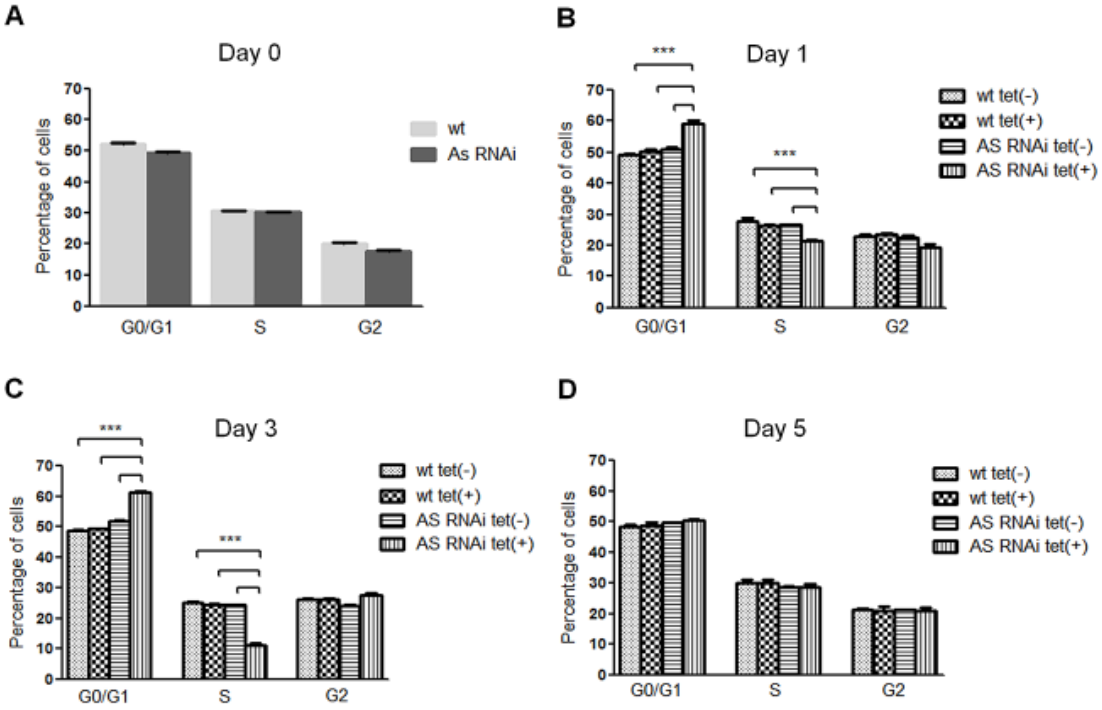

Figure 7. *In vitro* effect of RNAi-mediated AS downregulation on *T. brucei* cell cycle. DNA content of $\approx2\times10^6$ wt and RNAi cell line parasites grown in completed HMI-9 medium with basal IMDM without asparagine, was collected before tetracycline induction, day 0 (A), and at day 1 (B), 3 (C), and 5 (D) post-induction, for cell cycle analysis. Samples were analysed by flow cytometry and the percentage of cells in each phase of the cell cycle were determined using FlowJo software. Each bar represents the average from three replicates. Error bars indicate standard deviation of these measurements. The statistics were calculated by one-way ANOVA (*** $p\leq0.001$ and ** $p\leq0.01$).
doi:10.1371/journal.pntd.0002578.g007

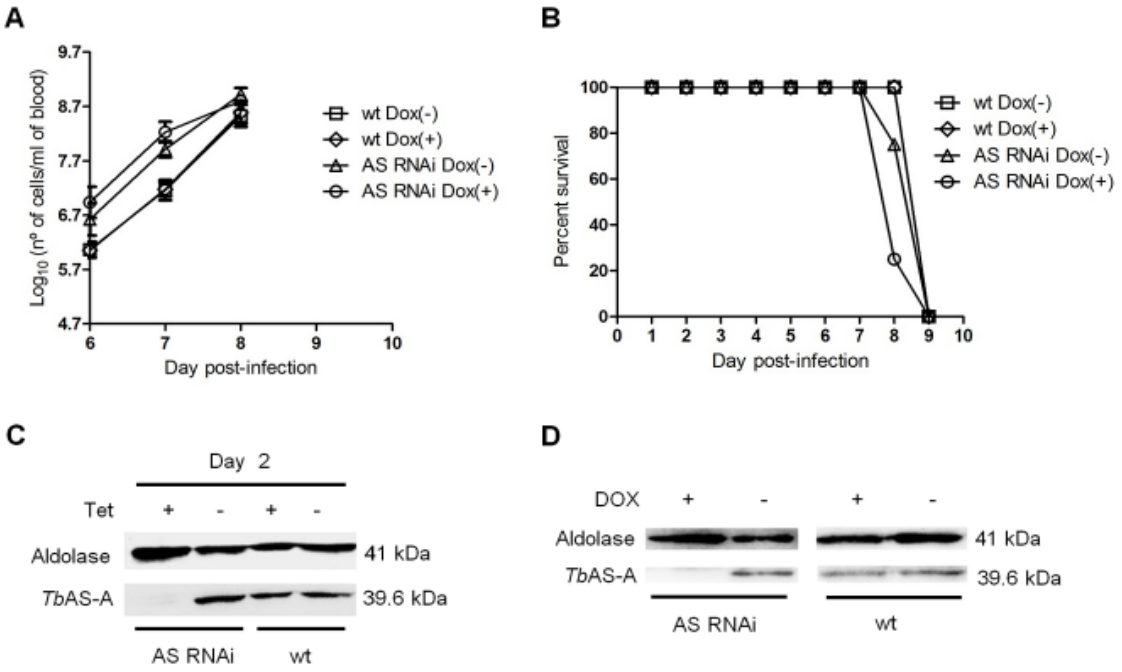

Figure 8. *In vivo* effect of RNAi against *Tb*AS-A. (A) Groups of 4 mice were infected intraperitoneally, with 1×10^4 control wt parental cell line (open squares and open diamonds) or a representative AS RNAi clone (open triangles and open circles). The mice were either untreated (open squares and open triangles) or treated with 1 mg/ml doxycycline (Dox) (open diamonds and open circles) in the water supply. Parasitemia was quantified at the times indicated. Error bars indicate standard deviation of the means of three mice for wt cell lines, and four mice in the case of AS RNAi cell lines. The detection limit for this assay is 5×10^4 trypanosomes per ml of blood. Mice were euthanized when parasitemia reached 1×10^8 cells/ml. (B) Kaplan–Meier survival analysis of mice infected with wt parental cell line and AS RNAi cell line in the absence or presence of doxycycline. Data are representative of three independent experiments. Western blot analysis of the AS-A levels in trypanosomes injected in mice, after 48 h of *in vitro* tetracycline induction (C), and in trypanosomes isolated from mice, before being euthanized (D).
doi:10.1371/journal.pntd.0002578.g008

Normal *T. brucei* parasites also showed a statistically significant slower growth under conditions of asparagine limitation ($p\leq0.01$; data not shown) (compare Fig. 6C, with A, E, G). It is therefore possible that even when the parasite has AS, it also requires external asparagine for optimal *in vitro* growth.

AS-A is dispensable for *T. brucei* infectivity in mice

To test whether AS-A is important for parasite infection in a disease model, two groups of mice ($n=4$) were inoculated with the parental cell line, and other two groups with RNAi cells. Two mice groups were fed with water containing doxycycline to induce down-regulation of *Tb*AS-A, while the remaining mice were kept as non-induced controls. Within six days of inoculation, all mice from the different groups developed high levels of parasitemia (Fig. 8A), and all had to be euthanized after seven or eight days post-infection (Fig. 8B). The results confirm that the asparagine in mouse blood is sufficient to compensate for the ≈87% downregulation of AS-A (Fig. 8C, D).

To assess the contribution of blood L-asparagine *in vivo*, mice were treated with L-asparaginase [50]. L-asparaginase treatment did not affect growth of normal parasites in mice (Fig. 9A) and consequently did not extend animal survival (Fig. 9B). However L-asparaginase treatment in mice infected with *Tb*AS-A RNAi-induced parasites caused a decrease in the parasitemia (Fig. 9D), thus leading to an increase of mice survival (Fig. 9E). Even so, the infection resulted in death. As happened *in vitro*, RNAi revertants appeared during the course of infection in asparaginase-treated, but not untreated, mice (Fig. 9F). Parasites extracts from wt infected mice were used as controls (Fig. 9C).

Discussion

In this study we demonstrated that trypanosomes AS-A use both ammonia or glutamine as nitrogen donors for the ATP dependent conversion of aspartate into asparagine. Such hybrid activity was only previously demonstrated for type B enzymes, which prefer glutamine to ammonia [15–19]. The small differences in K_m of *Tb*AS-A and *Tc*AS-A for ammonia and glutamine (1.5 and 2 fold, respectively) are lower than the difference found in most AS-B enzymes, with the exception of the human enzyme, which has similar affinities for both [16–20]. Purified *E. coli* AS-A used only ammonia as the nitrogen source, and results from *Klebsiella aerogenes* also suggested that AS-A preferentially uses ammonia as substrate [5,21,22]. The conclusions for AS-A enzymes of these two Gram-negative organisms relied on both biochemical and genetic analysis, but given technical limitations at the time, and the fact that background enzyme activity was seen in the absence of both ammonia and glutamine, some re-examination in bacteria would be worthwhile. Moreover the overall K_m values of trypanosomes AS-A for aspartate, are 6 up to 20 fold higher than the ones found in the literature for prokaryotic asparagine synthetase type A [5,21,22]. *Trypanosoma* AS-A structures were not yet been solved

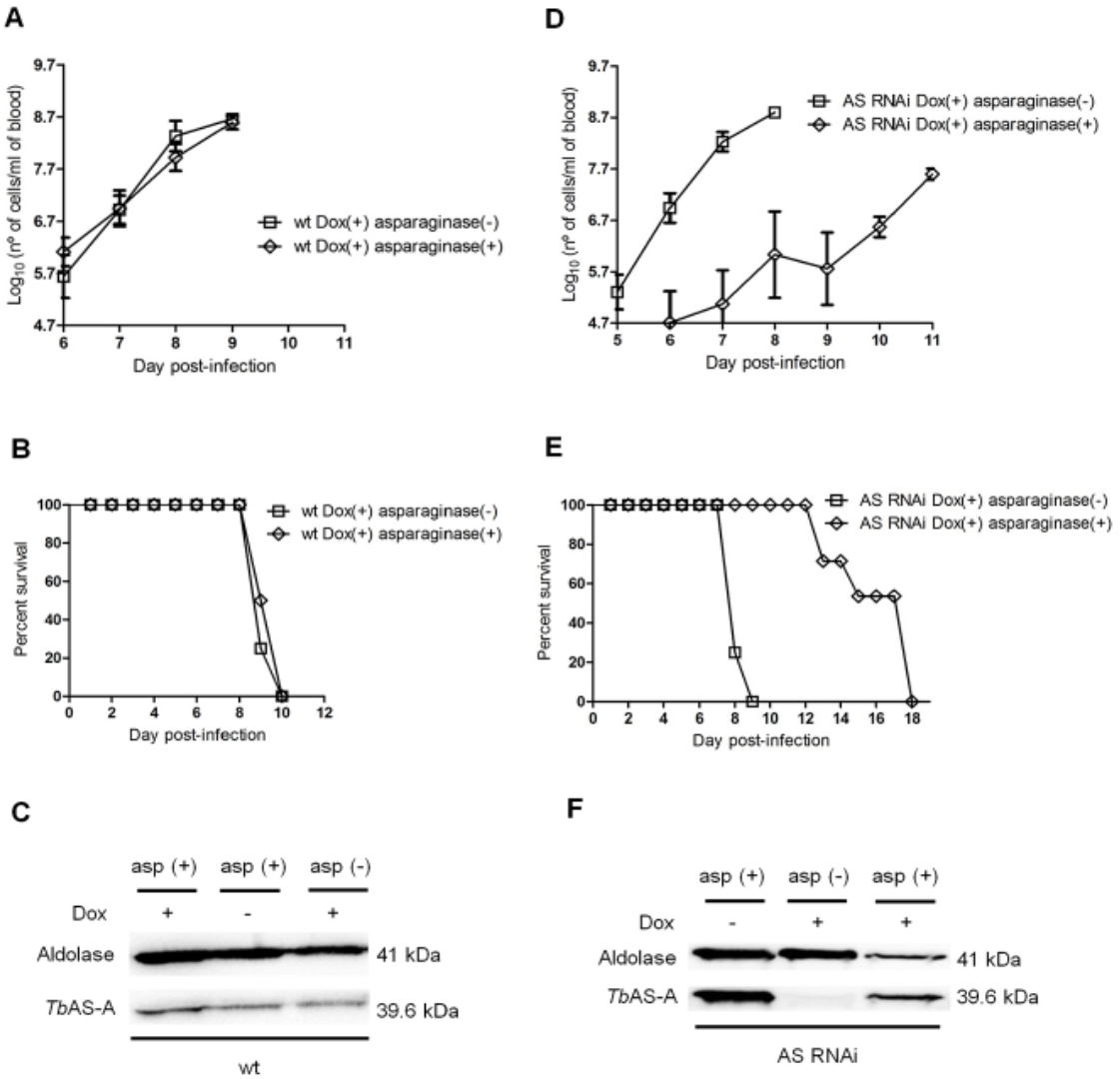

Figure 9. ***In vivo*** **RNAi against** ***Tb*****AS-A in mice undergoing** ***E. coli*** **L-asparaginase treatment.** Time course of the parasitemia of two groups of 4 mice infected intraperitoneally, with 1×10^4 of RNAi induced [using 1 mg/ml of doxycycline, Dox (+)] wt parental cell line (A) or a representative AS RNAi cell line (D) either untreated (open squares) or treated daily every 2 days (open diamonds) with 50 IU *E. coli* L-asparaginase/mouse. Parasitemia was quantified in peripheral tail blood at the times indicated. Error bars indicate standard deviation, and data are representative of two independent experiments using two different AS RNAi clones. The detection limit for this assay is 5×10^4 trypanosomes/ml of blood. Mice were culled when parasitemia reached 1×10^8 cells/ml. Kaplan–Meier survival plot of mice infected with RNAi induced wt cell line (B) or AS RNAi cell line (E) either untreated (open squares) or treated (open diamonds) with *E. coli* L-asparaginase. (F) Western blot analysis of AS-A levels in trypanosomes isolated from mice, before being euthanized. (C) Wt cell extracts, also collected when mice were culled, were use as negative control.
doi:10.1371/journal.pntd.0002578.g009

and our protein homology models are not completely enlightening, nevertheless we can speculate that such differences may result in the fact that parasite enzymes were expressed and purified as recombinant proteins in bacteria and not purified directly from trypanosomes extracts. As a consequence, differences in protein post-transcriptional processing and/or changes in protein conformation cannot be excluded.

Our results suggest that bloodstream-form parasites rely on two major sources of asparagine to ensure normal proliferation: uptake from the extracellular medium and biosynthesis by AS-A. Bloodstream form proliferation, either *in vitro* or *in vivo*, was only significantly affected when both asparagine sources were compromised. Also consistent with this idea, in the published RNAi screen, a very slight (possibly insignificant) growth disadvantage was seen in bloodstream forms depleted of AS-A [56]. In the same way, our *in vitro* results are corroborated with previous studies, as mammalian cells with low expression of AS are similarly susceptible to asparagine depletion [57–59], and asparaginase

isolated from *E. coli* and *Erwinia carotovora* act as potent anti-leukemic agents [60].

In the trypanosomes genome there is a second open reading frame (Tb927.3.4060) coding for a putative AS domain. However this is apparently not a classical AS, despite the presence of a good Pfam AS domain (PF0073) at the C-terminus. A BLASTp search using the *T. brucei* sequence revealed a variety of proteins of unknown function that aligned not only across the AS domain, but also in the N-terminal region, which contains N-terminal aminohydrolase domains. Best matches originate from extremely diverse eukaryotes including a plant, an alga, a member of the fungi and an amoeba. BLASTp against the *Saccharomyces cerevisiae* predicted proteome yielded YML096W, and the reciprocal BLASTp on the trypanosome genome indeed gave Tb927.3.4060 as best match. The function of YML096W is not known, and in a trypanosome RNAi screen no growth defect was seen for Tb927.3.4060 [56].

The capacity of trypanosomes to grow using asparagine from the extracellular environment, and the lack of growth defect when the levels of AS-A are reduced, show that only a combination therapy using both a *Tb*AS-A inhibitor and an extracellular asparagine depletor (e.g. L-asparaginase) or an asparagine transport blocker could inhibit parasite growth. This is not appropriate for African sleeping sickness treatment. A combination that absolutely required simultaneous activities of two different drugs would be wide open to resistance development, and drug combination including an intravenously-introduced enzyme is likely to be both too expensive and logistically inappropriate for treatment of African trypanosomiasis. Moreover, L-asparaginase treatment in cancer results in serious adverse events [61–63]. We therefore conclude that AS-A is not a good candidate as a sleeping sickness drug target. Its role in *Trypanosoma cruzi*, however, remains to be established.

Supporting Information

Figure S1 RNAi vectors used to generate RNAi-mediated *Tb*AS-A downregulation. (A) pHD1144 vector for stem-loop cloning (pSP72 vector with a stuffer fragment); (B) pHD1145 inducible polymerase I vector for insertion of ready-made stem-loops (pHD677 vector without a T7 promoter and with an inducible EP1 promoter and hygromycin resistance cassette, insertion into ribosomal spacer).
(TIF)

Figure S2 Validation of antibodies against *Tb*AS-A. Immunofluorescence analysis of *T. brucei* wt or a representative AS RNAi clone grown in the presence or absence of tetracycline. RNAi induced and uninduced cells were grown for 48 h, then fixed and probed with rat polyclonal anti-*Tb*AS-A (A) or rabbit polyclonal anti-*Tb*AS-A (B) antibody and co-stained with DAPI. Bars, 5 µm. Quantification of *Tb*AS-A fluorescence levels in induced cells (AS RNAi tet(+), $n = 30$) and uninduced cells (AS RNAi tet(−), $n = 30$), using the rat and the rabbit polyclonal anti-*Tb*AS-A antibodies (C). Data representative of two independent experiments using two different clones. ImageJ software (version 1.43u) was used for fluorescence quantification. p value was calculated by Student's t test (*** $p \leq 0.001$ and ** $p \leq 0.01$).
(TIF)

Figure S3 *Tb*AS-A cellular localization in *T. brucei* bloodstream forms. Immunofluorescence analysis by confocal microscopy of *Tb*AS-A (red) in bloodstream forms. Aldolase (glycosome marker), GRASP (golgi marker), BiP (endoplasmic reticulum marker) and MitoTracker (labels mitochondria) are in green. DAPI locate nuclear and kinetoplast mitochondrial DNA (blue). Bars, 5 µm. Images are maximal Z-projections of 50 contiguous stacks separated by 0.1 µm.
(TIF)

Acknowledgments

We would like to thank Dr. Jay Bangs from University of Wisconsin-Madison Medical School, USA, for providing us BiP antibody, Dr. Paul Michels from Université Catholique de Louvain, Belgium, for sending us enolase antibody and Dr. Graham Warren from Yale University School of Medicine, USA, for the GRASP antibody. We also thank Claudia Helbig for assistance in Heidelberg.

Author Contributions

Conceived and designed the experiments: IL JF JT ACdS. Performed the experiments: IL JF NS JT. Analyzed the data: IL JF SMR CC JT ACdS. Contributed reagents/materials/analysis tools: CC SMR NR. Wrote the paper: IL JF CC SMR JT ACdS.

References

1. Richards NG, Schuster SM (1998) Mechanistic issues in asparagine synthetase catalysis. Adv Enzymol Relat Areas Mol Biol 72: 145–198.
2. Blaise M, Frechin M, Olieric V, Charron C, Sauter C, et al. (2011) Crystal structure of the archaeal asparagine synthetase: interrelation with aspartyl-tRNA and asparaginyl-tRNA synthetases. J Mol Biol 412: 437–452.
3. Roy H, Becker HD, Reinbolt J, Kern D (2003) When contemporary aminoacyl-tRNA synthetases invent their cognate amino acid metabolism. Proc Natl Acad Sci U S A 100: 9837–9842.
4. Nakamura M, Yamada M, Hirota Y, Sugimoto K, Oka A, et al. (1981) Nucleotide sequence of the asnA gene coding for asparagine synthetase of E. coli K-12. Nucleic Acids Res 9: 4669–4676.
5. Reitzer LJ, Magasanik B (1982) Asparagine synthetases of Klebsiella aerogenes: properties and regulation of synthesis. J Bacteriol 151: 1299–1313.
6. Blattner FR, Plunkett G, 3rd, Bloch CA, Perna NT, Burland V, et al. (1997) The complete genome sequence of Escherichia coli K-12. Science 277: 1453–1462.
7. Sugiyama A, Kato H, Nishioka T, Oda J (1992) Overexpression and purification of asparagine synthetase from Escherichia coli. Biosci Biotechnol Biochem 56: 376–379.
8. Gowri VS, Ghosh I, Sharma A, Madhubala R (2012) Unusual domain architecture of aminoacyl tRNA synthetases and their paralogs from Leishmania major. BMC Genomics 13: 621.
9. Humbert R, Simoni RD (1980) Genetic and biomedical studies demonstrating a second gene coding for asparagine synthetase in Escherichia coli. J Bacteriol 142: 212–220.
10. Andrulis IL, Chen J, Ray PN (1987) Isolation of human cDNAs for asparagine synthetase and expression in Jensen rat sarcoma cells. Mol Cell Biol 7: 2435–2443.
11. Andrulis IL, Shotwell M, Evans-Blackler S, Zalkin H, Siminovitch L, et al. (1989) Fine structure analysis of the Chinese hamster AS gene encoding asparagine synthetase. Gene 80: 75–85.
12. Ramos F, Wiame JM (1980) Two asparagine synthetases in Saccharomyces cerevisiae. Eur J Biochem 108: 373–377.
13. Merchant SS, Prochnik SE, Vallon O, Harris EH, Karpowicz SJ, et al. (2007) The Chlamydomonas genome reveals the evolution of key animal and plant functions. Science 318: 245–250.
14. Coruzzi GM (2003) Primary N-assimilation into Amino Acids in Arabidopsis. Arabidopsis Book 2: e0010.
15. Boehlein SK, Richards NG, Schuster SM (1994) Glutamine-dependent nitrogen transfer in Escherichia coli asparagine synthetase B. Searching for the catalytic triad. J Biol Chem 269: 7450–7457.
16. Duff SM, Qi Q, Reich T, Wu X, Brown T, et al. (2011) A kinetic comparison of asparagine synthetase isozymes from higher plants. Plant Physiol Biochem 49: 251–256.
17. Ramos F, Wiame JM (1979) Synthesis and activation of asparagine in asparagine auxotrophs of Saccharomyces cerevisiae. Eur J Biochem 94: 409–417.
18. Horowitz B, Meister A (1972) Glutamine-dependent asparagine synthetase from leukemia cells. Chloride dependence, mechanism of action, and inhibition. J Biol Chem 247: 6708–6719.
19. Patterson MK Jr OG (1968) Asparagine biosynthesis by the Novikoff Hepatoma isolation, purification, property, and mechanism studies of the enzyme system. J Biol Chem 243: 376–380.

20. Ciustea M, Gutierrez JA, Abbatiello SE, Eyler JR, Richards NG (2005) Efficient expression, purification, and characterization of C-terminally tagged, recombinant human asparagine synthetase. Arch Biochem Biophys 440: 18–27.
21. Cedar H, Schwartz JH (1969) The asparagine synthetase of Escherichia coli. II. Studies on mechanism. J Biol Chem 244: 4122–4127.
22. Cedar H, Schwartz JH (1969) The asparagine synthetase of Escherhic coli. I. Biosynthetic role of the enzyme, purification, and characterization of the reaction products. J Biol Chem 244: 4112–4121.
23. Larsen TM, Boehlein SK, Schuster SM, Richards NG, Thoden JB, et al. (1999) Three-dimensional structure of Escherichia coli asparagine synthetase B: a short journey from substrate to product. Biochemistry 38: 16146–16157.
24. Nakatsu T, Kato H, Oda J (1998) Crystal structure of asparagine synthetase reveals a close evolutionary relationship to class II aminoacyl-tRNA synthetase. Nat Struct Biol 5: 15–19.
25. Nakatsu T, Kato H, Oda J (1996) Crystallization and preliminary crystallographic study of asparagine synthetase from Escherichia coli. Acta Crystallogr D Biol Crystallogr 52: 604–606.
26. Boehlein SK, Stewart JD, Walworth ES, Thirumoorthy R, Richards NG, et al. (1998) Kinetic mechanism of Escherichia coli asparagine synthetase B. Biochemistry 37: 13230–13238.
27. Luehr CA, Schuster SM (1985) Purification and characterization of beef pancreatic asparagine synthetase. Arch Biochem Biophys 237: 335–346.
28. Huang XH, HM; and Raushel, F (2001) Channeling of substrates and intermediates in enzyme-catalyzed reactions. Annual Review in Biochemistry 70: 149–180.
29. Berriman M, Ghedin E, Hertz-Fowler C, Blandin G, Renauld H, et al. (2005) The genome of the African trypanosome Trypanosoma brucei. Science 309: 416–422.
30. El-Sayed NM, Myler PJ, Bartholomeu DC, Nilsson D, Aggarwal G, et al. (2005) The genome sequence of Trypanosoma cruzi, etiologic agent of Chagas disease. Science 309: 409–415.
31. El-Sayed NM, Myler PJ, Blandin G, Berriman M, Crabtree J, et al. (2005) Comparative genomics of trypanosomatid parasitic protozoa. Science 309: 404–409.
32. Legros D, Ollivier G, Gastellu-Etchegorry M, Paquet C, Burri C, et al. (2002) Treatment of human African trypanosomiasis–present situation and needs for research and development. Lancet Infect Dis 2: 437–440.
33. Castro JA, de Mecca MM, Bartel LC (2006) Toxic side effects of drugs used to treat Chagas' disease (American trypanosomiasis). Hum Exp Toxicol 25: 471–479.
34. Alsford S, Kelly JM, Baker N, Horn D (2013) Genetic dissection of drug resistance in trypanosomes. Parasitology: 1–14.
35. MacGregor P, Szoor B, Savill NJ, Matthews KR (2012) Trypanosomal immune evasion, chronicity and transmission: an elegant balancing act. Nat Rev Microbiol 10: 431–438.
36. Radwanska M, Guirnalda P, De Trez C, Ryffel B, Black S, et al. (2008) Trypanosomiasis-induced B cell apoptosis results in loss of protective anti-parasite antibody responses and abolishment of vaccine-induced memory responses. PLoS Pathog 4: e1000078.
37. Akerley BJ, Rubin EJ, Novick VL, Amaya K, Judson N, et al. (2002) A genome-scale analysis for identification of genes required for growth or survival of Haemophilus influenzae. Proc Natl Acad Sci U S A 99: 966–971.
38. Boyce JD, Wilkie I, Harper M, Paustian ML, Kapur V, et al. (2002) Genomic scale analysis of Pasteurella multocida gene expression during growth within the natural chicken host. Infect Immun 70: 6871–6879.
39. Schlecker T, Schmidt A, Dirdjaja N, Voncken F, Clayton C, et al. (2005) Substrate specificity, localization, and essential role of the glutathione peroxidase-type tryparedoxin peroxidases in Trypanosoma brucei. J Biol Chem 280: 14385–14394.
40. Lanham SM (1968) Separation of trypanosomes from the blood of infected rats and mice by anion-exchangers. Nature 218: 1273–1274.
41. Sheng S, Kraft JJ, Schuster SM (1993) A specific quantitative colorimetric assay for L-asparagine. Anal Biochem 211: 242–249.
42. Fresquet V, Thoden JB, Holden HM, Raushel FM (2004) Kinetic mechanism of asparagine synthetase from Vibrio cholerae. Bioorg Chem 32: 63–75.
43. Kakkar T, Boxenbaum H, Mayersohn M (1999) Estimation of Ki in a competitive enzyme-inhibition model: comparisons among three methods of data analysis. Drug Metab Dispos 27: 756–762.
44. Larkin MA, Blackshields G, Brown NP, Chenna R, McGettigan PA, et al. (2007) Clustal W and Clustal X version 2.0. Bioinformatics 23: 2947–2948.
45. Bond CS, Schuttelkopf AW (2009) ALINE: a WYSIWYG protein-sequence alignment editor for publication-quality alignments. Acta Crystallogr D Biol Crystallogr 65: 510–512.
46. Arnold K, Bordoli L, Kopp J, Schwede T (2006) The SWISS-MODEL workspace: a web-based environment for protein structure homology modelling. Bioinformatics 22: 195–201.
47. Kiefer F, Arnold K, Kunzli M, Bordoli L, Schwede T (2009) The SWISS-MODEL Repository and associated resources. Nucleic Acids Res 37: D387–392.
48. Peitsch MC, Wells TN, Stampf DR, Sussman JL (1995) The Swiss-3DImage collection and PDB-Browser on the World-Wide Web. Trends Biochem Sci 20: 82–84.
49. Cooney DA, Capizzi RL, Handschumacher RE (1970) Evaluation of L-asparagine metabolism in animals and man. Cancer Res 30: 929–935.
50. Goldberg AI, Cooney DA, Glynn JP, Homan ER, Gaston MR, et al. (1973) The effects of immunization to L-asparaginase on antitumor and enzymatic activity. Cancer Res 33: 256–261.
51. Hannaert V, Albert MA, Rigden DJ, da Silva Giotto MT, Thiemann O, et al. (2003) Kinetic characterization, structure modelling studies and crystallization of Trypanosoma brucei enolase. Eur J Biochem 270: 3205–3213.
52. Clayton CE (1987) Import of fructose bisphosphate aldolase into the glycosomes of Trypanosoma brucei. J Cell Biol 105: 2649–2654.
53. Bangs JD, Uyetake L, Brickman MJ, Balber AE, Boothroyd JC (1993) Molecular cloning and cellular localization of a BiP homologue in Trypanosoma brucei. Divergent ER retention signals in a lower eukaryote. J Cell Sci 105 (Pt 4): 1101–1113.
54. He CY, Ho HH, Malsam J, Chalouni C, West CM, et al. (2004) Golgi duplication in Trypanosoma brucei. J Cell Biol 165: 313–321.
55. Chen Y, Hung CH, Burderer T, Lee GS (2003) Development of RNA interference revertants in Trypanosoma brucei cell lines generated with a double stranded RNA expression construct driven by two opposing promoters. Mol Biochem Parasitol 126: 275–279.
56. Alsford S, Turner DJ, Obado SO, Sanchez-Flores A, Glover L, et al. (2011) High-throughput phenotyping using parallel sequencing of RNA interference targets in the African trypanosome. Genome Res 21: 915–924.
57. Scotti C, Sommi P, Pasquetto MV, Cappelletti D, Stivala S, et al. (2010) Cell-cycle inhibition by Helicobacter pylori L-asparaginase. PLoS One 5: e13892.
58. Ueno T, Ohtawa K, Mitsui K, Kodera Y, Hiroto M, et al. (1997) Cell cycle arrest and apoptosis of leukemia cells induced by L-asparaginase. Leukemia 11: 1858–1861.
59. Broome JD (1963) Evidence that the L-asparaginase of guinea pig serum is responsible for its antilymphoma effects. I. Properties of the L-asparaginase of guinea pig serum in relation to those of the antilymphoma substance. J Exp Med 118: 99–120.
60. Beard ME, Crowther D, Galton DA, Guyer RJ, Fairley GH, et al. (1970) L-asparaginase in treatment of acute leukaemia and lymphosarcoma. Br Med J 1: 191–195.
61. Appel IM, Hop WC, van Kessel-Bakvis C, Stigter R, Pieters R (2008) L-Asparaginase and the effect of age on coagulation and fibrinolysis in childhood acute lymphoblastic leukemia. Thromb Haemost 100: 330–337.
62. Cohen H, Bielorai B, Harats D, Toren A, Pinhas-Hamiel O (2010) Conservative treatment of L-asparaginase-associated lipid abnormalities in children with acute lymphoblastic leukemia. Pediatr Blood Cancer 54: 703–706.
63. van den Berg H (2011) Asparaginase revisited. Leuk Lymphoma 52: 168–178.

2.1.2. *Leishmania infantum* asparagine synthetase A is dispensable for parasites survival and infectivity

A growing interest in asparagine (Asn) metabolism has currently been observed in cancer and infection fields. Asparagine synthetase (AS) is responsible for the conversion of aspartate into Asn in an ATP-dependent manner, using ammonia or glutamine as a nitrogen source. There are two structurally distinct AS: the strictly ammonia dependent, type A, and the type B, which preferably uses glutamine. Absent in humans and present in trypanosomatids, AS-A was worthy of exploring as a potential drug target candidate. Appealingly, it was reported that AS-A was essential in *Leishmania donovani*, making it a promising drug target. In the work herein we demonstrate that *Leishmania infantum*AS-A, similarly to *Trypanosoma* sp and *L. donovani*, is able to use both ammonia and glutamine as nitrogen donors. Moreover, we have successfully generated *LiASA* null mutants by targeted gene replacement in *L. infantum* and these parasites do not display any significant growth or infectivity defect. Indeed, a severe impairment of *in vitro* growth was only observed when null mutants were cultured in asparagine limiting conditions. Altogether our results demonstrate that despite being important under asparagine limitation, *Li*AS-A is not essential for parasite survival, growth or infectivity in normal *in vitro* and *in vivo* conditions. Therefore we exclude AS-A as a suitable drug target against *L. infantum* parasites.

Reprinted from PLoS Neglected Tropical Diseases *in press* doi: 10.1371/journal.pntd.0004365

"Leishmania infantum asparagine synthetase A is dispensable for parasites survival and infectivity"

Short Title: "AS-A is dispensable for *L. infantum* infectivity"

Joana Faria[1,2], Inês Loureiro[1,2] , Nuno Santarém[1,2] , Sandra Macedo-Ribeiro[2,3], Joana Tavares[1,2*] and Anabela Cordeiro-da-Silva[1,2,4*]

[1]Parasite Disease Group, Instituto de Biologia Molecular e Celular da Universidade do Porto, Portugal
[2]Instituto de Investigação e Inovação em Saúde, Universidade do Porto, Porto, Portugal
[3]Protein Crystallography Group, Instituto de Biologia Molecular e Celular da Universidade do Porto, Portugal
[4]Departamento de Ciências Biológicas, Faculdade de Farmácia, Universidade do Porto, Portugal

[*] Corresponding authors:
(JT) E-mail: jtavares@ibmc.up.pt and (ACdS) E-mail: cordeiro@ibmc.up.pt

Keywords: Asparagine synthetase A; *Leishmania infantum*; gene knock-out; asparagine metabolism; glutamine

Abstract

A growing interest in asparagine (Asn) metabolism has currently been observed in cancer and infection fields. Asparagine synthetase (AS) is responsible for the conversion of aspartate into Asn in an ATP-dependent manner, using ammonia or glutamine as a nitrogen source. There are two structurally distinct AS: the strictly ammonia dependent, type A, and the type B, which preferably uses glutamine. Absent in humans and present in trypanosomatids, AS-A was worthy of exploring as a potential drug target candidate. Appealingly, it was reported that AS-A was essential in *Leishmania donovani*, making it a promising drug target. In the work herein we demonstrate that *Leishmania infantum*AS-A, similarly to *Trypanosoma* sp and *L. donovani*, is able to use both ammonia and glutamine as nitrogen donors. Moreover, we have successfully generated *LiASA* null mutants by targeted gene replacement in *L. infantum* and these parasites do not display any significant

growth or infectivity defect. Indeed, a severe impairment of *in vitro* growth was only observed when null mutants were cultured in asparagine limiting conditions. Altogether our results demonstrate that despite being important under asparagine limitation, *Li*AS-A is not essential for parasite survival, growth or infectivity in normal *in vitro* and *in vivo* conditions. Therefore we exclude AS-A as a suitable drug target against *L. infantum* parasites.

Author Summary

It was recently described that asparagine synthetase A (AS-A) of trypanosomatids uses not only ammonia but also glutamine for asparagine formation, which was a surprising feature for a type A AS. Interestingly, *Leishmania donovani* AS-A was reported to be essential for parasite survival, and once a human homologue was absent, this is enzyme emerged as a novel drug target candidate. *Leishmania infantum* encodes for a functional AS-A enzyme, which also uses either ammonia or glutamine as nitrogen donor for asparagine synthesis. In *L. infantum*, *ASA* ablation drives parasites auxotrophic to asparagine, however, *Li*AS-A is not detrimental for parasite survival, growth or infectivity. AS-A is therefore unlikely to be a suitable drug target against *Leishmania* parasites.

Introduction

Leishmaniasis is a vector borne human disease, caused by several species of digenetic protozoan parasites belonging to genus *Leishmania*. The clinical presentations of this neglected tropical disease vary from selfhealing cutaneous manifestations to potentially fatal, if untreated, visceral ailment [1]. The most severe form of the disease, designated as visceral leishmaniasis (VL) is mainly associated to *Leishmania donovani* or *Leishmania infantum*. Due to the absence of human vaccines, VL control relies mainly on chemotherapy and appropriate vector control [2]. The traditional therapeutic options are associated with significant limitations (cost, toxicity, complex administration regimes, resistance) averting disease control in endemic areas [3]. As consequence, according to World Health Organization between 20,000 and 30,000 people (mostly children) die every year, rendering the search for novel chemotherapeutic options a priority [4].

Asparagine (Asn) metabolism has been under the spotlight in the recent years. Asn is the last nonessential amino acid to be synthesised from glucose metabolism [5]. For many years it seemed it was not involved in any other pathway but protein synthesis in mammalian cells, contrasting with the other 19 common amino acids [6]. Nonetheless, several recent studies suggest Asn somehow coordinates cell responses with metabolic reserves and ultimately regulates cell fate [5]. In many pathogenic microorganisms, functional studies on

L-asparaginase and Asn transporters have implicated Asn metabolism in survival, invasion and/or virulence [7-14].

Asparagine synthetase (AS) is another key player in Asn metabolism, it catalyses Asn formation from aspartate in an ATP dependent manner using ammonia or glutamine as nitrogen donors. The reaction mechanism comprises two crucial steps: 1) the formation of β-aspartylAMP, in which β-carboxylate group of aspartate is activated by ATP; 2) nucleophilic attack by an ammonium ion. This mechanism mirrors the close evolutionary relation to aminoacyl-tRNA synthetase enzymes [15]. There are two structurally distinct types of AS: A and B [16]. Type B (AS-B, EC. 6.3.5.4) uses preferably glutamine over ammonia and can be found in prokaryotes and eukaryotes (mammalian cells, yeasts, *Chlamydomonas reinhardtii*, higher plants) [17-23]. Type A (AS-A, EC. 6.3.1.1) are found mainly in prokaryotes (*Escherichia coli* [24] and *Klebsiella aerogenes* [25]) or in archaea (*Pyrococcus abyssi* [26]) and described as strictly ammonia dependent. Surprisingly, kinetoplastids and other protozoans, despite being eukaryotes, possess not only a putative AS-B but also a bacterial type AS-A [27-29]. Moreover AS-A from *Trypanosoma brucei*, *Trypanosoma cruzi* [28] and *L. donovani* [29] parasites were reported to use glutamine as nitrogen donor as well.

Several roles have been associated to bacterial AS. For instance, in *Pasteurella multocida*, AS-A is significantly upregulated during host infection, in *Mycobacterium smegmatis* AS-B is involved in natural resistance to antibiotics and in *Mycobacterium tuberculosis*, AS-B was reported to be required for *in vitro* growth [30-33].

Recently our group showed that in *T. brucei* bloodstream forms AS-A knockdown has no impact on parasites growth or infectivity, except upon Asn deprivation. These results suggest Asn main sources are AS-A mediated synthesis and extracellular uptake [28]. Surprisingly, in *L. donovani*, AS-A was claimed to be essential for parasites survival and emerged as a promising drug target due to the absence of a human homologue [29]. Additionally, these results also suggest that Asn homeostasis could be differently regulated among trypanosomatids. These parasites present different amino acid requirements for either energetic or osmotic functions in different stages of their life cycles and as a reflex of the different environmental stimuli they receive in the vector or mammalian host [34]. Across trypanosomatids' species, the amino acid transporters (AAT) repertoire has a high interspecific variation, regarding number, affinity, specificity and capacity [34]. For instance, in the case of cysteine, a crucial amino acid for thiol biosynthesis, *Leishmania major* contrarily to *T. brucei*, fails to uptake it at a rate that ensures the intracellular pool is enough for optimal growth. Therefore, these parasites rely mainly on pathways that enable cysteine synthesis [35].

In this work, we have biochemically characterized *L. infantum* AS-A (*Li*AS-A), and to gain further insights on AS-A essentiality across different *Leishmania* species, we have performed gene replacement studies in *L. infantum.*

Methods

Ethics statement. All experiments were carried out in accordance with the IBMC.INEB Animal Ethics Committee and the Portuguese National Authority for Animal Health (DGAV) guidelines, according to the statements on the directive 2010/63/EU of the European Parliament and of the Council. DGAV approved the animal experimentation presented in this manuscript under the license DGAV number 25268/2013-10-02.

Chemicals and reagents. L-asparagine, L-aspartic acid sodium salt monohydrate, L-glutamine, L-glutamatic acid salt hydrate, ATP disodium salt hydrate, AMP disodium salt, sodium pyrophosphate decahydrate, ninhydrin, dNTPs, ammonium chloride, magnesium chloride, tween-20, tris-base, urea, thiourea, DTT, triton X-100 and IPTG (isopropyl-β-D-thiogalactopyranoside) were purchased from Sigma. Oligonucleotide primers were obtained from STAB VIDA. Restriction endonucleases were from New England Biolabs. Polyclonal antibodies against *Li*AS-A were obtained in rabbits inoculated with purified recombinant His-tagged *Li*AS-A. *E. coli* L-asparaginase was purchased from Prospec.

Parasites. *L. infantum* (MHOM/MA/67/ITMAP-263) promastigote forms were grown at 26ºC in complete RPMI 1640 medium [36]. For *in vitro* and *in vivo* characterization, different cell lines were firstly recovered from the spleen of infected BALB/c to restore virulence, and subsequently maintained in culture no longer than 10 passages [36]. Axenic amastigotes were grown in MAA complete medium [36], at 37ºC, 5% CO_2. Depending on the analysis, protein extracts were prepared as follows: 1) 1 x 10^7 late-stationary promastigotes were resuspended in T8 lysis buffer (tris-base 0.6%, urea 42%, thiourea 15%, DTT 0.3%, triton X-100 1%); or 2) 1 x 10^8 promastigotes or axenic amastigotes were resuspended in 100 µL of PBS containing protease inhibitor (Roche) and following 6 freezing/thaw cycles, the parasite suspensions supernatants were recovered and then quantified using Bio-Rad DC Protein Assay (Biorad).

AS-A protein alignments and *Li*AS-A/*Lm*AS-A homology models. *Ec*AS-A, *Li*AS-A, *Lm*AS-A, *Tb*AS-A and *Tc*AS-A protein alignments were performed using the ClustalW program [37]. Aline program, *Version 011208* [38], was used for editing protein sequence alignments. *Li*AS-A and *Lm*AS-A homology models were obtained with SWISS-

MODEL, using *Ec*AS-A crystal structure (Protein Data Bank (PDB) 12AS [15]) as a template (percentage of sequence identity of ~50-60% in both cases) [39-41]. The 3D models were illustrated using PyMOL program (The PyMOL Molecular Graphics System, Version 1.3, Schrödinger, LLC).

Cloning *ASA* genes. Asparagine synthetase A (*ASA*) from *L. infantum* (LinJ.26.0790; chromosome LinJ.26; 234298 - 235360) was obtained by performing PCR on genomic DNA, extracted using DNAzol (Invitrogen) [42-44], using primers 1 + 2 (Table S1). PCR conditions were as follows: initial denaturation (2 min at 94ºC), 35 cycles of denaturation (30 s at 94ºC), annealing (30 s at 50ºC) elongation (2 min at 68ºC) and a final extension step (10 min at 68ºC). Another restriction strategy was required to clone the gene into a *Leishmania* overexpression vector – pSPα*BLAST*α, and the sequence was amplified using primers 3 + 4 (Table S1). PCR conditions were as follows: initial denaturation (2 min at 94ºC), 30 cycles of denaturation (15 s at 94ºC), annealing (30 s at 55ºC) elongation (1 min at 72ºC) and a final extension step (10 min at 72ºC). All PCR products were cloned into a pGEM-T Easy vector (Promega) and sent for sequencing.

Expression and purification of poly-His-tagged recombinant *Li*AS-A. The *LiASA* gene was excised from the pGEM-T Easy vector (using NdeI/EcoRI), and subcloned into pET28a(+) expression vector (Novagen). The resulting construct presented a poly-His tag (6x Histine residues) at the N-terminal and was transformed into *E. coli* BL21DE3. The recombinant protein was expressed by induction of log-phase cultures with 0.5 mM of IPTG at 18ºC O/N. Bacteria were harvested and resuspended in buffer A (0.5 M NaCl, 20 mM Tris.HCl, pH 7.6). The sample was sonicated, according to the following conditions: output 4, duty cycle 50%, 10 cycles with 15 s each (Branson sonifier 250), followed by centrifugation to obtain the bacterial crude extract. For enzymatic activity experiments and rabbit polyclonal antibody production, the recombinant enzyme was purified in one step using Ni^{2+} resin (Qiagen) pre-equilibrated in buffer A. The column was washed sequentially with buffer A, bacterial crude extract, and buffer A with increasing concentrations of imidazole. *Li*AS-A was eluted in the fractions of buffer A containing 100 to 500 mM of imidazole. Dialysis was performed against PBS.

For additional activity tests, oligomeric form and Stokes' radius assessment, a deeper purification was performed. Firstly, the enzyme was purified by affinity chromatography, using a Histrap HP column (GE Healthcare), charged with nickel sulphate and equilibrated in buffer A, and posteriorly mounted in an AKTAPrimer Plus (GE Healthcare) system, at 4ºC. Secondly, it was purified by size exclusion chromatography, in

a Hiprep 26/60 Sephacryl S-200 column (GE Healthcare), previously equilibrated with running buffer (150 mM NaCl, 20 mM Tris, pH 7.6). The last purification step was a preparative ion exchange chromatography, using an UNO Q-1 (Bio-Rad, Cat. No 720-0001) column, mounted in a BioLogic DuoFlow (Bio-Rad) device, at 4ºC. The fractions were finally analysed by analytic size exclusion chromatography and analytic ion exchange chromatography, using AktaPurifier10 system (GE Healthcare), using Superose 12 10/300GL (GE Healthcare) column and a UNO Q-1 (Bio-Rad, Cat. No 720-0001) column, respectively. The final fractions were concentrated using Millipore centrifugal filter 30K (Amicon Ultra).

Concentration was determined measuring the absorbance at 280 nm using the theoretical molar extinction coefficient of 46910 $M^{-1}.cm^{-1}$ for *Li*AS-A, making use of NanoDrop ND-1000 Spectrophotometer (NanoDrop Technologies). The purified recombinant protein was resolved in SDS/PAGE and stained with Coomassie Brilliant Blue G-250 (Biorad).

For estimation of the *Li*AS-A oligomeric state the purified recombinant protein was analysed by analytic size exclusion chromatography, using the above described conditions. Blue dextran (2,000 kDa), catalase (MW 232 kDa, Stokes radius (SR) 5.22 nm), aldolase (MW 158 kDa, SR 4.81 nm), albumin (MW 67 kDa, SR 3.55 nm), ovalbumin (MW 43 kDa, SR 3.05 nm), chymotrypsinogen A (MW 25 kDa, SR 2.09 nm) and ribonuclease (MW 13.7 kDa, SR 1.64 nm) were used as standards. A calibration curve relating Log (MW) or Log(SR) with K_{av} was performed (K_{av} is $(V_e-V_0)/(V_t-V_0)$, in which V_e is elution volume, V_0 is the exclusion volume given by blue dextran and V_t is the total volume of the column).

Differential scanning fluorimetry. In a 96-well, thin-walled white PCR plate, 5 µl of *Li*AS-A (2.4 µM) were mixed with 5 µl of 10x SYPRO Orange (λ_{exc} 485 nm; λ_{em} 625 nm) and 40 µl of water or the ligands and ligands combinations to be tested. Plates were then sealed and placed into a BioRad iCycler5 PCR instrument. Measurements were taken every minute in 0.5ºC increments from 25º to 95ºC. Subsequent analysis of the fluorescent data using Biorad iCycler iQ Optical System *Software* Version 3.1 yielded the protein melting temperature (T_m) for *Li*AS-A.

Western-blot analysis. Western-blot was performed aiming different purposes: (1) His-tag labelling of recombinant proteins, (2) *Li*AS-A labelling in total soluble parasite extracts to assess protein expression throughout the life cycle, (3) *Li*AS-A labelling in mutants and (4) to assess protein distribution upon digitonin fractionation. One µg of recombinant *Li*AS-A, 20 µg of total soluble extracts from both promastigote and amastigote

forms, or 1 x 10^7 parasites were resolved in SDS-PAGE and transferred onto a nitrocellulose membrane (TransBlot Turbo, Bio-Rad), which was blocked, probed, washed and developed as previously described [28]. The following primary antibodies were used: rabbit anti-His-tag (MicroMol-413, 1:1000), mouse anti-α-tubulin (clone DM1A, Neomarkers, 1:1000), rabbit anti-*Li*AS-A (1:1000), rabbit anti-*Li*CS (cysteine synthase, 1:2000), rabbit anti-*Ld*HGPRT (hypoxanthine guanine phosphoribosyl transferase, 1:2000), and rabbit anti-*Tb*Enolase (1:5000). *Horseradish* peroxidase-conjugated goat anti-rabbit or goat anti-mouse IgG (Amersham) (1:5000 for 1 h, at RT) were used as the secondary antibody. ImageJ software (version 1.43u) was used for protein semi-quantification.

Enzymatic Assay. A 150 µl enzymatic mixture containing 85 mM Tris.HCl, 8.4 mM magnesium and varying concentration of aspartate, ammonia and ATP was assayed. The assay was performed as previously described [28], and ultimately absorbance at 340 nm was measured [45]. To determine the optimal conditions for kinetic parameter determination, reaction linearity was checked by varying enzyme concentration and time. The final reaction condition used 7.5 µg of enzyme per assay and 15 min incubation at 37ºC. A pH range of 7.0 to 9.0 was assessed, and pH 7.6 was selected as the optimal one to perform the following enzyme assays. To determine the K_m of each substrate a certain range of concentration was used and the remaining substrates were maintained in excess. For aspartate, ammonia, ATP and glutamine, the following concentrations were used: 1.25 to 20, 0.78 to 50, 0.625 to 10 and 1.56 to 25 mM, respectively.

Generation of *LiASA* null mutants. A targeted gene replacement strategy was used for *L. infantum ASA* gene knock-out. Briefly, *ASA* flanking regions were amplified from *L. infantum* genomic DNA and were linked to neomycin phosphotransferase (*NEO*) or hygromycin phosphotransferase (*HYG*) genes using a fusion PCR approach. The 5' and 3' UTR were amplified using primers 1 + 2 and 3 + 4 (Table S2), respectively. *NEO* and *HYG* were amplified from pSP72*αNEOα* and pGL345*HYG* templates, using primers 5 + 6 and 7 + 8 (Table S2) respectively, which possess around 30 nucleotides of the 5' UTR in the sense primer and the first 30 nucleotides of the 3' UTR in the antisense primer. 5' UTR_*NEO*_3' UTR and 5' UTR_*HYG*_3' UTR constructs were obtained using primers 1 + 4 (Table S2). Mid-log promastigotes were transfected with approximately 10 µg of linear construct, obtained by fusion PCR, using an AMAXA Nucleofector II device with Human T-cell nucleofector kit (Lonza). The day after transfection drug selection was carried out at 20 µg/mL of G418 (Invitrogen) and 50 µg/mL of hygromycin B (InVivoGen). Parasite cloning was performed by diluting the parasite suspension to a concentration of 0.5 cells/well, using

SDM culture medium. The drug concentrations for clone maintenance correspond to half of the selection concentrations.

Generation of *LiASA* overexpressor (OE) and null mutants' complementation. *LiASA* gene was excised from the pGEM-T Easy vector (using XbaI/NdeI) and subcloned into pSP72*αBLASTα* vector. Mid-log promastigotes, WT and dKO mutants, were transfected with approximately 10 µg of plasmid DNA as above in order to generate an overexpressing line (OE) or complemented null mutants, respectively. Drug selection was carried out at 30 µg/ml of blasticidin (InVivoGen).

PCR and Southern-blot analysis of *LiASA* mutants. *LiASA* mutants were analysed by PCR using Taq polymerase (NZYTech) for the following events: *LiASA* presence; *NEO* 5' integration; *NEO* 3' integration; *HYG* 5' integration and *HYG* 3' integration, using primers pairs 9 + 10, 11 + 12, 13 + 14, 15 + 16 and 17 + 18 (Table S2), respectively. Additionally, a non-related gene from chromosome 28, encoding a putative ribose-5-phosphate isomerase B (*RPIB*, ~570 bp) was used as control, using primers 19 + 20 (Table S2). For Southern-blot analysis, total genomic DNA was extracted. Ten µg of genomic DNA were digested O/N with a 5 fold excess of SacI and NdeI, at 37ºC and samples were run O/N in an agarose gel. The gel was sequentially incubated with 0.25 M HCl, 1.5M NaCl 0.5M NaOH and 3M NaCl 0.5M Tris.HCl pH 7. DNA was then transferred O/N onto a Nylon membrane (Amersham), using 10x SSC (saline sodium citrate: 300 mM sodium citrate, 1 M NaCl). Nucleic acids fixation was achieved at 65ºC for 5 hours. Hybridization and revelation were undertaken using Gene Images AlkPhos Direct Labelling and Detection System kit (GE Healthcare Amersham). Pre-hybridisation, hybridisation and washes took place at 65ºC, probe labelling and membrane stripping were performed according to the manufacturer instructions. The blots were probed sequentially with 5' UTR, *LiASA*, *HYG* and *NEO*, which were PCR amplified, using primers 1 + 2, 9 + 10, 7 + 8 and 5 + 6 (Table S2), respectively.

***In vitro* growth of *LiASA* mutants.** Cultures were launched and monitored microscopically every 24h for 8 days or were maintained in log phase by subculturing every 2 days and cumulative growth was assessed for 5 consecutive passages. The growth experiments were performed in complete RPMI (cRPMI) or Asn depleted cRPMI (cRPMI + L-asparaginase) obtained by cRPMI O/N incubation with 1250 U/L of L-asparaginase at 37ºC. Growth curves were also undertaken in a serum-free RPMI (sfRPMI [46]) incubated with L-asparaginase, that was removed afterwards by flowing the medium through a 3 kDa

Millipore centrifugal filter (Amicon Ultra), generating an Asn free medium (sfRPMI + L-asparaginase). Asn was directly added to the Asn free sfRPMI (cf = 380 µM) to generate complemented sfRPMI (sfRPMI + L-Asparaginase + Asn). Finally, growth curves were performed in complete M199 (cM199) [29] or cM199 supplemented with Asn (cf = 380 µM). Growth curves of *LiASA* mutants and WT were seeded at 1 x 10^6 parasites/ml at 26ºC, except in the case ofsfRPMI, whose initial parasite density was 2 x 10^6 parasites/ml, grown with agitation. Before launching growth curves, the parasites were maintained in log phase for 2-3 passages in the absence of selection drugs.

***In vivo* infectivity of *LiASA* mutants.** Five to six weeks old female BALB/c mice were obtained from Charles River. For each mouse injection, 1 x 10^8 promastigotes recovered from 4 days old stationary culture were washed, resuspended in PBS, and injected intraperitoneally. Mice of each group (n=4) were sacrificed at 2 weeks post-infection. The parasite burden in the spleen and liver was determined by limiting dilution as previously described [47].

Digitonin Fractionation. For each sample condition, 1 x 10^8 promastigotes were washed once with cold trypanosome homogenisation buffer (THB), composed by 25 mM Tris, 1 mM EDTA and 10% sucrose, pH 7.8. Just before cell lyses, peptidase inhibitor (Roche) and different digitonin (Calbiochem) quantities (final concentrations of 12.5, 25, 50, 100, 200, 500 and 1000 µg/ml) were added to 250 µl of cold THB, for cell pellet resuspension. Untreated cells and those completely permeabilised (total release, the result of incubation in 1% Triton X-100) were used as controls. Each sample was incubated 60 min on ice, and then centrifuged at 13,000 rpm, 4°C, for 10 min. Supernatants were taken off into new pre-cold tubes and 250 µl of cold THB was added to each pellet and then mixed. All fractions were analysed by WB.

Immunofluorescence. *L. infantum* mid-log promastigotes were fixed, permeabilised and stained as previously described [48]. Cells were incubated with primary antibody O/N at 4ºC. The following primary antibodies were used: rabbit anti-*Li*AS-A (1:1000) and sheep anti-*Li*TDR1 (thiol-dependent reductase 1, 1:2000). Subsequently, slides were incubated for 1h at RT in a dark humidified atmosphere with a secondary antibody (1:500). The following secondary antibodies were used: goat anti-rabbit Alexa Fluor 488 or 568 and donkey anti-sheep Alexa Fluor 488 (Molecular probes, Life Technologies). In the case of Mitotracker Orange (Invitrogen), we stained the parasites by adding 1 µM to culture medium (without FBS) for 1h at 26ºC, prior to the above described

procedure. Slides were stained and mounted with Vectashield-DAPI (Vector Laboratories, Inc.). Images were captured using fluorescence microscope AxioImager Z1 (Carl Zeiss), equipped with a Axiocam MR v. 3.0 camera (Carl Zeiss), using either 63x (Plan-Apochromat 63x/1.40 Oil DIC) or 100x (Plan-Apochromat 100x/1.40 Oil DIC) objective. Images analysis and deconvolution was performed using ImageJ software (v. 1.47) and image deconvolution lab plugin (2010 Biomedical Imaging Group, EPFL, Switzerland) with Richardson-Lucy algorithm.

Statistical Analysis. For statistical analysis, one-way ANOVA and two-tailed Student's test were used. Statistical analysis was performed using GraphPad Prism Software (version 5.0): statistical significance $p < 0.05$ (*), $p < 0.01$ (**), $p < 0.001$ (***), $p < 0.0001$ (****).

Results

***Li*AS-A and *Lm*AS-A sequence alignment and homology models.** The open reading frames (ORFs) encoding putative AS-A and AS-B enzymes were identified in the genomes of *L. infantum* JPCM5 (LinJ.26.0790; LinJ.29.1590) and *L. major* Friedlin (LmjF.26.0830; LmjF.29.1490) [42-44]. The *ASA* amplified sequence from *L. infantum* strain matched 100% the annotated sequence from JPCM5 genome. To obtain structural and functional insights on AS-A enzymes, we have performed *in silico* analysis using the *L. infantum* (*Li*AS-A), *L. major* (*Lm*AS-A), *T. brucei* (*Tb*AS-A), *T. cruzi* (*Tc*AS-A) and *E. coli* (*Ec*AS-A) sequences that generate polypeptides containing 353, 353, 351, 348 and 330 residues, respectively (Fig. 1A). Overall, the sequence alignment shows a high conservation of the main structural features, including the active site residues (Fig. 1A). Indeed, the amino acids involved in Asn binding are strictly conserved across species, whereas in the case of AMP binding pocket, the majority of residues are conserved with a few exceptions. For instance, in the case of *Li*AS-A and *Lm*AS-A, there is a sole residue replacement, namely *Ec*AS-A L109, corresponding to I111 in both cases. This residue is not involved in polar interactions with AMP molecule, but instead integrates the outer wall of the nucleotide binding pocket [15].

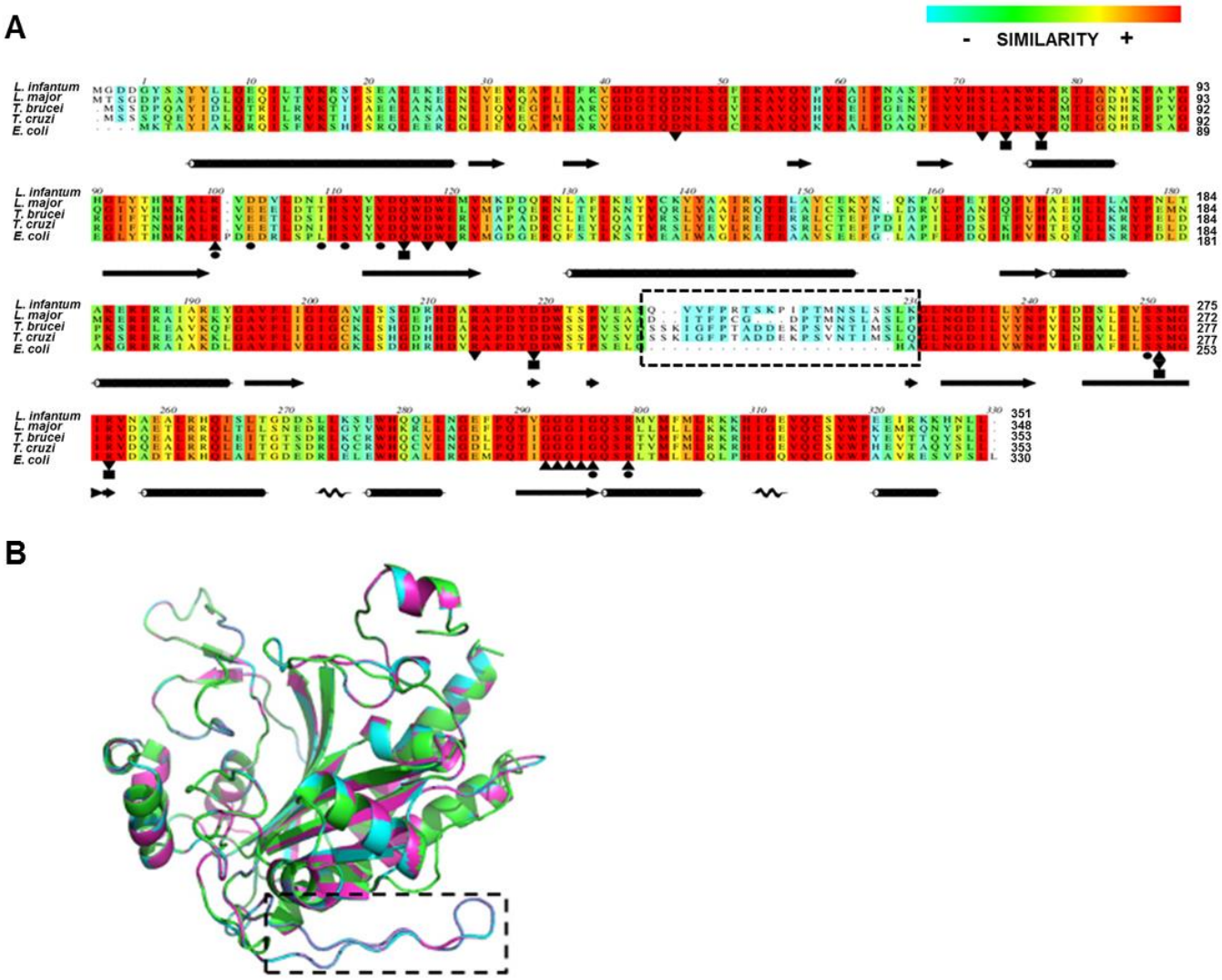

Fig. 1. Multiple-sequence alignment of prokaryote and eukaryote AS-A proteins and 3D homology models of *Li*AS-A and *Lm*AS-A. A) Alignment of *Li*AS-A (NCBI-Gene ID: 5069795/ LinJ.26.0790), *Lm*AS-A (NCBI-Gene ID: 5652811/LmjF.26.0830), *Tb*AS-A (NCBI-GeneID:3658321/ Tb927.7.1110), *Tc*AS-A (NCBI-GeneID:3534325/Tc00.1047053503625.10) and *Ec*AS-A (NCBI-GeneID:948258/pdb:12AS). A pre-established colour pattern was used, according to ALSCRIPT Calcons (Aline version 011208): red, identical residues; orange to blue, scale of conservation of amino acid properties in each column alignment; white, dissimilar residues). Secondary structure components of *Ec*AS-A crystal structure (black) are represented above the alignment. In all sequences, binding residues for several ligands were represented: AMP (circles), asparagine (squares), ATP (triangle) and aspartate (inverted triangle). **B)** Superposition of *Ec*AS-A structure (green) (PDB accession code 12AS), with *Li*AS-A (blue) and *Lm*AS-A (purple) homology models (obtained from the SWISS-MODEL server, using PDB 12AS as a template). The dashed box points a structurally divergent region.

Analysing the homology models of *Li*AS-A and *Lm*AS-A (Fig. 1B) obtained by superimposition with *Ec*AS-A crystal structure (*PDB* 12AS [15]), there is a divergent region

highlighted with a dashed rectangle (Fig. 1B) in *L. infantum* and *L. major* enzymes, which is strictly conserved in these two species. This region also exists in trypanosomes, although little conservation is found when comparing to *Leishmania* spp. (Fig. 1A, [28, 29]).

Enzymatic characterization of *Li*AS-A. Recombinant *Li*AS-A , comprising a 6 histidine N-terminal tag, was expressed in *E. coli* and purified by affinity chromatography in native conditions in order to evaluate and characterize its enzymatic activity. The protein presented the expected MW for the monomer, ~42 kDa, as presented on figure 2A and 2B, with either Coomassie staining or Western-blot analysis with an anti-HisTag antibody, respectively. Subsequently, *Li*AS-A was further purified sequentially by size exclusion and ion exchange chromatographies, and the final fractions were analysed by analytic size exclusion chromatography (Fig. 2C). Using the latter chromatography and calibration standards, Stokes' radius (~3.52 nm, Fig. 2D) and MW (~78.8 kDa, Fig. 2E) were extrapolated in the protein native state. *Li*AS-A corresponds to a homodimer, as predicted.

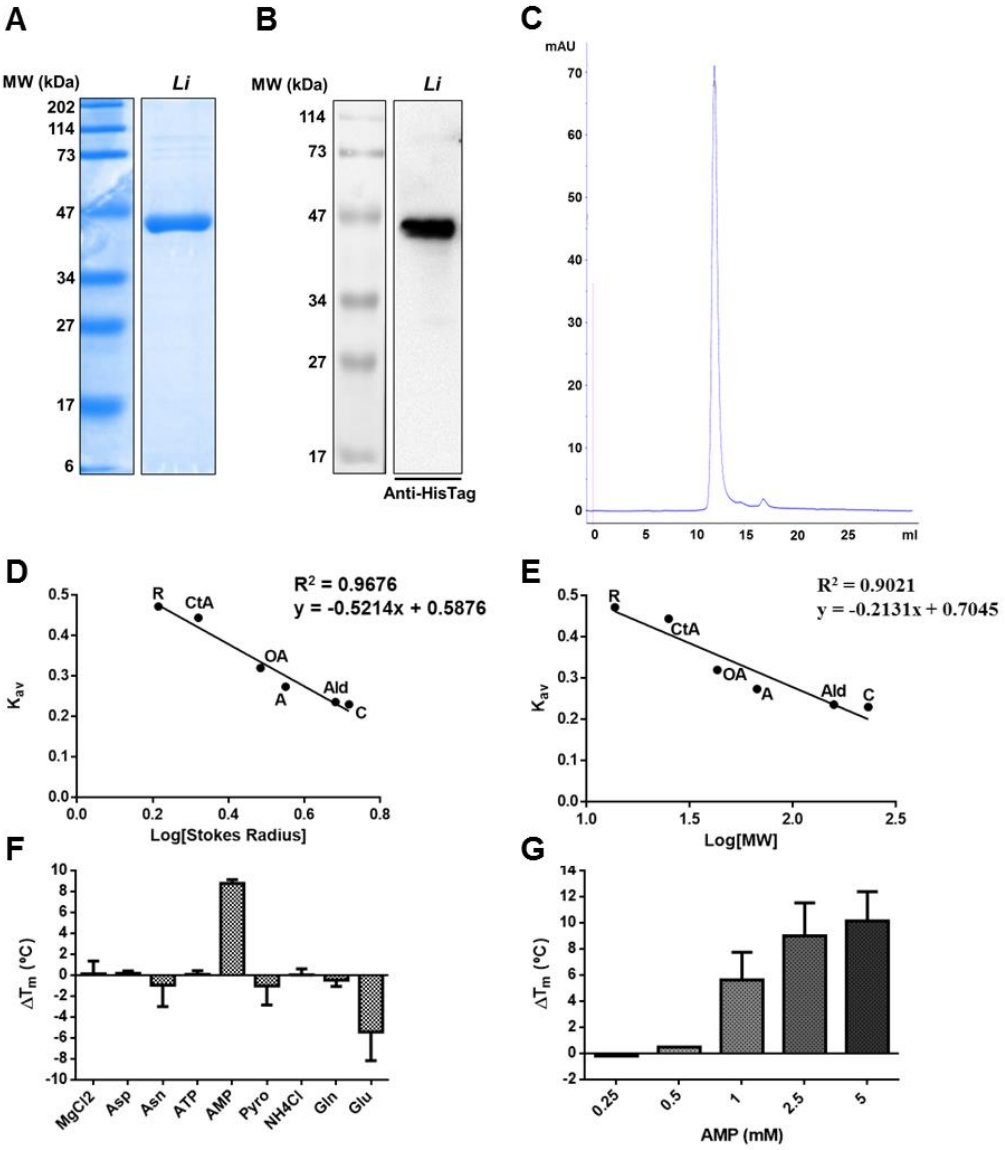

Fig. 2. Analysis of recombinant *Li*AS-A. A) Coomassie blue stained 12% SDS-PAGE gel of 10 µg of recombinant *Li*AS-A post affinity chromatography purification. **B)** Western-blot analysis of 1 µg of purified recombinant *Li*AS-A using a rabbit anti-HisTag monoclonal antibody (1:1000). MW, molecular weight marker. **C)** Analytic size exclusion chromatogram of recombinant *Li*AS-A after purification by affinity, size exclusion and ion exchange chromatographies. **D and E)** Calibration curve for *Li*ASA Stokes' radius and MW determination, respectively. K_{av} was determined considering the elution volume of the proteins used as standards, the total volume of the column and the exclusion volume given by the elution of blue dextran. The used standards were as follows: ribonuclease (R), chymotrypsinogen A (CtA), ovalbumin (OA), albumin (A), aldolase (Ald), catalase (C). Data is representative of two independent experiments. . **F and G)** Differential scanning fluorimetry analysis of recombinant *Li*AS-A in the presence of several ligands, expressed in T_m variation (ΔT_m - ºC) determined as T_m (protein + ligand) – T_m (protein without ligand). **F)** Single ligand effect at 1 mM concentration: ATP, AMP, pyrophosphate (Pyro), ammonium chloride (NH_4Cl), magnesium chloride ($MgCl_2$), asparagine (Asn), aspartate (Asp), glutamate (Glu), glutamine (Gln). **G)** Concentration dependent effect of AMP in *Li*AS-A

stabilization. These results represent the mean values of two independent experiments plus the standard deviation.

For the characterization of the enzymatic activity of recombinant *Li*AS-A , a specific colorimetric assay that quantifies Asn formation was used [28, 45]. The optimal pH for the enzymatic activity was 7.6. The kinetic characterization of the enzyme was undertaken in steady-state conditions, using a fixed concentration of 8.4 mM of Mg^{2+} (Table 1). *Li*AS-A displayed ammonia and glutamine dependent activity.

Table 1. Kinetic parameters of *Li*AS-A for aspartate, ATP, ammonia and glutamine

Substrate	***L. infantum***		
	K_m **(mM)**	k_{cat} **(s^{-1})**	K_{sp}*** ($M^{-1}.s^{-1}$)**
Aspartate	6.21 ± 1.15	9.19 ± 0.69	1.48 x 10^3
ATP	1.47 ± 0.04	4.18 ± 0.02	2.84 x 10^3
Ammonia dependent activity			
Ammonia	1.12 ± 0.16	7.46 ± 0.33	6.66 x 10^3
Glutamine dependent activity			
Glutamine	1.71 ± 0.28	4.51 ± 0.19	2.64 x 10^3

*Specificity Constant (k_{cat} / K_m)
The values are means ± standard deviations obtained from 3 independent experiments

When comparing K_m values for ammonia and glutamine, no statistical significant difference is found (p = 0.03), but there is significance in the differences found in k_{cat} (p = 1.80 x 10^{-4}). In order to discard the possibility that utilization of glutamine as a substrate was an artefact resulting from contamination with *Ec*AS-B (*Ec*AS-B ~120 kDa), highly purified fractions of *Li*AS-A (*Li*AS-A ~84 kDa) were tested and glutamine utilization were clear in all protein samples tested.

Differential scanning fluorimetry was also used in order to further understand the relevance of the different substrates for thermal stabilization of the enzyme. AS-A forms a

crucial β-AspartylAMP-Mg^{2+} intermediate, which then undergoes a nucleophilic attack of ammonia, forming Asn and releasing AMP e pyrophosphate [15]. According to our data, ammonia can be free or glutamine-derived, although the glutaminase domain of *Li*AS-A remains to be identified. Looking at the differential scanning fluorimetry data, AMP leads to a 10 degrees shift in *Li*AS-A T_m, thermally stabilising this protein (Fig. 2F) in a concentration dependent fashion(Fig. 2G).

***LiASA* null mutants generation by targeted gene replacement.** A targeted gene replacement strategy was used for inactivation of the *ASA* gene of *L. infantum*. Two constructs, obtained by fusion PCR, linking *NEO* or *HYG* to the 5' and 3' UTRs of the *LiASA* gene were used to remove the first and second *LiASA* allele, respectively. Two sKO mutants (clones A and B) were transfected with the *HYG* construct. We successfully obtained 5 dKO mutants, 3 from clone A (A1, A2 and A3) and 2 from clone B (B1 and B2). The integration of the resistance markers in the expected locus was confirmed by PCR using primers upstream of the 5' UTR or downstream of the 3'UTR coupled with primers in their ORFs (the strategy is illustrated on Fig. 3A). *NEO* 5' and 3' integration was positive in both sKO and dKO mutants, as for *HYG*, only in dKO parasites, as expected (Fig. 3B). Also by PCR analysis, we could not amplify *LiASA* ORF in null mutants (a non-related gene – *LiRPIB*- was amplified as control – Fig. 3B).

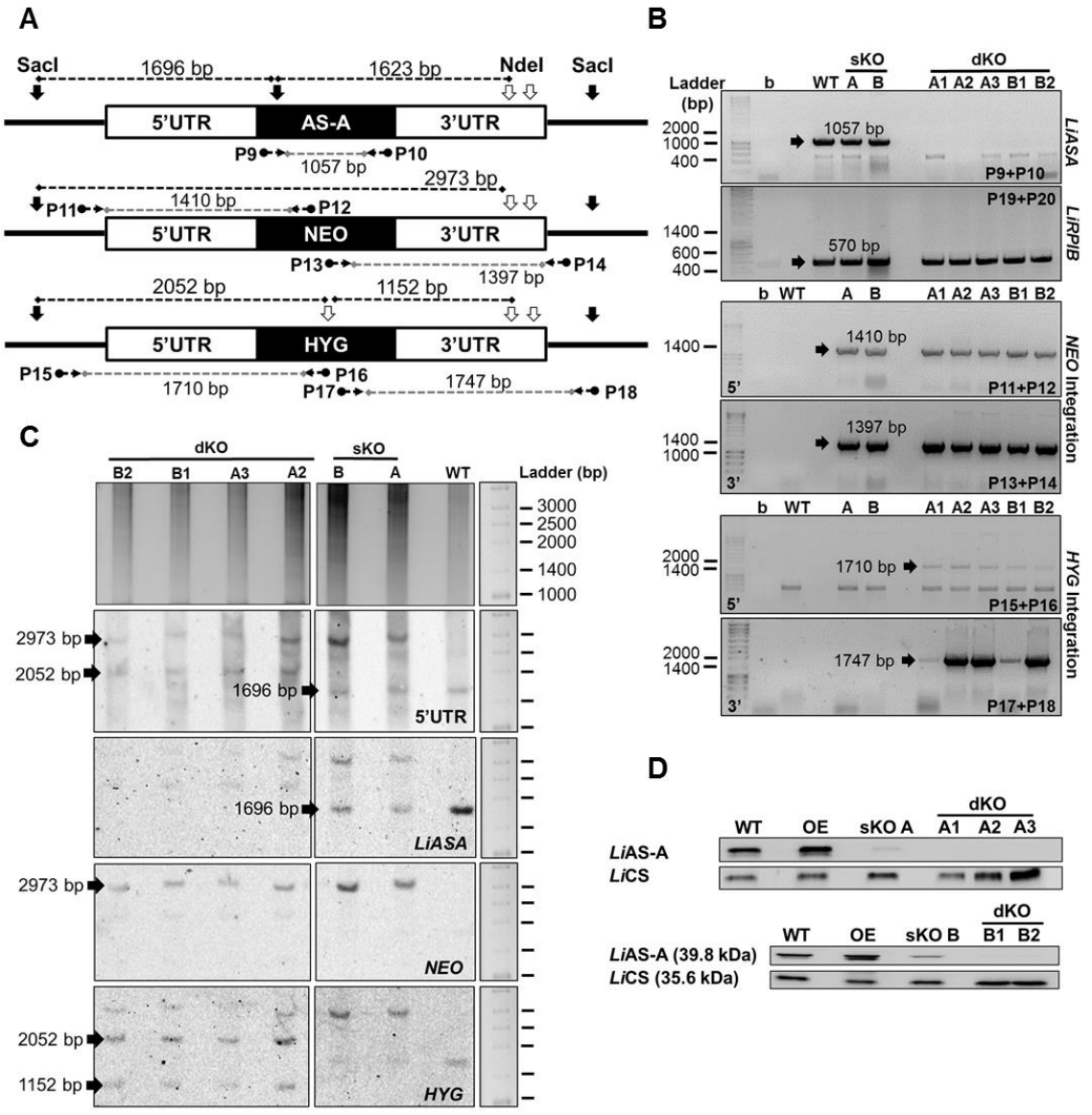

Fig. 3. Genetic and post-translational analysis of the *LiASA* mutants. A) *LiASA* locus schematics: *ASA* allele and targeted gene replacement cassettes, containing *NEO* and *HYG* resistance genes. Horizontal black arrows and numbers represent the primer pairs used to assess the genotype of the mutants: the grey dashed line represents the expected PCR fragment. Southern-blot approach, upon digestion with NdeI (vertical black contoured arrows) and SacI (vertical black full coloured arrows) is also represented: dashed black lines represent the expected digestion fragments. **B)** PCR analysis of *LiASA* mutants to assess *LiASA* presence, *NEO* 5' and 3' integration and *HYG* 5' and 3' integration. Additionally, non-related *LiRPIB* gene from chromosome 28 was amplified as a control. b, blank. **C)** Southern-blot analysis of 10 µg of *LiASA* mutants (*versus* WT) genomic DNA, previously digested with NdeI and SacI, and probed using 5' UTR. Subsequently, the blot was stripped and reprobed 3 additional times, using *LiASA*, *NEO* and *HYG*. **D)** Western-blot analysis of *Li*AS-A expression in promastigote mutants (*versus* WT) using *Li*CS as loading control (cysteine synthase). OE, overexpressor.

Southern-blot analysis confirmed the genotypes: the expected fragments upon digestion with SacI and NdeI are represented on figure 3A. A first hybridisation was performed using 5' UTR as a probe: in WT a single band of ~1696 bp corresponding to *LiASA* was generated, with twice the intensity observed in the sKO mutants that possess a single copy, and absent in the dKO mutants, confirming the successful gene removal (Fig. 3C). In both sKO and dKO clones, a band of ~2973 bp was generated corresponding to *NEO*, and then only in dKO clones, a band of ~2052 bp corresponding to *HYG* was observed (Fig. 3C). The blot was then stripped and reprobed three additional times to confirm each one of the bands (faint bands of incomplete stripping can be observed), sequentially using *LiASA*, *NEO* and *HYG*. All the mutants were also analysed by Western-blot, showing a protein reduction in sKO mutants and a complete absence in the dKO clones (Fig. 3D). *LiASA* gene was cloned into a pSP72*αBLASTα* vector in order to obtain an overexpressor mutant (OE) as well (Fig. 3D).

AS-A is localized in the cytosol of *L. infantum* promastigotes. Rabbit polyclonal antibodies produced against recombinant *Li*AS-A recognised a major band in total WT promastigotes extract with the expected molecular weight (~39.8 kDa [web.expasy.org/protparam], Fig. S1A), but not in a dKO mutant (dKO A2). Prior to immunolocalisation studies, *Li*AS-A antibody was also validated (Fig. S1B) by performing an IFA and comparing the labelling intensity in WT promastigotes *versus LiASA* null mutants and OE. A positive correlation between protein level and fluorescence intensity was found on WT *versus* OE (Fig. S1C). As expected, no specific labelling was detected for the *Li*AS-A null mutants (Fig. S1B and S1C).

Using α-tubulin (~50 kDa) as loading control we compared the expression levels of *Li*AS-A in different developmental stages*:* promastigotes (logarithmic, early stationary and late stationary phase) and axenic amastigotes (Fig. 4A). No significant differences were observed.

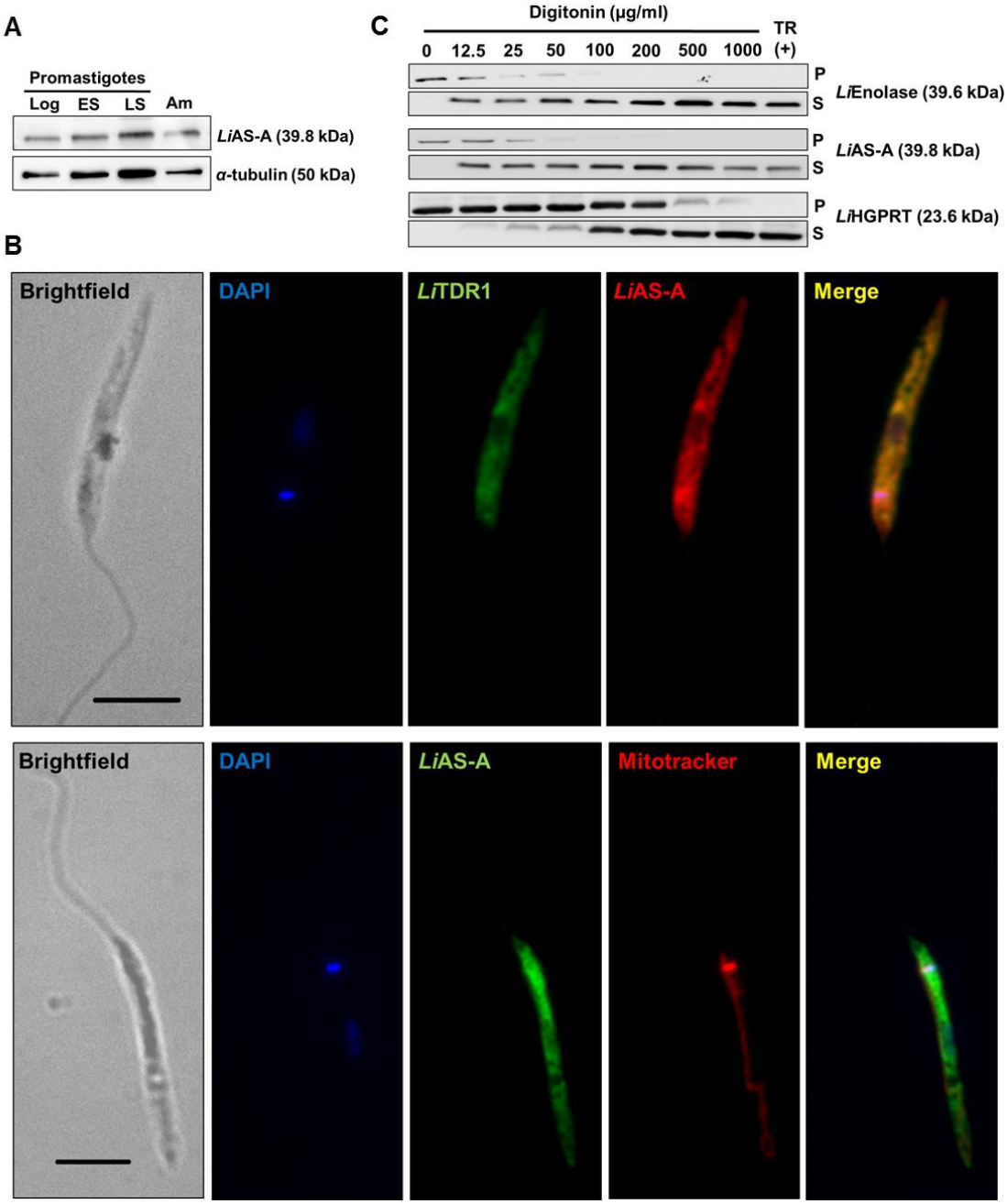

Fig. 4. *Li*AS-A expression and localization in *L. infantum*. A) AS-A expression in different stages of *L. infantum* life cycle. Promastigote forms: logarithmic phase (Log), early stationary phase (ES), late stationary phase (LS); axenic amastigote forms (Am). Twenty µg of total extract were analysed by Western-blot and probed with rabbit polyclonal anti-*Li*AS-A. α-tubulin (mouse monoclonal antibody) was used as loading control. These results are representative of 3 independent experiments. **B)** Immunofluorescence analysis showing AS-A (red upper panel; green lower panel) localization in *L. infantum* promastigote form. Nucleus and kinetoplast DNA, cytosol and mitochondria were stained with DAPI (blue), sheep anti-*Li*TDR1 (thiol-dependent reductase in green) and Mitotracker Orange CMTMROS (red), respectively. Images were acquired with a 100x objective, using a Zeiss AxioImager Z1. The scale bar corresponds to 5 µm. Data is representative of 4 independent experiments. **C)** Digitonin fractionation of mid-log *L. infantum* promastigotes. Pellet (P) and

supernatant (S) fractions obtained using increasing concentrations of digitonin or positive control with 1% of Triton X-100 (TR – Total Release) were subjected to Western-blot analysis and probed with antibodies against *Li*Enolase (cytosolic marker) and hypoxanthine guanine phosphoribosyltransferase *Li*HGPRT (glycosomal marker). Data is representative of 5 independent experiments.

Immunofluorescence analysis showed that in promastigotes *Li*AS-A co-localises with *Li*TDR1 (thiol-dependent reductase 1), which is a cytosolic protein involved in thiol metabolism [49] (Fig. 4B, upper panel). *Li*AS-A subcellular localisation in promastigotes was also assessed by digitonin fractionation. The fractioning profile was evaluated using antibodies for proteins present in different subcellular compartments, namely, anti-*Tb*Enolase (*Li*Enolase *versus Tb*Enolase 79% identity, *Li*Enolase 39.6 kDa) as cytosolic marker [50], and anti-*Ld*HGPRT (hypoxanthine guanine phosphoribosyltransferase, 23.6 kDa) as glycosomal marker [51]. *Li*Enolase (Fig. 4C) can be found in the supernatant for digitonin concentrations as low as 12.5 µg/ml, and retained in the pellets up to 25-50 µg/ml. *Li*HGPRT (Fig. 4C), which localises to the glycosomes, is detected in the supernatant in appreciable amounts for higher digitonin concentrations and is retained longer in the pellet (up to 200-500 µg/ml, and residually at 1000 µg/ml of digitonin). As expected, *Li*AS-A presents a profile similar to *Li*Enolase, supporting a cytosolic location (Fig. 4C).

Intriguingly, *Ld*AS-A was reported to have dual localisation between the cytoplasm and mitochondria in promastigote form [29]. Due to the high identity (~99%) between both enzymes, we investigated whether *Li*AS-A also localised to the mitochondria. Immunofluorescence analysis of *Li*AS-A subcellular distribution on promastigotes labelled with mitotracker showed no evidence of mitochondrial location (Fig. 4B, lower panel). Moreover, by using tools for protein localisation prediction (TargetP, CELLO, MITOPROT and Predotar), mitochondria localisation seems unlikely and actually, CELLO predicts cytoplasmic localisation. In conclusion, our data shows *Li*AS-A localises to the cytosol.

***Li*AS-A is required for promastigotes growth only in asparagine limiting conditions.** All mutants displayed similar growth patterns comparing to WT promastigotes in cRPMI (Fig. 5A). However, in Asn depleted medium, achieved upon L-asparaginase treatment (cRPMI + L-asparaginase), the behaviour was quite different for some of the mutants. Parasites overexpressing *Li*AS-A displayed a significant higher growth during log phase when comparing to the WT, whereas the dKO mutants (clones A2 and B1) displayed a major growth defect (Fig. 5B). The complementation of these null mutants with an episome (pSP72α*BLAST*α) carrying *LiASA* gene rescued the growth (Fig. 5B). Moreover, an upregulation in *Li*AS-A levels could be observed in these mutants in Asn limiting conditions (Fig. 5C). Western-blot analysis also showed that in the same conditions, an upregulation

in *Li*AS-A could also be observed over time in the sKO parasites (clones A and B), enabling the growth recovery in these mutants (Fig. 5B, C, D and Table S3). This recovery was faster in sKO clone B that had higher basal levels of *Li*AS-A than clone A (Fig. 5B and 5C). We also evaluated the cumulative growth under constant multiplicative conditions, in which high amino acids levels are required. For that, parasites were maintained in log phase in Asn replete or Asn depleting conditions, and the same patterns were observed (Fig. S2).

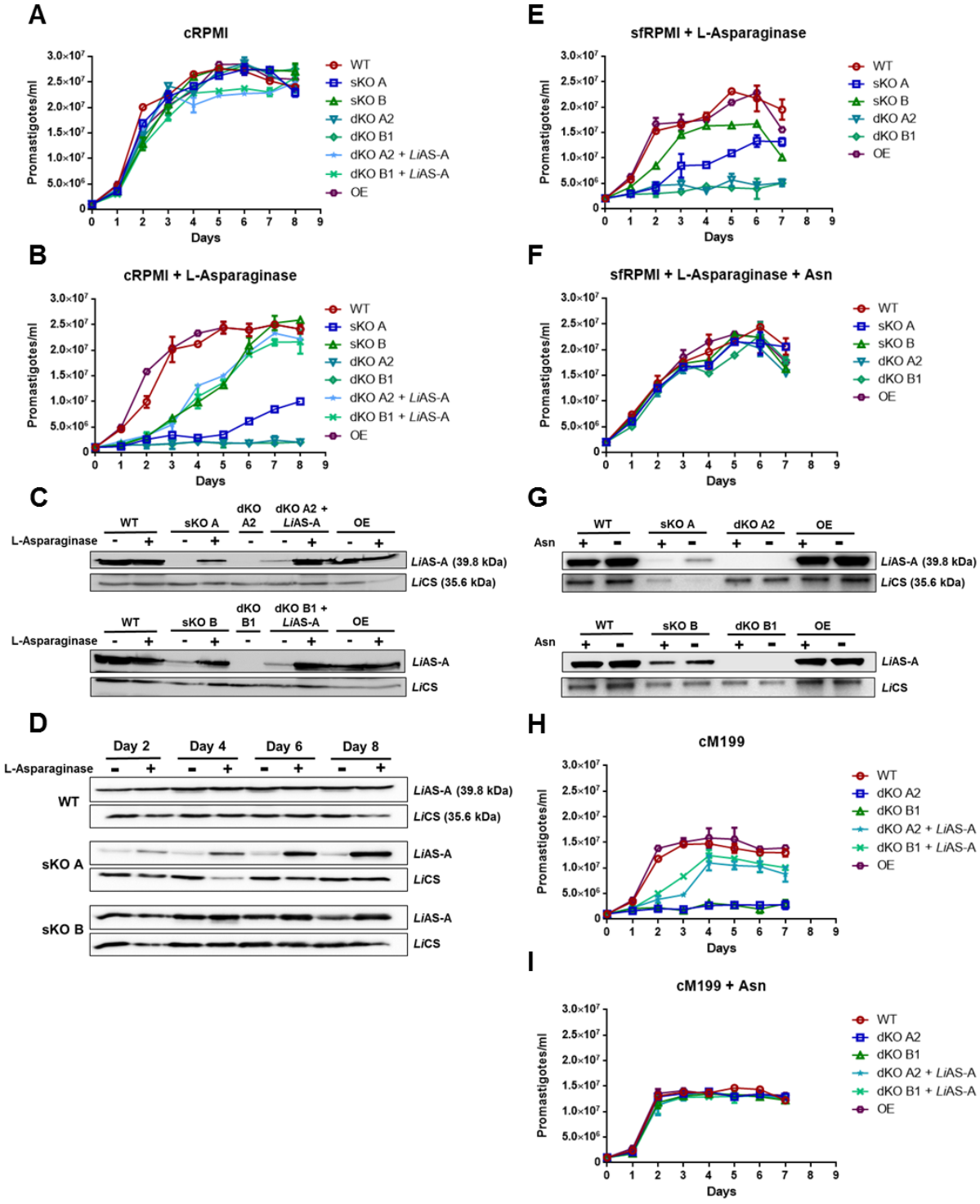

Fig. 5*. In vitro* growth of *LiASA* mutants in normal or Asn depleted medium and respective *Li*AS-A expression levels. A and B) *L. infantum* promastigote growth curves in cRPMI or cRPMI + L-asparaginase, respectively, including dKO mutants (clones A2 and B1) complemented with pSPα*BLAST*α carrying *LiASA* gene. In B, a significant growth difference in comparison to WT ($p < 0.05$, Graphpad Prism 5.0 version) was found for sKO A, sKO B, dKO A2 and B1, dKO A2 + *Li*AS-A, dKO B1 + *Li*AS-A and OE mutants for days 1 to 8, days 1 to 6, days 1 to 8, days 2 to 6, days 2 to 7 and day 3, respectively. **C)** Western-blot analysis of *Li*AS-A expression in 7 days old *LiASA* mutants (*versus* WT) cultured in cRPMI and cRPMI + L-asparaginase. **D)** Western-blot analysis of *Li*AS-A expression levels over time in WT, and clones A and B cultured in cRPMI (lane L-asparaginase -) or cRPMI + L-asparaginase (lane L-asparaginase +). **E and F)** *L. infantum* promastigote growth curves in sfRPMI + L-asparaginase or sfRPMI + L-asparaginase + Asn, respectively. sfRPMI was Asn depleted through incubation with L-asparaginase, which was then removed by flowing the medium through an Amicon Column of 3 kDa pore (sfRPMI + L-asparaginase). Asn was then added directly to the medium (sfRPMI + L-asparaginase + Asn). In E, a significant growth difference in comparison to WT ($p < 0.05$, Graphpad Prism 5.0 version) was found for sKO A, sKO B and dKO A2 and B1 mutants for days 2 to 7, days 2 and 5 to 7 and days 2 to 7, respectively. **G)** Western-blot analysis of *Li*AS-A expression in 7 days old *LiASA* mutants (*versus* WT) cultured in sfRPMI + L-asparaginase (lane Asn -) and sfRPMI + L-asparaginase + Asn (lane Asn +). **H and I)** *L. infantum* promastigote growth curves in cM199 and cM199 + Asn, respectively, including dKO mutants complemented with pSPα*BLAST*α carrying *LiASA* gene. In H, a significant growth difference in comparison to WT ($p < 0.05$, Graphpad Prism 5.0 version) was found for dKO A2 and B1, dKO A2 + *Li*AS-A and dKO B1 + *Li*AS-A mutants for days 1 to 7, days 2 and 3, days 1 to 3, respectively. The results (A-I) are representative of 2 independent experiments. For the Western-blot analysis displayed in C, D and G, $1x10^7$ parasites were used for total extract preparation and *Li*CS (cysteine synthase) was used as loading control. OE, overexpressor.

To ensure the defective growth phenotype of sKO and dKO parasites in L-asparaginase treated medium was due to Asn depletion, we supplemented this medium with Asn. Surprisingly the addition of this amino acid to L-asparaginase treated RPMI medium fails to reverse the observed growth delay/arrest phenotype. The fact that L-asparaginase was not inactivated or neutralized, and consequently may have remained active, may explain this result. Consequently, we used another strategy by undertaking growth curves in a serum free medium (sfRPMI [46]) incubated with L-asparaginase that was removed afterwards using a 3 kDa Amicon column. In sfRPMI devoid of Asn (sfRPMI + L-asparaginase), the same growth defect of the sKO and dKO mutants was observed (Fig. 5E). And then again, in the sKO clones the upregulation of *Li*AS-A allowed the growth rescue (Fig. 5G, Table S3). When adding back Asn (sfRPMI + L-Asparaginase + Asn), all mutants grew in a similar fashion (Fig. 5F). In the absence of drug pressure and in normal conditions, parasites provided of an episome carrying *LiASA* (OE) hardly overexpress AS-A, however, under Asn depleting conditions, they upregulate its expression (comparing to

the levels in the WT, there is an increase from ~130% to ~300% and from ~110 to ~130%, in panels C and G, respectively, and Table S3).

Moreover, besides the experiments using L-asparaginase treatment, we have also performed growth curves in a medium formally lacking Asn – complete M199 (cM199) - in order to further confirm Asn auxotrophy upon *ASA* ablation. In this medium, null mutants presented a growth defect comparable to the one observed in cRPMI + L-asparaginase, which again was reversed when these mutants were complemented with an ectopic copy of *ASA* gene (Fig. 5B *versus* 5H). The addition of Asn to the final concentration of 380 µM (like in RPMI) rescues the growth defect displayed by the null mutants in cM199 (Fig. 5I). Interestingly, the experiments to assess *Li*AS-A essentiality in *L. donovani* were performed in cM199 [29], therefore the inability to generate *LdASA* null mutants may be due to the performance of those attempts in Asn limiting conditions.

In conclusion, *ASA* deletion renders parasites auxotrophic to Asn, but is dispensable for parasite growth in normal conditions.

***In vivo* infectivity of *LiASA* mutants.** Notwithstanding, we intended to evaluate the impact of *LiASA* ablation on, *in vivo* infectivity. Five to six old female BALB/c mice were infected and were sacrificed at 2 weeks post-infection. The parasite burden in the spleen (Fig. 6A) and liver (Fig. 6B) was not statistically different in *LiASA* mutants when compared to the WT. The same scenario was observed for sKO A and dKO A2 mutants. No differences in *Li*AS-A expression levels were found when comparing parasites used in mice infection (Culture) to parasites recovered from spleen (S) or liver (L) (Fig. 6C). Thus, *Li*AS-A ablation does not compromise parasite infectivity in the context of an acute *in vivo* infection.

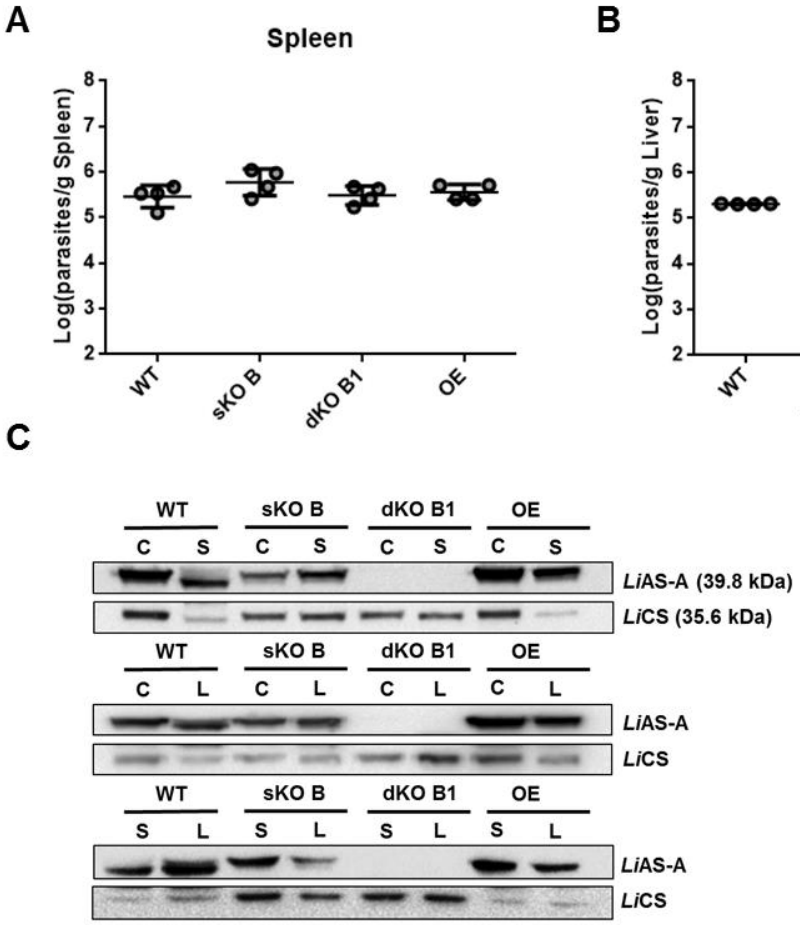

Fig. 6. ***In vivo*** **infectivity of *LiASA* mutants in mice. A and B)** Stationary promastigotes were intra-peritoneally injected in BALB/c mice that were sacrificed 2 weeks post infection, in order to determine parasite burden in spleen (A) and liver (B). The values represent the means of four independent animals ± standard deviation **C)** Western-blot analysis of *Li*AS-A levels in WT and *LiASA* mutants: parasites maintained in culture (C) comparing with parasites recovered from spleen (S) or liver (L). The data is representative of 2 independent experiments carried out with 2 different clones for each genotype. For the Western-blot analysis displayed in C, $1x10^7$ parasites were used for total extract preparation and *Li*CS (cysteine synthetase) was used as loading control. OE, overexpressor.

Discussion

Despite being eukaryotes, trypanosomatids, present AS-A enzymes of bacterial origin. Moreover, these enzymes are aminoacyl-tRNA synthetase paralogs, displaying an AsnRS catalytic core with conserved class II motifs, yet lacking the tRNA binding domain [27]. In this work, we have demonstrated that *Li*AS-A is able to synthesise Asn using either ammonia or glutamine as nitrogen donors, as previously described for *Tb*AS-A, *Tc*AS-A and *Ld*AS-A [28, 29]. K_m values for aspartate and ATP are close to the ones determined for *Tb*AS-A and *Tc*AS-A [27]. As for ammonia, the K_m value found for *Li*AS-A is 5 fold lower in

comparison to *Tb*AS-A, *Tc*AS-A and *Ld*AS-A [27, 28]. In the case of *Ld*AS-A, the K_m values for aspartate were around 10 fold lower [29] than the ones obtained for *Li*AS-A. Regarding the high conservation of the active sites among *Leishmania* AS-A enzymes, we cannot exclude that the observed kinetic differences may be due to the differences in the amount of protein that is properly folded, especially taking into account they are expressed in a heterologous system. Moreover, it is important to emphasize that the kinetic determinations for *Ld*AS-A were performed using a different experimental set up. Importantly, *Tb*AS-A and *Tc*AS-A use preferably ammonia [28], whereas *Li*AS-A seems to use both roughly in the same extent (Table 1). AS-A activity in trypanosomatids more resembles AS-B enzymes, concerning both the optimal pH for enzymatic activity (7.6 instead of 8) and also the ability to use both nitrogen donors. AS-B enzymes use preferably glutamine, with exception of the human enzyme that presents approximately the same affinity for both nitrogen sources [18, 19, 25, 52-57]. This biochemical feature, so far only described for trypanosomatids AS-A enzymes [28, 29], becomes particularly interesting in the context of the presence of an ORF encoding a hypothetical, yet non-classical, AS-B, in the genome of these organisms (*L. infantum* [LinJ.29.1590], *L. major* [LmjF.29.1490], *T. brucei* [Tb927.3.4060] and *T. cruzi* [Tc00.1047053510001.40]) [42-44]. These sequences contain a Pfam AS domain (pfam00733) and glutamine hydrolysing domains in the C and N-terminus, respectively. BLASTp analysis of *L. infantum* sequence, for instance, revealed several hits that corresponded to hypothetical proteins from a broad range of eukaryotes. However, we have no evidence AS-B is functional at all.

Much remains to be disclosed regarding the AS-A enzymes from trypanosomatids, for instance, we still lack information on their glutamine binding and hydrolysing sites. *Tb*AS-A crystallisation only emphasised the high conservation of Asn and AMP binding pockets, as the only divergent region from *Ec*AS-A (a 19 residues insertion, also present in *Li*AS-A and *Lm*AS-A, Fig. 1) was not visible in the experimental electron density maps and therefore likely disordered [29]. This insertion displays little conservation when comparing *Leishmania* and trypanosomes, and its role on a structural or functional level is still unclear.

AS-A is a key enzyme in Asn metabolism that was proposed as a potential drug target due to its absence in the human host. Moreover, AS-A was reported to be essential for *L. donovani* survival, contrasting with *T. brucei* bloodstream forms, as in the latter it was shown to be dispensable for both *in vitro* growth and infectivity. These findings pointed to a differently regulated Asn homeostasis across trypanosomatids. In *L. infantum*, our efforts to generate *ASA* null mutants were successful, indicating the gene is not essential for survival. Moreover, the null mutants did not present any growth or infectivity defect. Our *in vitro* growth data demonstrate that upon *LiASA* deletion, promastigotes become dependent on

extracellular Asn for optimal growth (Fig. 5). These results suggest that even if AS-B is functional, it does not compensate *Li*AS-A activity, as *LiASA* null mutants fail to grow in Asn limiting conditions. Additionally, WT parasites grew normally in Asn depleted medium without AS-A upregulation, suggesting Asn synthesis by basal AS-A suffices the cellular needs, although the mutants overexpressing this enzyme had a metabolic advantage in an Asn deprivation environment during log phase (Fig. S2B and S2E). We can actually infer the parasite can both synthesise and take up this amino acid, and the latter fully compensates the former. Furthermore, our results indicate that *Li*AS-A levels are regulated according to Asn availability, and it was equally surprising to see how fast and efficiently sKO mutants were able to upregulate AS-A when cultured in Asn limiting conditions (Fig. 5D). It is also noteworthy that the two sKO mutants displayed a substantial difference in AS-A levels, which has also been observed among other sKO mutants generated in this study. A possible explanation might be that the two allelic copies may differently affect *ASA* expression.

In trypanosomatids, much remains to be unravelled concerning amino acid transporters (AATs) and mostly the pathways involved in amino acid sensing and regulation of their synthesis and uptake [34]. Very few data is available in the literature concerning Asn transport in these parasites. In *T. brucei*, a protein presenting putative orthologues in *Leishmania* [42-44] was characterized as a transporter of several neutral amino acids, including asparagine (*Tb*AATP1) [58]. In mammalian cells, AS-B is a transcriptional target of the well characterized GCN2/eIF2α/ATF4 axis, in response to amino acid starvation [59, 60]. The phosphorylation of eIF2 leads to a repression of general protein synthesis, as well as an activation of gene-specific translation. In *Saccharomyces cerevisiae*, GCN2, which is activated by amino acid, glucose or purine deprivation, is the only eIF2 kinase, contrasting with mammals that possess some additional three, HRI, PKR and PEK/PERK [61]. *T. brucei* and *L. donovani* PERK orthologues [62, 63] have been implicated in the response to ER stress and their activation leads to a decrease in the overall translation [62]. At the moment, it is still not clear whether phosphorylation of eIF2 in trypanosomatids would result in a downstream signalling cascade, as bZIP type transcription factors, that could act like GCN4 or ATF4, are absent in these organisms [64].

The close relation between *L. infantum* and *L. donovani* species and the 99% identity of AS-A between both makes the discrepant phenotype intriguing. In the literature, several cases in which knocking out a gene can have different impact on virulence depending on the species can be found. [65]. Nevertheless, to our knowledge, there is no documented example among cutaneous or among visceral species of a gene that is detrimental for survival in one species and dispensable in other closely related species.

However, we did find a case of differences at a strain level for instance [66]. Nonetheless, firstly we must highlight that *LdASA* essentiality was claimed solely based on the consecutive failure in the removal of the second gene copy [29]. Secondly, our results suggest that the medium in which the experiments were performed, cM199, may explain this difference. The former lacks Asn and *LiASA* null mutants could not grow unless upon Asn supplementation (Fig. 5H and 5I). These results reinforce the importance of the medium composition when attempting gene knock-out of metabolic enzymes, and supplementation may be detrimental when potentially generating auxotrophs [67, 68].

LiASA dKO mutants displayed no compromised infectivity in mice, suggesting that in intracellular amastigote form, either AS-B is functional or, most likely, parasites are able to uptake Asn in such an extent that compensates the lack of intracellular synthesis. *In vivo* treatment with L-asparaginase, which induces a decrease in Asn bloodstream levels, has been successfully used for years in the treatment of acute lymphoblastic leukemia [69] and recently it was proposed as a promising strategy to treat bacteremia caused by group A *Streptococcus* and eventually other extracellular bacteria [13]. However, if for some extracellular pathogens, L-asparaginase treatment seems promising, in the case of an obligate intracellular microorganism, even when simultaneously inhibiting the microbial AS-A, several issues may arise, namely the potential contribution of the host cell for Asn *de novo* synthesis.

Taken all together, we conclude AS-A is not a suitable drug target candidate in *L. infantum*, and therefore, with regard to drug development, such a protein target becomes pointless against *Leishmania*.

Acknowledgements

We would like to thank Dr. Paul Michels from Université Catholique de Louvain, Belgium, for providing *Tb*enolase antibody; Professor Graham Coombs, Strathclyde University, Glasgow, for *Lm*CS antibody; Professor Buddy Ullman, School of Medecine, Oregan Health and Science University, USA, for *Ld*HGPRT antibody; Dr Christine Clayton, Zentrum fur Molekulare Biologie der Universitat Heidelberg, Germany, for *Tb*Aldolase antibody and Professor Ana Tomás, IBMC, Portugal, for providing mTXNPx antibody. We would also like to thank Professor Jeremy Mottram, University of Glasgow, for pGL345*HYG* and Dr Marc Ouellette, Centre de Recherche en Infectiologie, of Laval University, Canada, for pSPα*NEO*α and pSPα*BLAST*α. Moreover, a special acknowledgement to Dr Frederico Silva, Protein Purification Unit, IBMC, Portugal, for technical support and critical discussion and Professor Pedro Pereira, IBMC, Portugal for critical discussion.

Conflict of Interest

The authors declare no conflict of interest.

Author Contributions

JF IL JT NS and ACdS conceived and designed the experiments. JF and IL performed the experiments and analyzed the data. JF IL JT NS SMR ACdS critically discussed the results. ACdS and SMR contributed with reagents, materials and analysis tools. JF IL JT NS SMR ACdS wrote the paper. All the authors reviewed the results and approved the final version of the manuscript.

Funding

The research leading to these results has received funding from: the European Community's Seventh Framework Programme under grant agreement No.602773 (Project KINDRED) and Fundação para a Ciência e Tecnologia (FCT)/Ministério da Educação e Ciência (MEC) cofunded by FEDER, partnership agreement PT2020, through the Research Unit No.4293. The COST Action CM1307: Targeted chemotherapy towards diseases caused by endoparasites has also contributed for this work. We would like to acknowledge FTC for supporting Joana Faria (SFRH/BD/79712/2011) and Inês Loureiro (SFRH/BD/64528/2009). Inês Loureiro was also supported by the European Community's Seventh Framework Programme (KINDRED-PR300102-BD). JT is an Investigator FCT funded by National funds through FCT and co-funded through European Social Fund within the Human Potential Operating Programme. Nuno Santarem is supported by a fellowship from the European Community's Seventh Framework Programme under grant agreements No. 602773 (Project KINDRED).

References

[1] Mougneau E, Bihl F and Glaichenhaus N (2011) Cell biology and immunology of Leishmania. Immunological Reviews 240: 286–296.

[2] Kedzierski L (2010) Leishmaniasis vaccine: where are we today? Journal of Global Infectious Diseases 2: 177–185.

[3] Maltezou HC (2010) Drug resistance in visceral leishmaniasis. Journal of Biomedicine and Biotechnology 617521.

[4] Leishmaniasis. 2014. Available: http://www.who.int/topics/leishmaniasis/en/. Accessed July 12, 2015.

[5] Zhang J, Fan J, Venneti S, Cross JR., Takagi T, Bhinder B, *et al.* (2014) Asparagine plays a critical role in regulating cellular adaption to glutamine depletion. Molecular Cell 56: 205-218.

[6] Ubuka T and Meister A (1971) Studies on the utilization of asparagine by mouse leukemia cells. Journal of National Cancer Institute 46: 291-298.

[7] Hofreuter D, Novik V, Galan JE (2008) Metabolic diversity in *Campylobacter jejuni* enhances specific tissue colonization. Cell Host Microbe 4: 425–433.

[8] Kullas AL., McClelland M, Yang HJ, Tam JW, Torres A, Porwollik S, *et al.* (2012) L-asparaginase II produced by *Salmonella typhimurium* inhibits T cell responses and mediates virulence. Cell Host Microbe 12: 791–798.

[9] Leduc D, Gallaud J, Stingl K, de Reuse H (2010) Coupled amino acid deamidase-transport systems essential for *Helicobacter pylori* colonization. Infection and Immunity 78: 2782–2792.

[10] Scotti C, Sommi P, Pasquetto MV, Cappelletti D, Stivala S, Mignosi P, *et al.* (2010) Cell cycle inhibition by *Helicobacter pylori* L-asparaginase. PLoS One 5: e13892.

[11] Shibayama K, Takeuchi H, Wachino J, Mori S, Arakawa Y (2011) Biochemical and pathophysiological characterization of *Helicobacter pylori* asparaginase. Microbiology and Immunology 55: 408–417.

[12] Gouzy A, Larrouy-Maumus G, Bottai D, Levillain F, Dumas A, Wallach JB *et al.* (2014) *Mycobacterium tuberculosis* exploits asparagine to assimilate nitrogen and resists stress during infection. Plos Pathogens 10: e1003928.

[13] Baruch M, Belotserkovsky I, Hertzog BB, Ravins M, Dov E, McIver KS *et al.* (2014) An extracellular bacterial pathogen modulates host metabolism to regulate its own sensing and proliferation. Cell 156: 97-108.

[14] Gesbert G, Ramond E, Rigard M, Frapy E, Dupuis M, Dubail I. *et al.* (2014) Asparagine assimilation is critical for intracellular replication and dissemination of *Francisella*. Cellular Microbiology 16: 434-449.

[15] Nakatsu T, Kato H, Oda J (1998) Crystal structure of asparagine synthetase reveals a close evolutionary relationship to class II aminoacyl-tRNA synthetase. Nature Structural Biology 5: 15-19.

[16] Sugiyama A, Kato H, Nishioka T, and Oda J (1992) Overexpression and purification of asparagine synthetase from *Escherichia coli*. Bioscience, Biotechnology and Biochemistry 56: 376-379.

[17] Humbert R, Simoni RD (1980) Genetic and biomedical studies demonstrating a second gene coding for asparagine synthetase in *Escherichia coli*. Journal of Bacteriology 142: 212-220.

[18] Andrulis IL, Chen J, Ray PN (1987) Isolation of human cDNAs for asparagine synthetase and expression in Jensen rat sarcoma cells. Molecular Cell Biology 7: 2435-2443.

[19] Andrulis, I. L., Shotwell, M., Evans-Blackler, S., Zalkin, H., Siminovitch, L., Ray, P. N. (1989) “Fine structure analysis of the Chinese hamster AS gene encoding asparagine synthetase.”, *Gene*, 80, 75-85.

[20] Ramos F, Wiame JM (1980) Two asparagine synthetases in *Saccharomyces cerevisiae*. *European* Journal of Biochemistry 108: 373-377.

[21] Merchant SS, Prochnik SE, Vallon O, Harris EH, Karpowicz SJ, *et al*. (2007) The *Chlamydomonas* genome reveals the evolution of key animal and plant functions. Science 318: 245-250.

[22] GC (2003) Primary N-assimilation into amino acids in Arabidopsis. The Arabidopsis Book: American Society of Plant Biologists, Rockville. 17 p.

[23] Scofield MA, Lewis W, Schuster SM (1990) Nucleotide sequence of *Escherichia coli* asnB and deduced amino acid sequence of asparagine synthetase B. Journal Biological Chemistry 265: 12895-12902.

[24] Nakamura M, Yamada M, Hirota Y, Sugimoto K, Oka A, Takanami M (1981) Nucleotide sequence of the asnA gene coding for asparagine synthetase of *E. coli* K-12. Nucleic Acids Research 9: 4669-4676.

[25] Reitzer LJ, Magasanik B (1982) Asparagine synthetases of *Klebsiella aerogenes*: properties and regulation of synthesis. Journal of Bacteriology 151: 1299-1313.

[26] Blaise M, Frechin M, Olieric V, Charoon C, Sauter C, Lirber B, *et al.* (2011) Crystal structure of the archaeal asparagine synthetase: interrelation with aspartyl-tRNA and asparaginyl-tRNA synthetases. Journal of Molecular Biology 412: 437-452.

[27] Gowri VS, Ghosh I, Sharma A, Madhubala R (2012) Unusual domain architecture of aminoacyl tRNA synthetases and their paralogs from *Leishmania major*. BMC Genomics 13: 621.

[28] Loureiro I, Faria J, Clayton C, Ribeiro SM, Roy N, Santarém N, *et al.* (2013) Knockdown of Asparagine Synthetase A Renders *Trypanosoma brucei* Auxotrophic to Asparagine. Plos Neglected Tropical Diseases 7: e2578.

[29] Manhas R, Tripathi P, Khan S, Lakshmi BS, Lal SK., Gowri VS, *et al.* (2014) Identification of functional characterization of a novel bacterial type asparagine synthetase A: a tRNA synthetase paralog from *Leishmania donovani.* Journal of Biological Chemistry289: 12096-12108.

[30] Boyce JD, Wilkie I, Harper M, Paustian ML, Kapur V, Adler B (2002) Genomic scale analysis of *Pasteurella multocida* gene expression during growth within the natural chicken host. Infection and Immunity 70: 6871-6879.

[31] Ren H, Liu J (2006) AsnB is involved in natural resistance of *Mycobacterium smegmatis* to multiple drugs. Antimicrobial Agents and Chemotherapy 50: 250-255.

[32] Sassetti CM, Boyd DH, Rubin EJ (2003) Genes required for mycobacterial growth defined by high density mutagenesis. Molecular Microbiology 48: 77-84.

[33] Griffin JE, Gawronski JD, Dejesus MA, Ioerger TR., Akerley BJ, Sassetti CM (2011) High-resolution phenotypic profiling defines genes essential for mycobacterial growth and cholesterol catabolism. PLoS Pathogens 7: e1002251.

[34] Jackson AP (2007) Origins of amino acid transporter loci in trypanosomatid parasites. BMC Evolutionary Biology 7 doi:10.1186/1471-2148-7-26.

[35] Williams RAM, Westrop GD, Coombs GH (2009) Two pathways for cysteine biosynthesis in *Leishmania major.* Biochemical Journal 420: 451-462.

[36] Moreira D, Santarém N, Loureiro I, Tavares J, Silva AM, Amorim AM *et al.* (2012) Impact of Continuous Axenic Cultivation in *Leishmania infantum* Virulence. Plos Neglected Tropical Diseases 6: e1469.

[37] Larkin MA, Blackshields G, Brown NP, Chenna R, McGettigan PA, McWilliam H, *et al.* (2007) Clustal W and Clustal X version 2.0. Bioinformatics 23: 2947-2948.

[38] Bond CS, Schuttelkopf AW (2009) ALINE: a WYSIWYG protein-sequence alignment editor for publication-quality alignments. Acta Crystallographic D Biological Crystallogaphyr 65: 510-512.

[39] Arnold K, Bordoli L, Kopp J, Schwede T (2006) The SWISS-MODEL workspace: a web-based environment for protein structure homology modelling. Bioinformatics 22: 195-201.

[40] Kiefer F, Arnold K, Kunzli M, Bordoli L, Schwede T (2009) The SWISS-MODEL Repository and associated resources. Nucleic Acids Research 37: D387-392.

[41] Peitsch MC, Wells TN, Stampf DR, Sussman JL (1995) The Swiss-3DImage collection and PDB-Browser on the World-Wide Web. Trends Biochemical Science 20: 82-84.

[42] Ivens AC, Peacock CS, Worthey EA, Murphy L, Aggarwal G (2005) The Genome of the Kinetoplastid Parasite, *Leishmania major.* Science 309: 436-442.

[43] El-Sayed NM, Myler PJ, Blandin G, Berriman M, Crabtree J, *et al.* (2005) Comparative genomics of trypanosomatid parasitic protozoa. Science 309: 404-409.

[44] Aurrecoechea C, Brestelli J, Brunk BP, Fischer S, Gajria B (2010) EuPathDB: a portal to eukaryotic databases. Nucleic Acid Research 38: D415-419.

[45] Sheng S, Kraft JJ, Schuster SM (1993) A specific quantitative colorimetric assay for L-asparagine. Analytical Biochemistry 211: 242-249.

[46] Santarém N, Racine G, Silvestre R, Cordeiro-da-Silva A, Ouellette M (2013) Exoproteome dynamics in *Leishmania infantum.* Journal of Proteomics 84: 106-18.

[47] Silvestre R, Cordeiro-da-Silva A, Santarém N, Vergnes B, Sereno D, Quaissi A (2007) SIR2-deficient *Leishmania infantum* induces a defined IFN-gamma/IL-10 pattern that correlates with protection. Journal of Immunology 179: 3161-3170.

[48] Cull B, Godinho JLP, Rodrigues JCF, Frank B, Schurigt U, Williams RAM, *et al.* (2015) Glycosome turnover in *Leishmania major* is mediated by autophagy. Autophagy 12: 2143-2157.

[49] Silva AM, Tavares J, Silvestre R, Quaissi A, Coombs GH, Cordeiro-da-Silva A (2012) Characterization of *Leishmania infantum* thiol-dependent reductase 1 and evaluation of its potential to induce immune protection. Parasite Immunology 34: 345-350.

[50] Gupta R, Kumar V, Kushawaha PK, Tripathi CP, Joshi S, Sahasrabuddhe AA, *et al.* (2014) Characterization of glycolytic enzymes-rAldolase and rEnolase of *Leishmania donovani*, identified as Th1 stimulatory proteins, for their immunogenicity and immunoprophylactic efficacies against experimental visceral leishmaniasis. Plos one 9: e86073.

[51] Shih S, Hwang HY, Carter D, Stenberg P, Ullman B (1998) Localization and targeting of the *Leishmania donovani* Hypoxanthine-Guanine Phosphoribosyltransferase to the glycosome. Journal of Biological Chemistry 273: 1534-1541.

[52] Cedar H, Schwartz JH (1969) The asparagine synthetase of *Escherichia coli*. II. Studies on mechanism. Journal of Biological Chemistry 244: 4122-4127.

[53] Cedar H, Schwartz JH (1969) The asparagine synthetase of *Escherichia coli*. I. Biosynthetic role of the enzyme, purification, and characterization of the reaction products. Journal of Biological Chemistry 244: 4112-4121.

[54] Larsen TM, Boehlein SK, Schuster SM, Richards NG, Thoden JB, Holden HM, et al. (1999) Three-dimensional structure of *Escherichia coli* asparagine synthetase B: a short journey from substrate to product. Biochemistry 38: 16146-16157.

[55] Boehlein SK, Richards NG, Schuster SM (1994) Glutamine-dependent nitrogen transfer in *Escherichia coli* asparagine synthetase B. Searching for the catalytic triad. Journal of Biological Chemistry 269: 7450-7457.

[56] Duff SM, Qi Q, Reich T, Wu X, Brown T, Crowley JH, *et al.* (2011) A kinetic comparison of asparagine synthetase isozymes from higher plants. Plant Physiology and Biochemistry 49: 251-256.

[57] Horowitz B, Meister A (1972) Glutamine-dependent asparagine synthetase from leukemia cells. Chloride dependence, mechanism of action, and inhibition. Journal of Biological Chemistry 247: 6708-6719.

[58] Ebikeme C (2007) Amino Acid Transporters & Amino Acid Metabolism in *Trypanosoma brucei* brucei. Doctor of Philosophy Thesis, Division of Infection & Immunity Faculty of Biomedical & Life Sciences-University of Glasgow.

[59] Horiguchi M, Koyanagi S, Okamoto A, Suzuki SO, Matsunaga M, and Ohdo S (2012) Stress regulated transcription factor ATF4 promotes neoplastic transformation by suppressing expression of the INK4a/ARF cell senescence factors. Cancer Research 72: 395-401.

[60] Ye J, Kumanova M, Hart LS, Sloane K, Zhang H, De Panis DN, *et al.* (2010) The GCN2-ATF4 pathway is critical for tumour cell survival and proliferation in response to nutrient deprivation. The EMBO Journal 29: 2082-2096.

[61] Lahav T, Sivam D, Volpin H, Ronen M, Tsigankov P, Green A, *et al.* (2011) Multiple levels of gene regulation mediate differentiation of the intracellular pathogen *Leishmania*. FASEB Journal 25: 515-525.

[62] Gosline SJC, Nascimento M, McCall L, Zilberstein D, Thomas DY, Matlashewski G, *et al.* (2011) Intracellular Eukaryotic Parasites Have a Distinct Unfolded Protein Response. Plos One 6: e19118.

[63] Chow C, Cloutier S, Dumas C, Chou M, Papadopoulou B (2011) Promastigote to amastigote differentiation of *Leishmania* is markedly delayed in the absence of PERK eIF2alpha kinase-dependent eIF2alpha phosphorylation. Cellular Microbiology 13: 1059-1077.

[64] Moraes MCS, Jesus TCL, Hashimoto NN, Dey M, Schwartz KJ, Alves VS, *et al.* (2007) Novel Membrane-Bound eIF2 Kinase in the Flagellar Pocket of *Trypanosoma brucei.* Eukaryotic Cell 6: 1979-1991.

[65] Turco SJ, Spaeth GF, Beverley SM (2001) Is lipophosphoglycan a virulence factor? A surprising diversity between Leishmania species. Trends in Parasitology 5: 223-226.

[66] Cruz AK, Titus R, Beverley SM (1993) Plasticity in chromosome number and testing of essential genes in *Leishmania* by targeting. PNAS 90: 1599-1603.

[67] Nare B, Hardy LW, Beverley SM (1997) The Roles of Pteridine Reductase 1 and Dihydrofolate Reductase-Thymidylate Synthase in Pteridine Metabolism in the Protozoan Parasite *Leishmania major*. The Journal of Biological Chemistry 272(21): 13883-13891.

[68] Wilson ZN, Gilroy CA, Boitz JM, Ullman B, Yates PA (2012) Genetic Dissection of Pyrimidine Biosynthesis and Salvage in *Leishmania donovani. Journal of Biological Chemistry, 287(16): 12759-12770.*

[69] Avramis VI (2012) Asparaginases: biochemical pharmacology and modes of drug resistance. Anticancer Research 32: 2423-2437.

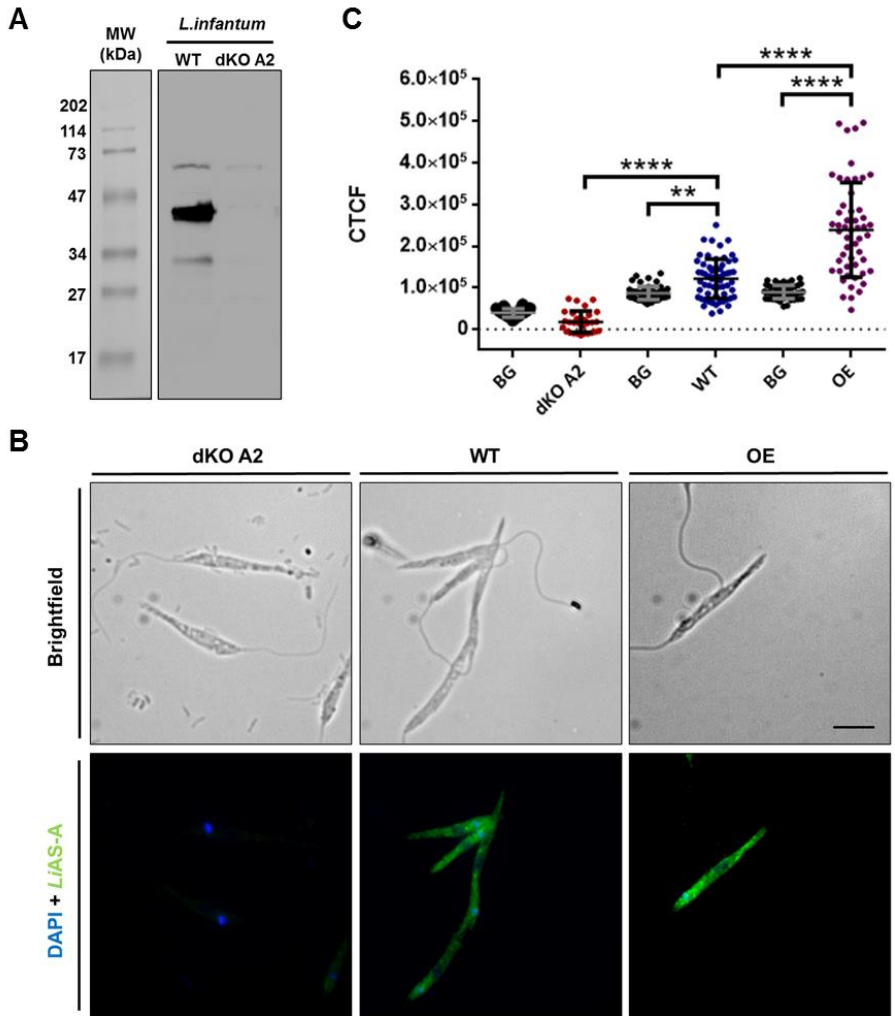

Fig. S1. Rabbit polyclonal anti-*Li*AS-A antibody validation. A) Western-blot analysis of WT and *LiASA* null mutant (clone A2) promastigotes extracts using rabbit polyclonal anti-*Li*AS-A (1:1000). **B)** Representative immunofluorescence images of different genotypes (WT, dKO clone A2 and OE) of mid-log *L. infantum* promastigotes, using rabbit polyclonal anti-*Li*AS-A antibody (1:1000). Upper and lower panels present brightfield and *Li*AS-A (green) + DAPI (blue) stained images, respectively. Images were acquired with a 100x objective, using a Zeiss AxioImager Z1. The scale bar corresponds to 5 µm. **C)** Fluorescence intensity quantification in WT, dKO clone A2 and OE parasites when stained with anti-*Li*AS-A antibody (1:1000). The values are expressed in CTCF (corrected total cell fluorescence), and background (BG) values are displayed as well. The quantification was performed on images acquired with 63x objective, using a Zeiss AxioImager Z1 and the same exposure time for all genotypes (*Li*AS-A 400 ms; DAPI 100 ms). Twenty different fields for each genotype were analysed in duplicate, and the fluorescence of an average of 50-100 parasites was quantified using ImageJ (v 1.47) software. Statistical analysis was performed using Graphpad Prism 5.0 version: statistical significance $p < 0.05$ (*), $p < 0.01$ (**), $p < 0.001$ (***), $p < 0.0001$ (****). The results (A-C) are representative of 2 independent experiments

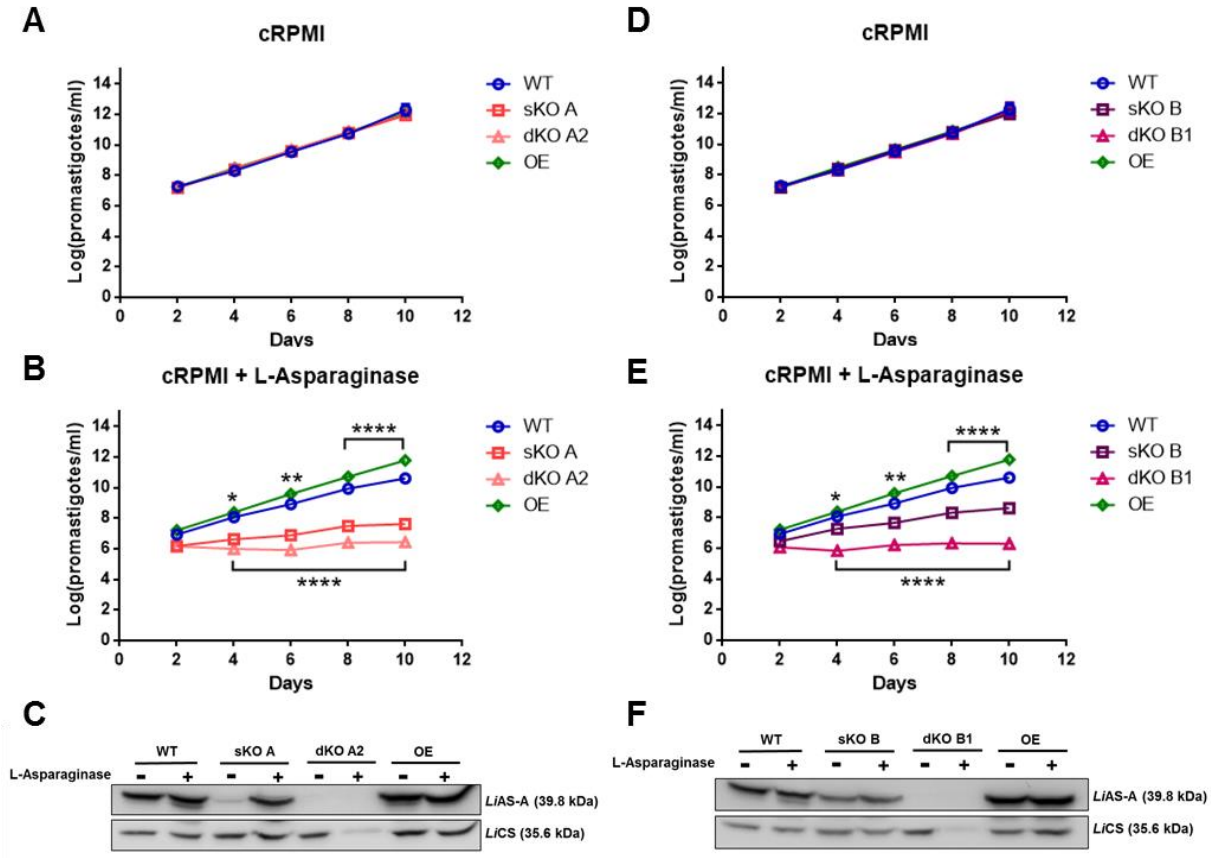

Fig. S2*.* Cumulative *in vitro* growth of logarithmic *LiASA* mutants in normal or Asn depleted medium. A/D and B/E) *L. infantum* promastigotes growth curves of *LiASA* mutants (*versus* WT), cultured in cRPMI and cRPMI + L-asparaginase, respectively. Parasites were maintained in logarithmic phase by subculturing every 2 days. The results correspond to mean values of duplicates ± standard deviation. Statistical analysis was performed using Graphpad Prism 5.0 version: statistical significance $p < 0.05$ (*), $p < 0.01$ (**), $p < 0.001$ (***), $p < 0.0001$ (****). **C and F)** Western-blot analysis of *Li*AS-A expression levels in 8 days old promastigotes, cultured in cRPMI and cRPMI + L-asparaginase. In A-F panels, the results are representative of two independent experiments. For the Western-blot analysis displayed in C and F, $1x10^7$ parasites were used for total extract preparation and *Li*CS (cysteine synthase) was used as loading control.

Table S1. Oligonucleotides sequences used to obtain *Li*AS-A recombinant protein (P1-P2) and pSPα*BLASTα**LiASA* (P3-P4)

Primer	Sequence
1	5' CAATTTGCATATGTCGTCCAGTCCGCAG 3'
2	5' CCCAAGCGAATTCTTACAATAAAGAGTAC 3'
3	5' GTCTAGAATGTCGTCCAGTCCGCAGGAGTACATTGA 3'
4	5' GCATATGTTACAATAAAGAGTACTGCGCCGTGACC 3'

Table S2. Oligonucleotides sequences used to obtain gene replacement cassettes (P1-P8) and to confirm *LiASA* mutants' genotype (P9-P20)

Primer	Sequence
1	5' CAGCCTGGAGGAGAACATTG 3'
2	5' GGGATGAATGGAGGGGTGTTG 3'
3	5' CCACAAAATGCCAGGGAGAAG 3'
4	5' GTAATCGTCCACGCCAGAAG 3'
5	5' CCTTTTATTCAACACCCCTCCATTCATCCCATGATTGAACAAGATGGATT 3'
6	5' CTGCAGAGAGCTTCTCCCTGGCATTTTGTGGTCAGAAGAACTCGTCAAGAAGGCGATAG 3'
7	5' GTCGCCAAGCCCTTTTATTCAACACCCCTCCATTCATCCCATGAAAAAGCCTGAACTCAC 3'
8	5' CTGCAGAGAGCTTCTCCCTGGCATTTTGTGGCTATTCCTTTGCCCTCGGACGAGTG 3'
9	5' TCGTCCAGTCCGCAGGAGTACA 3'
10	5' ACAATAAAGAGTACTGCGCCGTGACC 3'
11	5' CGGGTCCACGATTCACTGGAAG 3'
12	5' CAGGTAGCCGGATCAAGCGTATGC 3'
13	5' CGAGCACGTACTCGGATGGAAG 3'
14	5' GACCTCAACAGGAGCAACCTAAAG 3'
15	5' AACTTTATGCGCAGCGTCAC 3'
16	5' GGCCCAAAGCATCAGCTCATC 3'
17	5' GCAGGCTCTCGATGAGCTGATG 3'
18	5' AGGAAGGAAACACGCAAAGGTC 3'
19	5' ATGCCGAAGCGTGTTGCTCTG 3'
20	5' TTAAGACCTCCACAACCGCTGAAG 3'

Table S3. *Li*AS-A levels quantification in *LiASA* mutants in *in vitro* Asn replete or depleting conditions

Mutants	Asn	cRPMI(C)	sfRPMI(G)
sKO A	**+**	0.05	0.01
	-	0.68	1.77
sKO B	**+**	0.66	0.52
	-	0.93	0.99
dKO A2	**+**	SBG	SBG
	-	ND	SBG
dKO B1	**+**	SBG	SBG
	-	ND	SBG
dKO A2 + *Li*AS-A	**+**	0.25	ND
	-	1.12	ND
dKO B1 + *Li*AS-A	**+**	0.41	ND
	-	1.07	ND
OE	**+**	1.30	1.10
	-	3.02	1.34

Results were normalized against *Li*CS (cysteine synthase) and are expressed in protein ratio against WT parasites cultivated in Asn non depleting conditions

Results in C and G correspond to the Western-blots depicted in these panels of the figure 5 (in the case of OE, the values correspond to the mean of 2 independent blots).

SBG – Similar to the background

ND – Non determined

2.2. Ribose-5-phosphate isomerase B

2.2.1. Ribose-5-phosphate isomerase B knockdown compromises *Trypanosoma brucei* bloodstream form infectivity

Ribose 5-phosphate isomerase is an enzyme involved in the non-oxidative branch of the pentose phosphate pathway, and catalyzes the inter-conversion of D-ribose 5-phosphate and D-ribulose 5-phosphate. Trypanosomatids, including the agent of African sleeping sickness namely *Trypanosoma brucei*, have a type B ribose-5-phosphate isomerase. This enzyme is absent from humans, which have a structurally unrelated ribose 5-phosphate isomerase type A, and therefore has been proposed as an attractive drug target waiting further characterization. In this study, *Trypanosoma brucei* ribose 5-phosphate isomerase B showed *in vitro* isomerase activity. RNAi against this enzyme reduced parasites' *in vitro* growth, and more importantly, bloodstream forms infectivity. Mice infected with induced RNAi clones exhibited lower parasitaemia and a prolonged survival compared to control mice. Phenotypic reversion was achieved by complementing induced RNAi clones with an ectopic copy of *Trypanosoma cruzi* gene. Our results present the first functional characterization of *Trypanosoma brucei* ribose 5-phosphate isomerase B, and show the relevance of an enzyme belonging to the nonoxidative branch of the pentose phosphate pathway in the context of *Trypanosoma brucei* infection.

Reprinted from PLoS Neglected Tropical Diseases 2015 Dec 8; 9(1): e2578. doi: 10.1371/journal.pntd.0003430

OPEN ACCESS Freely available online

PLOS | NEGLECTED TROPICAL DISEASES

Ribose 5-Phosphate Isomerase B Knockdown Compromises *Trypanosoma brucei* Bloodstream Form Infectivity

Inês Loureiro[1], Joana Faria[1], Christine Clayton[2], Sandra Macedo-Ribeiro[3], Nuno Santarém[1], Nilanjan Roy[4], Anabela Cordeiro-da-Siva[1,5‡*], Joana Tavares[1‡*]

1 Parasite Disease Group, Instituto de Biologia Molecular e Celular da Universidade do Porto, Porto, Portugal, 2 Zentrum für Molekulare Biologie der Universität Heidelberg, DKFZ-ZMBH cv Alliance, Heidelberg, Germany, 3 Protein Crystallography Group, Instituto de Biologia Molecular e Celular da Universidade do Porto, Porto, Portugal, 4 Ashok & Rita Patel Institute of Integrated Study & Research in Biotechnology & Allied Sciences, New Vallabh Vidyanagar, Dist-Anand, Gujarat, India, 5 Departamento de Ciências Biológicas, Faculdade de Farmácia da Universidade do Porto, Porto, Portugal

Abstract

Ribose 5-phosphate isomerase is an enzyme involved in the non-oxidative branch of the pentose phosphate pathway, and catalyzes the inter-conversion of D-ribose 5-phosphate and D-ribulose 5-phosphate. Trypanosomatids, including the agent of African sleeping sickness namely *Trypanosoma brucei*, have a type B ribose-5-phosphate isomerase. This enzyme is absent from humans, which have a structurally unrelated ribose 5-phosphate isomerase type A, and therefore has been proposed as an attractive drug target waiting further characterization. In this study, *Trypanosoma brucei* ribose 5-phosphate isomerase B showed *in vitro* isomerase activity. RNAi against this enzyme reduced parasites' *in vitro* growth, and more importantly, bloodstream forms infectivity. Mice infected with induced RNAi clones exhibited lower parasitaemia and a prolonged survival compared to control mice. Phenotypic reversion was achieved by complementing induced RNAi clones with an ectopic copy of *Trypanosoma cruzi* gene. Our results present the first functional characterization of *Trypanosoma brucei* ribose 5-phosphate isomerase B, and show the relevance of an enzyme belonging to the non-oxidative branch of the pentose phosphate pathway in the context of *Trypanosoma brucei* infection.

Citation: Loureiro I, Faria J, Clayton C, Macedo-Ribeiro S, Santarém N, et al. (2015) Ribose 5-Phosphate Isomerase B Knockdown Compromises *Trypanosoma brucei* Bloodstream Form Infectivity. PLoS Negl Trop Dis 9(1): e3430. doi:10.1371/journal.pntd.0003430

Editor: Michael P. Pollastri, Northeastern University, United States of America

Received July 25, 2014; **Accepted** November 21, 2014; **Published** January 8, 2015

Data Availability: The authors confirm that all data underlying the findings are fully available without restriction. All relevant data are within the paper and its Supporting Information files except for the sequence of TbRpiB, TcRpiB from CL Brener Esmeraldo-like and non-Esmeraldo-like which are available from TriTrypdb.org under the accession numbers Tb927.11.8970, Tc00.1047053509199.24 and Tc00.1047053508601.119 respectively.

Funding: This work was funded by the European Community's Seventh Framework Programme under grant agreement No. 602773 (Project KINDRED). The COST Action CM1307 'Targeted chemotherapy towards diseases caused by endoparasites' and FEDER funds through the Operational Competitiveness Program – COMPETE and by National Funds through FCT – Fundação para a Ciência e a Tecnologia under the project PEst-C/SAU/LA0002/2011 have also contributed for this work. IL and JF were supported by fellowships from FCT reference SFRH/BD/64528/2009 and SFRH/BD/79712/2011, respectively. NS is supported by a fellowship from the European Community's Seventh Framework Programme under grant agreement No. 602773 (Project KINDRED). JT is an Investigator FCT funded by National funds through FCT and co-funded through European Social Fund within the Human Potential Operating Programme. The funders had no role in study design, data collection and analysis, decision to publish, or preparation of the manuscript.

Competing Interests: The authors have declared that no competing interests exist.

* cordeiro@ibmc.up.pt (ACdS); jtavares@ibmc.up.pt (JT)

‡ These authors contributed equally to this work.

Introduction

African sleeping sickness is a vector borne disease of mammals, caused by *Trypanosoma brucei* (*T. brucei*), for which the development of more effective, safe, and affordable chemotherapies remains a major goal. Vaccines are unlikely to be suitable [1–3], and therefore disease control relies exclusively on chemotherapy. The glucose-based metabolism is a key metabolic pathway for bloodstream forms, the mammalian infective stages. The absence of a fully functional mitochondrion along with a remarkable high proliferation rate makes parasites entirely dependent on glucose [4,5]. The glucose-based metabolism comprises two pathways: the glycolytic pathway and the pentose phosphate pathway (PPP). Despite using the same substrate, the pathways have different functions. Glycolysis catabolizes glucose for ATP requirements, while PPP includes an oxidative branch, mainly involved in the maintenance of cell redox homeostasis, and a non-oxidative branch in which ribose 5-phosphate is produced for nucleotide and nucleic acid synthesis. Enzymes involved in the PPP non-oxidative branch include ribose-5-phosphate isomerase, ribulose-5-phosphate epimerase, transaldolase and transketolase, and in contrast with enzymes involved in the glycolysis [6–15] or in the oxidative PPP [16,17], have been less studied. In *T. brucei*, enzymes of the non-oxidative branch downstream ribose-5-phosphate isomerase are apparently developmentally regulated [18]. Ribose 5-phosphate epimerase and transketolase activities were only detected in procyclics, the parasite form present in the insect vector. This suggests that in the mammalian host, bloodstream forms constrain sugar metabolism to the production of ribose-5-phosphate and NADPH via the oxidative phase of the

Author Summary

Within the non-oxidative branch of the pentose phosphate pathway, ribose 5-phosphate isomerase catalyzes the inter-conversion of ribose 5-phosphate and ribulose 5-phosphate. There are two types of ribose 5-phosphate isomerase, namely A and B. The presence of type B in *Trypanosoma brucei*, and its absence in humans, make this protein a promising drug target. African sleeping sickness is a serious parasitic disease that relies on limited chemotherapeutic options for control. In our study, a functional characterization of *Trypanosoma brucei* ribose 5-phosphate isomerase B is reported. Biochemical studies confirmed enzyme isomerase activity and its downregulation by RNAi affected mainly parasites infectivity *in vivo*. Overall this study shows that ribose 5-phosphate isomerase depletion is detrimental for parasites infectivity under host pressure.

PPP, most likely to meet the remarkably high proliferation rate of these parasites [19], and/or to protect themselves against a variety of reactive oxygen and nitrogen species [20,21] in a context of an *in vivo* infection.

Ribose-5-phosphate isomerase (Rpi) catalyzes the inter-conversion between ribulose-5-phosphate (Ru5P) and ribose 5-phosphate (R5P). Contrary to trypanosomatids, which have a Rpi type B (RpiB), the presence of a structurally unrelated Rpi type A (RpiA) in humans together with the adverse phenotype observed in *rpiA*$^{-}$/*rpiB*$^{-}$ knockout *Escherichia coli* (*E. coli*) [22] have led to suggest RpiB as an attractive drug target candidate that waits further characterization.

In this study, we investigate the importance of RpiB in *T. brucei* bloodstream form viability and infectivity.

Materials and Methods

Ethics statement

All experiments were carried out in accordance with the IBMC.INEB Animal Ethics Committees and the Portuguese National Authorities for Animal Health guidelines, according to the statements on the directive 2010/63/EU of the European Parliament and of the Council. IL, JT and ACS have an accreditation for animal research given from Portuguese Veterinary Direction (Ministerial Directive 1005/92).

Parasite culture

Procyclic and bloodstream *T. brucei* Lister 427 were cultivated in MEM-Pros and HMI-9 medium, respectively, as previously described [23]. Bloodstream forms containing pHD1313 [24] were maintained with 0.2 μg/ml phleomycin.

Cloning of trypanosomes *RPIB* genes

Ribose 5-phosphate isomerase B genes from *T. brucei* (*TbRPIB*) and *T. cruzi* (*TcRPIB*) were obtained by performing PCR on genomic DNA from *Trypanosama brucei* TREU927 and *Trypanosoma cruzi* CL Brener Non-Esmeraldo-like. Fragments of the open reading frames of *TbRPIB* (Tb927.11.8970; chromosome Tb927_11_v5 from 2,462,183 to 2,463,307) and *TcRPIB* (Tc00.1047053508601.119; chromosome TcChr30-P from 475,724 to 476,203) were PCR-amplified using a Taq DNA polymerase with proofreading activity (Roche). The primers were as follows: sense primer 5′ - CAATTTCCATATGACGCG-CAAGGTGGC - 3′ and antisense primer 5′ - CCCAAG-CAAGCTTCTAACAACCATTCG - 3′, sense primer 5′ - CAATTTCCATATGACGCGCCGAGTCGC - 3′ and antisense primer 5′ - CCCAAGCGAATTCTCATTTTACCCCTTTG - 3′, respectively. PCR conditions were as follows: initial denaturation (2 min at 94°C), 35 cycles of denaturation (30 s at 94°C), annealing (30 s at 40°C) and elongation (2 min at 68°C) followed by a final extension step (10 min at 68°C); initial denaturation (2 min at 94°C), 35 cycles of denaturation (30 s at 94°C), annealing (30 s at 58°C) elongation (2 min at 68°C) and a final extension step (10 min at 68°C), respectively. The PCR products were isolated from a 1% agarose gel, purified by the Qiaex II protocol (Qiagen), and cloned into a pGEM-T Easy vector (Promega) and sent to Eurofins MWG (Germany) for sequencing. All fragments were checked against the *T. brucei* and *T. cruzi* genome sequence database (http://www.genedb.org) using Blast to ensure their specificity.

Expression and purification of poly-His-tagged recombinant *Tb*RpiB and *Tc*RpiB

The *TbRPIB* and *TcRPIB* genes were excised from the pGEM-T Easy vector (using NdeI/EcoRI restriction enzyme combination), gel purified and subcloned into pET28a(+) expression vector (Novagen). The resulting constructs presented a poly-His tag (6× Histidine residues) at the N-terminal and were used to transform *E. coli* BL21DE3 cells. Both recombinant proteins were expressed by induction of log-phase cultures (500 ml; OD_{600} = 0.6) with 0.5 mM IPTG (isopropyl-β-D- thiogalactopyranoside) for 3 h at 37°C and agitation at 250 rpm/min. Bacteria were harvested by centrifugation (4000 rpm, for 40 min, at 4°C), resuspended in 20 ml of buffer A (0.5 M NaCl, 20 mM Tris.HCl, pH 7.6). The sample was sonicated, according to the following conditions: output 4, duty cycle 50%, 10 cycles with 15 s each. Centrifugation (4000 rpm, for 60 min, at 4°C) was followed to obtain the bacterial crude extract. The recombinant enzymes were purified in one step using Ni^{2+} resin (ProBond) pre-equilibrated in buffer A. The column was washed sequentially with 2–3 ml of the buffer A, 20 ml of the bacterial crude extract, 2 ml of buffer A 25 mM imidazole, 2 ml of buffer A 30 mM imidazole, 2 ml of buffer A 40 mM imidazole, 2 ml of buffer A 40 mM imidazole, 2 ml of buffer A 50 mM imidazole, 10 ml of buffer A 100 mM imidazole, 5 ml of buffer A 500 mM imidazole and 8 ml of buffer B (1 M imidazole, 0.5 M NaCl, 200 mM Tris, pH 7.6). *Tb*RpiB and *Tc*RpiB were eluted in the fractions of buffer A containing between 100 and 500 mM of imidazole. Dialysis was performed against 100 mM Tris/HCl (pH 7.6).

To generate rat polyclonal antibody against *Tb*RpiB, and rabbit polyclonal antibodies against *Tb*RpiB and *Tc*RpiB, each animal was first immunized with 150 μg of recombinant protein. After 2 weeks, 4 boosts with 100 μg of recombinant *Tb*RpiB or *Tc*RpiB were given weekly. The collected blood samples were centrifuged to obtain the sera.

Protein alignments and homology models

Multiple sequence alignments were performed in ClustalW [25] and images prepared with Aline, Version 011208 [26]. Homology models were obtained in SWISS-MODEL, using PDB accession code 3K7S as a template [27–29]. 3D structures were rendered with PyMOL (The PyMOL Molecular Graphics System, Version 1.3, Schrödinger, LLC).

Enzyme assays

*Tb*RpiB activity was assessed through *Km* determination for R5P and Ru5P, through 4-deoxy-4-phospho-D-erythronohydroxamic acid (4-PEH) (kindly provided by Dr. Laurent Salmon) inhibitory capacity against *Tb*RpiB, and through 4-PEH inhibition

mechanism characterization. Firstly, to determine the *Km* for R5P and to characterize 4-PEH-inhibition mechanism, a direct spectrophotometric method at 290 nm [30] was used, to quantify Ru5P formation. *Km* determination was performed at R5P concentrations in a range between 3.1 and 50 mM in Tris/HCl (pH 7.6). For 4-PEH inhibition mechanism characterization, the experiment was performed in the presence of 0.5 µg of enzyme and 0.1, 0.4, 0.7 or 1 mM of inhibitor. All inhibitors were tested in the presence of 3.1 mM R5P. A negative control was made using heat inactivated enzyme. The *Tc*RpiB enzyme was used as a positive control [31]. A calibration curve for Ru5P, using the referred method, was established to determine enzyme activity. An absorbance of 0.0381 at 290 nm was considered for 1 mM Ru5P. To determine the *Km* for Ru5P and to test 4-PEH inhibition as well, a modification of Dische's Cysteine-Carbazole method was used [32]. To determine *Km*, an incubation mixture contained 5 µl of 0.05 µg of enzyme in buffer A [100 mM Tris/HCl (pH 8.4), 1 mM EDTA and 0.5 mM 2-mercaptoethanol] plus 5 µl of Ru5P, giving final concentrations between 0.625 and 10 mM Ru5P, was used. For inhibition assay, Ru5P concentration used was 1.25 mM. Incubation was done for 10 min at room temperature. Following incubation, 15 µl of 0.5% cysteinium chloride, 125 µl of 75% (v/v) sulfuric acid and 5 µl of a 0.1% solution of carbazole in ethanol were added. After 30 min standing at room temperature, the A_{546} was determined. A blank without enzyme was run for each substrate or inhibitor concentration. Reaction linearity was checked varying enzyme concentration and time. To estimate the remaining Ru5P, a calibration curve was generated. In this assay conditions, 1 mM of Ru5P gave an A_{546} of 0.270 in a final reaction volume of 155 µl.

Immunofluorescence

For anti-*Tb*RpiB antibodies validation, cells from log-phase cultures of *T. brucei* RNAi cell lines and wt strain were centrifuged and resuspended at 10^6/ml in PBS. The cells were fixed in µ-Chamber 12 well (Ibidi) for 15 min, at room temperature, in PBS containing 4% p-formaldehyde, washed twice with PBS, and then permeabilized in PBS containing 0.1% of Triton X-100. The coverslips were incubated in PBS containing 10% FCS during 60 min, at room temperature, in a humidified atmosphere and washed twice with PBS/2% FCS. Then, incubated with primary rat or rabbit polyclonal antibodies against *Tb*RpiB (1:100 and 1:1000 respectively, both diluted in blocking solution) overnight, at 4°C, followed by two washes with PBS/2% FCS (5 min each one). Subsequently, cells were incubated with Alexa Fluor 647 conjugated goat anti-rat or Alexa Fluor 488 conjugated goat anti-rabbit secondary antibodies (Molecular probes from Life technologies) (1:500 diluted in blocking solution) for 1 h at room temperature in an humidified atmosphere, then washed twice with PBS. The coverslips were then stained and mounted with Vectashield-DAPI (Vector Laboratories, Inc.). Images were captured using fluorescence microscope AxioImager Z1 and software Axiovision 4.7 (Carl Zeiss, Germany). Pseudo-coloring of images were carried out using ImageJ software (version 1.43u). In case of *Tb*RpiB immunolocalization, bloodstream form *T. brucei* wt cells were probed using primary rat anti-*Tb*RpiB (1:100 diluted in blocking solution) and primary rabbit polyclonal antibody against aldolase (glycosome marker, 1:5000 diluted in blocking solution). Cells were then incubated with biotin conjugated goat anti-rat (1:500 diluted in blocking solution) (BD Pharmingen) for 1 h room temperature in a humidified atmosphere, then washed twice with PBS/2% FCS. Subsequently, cells were incubated with Alexa Fluor 647 conjugated goat anti-rabbit (Molecular probes, Life technologies) and Streptavidin-FITC (BD Pharmingen) secondary antibodies (1:1000 diluted in blocking solution) for 1 h at room temperature in an humidified atmosphere, then washed twice with PBS. Vertical stacks were captured, using an confocal microscope Leica TCS SP5II and LAS 2.6 software (Leica Microsystems, Germany). Mean fluorescence intensity of aldolase and RpiB was determined in each stack for the projected co-localization areas. Quantifications were carried out using ImageJ software (version 1.43u).

Digitonin permeabilization

For each sample condition, bloodstream cells were washed once with cold trypanosome homogenisation buffer (THB), composed by 25 mM Tris, 1 mM EDTA and 10% sucrose, pH = 7.8. Just before cell lyses, leupeptin (final concentration of 2 µg/ml) and different digitonin quantities (final concentrations of 5, 12.5, 25, 50, 100, 150 and 200 ug/ml) were added to 500 µl of cold THB, for cell pellet resuspension. Untreated cells (0 µg/ml of digitonin) and those completely permeabilized (total release, the result of incubation in 0.5% Triton X-100) were used for comparison. Each sample condition was incubated 60 min on ice, and then centrifuged at 2000 rpm, 4°C, for 10 min. Supernatants were taken and 500 µl of cold THB was added to each pellet. All fractions were analysed through Western blot for Rpi (10^8 cells per well; 1:1000 polyclonal rabbit anti-*Tb*RpiB as primary antibody), enolase (10^7 cells per well; 1:5000 polyclonal rabbit anti-enolase as primary antibody) and aldolase (10^7 cells per well; 1:5000 polyclonal rabbit anti-aldolase as primary antibody). HRP-conjugated goat anti-rabbit (1:5000) was used as secondary antibody.

Generation of transgenic RNAi cell lines

TbRPIB fragment (sense oligo with a BglII – SphI linker 5′ – GAGAAGATCTGCATGCGCGCAAGGTGGCTATCGGTG - 3′, and an antisense oligo with a ClaI – SalI 5′ – GCTAGCTA-CAGCTGACGGTCCTCCCCGCTGTATG – 3′) was cloned twice in opposite direction on either sides of a "stuffer" of the pHD1144 vector. The resulting construct obtained through HindIII and BglII digestion was cloned into pHD1145. The final construct was transfect into bloodstream forms with pHD1313, and stable individual clones were selected with 7.5 µg/ml of hygromycin. For functional complementation, *TcRPIB* fragment (sense oligo with a HindIII linker 5′ - GAAGCTTAT-GACGCGCCGAGTCGCAAT - 3′, and an antisense oligo with a BglII linker 5′ - AGATCTTCATTTTACCCCTTTGTTCC - 3′), was cloned in pHD1034 vector (digested with HindIII and BamHI). After transfection [33], individual clones were selected with 0.2 µg/ml of puromycin.

In vitro and *in vivo* analysis of *Tb*RpiB RNAi

For *in vitro* growth curves, cell lines were seeded at 2×10^5 parasites/ml of complete HMI-9 medium, in the absence and presence of 100 ng/ml of tetracycline (tet). Every 24 h, until day 10, cell growth was monitored microscopically. For *in vivo* infections, after 24 h in the absence of selective drugs, and then a further 48 h of tet induction, 10^4 wt and transgenic parasites were inoculated intraperitoneally in 6–8 weeks old BALB/c mice (n = 3–8). 48 h prior infection, the RNAi induced mice were treated with 1 mg/ml doxycycline hyclate and 5% sucrose containing water [34], while RNAi non-induced mice were given standard water. Parasitaemia was measured daily from the six day post-infection through tail blood extraction, during a period which all mice in the group were alive.

Northern blot analysis

Total RNA was isolated from ≈2×10^7 bloodstream forms using Trizol reagent (Life Technologies). 10 µg RNA were directly separated by overnight formaldehyde agarose-gel electrophoresis, transferred onto a nylon membrane by capillarity and fixed by UV irradiation. The membrane was prehybridized in a hybridization bottle in 5× SSC, 0.5% SDS with salmon sperm DNA (200 µg/ml) and 1× Denhardt's solution for 2 hours at 65°C. *TbRPIB* and signal recognition particle (*SRP*; Tb927.8.2861_7SL) probes were generated by PCR in the presence of [^{32}P]-labelled dCTP using Prime-It RmT random primer labelling kit (Stratagene) followed by purification using QIAquick Nucleotide Removal Kit (QIAGEN). Denaturated radioactive probes were added to the prehybridization solution at 65°C and incubated overnight. After rinsing the membrane twice for 5 min. with 2× SSC/0.1% SDS, the probes were washed out with two washes of 30 minutes in 0.1× SSC/0.1% SDS at 65°C and the membrane exposed on a Fugifilm FLA-3000 reader screen. ImageJ software (version 1.43u) was used for RNA quantification.

Protein extracts and western blot analysis

Cell free extracts were obtained in RIPA buffer (20 mM Tris-HCl (pH 7.5), 150 mM NaCl, 1 mM Na_2EDTA, 1 mM EGTA, 1% NP-40, 1% sodium deoxycholate, 2.5 mM sodium pyrophosphate, 1 mM b-glycerophosphate, 1 mM Na_3VO_4), with freshly-added complete protease inhibitor cocktail (Roche Applied Science). The total protein amount was quantified using Biorad Commercial Kit (Reagents A, B and S) and the samples were then kept at -80°C. For analysis of parasites collected from mice, trypanosomes were purified from mouse blood using a DE-52 (Whatman) column [35].

For Western blotting, 10 µg of recombinant *Tb*RpiB and *Tc*RpiB proteins were resolved in 15% SDS/PAGE (Tris-Tricine gel), while 30 µg of total soluble cell extract and 10^7 parasites were resolved in 12% Tris-Glycine SDS/PAGE, and all were then transferred on to a nitrocellulose Hy-bond ECL membrane (Amersham Biosciences). The membrane was blocked in 5% (w/v) non-fat dried skimmed milk in PBS/0.1% Tween-20 (blocking solution), followed by incubation with an anti-His-tag rabbit antibody (MicroMol-413) (1:1000) or a combination of an anti-*Tb*RpiB rabbit antibody (1:1000) with an anti-aldolase rabbit antibody (1:5000) in blocking solution at 4°C overnight, respectively. Blots were washed with PBS/0.1% Tween-20 (3 times 15 min). Horseradish peroxidase-conjugated goat anti-rabbit IgG (Amersham) (1:5000 for 1 h, at room temperature) was used as the secondary antibody. The membranes were developed using SuperSignal WestPico Chemiluminescent Substrate (Pierce). ImageJ software (version 1.43u) was used for protein bands semi-quantification.

Statistical analysis

Student's t-test and Graphpad Prism Software (version 5.0) were used. p values ≤0.05 were considered to be statistically significant (* $p\leq0.05$, ** $p\leq0.01$, *** $p\leq0.001$).

Results

*Tb*RpiB biochemical properties

An open reading frame with sequence similarity to RpiB was identified both in *T. brucei* (Tb927.11.8970) and in *T. cruzi* (Tc00.1047053508601.119) genomes. Protein sequence alignment using ClustalW [25] revealed 67% identity for *Tb*RpiB *versus* *Tc*RpiB, and both proteins show no similarity with human ribose 5–phosphate isomerase A. *Tc*RpiB and *Tb*RpiB contain 159 and 155 amino acids residues per monomer, respectively. Protein multiple sequence alignment of RpiB from *T. cruzi* CL Brener Esmeraldo-like (Tc00.1047053509199.24; PDB accession code 3K7S [36]), *T. cruzi* CL Brener Non-Esmeraldo-like (Tc00.1047053508601.119) and *T. brucei* (Tb927.11.8970) is shown in S1A Fig. The scale colour, from cyan (low-similarity residues) to red (high-similarity residues), underlines the degree of similarity between the three protein sequences, also seen in the *Tc*RpiB (Esmeraldo like strain) ribbon representation (S1B Fig.). The superposition of *Tc*RpiB (Esmeraldo like strain) structure (grey) (PDB code 3K7S), with the homology models generated for *Tc*RpiB (Non Esmeraldo like strain) (purple) and *Tb*RpiB (blue) show a high structural homology and strict conservation of the residues involved in R5P binding pocket (S1A, C Fig.).

Biochemical studies were performed using histidine-tagged fusion *Tb*RpiB and *Tc*RpiB (positive control) proteins expressed in *E. coli* and purified under non-denaturing conditions (Figs. 1A, S2A). The *T. brucei* and *T. cruzi* [31] enzymes have *in vitro* ribose 5-phosphate isomerase activity, as these proteins can use both R5P and Ru5P as substrates. For R5P, *T. brucei* protein showed a significantly higher K_m (2.8 fold increase, $p<0.05$), but not a lower maximum velocity (V_{max}) or catalytic constant (k_{cat}) compared to *T. cruzi* enzyme (Table 1 and S2B Fig.). For Ru5P, the K_m of the *T. brucei* protein was not significantly different from that of the *T. cruzi* enzyme value, but the V_{max} and k_{cat} were higher (≈1.5 fold, $p<0.05$) (Table 1 and S2B Fig.). Both the *T. brucei* and the *T. cruzi* enzymes exhibited significant lower K_ms for Ru5P than for R5P, (5.2 fold, $p<0.05$ and 3.7 fold, $p<0.01$, respectively), suggesting the reaction occurs preferentially from Ru5P to R5P. The turnover values (k_{cat}) were found to be significantly higher for Ru5P than for R5P, in both *T. brucei* ($p=0.001$) and *T. cruzi* ($p<0.001$) enzymes (Table 1 and S2B Fig.).

The reaction mechanism of ribose 5-phosphate isomerase involves two steps: an initial opening of the furanose ring of R5P, followed by the aldolase-ketose isomerisation, via a cis-enediolate high energy intermediate [31]. 4-PEH has been described to act as a competitive inhibitor which compromises the binding of 1,2-*cis*-enediolate intermediate [37]. The inhibitory capability of 4-PEH was screened *in vitro*, resulting in an IC50 of 0.8 mM and 0.7 mM for *Tb*RpiB (Fig. 1B) and *Tc*RpiB (S2C Fig.), respectively, with K_i values of 2.2 (Fig. 1C) and 1.6 mM (S2D Fig.). 4-PEH showed, as expected, a competitive inhibition behaviour, once using increasing concentrations of inhibitor, a progressive increase in the K_m for R5P without V_{max} alteration was observed (Figs. 1D, S2E). The inhibitor behaviour, and also the IC_{50} and the K_i values are in agreement to what was described before for *T. cruzi* enzyme [31,36]. 4-PEH was also reported as a potent inhibitor against *Mycobacterium tuberculosis* RpiB [37].

Undoubtedly, *Tb*RpiB has isomerase activity and uses preferentially ribulose 5-phosphate as a substrate.

*Tb*RpiB expression and subcellular localization

Rabbit and rat polyclonal antibodies were generated against the *Tb*RpiB recombinant protein. Antibody specificity was validated, as induction of RpiB RNAi resulted in a decrease in the fluorescence intensity of bloodstreams when compared to non-induced parasites (S3A, B, C Fig.). Similarly a significant decrease on RpiB levels in the extracts of *Tb*RpiB RNAi induced parasites is shown by Western blot. Rat and rabbit antibodies specificity against RpiB can be appreciated on the whole Western blot membranes (S3D, E Fig.). Using rabbit polyclonal antibody against parasite extracts, *Tb*RpiB was found more abundant in procyclic forms than in bloodstream forms (Fig. 2A). To ascertain RpiB subcellular localization in bloodstream forms,

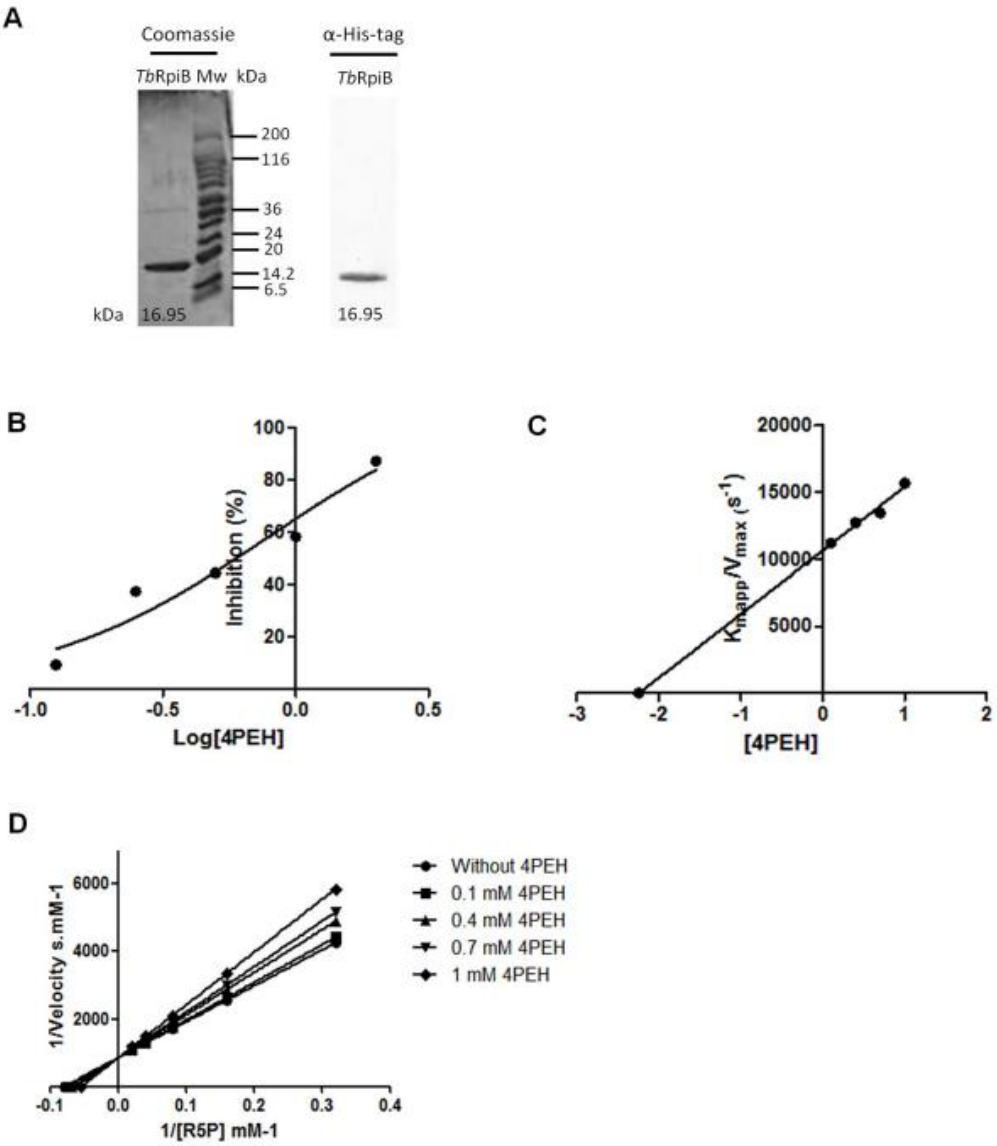

Fig. 1. Biochemical properties of *Tb*RpiB expressed in *E. coli*. (A) 10 μg of *Tb*RpiB recombinant protein analyzed by SDS-PAGE and Coomassie blue staining. Mw, molecular weight marker. Western blot analysis of his-tagged recombinant protein probed with rabbit anti-histidine monoclonal antibody (MicroMol-413) (1:1000). (B) Inhibition (%) of *Tb*RpiB activity by 4PEH. (C) Plot of K_{mapp}/V_{max} *versus* 4PEH concentrations; K_i corresponds to the symmetric value of the X-axis intersection. (D) Plots showing the effect of different 4PEH concentrations on the inverse of the initial velocity *versus* the inverse of several concentrations of R5P. (B–D) The values correspond to the means ± standard deviation of two replicates, and data is representative of three independent experiments.
doi:10.1371/journal.pntd.0003430.g001

two complementary approaches, immunofluorescence and digitonin fractionation, were performed. Fluorescent confocal microscopy analysis suggests that *Tb*RpiB despite being localized mainly in the cytosol can be also found in glycosomes due to colocalization with the glycosomal marker, aldolase [38] (Fig. 2B). Upon digitonin fractionation, RpiB showed an intermediate pattern between the glycosomal marker, aldolase (still partially in the pellet after 200 μg/ml digitonin treatment) and the cytosolic marker, enolase (almost all in supernatant with 25 μg/ml digitonin), being practically released with 100 μg/ml digitonin (Fig. 2C). In conclusion, RpiB localizes mainly in the cytosol of bloodstream forms.

In vitro and *in vivo* analysis of *Tb*RpiB RNAi

To assess if *Tb*RpiB targeting affects *in vitro* bloodstream forms growth, RNAi against RpiB was induced. This resulted in a lower

Table 1. *Tb*RpiB kinetic parameters.

	R5P to Ru5P	Ru5P to R5P
K_m (mM)	12.50±4.43	2.39±0.94
$V_{max} \times 10^{-3}$(mM.s^{-1})	1.17±0.16	5.84±0.79
k_{cat} (s^{-1})	12.00±1.58	39.44±5.32
k_{cat}/K_m (M^{-1}.s^{-1})	9.60×10^2	1.64×10^4

The values are the means ± standard deviation obtained from 3 independent experiments.
doi:10.1371/journal.pntd.0003430.t001

mRNA and protein levels 1 and 2 days post-induction (Fig. 3A and B, respectively). Using ImageJ software we estimate a decrease of approximately 93% of protein levels at 48 h RNAi post-induction. The growth of *Tb*RpiB RNAi tet(-) and wt tet(-) cell lines was shown to be similar (Fig. 3C). A significant decrease of *in vitro* cell proliferation of induced *versus* non-induced RNAi cell lines was seen only after day 4 of the cumulative growth curve (Fig. 3C).

To test the importance of RpiB for parasite infectivity in a disease model, two groups of BALB/c mice were inoculated with the wt parental cell line and other two groups with the RNAi cell line. Some mice were fed with water containing doxycycline (Dox) to induce downregulation of *Tb*RpiB, whilst the remaining mice were kept as non-induced controls. A Western blot confirmed the reduction of the protein level in 48 h RNAi induced parasites used for mice infections (Fig. 4A). Blood samples were taken from all mice at daily intervals to chart parasitaemia (Fig. 4B). Animals achieving a parasitaemia greater than 10^8 trypanosomes per millilitre were euthanized. *In vivo* growth of the *Tb*RpiB RNAi Dox(-) trypanosomes was not significantly different from that of wt Dox(-) parasites. However a significant decrease in the parasitaemia of induced *versus* non-induced RNAi cell lines was seen. Within 6 days of inoculation, contrary to mice infected with induced RNAi cell line (in which overall parasitaemias remained below the detection limit, 5×10^4 trypanosomes/ml), mice infected with control parasites developed high levels of parasitaemia. As a consequence, and in contrast to mice infected with wt and *Tb*RpiB RNAi Dox(-) parasites, which were culled sooner (between eighth to thirteenth day post-infection), *Tb*RpiB RNAi Dox(+) were euthanized from the eighteenth day post-infection (Fig. 4C). Eventually parasitaemia also increased in the *Tb*RpiB RNAi Dox(+) mice, due to the emergence of "RNAi revertants" (Fig. 4D) [39–42]. In this way, ribose 5-phosphate isomerase B despite being dispensable *in vitro*, confers optimal *in vitro* growth and is highly relevant for mice infections.

Complementation of *Tb*RpiB RNAi phenotype

Functional complementation of *T. brucei* RNAi cell lines with the *T. cruzi* homologue was performed, since *Tc*RpiB has *in vitro* isomerase activity and *TcRPIB* nucleotide sequence is sufficiently different to avoid *Tb*RpiB RNAi. Western blot analysis confirmed *Tb*RpiB downregulation only in induced RNAi parasites, and *Tc*RpiB expression exclusively in complemented parasites (Fig. 5A). Cells with RNAi and complemented with *Tc*RpiB grew equally *in vitro* (Fig. 5B), and were almost as virulent *in vivo* (Fig. 5C, D), as the wild-type. RNAi revertants appeared during the course of infection in induced *Tb*RpiB RNAi infected mice, but not in induced complemented *Tb*RpiB RNAi infected mice (Fig. 5E). As a result, complementation restored *in vitro* and *in vivo* phenotypes.

Discussion

In this study we demonstrated that *Tb*RpiB, like the related *Tc*RpiB and *Leishmania donovani* RpiB (*Ld*RpiB) enzymes, has *in vitro* ribose 5-phosphate isomerase activity [31,43]. Based on the theoretical homology model, *Tb*RpiB is predicted to be dimeric. Although the dimer comprises a complete functional unit, tetramers are observed in all available RpiB structures except that of *Mycobacterium tuberculosis* RpiB [36]. Similarly to *T. cruzi*, *Clostridium thermocellum* and *Pisum sativum* Rpi enzymes, *Tb*RpiB has the ability of using both R5P or Ru5P as substrates, but with remarkable preference for Ru5P [31,44,45]. However, the differences in affinity are more pronounced in trypanosomes enzymes. Indeed, these differences were higher for *Tb*RpiB compared to *Tc*RpiB. Analysis of the three enzymes from trypanosomatids (*Tc*RpiB, *Ld*RpiB and *Tb*RpiB) shows that *Tb*RpiB and *Ld*RpiB have the highest K_m and k_{cat} value for R5P substrate, respectively [31,43]. Nevertheless, we can speculate that such differences may result in part by the fact that parasite enzymes were expressed and purified as recombinant proteins in bacteria and not purified directly from trypanosomes extracts. Consequently, differences in protein post-transcriptional processing and/or changes in protein conformation cannot be excluded.

RpiB is expressed on *T. brucei* procyclic and bloodstream forms, and our data indicate its higher expression in procyclics. Interestingly, a previous study has shown higher levels of *TbRPIB* mRNA (Tb927.11.8970) in logarithmic phase procyclic forms compared to bloodstream forms [46]. However, its biological meaning, if any, remains to be elucidated.

Regarding RpiB subcellular localization in bloodstream forms, the protein despite found mainly in the cytosol is also present in glycosomes. This might explain why a previous proteomic analysis failed to find *Tb*RpiB enzyme in purified glycosomes [47]. The glycosomal localization observed within the dual-localization can be justified by the presence of a peroxisomal targeting signal, PTS2 (-KVAIGADHI-), at the N-terminus [48]. Moreover, other enzymes of the hexose-monophosphate pathway, although present in glycosomes, were also found mainly within the cytosol (e.g. glucose-6-phosphate dehydrogenase, 6-phosphogluconolactonase and transketolase) [49,50].

*Tb*RpiB is clearly needed for optimal *in vitro* parasite growth, although we do not know whether it is essential for survival since some protein remained after RNAi. Nevertheless, our results show that *Tb*RpiB is important for parasites infectivity *in vivo*, through the appearance of RNAi revertants and reversion of the phenotype in complemented parasites. Infectivity defects of bloodstreams with reduced levels of *Tb*RpiB were shown on a monomorphic *T. brucei* strain. This strain is abnormally virulent and typically mice do not survive longer than ≈10 days. In the future, it would be interesting to test the role of RpiB in a more chronic infection, as the one caused by pleomorphic strains. Interfering with the PPP

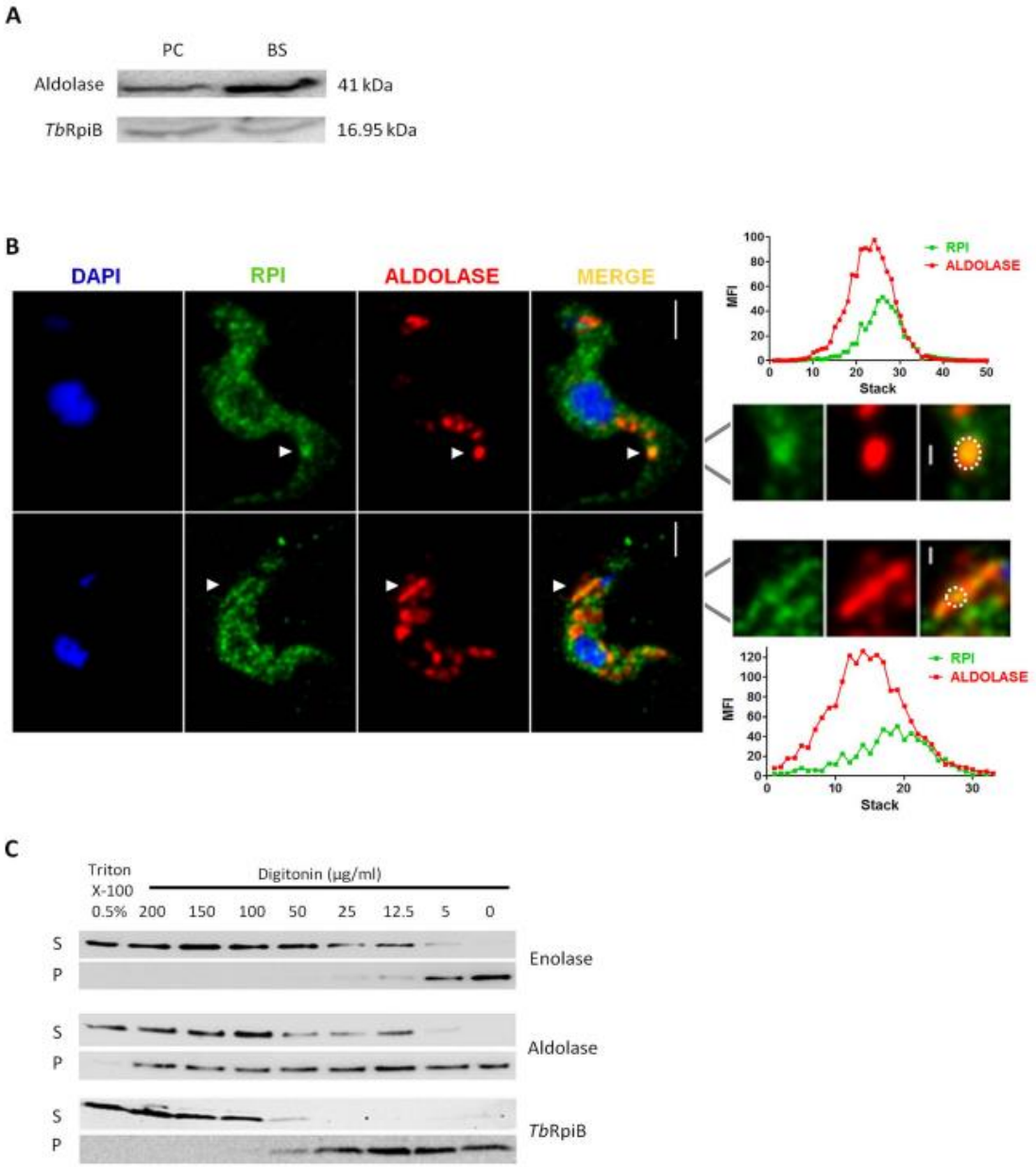

Fig. 2. *Tb*RpiB expression within life cycle stages and localization in bloodstream forms. (A) RpiB expression in *T. brucei* life-cycle stages; 30 µg of protein from bloodstream (BS) and procyclic (PC) total lysates was analysed by Western blot probed with rabbit anti-*Tb*RpiB (1:1000) and anti-aldolase (loading control; 1:5000) polyclonal antibodies. Data is representative of three independent experiments. (B) Immunofluorescence analysis by confocal microscopy of bloodstream forms *Tb*RpiB. Nuclear and kinetoplast DNA labelled by DAPI staining (blue). RpiB (green) and aldolase (red) were labelled respectively with rat anti-*Tb*RpiB (1:100) and rabbit anti-aldolase (1:5000) antibodies. White arrowheads indicate RpiB and aldolase co-localization areas that are magnified in the right panels. Mean fluorescence intensity (MFI) of aldolase (red) and RpiB (green) in these co-localization areas (white dotted circle) were determine for each stack. Images are maximal Z-projections of 50 and 33 contiguous stacks separated by 0.1 µm. Scale Bars: 2.5 (top left panel), 5 (below left panel), 0.5 (top right panel) and 1 µm (below right panel). (C) Supernatant (S) and pellet (P) fractions obtained with different concentrations of digitonin were subjected to Western blot analysis and probed with rabbit antibodies against *Tb*RpiB (1:1000), enolase (cytoplasmic marker; 1:5000), and aldolase (glycosome marker; 1:5000). Data is representative of two independent experiments. Untreated cells and those completely permeabilized by incubation with 0.5% Triton X-100 [total release (TR)] were used as controls. doi:10.1371/journal.pntd.0003430.g002

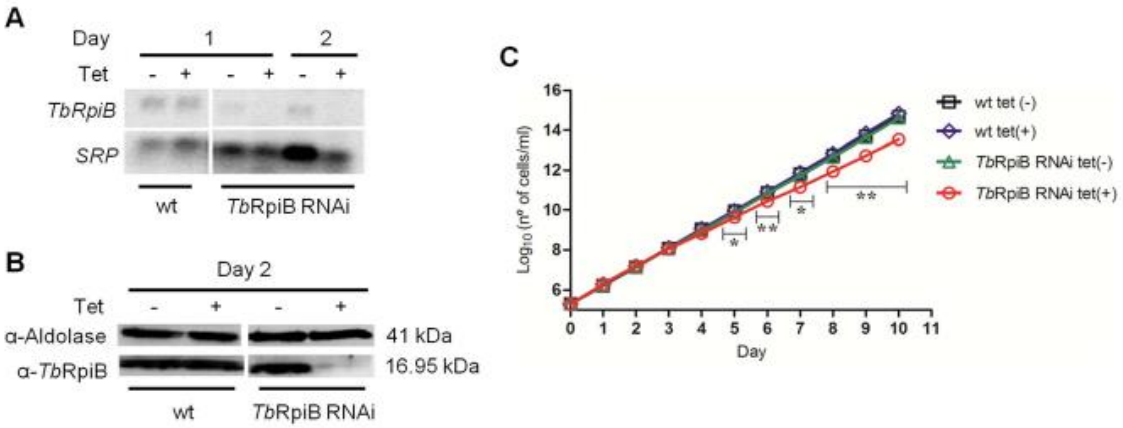

Fig. 3. ***In vitro*** **effect of RNAi-mediated RpiB downregulation on** ***T. brucei*** **bloodstream forms.** (A) Northern and (B) Western blot analysis of mRNA and protein levels, respectively, upon RpiB RNAi. *SRP* and aldolase used as loading controls, respectively. Rabbit anti-*Tb*RpiB (1:1000) and anti-aldolase (1:5000) polyclonal antibodies were used as primary antibodies. (C) Growth curve of a wt *versus* a representative RpiB RNAi cell line. Black squares and blue diamonds represent wt growth in the absence or presence of tetracycline (tet) while green triangles and red circles represent RpiB RNAi clone growth in the absence or presence of tet, respectively. Cumulative cell numbers (product of cell number and total dilution) are plotted. Values represent averages from three independent experiments using one representative RpiB RNAi clone and error bars indicate standard deviation. Statistical differences between non-induced and induced *Tb*RpiB RNAi clone are depicted (* $p \leq 0.05$, ** $p \leq 0.01$).
doi:10.1371/journal.pntd.0003430.g003

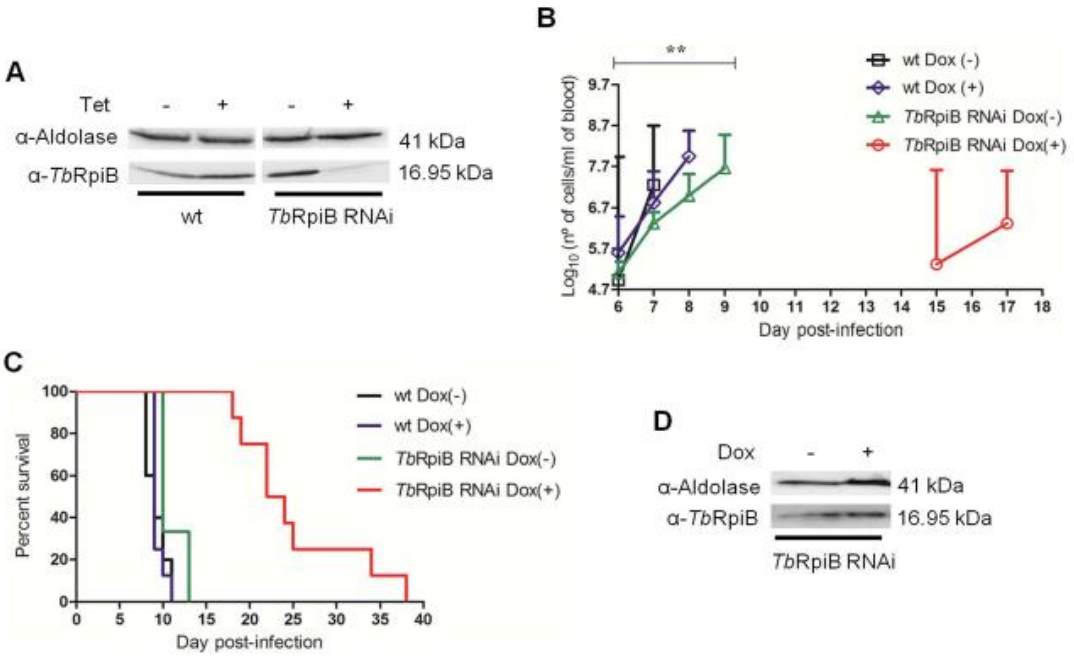

Fig. 4. ***In vivo*** **effect of RNAi-mediated RpiB downregulation on** ***T. brucei*** **bloodstream forms.** (A) Western blot analysis of Rpi protein levels in bloodstream forms 48 h after tet induction, which were used for mice infections. (B) Groups of mice (n = 3–7) were infected intraperitoneally with 10^4 control wt (black squares and blue diamonds) or a representative RNAi clone (green triangles and red circles). The mice were either untreated (black squares and green triangles) or treated with 1 mg/ml Dox (blue diamonds and red circles) in the water supply. Parasitaemias of each group are shown for the period of time in which there is no mice death. Values are means and errors bars indicate + standard deviation. 5×10^4 trypanosomes/ml of blood is the detection limit. Mice were culled when parasitaemia reached 10^8 cells/ml. (C) Kaplan–Meier survival analysis of mice infected with non-induced and induced wt cell line (black and blue line, respectively) *versus* a non-induced and induced representative RNAi clone (green and red line, respectively). Parasitaemias and survival curve are representative of two independent experiments using two different RNAi clones. (D) Western blot analysis of RpiB levels in a representative non-induced and Dox-induced RNAi clone collected from mice before being euthanized confirmed the appearance of RNAi revertants. Statistical differences between non-induced and induced *Tb*RpiB RNAi clone are depicted (** $p \leq 0.01$).
doi:10.1371/journal.pntd.0003430.g004

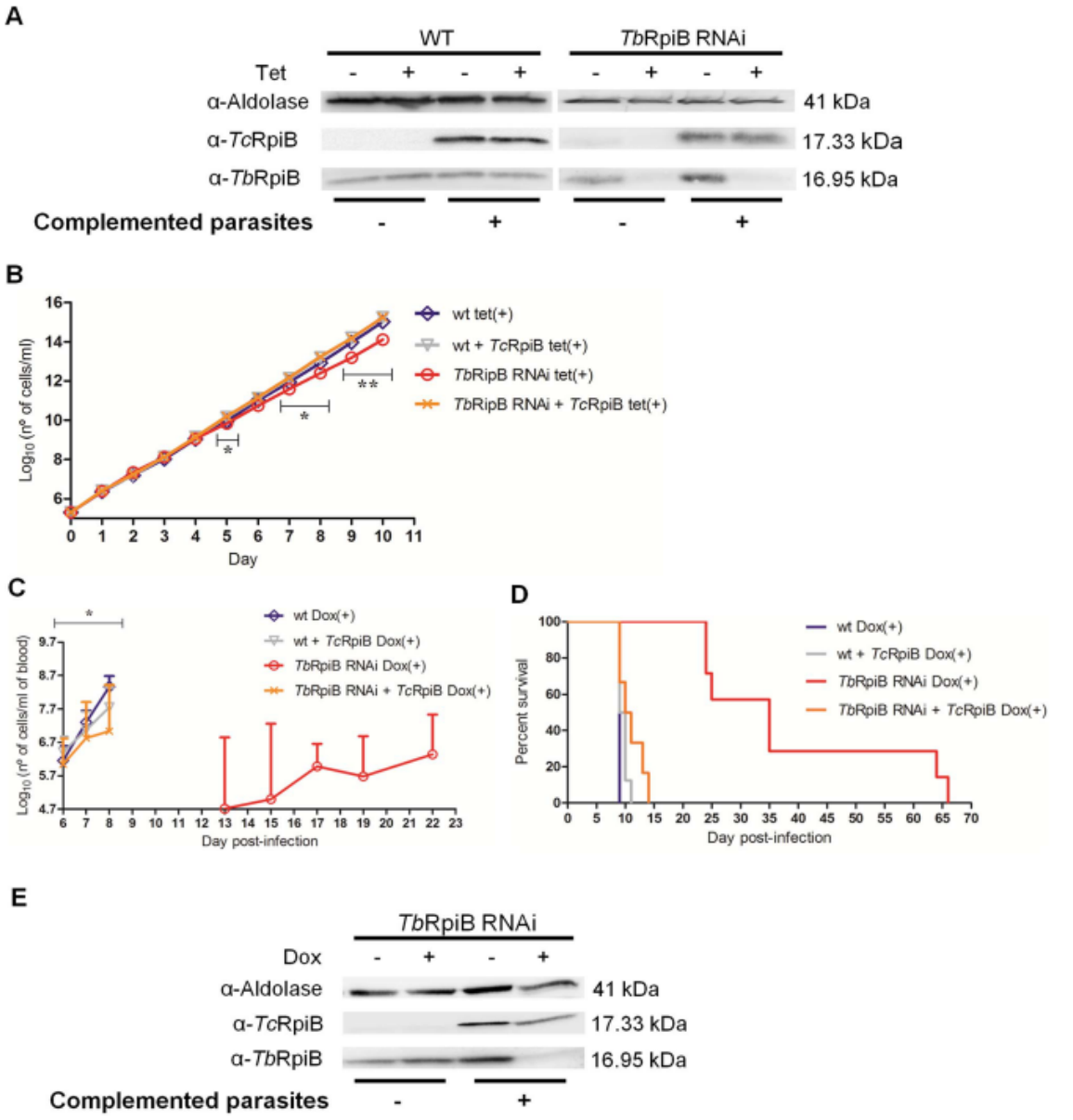

Fig. 5. Rescue of RpiB RNAi mediated defect by expression of *Tc*RpiB. (A) Western blot analysis of *Tb*RpiB and *Tc*RpiB levels in bloodstream forms 48 h after tetracycline (tet) induction reveal a decrease of RpiB in non-complemented and complemented *Tb*RpiB RNAi cells, contrary to wt controls. Parasite extracts were probed sequentially, with rabbit anti-*Tb*RpiB (1:1000) and anti-aldolase (loading control; 1:5000), and with anti-*Tc*RpiB (1:1000) primary antibodies. (B) *In vitro* cumulative growth of induced non-complemented and complemented wt bloodstream forms (blue diamond and grey down triangle, respectively) *versus* an induced non-complemented and complemented representative *Tb*RpiB RNAi clone (red circle and orange cross, respectively). Values represent an average of parasite numbers ± standard deviation of two independent experiments from a representative RNAi clone. (C) Groups of mice (n = 6–8) were infected intraperitoneally with 1×10^4 RNAi induced non-complemented and complemented wt parental cell line (blue diamond and grey down triangle, respectively) *versus* non-complemented and complemented representative *Tb*RpiB RNAi clone (red circle and orange cross, respectively). Mice were treated with 1 mg/ml Dox in the water supply. Mice were culled when parasitaemia reached 10^8 cells/ml. The mean value of the parasitaemias for each group of mice + standard deviation is shown. (D) Kaplan–Meier survival analysis of mice infected with Dox induced non-complemented and complemented wt cell line (blue and grey lines, respectively) *versus* induced non-complemented and complemented representative *Tb*RpiB RNAi clone (red and orange lines, respectively). Data are representative of two independent experiments of two different RNAi clones. (E) Western blot analysis of RpiB levels in a representative non-complemented and complemented *Tb*RpiB RNAi clone isolated from mice blood before being euthanized, showing the emergence of RNAi revertants only in induced non-complemented RNAi clones. Statistical differences between non-complemented and complemented induced *Tb*RpiB RNAi clone are depicted (* $p \leq 0.05$, ** $p \leq 0.01$).
doi:10.1371/journal.pntd.0003430.g005

non-oxidative branch showed to be detrimental under host pressure, in these highly proliferative parasitic forms, which can be due to a defective production of ribose 5-phosphate towards nucleotide and nucleic acid synthesis. Moreover, another enzyme capable of producing ribose 5-phosphate, ribokinase, is essential for parasites survival since attempts to remove the two alleles were unsuccessful [51].

*Tb*RpiB is not the first protein reported as dispensable under standard laboratory culture conditions but crucial for parasites growth in the animal host [52,53]. In rich culture conditions, parasites may uptake essential nutrients from the extracellular medium, which may not be as available in blood. Moreover, *in vivo*, parasites need to deal with pressure from the host immune response.

As for other proteins [54,55], our *in vitro* results differ from the ones achieved in RNA interference target sequencing (RITseq) screen [56]. Indeed, proteins described to be significantly important for parasites fitness by Alsford and colleagues [56] were not in others studies [54,55]. Despite large-scale RNAi screens have already proved useful, caution should be taken due to some level of false negatives and positives, inherent to high-throughput approaches and more importantly due to off-target effects [57]. Furthermore, variations between different large-scale RNAi screenings were already been reported and explained by the use of different *T. brucei* strains, RNAi constructs and methods for assessing cell growth highlighting the importance of using complementary approaches in such studies [58]. Despite all, both studies are in agreement and show a role for *Tb*RpiB on parasites growth.

To further investigate if bloodstream forms deleted of RpiB are completely cleared in mice, studies with gene knockout parasites should be done.

Overall our results clearly show a role of RpiB for bloodstream *in vitro* optimal growth and more importantly *in vivo* infectivity, but also suggest a conserved role among different *Trypanosoma* species. In conclusion *Tb*RpiB emerges as a new potential therapeutic target against African sleeping sickness.

Supporting Information

S1 Fig. Sequence alignment and ribbon representation of RpiB protein from trypanosomes. (A) ClustalW alignment of RpiB from *T. cruzi* CL Brener Esmeraldo-like (Tc00.1047053509199.24; PDB accession code 3K7S), *T. cruzi* CL Brener Non-Esmeraldo-like (Tc00.1047053508601.119) and *T. brucei* (Tb927.11.8970). The residues are colored according to ALSCRIPT Calcons (Aline version 011208) using a predefined colour scheme (red: identical residues; orange to blue: scale of conservation of amino acid properties; white: dissimilar residues). Secondary structure of *Tc*RpiB crystallographic model (PDB code 3K7S) (grey) and the theoretical homology models *Tc*RpiB (Tc00.1047053508601.119) (purple) and *Tb*RpiB (Tb927.11.8970) (blue) are depicted above the alignment. Black circles indicate R5P binding residues. (B) Ribbon representation of *Tc*RpiB Esmeraldo-like (PDB code 3K7S) colored according to the sequence similarity with *Tc*RpiB Non-Esmeraldo-like and *Tb*RpiB as shown in (A). (C) Superposition of *Tc*RpiB structure (PDB code 3K7S) (grey) with *Tc*RpiB (Tc00.1047053508601.119) (purple) and *Tb*RpiB (Tb927.11.8970) (blue) homology models. Ligand color scheme: R5P is shown in yellow (oxygen, pink; phosphorous orange).
(TIF)

S2 Fig. Biochemical properties of *Tc*RpiB (Tc00.1047053508601.119) expressed in *E. coli*. (A) 10 μg of *Tc*RpiB recombinant protein analyzed by SDS-PAGE and Coomassie blue staining. Mw, molecular weight marker. Western blot analysis of his-tagged recombinant protein probed with rabbit anti-histidine monoclonal antibody (MicroMol-413) (1:1000). (B) Kinetic parameters of direct (R5P to Ru5P) and inverse (Ru5P to R5P) reaction. The values are the means ± standard deviation obtained from 3 independent experiments. (C) Inhibition (%) of *Tc*RpiB activity by 4PEH. (D) Plot of K_{mapp}/V_{max} *versus* 4PEH concentrations; K_i corresponds to the symmetric value of the X-axis intersection. (E) Plot showing the effect of different 4PEH concentrations on the inverse of the initial velocity *versus* the inverse of several concentrations of R5P. (C–E) The values correspond to the means ± standard deviation of two replicates, and data is representative of three independent experiments.
(TIF)

S3 Fig. Validation of antibodies against *Tb*RpiB. Immunofluorescence analysis of *T. brucei* wt or a representative Rpi RNAi clone in the presence or absence of tetracycline (tet). RNAi induced and uninduced cells were grown for 48 h, then fixed and probed with rat polyclonal anti-*Tb*RpiB (A) or rabbit polyclonal anti-*Tb*RpiB (B) antibody and co-stained with DAPI. Bars, 5 μm. (C) Quantification of *Tb*RpiB fluorescence levels in induced cells [Rpi RNAi tet(+), $n = 30$] and uninduced cells [Rpi RNAi tet(−), $n = 30$], using the rat and the rabbit polyclonal anti-*Tb*RpiB antibodies. Data representative of two independent experiments using two different clones. ImageJ software (version 1.43u) was used for fluorescence quantification. p value was calculated by Student's t test (*** $p \leq 0.001$, for both $p < 0.001$). (D, E) Whole membrane resulting from Western blot analysis of RpiB levels, in *T. brucei* wt or a representative Rpi RNAi clone, in the presence or absence of tet. The membrane was probed with rat anti-*Tb*RpiB (1:100) (D) or rabbit anti-*Tb*RpiB (1:1000) (E), and after membrane stripping, with rabbit anti-aldolase (1:5000) for loading control.
(TIF)

Acknowledgments

We would like to thank Dr. Paul Michels from Université catholique de Louvain, Belgium, for sending us enolase antibody and Dr. Laurent Salmon from Laboratoire de Chimie Universite de Paris-Sud XI, France for providing 4-deoxy-4-phospho-D-erythronohydroxamic acid (4-PEH) inhibitor. We also thank Claudia Helbig for assistance in Heidelberg.

Author Contributions

Conceived and designed the experiments: IL JF JT ACdS. Performed the experiments: IL JF JT. Analyzed the data: IL JF SMR CC JT ACdS NS. Contributed reagents/materials/analysis tools: CC SMR NR NS. Wrote the paper: IL JF CC SMR JT ACdS.

References

1. MacGregor P, Szoor B, Savill NJ, Matthews KR (2012) Trypanosomal immune evasion, chronicity and transmission: an elegant balancing act. Nat Rev Microbiol 10: 431–438.
2. Radwanska M, Guirnalda P, De Trez C, Ryffel B, Black S, et al. (2008) Trypanosomiasis-induced B cell apoptosis results in loss of protective anti-parasite antibody responses and abolishment of vaccine-induced memory responses. PLoS Pathog 4: e1000078.
3. Lejon V, Mumba Ngoyi D, Kestens L, Boel L, Barbe B, et al. (2014) Gambiense human african trypanosomiasis and immunological memory: effect on phenotypic lymphocyte profiles and humoral immunity. PLoS Pathog 10: e1003947.

4. Clayton CE, Michels P (1996) Metabolic compartmentation in African trypanosomes. Parasitol Today 12: 465–471.
5. Hellemond JJ, Bakker BM, Tielens AG (2005) Energy metabolism and its compartmentation in Trypanosoma brucei. Adv Microb Physiol 50: 199–226.
6. Albert MA, Haanstra JR, Hannaert V, Van Roy J, Opperdoes FR, et al. (2005) Experimental and in silico analyses of glycolytic flux control in bloodstream form Trypanosoma brucei. J Biol Chem 280: 28306–28315.
7. Chambers JW, Fowler ML, Morris MT, Morris JC (2008) The anti-trypanosomal agent lonidamine inhibits Trypanosoma brucei hexokinase 1. Mol Biochem Parasitol 158: 202–207.
8. Willson M, Sanejouand YH, Perie J, Hannaert V, Opperdoes F (2002) Sequencing, modeling, and selective inhibition of Trypanosoma brucei hexokinase. Chem Biol 9: 839–847.
9. Chudzik DM, Michels PA, de Walque S, Hol WG (2000) Structures of type 2 peroxisomal targeting signals in two trypanosomatid aldolases. J Mol Biol 300: 697–707.
10. Azema L, Lherbet C, Baudoin C, Blonski C (2006) Cell permeation of a Trypanosoma brucei aldolase inhibitor: evaluation of different enzyme-labile phosphate protecting groups. Bioorg Med Chem Lett 16: 3440–3443.
11. Caceres AJ, Michels PA, Hannaert V (2010) Genetic validation of aldolase and glyceraldehyde-3-phosphate dehydrogenase as drug targets in Trypanosoma brucei. Mol Biochem Parasitol 169: 50–54.
12. Helfert S, Estevez AM, Bakker B, Michels P, Clayton C (2001) Roles of triosephosphate isomerase and aerobic metabolism in Trypanosoma brucei. Biochem J 357: 117–125.
13. Aronov AM, Suresh S, Buckner FS, Van Voorhis WC, Verlinde CL, et al. (1999) Structure-based design of submicromolar, biologically active inhibitors of trypanosomatid glyceraldehyde-3-phosphate dehydrogenase. Proc Natl Acad Sci U S A 96: 4273–4278.
14. Subramaniam C, Veazey P, Redmond S, Hayes-Sinclair J, Chambers E, et al. (2006) Chromosome-wide analysis of gene function by RNA interference in the african trypanosome. Eukaryot Cell 5: 1539–1549.
15. Bressi JC, Choe J, Hough MT, Buckner FS, Van Voorhis WC, et al. (2000) Adenosine analogues as inhibitors of Trypanosoma brucei phosphoglycerate kinase: elucidation of a novel binding mode for a 2-amino-N(6)-substituted adenosine. J Med Chem 43: 4135–4150.
16. Cordeiro AT, Thiemann OH, Michels PA (2009) Inhibition of Trypanosoma brucei glucose-6-phosphate dehydrogenase by human steroids and their effects on the viability of cultured parasites. Bioorg Med Chem 17: 2483–2489.
17. Dardonville C, Rinaldi E, Barrett MP, Brun R, Gilbert IH, et al. (2004) Selective inhibition of Trypanosoma brucei 6-phosphogluconate dehydrogenase by high-energy intermediate and transition-state analogues. J Med Chem 47: 3427–3437.
18. Cronin CN, Nolan DP, Voorheis HP (1989) The enzymes of the classical pentose phosphate pathway display differential activities in procyclic and bloodstream forms of Trypanosoma brucei. FEBS Lett 244: 26–30.
19. Comini MA OC, Cazzulo JJ (2013) Drug Targets in Trypanosomal and Leishmanial Pentose Phosphate Pathway. In: Jäger T KO, Flohé L, editor. Trypanosomatid Diseases: Molecular Routes to Drug Discovery. Wiley-VCH Verlag GmbH & Co. KGaA, Weinheim, Germany. pp. 297–313.
20. Husain A, Sato D, Jeelani G, Soga T, Nozaki T (2012) Dramatic increase in glycerol biosynthesis upon oxidative stress in the anaerobic protozoan parasite Entamoeba histolytica. PLoS Negl Trop Dis 6: e1831.
21. Ralser M, Wamelink MM, Kowald A, Gerisch B, Heeren G, et al. (2007) Dynamic rerouting of the carbohydrate flux is key to counteracting oxidative stress. J Biol 6: 10.
22. Sorensen KI, Hove-Jensen B (1996) Ribose catabolism of Escherichia coli: characterization of the rpiB gene encoding ribose phosphate isomerase B and of the rpiR gene, which is involved in regulation of rpiB expression. J Bacteriol 178: 1003–1011.
23. Schlecker T, Schmidt A, Dirdjaja N, Voncken F, Clayton C, et al. (2005) Substrate specificity, localization, and essential role of the glutathione peroxidase-type tryparedoxin peroxidases in Trypanosoma brucei. J Biol Chem 280: 14385–14394.
24. Alibu VP, Storm L, Haile S, Clayton C, Horn D (2005) A doubly inducible system for RNA interference and rapid RNAi plasmid construction in Trypanosoma brucei. Mol Biochem Parasitol 139: 75–82.
25. Larkin MA, Blackshields G, Brown NP, Chenna R, McGettigan PA, et al. (2007) Clustal W and Clustal X version 2.0. Bioinformatics 23: 2947–2948.
26. Bond CS, Schuttelkopf AW (2009) ALINE: a WYSIWYG protein-sequence alignment editor for publication-quality alignments. Acta Crystallogr D Biol Crystallogr 65: 510–512.
27. Arnold K, Bordoli L, Kopp J, Schwede T (2006) The SWISS-MODEL workspace: a web-based environment for protein structure homology modelling. Bioinformatics 22: 195–201.
28. Kiefer F, Arnold K, Kunzli M, Bordoli L, Schwede T (2009) The SWISS-MODEL Repository and associated resources. Nucleic Acids Res 37: D387–392.
29. Peitsch MC, Wells TN, Stampf DR, Sussman JL (1995) The Swiss-3DImage collection and PDB-Browser on the World-Wide Web. Trends Biochem Sci 20: 82–84.
30. Wood T (1970) Spectrophotometric ass for D-ribose-5-phosphateketol-isomerase and for D-ribulose-5-phosphate 3-epimerase. Anal Biochem 33: 297–306.
31. Stern AL, Burgos E, Salmon L, Cazzulo JJ (2007) Ribose 5-phosphate isomerase type B from Trypanosoma cruzi: kinetic properties and site-directed mutagenesis reveal information about the reaction mechanism. Biochem J 401: 279–285.
32. Domagk GF, Alexander WR, Doering KM (1974) Protein structure and enzymatic activity, XIV. Purification and properties of ribosephosphate isomerase from skeletal muscle. Hoppe Seylers Z Physiol Chem 355: 781–786.
33. Burkard G, Fragoso CM, Roditi I (2007) Highly efficient stable transformation of bloodstream forms of Trypanosoma brucei. Mol Biochem Parasitol 153: 220–223.
34. Rothberg KG, Burdette DL, Pfannstiel J, Jetton N, Singh R, et al. (2006) The RACK1 homologue from Trypanosoma brucei is required for the onset and progression of cytokinesis. J Biol Chem 281: 9781–9790.
35. Lanham SM (1968) Separation of trypanosomes from the blood of infected rats and mice by anion-exchangers. Nature 218: 1273–1274.
36. Stern AL, Naworyta A, Cazzulo JJ, Mowbray SL (2011) Structures of type B ribose 5-phosphate isomerase from Trypanosoma cruzi shed light on the determinants of sugar specificity in the structural family. FEBS J 278: 793–808.
37. Roos AK, Burgos E, Ericsson DJ, Salmon L, Mowbray SL (2005) Competitive inhibitors of Mycobacterium tuberculosis ribose-5-phosphate isomerase B reveal new information about the reaction mechanism. J Biol Chem 280: 6416–6422.
38. Clayton CE (1987) Import of fructose bisphosphate aldolase into the glycosomes of Trypanosoma brucei. J Cell Biol 105: 2649–2654.
39. Chen Y, Hung CH, Burderer T, Lee GS (2003) Development of RNA interference revertants in Trypanosoma brucei cell lines generated with a double stranded RNA expression construct driven by two opposing promoters. Mol Biochem Parasitol 126: 275–279.
40. Lecordier L, Walgraffe D, Devaux S, Poelvoorde P, Pays E, et al. (2005) Trypanosoma brucei RNA interference in the mammalian host. Mol Biochem Parasitol 140: 127–131.
41. Jetton N, Rothberg KG, Hubbard JG, Wise J, Li Y, et al. (2009) The cell cycle as a therapeutic target against Trypanosoma brucei: Hesperadin inhibits Aurora kinase-1 and blocks mitotic progression in bloodstream forms. Mol Microbiol 72: 442–458.
42. Loureiro I, Faria J, Clayton C, Ribeiro SM, Roy N, et al. (2013) Knockdown of asparagine synthetase A renders Trypanosoma brucei auxotrophic to asparagine. PLoS Negl Trop Dis 7: e2578.
43. Kaur PK, Dinesh N, Soumya N, Babu NK, Singh S (2012) Identification and characterization of a novel Ribose 5-phosphate isomerase B from Leishmania donovani. Biochem Biophys Res Commun 421: 51–56.
44. Yoon RY, Yeom SJ, Kim HJ, Oh DK (2009) Novel substrates of a ribose-5-phosphate isomerase from Clostridium thermocellum. J Biotechnol 139: 26–32.
45. Skrukrud CL, Gordon IM, Dorwin S, Yuan XH, Johansson G, et al. (1991) Purification and characterization of pea chloroplastic phosphoriboisomerase. Plant Physiol 97: 730–735.
46. Jensen BC, Sivam D, Kifer CT, Myler PJ, Parsons M (2009) Widespread variation in transcript abundance within and across developmental stages of Trypanosoma brucei. BMC Genomics 10: 482.
47. Colasante C, Ellis M, Ruppert T, Voncken F (2006) Comparative proteomics of glycosomes from bloodstream form and procyclic culture form Trypanosoma brucei brucei. Proteomics 6: 3275–3293.
48. Opperdoes FR, Szikora JP (2006) In silico prediction of the glycosomal enzymes of Leishmania major and trypanosomes. Mol Biochem Parasitol 147: 193–206.
49. Stoffel SA, Alibu VP, Hubert J, Ebikeme C, Portais JC, et al. (2011) Transketolase in Trypanosoma brucei. Mol Biochem Parasitol 179: 1–7.
50. Duffieux F, Van Roy J, Michels PA, Opperdoes FR (2000) Molecular characterization of the first two enzymes of the pentose-phosphate pathway of Trypanosoma brucei. Glucose-6-phosphate dehydrogenase and 6-phosphogluconolactonase. J Biol Chem 275: 27559–27565.
51. Kerkhoven EJ, Achcar F, Alibu VP, Burchmore RJ, Gilbert IH, et al. (2013) Handling uncertainty in dynamic models: the pentose phosphate pathway in Trypanosoma brucei. PLoS Comput Biol 9: e1003371.
52. Ong HB, Sienkiewicz N, Wyllie S, Patterson S, Fairlamb AH (2013) Trypanosoma brucei (UMP synthase null mutants) are avirulent in mice, but recover virulence upon prolonged culture in vitro while retaining pyrimidine auxotrophy. Mol Microbiol 90: 443–455.
53. Vigueira PA, Paul KS (2011) Requirement for acetyl-CoA carboxylase in Trypanosoma brucei is dependent upon the growth environment. Mol Microbiol 80: 117–132.
54. Signorell A, Rauch M, Jelk J, Ferguson MA, Butikofer P (2008) Phosphatidylethanolamine in Trypanosoma brucei is organized in two separate pools and is synthesized exclusively by the Kennedy pathway. J Biol Chem 283: 23636–23644.
55. Mackey ZB, Koupparis K, Nishino M, McKerrow JH (2011) High-throughput analysis of an RNAi library identifies novel kinase targets in Trypanosoma brucei. Chem Biol Drug Des 78: 454–463.
56. Alsford S, Turner DJ, Obado SO, Sanchez-Flores A, Glover L, et al. (2011) High-throughput phenotyping using parallel sequencing of RNA interference targets in the African trypanosome. Genome Res 21: 915–924.
57. Mohr SE, Perrimon N (2012) RNAi screening: new approaches, understandings, and organisms. Wiley Interdiscip Rev RNA 3: 145–158.
58. Jones NG, Thomas EB, Brown E, Dickens NJ, Hammarton TC, et al. (2014) Regulators of Trypanosoma brucei cell cycle progression and differentiation identified using a kinome-wide RNAi screen. PLoS Pathog 10: e1003886.

2.2.2. Disclosing ribose-5-phosphate isomerase B essentiality in trypanosomatids

Ribose-5-phosphate isomerase (RPI) belongs to the non-oxidative branch of the pentose phosphate pathway, catalysing the inter-conversion of D-ribose-5-phosphate and D-ribulose-5-phosphate. Trypanosomatids encode a type B RPI, whereas humans have a structurally unrelated type A, making RPIB worthy of exploring as a potential drug target.

Null mutants generation in *Leishmania infantum* was only possible when an episomal copy of *RPIB* gene was provided, and the latter was preserved both *in vitro* and *in vivo* in the absence of drug pressure. This suggests the gene is essential for parasite survival. Importantly, the inability to remove the second allele of *RPIB* gene in sKO mutants complemented with an episomal copy of *RPIB* carrying a mutation that abrogates isomerase activity suggests the essentiality is due to its metabolic function. *In vitro*, sKO promastigotes exhibited no defect in growth, metacyclogenesis or macrophages infection, however, an impairment in intracellular amastigotes' replication was observed. Additionally, mice infected with sKO mutants presented a reduced parasite burden in the liver, rescued by RPIB complementation. Moreover, *T. brucei* is reluctant to complete *RPIB* gene removal, and mice experienced an extended survival upon infection with sKO mutants. Overall, our results genetically validate RPIB as a drug target candidate in trypanosomatids.

Submitted

"Disclosing ribose-5-phosphate isomerase B essentiality in trypanosomatids"

Joana Faria[1,2], Inês Loureiro[1,2], Nuno Santarém[1,2], Pedro Cecílio[1,2], Sandra Macedo-Ribeiro[2,3], Joana Tavares[1,2†*] & Anabela Cordeiro-da-Silva[1,2,4†*]

[1]Parasite Disease Group, Instituto de Biologia Molecular e Celular da Universidade do Porto, Portugal
[2]Instituto de Investigação e Inovação em Saúde, Universidade do Porto, Porto, Portugal
[3]Protein Crystallography Group, Instituto de Biologia Molecular e Celular da Universidade do Porto, Portugal
[4]Departamento de Ciências Biológicas, Faculdade de Farmácia, Universidade do Porto, Portugal

[*]Corresponding authors: jtavares@ibmc.up.pt or cordeiro@ibmc.up.pt
[†]These authors contributed equally to this work

Abstract

Ribose-5-phosphate isomerase (RPI) belongs to the non-oxidative branch of the pentose phosphate pathway, catalysing the inter-conversion of D-ribose-5-phosphate and D-ribulose-5-phosphate. Trypanosomatids encode a type B RPI, whereas humans have a structurally unrelated type A, making RPIB worthy of exploring as a potential drug target. Null mutants generation in *Leishmania infantum* was only possible when an episomal copy of *RPIB* gene was provided, and the latter was preserved both *in vitro* and *in vivo* in the absence of drug pressure. This suggests the gene is essential for parasite survival. Importantly, the inability to remove the second allele of *RPIB* gene in sKO mutants complemented with an episomal copy of *RPIB* carrying a mutation that abrogates isomerase activity suggests the essentiality is due to its metabolic function. *In vitro*, sKO promastigotes exhibited no defect in growth, metacyclogenesis or macrophages infection, however, an impairment in intracellular amastigotes' replication was observed. Additionally, mice infected with sKO mutants presented a reduced parasite burden in the liver, rescued by RPIB complementation. Moreover, *T. brucei* is reluctant to complete *RPIB* gene removal, and mice experienced an extended survival upon infection with sKO mutants. Overall, our results genetically validate RPIB as a drug target candidate in trypanosomatids.

Introduction

Some clinically relevant pathogens can survive and replicate in macrophages (MØ). However, only the protozoan *Leishmania* and *Coxiella* bacteria are known to thrive in fully mature phagolysosomes[1, 2]. Mammals become infected with *Leishmania* through the bite of an infected sand fly, which injects non-replicative metacyclic promastigotes in the skin, later phagocytosed by MØ[2]. Upon delivery to the phagolysosome, the internalized promastigotes differentiate into amastigotes[3]. The latter are able to rapidly re-infect other phagocytic cells (MØ or dendritic cells), as well as some non-phagocytic cells (fibroblasts), leading to several possible disease outcomes, like acute disease (ranging from self-healing cutaneous infections to fatal if untreated visceral forms), as well as chronic or latent infections[3].

Leishmaniasis is an important worldwide human health problem, affecting approximately 12 million people, with 1.3 million new cases every year[4]. Visceral leishmaniasis (VL), the most severe form of the disease, is mainly associated to infections by *Leishmania donovani* or *Leishmania infantum*. Currently, VL control relies mainly on chemotherapy and vector control, both presenting several limitations that hinder disease eradication in endemic areas[5]. Traditional chemotherapy is often associated with high cost, toxicity, complex administration regimes and the emergence of resistance[5]. Consequently, approximately 20,000 to 30,000 people die every year[4], rendering the search for novel chemotherapeutic options a priority.

The Pentose Phosphate Pathway (PPP) is a key metabolic pathway that relies on the use of glucose and is classically divided into two branches: an oxidative and a non-oxidative branch. In these organisms, enzymes from the oxidative branch, namely glucose-6-phosphate dehydrogenase (G6PD), 6-phosphogluconolactonase (6PGL) and 6-phosphogluconate dehydrogenase (6PGDH) play an important housekeeping role and are related to their cyanobacteria and plant orthologues[6, 7]. The non-oxidative PPP is responsible for the interconversion of phosphorylated saccharides, giving rise to products (ribose-5-phosphate - R5P), intermediates (glyceraldehyde-3-phosphate - G3P, fructose-6-phosphate - F6P) and cofactors (NADPH) used to synthesize nucleic acids and lipids and to maintain redox homeostasis[8]. Curiously, the enzymes involved in the non-oxidative branch, such as ribose-5-phosphate isomerase B (RPIB), ribose-5-phosphate-3-epimerase (RPE), transketolase (TKT) and transaldolase (TAL), constitute a more heterogeneous group, comprising a member that lacks any mammalian orthologue (RPIB[9]) and others (RPE and TKT) that are developmentally regulated and dispensable in a species-specific manner[10-14].

RPI enzymes catalyse the interconversion of ribose 5-phosphate (R5P) and ribulose 5-phosphate (Ru5P), depending on the substrate and product concentrations[15]. Two types

of RPI enzymes can be found: type A (RPIA) is represented in all kingdoms of life, contrasting with the type B (RPIB) that is restricted to some bacteria and protozoans[15]. Trypanosomatids possess a RPI type B with no mammalian homologue[9, 16-18]. Indeed, we have recently demonstrated that in *T. brucei* bloodstream forms RPIB knockdown induces a dramatic impairment on parasite infectivity[18].

Taken all together, RPIB was suitable to be investigated as a drug target candidate in *Leishmania*. Thus, to evaluate the importance of this protein for *Leishmania* survival and infectivity, we have performed target gene replacement studies in *L. infantum*, and characterized the generated mutants. Target gene replacement studies were also undertaken in *T. brucei.*

Results

***Li*RPIB and *Lm*RPIB sequence alignment.** The open reading frames (ORFs) encoding a putative RPIB enzyme were identified in the genomes of *L. infantum* JPCM5 (LinJ.28.2100) and *L. major* Friedlin (LmjF.28.1970)[19, 20]. The *RPIB* amplified sequences from these strains matched 100% the annotated sequences. RPIB sequences of *L. infantum (Li*RPIB), *L. major* (*Lm*RPIB), *T. brucei* (*Tb*RPIB) and *T. cruzi* (*Tc*RPIB) generate polypeptides containing 172, 172, 155 and 159 amino acids, respectively (Fig. 1a). *Li*RPIB displays a 93% sequence identity with *Lm*RPIB, and around 50% to RPIB of trypanosomes. *Li*RPIB shows only around 12% similarity to human RPIA. The amino acids involved in isomerisation (Cys69), phosphate stabilization (Arg113, Arg137, Arg141) and ring opening (His102, His138) have been identified in *Tc*RPIB[16] and are strictly conserved in *Li*RPIB, *Lm*RPIB and *Tb*RPIB (Fig. 1a).

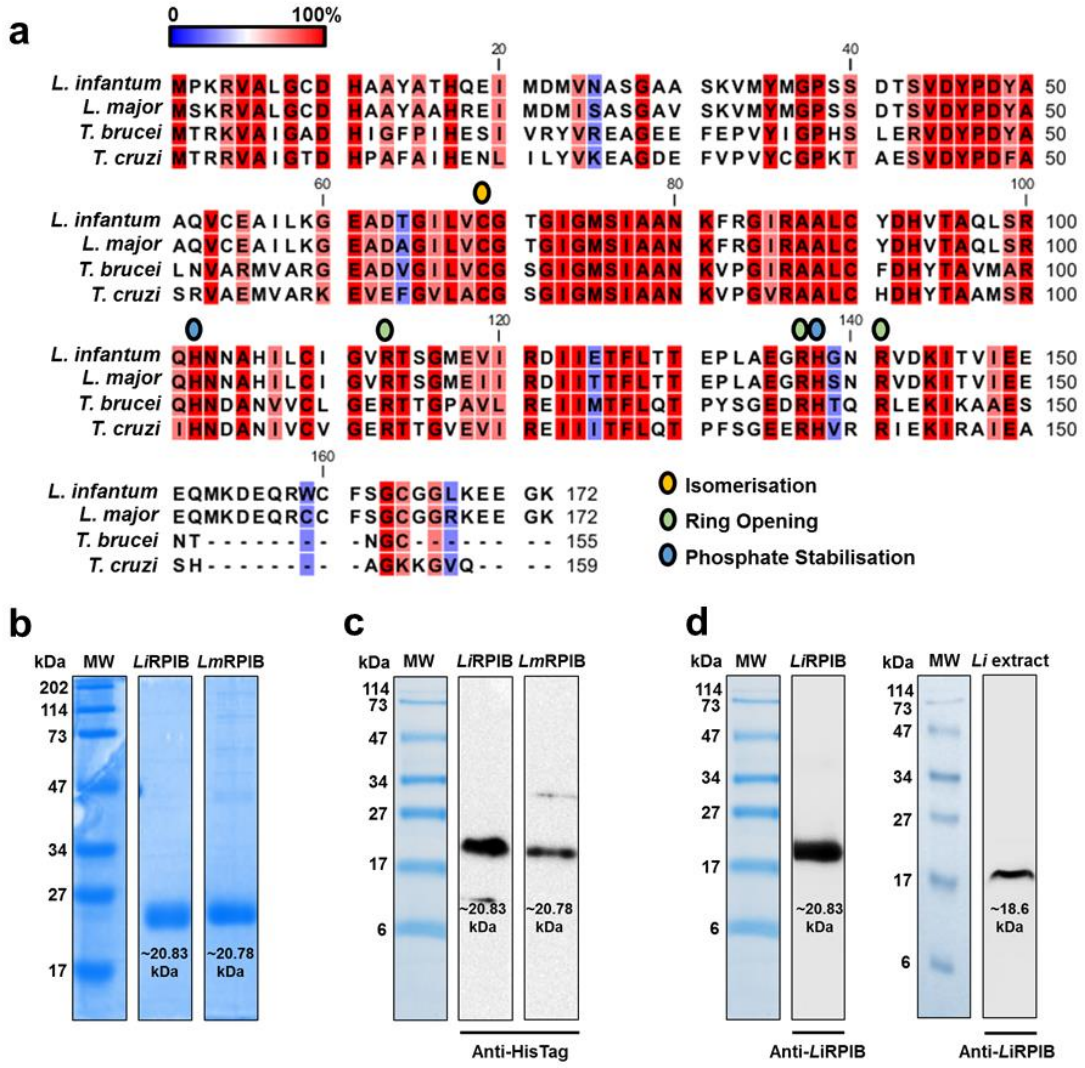

Figure 1. Multiple-sequence alignment of RPIB proteins from trypanosomatids and analysis of recombinant *Li*RPIB and *Lm*RPIB. (a) Alignment of *Li*RPIB (NCBI-Gene ID: 5070424/ LinJ.28.2100), *Lm*RPIB (NCBI-Gene ID: 5653408/LmjF.28.1970), *Tb*RPIB (NCBI-Gene ID: 3664062/ Tb927.11.8970) and *Tc*RPIB (NCBI-Gene ID: 3542840/TcCLB.508601.119). The amino acid conservation is coloured in blue (low conservation) to red (high conservation). Yellow, light green and light blue indicate the residues involved in the isomerisation, ring opening and phosphate stabilisation respectively. **(b)** Coomassie blue stained SDS-PAGE gel of 10 µg of recombinant *Li*RPIB and *Lm*RPIB post affinity chromatography purification. **(c)** Western-blot analysis of 1 µg of purified recombinant *Li*RPIB and *Lm*RPIB using a rabbit anti-HisTag monoclonal antibody (1:1000). (**d)** Western-blot analysis of recombinant *Li*RPIB or whole *L. infantum* promastigote extract using a rabbit polyclonal anti-*Li*RPIB (1:1000). MW, molecular weight marker.

Enzymatic characterization of *Li*RPIB and *Lm*RPIB. *Li*RPIB and *Lm*RPIB recombinant proteins, containing a 6-histidine N-terminal tag, were expressed in *Escherichia coli* and purified by affinity chromatography under native conditions. Coomassie

staining and Western-blot analysis with an anti-HisTag antibody, are represented on figure 1b and 1c, respectively, showing both proteins present the predicted MW for the monomer (*Li*RPIB ~20.83, *Lm*RPIB ~20.78 kDa). The Coomassie staining also demonstrates that the purified recombinant proteins possess a suitable purity level to proceed to enzymatic studies. Additionally, recombinant *Li*RPIB was used to immunise rabbits to produce polyclonal anti-*Li*RPIB antibodies. Those antibodies do recognise the recombinant protein and a single band in *L. infantum* promastigotes extract with the expected MW (~18.6 kDa, [web.expasy.org/protparam]) (Fig. 1d). Both *Li*RPIB and *Lm*RPIB catalyse the conversion of R5P into Ru5P (direct reaction) or Ru5P into R5P (inverse reaction) *in vitro*, with similar kinetic constants, as shown in Table S1. The inverse reaction, which generates R5P, seems to be favoured, with both enzymes presenting lower K_m values and higher v_{max} and k_{cat}.

RPIB has a dual localisation in *L. infantum* promastigotes. The rabbit anti-*Li*RPIB polyclonal antibody was also validated by IFA, as the fluorescence intensity of WT promastigotes *versus LiRPIB* mutants (single knockout (sKO; clone 15) and overexpressing line (OE)) was measured and a positive correlation between protein levels and labelling intensity was found (Fig. S1).

Using α-tubulin as a loading control, we compared RPIB expression in different stages of the parasite life cycle. RPIB was found to be more expressed in amastigotes (5 fold increase) followed by logarithmic promastigotes (3 fold increase) when compared to late stationary promastigotes (Fig. 2a).

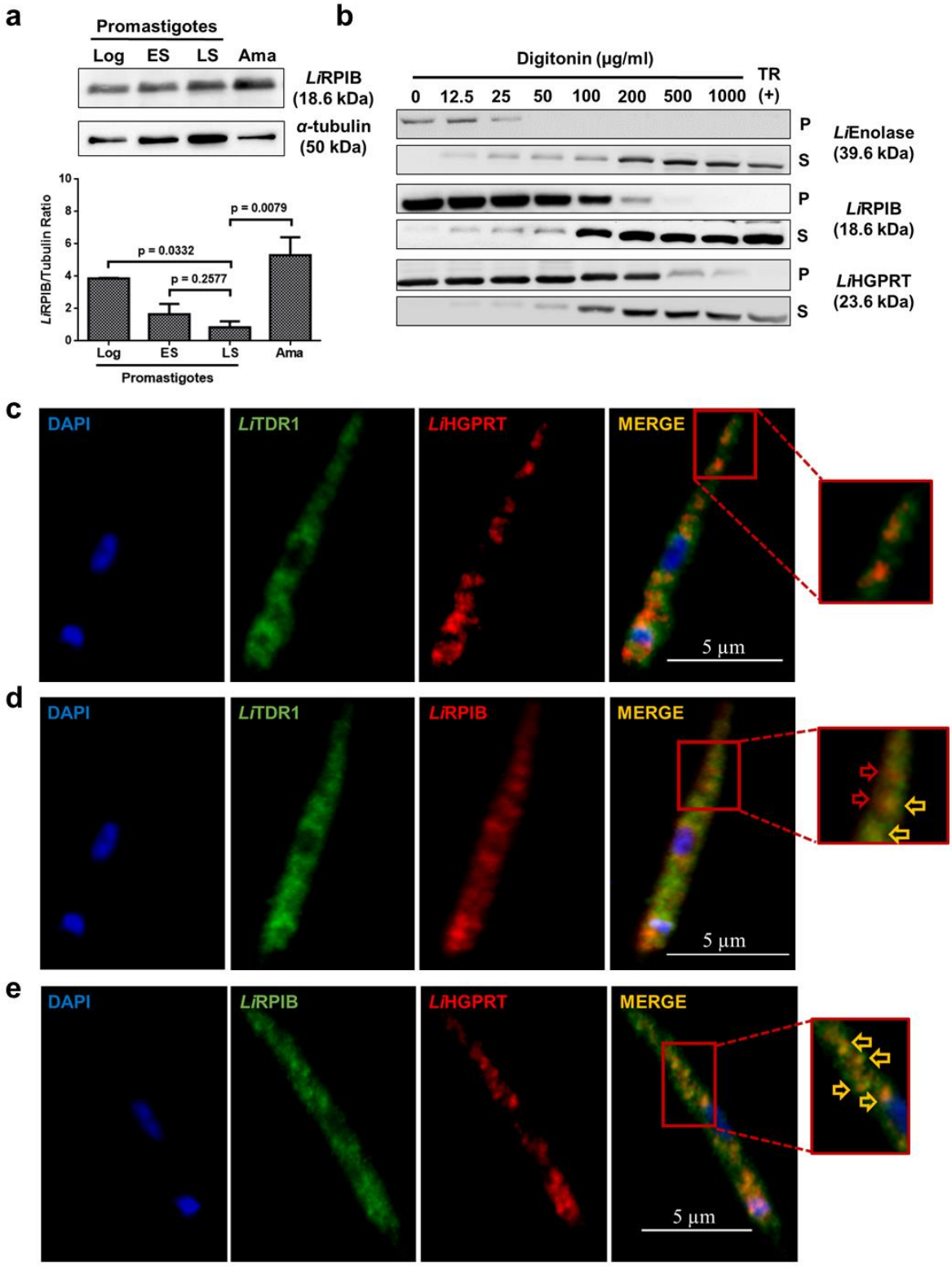

Figure 2. RPIB expression and localization in *L. infantum*. (a) RPIB expression in different stages of *L. infantum* life cycle. Promastigote forms: logaritmic phase (Log), early stationary phase (ES), late stationary phase (LS); axenic amastigote forms (Ama). Twenty µg of total extracts were analysed by Western-blot and probed with rabbit polyclonal anti-*Li*RPIB. α-tubulin (mouse monoclonal antibody) was used as loading control. Quantification expressed in *Li*RPIB/tubulin ratio, is presented in the lower panel. Two-tailed unpaired *t* test

was performed: statistical significance $p < 0.05$. **(b)** Digitonin fractionation of mid-log *L. infantum* promastigotes. Pellet (P) and supernatant (S) fractions obtained using increasing concentrations of digitonin or positive control with 1% of Triton X-100 (TR – Total Release) were subjected to Western-blot analysis and probed with antibodies against *Li*RPIB, *Li*Enolase (cytosolic marker) and hypoxanthine guanine phosphoribosyltransferase *Li*HGPRT (glycosomal marker). **(c-e)** Immunofluorescence analysis showing *Li*RPIB (red in c; green in e) localization in *L. infantum* promastigote form. Nucleus and kinetoplast DNA, cytosol and glycosomes were stained with DAPI (blue), sheep anti-*Li*TDR1 (thiol-dependent reductase 1, green) and rabbit anti-*Li*HGPRT (red), respectively. On panel d, red arrows in the zoomed areas correspond to sites of exclusive *Li*RPIB staining. On panels d and e, yellow arrows in the zoomed areas point to colocalisation sites. Images are maximal Z-projections of 30 to 35 contiguous stacks separated by 0.1 µm and were acquired with a 63x objective, using a LEICA SP5II confocal microscope. The scale bar corresponds to 5 µm. Data displayed on a-e are representative of 3 independent experiments.

To determine *Li*RPIB subcellular localization, we resorted to *in silico* prediction and performed digitonin fractionation and immunofluorescence analysis. Bioinformatics tools, Wolf Psort and CELLO, predicted a cytosolic localization for RPIB. Digitonin fractionation followed by Western-blot analysis was performed in promastigotes. The following antibodies were used to detect the fractioning pattern of proteins located in different subcellular compartments, namely, anti-*Tb*Enolase (*Li*Enolase *versus* *Tb*Enolase 79% identity, *Li*Enolase 39.6 kDa) as a cytosolic marker[21] and anti-*Ld*HGPRT (hypoxanthine guanine phosphoribosyl transferase, *Li*HGPRT 23.6 kDa) as a glycosomal marker[22]. Enolase (Fig. 2b) was found in the supernatant for digitonin concentrations as low as 12.5 µg/ml, and retained in the pellets up to 12.5-25 µg/ml. HGPRT, in its turn, is longer retained in the pellet fractions (significantly up to 200 µg/ml of digitonin, and detected up to 1000 µg/ml), being detected in the supernatant only at 100 µg/ml. RPIB is less retained in the pellet fraction than HGPRT , however, it appears in the supernatant in a similar fashion to enolase. To further elucidate RPIB localization, we have also performed immunofluorescence analysis in promastigotes and confocal microscopy. TDR1 (thiol-dependent reductase 1)[23] and HGPRT were labelled as cytosolic and glycosomal markers, respectively. Representative images of the labelling with these two markers are shown on figure 2c (also on Fig. S2a). RPIB labelling profile and the partial co-localization with the cytosolic marker TDR1 indicates the protein is mainly localized in the cytosol (Fig. 2d and S2b). However, some co-localization with the glycosomal marker, HGPRT, was frequently seen, suggesting this protein might have a dual localization (Fig. 2e and S2c). Indeed, in all the parasites we have analysed, partial RPIB co-localisation with TDR1 or HGPRT was always observed.

In conclusion, RPIB despite mostly localised in the cytosol of promastigotes can also be found in association to the glycosomes.

***LiRPIB* facilitated null mutants generation by targeted gene replacement.** A targeted gene replacement strategy was used for *RPIB* gene inactivation in *L. infantum*. The first transfection allowed the removal of one of the gene alleles generating sKO clones resistant to either neomycin *(NEO)* or hygromycin *(HYG),* depending on the cassette that was used. When attempting to remove the second gene allele, independently of using a *HYG* or *NEO*, no null mutants were obtained in a total of four independent attempts. Some of the mutants obtained following the dKO attempt were likely aneuploid (Table S2), as by PCR and by Southern-blot (data not shown), parasites carry both resistance cassettes and the gene at the target locus. The consecutive inability to remove the second allele, coupled with the constant aneuploidy generation was suggestive of gene essentiality. Therefore, a *HYG* construct has been transfected in parallel into parasites with the following genotypes: WT, sKO*NEO* (sKO 15) and sKO*NEO* complemented (sKO P15) with an episome carrying the *RPIB* gene (pSP*αBLASTαRPIB*). This approach enabled the generation of sKO mutants from the WT, dKO mutants only in the complemented sKO, and once more failed to generate mutants that were truly null to *RPIB*. The WT parasites were transfected with the pSP*αBLASTαRPIB* plasmid to generate an overexpressing cell line.

The genotype of the facilitated null mutants (dKO P15.3, dKO P15.14 and dKO P15.15) was confirmed by PCR (Fig. 3b) and Southern-blot (Fig. 3c), whose strategies are illustrated on figure 3a. By PCR, the successful integration of the selectable markers, *RPIB* presence in the episome and absence in the chromosomic locus were verified. The genotypes were further confirmed by Southern-blot. A first hybridization was performed using 3' UTR as a probe: the bands of ~7547 bp, ~3958 bp and ~4574 bp correspond to *RPIB, NEO* and *HYG,* respectively (Fig. 3c). The blot was then stripped and reprobed three additional times to confirm each of the bands. Reprobing with *RPIB* gene confirmed its presence in the chromosomes of WT, OE, sKO 15 and sKO P15 (~7547 bp) and in the episome in OE, sKO P15 and facilitated null mutants (~3606 bp) (Fig. 3c). All the clones were also analysed by Western-blot and shown RPIB reduction in sKO mutants, an overexpression in sKO P15 and OE mutants (Fig. 3d).

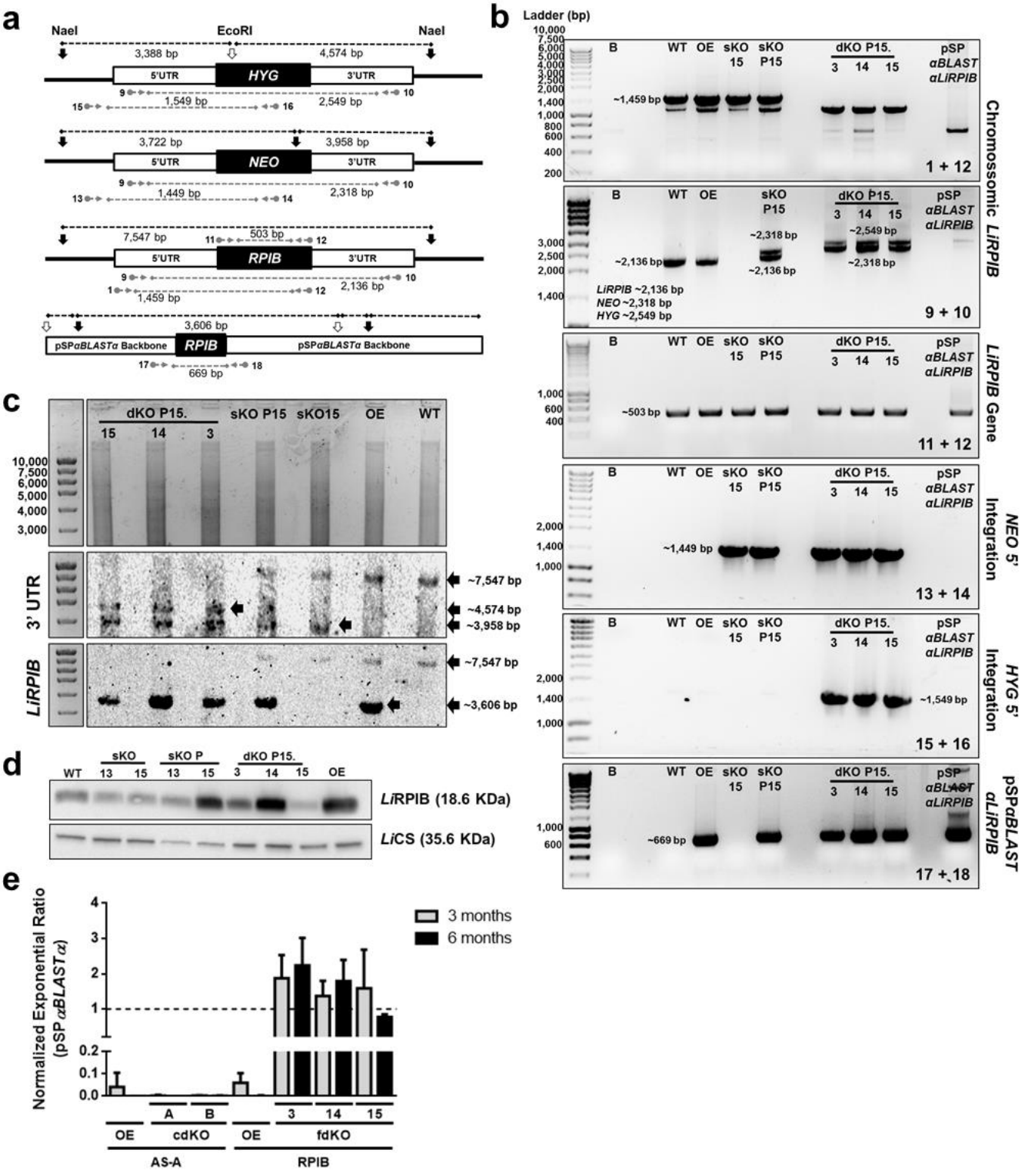

Figure 3. Genetic and post-translational analysis of the *LiRPIB* mutants. (a) *LiRPIB* locus (*RPIB* allele, targeted gene replacement cassettes, containing *NEO* and *HYG*) and pSP*αBLASTαLiRPIB* schematics. Horizontal grey arrows and numbers represent the primer pairs (sequence on Table S4) used to assess the genotype of the mutants: the grey dashed line represents the expected PCR fragment. Southern-blot approach, upon digestion with EcoRI (vertical black contoured arrows) and NaeI (vertical black full coloured arrows) is also

represented: dashed black lines represent the expected digestion fragments. **(b)** PCR analysis of *LiRPIB* mutants to assess *LiRPIB, NEO* and *HYG* presence in chromosome 28, as well as pSP*αBLASTαLiRPIB* presence. B, blank. **(c)** Southern-blot analysis of 10 µg of *LiRPIB* mutants (*versus* WT) genomic DNA, previously digested with EcoRI and NaeI, and probed using 3' UTR. Following, the blot was stripped and reprobed using *LiRPIB*. **(d)** Western-blot analysis of *Li*RPIB expression in promastigote mutants (*versus* WT), using *Li*CS (cysteine synthase) as loading control. **(e)** pSP*αBLASTα* quantification by qPCR using 10 ng of genomic DNA from *LiRPIB* OE and facilitated null mutants (fdKO) P15.3, P15.14 and P15.15 and from *LiASA* OE and complemented null mutants (cdKO) clones A and B. We used DNA of each one of the mutants left in culture for 3 and 6 months in the absence of blasticidin and calibrated against the correspondent mutant maintained in culture in the presence of the drug. rRNA45 was used a reference gene. The results correspond to means plus standard deviation of two independent experiments.

The facilitated dKO mutants were subcultured weekly for 6 months in the presence or absence of blasticidin drug pressure. In the absence of drug pressure, *LiRPIB* facilitated mutants (fdKO) did not lose the plasmid, as assessed by qPCR (Fig. 3e). Contrarily, *Li*RPIB OE, as well as an unrelated non-essential protein (asparagine synthase A; AS-A) OE and its correspondent complemented null mutants (in which pSP*αBLASTα* was also used as a vector; cdKO), lost the plasmid.

In conclusion, our results indicate RPIB is essential for *L. infantum* survival.

***Li*RPIB is important for the replication of intracellular amastigotes.** Several experiments using the different mutants were conducted *in vitro* to assess whether *Li*RPIB would have a role in promastigotes growth and metacyclogenesis, MØ infection or intracellular amastigote replication.

All promastigotes mutants grew in a similar fashion to the WT (Fig. 4a), including in logarithmic phase (Fig. 4b). The expression of metacyclogenesis markers (Histone H4, SHERP, MET-1[24]) in stationary cultures was not statistically different from the WT (Fig. 4c). Moreover, all the clones successfully differentiated into axenic amastigotes and apparently enter bone marrow derived MØ normally, as observed at 4 hours post infection, either by FACS (Fig. 4d) or microscopic analysis. Indeed, no differences in the percentage of infected cells nor the numbers of parasites per infected cell were seen at 4 and 24 hours post-infection between WT and mutant parasites (Fig 4e-f). While the percentage of infected cells remained similar during the experiment for all the mutants, cells infected with sKO presented a statistically significant decrease in the average of amastigotes per cell at 72 hours post-infection (Fig. 4g). This reduction is due to an increase in the percentage of cells with one amastigote and a decrease in the percentage of cells containing, at least, three

amastigotes (Fig. 4h-i). Importantly, this phenotype is not observed in complemented sKO (sKO P15).

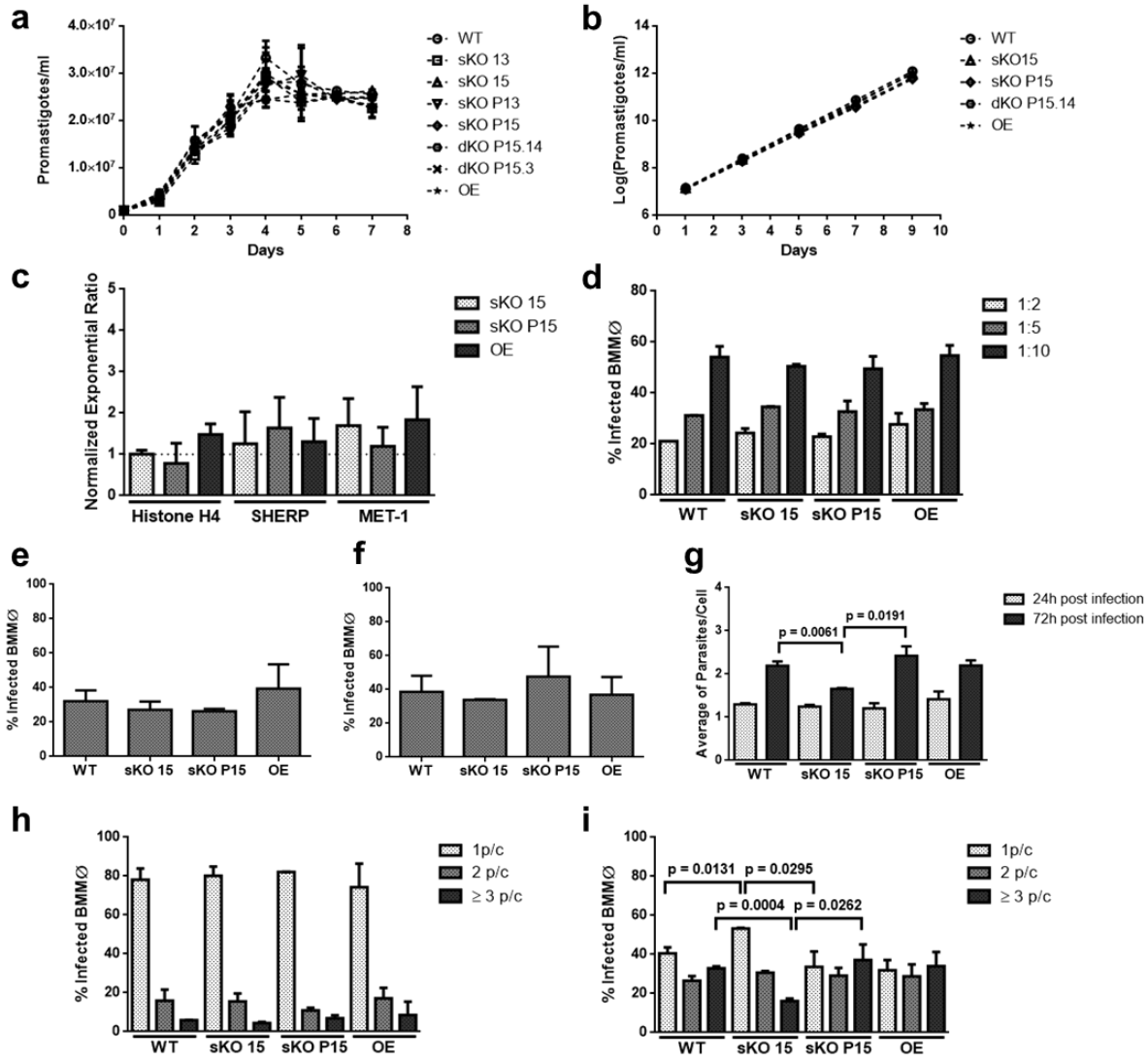

Figure 4*. In vitro* characterization of *LiRPIB* mutants: promastigotes growth, metacyclogenesis, MØ invasion and intracellular amastigote replication. (a and b) *L. infantum* promastigotes growth curves of *LiRPIB* mutants (*versus* WT), cultured in cRPMI. In b, parasites were maintained in logarithmic phase by subculturing every 2 days. Data correspond to mean values of duplicates ± standard deviation. **(c)** Histone H4, SHERP and MET-1 gene expression levels quantification by qRT-PCR. Prior, total RNA from WT and *LiRPIB* mutants stationary promastigotes was extracted and converted into cDNA. rRNA45 was used as reference gene. Calibration was performed against WT. Data correspond to mean values of duplicates plus standard deviation. **(d)** Percentage of infected bone marrow derived MØ determination by FACS analysis using CFSE-labelled WT or *LiRPIB* mutants stationary promastigotes, at 4 hours post infection. Infections were performed using a ratio of 2, 5 or 10 parasites per cell. Data correspond to mean values of duplicates plus standard deviation. **(e and f)** Percentage of infected bone marrow derived MØ at 24 (e) and 72 (f) hours post infection. **(g)** Average of amastigotes per cell in bone marrow derived MØ at 24

and 72 hours post infection. **(h and i)** Percentage of infected bone marrow derived MØs that contain 1, 2 or ≥ 3 parasites, at 24 (h) and 72 (i) hours post infection. a-j are representative of 2 independent experiments. In e-i, WT or *LiRPIB* mutants stationary promastigotes were used in a ratio of 10 parasites per cell. In the appropriate timepoints, the cells were Giemsa stained and microscopically analysed. Data correspond to mean values of duplicates plus standard deviation. Two-tailed unpaired *t* test was performed: statistical significance $p < 0.05$.

In conclusion, the *in vitro* results suggest that *Li*RPIB might be important for the replication of intracellular amastigotes.

***Li*RPIB has a role in mice infection.** To evaluate the role of RPIB on parasites infectivity, BALB/c mice were infected with WT or *LiRPIB* mutant promastigotes and the parasite burdens in the spleen and liver determined at two (acute phase) and eight weeks (chronic phase) post infection. At two weeks post infection, no differences in the splenic parasite loads were detected, while in the liver, animals infected with sKO mutants (clones 13 and 15) presented reduced parasite loads (Fig. 5a-b). Importantly, these differences were not seen in animals infected with sKO lines complemented with episomal *RPIB* (clones sKO P13 and sKO P15). Western-blot analysis of parasites recovered from the spleen and the liver in acute phase demonstrates RPIB downregulation in sKO and overexpression in the complemented sKO. A representative Western-blot and the respective quantification are shown on figure 5c-d. In the chronic phase, there is a partial clearance of the parasite burden in the liver compared to acute phase, but overall both WT and mutant parasites persist in both organs. Mutant parasites recovered from the spleen and the liver of chronically infected animals were analysed by qPCR for the presence of the episome carrying *RPIB*. While the OE has lost the episome over time, the same did not occur with the facilitated null mutant clone P15.14 (Fig. 5e), suggesting RPIB is also essential in amastigote form.

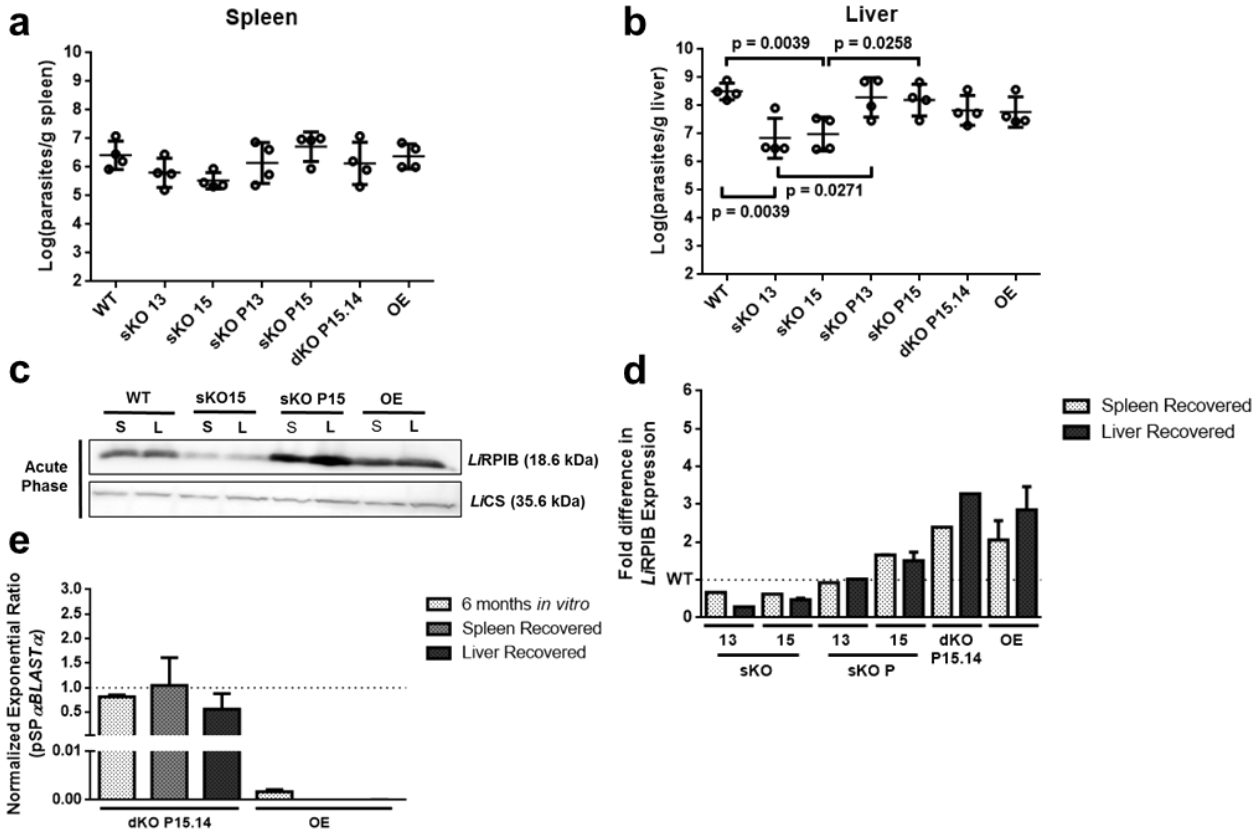

Figure 5. Infectivity of *LiRPIB* mutants in mice. (a and b) 1 x 10^8 early stationary promastigotes were intra-peritoneally injected in BALB/c mice that were sacrificed 2 weeks post infection. The parasite burden in spleen (a) and liver (b) was assessed by the limiting dilution method. The values represent the means of four animals ± standard deviation. Two-tailed unpaired *t* test was performed: statistical significance $p < 0.05$. (**c and d)** Western-blot analysis of RPIB levels in WT and *LiRPIB* mutants recovered from spleen (S) or liver (L). 1x10^7 parasites were used for total extract preparation and *Li*CS (cysteine synthase) was detected as loading control. The fold difference in *of* RPIB expression in *LiRPIB* mutants in comparison to WT recovered from the spleen and liver at 2 weeks post infection is shown in d. The results correspond to means plus standard deviation of two independent experiments. In c a representative Western-blot is shown. **E)** pSP*αBLASTα* quantification by qPCR using 10 ng of genomic DNA from *LiRPIB* OE and facilitated null mutant P15.14 that were left in culture for 6 months in the absence of blasticidin or recovered from spleen or liver 2 months post infection relative to the respective mutant maintained in culture under drug pressure. rRNA45 was used as reference gene. The results correspond to means plus standard deviation of two independent experiments.

These data suggest RPIB is important during *Leishmania* mouse infection, particularly in the liver.

***Li*RPIB essentiality is dependent on its isomerase function.** We consider that assessing whether protein essentiality is due to the annotated metabolic function is particularly important in the context of a drug target validation. *T. cruzi* RPIB isomerase activity is abrogated by replacing cysteine 69 by an alanine without compromising the overall 3D conformation[16]. Therefore, we thought of evaluating whether the same mutation would abrogate *Li*RPIB isomerase activity and whether the second RPIB allele removal in a single KO complemented with a plasmid carrying the mutated RPIB (sKO P15 ^{C69A}) would be successful. This experimental approach would disclose whether protein essentiality is independent (Fig. $6a_6$) or dependent (Fig. $6a_7$) on RPIB isomerase function, respectively.

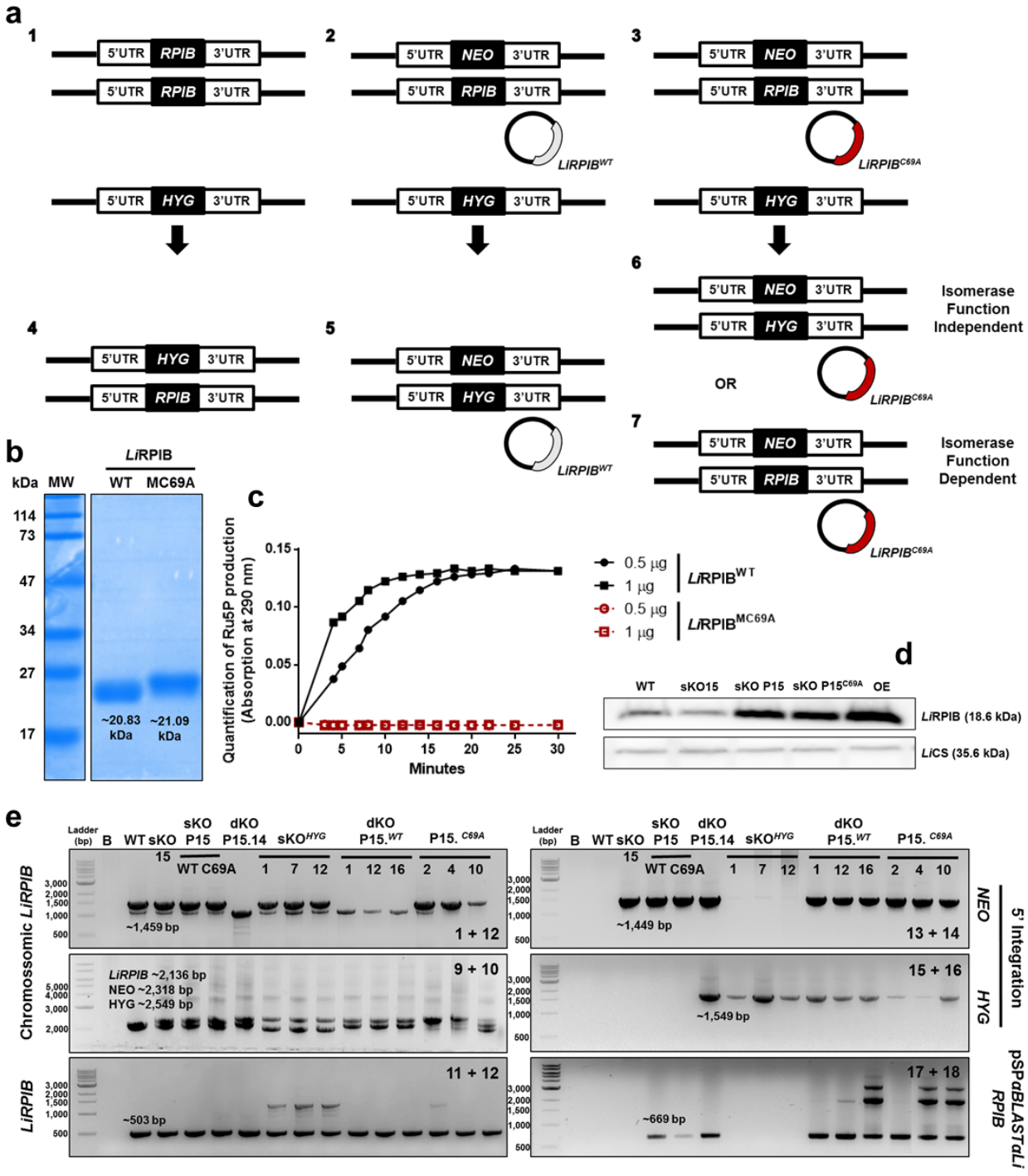

Figure 6. Assessing whether *Li*RPIB essentiality depends on its isomerase function. **(a)** Schematic overview of the strategy used to determine if *Li*RPIB essentiality depends on its isomerase function. The strategy was to transfect WT (1), sKO 15 provided of pSP72*αBLASTαRPIBWT* (sKO P15^{WT}, 2) or pSP72*αBLASTαRPIBC69A* (sKO P15^{C69A}, 3), with a *HYG* containing construct. Two series of mutant's generation had to be successful for conclusions to be extracted: sKO*HYG* mutants' generation from WT transfection (4), validating the construct, and facilitated null mutants generation from sKO P15^{WT} transfection (5). Therefore, whether we were able to remove the second *RPIB* allele or not when transfecting sKO P15^{C69A} would determine whether the protein essentiality was independent

(6) or dependent (7) on the isomerase function, respectively. **(b)** Coomassie blue stained SDS-PAGE gel of 10 µg of recombinant *Li*RPIB^{WT} and *Li*RPIB^{C69A} post affinity chromatography purification. **(c)** Measurement of *Li*RPIB^{WT} and *Li*RPIB^{C69A} activity, catalysing the direct reaction (R5P -> Ru5P), using either 25 or 50 mM of R5P and 0.5 or 1 µg of enzyme and the direct spectrophotometric method at 290 nm. The data are representative of 2 independent experiments. **(d)** Western-blot analysis of *Li*RPIB expression in WT, sKO 15, sKO P15^{WT}, sKO P15^{C69A} and OE, before the transfection scheme represented in A. 1x10^7 parasites were used for total extract preparation and *Li*CS (cysteine synthase) was used as loading control. **(e)** PCR analysis of *LiRPIB* mutants to assess *LiRPIB, NEO* and *HYG* presence in chromosome 28, as well as pSP*αBLASTαLiRPIB* presence. See primers sequences on Table S4 and the expected fragments and annealing sites on figure 3A. B, blank.

For this purpose, a mutated recombinant *Li*RPIB^{C69A} protein was expressed to confirm the inactivation of the isomerase function. The recombinant protein possessed the expected MW (~21.09 kDa, Fig. 6b) and failed to convert R5P into Ru5P (Fig. 6c) or Ru5P into R5P. The sKO 15 was complemented with pSP72*αBLASTαRPIBC69A,* and the expression levels of RPIB in sKO P15^{WT} and sKO P15^{C69A} were found to be similar (Fig. 6d). Afterwards, WT (Fig. 6a$_1$) and sKO 15 provided of pSP72*αBLASTαRPIBWT* (sKO P15^{WT}, Fig. 6a$_2$) or pSP72*αBLASTαRPIBC69A* (sKO P15^{C69A}, Fig. 6a$_3$) were transfected with a *HYG* construct (Fig. 6a). As controls, two mutant series were successfully generated: sKO*HYG* mutants from WT transfection (Fig. 6a$_4$) and facilitated null mutants from sKO P15^{WT} transfection (Fig. 6a$_5$). Eleven out of 12 (Table S2) facilitated null mutants from sKO P15^{WT} transfection were obtained, while no facilitated null mutants were obtained with sKO P15^{C69A}. PCR analysis of representative mutants of each series is shown on figure 6e, following the same strategies depicted on figure 3a. The previously generated facilitated null mutant clone P15.14 was used as positive control.

These data indicate *Li*RPIB essentiality is due to its isomerase function.

RPIB essentiality is conserved across trypanosomatids. Taking into account RPIB essentiality in *L. infantum*, and a previous report of its importance for *T. brucei* bloodstream forms infectivity[18], we investigated whether essentiality would be preserved in this organism. To obtain *TbRPIB* null mutants, a target gene replacement strategy was also applied. One *TbRPIB* allele was replaced by *HYG* giving rise to sKO mutants right in the first attempt. PCR and Southern blot, whose approach is represented on figure 7a, confirmed the correct insertion of the cassette (Fig. 7b and d), and Western-blot shows a reduction in *Tb*RPIB protein levels of approximately 50% in sKO cell lines compared to the WT (Fig. 7c). For the generation of *TbRPIB* dKO mutants, sKO parasites were transfected either with a *BLEO* construct or with a *NEO* construct, with no success. The *NEO* construct

reliability was assessed by simultaneous transfection of WT and sKO mutant. Resistant parasites were only obtained for the WT but not for the sKO (Fig. 7e), enabling the generation of sKO but not null mutants. Therefore, we have characterized the generated sKO cell lines. No significant differences were found on the *in vitro* growth of *TbRPIB* sKO bloodstream forms compared to WT (Fig. 7f). *In vivo*, *TbRPIB* sKO showed a reduced infectivity evaluated by the parasitemia (Fig. 7g) and by the increase of mice life span (Fig. 7h) when compared to WT parasites.

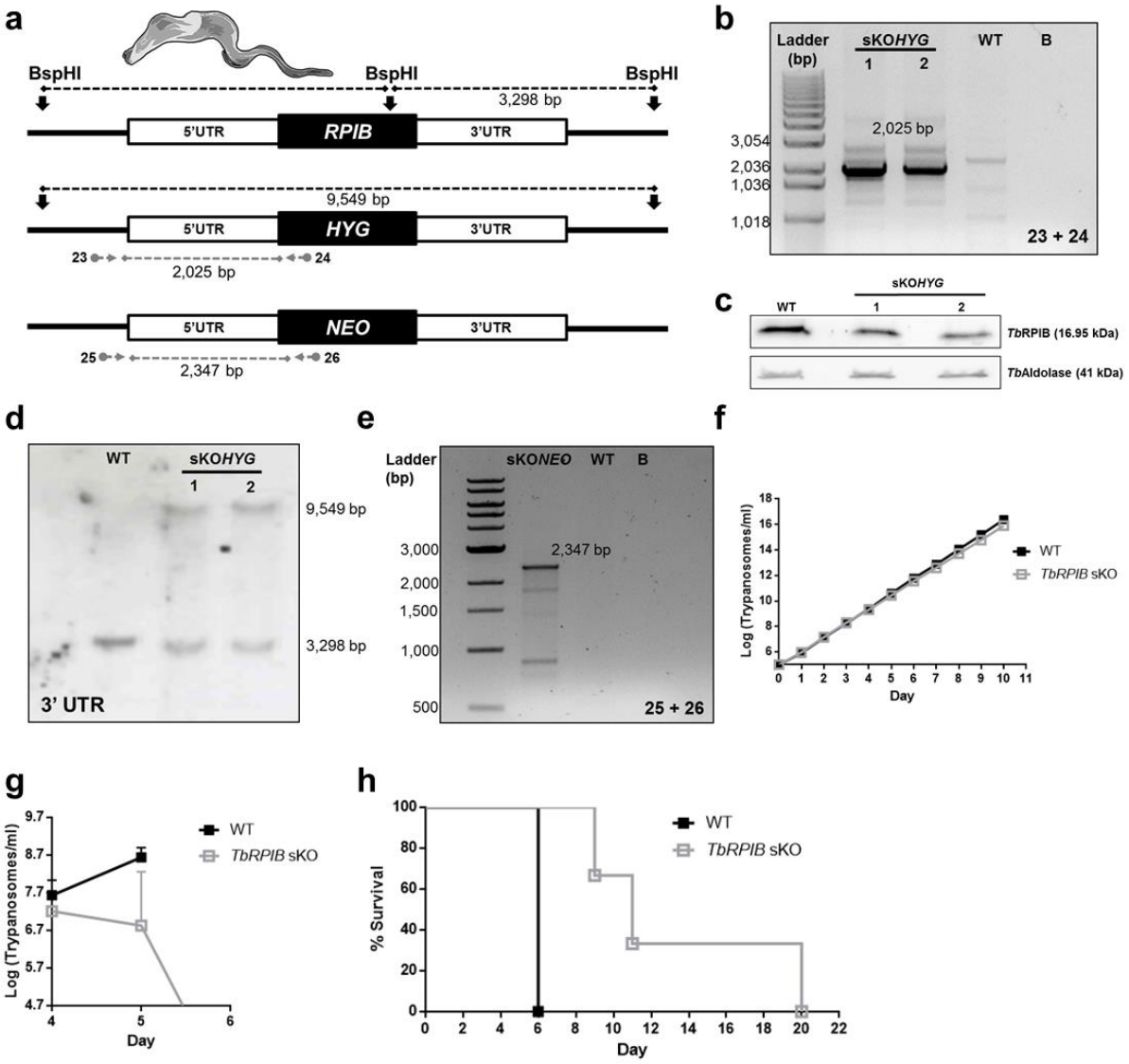

Figure 7. *TbRPIB* mutants generation and their *in vitro* and *in vivo* characterization. **(a)** *TbRPIB* locus schematics: *RPIB* allele, targeted gene replacement cassettes, containing *NEO* and *HYG* genes. Horizontal grey arrows and numbers represent the primer pairs used to assess the genotype of the mutants: the grey dashed line represents the expected PCR fragment. Southern-blot approach, upon digestion with BspHI (vertical black full coloured arrows) is also represented: dashed black lines represent the expected digestion fragments. **(b)** PCR analysis of *TbRPIB* sKO mutants to assess *HYG* 5' integration. B, blank. **(c)** Southern-blot analysis of 10 µg of *TbRPIB* mutants (*versus* WT) genomic DNA, previously

digested with BspHI, and probed using 3' UTR. **(d)** Western-blot analysis of RPIB expression in bloodstream mutants (*versus* WT) using aldolase as loading control. **(e)** PCR analysis of *TbRPIB* sKO mutant to assess *NEO* 5' integration. B, blank. **(f)** Growth curve of WT *versus* a representative sKO cell line. Black and grey squares represent WT and sKO growth, respectively. Cumulative cell numbers (product of cell number and total dilution) are plotted. Values represent averages from two independent experiments using one representative sKO clone and ± error bars indicate standard deviation. **(g)** Groups of mice (n=3) were infected intraperitoneally with 1 x 10^4 control WT (black squares) or a representative sKO clone (grey squares). Parasitemias of each group are shown from 4^{th} to 6^{th} day post-infection. Values are means and errors bars indicate + standard deviation. 5 × 10^4 trypanosomes/ml of blood is the detection limit. For *TbRPIB* sKO, the mean of parasitemia at day 6 was below the detection limit and therefore not seen in the graphic. Mice were culled when parasitemia reached 1 x 10^8 cells/ml. **(h)** Kaplan–Meier survival analysis of mice infected with WT *versus* a representative sKO clone (black and grey line, respectively). Parasitemias and survival curve are representative of two independent experiments using two different sKO clones.

Our data strongly suggest that a functional copy of *TbRPIB* gene is essential for parasites survival and that 50% decrease in RPIB levels is sufficient to compromise parasites infectivity.

Discussion

Trypanosomatids genomes have sequences that encode for a putative RPIB and recombinant enzymes from *L. donovani*[17], *T. brucei*[18] and *T. cruzi*[9] have been formally demonstrated to have *in vitro* isomerase activity by catalyzing the interconversion of R5P and Ru5P. In this work we have demonstrated the same applies to *L. infantum* and *L. major* homologues. *Leishmania* enzymes share over 90% identity among them, and only around 50% to RPIB of trypanosomes. Nevertheless, the protein residues so far associated to isomerization, ring opening and phosphate charge stabilization are strictly conserved. The K_m values for both R5P and Ru5P were similar between *Leishmania* and trypanosomes, however, k_{cat} values are considerably higher for *Leishmania*, in both direct and inverse reactions (Table 1 *versus* [9, 17-18]). A decrease in K_m and an increase in k_{cat} were consistently observed for Ru5P in comparison to R5P (Table S1), suggesting that the conversion of Ru5P into R5P is favored, which might be explained by the important role of R5P as a building block for nucleic acid synthesis.

Trypanosomatids have unique organelles to respond to their specific life cycle needs. Among those are glycosomes, peroxisome-related organelles that comprise enzymes of important metabolic pathways such glycolysis, PPP, among others[25]. This compartmentation of metabolic pathways can prevent the accumulation of toxic intermediates[26] or enable a fast metabolic adaptation to environmental changes[25]. *Lm*RPIB

possesses a peroxisome targeting sequence 2 (PTS-2) a glycosomal signal peptide sequence (–RVALGCDHA–[27]) that is conserved in *L. infantum* and *L. donovani*. Our study suggests a dual localisation despite most RPIB is detected in the cytosol of *L. infantum* promastigotes, it also localises in a certain extent to the glycosomes, similarly to what we have described for *Tb*RPIB[18]. Moreover, other enzymes of the same pathway have been described to display the same pattern, for instance, the enzymes immediately upstream or downstream to RPIB, 6PGDH and TKL respectively[11-12, 27-29]. However, recent proteomic analysis of *L. donovani* glycosomes failed to detect RPIB[30]. This same analysis detected HGPRT (PTS-1), aldolase (PTS-2), as well as some enzymes of PPP, namely putative G6PD, TKL, putative RPE (PTS-1), putative 6PGDH and putative TAL (non-identified signal peptide), or other related proteins like putative ribokinase (PTS-2). We wonder whether this is due to RPIB amount in the glycosomes, or the fact it does not seem to be present in all the glycosomes (Fig. 2e, S2c).

To assess the importance of RPIB for *L. infantum* survival and infectivity, we tried to generate null mutants. Consecutive inability to obtain mutants null to RPIB, coupled with constant aneuploidy generation were suggestive of gene essentiality[31, 32]. We have used a classical approach to demonstrate it[33, 34], by providing the sKO parasites an episomal copy of *RPIB* and successfully removed the second gene copy, generating facilitated null mutants. Moreover, the plasmid was not lost even in the long-term absence of drug pressure *in vitro* (Fig. 3e) and *in vivo* (Fig. 5e) further supporting RPIB essentiality for *L. infantum* survival in both promastigote and amastigote forms.

Due to the impossibility of generating mutants truly null to *RPIB*, we have performed phenotypic studies using the sKO lines that present a 50% downregulation of the protein levels. *In vitro,* sKO promastigotes grow, undergo metacyclogenesis, enter macrophages and differentiate normally. However, our data point to a defective replication of the intracellular amastigotes. Indeed, in these experimental conditions, amastigotes replication can be evaluated as the number of parasites per cell significantly increases from 24 to 72 hours post-infection in the WT. Importantly, MØ infected with sKO mutants showed a reduced number of amastigotes per cell at 72h post-infection and this phenotype was rescued by complementation with episomal *RPIB*. It is noteworthy that probably the remaining protein amount suffices the parasite needs for a minimal intracellular replication and therefore the overall effect is not dramatic. Actually, *in vivo*, there was no parasite clearance, not even at later stages of infection (data not shown), meaning that the parasites persist. This type of phenotype is frequently described in *Leishmania* mutants for enzymes involved in energy metabolism, for instance, glucose transporter knockout in *L. mexicana*[35] and gluconeogenic enzyme fructose-1,6-bisphosphatase (FBPase) knockout in *L. major*[36],

as promastigotes infect and differentiate, but the resulting amastigotes do not replicate falling to generate normal lesions in mice.

The higher expression of RPIB in amastigotes (Fig. 2a), in accordance with a whole genome transcriptomic analysis[37], and its importance for intracellular amastigote replication (Fig. 4g-i) suggests a major role in this stage.

Moreover, RPIB knockdown in *T. brucei* bloodstream forms impacts their infectivity, with an appreciable extension of mice survival[18]. The defective phenotype observed *in vivo* for the *TbRPIB* sKO mutants (Fig. 7g-h) was less dramatic when compared to the one with RNAi[18]. This might be explained by the more pronounced RPIB downregulation achieved with the RNAi system. Three independent attempts to generate dKO mutants have failed, suggesting that RPIB is essential for *T. brucei* survival. A *TbRPIB* conditional knockout would ultimately prove gene essentiality[38]. Nevertheless, our results support that RPIB is a potential therapeutic target against both *Leismania* and *T. brucei* infections.

Several enzymes have been reported to exhibit protein moonlighting in trypanosomatids[39-41], particularly in carbohydrates metabolism[40]. In this sense, in a drug discovery perspective, it is crucial to assess if the expected metabolic function is the one that is detrimental for parasite survival and/or infectivity and therefore the one to be targeted by inhibitory molecules. We have unequivocally demonstrated that RPIB isomerase function is indispensable for *L. infantum* survival (Fig. 6).

We can only speculate why an enzyme involved in the non-oxidative branch of PPP, in which substrate interconversion takes place, is essential. Amastigotes are known to have complex nutritional requirements, which may have precluded their establishment in early endosomal or non-hydrolytic vacuoles of MØ[42], where the levels of amino acids and sugars do not suffice the parasite demands[43, 44]. Inclusively, the variable nutritional composition of host cells phagolysosomes might be one of the reasons why *Leishmania* promastigotes fail to differentiate and the ensuing amastigotes to replicate in neutrophils[2], but do it successfully in MØs[42]. Actually, this may also explain why sKO mutants exhibit a more pronounced infectivity defect in the liver when comparing to the spleen.

Many *Leishmania* auxotrophs do not exhibit any loss of virulence and manage to persist in animal hosts, suggesting that the apparently hostile environment of the phagolysosome is somehow a permissive niche[42]. Importantly, amastigotes undergo a "stringent metabolic response", characterized by a sharp decrease in glucose uptake that allows a more efficient energy metabolism, associated to a decrease of energy expense in anabolic processes and redirecting the carbon to intracellular carbohydrate reserves[45]. It has been proposed it facilitates a long-term amastigote survival in the nutrient-limited environment of the phagolysosome, but simultaneously and paradoxically increasing the

dependency on carbohydrates uptake and metabolism, as they become dependent on mitochondrial metabolism for glutamate and glutamine synthesis[45]). If glucose uptake and carbohydrates availability in the phagolysosome is reduced for amastigote forms, the same should apply to ribose, in particular. Ribose can be imported[46] and metabolized[47] by *Leishmania* promastigotes and apart from its importance for nucleic acid synthesis it can also be a relevant source of energy for intracellular amastigotes[48]. Interestingly, organisms such as yeast present an alternative NADP-independent pathway for R5P synthesis, designated riboneogenesis pathway[49]. Although it has not been formally shown to be operational in trypanosomes, *Leishmania* lacks a sequence encoding for the putative key enzyme of the process[13]. The decrease of glucose and ribose import along with the absence of an alternative pathway for RPIB generation would render the parasites more dependent in enzymes that ultimately generate this metabolite.

Apart from the effects of R5P pool diminishment, absence of RPIB may lead to the potential accumulation of Ru5P. Indeed, if the upstream enzymes are regulated by end products concentration, then the oxidative branch could become less operational leading to a decrease in NADPH production, which could render the parasites more susceptible to reactive oxygen species. Moreover, Ru5P accumulation could trigger another sort of outcome, considering observations made in hepatocarcinoma cells, upon human RPIA knockdown[50]. In this study, the accumulated Ru5P is converted into xylulose-5P by RPE. This metabolite can activate PP2A activity[51], which negatively regulates ERK signalling for cell proliferation. Whether this sort of regulation takes place in *Leishmania* has not been described, however, it does encode for putative RPE[19, 20], PP2A[52] and several MAP kinases[53].

In summary, RPIB, which lacks a human homologue, is essential for *L. infantum* survival and infectivity. We have indications this can also be the case in *T. brucei*, thus in a broader perspective, RPIB can be a potential drug target in trypanosomatids. The fact that a simple *in vitro* activity assay could be used for the screening of inhibitory molecules coupled to the existence of structural data[16], reinforce this protein to be a good target candidate. However, further studies approaching its druggability should be carried out in the future.

Materials and Methods

Ethics statement. All experiments were approved by the IBMC.INEB Animal Ethics Committees and the Portuguese National Authorities for Animal Health guidelines, according to the statements on the directive 2010/63/EU of the European Parliament and of the Council.

Chemicals and reagents. D-ribose-5-phosphate disodium salt hydrate, D-ribulose-5-phosphate disodium salt, EDTA, cysteinium chloride, tetracyclin, carbazole, sulphuric acid, dNTPs, tween-20, tris-base, urea, thiourea, DTT, 2-mercaptoethanol, triton X-100 and IPTG (isopropyl-β-D- thiogalactopyranoside) were purchased from Sigma. Oligonucleotide primers were obtained from STAB VIDA. Restriction endonucleases were from New England Biolabs. Polyclonal antibodies against *Li*RPIB and *Tb*RPIB were obtained in rabbits inoculated with purified recombinant His-tagged *Li*RPIB and *Tb*RPIB, respectively.

Parasites. *L. infantum* (MHOM/MA/67/ITMAP-263) promastigote and axenic amastigote forms were cultured in complete RPMI 1640 medium at 26ºC or in complete MAA medium at 37ºC, 5% CO2, respectively, as previously described[24]. For *in vitro* and *in vivo* characterization, different cell lines were firstly recovered from the spleen of infected BALB/c to restore virulence, and posteriorly maintained in culture no longer than 10 passages[24]. *T. brucei brucei* Lister 427 bloodstream forms were cultivated in HMI-9 medium, as previously described[54]. Depending on the analysis, protein extracts were prepared as follows: 1) 1 x 10^7 late-stationary *L. infantum* promastigotes or *T. b. brucei* bloodstream forms were resuspended in T8 lysis buffer (tris-base 0.6%, urea 42%, thiourea 15%, DTT 0.3%, triton X-100 1%); or 2) 1 x 10^8 promastigotes or axenic amastigotes were resuspended in 100 µL of PBS containing protease inhibitor (Roche) and following 6 freezing/thaw cycles, the parasite suspensions supernatants were recovered and then quantified using Bio-Rad DC Protein Assay (Biorad). All the samples were stored at -80ºC.

RPIB protein alignments. *Li*RPIB, *Lm*RPIB, *Tb*RPIB and *Tc*RPIB protein alignments were performed using the ClustalW program[55] or CLC Sequence Viewer v. 6.9.

RPIB *in silico* localization prediction. *Li*RPIB subcellular localisation prediction was performed using WoLF PSORT[56] and CELLO[57].

Cloning *RPIB* genes. Ribose 5-phosphate isomerase B from *L. infantum* (*LiRPIB*) and *L. major* (*LmRPIB*) was obtained by performing PCR on genomic DNA, extracted using DNAzol (Invitrogen) from *L. infantum* (MHOM/MA/67/ITMAP-263) and *L. major* strain Friedlin. Fragments of the open reading frames of *LiRPIB* (LinJ.28.2100; chromosome LinJ.28; 781,581-782,099) and *LmRPIB* (LmjF.28.1970; chromosome LmjF.28; 766,756-767,274)[19, 20] were PCR-amplified, using primers 1 + 2 and 3 + 4 (Table S3), respectively. PCR conditions were as follows: initial denaturation (2 min at 94ºC), 35 cycles of denaturation (30 s at 94ºC), annealing (30 s at 45ºC,) elongation (2 min at 68ºC) and a final extension step (10 min at 68ºC). In the case of *LiRPIB*, another restriction strategy was required to clone the gene into a *Leishmania* overexpression vector – pSPα*BLAST*α (primers 7 + 8, table S3). PCR conditions were as follows: initial denaturation (2 min at 94ºC), 30 cycles of denaturation (15 s at 94ºC), annealing (30 s at 62ºC,) elongation (1 min

at 72ºC) and a final extension step (10 min at 72ºC). In order to obtain *LiRPIB* with a point mutation on Cys69 (replaced by an alanine, C69A) – *LiRPIBC69A*, primers 5 + 6 and 7 + 6 (Table S3) were used to amplify fragments of the ORF containing XbaI/AgeI or NheI/AgeI restriction sites and the desired point mutation, that were then cloned into pGEM-T in order to ultimately clone them into pET28a(+) (Novagen) and pSPα*BLAST*α vectors, respectively. PCR conditions were as follows: initial denaturation (2 min at 94ºC), 35 cycles of denaturation (15 s at 94ºC), annealing (30 s at 62ºC,) elongation (30 s at 72ºC) and a final extension step (10 min at 72ºC). All the PCR products were obtained using a Taq DNA polymerase with proofreading activity (Roche), isolated, cloned into a pGEM-T Easy vector (Promega) and sequenced.

Expression and purification of recombinant *Li*RPIB (WT and C69A) and *Lm*RPIB. The *LiRPIB*^{WT}, *LiRPIB*^{C69A} and *LmRPIB* genes were excised from the pGEM-T Easy vector (using NdeI/EcoRI, NheI/SacI and NdeI/EcoRI, respectively), gel purified and subcloned into pET28a(+) expression vector. The resulting constructs presented a 6-histidine tag at the N-terminal and were transformed into *E. coli* BL21DE3 cells. Proteins were purified by affinity chromatography as previously described[18]. Concentration was determined measuring the absorbance at 280 nm using the theoretical molar extinction coefficient of 12950, 12950 and 7450 $M^{-1}.cm^{-1}$ for *Li*RPIB^{WT}, *Li*RPIB^{C69A} and *Lm*RPIB, respectively, making use of NanoDrop ND-1000 Spectrophotometer (NanoDrop Technologies). Purified recombinant proteins were resolved in SDS/PAGE stained with Coomassie Brilliant Blue G-250 (Biorad).

Western-blot analysis. One µg of *Li*RPIB^{WT}, *Li*RPIB^{C69A} and *Lm*RPIB recombinant proteins, 20 µg of total soluble extracts from both promastigote and amastigote forms, or 1 x 10^7 parasites were resolved in SDS-PAGE and transferred onto a nitrocellulose membrane (TransBlot Turbo, Bio-Rad), which was blocked, probed, washed and developed as previously described[18]. The following primary antibodies were used: rabbit anti-His-tag (MicroMol-413, 1:1000), mouse anti-α-tubulin (clone DM1A, Neomarkers, 1:1000), rabbit anti-*Li*RPIB (1:500 or 1:1000), rabbit anti-*Tb*RPIB (1:1000), rabbit anti-*Li*CS (cysteine synthase, 1:2000), rabbit anti-*Ld*HGPRT (hypoxanthine guanine phosphoribosyl transferase, 1:2000), rabbit anti-*Tb*Enolase (1:5000) and rabbit anti-*Tb*Aldolase (1:5000). *Horseradish* peroxidase-conjugated goat anti-rabbit or goat anti-mouse IgG (Amersham) (1:5000 for 1 h, at RT) were used as the secondary antibody. ImageJ software (version 1.43u) was used for protein semi-quantification.

Enzymatic Assay. To determine the K_m for R5P and for Ru5P, a direct spectrophotometric method at 290 nm or a modification of Dische's Cysteine-Carbazole method were used, respectively[9]. The experimental set up was performed as previously[18].

Generation of *LiRPIB* overexpressor (OE) and facilitated null mutants. A targeted gene replacement strategy was used for *L. infantum RPIB* gene knockout. All the primers sequences for gene replacement cassettes and mutants' genotype confirmation are specified on table S4. Briefly, *RPIB* flanking regions were amplified from *L. infantum* genomic DNA and were linked to neomycin phosphotransferase (*NEO*) or hygromycin phosphotransferase (*HYG*) genes using a fusion PCR approach. The 5' and 3' UTR were amplified using primers 1 + 2 and 3 + 4, respectively. *NEO* and *HYG* were amplified from pSP72*αNEOα* and pGL345*HYG* templates, using primers 5 + 6 and 7 + 8 respectively, which possess around 30 nucleotides of the 5' UTR in the sense primer and the first 30 nucleotides of the 3' UTR in the antisense primer. 5'UTR_*NEO*_3'UTR and 5'UTR_*HYG*_3'UTR constructs were obtained using primers 9 + 10. To obtain an episomal copy of *RPIB*, *LiRPIB*^{WT} *or LiRPIB*^{C69A}*,* genes were excised from the pGEM-T Easy vector (using XbaI/NdeI), gel purified and subcloned into pSP72*αBLASTα* vector. Approximately 10 µg of either linear fragments obtained by fusion PCR or plasmid were purified, concentrated and transfected into 5 x 10^7 mid-log promastigotes, using an Amaxa Nucleofector II device with human T-cell nucleofector kit (Lonza). The day after transfection drug selection was carried out at 20 µg/mL of G418 (Invitrogen), 50 µg/mL of hygromycin B (InVivoGen) and/or 30 µg/mL blasticidin (InVivoGen). Parasites cloning, except for transfections with episomes was performed by diluting the parasite suspension to a concentration of 0.5 cells per well in 96-well plates using SDM culture medium. Mutants overexpressing *LiRPIB* (OE) were obtained by transfecting WT parasites with pSP72*αBLASTα LiRPIB*^{WT}*.* The facilitated null mutants were generated by complementing sKO mutants with pSP72*αBLASTαLiRPIB*^{WT}, followed transfection with 5'UTR_*HYG*_3'UTR.

Generation of *TbRPIB* mutants. Three different DNA cassettes were generated. The DNA fragments consisted ORFs of the resistance genes (hygromycin, bleomycin and neomycin), flanked by the 5' and 3' UTRs of the *TbRPIB* gene. For the generation of sKO mutants, the plasmid used was the *pGL345-HYG* plasmid modified with the 5′ (924 bp, primers 19 + 20, Table S4) and 3' (997 bp, primers 21 + 22, Table S4) *RPIB* flanks obtained through PCR from *T. brucei* genomic DNA template. The primers contained *Hin*dIII/*Sal*I and *Sma*I/*Bgl*II restriction sites were used for cloning into the appropriate pre-digested pGL345*HYG*. To remove the second allele**,** pGL345*BLEO* or pGL345*NEO* plasmids were constructed by replacing the *HYG* with *BLEO* or *NEO*, respectively, in the plasmid used to obtain the sKOs, employing *Spe*I/*Bam*HI restriction enzymes. Thereafter the final plasmids were digested with HindIII and BglII to obtain the final DNA fragment for transfection. Transfection was performed as described for *LiRPIB* mutants, using 10 µg of

DNA. Selection was undertaken using 7.5 µg/ml, 0.2 µg/ml and 5 µg/ml of hygromycin, bleomycin or neomycin, respectively.

PCR and Southern-blot analysis of *RPIB* mutants. *LiRPIB* mutants were analysed by PCR (NZYTech or Invitrogen Taq Polymerase) for the presence of the following events: *LiRPIB* and selectable markers, *LiRPIB*, *LiRPIB* 5' integration, *NEO* 5' integration, *HYG* 5' integration and pSP72*αBLASTαLiRPIB*, using primers pairs 9 + 10, 11 + 12, 1 + 12 and 9 + 12, 13 + 14, 15 + 16 and 17 + 18, respectively (Table S4). *TbRPIB* mutants were analysed by PCR for the following events: *HYG* and *NEO* 5' integration, using primers pairs 23 + 24, 25 + 26, respectively (Table S4). For Southern blot (SB) analysis, total genomic DNA was extracted. Ten µg of genomic DNA were digested O/N with a 5 fold excess of EcoRI and NaeI (*Li*RPIB mutants) or BspHI (*TbRPIB* mutants) at 37ºC and samples were run O/N in a 0.8% agarose gel. The transfer into a nylan membrane, nucleic acid fixation, hybridisation and revelation were performed as previously described[58]. In the case of *LiRPIB* mutants, the blots were probed sequentially with 3' UTR, *LiRPIB* (Fig. 3), *NEO* and *HYG*, which were PCR amplified, using primers 3 + 4, 11 + 12, 5 + 6 and 7 + 8 (Table S4), respectively. In the case of *TbRPIB* mutants, the blots were probed with 3' UTR (Fig. 7d), amplified using primers 21 + 22 (Table S4).

Real-Time quantitative PCR (qPCR) analysis of *LiRPIB* mutants. qPCR analysis was used to assess the expression of metacyclogenesis markers in *LiRPIB* promastigote mutants, as well as pSP72*αBLASTαLiRPIB*^{WT} copy number. Concerning metacyclogenesis markers expression (MET1, Histone H4, SHERP (small hydrophilic endoplasmic reticulum associated protein)), total RNA extraction, reverse transcription and qPCR were performed as previously[24]. To assess pSP72*αBLASTαLiRPIB*^{WT} copy number, 10 ng of genomic DNA, primers 17 + 18 (Table S4), and purified plasmid (as positive control) were used. In both cases, rRNA45 was used as reference gene and qPCR reactions were run in duplicate for each sample on a Bio-Rad My Cycler iQ5(BioRad).

***In vitro* growth of *RPIB* mutants.** Growth curves of *LiRPIB* mutants and WT were seeded at 1 x 10^6 parasites/ml. Cultures were launched and monitored microscopically every 24h for 7 days or maintained in log phase by subculturing every 2 days and cumulative growth assessed for 5 consecutive passages. Before launching growth curves, the parasites were maintained in log phase for 2-3 passages in the absence of selection drugs. For *TbRPIB* mutants and WT *in vitro* growth curves, cell lines were seeded at 1 x 10^5 parasites/ml of complete HMI-9 medium, after 48h in the absence of selective drugs. Every 24h, until day 10, cell growth was monitored microscopically.

***In vitro* bone marrow derived macrophages (BMMø) infection by *LiRPIB* mutants.** Cell suspension of bone marrow was obtained by flushing the femurs of

susceptible BALB/c mice and then cultured in 96-well plates (1 x 10^5 cells per well) or in 24-well plates containing cover glasses (3.5 x 10^5 cells per well) in LCCM supplemented DMEM, as previously[24]. For FACS analysis, CFSE labelled promastigotes[24] were incubated with the BMMø at a ratio of 2:1, 5:1 and 10:1 during 4 hours and then cells were washed to remove non-internalized parasites. The infection rates were determined at 4, 24 and 48 hours post-infection using the BD FACS Canto II cytometer and analysed by FlowJo software. For microscopic analysis, at day 7 of culture, promastigotes were incubated with the BMMø at a 10:1 ratio and again after 4 hours, infection was stopped. Infection ratios and number of parasites per cell were assessed at 4, 24 and 72 hours post infection. In those timepoints, cells were fixed with 3% *p*-formaldehyde (PFA), Giemsa stained and cover glasses were mounted on slides, using Vectashield (Vector Labs). Microscopic analysis was performed using a Nikon eclipse 80i (Nikon).

***In vivo* infectivity of *RPIB* mutants.** To characterize *LiRPIB* mutants, five to six weeks old female BALB/c mice were obtained from Charles River. For mouse infections, promastigotes from 4 days old stationary cultures were collected, washed, resuspended in PBS to a final amount of 1 x 10^8 parasites/animal, and injected intraperitoneally. Mice were sacrificed at 2 or 8 weeks post-infection. The parasite burden in the spleen and liver was determined by limiting dilution as previously described[59]. To characterize *TbRPIB* mutants, after 48h in the absence of selective drugs, 1 x 10^4 WT and sKO parasites were inoculated intraperitoneally in 6–8 weeks old BALB/c mice. Parasitemia was measured at fourth, fifth and sixth day post-infection through tail blood extraction.

Digitonin Fractionation. This procedure has been performed as previously described[58]. All fractions were analysed by WB.

Immunofluorescence. *L. infantum* mid-log promastigotes were fixed, permeabilised and stained as previously described[60]. Parasites were spread on 8 well-IF slides (Polysciences) or 18 well-IF slides (Ibidi) for wide field and confocal microscopy, respectively. The following primary antibodies were used: rabbit anti-*Li*RPIB (1:500), sheep anti-*Li*TDR1 (1:500) and rabbit anti-*Li*HGPRT (1:500). The following secondary antibodies were used: goat anti-rabbit Alexa Fluor 488 or Alexa Fluor 568 and donkey anti-sheep Alexa Fluor 488 (Molecular probes, Life Technologies). In the case of RPIB and HGPRT colocalisation studies, parasites were sequentially incubated with rabbit anti-*Li*RPIB O/N at 4ºC, unconjugated sheep anti-rabbit for 60 min at RT, donkey anti-sheep Alexa Fluor 488 for 60 min at RT, rabbit anti-*Li*HGPRT for 2 hours at RT and goat anti-rabbit Alexa Fluor 568 for 60 min at RT (sequential staining's lacking only anti-*Li*RPIB or anti-*Li*HGPRT as well as single stainings of each one of these proteins were performed simultaneously as controls). Images were captured using wide field fluorescence microscope AxioImager Z1

(Carl Zeiss) and confocal Leica TCS SP5II microscope (Leica) for antibody validation and colocalisation studies, respectively. Images were analysed using ImageJ (version 1.47) or Fiji (version 1.45) software's.

Statistical Analysis. For statistical analysis, two-tailed unpaired *t* test was used. Statistical analysis was performed using GraphPad Prism Software (version 5.0) and significance was found when $p < 0.05$.

References

1. Rabinovitch, M., Veras, P. S. Cohabitation of *Leishmania amazonensis* and *Coxiella burnetii*. *Trends in Microbiology*, **4,** 158-161 (1996)

2. van Zandbergen, G. *et al*. Cutting edge: neutrophil granulocyte serves as a vector for *Leishmania* entry into macrophages. *Journal of Immunology*, **173(11),** 6521-5 (2004)

3. Antoine, J. C., Prina, E., Courret, N., Lang, T. *Leishmania* spp.: on the interactions they establish with antigen-presenting cells of their mammalian hosts. *Advances in Parasitology*, **58,** 1-68 (2004)

4. WHO Leishmaniasis, Fact sheet No 375 (2014)

5. Maltezou, H. C. Drug resistance in visceral leishmaniasis. *Journal of Biomedicine and Biotechnology*, **617521** (2010)

6. Krepinsky, K., Plaumann, M., Martin, W., Schnarrenberger, C. Purification and cloning of choroplast 6-phsophogluconate dehydrogenase from spinach. Cyanobacterial genes for chloroplast and cytosolic isoenzymes encoded in eukaryotic chromosomes. *European Journal of Biochemistry*, **268,** 2678-2686 (2001)

7. Hannaert, V., Bringaud, F., Opperdoes, F. R., Michels, P. A. Evolution of energy metabolism and its compartmentation in Kinetoplastida. *Journal of Molecular Biology*, **331,** 653-665 (2003)

8. Stryer L. Biochemistry, 4th edition, Freeman, New York, 559-565 (1999)

9. Stern, A. L., Burgos, E., Salmon, L., Cazzulo, J. J. Ribose-5-phosphate isomerase type B from *Trypanosoma cruzi*: kinetic properties and site directed mutagenesis reveal information about the reaction mechanism. *Biochemical Journal*, **401,** 279-285 (2007)

10. Maugeri, D. A., Cazzulo, J. J., Burchmore, R. J., Barrett, M. P., Ogbunude, P. O. Pentose phosphate metabolism in *Leishmania mexicana*. *Molecular Biochemical Parasitology*, **130,** 117-125 (2003)

11. Maugeri, D. A., Cazullo, J. J. The pentose phosphate pathway in *Trypanosoma cruzi*. *FEBS Microbiology Letters*, **234,** 117-123 (2004)

12. Veitch, N. J., Maugeri, D. A., Cazzulo, J. J., Lindqvist, Y., Barrett, M. P. Transketolase from *Leishmania mexicana* has a dual subcellular localisation. *Biochemical Journal*, **382,** 759-767 (2004)

13. Opperdoes, F. R., Coombs, G. H. Metabolism of *Leishmania*: proven and predicted. *Trends in Parasitology*, **23,** 149-158 (2007)

14. Stoffel, S. A. *et al*. Transketolase in *Trypanosoma brucei*. *Molecular Biochemical Parasitology*, **179,** 1-7 (2011)

15. Sorensen, K. I., Hove-Jensen, B. Ribose catabolism of *Escherichia coli*: characterization of RpiB gene encoding ribose-5-phosphate isomerase Band of the RpiR gene, which is involved in the regulation of RpiB expression. *Journal of Bacteriology*, **178,** 1003-1011 (1996)

16. Stern, A. L., Naworyta, A., Cazzulo, J. J., Mowbray, S. L. Structures of type B ribose-5-phosphate isomerase from *Trypanosoma cruzi* shed light on the determinants of sugar specificity in the structural family. *FEBS Journal*, 278, 793-808 (2011)

17. Kaur, P. K., Dinesh, N., Soumya, N., Babu, N. K., Singh, S. Identification and characterization of a novel ribose-5-phosphate isomerase B from *Leishmania donovani*. *Biochemical and Biophysical Research Communications*, **421,** 51-56 (2012)

18. Loureiro, I. *et al.* Ribose-5-phosphate isomerase B knockdown compromises *Trypanosoma brucei* bloodstream form infectivity. *Plos Neglected Tropical Diseases*, **9(1),** e3430 (2015)

19. El-Sayed, N. M. *et al*. Comparative genomics of trypanosomatid parasitic protozoa. *Science*, **309,** 404-409 (2005)

20. Ivens, A. C. *et al*. The Genome of the Kinetoplastid Parasite, *Leishmania major. Science*, **309,** 436-442 (2005)

21. Gupta, R. *et al.* Characterization of glycolytic enzymes-rAldolase and rEnolase of *Leishmania donovani*, identified as Th1 stimulatory proteins, for their immunogenicity and immunoprophylactic efficacies against experimental visceral leishmaniasis. Plos one, **9,** e86073 (2014)

22. Shih, S., Hwang, H. Y., Carter, D., Stenberg, P., Ullman, B. Localization and targeting of the *Leishmania donovani* Hypoxanthine-Guanine Phosphoribosyltransferase to the glycosome. *Journal of Biological Chemistry*, **273,** 1534-1541 (1998)

23. Silva, A. M. *et al.* Characterization of *Leishmania infantum* thiol-dependent reductase 1 and evaluation of its potential to induce immune protection. *Parasite Immunology*, **34,** 345-350 (2012)

24. Moreira, D. *et al.* Impact of Continuous Axenic Cultivation in *Leishmania infantum* Virulence. *Plos Neglected Tropical Diseases*, **6,** e1469 (2012)

25. Michels, P. A. M., Bringaud, F., Herman, M., Hannaert, V. Metabolic functions of glycosomes in trypanosomatids. *Biochimica et Biophysica Acta (BBA) - Mol Cell Res*, **1763 (12),** 1463-1477 (2006)

26. Haanstra, J. R. *et al.* Compartmentation prevents a lethal turbo-explosion of glycolysis in trypanosomes. *PNAS*, **105(46),** 17718-17723 (2008)

27. Opperdoes, F. R., Szikora, J. P. *In silico* prediction of the glycosomal enzymes of *Leishmania major* and trypanosomes. *Molecular Biochemical Parasitology*, **147,** 193-206 (2006)

28. Heise, N., Opperdoes, F. R. Purification, localisation and characterization of glucose-6-phosphate dehydrogenase of *Trypanosoma brucei*. *Molecular Biochemical Parasitology*, **99,** 21-32 (1999)

29. Duffieux, F., Van Roy, J., Michels, P. A., Opperdoes, F. R. Molecular characterization of the first two enzymes of the pentose phosphate pathway of *Trypanosoma brucei*. *Journal of Biological Chemistry*, **275,** 27,559-27,565 (2000)

30. Jamdhade, M. D. *et al.* Comprehensive proteomic analysis of glycosomes from *Leishmania donovani*. *Journal of Integrative Biology*, **19(3),** 157-169 (2015)

31. Cruz, A. K., Titus, R., Beverley, S. M. Plasticity in chromosome number and testing essential genes in *Leishmania* by targeting. *PNAS*, **90,** 1599-1603 (1993)

32. Mukherjee, A., Langston, L. D., Ouellette, M. Intrachromosomal tandem duplication and repeat expansion during attempts to inactivate the subtelomeric essential gene *GSH1* in *Leishmania*. *Nucleic Acid Research*, **39(17),** 7499-7511 (2011)

33. Dacher, M. *et al*. Probing druggability and biological function of essential proteins in *Leishmania* combining facilitated null mutant and plasmid shuffle analyses. *Molecular Microbiology*, **93(1),** 146-166 (2014)

34. Pedrosa, A. L., Cruz, A. K. The effect of location and direction of an episomal gene on the restoration of a phenotype by functional complementation in *Leishmania*. *Molecular and Biochemical Parasitology*, **122,** 141-148 (2002)

35. Rodríguez-Contreras, D., Landfear, S. M. Metabolic changes in glucose transporter-deficient *Leishmania mexicana* and parasite virulence. *Journal of Biological Chemistry*, **281(29),** 20,068-20,076 (2006)

36. Naderer, T. *et al*. Virulence of *Leishmania major* in macrophages and mice requires the gluconeogenic enzyme fructose-1,6-bisphosphatase. *PNAS*, **103(14),** 5502-5507 (2006)

37. Rochette, A., Raymond, F., Corbeil, J., Ouellette, M., Papadopoulou, B. Whole-genome comparative RNA expression profiling of axenic and intracellularamastigote forms of *Leishmania infantum*. *Molecular and Biochemical Parasitology*, **165(1),** 32-47 (2009)

38. Wyllie, S. *et al*. Dissecting the essentiality of the bifunctional trypanothione synthetase-amidase in *Trypanosoma brucei* using chemical and genetic methods. *Molecular microbiology*, **74(3),** 529-40 (2009)

39. Castro, H. *et al.* *Leishmania* Mitochondrial Peroxiredoxin Plays a Crucial Peroxidase-Unrelated Role during Infection: Insight into Its Novel Chaperone Activity. *Plos Pathogens*, **7,** e1002325 (2011)

40. Gómez-Arreaza, A. *et al*. Extracellular functions of glycolytic enzymes of parasites: unpredicted use of ancient proteins. *Molecular and Biochemical Parasitology*, **193,** 75-81 (2014)

41. Teixeira, F. *et al.* 2015. Mitochonrdial peroxiredoxin functions as crucial chaperone reservoir in *Leishmania infantum*. *PNAS*, **112(7),** E616-624 (2015)

42. McConville, M. J., de Souza, D., Saunders, E., Likic, V. A., Naderer, T. Living in the phagolysosome: metabolism of *Leishmania* amastigotes. *TRENDS in Parasitology*, **23(8),** 368-375 (2007)

43. Lorenz, M. V., Bender, J. A., Fink, J. R. Transcriptional response to *Candida albicans* upon internalization by macrophages. *Eukaryotic Cell*, **3(5),** 1076-1087 (2004)

44. Muñoz-Elías, E. J., McKinney, J. D. *Mycobacterium tuberculosis* isocitrate lyases 1 and 2jointly required for in vivo growth and virulence. *Nature Medicine*, **11(6),** 638-644 (2005)

45. Saunders, E. C. *et al.* Induction of a stringent metabolic response in intracellular stages of *Leishmania mexicana* leads to increased dependence on mitochondrial metabolism. *Plos Pathogens*, **10(1),** e1003888 (2014)

46. Naula, C. M., Logan, F. M., Wong, P. E., Barrett, P. M., Burchmore, R. J. A glucose transporter can mediate ribose uptake. *Journal of Biological Chemistry*, **285(39),** 29,721-29,728 (2010)

47. Berens, R. L., Deutsch-King, L. C., Marr, J. J. *Leishmania donovani* and *Leishmania braziliensis*: hexokinase, glucose-6-phosphate dehydrogenase, and pentose phosphate shunt activity. *Experimental Parasitology*, **49(1),** 1-8 (1980)

48. Burchmore, R. J., Barrett, M. P. Life in vacuoles – nutrient acquisition by *Leishmania* amastigotes. *International Journal of Parasitology*, **12,** 1311-1320 (2001)

49. Clasquin, M. F. *et al.* Riboneogenesis in yeast. *Cell*, **145(6),** 969-980 (2011)

50. Ciou, S. C. *et al.* Ribose-5-phosphate isomerase A regulates hepatocarcinogenesis *via* PP2Aand ERK signalling. *International Journal of Cancer*, **137,** 104-115 (2014)

51. Kabashima, T., Kawaguchi, T., Wadzinski, B. E., Uyeda, K. Xylulose 5-phosphate mediates glucose-induced lipogenesis by xylulose 5-phosphate-activated protein phosphatase in rat liver. *PNAS*, **100,** 5107-5112 (2003)

52. Brenchley, R. *et al.* The TryTryp Phosphatome: analysis of the protein phosphatase catalytic domains. *BMC Genomics*, **8(434)** (2007)

53. Parsons, M., Worthey, E. A., Ward, P. N., Mottram, J. C. Comparative analysis of the kinomes of three pathogenic trypanosomatids: *Leishmania major, Trypanosoma brucei and Trypanosoma cruzi. BMC Genomics*, **6(127) (**2005)

54. Schlecker, T. *et al.* Substrate specificity, localization, and essential role of the glutathione peroxidase-type tryparedoxin peroxidases in *Trypanosoma brucei. The Journal of Biological Chemistry*, **280(15),** 14,385-14,394 (2005)

55. Larkin, M. A. *et al*. Clustal W and Clustal X version 2.0. *Bioinformatics*, **23,** 2947-2948 (2007)

56. Horton, P. *et al*. WoLF PSORT: protein localization predictor. *Nucleic Acid Research*, **35,** 585-587 (2007)

57. Yu, C. S., Chen, Y. C., Lu, C. H., Hwang, J. K. Prediction of protein subcellular localization. *Proteins*, **64,** 643–651 (2006)

58. Faria, J. *et al*. *Leishmania infantum* Asparagine Synthetase A Is Dispensable for Parasites Survival and Infectivity. *Plos Neglected Tropical Diseases* (*in press*) (2015) doi: 10.1371/journal.pntd.0004365

59. Silvestre, R. *et al.* SIR2-deficient *Leishmania infantum* induces a defined IFN-gamma/IL-10 pattern that correlates with protection. *Journal of Immunology*, **179,** 3161-3170 (2007)

60. Cull, B. *et al.* Glycosome turnover in *Leishmania major* is mediated by autophagy. *Autophagy*, **12,** 2143-2157 (2015)

Acknowledgements

We would like to thank Dr. Paul Michels from Université Catholique de Louvain, Belgium, for providing *Tb*enolase antibody; Professor Graham Coombs, Strathclyde University, Glasgow, for *Lm*CS antibody; Professor Buddy Ullman, School of Medecine, Oregan Health and Science University, USA, for *Ld*HGPRT antibody; Dr Christine Clayton, Zentrum fur Molekulare Biologie der Universitat Heidelberg, Germany, for *Tb*Aldolase antibody.. We would also like to thank Professor Jeremy Mottram, University of Glasgow, for pGL345*HYG* and Dr Marc Ouellette, Centre de Recherche en Infectiologie, of Laval University, Canada, for pSPα*NEO*α and pSPα*BLAST*α.

Conflict of Interest

The authors declare no conflict of interest.

Author Contributions

JF IL JT NS and ACS conceived and designed the experiments. JF IL and PC performed the experiments and analyzed the data. JF IL PC JT NS SMR ACS critically discussed the results. ACS and SMR contributed with reagents, materials and analysis tools. JF IL JT NS SMR ACS wrote the paper. All the authors reviewed the results and approved the final version of the manuscript.

Additional information

The research leading to these results has received funding from the European Community's Seventh Framework Programme under grant agreement No.602773 (Project KINDRED).'The COST Action CM1307: Targeted chemotherapy towards diseases caused by endoparasites has also contributed for this work. We would like to acknowledge Fundação para a Ciência e Tecnologia (FTC) for supporting Joana Faria (SFRH/BD/79712/2011) and Inês Loureiro (SFRH/BD/64528/2009). Inês Loureiro was also supported by the European Community's Seventh Framework Programme (KINDRED-PR300102-BD). JT is an Investigator FCT funded by National funds through FCT and co-funded through European Social Fund within the Human Potential Operating Programme. Nuno Santarem and Pedro Cecílio are supported by fellowships from the European Community's Seventh Framework Programme under grant agreements No. 602773 (Project KINDRED) and No. 603181 (Project MuLeVaClin), respectively.

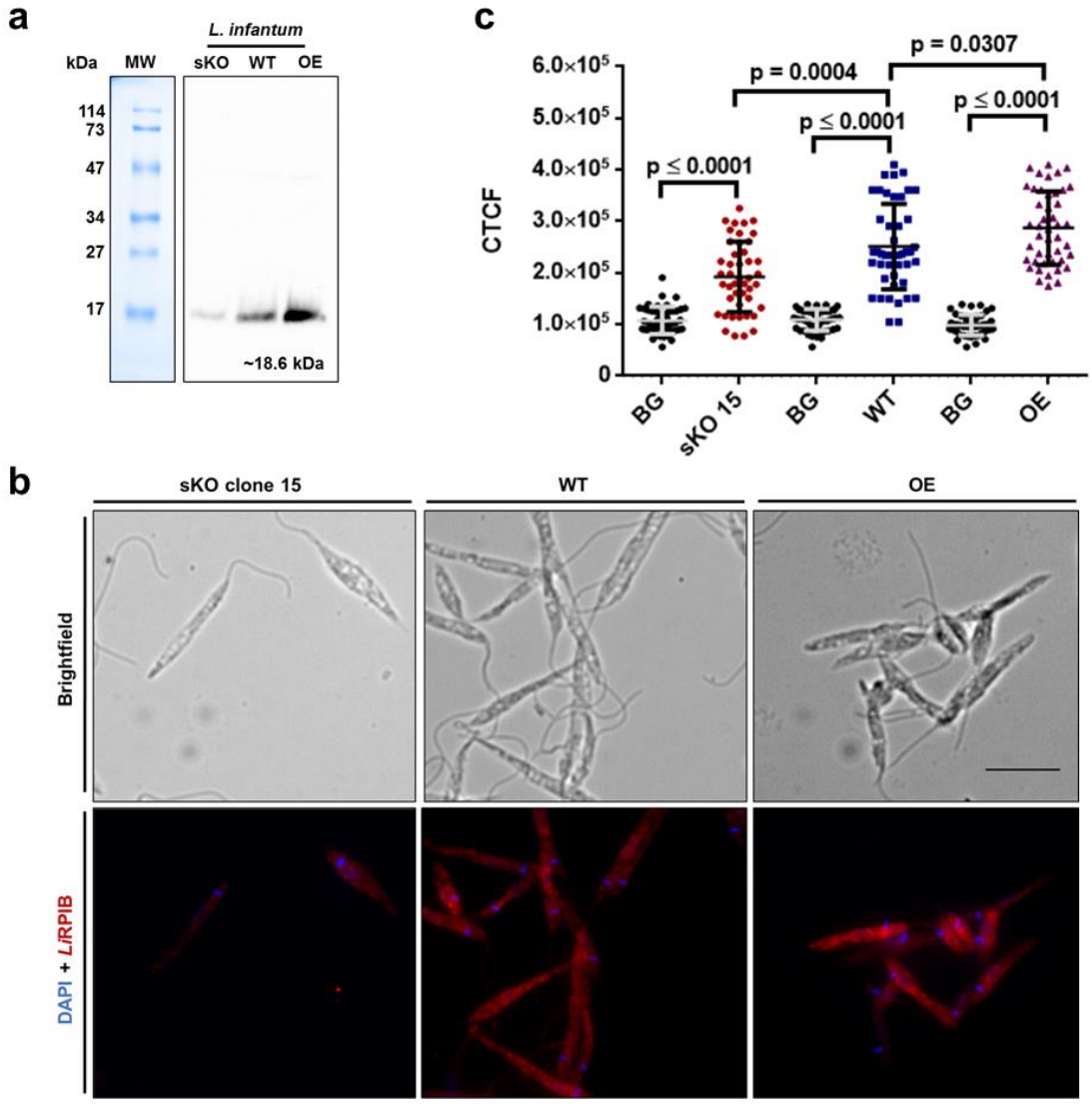

Figure S1. Rabbit polyclonal anti-*Li*RPIB antibodies validation. (a) Western-blot analysis of WT, *LiRPIB* sKO 15 and OE promastigotes extracts using rabbit polyclonal anti-*Li*RPIB (1:500). **(b)** Representative immunofluorescence images of different genotypes (WT, sKO 15 and OE) of mid-log *L. infantum* promastigotes, using rabbit polyclonal anti-*Li*RPIB antibody (1:500). Upper and lower panels present brightfield and *Li*RPIB (red) + DAPI (blue) stained images, respectively. Images were acquired with a 63x objective, using a Zeiss AxioImager Z1. The scale bar corresponds to 5 µm. **(c)** Fluorescence intensity quantification in WT, sKO 15 and OE parasites when stained with anti-*Li*RPIB antibody (1:500). The values are expressed in CTCF (corrected total cell fluorescence), and background (BG) values are displayed as well. The quantification was performed on images acquired with 63x objective, using a Zeiss AxioImager Z1 and the same exposure time for all genotypes (*Li*RPIB 300 ms; DAPI 100 ms). Twenty different fields for each genotype were analysed in duplicate, and the fluorescence of an average of 50-100 parasites was quantified using ImageJ (v 1.47) software. Two-tailed unpaired *t* test was performed: statistical significance $p < 0.05$. The results (a-c) are representative of 2 independent experiments.

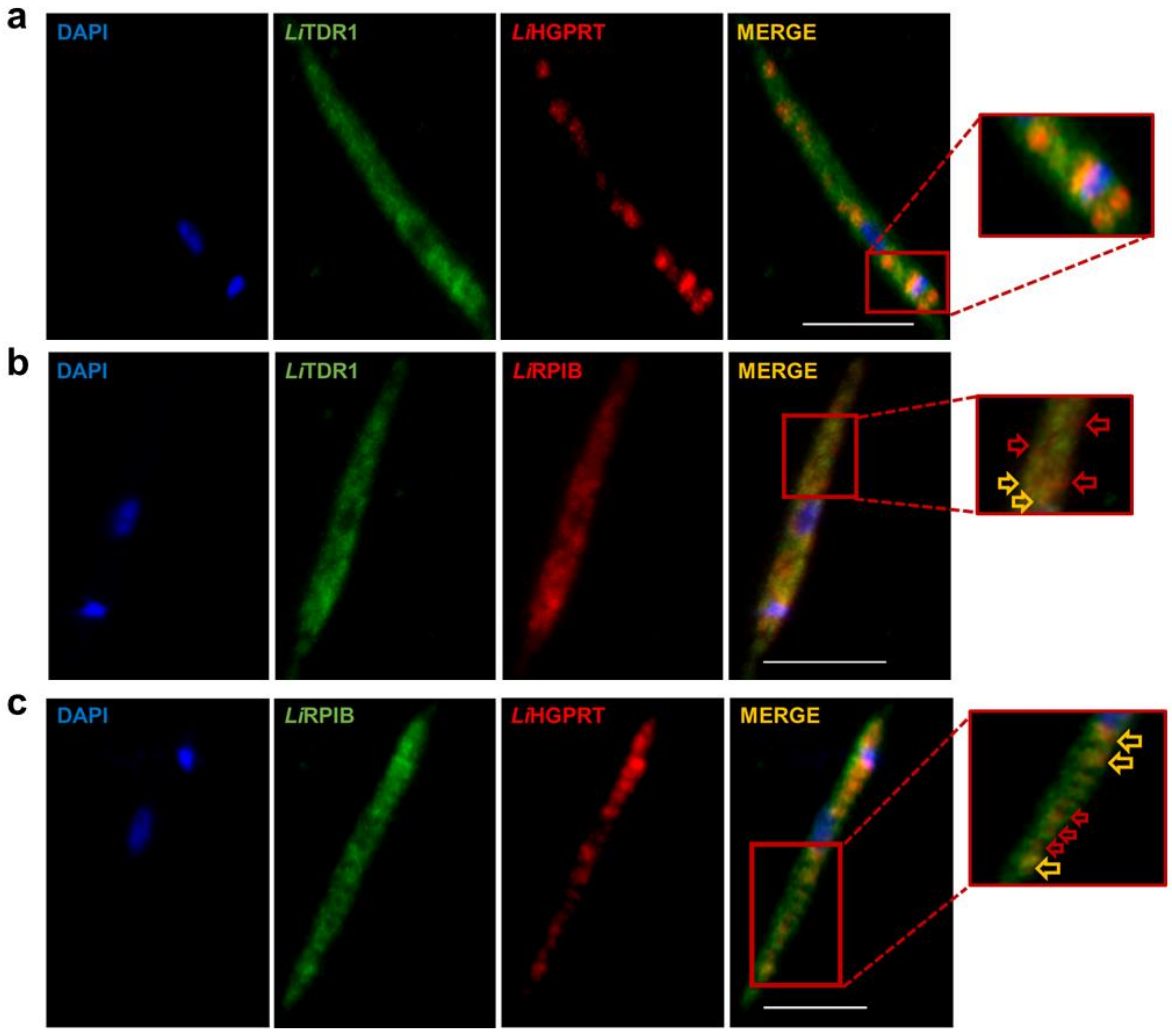

Figure S2. RPIB localization in *L. infantum*. (a-c) Immunofluorescence analysis showing RPIB (red in b; green in c) localization in *L. infantum* promastigotes. Nucleus and kinetoplast DNA, cytosol and glycosomes were stained with DAPI (blue), anti-*Li*TDR1 (thiol-dependent reductase 1, green) and anti-*Li*HGPRT (hypoxanthine guanine phosphoribosyltransferase, red), respectively. On panels b and c, yellow arrows in the zoomed areas point to colocalisation sites, and the red arrows point to sites of exclusive *Li*RPIB (b) or *Li*HGPRT (c) staining. Images were acquired with a 63x objective, using a LEICA SP5II confocal microscope. The scale bar corresponds to 5 µm. Data displayed on a-c are representative of 3 independent experiments.

Table S1. Kinetic parameters of *Li*RPIB and *Lm*RPIB for R5P and Ru5P in the direct and inverse reaction, respectively

Species	R5P -> Ru5P				Ru5P -> R5P			
	K_m (mM)	v_{max} (mM.s^{-1})	k_{cat} (s^{-1})	K_{sp}* (M^{-1}.s^{-1})	K_m (mM)	v_{max} (mM.s^{-1})	k_{cat} (s^{-1})	K_{sp}* (M^{-1}.s^{-1})
***Li*RPIB**	4.34 ± 0.62	$3.90 \times 10^{-3} \pm 1.44 \times 10^{-4}$	43.49 ± 1.61	1.00×10^{4}	2.82 ± 0.30	$1.55 \times 10^{-2} \pm 5.20 \times 10^{-4}$	115.30 ± 3.86	4.09×10^{4}
***Lm*RPIB**	5.59 ± 0.75	$3.86 \times 10^{-3} \pm 1.48 \times 10^{-4}$	43.11 ± 1.65	7.71×10^{3}	3.01 ± 0.54	$1.73 \times 10^{-2} \pm 9.86 \times 10^{-4}$	128.50 ± 7.33	4.27×10^{4}

* K_{sp} Specificity Constant (k_{cat}/ K_m)
The values are means ± standard deviations obtained from 3 independent experiments.

Table S2. Summary of the different cell lines obtained in several attempts to generate *LiRPIB* null mutants

Clone	Construct	dKO clones	Aneuploid clones
sKO*HYG* clone 4	*NEO*	0/12	6/12
sKO*HYG* clone 4	*NEO*	0/10	3/10
sKO*NEO* clone 13	*HYG*	0/7	3/7
sKO*NEO* clone 15	*HYG*	0/7	3/7
sKO*NEO* clone 15 + pSP72*αBLASTαLiRPIBWT*	*HYG*	11/12	1/12
sKO*NEO* clone 15 + pSP72*αBLASTαLiRPIBC69A*	*HYG*	0/11	7/11

Table S3. Oligonucleotides sequences used to obtain *Li*RPIBWT (P1 + P2), *Lm*RPIB (P3 + P4), *Li*RPIBC69A (P5 + P6) recombinant proteins, pSPα*BLASTα**LiRPIB* (P7 + P8) and pSPα*BLASTα**LiRPIB*^{C69A} (P7 + P6)

Primer	Sequence
1	5’ CAATTTCCATATGCCGAAGCGTGTTGC 3’
2	5’ CCCAAGCGAATTCTCTACTTTCCTTCC 3’
3	5’ CAATTTCCATATGTCGAAGCGTGTTGCTC 3’
4	5’ CGGATGCGAATTCTCACTTTCCTTCTTGG 3’
5	5' GGCTAGCATGCCGAAGCGTGTTGCTCTG 3'
6	5' TGCCGATACCGGTGCCTGCGACAAGGATAC 3'
7	5' GTCTAGAATGCCGAAGCGTGTTGCTCTG 3'
8	5' GCGCATATGTCACTTTCCTTCCTCCTTAAGACC 3'

Table S4. Oligonucleotides sequences used to obtain gene replacement cassettes (*L. infantum* P1-P10; *T. brucei* P19-P22) and to confirm *RPIB* mutants’ genotype (*L. infantum* P1, P9-18; *T. brucei* P23-P26)

Primer	Sequence
1	5' TTCGAGAGCGGGATGGAGAG 3'
2	5' AGGGTGGATGGCTGGATGAG 3'
3	5' CACAAGGCGATGGGTACAAG 3'
4	5' GCACACGAGGTGCAGCAATG 3'
5	5' AGCGCTCTCTCTCCATCCCGCTCTCGAAATGATTGAACAAGATGGATTGC 3'
6	5' GATGAGGCCAACGGCCTTGTACCCATCGCCTTGTGTCAGAAGAACTCGTC 3'
7	5' CACCACCAAGCGCTCTCTCTCCATCCCGCTCTCGAAATGAAAAAGCCTGAACTCAC 3'
8	5’ TATGATGAGGCCAACGGCCTTGTACCCATCGCCTTGTGCTATTCCTTTGCCCTCGGAC 3’
9	5’ AGGGTGGATGGCTGGATGAG 3’
10	5' GCACACGAGGTGCAGCAATG 3'
11	5' ATGCCGAAGCGTGTTGCTCTG 3'
12	5' TTAAGACCTCCACAACCGCTGAAG 3'
13	5' CCTGCTTCGTAGCCTGTGCAAGTC 3'
14	5' GTGGTCGAATGGGCAGGTAG 3'
15	5' AAGCGTTTGCGATGCTTCCTTC 3'
16	5' CGCCATGTAGTGTATTGACC 3'
17	5' CGCTTTCACTCTTCGAACAAACAC 3'
18	5' ACTATGCGGCATCAGAGCAG 3'
19	5’ CGAAGCTTTAAGCGGTGATTGAGCGT 3’
20	5’ CGGTCGACTGTTGATTGTAAAAGGA 3’
21	5’ CGCCCGGGATATTTGGTAAATGATAATC 3’
22	5’ CGAGATCTGCATACGTTCAGTGGTTGTT 3’
23	5’ AACATGCCCCACCCCTCCCC 3’
24	5’ GCTGCATCAGGTCGGAGACGC 3’
25	5’ AACATGCCCCACCCCTCCCC 3’
26	5’ GTGGTCGAATGGGCAGGTAG 3’

Chapter IV

Discussion and conclusions

1. Trypanosomatids encode a bacterial type AS-A

Trypanosomatids, despite eukaryotes, encode for AS-A enzymes of bacterial origin. These enzymes are aminoacyl-tRNA synthetase paralogues, displaying an AsnRS catalytic core with conserved class II motifs, yet lacking the tRNA binding domain (Gowri et al, 2012). *In silico* analysis comparing *Li*AS-A, *Lm*AS-A, *Tb*AS-A, *Tc*AS-A with *Ec*AS-A demonstrates there is a high conservation of the main structural features, including the active site residues. Indeed, the amino acids involved in Asn binding are strictly conserved across species, whereas in the case of AMP binding pocket, the majority of residues are conserved with a few exceptions. These organisms also encode a hypothetical, yet non-classical, AS-B: *L. infantum* [LinJ.29.1590], *L. major* [LmjF.29.1490], *T. brucei* [Tb927.3.4060] and *T. cruzi* [Tc00.1047053510001.40] (Aurrecoechea et al, 2010; El-Sayed et al, 2005; Ivens et al, 2005). The latter sequences contain a Pfam AS domain (pfam00733) and glutamine hydrolysing domains in the C and N-terminus, respectively.

1.1. AS-A atypical biochemical features

Our studies have demonstrated that *Li*AS-A, *Lm*AS-A, *Tb*AS-A and *Tc*AS-A can synthesize Asn in an ATP-dependent manner, curiously using either ammonia or glutamine as nitrogen donors (Faria et al, 2015b *in press*; Faria et al, unpublished data; Loureiro et al, 2013). The same has been observed for *Ld*AS-A (Manhas et al, 2014). *Li*AS-A K_m values for aspartate and ATP are close to the ones determined for *Tb*AS-A and *Tc*AS-A (Faria et al, 2015b *in press*; Loureiro et al, 2013). However, for ammonia, the K_m value found for *Li*AS-A is 5 fold lower in comparison to *Tb*AS-A, *Tc*AS-A and *Ld*AS-A (Loureiro et al, 2013; Manhas et al, 2014). In the case of *Ld*AS-A, the K_m values for aspartate were around 10 fold lower (Manhas et al, 2014) than the ones of *Li*AS-A. Regarding the high conservation of the active sites among AS-A enzymes from *Leishmania* and trypanosomes, we cannot exclude that the observed kinetic differences may be due to differences in the amount of protein that is properly folded, especially taking into account they are expressed in a heterologous system. Moreover, it is important to emphasize that in the case of *Ld*AS-A, the kinetic determinations were performed using a different experimental setup.

AS-A activity in trypanosomatids more resembles AS-B enzymes in several aspects. Indeed, beyond the ability of using both ammonia and glutamine as nitrogen donors their optimal pH for enzymatic activity is 7.6 instead of 8 (data not shown). AS-B enzymes preferably use glutamine over ammonia, with exception of the human enzyme that presents approximately the same affinity for both nitrogen sources (Andrulis et al, 1987; Andrulis et al, 1989; Ciustea et al, 2005; Humbert & Simoni, 1980; Merchant et al, 2007; Ramos & Wiame, 1980; Scofield et al, 1990). While *Tb*AS-A and *Tc*AS-A use preferably ammonia

(Loureiro et al, 2013), *Li*AS-A and *Lm*AS-A seem to use both practically in the same extent (Faria et al, 2015b *in press*; Faria et al, unpublished data). It is noteworthy that ideally these studies would have been performed with proteins purified from parasites extracts and not with recombinant enzymes expressed in *E.col*i.

When analysing the homology models of *Li*AS-A, *Lm*AS-A, *Tb*AS-A and *Tc*AS-A obtained by superimposition with *Ec*AS-A crystal structure (*PDB* 12AS (Nakatsu et al, 1998)), there is a divergent region (a 19 residues insertion) in trypanosomatids. This region is strictly conserved between *Li*AS-A and *Lm*AS-A enzymes but little conservation is found when comparing to others trypanosomes enzymes. Aiming at identifying the glutamine hydrolysing domain, we have attempted to crystallize *Li*AS-A, and also co-crystallize it with glutamine. However, our endeavours were unsuccessful. In the meantime, *Tb*AS-A was crystallized (Manhas et al, 2014), but it only emphasised the high conservation of Asn and AMP binding pockets, as the divergent region was not visible in the experimental electron density maps and therefore is likely disordered (Manhas et al, 2014). Furthermore, the structural or functional role of this insertion remains unclear.

1.2. Asn homeostasis in trypanosomatids

Asn metabolism has become very attractive in the last few years on cancer and infection fields. In the latter, it has been shown to play an important role on the survival, invasion and/or virulence of several pathogens (Baruch et al, 2014; Gesbert et al, 2014; Gouzy et al, 2014; Hofreuter et al, 2008; Kullas et al, 2012; Leduc et al, 2010; Nagaraj et al, 2015; Scotti et al, 2010; Shibayama et al, 2011). A key player in this metabolism is AS, and in trypanosomatids, the presence of a type A with no human's homologue made it appealing enough to investigate as a potential drug target. We have demonstrated that in *T. brucei*, AS-A knockdown renders the bloodstream forms auxotrophic to Asn, with no impact on growth or infectivity, except upon Asn deprivation. *In vitro* and *in vivo* studies in Asn replete and depleting conditions have shown that Asn can be obtained by two main sources: AS-A mediated synthesis and extracellular Asn uptake (Loureiro et al, 2013). Surprisingly, AS-A was proposed as a promising drug target in *Leishmania as* it was claimed to be essential for *L. donovani* survival due to the inability of generating null mutants (Manhas et al, 2014). This suggested a different regulation in Asn homeostasis in trypanosomatids. Such idea is conceivable as these organisms do have different amino acid requirements according to the developmental stage, reflecting the environmental pressure inflicted by the vector or the mammalian host (Jackson, 2007). Inclusively, whereas polyamine transporters are quite conserved, AATs repertoire is very diverse across trypanosomatids. Different species and life cycle stages may present AATs that

differ in number, affinity, specificity or capacity (Jackson, 2007). For instance, in *Leishmania*, arginine is an essential amino acid that fuels peptide and polyamine synthesis, whose homeostasis depends exclusively on external uptake (Darlyuk et al, 2009). However, in the case of cysteine, a crucial amino acid for thiol biosynthesis, contrarily to *T. brucei*, *L. major* fails to uptake it at a rate that ensures the intracellular pool is enough for optimal growth. Therefore, *Leishmania* parasites rely mainly on two pathways that enable cysteine *de novo* synthesis (Williams et al, 2009).

In order to evaluate AS relevance in *Leishmania* genus, we have performed gene replacement studies in *L. infantum*, and our efforts to generate *LiASA* null mutants were successful. Thus, the gene is not essential for survival nor was it for growth or infectivity. WT promastigotes grew normally in Asn depleted medium without AS-A upregulation, suggesting Asn synthesis by basal AS-A suffices the cellular needs, although the mutants overexpressing this enzyme had a metabolic advantage in Asn limiting conditions. Our *in vitro* data on growth demonstrated that *LiASA* deletion rendered parasites auxotrophic to Asn, as null mutants relied solely on Asn uptake to grow ((Faria et al, 2015b *in press*). This also indicated that despite it is unlikely that AS-B is functional, even if it is, its activity definitely does not compensate *ASA* ablation. Importantly, *Leishmania* promastigotes can then both synthesise and uptake this amino acid, and the latter fully compensates the first (Faria et al, 2015b *in press*). For instance in *Plasmodium*, the Asn granted by haemoglobin degradation and extracellular sources does not support *per se* an optimal parasite growth (Nagaraj et al, 2015). Actually, upon *ASB* ablation, a suboptimal blood-stage development and an even more dramatic effect on sexual and liver stages are observed. In the latter stage, the phenotype is probably due to limiting levels of Asn in the mammalian hepatocytes. The higher dependency of *Plasmodium* on Asn intracellular synthesis may be due to the great enrichment of its proteins on this amino acid (Nagaraj et al, 2015).

In the case of Asn uptake from the extracellular medium, not much information is available in trypanosomatids. In *T. brucei*, a protein presenting putative orthologues in *Leishmania* (Aurrecoechea et al, 2010; El-Sayed et al, 2005; Ivens et al, 2005) was characterized as a transporter of five neutral amino acids, including Asn (*Tb*AATP1) (Ebikeme, 2007).

It is interesting that trypanosomatids encode for AS-A and hypothetical AS-B enzymes regarding that: 1) our data on *Leishmania* promastigotes and *T. brucei* bloodstream forms suggest that AS-B may not be functional or at least has a negligible contribution for Asn synthesis even in Asn limiting conditions; 2) AS-A contrarily to what has been described for all the other bacterial type AS-A enzymes also uses glutamine as a nitrogen donor, in a fashion more concomitant with a type B AS. This may represent an

evolutionary upgrade, as one enzyme may have become sufficient to satisfy parasite demands and the other probably became redundant and eventually not functional. Especially in *Leishmania* enzymes, the fact that both ammonia and glutamine are used in the same extent may grant the parasite an opportunity to synthesize Asn using the more abundant nitrogen donor, depending on the environment. These parasites do experience dramatic environmental changes as they switch from one host to the other, or perhaps even by infecting different subsets of MØs, whose phagolysosome composition may be different as well. One of the great questions is how this may have occurred: 1) may this be the case of any sort of recombination? 2) did the divergent region play a role in this process?

Considering that AS-A is dispensable in promastigotes, unless upon Asn deprivation, did not immediately exclude AS-A as a drug target. Amastigotes thrive in a phagolysosome, in which the access to certain amino acids may be limited, as described for glutamate or glutamine for instance (Saunders et al, 2014). Nevertheless, when infecting BALB/c mice with *Li*ASA null mutants, no differences in the spleen and liver parasite burdens were observed in comparison to the WT. This means the null mutants found Asn levels that suffice their demands in the phagolysosome. Again we cannot exclude that AS-B is functional, although it appears unlikely.

In *T. brucei*, AS-A knockdown does not impact parasite infectivity as the parasite uptakes Asn directly from the bloodstream (Loureiro et al, 2013). In *Leishmania*, the scenario has multiple players, namely the ability of the host cell to uptake Asn from the extracellular medium and to synthesize it *via* AS-B. Moreover, since *Leishmania* infects MØs several phagosomes may be delivered to the phagolysosome, providing some extra nutrients, among which amino acids.

Figure 27 depicts a model of Asn metabolism in *L. infantum* based on t-RNA independent reactions.

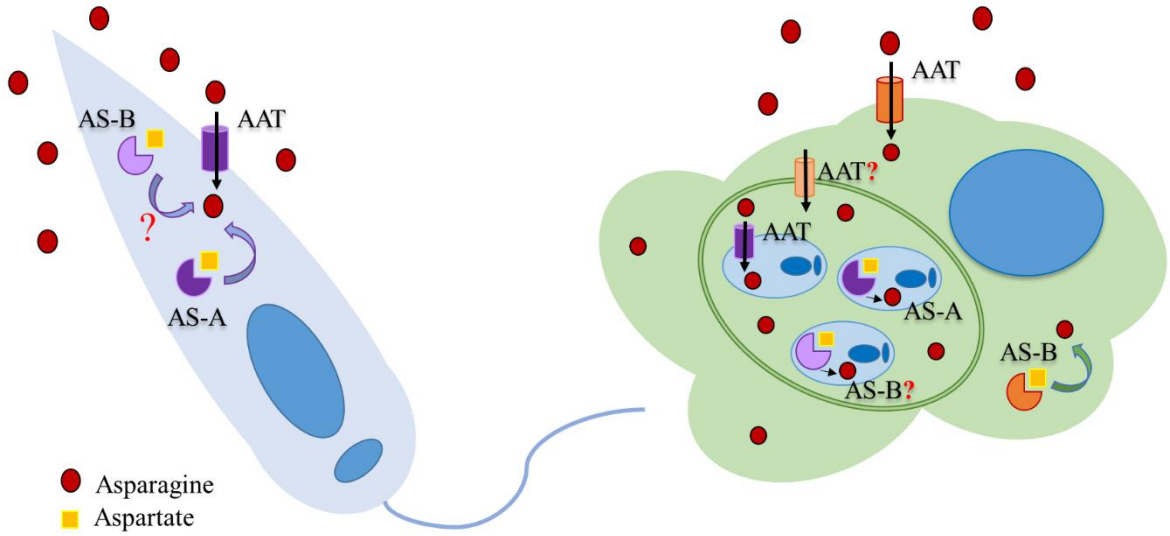

Figure 27. Asn homeostasis in *L. infantum*. The left and right panels represent promastigote and intracellular amastigote forms, respectively, the latter living inside the phagolysosome of MØs. Promastigotes are able to synthesize and uptake Asn in the same extent. AS-B is likely not functional in these forms. Intracellular amastigotes uptake Asn from the phagolysosome or synthesize it *via* AS-A. Again, AS-B can also play a role although it is unlikely. The host cell, MØs, is also able to uptake Asn and synthesize it *via* AS-B in this case. AAT, amino acid transporter; AS-A, asparagine synthetase A; AS-B, asparagine synthetase B. Red question marks indicate whether the transporter or the enzyme have not been identified/characterized.

1.3. The controversy on AS-A essentiality in *Leishmania*

The discrepancy on AS-A essentiality in *L. donovani* and *L. infantum* is intriguing due to the close relation between both species and the 99% identity between the two enzymes (Faria et al, 2015b *in press*; Manhas *et al*., 2014).

In the literature, there are several cases in which knocking out a gene can have different impact on virulence depending on the species. For instance, when knocking out LPG1, an enzyme involved in LPG synthesis, *L. major*, contrarily to *L. mexicana*, has its virulence dramatically reduced (Turco et al, 2001). However, to our knowledge, there is no documented example among cutaneous or among visceral species of a gene that is detrimental for survival in one species and dispensable in other closely related. But we did find a case of differences at a strain level, as null mutants of *L. major* DHFR were obtained in a lab strain but endeavours for the same accomplishment in virulent strains have lapsed (Cruz et al, 1993).

The most likely explanation comes from the fact that *L. infantum AS-A* null mutants do not growth in the medium M199, where the attempts to generate *AS-A* null mutants in *L. donovani* were made (Faria et al, 2015b *in press*; Manhas et al, 2014). Indeed, M199 lacks

Asn and the mutants' growth defect is rescued when this amino acid is provided. These results reinforce the importance of the medium composition when attempting gene knockout of metabolic enzymes, and supplementation may be detrimental when potentially generating auxotrophs (Nare et al, 1997; Wilson et al, 2012).

Nonetheless, we must discuss that AS-A essentiality in *L. donovani* was defined based on the consecutive failure in the removal of the second gene copy. According to the authors, when attempting to remove the second allele, there was aneuploidy generation, as resistance cassettes were integrated in the target locus, preserving a copy of the *LdASA* gene (Manhas et al, 2014). Ideally, essentiality should be confirmed by providing an ectopic copy of the gene to the sKO mutants and then attempt the second allele removal, which must be successful in these conditions, unless a technical limitation is obscuring the results. Additionally, if the ectopic copy is provided on a plasmid, the obtained facilitated null mutants must retain the vector even in the absence of drug pressure. We were surprised to realise that some of our sKO mutants in *L. infantum* displayed a quite bizarre profile: despite *NEO* cassette integration in the target locus and decreased levels of *Li*AS-A, assessed by PCR and western-blot, respectively, Southern-blot analysis showed several copies of the *NEO* were present (data not shown). Along with chromosome aneuploidy, DNA amplification by gene rearrangement, which is a highly dynamic and stochastic process, is one of the strategies *Leishmania* successfully explores in order to respond to environmental changes, such as drug pressure (Ubeda et al, 2014). Due to the massive genetic plasticity of these organisms, conclusions on essentiality must be taken cautiously, and consecutive inability to generate null mutants *per se* must not suffice.

1.4. Amino acids sensing in trypanosomatids

One of the most interesting observations in this study concerns the parasites ability to regulate AS-A levels depending on Asn availability. In particular, sKO mutants were able to upregulate AS-A presumably to restore Asn intracellular levels required for optimal growth. In Asn limiting conditions, these mutants had a growth delay followed by a partial or total recovery as AS-A levels increase over time. This indicates that parasites sense Asn levels and must have regulatory mechanisms oriented to the control of AS-A expression and probably Asn transporter as well.

In these parasites, much remains to be unravelled concerning the pathways involved in amino acid sensing and regulation of their synthesis and uptake (Jackson, 2007). In mammalian cells, AS-B is a transcriptional target of GCN2/eIF2α/ATF4 axis, in response to amino acid starvation. GCN2 phosphorylates eIF2 that subsequently leads to a repression of general protein synthesis, and the activation of gene-specific translation *via* ATF4

(Chamtranupong et al, 2015; Horiguchi et al, 2012; Ye et al, 2010, depicted on Fig. 25). In *Saccharomyces cerevisiae*, GCN2, which is activated by amino acid, glucose or purine deprivation, is the only eIF2 kinase, contrasting with mammals that possess some additional three, HRI, PKR and PEK/PERK (Chamtranupong et al, 2015; Lahav et al, 2011). *T. brucei* and *L. donovani* PERK orthologues have been implicated in the response to ER stress and their phosphorylation activity leads to a decrease in the overall translation (Gosline et al, 2011). Moreover in *L. donovani*, it has a role in the differentiation into amastigote form (Chow et al, 2011). *T. brucei* PERK orthologue localises to the flagellar pocket, is able to phosphorylate yeast and mammalian eIF2α, albeit *Tb*eIF2α is not a target of GCN2 or PERK *in vitro* (Moraes et al, 2007). At the moment, it is still not clear whether phosphorylation of eIF2 in trypanosomatids would result in a downstream signalling cascade, as bZIP type transcription factors that could act like GCN4 or ATF4, are absent in these organisms (Moraes et al, 2007). To the date, it seems this signalling may only lead to a general downregulation of translation upon specific stimuli (Moraes et al, 2007).

As previously addressed, these organisms lack transcriptional regulation of gene expression in a great extent, relying mostly on post-transcriptional mechanisms (Clayton, 2002; Requena, 2011; Alsford et al, 2012). This encompasses modulation of mRNA stability (Brittingham et al, 2001; Muller et al, 2010a; Muller et al, 2010b) or protein translation rate (Boucher et al, 2002; Zeiner et al, 2003).

Related or not, in several Western-blots, the appearance of two close bands that react with polyclonal anti-*Li*AS-A antibody were consistently observed (in some cases more clearly than others). We questioned the possibility of a post-translational modification. In *L. donovani*, a phosphoproteomic study identified two phosphorylated isoforms, but only in amastigotes (Morales et al, 2008). We did check for cleavage sites, and for calpain for instance, we have used GPS-CCD (Liu et al, 2011), which predicted 5 possible sites. Three of this hypothetic cleavage sites could generate peptides with 39.7, 39.6 and 39.5 kDa (*versus* 39.8 kDa), which could explain the two bands we consistently observe. Inclusively, other of those predicted sites could generate a 32.21 kDa peptide, and interestingly, we often got a band around that size in our extracts. However, the biological significance remains non-identified.

Taken all together, we believe that the AS-A expression regulation most likely relies on a novel mechanism in comparison to higher eukaryotic cells. Unravelling such mechanisms may have biological relevance, as it may be *per se* a source of novel drug target candidates.

1.5. Asn unexpected roles challenge preconceived notions

GCN2/eIF2α/ATF4 pathway has been shown to be activated in primary solid tumours, contrasting with GCN2- or ATF4-deficient cells that failed to generate tumours *in vivo* (Horiguchi et al, 2012; Ye et al, 2010). These observations support that the maintenance of Asn production is critical for solid tumour progression (Zhang et al, 2014b). These results also point AS-B as a potential drug target in solid tumours, but so far its inhibition has only been tested in L-asparaginase-refractory cases of acute leukemia (Horiguchi et al, 2012; Ye et al, 2010; Zhang et al, 2014b). For a long time, Asn was strictly associated to protein synthesis in mammalian cells (Ubuka et al, 1971; Zhang et al, 2014b). However, recent studies point to an additional role, surprisingly as a signalling molecule. Therefore, Asn has joined the growing list of metabolites that cells utilize to coordinate cell responses with metabolic reserves, ultimately regulating cell fate.

It appears that this amino acid is a critical suppressor of apoptosis in many human tumours (Zhang et al, 2014b). Proliferating cells utilize glutamine to maintain anaplerosis of the TCA cycle, the production of nucleotides and non-essential amino acids (Wise & Thompson, 2010). Inclusively, many cancer cells are dependent on glutamine for cell survival and growth (Wise et al, 2008). Actually, glutamine deprivation in cancer cells lead to cell cycle arrest, a general reduction in the protein translation rate and translation of stress response RNAs that ultimately result in apoptosis (Zhang et al, 2014b). Supplementation with a single amino acid, Asn, was sufficient to suppress apoptosis, however, it failed to restore the levels of TCA cycle intermediates or other non-essential amino acids, supporting the model that anaplerosis *per se* is not required for survival (Zhang et al, 2014b). Indeed, the cells experience long term survival despite cell cycle arrest. Moreover, even in glutamine replete conditions, AS-B inhibition or Asn depletion alone leads to apoptosis even if glutamine and other non-essential amino acids supplies are abundant (Zhang et al, 2014b). Altogether, these results suggest that Asn not only suppresses apoptosis as it promotes cellular adaptions to the depletion of glutamine and other non-essential amino acids.

Therefore, in cancer the challenging notion that Asn is a signalling molecule has emerged and repeatedly gains ground. However, to our knowledge, nothing similar has been addressed in pathogens. But we did make an interesting observation in our studies regarding Asn availability. Indeed, *LiASA* null mutants do not grow in L-asparaginase treated cRPMI, however, they did not die either, at least for a month. By that time, Asn supplementation was provided and parasites immediately started multiplying again. Of course we cannot claim this to be a specific effect, as we did not perform any control with another non-essential amino acid. A hibernatory state has been described in *P. falciparum* for instance regarding isoleucine (Babbitta et al, 2012). *Plasmodium* is auxotrophic to

isoleucine and its extracellular depletion makes the parasite slow down its metabolism and progress through life cycle at a reduced rate. These parasites lack canonical eukaryotic nutrient stress response pathways and manage to circumvent isoleucine restriction by hibernating and waiting for a potential nutrient repletion. Actually in the case of *Plasmodium*, proteolysis played an important role for the maintenance of parasite viability during such state, and autophagy may also contribute (Babbitta et al, 2012). Whether this takes place in *Leishmania*, again we have not explored, but we did observe morphological changes in *LiASA* null promastigotes, especially concerning size, as they became much smaller and could be indeed "recycling" intracellular material during this possibly dormant state.

1.6. AS-A is not a suitable drug target

The results on BALB/c mice infection with *ASA* null or RNAi mutants in *L. infantum* and *T. brucei*, respectively, indicate that AS-A is not a suitable drug target in trypanosomatids, as the outcome of the infection is comparable to the WT parasites.

In vivo treatment with L-asparaginase, which induces a decrease in Asn bloodstream levels, has been successfully used for years in the treatment of acute lymphoblastic leukemia (ALL) (Avramis, 2012). Recently it was proposed as a promising strategy to treat bacteremia caused by GAS and eventually other extracellular bacteria (Baruch et al, 2014).

The simultaneous *Tb*AS-A knockdown and L- asparaginase treatment prolonged BALB/c mice survival (Loureiro et al, 2013). This suggested that simultaneous inhibition of the parasite AS-A and L-asparaginase treatment could be a possible therapeutic strategy (Loureiro et al, 2013). In *Plasmodium*, a similar proposal has been made (Nagaraj et al, 2015). In the case of *Leishmania* infection, *in vitro* preliminary data in Asn depleting conditions suggest that intracellular levels of Asn could be maintained by Asn *de novo* synthesis by the host MØs (data not shown). Also *in vivo*, the MØs phagocytic capacity may continuously provide nutritional supplies to the phagolysosome. Therefore, L-asparaginase treatment coupled with AS-A inhibition would probably be unsuccessful in an *in vivo* model of VL. Besides, L-asparaginase is very expensive and has several adverse effects (Avramis, 2012). A more suitable strategy to all three organisms could be simultaneous inhibition of AS-A (AS-B in *Plasmodium* case) and Asn transporter.

Regardless, a drug combination approach such as this would not be appropriate to treat neglected tropical diseases, not only due to the financial implications, but also the higher likelihood for drug resistance emergence. Taken all together, we conclude *Li*AS-A is not a suitable drug target against trypanosomatids.

2. Trypanosomatids RPIB

Trypanosomatids, despite being eukaryotes, encode for type B RPI enzymes. *Li*RPIB, *Lm*RPIB, *Tb*RPIB and *Tc*RPIB generate polypeptides containing 172, 172, 155 and 159 amino acids, respectively. *Li*RPIB displays a 93% sequence identity with *Lm*RPIB, and around 50% to RPIB of trypanosomes. Importantly, human RPIA and RPIB enzymes from trypanosomatids are not homologues. The amino acids involved in isomerisation, phosphate stabilization and ring opening have been identified in *Tc*RPIB (Stern et al, 2011) and are strictly conserved in *Li*RPIB, *Lm*RPIB and *Tb*RPIB.

2.1. RPIB has classical isomerase activity

Recombinant enzymes from *L. donovani* (Kaur et al, 2012) and *T. cruzi* (Stern et al, 2007) have been formally demonstrated to have *in vitro* isomerase activity by catalyzing the interconversion of R5P and Ru5P. We have demonstrated the same applies to *L. infantum*, *L. major* and *T. brucei* (Faria et al, 2015a *submitted*; Loureiro et al, 2015) homologues. The K_m values for both R5P and Ru5P were close between *Leishmania* and trypanosomes, however, K_{cat} values are considerably higher for *Leishmania*, in both direct and inverse reactions (Faria et al, 2015a *submitted*; Kaur *et al.*, 201 Kaur et al, 2012; Loureiro et al, 2015; Stern et al, 2007). A decrease in K_m and an increase in K_{cat} were consistently observed for Ru5P in comparison to R5P, suggesting that the conversion of Ru5P into R5P is favored, which might be explained by the important role of R5P as a building block for nucleic acid synthesis.

2.2. RPIB has a dual localisation

Trypanosomatids have several unique organelles in order to respond to their specific lifestyle needs. Among those are glycosomes, peroxisome-related organelles that comprise enzymes of important metabolic pathways such as glycolysis, PPP, β-oxidation, gluconeogenesis, purine salvage and biosynthesis of pyrimidines, both lipids and squalenes (Michels et al, 2006). This compartmentation of metabolic pathways can prevent the accumulation of toxic intermediates (Haanstra et al, 2008) or enable a fast metabolic adaptation to environmental changes (Michels et al, 2006). *Lm*RPIB possesses a PTS-2 signal sequence (–RVALGCDHA–, Opperdoes et al, 2006), which is conserved in *L. infantum* and *L. donovani*. However, recent proteomic analysis of *L. donovani* glycosomes failed to detect RPIB in these organelles (Jamdhade et al, 2015). The same analysis detected HGPRT (PTS-1), aldolase (PTS-2), as well as some enzymes of PPP that are upstream RPIB, namely putative G6PD (PTS-1), putative 6PGDH (non-identified), or

enzymes downstream RPIB, such as TKL (PTS-1), putative RPE (PTS-1) and putative TAL (non-identified signal peptide), or other related proteins like putative ribokinase (PTS-2 signal peptide). Our localisation studies in *L. infantum* promastigotes suggest a dual localisation with a higher content in the cytosol, similarly to *T. brucei* bloodstream forms (Faria et al, 2015a *submitted;* Loureiro et al, 2015). Other enzymes of the same pathway have been described to display dual localisation in *Leishmania* (Duffieux et al, 2000; Heise & Opperdoes, 1999; Opperdoes & Szikora, 2006), inclusively, the enzyme immediately upstream, 6PGDH (Heise & Opperdoes, 1999), and the one immediately downstream, TKL (Maugeri et al, 2004; Veitch et al, 2004) that localise predominantly to cytosol but also to glycosomes.

We have not quantified the amount of RPBI that is in the cytosol or the glycosomes, as well as if the distribution changes throughout the parasite life cycle.

Targeting studies with reporter proteins have demonstrated that changes in the PTS-1, as well as modifications in the vicinity, can cause dual localization, probably due to a reduced affinity for the PTS-1 receptor (Lametschwandtner et al, 1998; Sommer et al, 1992). Only recently, the crystal structure of PTS-2 bound to its receptor has been solved, providing a structural framework for studying the import of PTS-2 cargo into peroxisomes and glycosomes (Pan et al, 2013). However, the biological relevance of this dual localization to the parasites remains unanswered.

2.3. RPIB is essential for *L. infantum* survival

To assess the importance of RPIB for *L. infantum* survival and infectivity, we tried to generate null mutants. Attempts to generate dKO lines from reliable sKO mutants have consecutively failed, suggesting gene essentiality for parasite survival. That was also supported by constant aneuploidy generation in the resultant mutants. Although, whether there was a whole genome amplification (Cruz et al, 1993), a chromosomal amplification (Cruz et al, 1993) or intrachromossomal tandem duplication (Mukherjee et al, 2011) remains to be addressed. We have used a classical approach to demonstrate gene essentiality (Pedrosa & Cruz, 2002), as facilitated null mutants were successfully generated. Moreover, the plasmid was not lost even in long-term absence of drug pressure. *L. infantum* promastigotes have preserved the plasmid in the absence of blasticidin over more than one year now as control lines have lost it long before. Facilitated null mutants recovered from chronically infected mice also preserved the vector carrying *RPIB* in opposition to the overexpressing line for instance, suggesting that the gene is detrimental for amastigotes as well.

In *Leishmania*, the absence of conditional knockout systems, previously addressed in the first chapter of this dissertation, render gene replacement studies dependent on very limiting approaches. It is debatable in the field whether the above described approach gives the ultimate proof of essentiality, as some defend this can merely mean that the ectopic gene provides an advantage for *in vitro* or *in vivo* growth (Dacher et al, 2014). It would be interesting to use pXNG vector in this context to address essentiality (Dacher et al, 2014; Murta et al, 2009). Moreover, with the recent advances in inducible expression systems and CRISPR/Cas9 technology, a new era may begin in *Leishmania* genetic manipulation (Kraeva et al, 2014; Sollelis et al, 2015; Zhang et al, 2015).

2.4. *RPIB* partial ablation has impact on *L. infantum* infections

Often, gene essentiality in *Leishmania* limits functional studies, as only facilitated null mutants can be achieved, thus, total absence of the protein of interest is never achieved. Sometimes the remaining protein levels in the sKO mutants are enough to grant parasites a normal development and no defects can be observed. There are some approaches that try to overcome this limitation like plasmid shuffle analysis (Dacher et al, 2014). Nevertheless, *RPIB* sKO mutants have some impairment *in vitro* and *in vivo,* therefore providing hints on the infection steps the protein may be important for.

In vitro, sKO promastigotes grow, undergo metacyclogenesis and infect host macrophages as the WT. The percentage of MØs infected by the mutants does not change over time. Moreover, the average of amastigotes per cell remained alike when comparing the sKO with the WT at 24 hours post infection, suggesting that differentiation into amastigotes occurs normally. In contrast, sKO mutants presented a lower average of amastigotes per cell at 72 hours post infection. This phenotype is reversed in complemented sKO mutants, which overexpresses RPIB. This suggests that RPIB is important for amastigote replication.

In vivo, BALB/c infected with the sKO mutants presented a lower parasite burden in the spleen and the liver at two weeks post infection, but statistical significance was only found for the latter. This effect was rescued in the complemented sKO mutants (Faria et al, 2015a *submitted*). In chronic infections (2 months post infection), no parasite clearance was observed in the mice infected with the sKO mutants.

Similarly, the ablation of other enzymes involved in energy metabolism such as glucose transporter in *L. mexicana* and the gluconeogenic enzyme FBPase in *L. major*, have led to defects exclusively in amastigote stage. In both cases, promastigotes invade and differentiate normally, but the resulting amastigotes fail to replicate, persisting in

infected mice, however failing to generate normal lesions (Naderer et al, 2006; Rodríguez-Contreras et al, 2006).

Our results point to a role of RPIB particularly in amastigotes development. This may help to explain why the enzyme is more expressed in this stage, which is in agreement with a whole genome transcriptomic analysis (Rochette et al, 2009). We can hypothesize the remaining protein (~50%) suffices the parasite needs for a minimal intracellular replication and therefore the overall effect is not dramatic. Inclusively *in vivo*, there is no parasite clearance even in later stages of infection. Actually even earlier, during infection and differentiation, we cannot exclude the protein may play a role, as only 50% of it may be enough to allow these steps to occur without disturbance. Moreover, the inability to inactivate *RPIB* in promastigotes indicates the gene is essential for survival of the insect infective form.

Again, the availability of conditional knockout/knockdown systems in *Leishmania* would facilitate functional studies on essential genes. Another alternative would be attempting plasmid shuffle (Dacher et al, 2014). Switching the episome carrying RPIB for one carrying a mutated version devoid of isomerase activity would be lethal, as we have proven this function to be essential for parasite survival.

2.5. RPIB isomerase function is indispensable for *L. infantum*

Although we cannot exclude RPIB may have an additional function, we have demonstrated that the isomerase function is essential for *L. infantum* survival.

One of the things that would be worthy of exploring concerns the metabolic implications of RPIB inactivation/inhibition. At this point, we can only speculate why an enzyme involved in the non-oxidative branch of PPP, in which interconversion reactions take place, is essential. As previously mentioned, considering the evidence for a role of RPIB in amastigotes development, we will focus on the metabolic particularities of these forms.

Leishmania amastigotes have nutritional requirements that are more complex than those of the majority of prokaryotes and fungal pathogens. Curiously, even though, *Leishmania* is one of the very few pathogens that infect MØs and does not escape or subvert the endocytic pathway, oddly dwelling in a mature phagolysosome (McConville et al, 2007). This compartment may appear very hostile. However, it may be a permissive niche regarding nutrient availability. But to benefit from this large nutrient supply, pathogens must establish successful strategies to counteract the host cell microbicidal mechanisms, and *Leishmania* has efficiently mastered it (McConville et al, 2015).

The phagolysosome compartment appears to be extremely dynamic fusing with phagocytic, endocytic, autophagic or endoplasmic reticulum vesicles that deliver a broad range of macromolecules that are hydrolysed into free sugars, lipids and amino acids. Amastigotes can uptake the nutrients or even directly internalize those host macromolecules and degrade them on their own (McConville et al, 2015; Fig. 28).

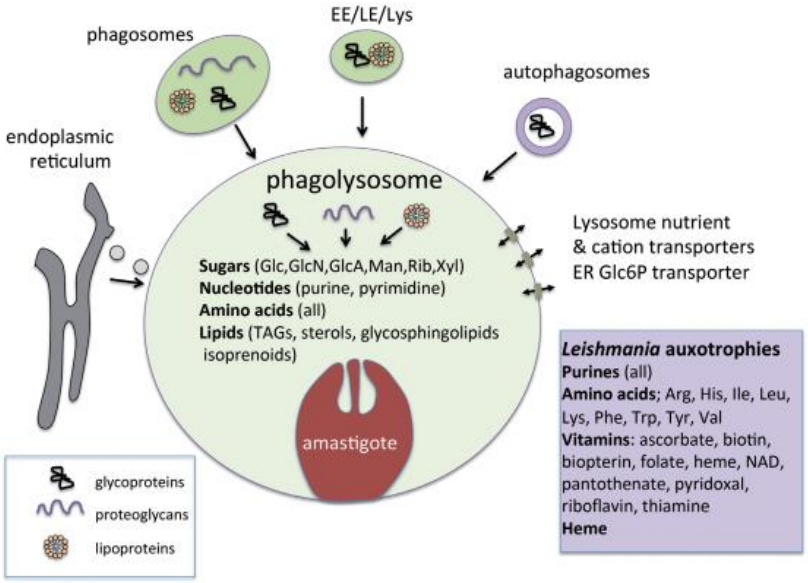

Figure 28. Nutrient availability within the phagolysosome of MØs. The phagolysosome contains several carbon sources, such as amino acids, sugars or lipids that are delivered *via* endocytic, autophagic or endoplasmic reticulum vesicles or lysosomal membrane transporters. Arg, arginine; EE, early endosome; Glc, glucose; Glc6P, glucose 6-phosphate; GlcA, glucuronic acid; GlcN, glucosamine; His, histidine; Ile, isoleucine; LE, late endosome; Leu, leucine; Lys, lysine; Man, mannose; Phe, phenylalanine; Rib, ribose; TAG, triacylglycerol; Trp, tryptophan; Tyr, tyrosine; Val, valine; Xyl, xylose. Adapted from McConville et al, 2015.

As promastigotes differentiate into amastigotes, there is a profound metabolic rearrangement, and the latter forms enter a stringent energy-sparing metabolic state (Saunders et al, 2014). Consequently, a decrease in glucose uptake accompanied by an increase in fatty acid utilization is observed. Carbon is redirected to intracellular reserves and processes like protein and lipid biosynthesis are minimized as they occur at a great energy expense. Despite the decrease in sugars uptake, the parasites are still dependent on carbohydrates, particularly on mitochondrial metabolism to produce glutamate and glutamine, which parasites salvage poorly from the phagolysosome (Saunders et al, 2014). This rearrangement is thought to make the parasites energetically more efficient and may underlie their resistance to stressful conditions, like pH or temperature and tolerance to nutrient limitation or excess (McConville et al, 2015; Saunders et al, 2014).

A very dramatic modification in amastigotes concerns the global downregulation of nutrient transporters as the stringent metabolic response is activated (Vince et al, 2011). Whereas promastigotes can exploit high concentrations of glucose and avoid excessive flux into the TCA cycle by secreting partially oxidized metabolites, this would be deleterious for intracellular parasites and could also affect the host cell physiology (McConville et al, 2015). Therefore in amastigotes, decreasing the nutrient uptake can minimize the reductive stress as well as prevent limiting (micro)nutrient exhaustion within the phagolysosome compartment (McConville et al, 2015; Saunders et al, 2014; Vince et al, 2011).

Besides its importance for nucleic acid synthesis, ribose can also be an important energy source for amastigotes (Burchmore & Barrett, 2001) as *Leishmania* can import (Maugeri et al, 2003) and metabolize it (Berens et al, 1980). A ribose transport system has been identified in promastigotes (Maugeri et al, 2003; Pastakia & Dwyer, 1987), and a glucose-transporter mutant also has a defective ribose import (Naula et al, 2010). The overall decrease in nutrient uptake in amastigotes as they enter the described metabolic stringency may render the parasites more dependent on RPIB for R5P synthesis. In this sense, it is important to look at alternative sources for R5P production. One of them is through the action of ribokinase (Feng et al, 2011; Jamdhade et al, 2015; Maugeri et al, 2003; Ogbunude et al, 2007) that directly phosphorylates ribose. However, it may not compensate RPIB activity, as it depends on the available ribose that is uptaken or that originates from intracellular catabolism, which again may be limiting in amastigotes. Ribokinase was reported to be essential in *T. brucei*, although trace amounts of the protein allow the fulfillment of its metabolic role such R5P production and phosphate homeostasis in the glycosomes (Kerkhoven et al, 2013). In *Leishmania*, its essentiality for parasite survival and contribution to amastigotes metabolism has not been addressed; only its upregulation upon glucose transport ablation has been reported in promastigotes (Feng et al, 2011).

Organisms like yeast have an alternative NADP-independent pathway for R5P synthesis. This so-called riboneogenesis pathway transforms glycolytic intermediates into sedoheptulose-1, 7-biphosphate, by a combined action of TKL and aldolase. Sedoheptulose-1, 7-biphosphate, through the action of sedoheptulose-1, 7-biphosphatase, is converted into S7P, which can be a substrate of TKL leading ultimately to R5P generation (Clasquin et al, 2011).

Trypanosomes encode a putative sedoheptulose-1, 7-biphosphatase, although riboneogenesis has not been formally shown to operate in these organisms (Creek et al, 2015; Opperdoes & Coombs, 2007). *Leishmania* in opposition to trypanosomes lacks this sequence: could this render it more dependent on RPIB function then?

Another possibility is that the absence/inhibition of RPIB may lead to the accumulation of Ru5P, which may modulate by negative feedback the activity of the upstream PPP enzymes. Two of those produce NADPH, and a decrease in their activity and consequently of NADPH production may render the parasites more susceptible to ROS. This sort of regulation is absent in several key enzymes of central carbon metabolism in trypanosomatids (Blangy et al, 1968; Newsholme et al, 1967).

Moreover, a study has demonstrated that human RPIA modulates hepatocarcinogenesis (Ciou et al, 2014), and its knockdown leads to Ru5P accumulation, which is further converted into X5P by RPE. It has been reported that X5P can activate PP2A (Kabashima et al, 2003), which negatively regulates ERK signalling for cell proliferation. Whether this sort of regulation takes place in *Leishmania* is unknown. However, *Leishmania* genome encodes for a RPE (Ivens et al, 2005; Jamdhade et al, 2015; Maugeri et al, 2003), PP2A (Brenchley et al, 2007) and MAP kinases (Parsons et al, 2005).

Figure 29 illustrates a model concerning RPIB critical role for *Leishmania* amastigotes survival and replication.

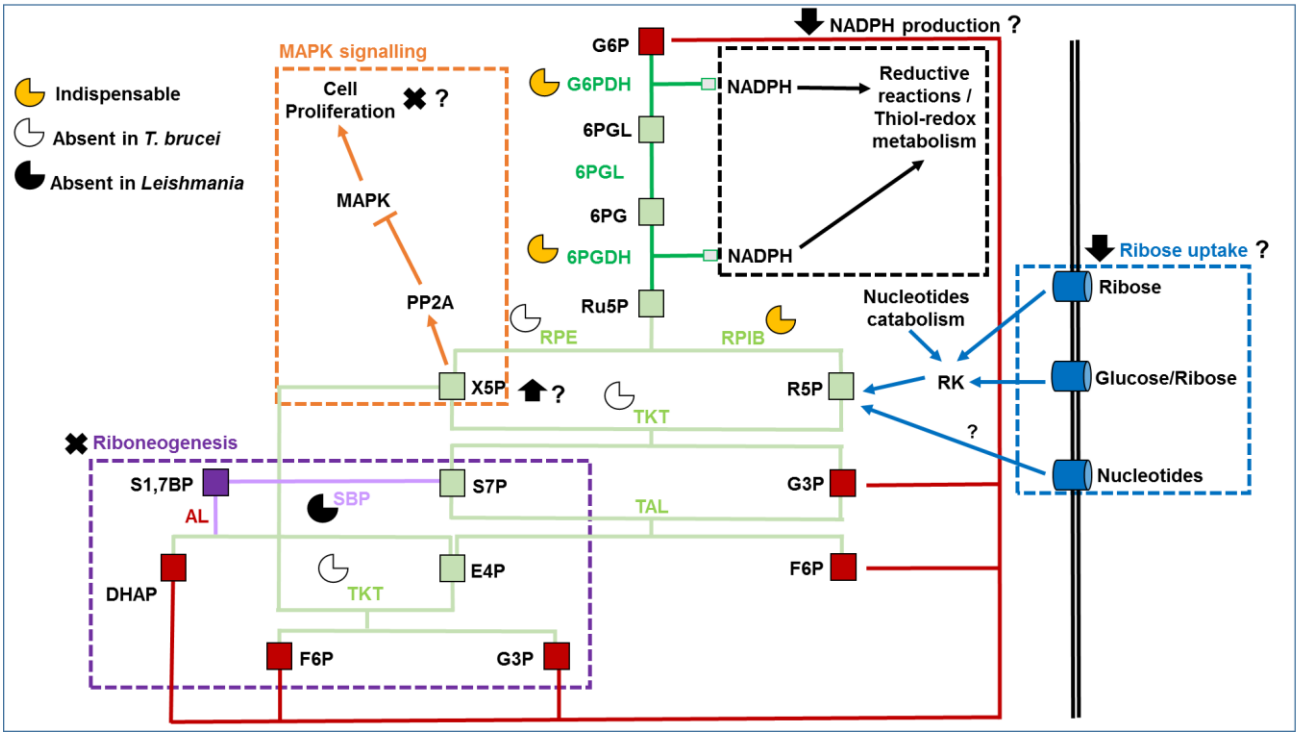

Figure 29. RPIB isomerase activity is detrimental for *Leishmania* parasites. The dashed rectangles represent steps that may be critical for the parasites in the absence of RPIB. Particularly in amastigotes there is a general decrease in nutrient uptake, thus a lower ribose import may render the parasites more dependent on RPIB function for R5P synthesis (dashed rectangle and arrows in blue). In *Leishmania*, the riboneogenesis pathway is absent, rendering the parasites more dependent on RPIB (dashed rectangle in purple). The accumulation of Ru5P may decrease the activity of the enzymes of the oxidative branch by negative feedback, leading to reduced levels of NADPH, ultimately rendering the parasites

more susceptible to ROS (dashed rectangle and arrows in black). The accumulation of Ru5P may also lead to increased levels of X5P, which may block cell proliferation by interfering with MAPK signaling. This has only been described in mammalian cells so far (dashed rectangle and arrows in orange). The red squares represent substrates and products that are shared with other pathways. The enzymes of the oxidative and non-oxidative branch are depicted in dark and light green, respectively: G6PDH, glucose-6-phosphate dehydrogenase; 6PGL, 6-phosphogluconolactonase; G6PDH, 6-phosphogluconate dehydrogenase; RPIB, ribose-5-phosphate isomerase B; RPE, ribose-5-phosphate epimerase; TKT, transketolase; TAL; transaldolase. Enzymes from glycolysis (AL, aldolase) and riboneogenesis (SBP, sedoheptulose biphosphatase) are represented in red and violet, respectively. Glycolysis, oxidative PPP, non-oxidative PPP and riboneogenesis metabolic flow are depicted with red, dark green, light green and violet lines. 6PG, 6-phosphogluconate; 6PGL, 6-phsophogluconalactone; DHAP, dihydroxyacetone phosphate; E4P, erythrose-4-phosphate; F6P, fructose-6-phosphate; G3P, glyceraldehyde-3-phosphate; G6P, glucose-6-phosphate; R5P, ribose-5-phosphate; Ru5P, ribulose-5-phosphate; S7P, sedoheptulose-7-phosphate; S1,7BP, sdoheptulose-1, 7-biphosphate; X5P, xylulose-5-phosphate. Modified from Comini et al, 2013.

2.6. RPIB essentiality appears to be conserved in trypanosomatids

RPIB knockdown in *T. brucei* bloodstream forms dramatically reduces their infectivity, resulting in the extension of mice survival. This phenotype is not due to any off-target effect as it was reversed by functional complementation with *Tc*RPIB whose mRNA sequence is sufficiently different to avoid RNAi (Loureiro et al, 2015). Moreover, three independent attempts to generate dKO mutants have failed, suggesting that RPIB is essential for parasite survival (Faria et al, 2015a *submitted*), although only a *TbRPIB* conditional knockout would be the ultimate proof. Using this system, parasites are engineered to express a regulable allele of the gene, which ceases to be expressed upon tetracycline removal, and a lethal phenotype should follow if the gene is indeed essential (Wyllie et al, 2009). The sKO mutants alone did not have any *in vitro* growth impairment but did display an infectivity defect *in vivo*. The latter was not as dramatic as the one observed in RNAi studies, probably because the protein knockdown is 50 and 90%, respectively (Faria et al, 2015a *submitted*; Loureiro et al, 2015).

These results point to a conservation of RPIB essentiality in trypanosomatids, reinforcing its potential as a drug target in these organisms.

2.7. Future perspectives on RPIB as a drug target

Target-based approach has not been as successful as initially expected over the years for several reasons previously listed in the second chapter of this dissertation. Those reasons concern normally poor membrane permeability or metabolic inactivation of the enzymatic inhibitors when tested against the whole parasites. Of course, in our view other

reasons may underlie such disappointing results: 1) the enzyme may be abundantly expressed and/or present a fast turnover; 2) the compound can have higher affinity for other targets that are dispensable for the parasite; 3) the *Leishmania* ability for DNA amplification may allow a higher expression of the molecular target; 4) protein moonlighting, in which the atypical function is the one detrimental for parasite survival.

In the case of the mammalian stage of *Leishmania*, a drug has to cross the host cell, the phagolysosome and the parasite membranes, and if the enzyme is inside an organelle, another membrane has to be crossed. In the case of RPIB, it displays a dual localization, as it localises mainly to the cytosol, but also in part to the glycosomes. We have not quantified the exact amount in each compartment, though, or whether the distribution changes during the parasite development. Another question is whether the localization in the glycosomes is essential for the parasite, as its activity inside the organelle may be harder to target. We could do a similar experiment to the one we have done to assess whether RPIB essentiality was dependent on the isomerase function, but instead of the mutated form devoid of isomerase function, we could use a truncated version lacking the PTS-2 signal peptide.

Another important issue to be addressed shortly is the enzyme druggability. The K_m values for both R5P and Ru5P are quite high and little physiological. This can be related to RPIB improper folding in the bacterial expression vector, the presence of the protein tag or even the sensitivity of the methods used for the activity determinations. We are currently trying to address the last two by cleaving the tag in the recombinant proteins, as well as trying to set up another assay, if possible, robust enough for a potential HTS scale up.

Moreover, an analogue of the isomerization intermediate, 4-PEH, has been proven to inhibit *Tb*RPIB and *Tc*RPIB (Loureiro et al, 2015; Stern et al, 2007). However, it also inhibits RPIA (Roos et al, 2005) and its anti-parasitic activity remains to be demonstrated. 4-PEH and several derivatives are extremely hydrophilic, but perhaps prodrugs can be developed to overcome this limitation as it has been done for *Tb*6PGDH (Ruda et al, 2010). The human RPIA crystal is not available yet, but *Tc*RPIB (Stern et al, 2011) has been crystallized and so has *Tb*RPIB and *Li*RPIB (unpublished data), which can be useful for rational drug design.

In summary, RPIB lacks a human homologue, is essential for survival and infectivity in *L. infantum* and likely in *T. brucei*. Furthermore it is a suitable drug target candidate, currently awaiting druggability studies.

Chapter V

Publications outside of the scope of this thesis

Original Research

Drug Discovery for Human African Trypanosomiasis: Identification of Novel Scaffolds by the Newly Developed HTS SYBR Green Assay for *Trypanosoma brucei*

Journal of Biomolecular Screening
1–12

DOI: 10.1177/1087057114556236
jbx.sagepub.com
SAGE

Joana Faria[1,3,§], Carolina B. Moraes[1,4,§], Rita Song[2], Bruno S. Pascoalino[4], Nakyung Lee[1], Jair L. Siqueira-Neto[1,¶], Deu John M. Cruz[1], Tanya Parkinson[5], Jean-Robert Ioset[5], Anabela Cordeiro-da-Silva[3,6], and Lucio H. Freitas-Junior[1,4]

Abstract

Human African trypanosomiasis (HAT) is a vector-transmitted tropical disease caused by the protozoan parasite *Trypanosoma brucei*. High-throughput screening (HTS) of small-molecule libraries in whole-cell assays is one of the most frequently used approaches in drug discovery for infectious diseases. To aid in drug discovery efforts for HAT, the SYBR Green assay was developed for *T. brucei* in a 384-well format. This semi-automated assay is cost- and time-effective, robust, and reproducible. The SYBR Green assay was compared to the resazurin assay by screening a library of 4000 putative kinase inhibitors, revealing a superior performance in terms of assay time, sensitivity, simplicity, and reproducibility, and resulting in a higher hit confirmation rate. Although the resazurin assay allows for comparatively improved detection of slow-killing compounds, it also has higher false-positive rates that are likely to arise from the assay experimental conditions. The compounds with the most potent antitrypanosomal activity were selected in both screens and grouped into 13 structural clusters, with 11 new scaffolds as antitrypanosomal agents. Several of the identified compounds had IC_{50} <1 μM coupled with high selectivity toward the parasite. The core structures of the scaffolds are shown, providing promising new starting points for drug discovery for HAT.

Keywords

anti-infective drugs, cell-based assays, ultrahigh-throughput screening, fluorescence methods

Introduction

Human African trypanosomiasis (HAT), also known as sleeping sickness, is a vector-transmitted disease caused by 2 subspecies of the digenetic protozoan parasite *Trypanosoma brucei*, namely, *T. b. gambiense* and *T. b. rhodesiense*. The disease is endemic in 36 Sub-Saharan Africa countries where the vector, the parasite, and the animal reservoir coexist. HAT has a fatal outcome if left untreated. Although the number of reported cases dropped from 37,385 in 1998 to 9689 in 2009, many remain unreported—and therefore untreated—due to the lack of specificity of the clinical diagnostic and the limited access to the infected populations.[1] In addition, *T. brucei* has an economic importance, because some subspecies are pathogenic to cattle, causing a wasting disease known as *nagana* and resulting in annual losses of US$1.5 billion in agricultural incomes.[2]

There are 2 *T. brucei* subspecies responsible for the disease in humans: *T. b. gambiense*, which is found in West Africa and responsible for more than 95% of the cases of the disease, and *T. b. rhodesiense* in East Africa, which is

[1]Center for Neglected Diseases Drug Discovery (CND3), Institut Pasteur Korea, Seongnam-si, Gyeonggi-do, South Korea
[2]MedChem & Chemical Biology Group, Institut Pasteur Korea, Seongnam-si, Gyeonggi-do, South Korea
[3]Parasite Disease Group, Instituto de Biologia Molecular e Celular, Universidade do Porto, Porto, Portugal
[4]Laboratório Nacional de Biociências (LNBio), Centro Nacional de Pesquisa em Energia e Materiais (CNPEM), Campinas—SP, Brazil
[5]Drugs for Neglected Diseases *initiative* (DNDi), Geneva, Switzerland
[6]Departamento de Ciências Biológicas, Faculdade de Farmácia, Universidade do Porto, Porto, Portugal
[§]These authors contributed equally to this work.
[¶]Present address: Skaggs School of Pharmacy and Pharmaceutical Science, University of California San Diego, La Jolla, CA, USA

Received Jun 22, 2014, and in revised form Sep 24, 2014. Accepted for publication Sep 27, 2014.

Supplementary material for this article is available on the *Journal of Biomolecular Screening* Web site at http://jbx.sagepub.com/supplemental.

Corresponding Author:
Lucio H. Freitas-Junior, CNPEM, Rua Giuseppe Maximo Scolfaro 10000, Campinas, 13087-100, Brazil.
Email: lucio.freitasjunior@lnbio.cnpem.br

responsible for the other 5% of the cases.[3] A third subspecies, *T. brucei brucei*, is unable to infect primates, although it is genotypically very similar to the 2 pathogenic subspecies, making it a good experimental model.

Because there are no vaccines available, drugs remain the main control strategy for HAT. There are 4 approved drugs for chemotherapy. Suramin, pentamidine, and melarsoprol are the most widely used and were developed before 1950. Eflornithine was approved in 1990, and since then advances in HAT treatment have been slow.[4] Furthermore, current treatments possess several limitations, such as limited efficacy and severe side effects due to toxicity, including mortality due to treatment.[1,5–7] Nifurtimox, a drug used for the treatment of Chagas disease, was introduced in 2009 in the World Health Organization's (WHO) List of Essential Medicines to be used as part of the nifurtimox–eflornithine combination therapy (NECT), providing a treatment less favorable toward the development of drug resistance and simpler to administer than the eflornithine monotherapy.[2,8]

High-throughput screening (HTS) of compound libraries using whole-cell assays is a well-established approach for drug discovery programs in neglected diseases. This kind of assay normally relies on simple pathogen viability readout, precluding the need for a validated target, which can be difficult to achieve; and, in contrast to a biochemical target-based assay, in this assay active compounds are discovered under physiologically relevant conditions. In addition, whole-cell-based assays have been quite successful in resulting in approved drugs for infectious diseases in general.[3,9,10] In spite of its compelling advantages, only recently were whole-cell-based assays reported in HTS format for *T. brucei*. Luciferase and resazurin-based cell viability assays were proposed in a 384-well format.[4,11–13] The latter was recently used to screen 87,296 compounds, resulting in 6 hits from 5 new chemical classes with activity confirmed against *T. b. rhodesiense*.[14]

In spite of its versatility and widespread use, the resazurin assay does possess some important limitations.[15] Resazurin accepts electrons from free radicals and from the electron transport chain within the inner mitochondrial membrane, generating ROS and interfering with energy homeostasis.[16,17] In addition, the resazurin screening assay for assessment of *T. brucei* viability in 384-well format assays has additional issues that might lead to misinterpretation of the results. Specifically, the assay requires long exposure of live parasites to resazurin at room temperature.[13] The long exposure to resazurin coupled with room temperature incubation could compromise *T. brucei* viability and could potentially interfere with compound activity during drug screening.

As an alternative to the resazurin assay, a SYBR Green–based whole-cell assay was developed for *T. brucei* in a 384-well format. SYBR Green is a cyanine dye that binds to nucleic acids, preferably to double-stranded DNA (dsDNA), thus providing an indirect assessment of cell number in a population. A SYBR Green–based whole-cell assay has been intensively used in antimalarial drug discovery.[18–22] Because *T. brucei* is an exclusively extracellular parasite, whole-cell assays based on quantitative detection of nucleic acids could be a feasible alternative.

Material and Methods

Cell culture: Bloodstream forms of *T. b. brucei* Lister 427 were cultured in HMI-9 medium as described previously.[23] The human acute leukemia monocyte cell line THP-1 (Korean Cell Line Bank No. 40202; Korean Cell Line Bank, Seoul, South Korea) was cultivated in RPMI medium (Welgene, Daegu, South Korea). Both culture media were supplemented with 10% heat-inactivated fetal bovine serum (FBS; Gibco, Carlsbad, CA), 100 U/mL penicillin, and 100 µg/mL streptomycin (Gibco). Cultures were kept in vented flasks in a humidified atmosphere of 5% CO_2 at 37 °C. Parasites were maintained in log-phase growth (between 1×10^5 and 1×10^6 parasites/mL) and subcultured every 24 h. THP-1 cultures were diluted every 3 or 4 days to maintain the cell density between 1×10^5 and 8×10^5 cells/mL. Both cells and parasites were kept for a maximum of 20 subcultured dilution cycles. All cultures were often tested for mycoplasma contamination, and only mycoplasma-negative cultures were used in this study.

Growth curves: For the determination of growth curves in 384-well plates, exponentially growing parasites were diluted in fresh HMI-9 complete media for the initial inoculums ($0.5–676.7\times10^3$ trypanosomes/mL). Fifty microliters of each inoculum were added to 384 plates (Greiner, Frickenhausen, Germany), followed by the addition of 10 µL 3% DMSO in phosphate buffered saline (PBS). Several wells were prepared per inoculum. Plates were incubated at 37 °C for 5 days, and parasites from 3 different wells per initial inoculum were harvested and counted daily in a Neubauer chamber for the determination of growth curves. Three independent experiments were performed.

Reference and library compounds: Melarsoprol was kindly provided by Gilles Courtemanche (Sanofi, Paris, France); pentamidine and eflornithine [D, L-α-difluoromethylornithine (DFMO)] were purchased from Sigma-Aldrich (St. Louis, MO). A library comprised of 4000 synthetic, kinase inhibitor-like compounds was purchased from BioFocus (Livingstone, NJ).[24,25]

Compound preparation: Prior to the addition to assay plates, library and reference compounds in 100% DMSO stocks were diluted in PBS in intermediate 384-well plates at 1:33 (v/v) in the case of the SYBR Green assay, and 1:17 (v/v) in the case of the resazurin assay, using a 384-channel pipetting head and a CyBi-Well pipettor (CyBio, Jena, Germany). Compound dilutions for dose–response curves (DRCs) were carried out manually in 100% DMSO in

384-well plates, followed by the same transfer and dilution scheme of intermediate plates described above. Unless otherwise noted, final DMSO concentration was 0.5% for test and control wells in both the resazurin and SYBR Green assays.

SYBR Green assay: Unless otherwise noted, trypanosomes in log-phase growth were suspended at 6×10^3 trypanosomes/mL in complete HMI-9 medium and, under continuous agitation, dispensed into 384-well black plates (Greiner) at 50 µL/well using a Wellmate dispenser (Thermo Scientific, Waltham, MA), followed by transfer of 10 µL of compounds from the intermediate plates as described above. Plates were incubated for 72 h at 37 °C and 5% CO_2, at which point the trypanosomes were lysed by the addition of 15 µL of 5× SYBR Green I (10,000× in DMSO; Invitrogen, Carlsbad, CA) in lysis solution [30 mM Tris pH 7.5, 7.5 mM EDTA, 0.012% saponin, and 0.12% Triton X-100, modified from Co et al.;[20] saponin was obtained from Sigma-Aldrich (Cat. No. S4521)]. The plates were agitated at 1700 rpm for 45 s using the MixMate plate mixer (Eppendorf, Hamburg-Eppendorf, Germany) and incubated in the dark for 1 h at room temperature, followed by reading on a Wallac Victor 3 plate reader (PerkinElmer, Waltham, MA), with excitation at 485 nm/emission at 530 nm during 3 min per plate.

Resazurin assay: The resazurin-based viability assay was performed as described[13] with minor modifications. Resazurin is the dye present in alamar blue, and commercial resazurin powders offer a more affordable alternative to the alamar blue reagent. Exponentially growing trypanosomes were diluted to 2×10^3 trypanosomes/mL in complete HMI-9 medium, plated at 55 µL/well in 384-well black plates using a Wellmate dispenser, and incubated at 37 °C and 5% CO_2. After 24 h, 5 µL of compound solutions were transferred from intermediate plates to assay plates as described above. After an additional 48 h incubation at 37 °C, 10 µL of 140 µM resazurinin in PBS were added to assay plates. Unless otherwise noted, plates were further incubated for 2 h at 37 °C followed by 22 h in the dark at room temperature. Plates were read on a Wallac Victor 3 (PerkinElmer) plate reader with excitation at 535 nm/emission at 590 mm during 3 min.

Cell Titer Glo assay: Occasionally, plates prepared following either the resazurin assay protocol or the SYBR Green assay protocol were developed with the luminescence-based adenosine triphosphate (ATP) measurement reagent Cell Titer Glo (Promega, Fitchburg, WI). The protocol was adapted from Sykes and Avery.[12] Briefly, 30 µL of culture were transferred from assay plates to flat-bottom 384-well white plates (Corning, Corning, NY), mixed with 30 µL of HMI-9, followed by the addition of 15 µL of Cell Titer Glo reagent (Promega). Plates were shaken for 2 min at 500 rpm in a Mixmate plate mixer and incubated for 10 min in the dark at room temperature. The luminescence signal was measured on a Victor 3 (PerkinElmer) plate reader. When Cell Titer Glo was specifically used for the development of plates prepared following the resazurin assay protocol, plates were removed from the incubator 74 h after trypanosome plating and then maintained for 22 h at room temperature in the dark prior to plating of Cell Titer Glo reagent.

Signal stability: After the development of plates with either the SYBR Green or resazurin assay protocol, DMSO and reference-drugs DRC plates were kept in the dark at either room temperature or 4 °C, and the fluorescence was measured daily to determine signal stability. For this purpose, 3 DMSO and/or DRC plates that result from independent parasite cultures and that had been assayed on different days were monitored by both methods.

Time-kill assays: Evaluation of compound antiparasitic activity throughout time was adapted from Jacobs et al.[26] and assessed as follows. Test and reference compounds were twofold serially diluted in 100% DMSO and transferred to assay plates following the same scheme described above. For each compound, 10 concentration points were prepared, and the initial concentrations in the assay plate were 40 µM for test compounds, 200 nM melarsoprol, 120 nM pentamidine, and 900 µM eflornithine. Parasites were plated following the SYBR Green assay protocol described above, and at every 12 or 24 h as indicated, duplicate plates were developed either with SYBR Green or with Cell Titer Glo as described above.

Library screening against trypanosomes: The BioFocus library was screened against *T. b. brucei* at 10 µM with both the SYBR Green and resazurin assays, in duplicate. Compounds were plated immediately after the parasites for the SYBR Green assay, and 24 h after the parasites for the resazurin assay. The whole library was screened in a single day for each replicate. Compounds with normalized antiparasitic activity equal to or greater than 80% were considered hits. The primary screening hits that were selective toward *T. b. brucei* (i.e., not toxic for human cell lines at 10 µM) were "cherry-picked" for confirmatory screening and potency assessment in dose–response curves. Hits were twofold serially diluted to yield 10-point curves starting at 40 µM. For all plates, 200 nM melarsoprol and 0.5% DMSO were used as positive and negative controls, respectively.

Counter-screening: The 4000-compound library had been previously screened against a panel of human cell lines in our laboratory (data not shown), and the cytotoxicity properties toward these cell lines were determined by a viability index (VI), calculated as follows: $VI = (A \times B \times C \times D) / 10^8$, where A, B, C, and D correspond to the normalized viability (%) of cultures of, respectively, the HeLa, Huh7.5, THP-1, and U2OS cell lines when exposed for 60 h to 10 µM of test compound in 0.5% DMSO. The normalized viability (%) of each cell line after compound exposure was determined by the resazurin method. Briefly, 1×10^4 cells/well were plated in 384-well black plates followed by compound treatment in a total volume of 60 µL. After

48 h incubation at 37 °C, resazurin was added to a final concentration of 10 µM, followed by a further 12 h incubation and plate reading as described above.

In confirmatory counter-screening, hit compounds had their potency against THP-1 cells determined in dose–response curves as described above for trypanosomes. Briefly, compounds were diluted and plated as described above, followed by plating of 1×10^4 THP-1 cells/well in RPMI containing 10% FBS, totaling a final volume of 60 µL/well. Plates were incubated at 37 °C and 5% CO_2 for 60 h prior to the addition of 5 µL of 130 µM resazurin in PBS, and they were incubated further for 12 h before reading.

Data analysis: The activity of test compounds was normalized against controls from the same plate according to the following formula: Activity (%) = $[1 - (F_{Cpd} - F_{Pos}) / (F_{Neg} - F_{Pos})] \times 100$, where F_{Cpd} corresponds to the emitted fluorescent signal expressed in arbitrary fluorescence units for the test compound; and F_{Neg} and F_{Pos} correspond to the mean fluorescent signal of the negative and the positive control wells, respectively. In time-kill experiments and THP-1 counter-screening, the positive control was replaced by the blank (complete media containing 0.5% DMSO). For estimation of the hit confirmation rate, compounds were considered "confirmed" when the normalized antiparasitic activity at 10 µM was ≥80%. For screening quality control purposes, the IC_{50}s of reference drugs as well as the coefficient of variability (CV) of control wells and the Z'-factor of each plate were monitored. The CV was calculated by the following equation: CV = (SD / MS) × 100, where SD and MS are the standard deviation of the signal and mean signal of the control wells from the same plate. The Z'-factor was calculated according to Zhang et al.[27] The detection limit (DL), expressed in trypanosomes per milliliter, was calculated according to the following equation: DL = $(3 \times SD_{Blank}) / S$, where SD_{Blank} corresponds to the standard deviation of the blank (HMI-9 medium); and S corresponds to the sensitivity of the method, or the slope of the standard curve of parasite concentration per milliliter versus fluorescence signal for each method. Dose–response curves were prepared using the function log(inhibitor) versus normalized response–variable slope from the GraphPad Prism software, version 5.00 for Windows (www.graphpad.com).

Chemical-clustering analysis: Hit compounds were clustered based on chemical scaffold and activity using the Pipeline Pilot software, version 8.5 (Accelrys; www.accelrys.com). For clustering, extended-connectivity fingerprints (ECFP-4 and ECFP-6) were used, and the predefined average number of molecules per cluster was 10.

Results

SYBR Green Assay Development and Comparison to Resazurin Assay

The resazurin assay has been so far the simplest and most affordable assay for HTS using African trypanosomes. While performing this assay in 384-well plates, we observed that *T. brucei* bloodstream forms presented a strongly reduced motility at the assay endpoint, even in untreated controls (**Suppl. Video S1** and **Suppl. Fig. S3**). The reduced motility was suggestive of decreased trypanosome viability, and it prompted us to hypothesize whether during the course of the resazurin assay development the parasite population had its viability reduced and consequently would be sensitized to compound action; this could potentially result in the selection of false-positive hits during HTS. To address this issue and provide an alternative HTS method, the SYBR Green assay was developed for *T. brucei* in a 384-well format.

During assay development, experimental conditions such as the initial inoculum of trypanosomes in 384-well plates, the incubation time to achieve optimal trypanosome growth, and the volume and the composition of the lysis solution were optimized. Growth curves for different initial inoculums (several densities ranging from 0.5 to 676.6×10^3 trypanosomes/mL) were performed to determine the most suitable inoculum density to achieve optimal trypanosome growth in 384-well plates. **Supplemental Figure S1A** shows that an initial inoculum of 6000 trypanosomes/mL results in a population range of $2–3 \times 10^6$ trypanosomes/mL (equivalent to the maximum culture density observed for this strain—data not shown) in the well after 72 h of growth. This trypanosome density was chosen as the initial inoculum for the development of the SYBR Green assay protocol. Because compounds are normally solubilized in DMSO, the maximum concentration tolerated by trypanosomes in assay conditions was found to be 0.5% DMSO (data not shown).

To ensure the optimal conditions to expose dsDNA after cell lysis, 4 different formulations of lysis buffer were tested on several inoculums that simulate the maximal range of trypanosome densities found in the well at assay endpoint (**Suppl. Fig. S1B**). The best combination was 0.01% saponin and 0.1% Triton X-100 in 15 µL of lysis solution per well, with less or more concentrated solutions resulting in decreased signal when parasite density ranges from 3×10^6 to 4×10^6 trypanosomes/mL. The temperature (room temperature or 37 °C) and the incubation period (1, 4, or 24 h) for signal development were also taken into account to ensure the best relationship between the stability and intensity of the SYBR Green signal. No significant differences or gain in assay quality were found, however, between the tested conditions; and, to secure a simpler and time-effective method, 1 h incubation at room temperature was chosen as the final incubation condition for SYBR Green signal development. For such conditions, the detection limit of the method was calculated as 2.05×10^4 trypanosomes/mL, approximately 3.5 times lower than the mean detection limit of resazurin (**Table 1**).

SYBR Green Assay as an Alternative to Resazurin Assay

After establishing the final experimental parameters, the SYBR Green and resazurin assays were compared regarding the main parameters analyzed in HTS campaigns: the

Table 1. Overview on the Performance Parameters for Both SYBR Green and Resazurin Methods for Final Assay Conditions.

Parameter	SYBR Green	Resazurin
Detection limit ($\times 10^4$ parasites/mL)[a]	2.05 ± 0.31	7.77 ± 6.01
Coefficient of variation of negative control (%)[a]	4.32 ± 1.01	8.47 ± 2.17
Z'-factor[a]	0.76 ± 0.06	0.71 ± 0.10
IC_{50} Melarsoprol (nM)[a]	7.98 ± 0.88	10.59 ± 0.70
IC_{50} Pentamidine (nM)[a]	5.57 ± 1.06	5.97 ± 0.40
Stability at 4 °C[a]	20 days	4 days
Stability at RT[a]	20 days	Less than 24 h
Assay total time	73 h	96 h
Estimated detection reagent cost per plate (US dollars)[b]	1.62	1.53[c]

RT, room temperature.
[a]The values correspond to the mean ± standard deviation obtained from 3 independent experiments.
[b]Products supplied by Life Technologies (Carlsbad, CA).
[c]US$17.61/plate for alamar blue.

Z'-factor, the coefficient of variation, and the IC_{50}s of reference drugs—in this case, melarsoprol and pentamidine. The results are summarized in **Table 1**.

The SYBR Green assay presented lower variability, as indicated by the coefficient of variation of the negative control (4.32% for the SYBR Green assay vs. 8.47% for the resazurin assay) and a considerably more stable signal at both 4 °C and room temperature. In addition, the SYBR Green assay is faster, requiring a total of 73 h for completion—saving around 24 h in comparison with the resazurin assay. Both assays are comparable in terms of assay Z'-factor; IC_{50} values for melarsoprol and pentamidine, which are in accordance with the literature;[13,28] and estimated cost of detection reagent (dye only) per plate. When alamar blue is considered instead of resazurin, however, the reagent cost per plate increases approximately 10 times (**Table 1**).

The SYBR Green Assay Detects Activity of Both Fast- and Slow-Killing Compounds at the Assay Endpoint

One limiting factor for SYBR Green assay sensitivity in monitoring antitrypanosomal activity would be the required time for DNA degradation after cell death. Time-kill experiments for reference drugs were performed using the SYBR Green assay protocol, and developed with either SYBR Green or Cell Titer Glo as detection reagents to better understand the dynamics of the SYBR Green assay for the detection of fast- and slow-killing compounds and the sensitivity of the method when compared to Cell Titer Glo. The activity of melarsoprol and pentamidine, fast trypanocidal compounds, and eflornithine, a slow-killing compound, was monitored throughout time (**Suppl. Fig. S2**). Cell Titer Glo was able to detect cell death caused by all 3 drugs earlier than SYBR Green. At the HTS assay endpoint (72 h), SYBR Green could detect compound activity equally efficiently as Cell Titer Glo for 100% efficacious concentrations, or slightly less efficiently for subefficacious concentrations. Thus, the SYBR Green assay is sufficiently sensitive to detect the antitrypanosomal activity of fast-killing compounds at the assay endpoint, and also of slow-killing compounds to some extent.

Comparison of the SYBR Green and Resazurin Assays in HTS of a Kinase-Focused Library

The primary screen of a commercial kinase-focused library of 4000 compounds was performed at 10 µM and in duplicate (2 independent runs) to minimize variation and permit robust comparison of both assays. A summary of the results is shown in both **Figure 1** and **Table 2**. The SYBR Green assay screen had a slightly better performance in terms of quality control parameters (**Table 2**), and the IC_{50}s for melarsoprol and pentamidine were within the expected range (**Suppl. Table S1**).

The binned distribution of compounds and controls per mean value of normalized activity showed a markedly different distribution pattern between the resazurin and SYBR Green assay screens (**Fig. 1A**). The greater variability of the negative control population in the resazurin assay was clear, because it was also evident that, for this method, the activity of compounds was mostly distributed in extremes (i.e., most compounds displayed either very high or very low activity); fewer compounds displayed activity in the intermediate range when compared to SYBR Green assay screen compound distribution.

The selected hits were further filtered for the removal of compounds that showed promiscuous cytotoxicity against human cell lines. Because this library had been previously screened against a panel of human cell lines (data not shown), only compounds that had a human cell line

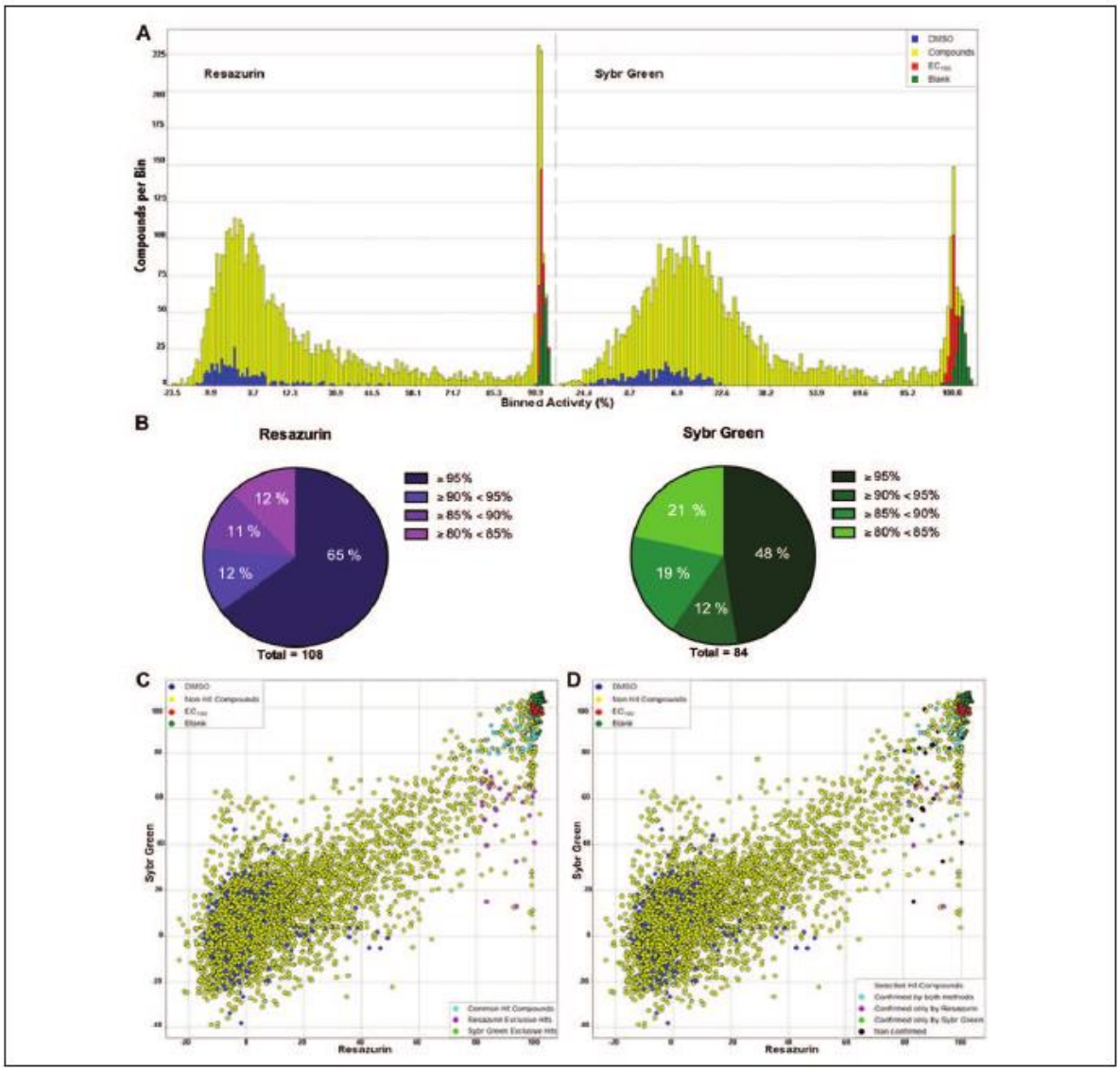

Figure 1. Comparison of antitrypanosomal activity profiles between the resazurin and SYBR Green assays. (**A**) Graphic representation of the library compounds distribution per normalized activity bin [Binned Activity (%), x-axis] for both resazurin and SYBR Green methods. The y-axis shows the number of compounds per bin. Blue, negative control wells (trypanosomes only); yellow, compound wells (trypanosomes and compound at 10 µM); red, positive control wells (trypanosomes and melarsoprol EC_{100} = 40 µM); and green, blank (complete media only). Two independent runs were undertaken for both methods. (**B**) Distribution of primary screening hits per activity bins as indicated in the legends for the resazurin assay screen (left) and SYBR Green assay screen (right) of 4000 compounds. The total number of hits selected is shown below the pie charts. (**C**) Whole screen compound and control activity correlation between the resazurin and SYBR Green methods, highlighting the selected hit compounds after primary screening. Data refer to each well-normalized activity (i.e., percent inhibition in relation to mean values of plate controls). Compounds with activity ≥80% and nontoxic to human cells (data not shown) were selected as hits. Dark blue: negative control wells; red, positive control wells; dark green, blank wells; yellow, nonhit compounds; light blue, nonexclusive (common to both screens) hit compounds; magenta, resazurin screen exclusive hit compounds; and light green, SYBR Green screen exclusive hit compounds. (**D**) Same as in (C), highlighting the results of activity confirmation screening. Selected hits were "cherry-picked" and tested in serial dilution in both assays, and they were considered "confirmed" when the normalized antitrypanosomal activity was ≥80% at 10 µM. The color code for wells is the same as in (C), except for the following: light blue, hits confirmed by both methods; magenta, hits confirmed only by the resazurin assay screen; light green, hits confirmed only by the SYBR Green assay screen; and black, hits that were not confirmed in either method. Among the primary screening selected hits, 5 compounds, which are pointed out in dark gray, were not available for hit confirmation. Data refer to 2 independent experiments.

Table 2. Comparison of SYBR Green and Resazurin Assays' Quality Control Parameters in the High-Throughput Screening of 4000 Compounds.

Parameter	SYBR Green	Resazurin
Z'-factor[a]	0.70 ± 0.04	0.67 ± 0.06
Coefficient of variation of negative control (%)[a]	2.32 ± 0.78	7.70 ± 1.94
Coefficient of variation of positive control (%)[a]	8.76 ± 2.00	6.32 ± 0.90
Coefficient of variation of blank (%)[a]	3.45 ± 2.20	6.06 ± 2.75

[a]Parameters were calculated for individual plates, and the values shown are the means ± standard deviations for all 26 compound plates run (2 runs of 13 plates each) with each assay.

viability index between 1.0 and 1.5 were further progressed for antitrypanosomal activity confirmatory screening.

The difference in activity pattern between the 2 assays reflected the number of hit compounds selected from both screens: 108 compounds with normalized activity ≥80% were selected as hits in the resazurin assay, whereas 84 compounds were selected as hits in the SYBR Green assay following the same selection criteria. This difference was also evidenced with hit compounds distribution per activity bins of 5% increments, showing the increased proportion (65%) of hits with very high activity (≥95%) in the resazurin assay screen, whereas the SYBR Green assay screen had 48% of the hits with activity ≥95% (**Fig. 1B**). Among the hit compounds, 82 were common to both resazurin and SYBR Green assays, 2 compounds were selected as exclusive hits of the SYBR Green assay, and 26 as exclusive hits of the resazurin assay (**Fig. 1C**).

Regarding the whole population of compounds and control wells, both assays were robust and resulted in reproducible data as shown in **Supplemental Table S2**. The correlation coefficient (r), determined for normalized activity between the first and second screening runs for each assay and including compounds and controls, was 0.94 for the resazurin assay and 0.82 for the SYBR Green assay, and the correlation was 0.92 between the resazurin assay runs and 0.73 between the SYBR Green assay runs. When only normalized activity of hit compounds was considered, the correlation between runs was 0.65 for the SYBR Green assay and 0.44 for the resazurin assay (**Suppl. Table S2**). This value was similar to the correlation between the resazurin and SYBR Green assay screens, considering the hit compounds' mean normalized activity of both runs (r, 0.48) (**Suppl. Table S2**). In summary, the correlation for the whole population of wells was higher in the resazurin assay screens; however, the SYBR Green assay had a better performance of correlation between runs when normalized activity of hit compounds was concerned.

Confirmatory and Counter-Screening for the Determination of Compounds With Selectivity Toward T. brucei

Among the 110 selected compounds, 3 compounds were not available for further studies: 2 hits were common to both assays, and 1 hit was exclusive of the resazurin assay. Thus, 79 compounds selected by both methods, 25 compounds selected only in the resazurin assay, and 2 selected only in the SYBR Green assay were tested for activity confirmation against *T. b. brucei* in dose–response curves to determine the compound potency. In parallel, the hits were also assayed against THP-1 cells to determine compound selectivity toward the parasites. A hit was considered confirmed when the normalized activity of the compound at 10 µM was ≥80% in the confirmatory screening.

Considering only the common hit compounds, the hit confirmation rate was 82.3% (65/79); when considering only the exclusive hits of this assay, the hit confirmation rate dropped to 64% (16/25). For the SYBR Green assay screen, the total hit confirmation rate was 86.4% (70/81) and thus higher than that of the resazurin assay screen. Both exclusive hit compounds for this assay confirmed, and regarding the common hits, the confirmation rate was 84.8% (67/79). One of the 2 SYBR Green exclusive hits was also confirmed by the resazurin assay, thus representing a missed hit or a false negative in the resazurin assay primary screening. From the 16 compounds selected as resazurin assay exclusive hits, 6 were also confirmed by SYBR Green assay. These compounds were also active in the SYBR Green assay primary screen, albeit with lower activity than in the resazurin assay primary screen, and therefore were excluded as hits in the SYBR Green assay screen due to the stringent activity cutoff applied in hit selection (**Fig. 1D**).

Potentiation of Compound Activity in the Resazurin Assay

The resazurin assay screen had a higher hit rate, and the hits had higher activity in comparison with the activity found in the SYBR Green assay screen. Furthermore, the resazurin assay screen had a higher rate of exclusive confirmed hits that could not be detected by the SYBR Green assay. These results could be explained by the fact that the SYBR Green assay may not detect slow-killing compounds within the assay time window; however, this claim is not supported by the time-kill assays performed with eflornithine (**Suppl.**

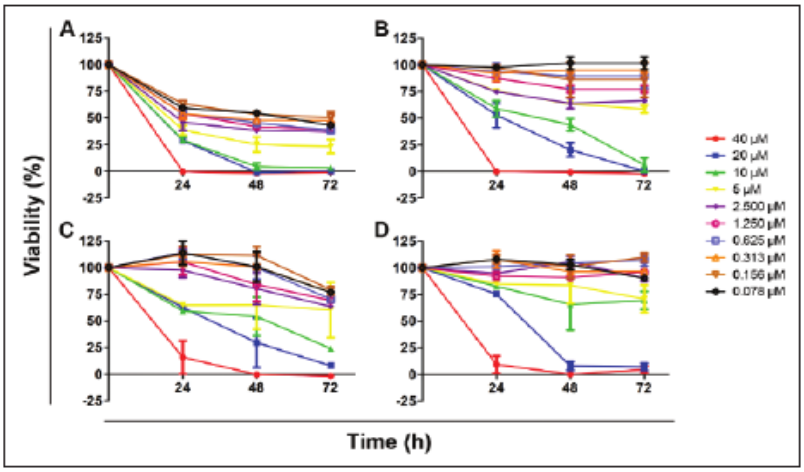

Figure 2. Some of the resazurin assay screen exclusive hits are slow-killing compounds, whereas others kill trypanosomes fast but have only minor activity at screening conditions with the SYBR Green assay. Nonexclusive (**A**) and resazurin exclusive hits (**B–D**) were tested in serial dilution in time-kill assays following the SYBR Green assay experimental conditions, except for the use of Cell Titer Glo as an alternative reagent for signal development and direct assessment of trypanosome viability. Representative compounds are shown. Two independent runs were undertaken.

Fig. S2). Alternatively, compound activity could potentially be exacerbated in the resazurin assay due to the possible reduction in parasite viability under the assay experimental conditions, as we first hypothesized. To further investigate why some compounds were exclusively selected and confirmed for antitrypanosomal activity by the resazurin assay only, and address the hypothesis of whether trypanosomes have reduced viability in the resazurin assay, some hit compounds were selected for further experiments: 9 compounds that were confirmed only by the resazurin assay, and 7 compounds that were confirmed by both assays. In the first set of experiments, parasites and compounds were plated and incubated following the SYBR Green assay protocol, and compound activity was measured every 24 h using either SYBR Green or Cell Titer Glo for signal development.

Representative examples of profiles obtained with hits common to both resazurin and SYBR Green assays (**Fig. 2A**), and hits exclusive to the resazurin assay (**Fig. 2B–D**), are shown. The plot for the common hit showed that at 10 µM (the concentration applied in the primary screening), this compound was able to kill 100% of the population with as little as 48 h of exposure, whereas 10 µM of resazurin assay screen exclusive hits plotted in **Figure 2B** could only reduce population viability to 0% after 72 h exposure, suggesting that indeed the SYBR Green assay screen preferentially detected fast-killing compounds. The other common hit compounds were also identified as fast-killing compounds, and in some cases they showed 100% antitrypanosomal efficacy after 24 h exposure, regardless of their potency (data not shown). Among the 7 compounds that had been confirmed only by resazurin assay, 2 other compounds presented the same pattern observed in **Figure 2B**, further suggesting that a potential limitation of SYBR Green assay may be less sensitivity toward slow-killing compounds. It is also important, however, to emphasize that these compounds can also be detected as active in the SYBR Green assay, albeit with reduced potency at the assay endpoint, presumably due to incomplete DNA degradation. The plots in **Figure 2C and 2D**, however, showed a different pattern: 10 µM of compound in **Figure 2C** had maximum activity of approximately 75% at 72 h exposure, demonstrating that although this compound can partially inhibit the growth of *T. brucei*, it could not be detected by the SYBR Green assay screen because the activity at 10 µM falls lower than the cutoff applied in the primary screening (normalized activity ≥80%). The compound in **Figure 2D**, however, showed a remarkably different activity pattern in the SYBR Green assay: at 20 µM, it reduced the population viability to nearly 5% at 48 h, in a concentration–time-to-kill kinetic similar to 20 µM of the common hit, shown in **Figure 2A**. At 10 µM, however, the compound in **Figure 2D** reduced population viability only to 69.49% (i.e., showed an activity of only approximately 30.51%, far lower than the 80% or more detected in the resazurin assay screening). Altogether, these results suggest that whereas the SYBR Green and resazurin assays may result in the detection of hits with different kinetics to kill trypanosomes, the resazurin assay is also selecting hits that are apparently very potent against trypanosomes under the resazurin assay conditions but only mildly potent under the SYBR Green assay conditions.

As a counterproof, all of the 16 confirmed hits were tested in a second set of experiments, but this time using the resazurin assay as the screening protocol and the Cell Titer Glo reagent as the reporter of cell viability.

The results summarized in **Figure 3** show the activity at 10 µM of these compounds obtained in both sets of experiments described above. Most nonexclusive hits had activity greater than 80% in all tested conditions, except for compound Hit ID 3, in which the activity at 10 µM was approximately 40% in the resazurin assay using resazurin for signal

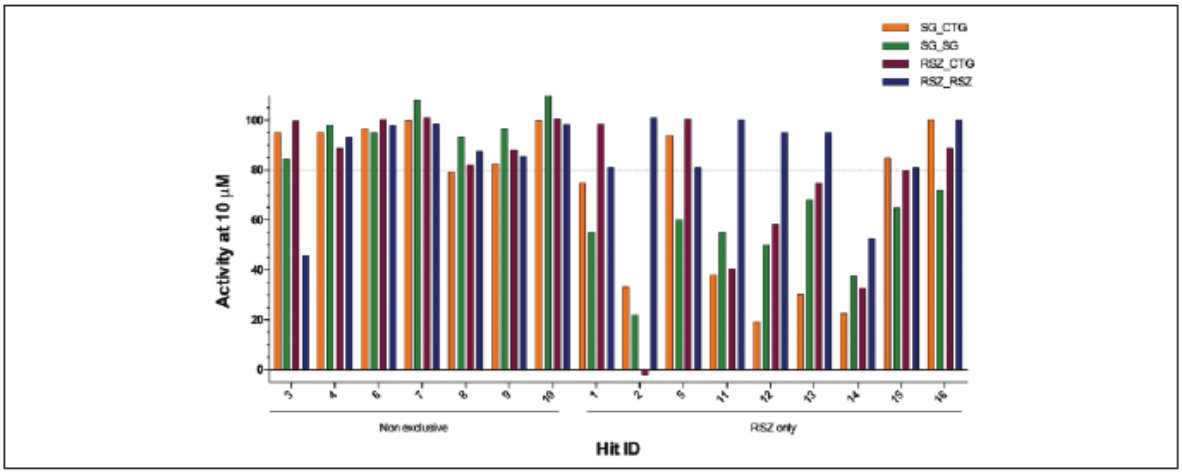

Figure 3. Some resazurin assay screen exclusive hits have pronounced activity in the presence of resazurin. Selected nonexclusive and resazurin assay screen exclusive hits (RSZ only) either were tested in serial dilution following the SYBR Green assay experimental conditions and developed with either Cell Titer Glo (SG_CTG, orange bars) or SYBR Green (SG_SG, green bars), or were tested following the resazurin assay experimental conditions and developed with either Cell Titer Glo (RSZ_CTG, purple bars) or resazurin (RSZ_RSZ, blue bars). A dotted line is shown at 80%, the activity cutoff applied in the selection of hits in the primary screening and used as activity confirmation criteria in the confirmatory dose response screening (shown here). Data refer to 2 independent replicates.

development (RSZ_RSZ). This can be attributed to the higher variation observed with the resazurin assay.

The resazurin assay screen exclusive hits can be classified in 2 major activity patterns: The first group of compounds (Hit ID 1, 5, 15, and 16) was active in all conditions, albeit moderately active (activity ranging from approximately 50% to 70%) only in the SYBR Green assay developed with SYBR Green (SG_SG) assay (**Fig. 3**), suggesting that they are slow-killing compounds, and in these cases there is a delay in the detection of cell death by the SYBR Green assay. A second group of compounds (Hit ID 2, 11, 12, and 13) were markedly highly active in the presence of resazurin only (RSZ_RSZ) (**Fig. 3**), regardless of the experimental protocol used in compound testing. Importantly, these compounds were only moderately active in the other assay setups tested, including the resazurin assay developed with Cell Titer Glo (RSZ_CTG), suggesting that, in these cases, compound activity was increased only in the presence of resazurin and differences in detection of antitrypanosomal activity between the resazurin and SYBR Green assays are not due to the speed with which the compound exerts its cidal effect.

Novel Scaffolds for Antitrypanosomal Drug Discovery

Despite the differences in the hit profile between the compound found in both assay protocols, the majority of the most potent hits were confirmed in both assays. The selectivity index toward trypanosomes (SI) varied from 3.9 to more than 512; indeed, 72% of the compounds presented an SI higher than 10 (data not shown).

The 72 confirmed compounds were analyzed for chemical clustering based on scaffold similarity, yielding 13 clusters. Among these, 11 clusters consisted of novel scaffolds with previously unknown antitrypanosomal activity (**Fig. 4**).

Discussion

The aim of this study was to develop a novel and improved drug-screening assay for drug discovery for HAT, and, in doing so, deliver new potential drug candidates. HTS of compound libraries using whole-cell assays is a simple and viable approach for early drug discovery programs in HAT; nevertheless, there are few reports based on whole-cell HTS assays for *T. brucei*. In the present work, we propose a novel, robust, suitable-to-automation, cost- and time-effective, simple, and reproducible 384-well-format HTS SYBR Green–based assay.

To validate the SYBR Green assay and, most importantly, discover new antitrypanosomal chemical entities, a kinase-focused library composed of 4000 compounds was screened against the *T. brucei* Lister 427 strain using both the SYBR Green and resazurin assays in HTS mode. The parallel screening of the same library in both assays allowed for comparison of the assays' performance in real HTS

conditions and also whether the hit profiling obtained in both screens would be considerably different.

A thorough comparison demonstrated that the SYBR Green assay is more sensitive, less variable, and faster to develop than the resazurin assay, all features of major importance in HTS. SYBR Green also had a better confirmation rate (approximately 86%) than the resazurin assay (75%), and some of the exclusively identified hits identified in the resazurin assay could not be confirmed or presented lower activity when rescreening with SYBR Green or Cell Titer Glo. This fact, allied with the increased activity of the selected hits in the resazurin assay, raised the hypothesis that this assay could lead to an additive "intrinsic activity" that further debilitates trypanosomes, thus decreasing the population viability and artificially increasing hit rates. Resazurin has been extensively used for monitoring *T. brucei* viability in drug assays in 96-well plates; however, no data regarding toxicity to trypanosomes are available in the literature. We suppose that in the 384-well-plate format, a longer exposure to resazurin (24 h) in comparison to the 96-well-plate format (4 h) and/or a relatively long incubation period at room temperature (22 h) could account for the reduced parasite motility observed at the resazurin assay endpoint (**Suppl. Video S1**), suggesting that parasite viability is reduced in these experimental conditions.

The practical effects of using a resazurin assay for HTS for HAT drug discovery can be speculated. Besides offering no advantage in terms of cost and time, the resazurin assay resulted in a higher rate of false positives. The greater assay variability could also result in a higher rate of false negatives in the resazurin assay. The resazurin assay, however, seems to be more sensitive for the detection of compounds that kill trypanosomes slowly. This could be due to cell membrane permeability kinetics, features that can be improved by chemical optimization of scaffolds; alternatively, it could (also) be due to the compound mechanism of action.

The major novelty of this study was the discovery of novel scaffolds with potent antitrypanosomal activity (**Fig. 4**). Kinase targets have been addressed by the pharmaceutical industry and offer potential for the development of new drugs in several therapeutic areas.[29] The library screened in this study is a focused set of approximately 4000 drug-like small molecules of structural features that favor interactions with kinases and/or phosphatases. Knowledge of the crucial role of protein kinases in cell survival in multicellular organisms has directed attention toward this enzyme class in parasitic protozoa to search for alternative drug targets to treat tropical diseases.[30,31]

Most of the 72 hit compounds identified here against *T. b. brucei* presented a high selectivity index toward trypanosomes. Among those, triazolopyridine-based inhibitors (**Fig. 4**, group 1) have been described as atypical kinase inhibitors, applicable to p38 mitogen-activated protein kinase (MAPK).[32] There are 3 major classes of MAPKs: ERK, p38, and JNK. So far, 2 ERK homologues (KFR1 and TbMAPK2) were identified in *T. brucei* along with 2 kinases that share features of both ERK and cyclin-dependent kinases (TbECK1 and TbMAPK5).[30,33] TbMAPK5 is involved in the growth and differentiation of bloodstream forms, and knockdown studies showed a reduction of the peak parasitemia in mice.[33] Extensive studies are needed, however, to determine the targets of the compounds reported in this article. Although not mandatory, knowledge of the target and its structure would facilitate the development of highly antiparasitic selective drugs. And, although some hits already have good potency, further medicinal chemistry optimization is necessary to improve activity and/or pharmacological properties and establish the structure–activity relationship (SAR). In conclusion, the contribution of this study is not only a novel HTS *T. brucei* viability assay that overcomes the limitations of the standard method but also attractive chemical scaffolds that will be valuable starting points for HAT drug development.

Acknowledgments

We would like to acknowledge Fundação para a Ciência e Tecnologia (FTC) for funding (SFRH/BD/79712/2011), Eunhye Kim and Luís Gaspar for technical support, and Gilles Courtemanche for kindly providing melarsoprol. This work was partially supported by a National Research Foundation of Korea (NRF) grant funded by the Korea government (MSIP; No. 2007-00559), Gyeonggi-do (No. K204EA000001-09E0100-00110), and KISTI.

Declaration of Conflicting Interests

The authors declared no potential conflicts of interest with respect to the research, authorship, and/or publication of this article.

Funding

The authors disclosed receipt of the following financial support for the research, authorship, and/or publication of this article: We would like to acknowledge Fundação para a Ciência e Tecnologia (FTC) for funding (SFRH/BD/79712/2011), Eunhye Kim and Luís Gaspar for technical support, and Gilles Courtemanche for kindly providing melarsoprol. This work was partially supported by the National Research Foundation of Korea (NRF) grant funded by the Korea government (MSIP; No. 2007-00559), Gyeonggi-do (No. K204EA000001-09E0100-00110), and KISTI.

References

1. Simarro, P. P.; Diarra, A.; Postigo, J. A. R.; et al. The Human African Trypanosomiasis Control and Surveillance Programme of the World Health Organization 2000–2009: The Way Forward. *PLoS Negl. Trop. Dis.* **2011**, *5*, e1007.
2. World Health Organization. Working to Overcome the Global Impact of Neglected Tropical Diseases; Crompton, D. W. T.; Peters, P., Eds.; Geneva: World Health Organization, **2010**.

3. Simarro, P. P.; Jannin, J.; Cattand, P. Eliminating Human African Trypanosomiasis: Where Do We Stand and What Comes Next? *PLoS Med.* **2008**, *5*, e55.
4. Docampo, R.; Moreno, S. N. J. Current Chemotherapy of Human African Trypanosomiasis. *Parasitol. Res.* **2003**, *90* Supp. 1, S10–S13.
5. Nok, A. J. Arsenicals (Melarsoprol), Pentamidine and Suramin in the Treatment of Human African Trypanosomiasis. *Parasitol. Res.* **2003**, *90*, 71–79.
6. Robays, J.; Nyamowala, G.; Sese, C.; et al. High Failure Rates of Melarsoprol for Sleeping Sickness, Democratic Republic of Congo. *Emerg. Infect. Dis.* **2008**, *14*, 966–967.
7. Balasegaram, M.; Young, H.; Chappuis, F.; et al. Effectiveness of Melarsoprol and Eflornithine as First-Line Regimens for Gambiense Sleeping Sickness in Nine Medecins Sans Frontieres Programmes. *Trans. R. Society Trop. Med. Hyg.* **2009**, *103*, 280–290.
8. Babokhov, P.; Sanyaolu, A. O.; Oyibo, W. A.; et al. A Current Analysis of Chemotherapy Strategies for the Treatment of Human African Trypanosomiasis. *Pathog. Glob. Health.* **2013**, *107*, 242–252.
9. Pink, R.; Hudson, A.; Mouriès, M.-A.; et al. Opportunities and Challenges in Antiparasitic Drug Discovery. *Nat. Rev. Drug Discov.* **2005**, *4*, 727–740.
10. Keller, T. H.; Shi, P.-Y.; Wang, Q.-Y. Anti-Infectives: Can Cellular Screening Deliver? *Curr. Opin. Chem. Biol.* **2011**, *15*, 529–533.
11. Mackey, Z. B.; Baca, A. M.; Mallari, J. P.; et al. Discovery of Trypanocidal Compounds by Whole Cell HTS of *Trypanosoma brucei*. *Chem. Biol. Drug Des.* **2006**, *67*, 355–363.
12. Sykes, M. L.; Avery, V. M. A Luciferase Based Viability Assay for ATP Detection in 384-Well Format for High Throughput Whole Cell Screening of *Trypanosoma brucei brucei* Bloodstream Form Strain 427. *Parasit. Vectors.* **2009**, *2*, 54.
13. Sykes, M. L.; Avery, V. M. Development of an Alamar Blue™ Viability Assay in 384-Well Format for High Throughput Whole Cell Screening of *Trypanosoma brucei brucei* Bloodstream Form Strain 427. *Am. J. Trop. Med. Hyg.* **2009**, *81*, 665–674.
14. Sykes, M. L.; Baell, J. B.; Kaiser, M.; et al. Identification of Compounds with Anti-Proliferative Activity Against *Trypanosoma brucei brucei* Strain 427 by a Whole Cell Viability Based HTS Campaign. *PLoS Negl. Trop. Dis.* **2012**, *6*, e1896.
15. Gould, M. K.; Vu, X. L.; Seebeck, T.; et al. Propidium Iodide-Based Methods for Monitoring Drug Action in the Kinetoplastidae: Comparison with the Alamar Blue Assay. *Anal. Biochem.* **2008**, *382*, 87–93.
16. Prutz, W. A.; Butler, J.; Land, E. J. Photocatalytic and Free Radical Interactions of the Heterocyclic N-Oxide Resazurin with NADH, GSH, and Dopa. *Arch. Biochem. Biophys.* **1996**, *327*, 239–248.
17. Ahmed, S. A.; Gogal, R. M. J.; Walsh, J. E. A New Rapid and Simple Non-Radioactive Assay to Monitor and Determine the Proliferation of Lymphocytes: an Alternative to [3H] Thymidine Incorporation Assay. *J. Immunol. Methods.* **1994**, *170*, 211–224.
18. Smilkstein, M.; Sriwilaijaroen, N.; Kelly, J. X.; et al. Simple and Inexpensive Fluorescence-Based Technique for High-Throughput Antimalarial Drug Screening. *Antimicrob. Agents Chemother.* **2004**, *48*, 1803–1806.
19. Johnson, J. D.; Dennull, R. A.; Gerena, L.; et al. Assessment and Continued Validation of the Malaria SYBR Green I-Based Fluorescence Assay for Use in Malaria Drug Screening. *Antimicrob. Agents Chemother.* **2007**, *51*, 1926–1933.
20. Co, E.-M. A.; Dennull, R. A.; Reinbold, D. D.; et al. Assessment of Malaria in Vitro Drug Combination Screening and Mixed-Strain Infections Using the Malaria Sybr Green I-Based Fluorescence Assay. *Antimicrob. Agents Chemother.* **2009**, *53*, 2557–2563.
21. Izumiyama, S.; Omura, M.; Takasaki, T.; et al. *Plasmodium Falciparum*: Development and Validation of a Measure of Intraerythrocytic Growth Using SYBR Green I in a Flow Cytometer. *Exp. Parasitol.* **2009**, *121*, 144–150.
22. Vossen, M. G.; Pferschy, S.; Chiba, P.; et al. The SYBR Green I Malaria Drug Sensitivity Assay: Performance in Low Parasitemia Samples. *Am. J. Trop. Med. Hyg.* **2010**, *82*, 398–401.
23. Hirumi, H.; Hirumi, K. Continuous Cultivation of *Trypanosoma brucei* Blood Stream Forms in a Medium Containing a Low Concentration of Serum Protein Without Feeder Cell Layers. *J. Parasitol.* **1989**, *75*, 985–989.
24. Harris, C. J.; Hill, R. D.; Sheppard, D. W.; et al. The Design and Application of Target-Focused Compound Libraries. *Comb. Chem. High Throughput Screen.* **2011**, *14*, 521–531.
25. Cruz, D. J. M.; Koishi, A. C.; Taniguchi, J. B.; et al. High Content Screening of a Kinase-Focused Library Reveals Compounds Broadly-Active Against Dengue Viruses. *PLoS Negl. Trop. Dis.* **2013**, *7*, e2073.
26. Jacobs, R. T.; Nare, B.; Wring, S. A.; et al. SCYX-7158, an Orally-Active Benzoxaborole for the Treatment of Stage 2 Human African Trypanosomiasis. *PLoS Negl. Trop. Dis.* **2011**, *5*, e1151.
27. Zhang, J.; Chung, T.; Oldenburg, K. A Simple Statistical Parameter for Use in Evaluation and Validation of High Throughput Screening Assays. *J. Biomol. Screen.* **1999**, *4*, 67–73.
28. Alsford, S.; Eckert, S.; Baker, N.; et al. High-Throughput Decoding of Antitrypanosomal Drug Efficacy and Resistance. *Nature.* **2012**, *482*, 232–236.
29. Cohen, P. Protein Kinases—the Major Drug Targets of the Twenty-First Century? *Nat. Rev. Drug Discov.* **2002**, *1*, 309–315.
30. Naula, C.; Parsons, M.; Mottram, J. C. Protein Kinases as Drug Targets in Trypanosomes and *Leishmania*. *Biochim. Biophys. Acta.* **2005**, *1754*, 151–159.
31. Sharlow, E.; Golden, J. E.; Dodson, H.; et al. Identification of Inhibitors of *Trypanosoma brucei* Hexokinases; Bethesda (MD): National Center for Biotechnology Information (US), 2010. Available from: http://www.ncbi.nlm.nih.gov/books/NBK63599/
32. McClure, K. F.; Abramov, Y. A.; Laird, E. R.; et al. Theoretical and Experimental Design of Atypical Kinase Inhibitors: Application to P38 MAP Kinase. *J. Med. Chem.* **2005**, *48*, 5728–5737.
33. Domenicali Pfister, D.; Burkard, G.; Morand, S.; et al. A Mitogen-Activated Protein Kinase Controls Differentiation of Bloodstream Forms of *Trypanosoma brucei*. *Eukaryot. Cell.* **2006**, *5*, 1126–1135.

Chapter VI

Bibliography

Addy M, Nandy A (1992) Ten years of kala-azar in West Bengal. Part I. Did post-kala-azar dermal leishmaniasis initiate the outbreak in 24-Parganas? *Bull World Health Organ* **70:** 341-346

Afonso L, Borges VM, Cruz H, Ribeiro-Gomes FL, Dos Reis GA, Dutra AN, et al. (2008) Interactions with apoptotic but not with necrotic neutrophils increase parasite burden in human macrophages infected with *Leishmania amazonensis*. Journal of Leukocyte Biology **84(2):** 389-96

Ahmed S, Colmenares M, Soong L, Goldsmith-Pestana K, Munstermann L, et al. (2003) Intradermal infection model for pathogenesis and vaccine studies of murine visceral leishmaniasis. *Infection and Immunity* **71:** 401-410

Akiyoshi B, Gull K (2013) Evolutionary cell biology of chromosome segregation: insights from trypanosomes. *Open Biology* **3(5):** 130023

Akiyoshi B, Gull K (2014) Discovery of unconventional kinetochores in kinetoplastids. *Cell* **156:** 1247-1258

Akopyants NS, Kimblin N, Secundino N, Patrick R, Peters N, Lawyer P, et al. (2009) Demonstration of genetic exchange during cyclical development of *Leishmania* in the sand fly vector. *Science* **324:** 265-268

Al-Mulla Hummadi YM, Al-Bashir NM, Najim RA (2006) *Leishmania major* and *Leishmania tropica*: II. Effect of an immunomodulator, S(2) complex on the enzymes of the parasites. *Experimental Parasitology* **112:** 85-91

Albert MA, Haanstra JR, Hannaert V, Van Roy J, Opperdoes FR, Bakker BM, et al. (2005) Experimental and *in silico* analyses of glycolytic flux control in bloodstream form *Trypanosoma brucei*. *The Journal of biological chemistry* **280:** 28306-28315

Alcolea PJ, Alonso A., Gómez MJ, Sánchez-Gorostiaga A, Moreno-Paz M, González-Pastor E et al. (2010) Temperature increase prevails over acidification in gene expression modulation of amastigote differentiation in *Leishmania infantum*. *BMC Genomics* **11:** 31

Ali BR, Pal A, Croft SL, Taylor RJ, Field MC (1999) The farnesyltransferase inhibitor manumycin A is a novel trypanocide with a complex mode of action including major effects on mitochondria. *Molecular and biochemical parasitology* **104:** 67-80

Alonso DP, Ferreira AFB, Ribolla PEM, Santos IKFDM, Cruz MDSPE, et al. (2007) Genotypes of the mannan-binding lectin gene and susceptibility to visceral leishmaniasis and clinical complications. *Journal of Infectious Diseases* **195:** 1212–1217

Alsford S, Eckert S, Baker N, Glover L, Sanchez-Flores A, Leung KF et al. (2012) High-throughput decoding of antitrypanosomal drug efficacy and resistance. *Nature* **482:** 232-236

Alsford S, Turner DJ, Obado SO, Sanchez-Flores A, Glover L, Berriman M et al. (2011) High-throughput phenotyping using parallel sequencing of RNA interference targets in the African trypanosome. *Genome Research* **21:** 915–924

Alsford S, duBois K, Horn D, Field MC (2012) Epigenetic mechanisms, nuclear architecture, and the control of gene expression in trypanosomes. *Expert Reviews in Molecular Medicine*, **14:** e13

Alvar J, Aparicio P, Aseffa A, Den Boer M, Canavate C, Dedet JP, et al. (2008) The relationship between leishmaniasis and AIDS: the second 10 years. *Clinical Microbiology Reviews* **21:** 334-359

Alvar J, Velez ID, Bern C, Herrero M, Desjeux P, Cano J, et al. (2012) Leishmaniasis worldwide and global estimates of its incidence. *PLoS One* **7(5):** e35671

Andrulis IL, Chen J, Ray PN (1987) Isolation of human cDNAs for asparagine synthetase and expression in Jensen rat sarcoma cells. *Molecular Cell Biology* **7:** 2435-2443

Andrulis IL, Shotwell M, Evans-Blackler S, Zalkin H, Siminovitch L, Ray PN (1989) Fine structure analysis of the Chinese hamster AS gene encoding asparagine synthetase. *Gene* **80:** 75-85

Anthony RL, Williams KM, Sacci JB, Rubin DC (1985) Subcellular and taxonomic specificity of monoclonal antibodies to New World Leishmania. *American Journal of Tropical Medicine and Hygiene* **34:** 1085-1094

Antoine JC, Prina E, Courret N, Lang T (2004) *Leishmania* spp.: on the interactions they establish with antigen-presenting cells of their mammalian hosts. *Advances in Parasitology* **58:** 1-68

Antoine JC, Prina E, Lang T, Courret N (1998) The biogenesis and properties of the parasitophorous vacuoles that harbour *Leishmania* in murine macrophages. Trends in Microbiology **6:** 392-401

Aquino DMC, Caldas AJM, Miranda JC, Silva AAM, Barral-Netto M, et al. (2010) Short report: epidemiological study of the association between anti-*Lutzomyia longipalpis* saliva antibodies and development of delayed-type hypersensitivity to *Leishmania* antigen. *American Journal of Tropical Medicine and Hygiene* **83:** 825-827

Arango-Duque G, Descoteaux A (2015) *Leishmania* survival in the macrophage: where the ends justify the means. *Current Opinion in Microbiology* **26:** 32-40

Arnau J, Lauritzen C, Petersen GE, Pedersen J (2006) Current strategies for the use of affinity tags and tag removal for the purification of recombinant proteins. *Protein expression and purification* **48:** 1-13

Aronov AM, Suresh S, Buckner FS, Van Voorhis WC, Verlinde CL, Opperdoes FR, et al. (1999) Structure-based design of submicromolar, biologically active inhibitors of trypanosomatid glyceraldehyde-3-phosphate dehydrogenase. *Proceedings of the National Academy of Sciences of the United States of America* **96:** 4273-4278

Ashutosh, Sundar S, Goyal N (2007) Molecular Mechanisms of antimony resistance in *Leishmania. Journal of Medical Microbiology* **56:** 143-153

Aulner N, Danckaert A, Rouault-Hardoin E, Desrivot J, Helynck O, Commere PH et al. (2013) High content analysis of primary macrophages hosting proliferating *Leishmania* amastigotes: application to anti-leishmanial drug discovery. *PLoS Neglected Tropical Diseases* **7(4):** e2154

Aurrecoechea C, Brestelli J, Brunk BP, Fischer S, Gajria B (2010) EuPathDB: a portal to eukaryotic databases. *Nucleic Acid Research* **38:** D415-419

Avramis VI (2012) Asparaginases: biochemical pharmacology and modes of drug resistance. *Anticancer Research* **32:** 2423-2437

Azema L, Lherbet C, Baudoin C, Blonski C (2006) Cell permeation of a *Trypanosoma brucei* aldolase inhibitor: evaluation of different enzyme-labile phosphate protecting groups. *Bioorganic & medicinal chemistry letters* **16:** 3440-3443

Babbitta, SE, Altenhofend, L, Cobboldd, SA, Istvana, ES, Fennellf, C, Doergf, C et al. (2012) *Plasmodium falciparum* responds to amino acid starvation by entering into a hibernatory state. *Proceedings of the National Academy of Sciences of the United States of America*, **109(47):** 3278-3287

Bacchi CJ, Brun R, Croft SL, Alicea K, Buhler Y (1996) *In vivo* trypanocidal activities of new S-adenosylmethionine decarboxylase inhibitors. *Antimicrobial agents and chemotherapy* **40:** 1448-1453

Badaró R, Jones TC, Lorenço R, Cerf BJ, Sampaio D, et al. (1986) A prospective study of visceral leishmaniasis in an endemic area of Brazil. *Journal of Infectious Diseases* **154:** 639-649

Baiocco P, Colotti G, Franceschini S, Ilari A (2009) Molecular basis of antimony treatment in leishmaniasis. *Journal of Medicinal Chemistry* **52:** 2603-2612

Baker N, Glover L, Munday JC, Aguinaga-Andrés D, Barrett MP, de Koning HP, et al. (2012) Aquaglyceroporin 2 controls susceptibility to melarsoprol and pentamidine in African Trypanosomes. *Proceedings of the National Academy of Sciences of the United States of America* **109(27):** 10996-11001

Baker N, Hamilton G, Wilkesb JM, Hutchinson S, Barrett MP, Horn D (2015) Vacuolar ATPase depletion affects mitochondrial ATPase function, kinetoplast dependency, and drug sensitivity in trypanosomes. *Proceedings of the National Academy of Sciences of the United States of America* **112(29):** 9112-9117

Bakker BM, Walsh MC, ter Kuile BH, Mensonides FI, Michels PA, Opperdoes FR, Westerhoff HV (1999) Contribution of glucose transport to the control of the glycolytic flux in *Trypanosoma brucei*. *Proceedings of the National Academy of Sciences of the United States of America* **96:** 10098-10103

Balber AE (1990) The pellicle and the membrane of the flagellum, flagellar adhesion zone, and flagellar pocket: functionally discrete surface domains of the bloodstream form of African trypanosomes. *Critic Reviews on Immunology* **10:** 177-201

Banuls AL, Hide M, Prugnolle F (2007) *Leishmania* and the leishmaniases: a parasite genetic update and advances in taxonomy, epidemiology and pathogenicity in humans. *Advances in Parasitology* **64:** 1-109

Barak E, Amin-Spector S, Gerliak E, Goyard S, Holland N, et al. (2005) Differentiation of *Leishmania donovani* in host-free system: analysis of signal perception and response. *Molecular Biochemical Parasitology* **141:** 99-108

Bari Au (2006) Chronology of cutaneous Leishmaniasis: An overview of the history of the disease. *Journal of Pakistan Association of Dermatologists* **16:** 24-27

Barrett MP (1997) The pentose phosphate pathway and parasitic protozoa. *Parasitology Today* **13:** 11-16

Baruch M, Belotserkovsky I, Hertzog BB, Ravins M, Dov E, McIver KS, et al. (2014) An extracellular bacterial pathogen modulates host metabolism to regulate its own sensing and proliferation. *Cell* **156:** 97-108

Bastien P, Blaineau C, Pages M (1992) Molecular karyotype analysis in *Leishmania*. *Subcellular Biochemistry* **18:** 131-187

Bates PA (2007) Transmission of *Leishmania* metacyclic promastigotes by phlebotomine sand flies. *International Journal of Parasitology* **37(10):** 1097-1106

Bates PA (2008) *Leishmania* sand fly interaction: progress and challenges. *Current Opinion on Microbiology* **11(4):** 340-344

Beachy SH, Repasky EA (2011) Toward establishment of temperature thresholds for immunological impact of heat exposure in humans. *International Journal of Hyperthermia* **27:** 344–352

Bello AR, Nare B, Freedman D, Hardy L, Beverley SM (1994) PTR1: a reductase mediating salvage of oxidized pteridines and methotrexate resistance in the protozoan parasite *Leishmania major*. *Proceedings of the National Academy of Sciences of the United States of America* **91:** 11442–11446

Ben Salah A, Buffet PA, Morizot G, Ben Massoud N, Zaatour A, Ben Alaya N, et al (2009) WR279,396, a third generation aminoglycoside ointment for the treatment of *Leishmania major* cutaneous leishmaniasis: a phase 2, randomized, double blind, placebo controlled study. *PLoS Neglected Tropical Diseases* **3:** e432

Berens RL, Deutsch-King LC, Marr JJ (1980) *Leishmania donovani* and *Leishmania braziliensis*: hexokinase, glucose-6-phosphate dehydrogenase, and pentose phosphate shunt activity. *Experimental Parasitology* **49(1):** 1-8

Berman JD (1997) Human leishmaniasis: clinical, diagnostic, and chemotherapeutic developments in the last 10 years. *Clinic Infectious Diseases* **24:** 684-703

Berman JD, Goad LJ, Beach DH, Holz GG Jr (1986) Effects of ketoconazole on sterol biosynthesis by *Leishmania mexicana* amastigotes in murine macrophage tumor cells. *Molecular Biochemical Parasitology* **20:** 85-92

Berman JJ (2008) Treatment of leishmaniasis with miltefosine: 2008 status. *Expert Opinion on Drug Metabolism and Toxicology* **4:** 1209-1216

Bern C, Adler-Moore J, Berenguer J, Boelaert M, den Boer M, Davidson RN, et al. (2006) Liposomal amphotericin B for the treatment of visceral leishmaniasis. *Clinic Infectious Diseases* **43:** 917-924

Berriman M, Ghedin E, Hertz-Fowler C, Blandin G, Renauld H, Bartholomeu DC et al. (2005) The genome of the African trypanosome *Trypanosoma brucei*. *Science* **309:** 416-422

Bertello LE, Goncalvez MF, Colli W, de Lederkremer RM. (1995) Structural analysis of inositol phospholipids from *Trypanosoma cruzi* epimastigote forms. *The Biochemical Journal* **310:** 255-61

Besteiro S, Williams RA, Morrison LS, Coombs GH, Mottram JC (2006) Endosome sorting and autophagy are essential for differentiation and virulence of *Leishmania major. Journal of Biological Chemistry* **281(16):** 11384-11396

Besteiro S, Williams RAM, Coombs GH, Mottram JC (2007) Protein turnover and differentiation in *Leishmania. International Journal of Parasitology* **37:** 1063-1075

Beverley SM (2003) Protozomics: trypanosomatid parasite genetics comes of age. *Nature Reviews Genetics* **4:** 11-19

Bhandari V, Sundar S, Dujardin JC, Salotra P (2014) Elucidation of Cellular Mechanisms Involved in Experimental Paromomycin Resistance in *Leishmania donovani. Antimicrobial Agents and Chemotherapy* **58(5):** 2580-2585

Bhattacharyya S, Ghosh S, Jhonson PL, Bhattacharya SK, Majumdar S (2001) Immunomodulatory role of interleukin-10 in visceral leishmaniasis: defective activation of protein kinase C-mediated signal transduction events. Infection and Immunity **69:** 1499-1507

Bhattacharya SK, Sinha PK, Sundar S, Thakur CP, Jha TK, Pandey K, Das VR, et al. (2007) Phase 4 trial of miltefosine for the treatment of Indian visceral leishmaniasis. *Journal of Infectious Diseases* **196:** 591-598

Bifeld E, Clos J (2015) The genetics of *Leishmania* virulence. *Medicinal Microbiological Immunology* **204(6):** 619-634

Blaise M, Frechin M, Olieric V, Charron C, Sauter C, Lorber B, et al. (2011) Crystal structure of the archaeal asparagine synthetase: interrelation with aspartyl-tRNA and asparaginyl-tRNA synthetases. *Journal of molecular biology* **412:** 437-452

Blangy D, Buc H, Monod J (1968) Kinetics of the allosteric interactions of phosphofructokinase from *Escherichia coli*. *Journal of molecular biology* **31:** 13-35

Boehlein SK, Richards NG, Schuster SM (1994) Glutamine-dependent nitrogen transfer in *Escherichia coli* asparagine synthetase B. Searching for the catalytic triad. *The Journal of biological chemistry* **269:** 7450-7457

Boehlein SK, Stewart JD, Walworth ES, Thirumoorthy R, Richards NG, Schuster SM (1998) Kinetic mechanism of *Escherichia coli* asparagine synthetase B. *Biochemistry* **37:** 13230-13238

Bogdan C, Donhauser N, Doring R, Rollinghoff M, Diefenbach A, Rittig MG (2000) Fibroblasts as host cells in latent leishmaniasis. *Journal of Experimental Medicine* **191(12):** 2121-30

Boucher N, Wu Y, Dumas C, Dube M, Sereno D, Breton M, Papadopoulou B (2002) A common mechanism of stage-regulated gene expression in *Leishmania* mediated by a conserved 3'-untranslated region element. *The Journal of biological chemistry* **277:** 19511-19520

Bour T, Akaddar A, Lorber B, Blais S, Balg C, Candolfi E, et al. (2009) Plasmodial aspartyl-tRNA synthetases and peculiarities in *Plasmodium falciparum*. *The Journal of biological chemistry* **284:** 18893-18903

Boyce JD, Wilkie I, Harper M, Paustian ML, Kapur V, Adler B (2002) Genomic scale analysis of *Pasteurella multocida* gene expression during growth within the natural chicken host. *Infection and Immunity* **70:** 6871-6879

Bray PG, Barrett MP, Ward SA, de Koning HP (2003) Pentamidine uptake and resistance in pathogenic protozoa: past, present and future. *Trends in Parasitology* **19:** 232-239

Brenchley R, Tariq H, McElhinney H, Szor B, Huxley-Jones J, Stevens R, et al. (2007) The TryTryp Phosphatome: analysis of the protein phosphatase catalytic domains. *BMC Genomics* **8:** 434

Brimacombe KR, Walsh MJ, Liu L, Vasquez-Valdivieso MG, Morgan HP, McNae I, et al. (2014) Identification of ML251, a Potent Inhibitor of *T. brucei* and *T. cruzi* Phosphofructokinase. *ACS medicinal chemistry letters* **5:** 12-17

Brittingham A, Miller MA, Donelson JE, Wilson ME (2001) Regulation of GP63 mRNA stability in promastigotes of virulent and attenuated *Leishmania chagasi*. *Molecular and Biochemical Parasitology* **112:** 51-59

Britto C, Ravel C, Bastien P, Blaineau C, Pages M, Dedet JP, et al. (1998) Conserved linkage groups associated with large-scale chromosomal rearrangements between Old World and New World *Leishmania* genomes. *Gene* 222: 107-117

Brotherton MC, Bourassa S, Légaré D, Poirier GG, Droit A, Ouellette M (2014) Quantitative proteomic analysis of amphotericin B resistance in *Leishmania infantum. International Journal of Parasitology: Drugs and Drug Resistance* **4:** 126-132

Bucheton B, Abel L, Kheir MM, Mirgani A, El-Safi SH, et al. (2003) Genetic control of visceral leishmaniasis in a Sudanese population: candidate gene testing indicates a linkage to the NRAMP1 region. *Genes and Immunity* **4:** 104-109

Bucheton B, Argiro L, Chevillard C, Marquet S, Kheir MM, et al. (2007) Identification of a novel G245R polymorphism in the IL-2 receptor beta membrane proximal domain associated with human visceral leishmaniasis. *Genes and Immunity* **8:** 79-83

Burchmore RJ, Barrett MP (2001) Life in vacuoles – nutrient acquisition by *Leishmania* amastigotes. *International Journal of Parasitology* **12:** 1311-1320

Caceres AJ, Michels PA, Hannaert V (2010) Genetic validation of aldolase and glyceraldehyde-3-phosphate dehydrogenase as drug targets in *Trypanosoma brucei*. *Molecular and biochemical parasitology* **169:** 50-54

Caffrey CR, Lima AP, Steverding D (2011) Cysteine peptidases of kinetoplastid parasites. *Advanced Experimental Medical Biology* **712:** 84-99

Callahan HL, Portal IF, Bensinger SJ, Grogl M (1996) *Leishmania* spp: temperature sensitivity of promastigotes *in vitro* as a model for tropism *in vivo*. *Experimental Parasitology* **84:** 400-409.

Calvo-Álvarez E, Stamatakis K, Punzón C, Álvarez-Velilla R, Tejería A, Escudero-Martínez JM, et al. (2015) Infrared fluorescent imaging as a potent tool for *in vitro*, *ex vivo* and *in vivo* models of visceral leishmaniasis. *PLoS Neglected Tropical Diseases* **9(3):** e0003666

Carrillo C, Canepa GE, Algranati ID, Pereira CA (2006) Molecular and functional characterization of a spermidine transporter (TcPAT12) from *Trypanosoma cruzi*. *Biochemical and Biophysical Research Communication* **344:** 936-940

Cavazzuti A, Paglietti G, Hunter WN, Gamarro F, Piras S, Loriga M, et al. (2008) Discovery of potent pteridine reductase inhibitors to guide antiparasite drug development. *Proceedings of the National Academy of Sciences of the United States of America* **105:** 1448-1453

Cecílio P, Pérez-Cabezas B, Santarém N, Maciel J, Rodrigues V, Cordeiro-da-Silva A (2014) Deception and manipulation: the arms of *Leishmania*, a successful parasite. *Frontiers in Immunology* **5:** 480

Cedar H, Schwartz JH (1969a) The asparagine synthetase of *Escherichia coli*. I. Biosynthetic role of the enzyme, purification, and characterization of the reaction products. *Journal of Biological Chemistry* **244:** 4112–4121

Cedar H, Schwartz JH (1969b) The asparagine synthetase of *Escherichia coli*. II. Studies on mechanism. *Journal of Biological Chemistry* **244:** 4122-4127

Chakravarty J and Sundar S (2010) Drug resistance in Leishmaniasis. *Clinical Microbiology Reviews* **19(1):** 111-126

Chamtranupong L, Wolfson RL, Sabatini DM (2015) Nutrient-sensing mechanisms across evolution. *Cell* 161: 67-83

Chappuis F, Rijal S, Soto A, Menten J, Boelaert M (2006) A meta-analysis of the diagnostic performance of the direct agglutination test and rK39 dipstick for visceral leishmaniasis. *BMJ* **333:** 723

Chappuis F, Sundar S, Hailu A, Ghalib H, Rijal S, Peeling RW, et al. (2007) Visceral leishmaniasis: what are the needs for diagnosis, treatment and control? *Nature Reviews Microbiology* **5(11):** 873-882

Charest H, Matlashewski G (1994) Developmental gene expression in *Leishmania donovani*: differential cloning and analysis of an amastigote-stage specific gene. *Molecular Cell Biology* **14:** 2975-2984

Chargui N, Amro A, Haouas N, Schonian G, Babba H, Schmidt S, et al. (2009) Population structure of Tunisian *Leishmania infantum* and evidence for the existence of hybrids and gene flow between genetically different populations. *International Journal of Parasitology* **39:** 801-811

Chattopadhyay A, Jafurulla M (2012) Role of membrane cholesterol in leishmanial infection. *Advanced Experimental Medical Biology* **749:** 201-213

Chow C, Cloutier S, Dumas C, Chou M, Papadopoulou B (2011) Promastigote to amastigote differentiation of *Leishmania* is markedly delayed in the absence of PERK eIF2alpha kinase-dependent eIF2alpha phosphorylation. *Cellular Microbiology* **13:** 1059-1077

Ciou SC, Chou YT, Liu YL, Nieh YC, Lu JW, Huang SF et al. (2014) Ribose-5-phosphate isomerase A regulates hepatocarcinogenesis *via* PP2Aand ERK signalling. *International Journal of Cancer* **137:** 104-115

Ciustea M, Gutierrez JA, Abbatiello SE, Eyler JR, Richards NG (2005) Efficient expression, purification, and characterization of C-terminally tagged, recombinant human asparagine synthetase. *Archives of biochemistry and biophysics* **440:** 18-27

Clasquin MF, Melamud E, Singer A, Gooding JR, Xu X, Dong A, et al. (2011) Riboneogenesis in yeast. *Cell* **145(6):** 969-980

Claustre S, Denier C, Lakhdar-Ghazal F, Lougare A, Lopez C, Chevalier N, et al. (2002) Exploring the active site of *Trypanosoma brucei* phosphofructokinase by inhibition studies: specific irreversible inhibition. *Biochemistry* **41:** 10183-10193

Clayton CE (2002) Life without transcriptional control? From fly to man and back again. *EMBO Journal* **21:** 1881-1888

Cleland WW (1967) Enzyme kinetics. *Annual review of biochemistry* **36:** 77-112

Coelho AC, Messier N, Ouellette M, Cotrim PC (2007) Role of the ABC transporter PRP1 (ABCC7) in pentamidine resistance in *Leishmania* amastigotes. *Antimicrobial Agents and Chemotherapy* **51:** 3030-3032

Coley AF, Dodson HC, Morris MT, Morris JC (2011) Glycolysis in the african trypanosome: targeting enzymes and their subcellular compartments for therapeutic development. *Molecular biology international* **2011:** 123702

Colotti G, Ilari A (2011) Polyamine metabolism in *Leishmania*: from arginine to trypanothione. *Amino Acids* **40:** 269-285

Comini MA, Guerrero SA, Haile S, Menge U, Lunsdorf H, Flohe L (2004) Validation of *Trypanosoma brucei* trypanothione synthetase as drug target. *Free radical biology & medicine* **36:** 1289-1302

Comini MA, Ortíz C, Cazzulo JJ (2013) Drug Targets in Trypanosomal and Leishmanial Pentose Phosphate Pathway. In *Trypanosomatid Diseases: Molecular Routes to Drug Discovery*, Jäger T KO, Flohé L (ed), pp 297-313. Wiley-VCH Verlag GmbH & Co. KGaA, Weinheim, Germany.

Cordeiro AT, Thiemann OH, Michels PA (2009) Inhibition of *Trypanosoma brucei* glucose-6-phosphate dehydrogenase by human steroids and their effects on the viability of cultured parasites. *Bioorganic & medicinal chemistry* **17:** 2483-2489

Coustou V, Besteiro S, Biran M, Diolez P, Bouchaud V, Voisin P, et al. (2003) ATP generation in the *Trypanosoma brucei* procyclic form: cytosolic substrate level is essential, but not oxidative phosphorylation. *The Journal of biological chemistry* **278:** 49625-49635

Creek, DJ, Mazet, M, Achcar, F, Anderson, J, Kim, DH, Kamour, R et al. (2015) “Probing the Metabolic Network in Bloodstream-Form *Trypanosoma brucei* Using Untargeted Metabolomics with Stable Isotope Labelled Glucose. *PLoS Pathogens* **11(3):** e1004689

Croan DG, Morrison DA and Ellis JT (1997) Evolution of the genus *Leishmania* revealed by comparison of DNA and RNA polymerase gene sequences. *Molecular Biochemical Parasitology* **89(2):** 149-159

Croft SL (2008) PKDL – A drug related phenomenon? *Indian Journal of Medical Research* **128:** 10-11

Croft SL and Olliaro P (2011) Leishmaniasis chemotherapy: challenges and opportunities." *Clinical Microbiology and Infection* **10:** 1478-1483

Croft SL, Sundar S, Fairlamb AH (2006) Drug Resistance in Leishmaniasis. *Clinical Microbiology Reviews* **19(1):** 111-126

Cronin CN, Nolan DP, Voorheis HP (1989) The enzymes of the classical pentose phosphate pathway display differential activities in procyclic and bloodstream forms of *Trypanosoma brucei*. *FEBS Letters* **244:** 26-30

Cruz A, Beverley SM (1990) Gene replacement in parasitic protozoa. *Nature* **348:** 171-173

Cruz AK, Titus R, Beverley SM (1993) Plasticity in chromosome number and testing essential genes in *Leishmania* by targeting. *Proceedings of the National Academy of Sciences of the United States of America* **90:** 1599-1603

Cull B, Godinho JLP, Rodrigues JCF, Frank B, Schurigt U, Williams RAM et al. (2015) Glycosome turnover in *Leishmania major* is mediated by autophagy. *Autophagy* **12:** 2143-2157

Cunningham ML, Fairlamb AH (1995) Trypanothione reductase from *Leishmania donovani*: Purification, characterisation and inhibition by trivalent antimonials. *European Journal of Biochemistry* **230:** 460-468

Cunningham ML, Titus RG, Turco SJ, Beverley SM. (2001) Regulation of differentiation to the infective stage of the protozoan parasite *Leishmania major* by tetrahydrobiopterin. *Science* **292:** 285-287

Cupolillo E, Medina-Acosta E, Noyes H, Momen H and Grimaldi G Jr. (2000) A revised classification for *Leishmania* and *Endotrypanum*. *Parasitology Today* **16(4):** 142-144

Curnow AW, Tumbula DL, Pelaschier JT, Min B, Soll D (1998) Glutamyl-tRNA(Gln) amidotransferase in *Deinococcus radiodurans* may be confined to asparagine biosynthesis. *Proceedings of the National Academy of Sciences of the United States of America* **95:** 12838-12843

Cyrino LT, Araujo AP, Joazeiro PP, Vicente CP, Giorgio S. (2012) *In vivo* and *in vitro Leishmania amazonensis* infection induces autophagy in macrophages. *Tissue Cell* **44(6):** 401-408

da Cunha e Silva NL, Hasson-Voloch A, De Souza W (1989) Isolation and characterization of a highly purified flagellar membrane fraction from trypanosomatids. *Molecular Biochemical Parasitology* **37:** 129-36

Dacher M, Morales MA, Pescher P, Leclercq O, Rachidi N, Prina E, et al. (2014) Probing druggability and biological function of essential proteins in *Leishmania* combining facilitated null mutant and plasmid shuffle analyses. *Molecular Microbiology* **93(1):** 146-166

Damasceno JD, Beverley SM, Tosi RLO (2015) A transposon-based tool for transformation and mutagenesis in trypanosomatid protozoa. *Methods Molecular Biology* **1201:** 235-245

Dardonville C, Rinaldi E, Barrett MP, Brun R, Gilbert IH, Hanau S (2004) Selective inhibition of *Trypanosoma brucei* 6-phosphogluconate dehydrogenase by high-energy intermediate and transition-state analogues. *Journal of medicinal chemistry* **47:** 3427-3437

Darlyuk I, Goldman A, Roberts SC, Ullman B, Rentsch D, Zilberstein D (2009) Arginine homeostasis and transport in the human pathogen *Leishmania donovani*. *Journal of Biological Chemistry* **284:** 19800-19807

David CV and Craft N (2009) Cutaneous and mucocutaneous leishmaniasis. *Dermatological Therapy* **22(6):** 491-502

Davies CR, Llanos-Cuentas EA, Campos P, Monge J, Leon E, Canales J (2000) Spraying houses in the Peruvian Andes with lambda-cyhalothrin protects residents against cutaneous

leishmaniasis. *Transactions of the Royal Society of Tropical Medicine and Hygiene* 94: 631-636

de A S Navarro MV, Gomes Dias SM, Mello LV, da Silva Giotto MT, Gavalda S, Blonski C, et al. (2007) Structural flexibility in *Trypanosoma brucei* enolase revealed by X-ray crystallography and molecular dynamics. *The FEBS journal* **274:** 5077-5089

De Doncker S, Hutse V, Abdellati S, Rijal S, Singh Karki BM, Decuypere S, et al. (2005) A new PCR-ELISA for diagnosis of visceral leishmaniasis in blood of HIV-negative subjects. *Transactions of the Royal Society of Tropical Medicine and Hygiene* **99:** 25-31

de Ibarra AA, Howard JG, Snary D (1982) Monoclonal antibodies to *Leishmania tropica major*: specificities and antigen location. *Parasitology* **85(Pt 3):** 523-531

De Koning HP (2001) Uptake of pentamidine in *Trypanosoma brucei brucei* is mediated by three distinct transporters: implications for cross-resistance with arsenicals. Molecular Pharmacology **59:** 586-592

De Menezes JPB, Guedes CES, Peterson ALOA, Fraga DBM, Veras PST (2015) Advances in develoment of new treatment for leishmaniasis. *Biomedical Research International* **2015:** 815023

De Trez C, Magez S, Akira S, Ryffel B, Carlier Y, et al. (2009) iNOS-producing inflammatory dendritic cells constitute the major infected cell type during the chronic *Leishmania major* infection phase of C57BL/6 resistant mice. *PLoS Pathogens* **5:** e1000494

Demicheli C, Frezard F, Mangrum JB, Farrell NP (2008) Interaction of trivalent antimony with a CCHC zinc finger domain: potential relevance to the mechanism of action of antimonial drugs. *Chemical Communications (Camb)* **39:** 4828-4830

Denton H, McGregor JC, Coombs GH (2004) Reduction of anti-leishmanial pentavalent antimonial drugs by a parasite-specific thiol-dependent reductase, TDR1. *Biochemical Journal* **381:** 405-412

Descoteaux, A, Moradin, N, Arango Duque G (2013) *Leishmania* dices away cholesterol for survival.” *Cell Host and Microbe* **13(3):** 245-247

Desjeux P, Alvar J (2003) *Leishmania*/HIV co-infections: epidemiology in Europe. *Annual Tropical Medical Parasitology* **97(Suppl 1):** 3-15

Diaz-Gandarilla JA, Osorio-Trujillo C, Hernandez-Ramirez VI, TalamasRohana P (2013) PPAR activation induces M1 macrophage polarization via cPLA(2)- COX-2 inhibition, activating ROS production against *Leishmania mexicana*. *Biomedical Research International* **2013:** 215283

Djikeng A, Shi H, Tschudi C, Ullu E (2001) RNA interference in *Trypanosoma brucei*: cloning of small interfering RNAs provides evidence for retroposon-derived 24-26-nucleotide RNAs. *RNA* **7:** 1522-1530

dos Santos Ferreira C, de Castro Pimenta AM, Demicheli C, Frezard F (2006) Characterization of reactions of antimoniate and meglumine antimoniate with a guanine ribonucleoside at different pH. *Biometals* 19: 573-581

Docampo R, Scott DA, Vercesi AE, Moreno SN. (1995) Intracellular Ca2+ storage in acidocalcisomes of *Trypanosoma cruzi*. *Biochemical Journal* **310:** 1005-1012

Dostalova A and Volf P (2012) *Leishmania* development in sand flies: parasite-vector interactions overview. *Parasites & Vectors* **5**: 276

Dow LE, Fisher J, O'Rourke KP, Muley A, Kastenhuber ER, Livshits G et al. (2015) Inducible *in vivo* genome editing with CRISPR-Cas9. *Nature Biotechnology*, **33(4):** 390-394

Drew ME, Langford CK, Klamo EM, Russell DG, Kavanaugh MP, Landfear SM. (1995) Functional expression of a myo-inositol/H+ symporter from *Leishmania donovani*. *Molecular and Cellular Biology* **15:** 5508-15

Drew ME, Morris JC, Wang Z, Wells L, Sanchez M, Landfear SM, et al. (2003) The adenosine analogue tubercidin inhibits glycolysis in *Trypanosoma brucei* as revealed by an RNA interference library. *The Journal of Biological Chemistry* **278:** 46596-46600

Dridi L, Ouameur AA, Ouellette M (2010) The high affinity S-Adenosylmethionine plasma membrane transporter of *Leishmania* is a member of the folate biopternin transporter (FBT) family. *The Journal of Biological Chemistry* **285(26):** 19767-19775

Duclert-Savatier N, Poggi L, Miclet E, Lopes P, Quazzani J, Chevalier N, et al. (2009) Insights into the enzymatic mechanism of 6-phosphogluconolactonase from *Trypanosoma brucei* using structural data and molecular dynamics simulation. *Journal of Molecular Biology* **388(5):** 1009-1021

Duffieux F, Van Roy J, Michels PA, Opperdoes FR (2000) Molecular characterization of the first two enzymes of the pentose-phosphate pathway of *Trypanosoma brucei*. Glucose-6-phosphate dehydrogenase and 6-phosphogluconolactonase. *The Journal of biological chemistry* **275:** 27559-27565

Dufour E, Gay F, Aguera K, Scoazec JY, Horand F, Lorenzi PL, et al.(2012) Pancreatic tumor sensitivity to plasma L-asparagine starvation. *Pancreas* **41:** 940-948

Dumas C, Ouellette M, Tovar J, Cunningham ML, Fairlamb AH, Tamar S, et al. (1997) Disruption of the trypanothione reductase gene of *Leishmania* decreases its ability to survive oxidative stress in macrophages. *EMBO Journal* 16: 2590-2598

Durand-Dubief M, and Bastin P (2003) TbAGO1, an Argonaute protein required for RNA interference, is involved in mitosis and chromosome segregation in *Trypanosoma brucei*. *BMC Biology* **1:** 2

Eastman RT, Buckner FS, Yokoyama K, Gelb MH, Van Voorhis WC (2006) Thematic review series: lipid posttranslational modifications. Fighting parasitic disease by blocking protein farnesylation. *Journal of lipid research* **47:** 233-240

Eberle C, Lauber BS, Fankhauser D, Kaiser M, Brun R, Krauth-Siegel RL, et al. (2011) Improved inhibitors of trypanothione reductase by combination of motifs: synthesis, inhibitory potency, binding mode, and antiprotozoal activities. *ChemMedChem* **6:** 292-301

Ebikeme C (2007) Amino Acid Transporters & Amino Acid Metabolism in *Trypanosoma brucei* brucei. Doctor of Philosophy Thesis, Division of Infection & Immunity Faculty of Biomedical & Life Sciences-University of Glasgow

Elias MC, Cunha JPC, de Faria FP, Mortara RA, Freymüller E, and Schenkman S (2007) Morphological events during the *Trypanosoma cruzi* cell cycle. *Protist* **158:** 147-157

El-Sayed NM, Myler PJ, Blandin G, Berriman M, Crabtree J, Aggarwal G, et al. (2005) Comparative genomics of trypanosomatid parasitic protozoa. *Science* **309:** 404-409

Erben ED, Fadda A, Lueong S, Hoheisel J, Clayton C (2014) A genome-wide tethering screen reveals novel potential post-transcriptional regulators in *Trypanosoma brucei. PLoS Pathogens* **10(6):** e1004178

Estévez AM and Simpson L (1999) Uridine insertion/deletion RNA editing in trypanosome mitochondria—a review. *Gene* **240:** 247-260

Fadok VA, Bratton DL, Konowal A, Freed PW, Westcott JY, Henson PM (1998) Macrophages that have ingested apoptotic cells *in vitro* inhibit proinflammatory cytokine production through autocrine/paracrine mechanisms involving TGF-beta, PGE2, and PAF. Journal of Clinical Investigation **101(4):** 890-898

Fairlamb AH, Henderson GB, Cerami A (1989) Trypanothione is the primary target for arsenical drugs against African trypanosomes. *Proceedings of the National Academy of Sciences of the United States of America* **86:** 2607-2611

Faria J, Loureiro I, Santarem N, Cecílio P, Macedo-Ribeiro S, Tavares J, et al. (2015a) Disclosing Ribose-5-Phosphate Isomerase B Essentiality in Trypanosomatids. (*submitted*);

Faria J, Loureiro I, Santarem N, Macedo-Ribeiro S, Tavares J, Cordeiro-da-Silva A (2015b) *Leishmania infantum* Asparagine Synthetase A Is Dispensable for Parasites Survival and Infectivity. *PLoS Neglected Tropical Diseases in press*

Faria J, Moraes CB, Song R, Pascoalino BS, Lee N, Siqueira-Neto JL, et al. (2015c) Drug discovery for human African trypanosomiasis: identification of novel scaffolds by the newly developed HTS/Sybr Green assay for *Trypanosoma brucei*. *Journal of Biomolecular Screening* **20(1):** 70-81

Faria MS, Reis FCG, Azevedo-Pereira RL, Morrison LS, Mottram JC, Lima AP (2011) *Leishmania* inhibitor of serine peptidase 2 prevents TLR4 activation by neutrophil elastase promoting parasite survival in murine macrophages. Journal of Immunology **186:** 411-422

Farr H and Gull K (2009) Functional studies of an evolutionarily conserved, cytochrome *b*5 domain protein reveal a specific role in axonemal organisation and the general phenomenon of post-division axonemal growth in trypanosomes. *Cell Motility and Cytoskeleton* **66:** 24-35

Feng X, Feistel T, Buffalo C, McCormack A, Kruvand E, Rodriguez-Contreras D, et al. (2011) Remodelling of protein and mRNA expression in *Leishmania mexicana* induced by deletion of glucose transporter genes. *Molecular Biochemical Parasitology* **175(1):** 39-48

Ferguson MA. (1997) The surface glycoconjugates of trypanosomatid parasites. *Philosophical Transactions of the Royal Society of London Series B, Biological Sciences* **352:** 1295-1302

Ferguson MA, Cross GA (1984) Myristylation of the membrane form of a *Trypanosoma brucei* variant surface glycoprotein. *The Journal of Biological Chemistry* **259:** 3011-3015

Ferguson MA, Homans SW, Dwek RA, Rademacher TW (1988) Glycosyl-phosphatidylinositol moiety that anchors *Trypanosoma brucei* variant surface glycoprotein to the membrane. *Science* **239:** 753-759

Fernandes AP, Coelho EA, Machado-Coelho GL, Grimaldi GJ, Gazzinelli RT (2012) Making an anti-amastigote vaccine for visceral leishmaniasis: rational, update and perspectives. *Current Opinion in Microbiology* **15:** 476-485

Ferreira Cdos S, Martins PS, Demicheli C, Brochu C, Ouellette M, Frezard F (2003) Thiol induced reduction of antimony(V) into antimony(III): a comparative study with trypanothione, cysteinyl-glycine, cysteine and glutathione. *Biometals* **16:** 441-446

Field MC and Carrington M (2009) The trypanosome flagellar pocket. *Nature Reviews Microbiology* **7(11):** 775-786

Flohe L (2012) The trypanothione system and its implications in the therapy of trypanosomatid diseases. *International journal of medical microbiology: IJMM* **302:** 216-220

Forestier CL, Machu C, Loussert C, Pescher P, Spath GF (2011) Imaging host cell-*Leishmania* interaction dynamics implicates parasite motility, lysosome recruitment, and host cell wounding in the infection process. *Cell Host Microbe* **9(4):** 319-330

Frade AF, de Oliveira LC, Costa DL, Costa CHN, Aquino D, Van Weyenbergh J, et al. (2011) TGFB1 and IL8 gene polymorphisms and susceptibility to visceral leishmaniasis. *Infection, Genetics and Evolution* **11:** 912-916

Frearson JA, Brand S, McElroy SP, Cleghorn LA, Smid O, Stojanovski L, et al. (2010) N-myristoyltransferase inhibitors as new leads to treat sleeping sickness. *Nature* **464:** 728-732

Frezard F, Demicheli C, Ribeiro RR (2009) Pentavalent antimonials: new perspectives for old drugs. *Molecules* **14:** 2317-2336

Fyfe PK, Oza SL, Fairlamb AH, Hunter WN (2008) *Leishmania* trypanothione synthetase-amidase structure reveals a basis for regulation of conflicting synthetic and hydrolytic activities. *The Journal of Biological Chemistry* **283:** 17672-17680

Gamarro F, Yu PL, Zhao J, Edman U, Greene PJ, Santi D (1995) *Trypanosoma brucei* dihydrofolate reductase-thymidylate synthase: gene isolation and expression and characterization of the enzyme. *Molecular and biochemical parasitology* **72:** 11-22

Garg M, Goyal N (2015) MAPK1 of *Leishmania donovani* modulates antimony susceptibility by down regulating P-glycoprotein efflux pumps. *Antimicrobial Agents and Chemotherapy* **59(7):** 3853-3863

Gaufichon L, Masclaux-Daubresse C, Tcherkez G, Reisdorf-Cren M, Sakakibara Y, Hase T, et al. (2013) *Arabidopsis thaliana* ASN2 encoding asparagine synthetase is involved in the control of nitrogen assimilation and export during vegetative growth. *Plant, cell & environment* **36:** 328-342

Gautam S, Kumar R, Maurya R, Nylen S, Ansari N, Rai M, et al. (2011) IL-10 neutralization promotes parasite clearance in splenic aspirate cells from patients with visceral leishmaniasis. *Journal of Infectious Diseases* **204(7):** 1134-1137

Genest PA, ter Riet B, Dumas C, Papadopoulou B, van Luenen HGAM and Borst P (2005) Formation of linear inverted repeat amplicons following targeting of an essential gene in *Leishmania*. *Nucleic Acids Research* **33:** 1699-1709

Gesbert G, Ramond E, Rigard M, Frapy E, Dupuis M, Dubail I, et al. (2014) Asparagine assimilation is critical for intracellular replication and dissemination of *Francisella*. *Cellular Microbiology* **16:** 434-449

Ghedin E, Zhang WW, Charest H, Sundar S, Kenney RT, et al. (1997) Antibody response against a *Leishmania donovani* amastigote-stage-specific protein in patients with visceral leishmaniasis. *Clinical and Diagnostic Laboratory Immunology* **4:** 530-535

Ghosh AK, Sardar AH, Mandal A, Saini S, Abhishek K, Kumar A et al. (2015) Metabolic reconfiguration of the central glucose metabolism: A crucial strategy of *Leishmania donovani* for its survival during oxidative stress. *FASEB Journal* **29(5):** 2081-2098

Gilinger G, Bellofatto V (2001) Trypanosome spliced leader RNA genes contain the first identified RNA polymerase II gene promoter in these organisms. *Nucleic Acids Research* **29:** 1556-1564

Ginger ML, Fairlamb AH & Opperdoes FR (2007) Comparative genomics of trypanosome metabolism. In *Trypanosomes: after the genome*, JD Barry JM, R McCulloch & A Acosta-Serrano (ed), pp 373-417. London: Horizon Bioscience

Glover L, Alsford S, Baker N, Turner DJ, Sanchez-Flores A, Hutchinson S et al. (2015) Genome-scale RNAi screens for high-throughput phenotyping in bloodstream-form African trypanosomes. *Nature Protocols* **10(1):** 106-133

Gluenz E, Hoog JL, Smith AE, Dawe HR, Shaw MK, Gull K (2010) Beyond 9+0: noncanonical axoneme structures characterize sensory cilia from protists to humans. *FASEB Journal* **24(9):** 3117-3121

Gomes R, Teixeira C, Teixeira MJ, Oliveira F, Menezes MJ, et al. (2008) Immunity to a salivary protein of a sand fly vector protects against the fatal outcome of visceral leishmaniasis in a hamster model. *Proceedings of the National Academy of Sciences of the United States of America* **105:** 7845-7850

González NS, Ceriani C, Algranati ID (1992) Differential regulation of putrescine uptake in *Trypanosoma cruzi* and other trypanosomatids. *Biochemical and Biophysical Research Communications* **188:** 120-128

Gonzalez-Salgado A, Steinmann ME, Greganova E, Rauch M, Mäser P, Sigel E, et al. (2012) myoInositol uptake is essential for bulk inositol phospholipid but not glycosylphosphatidylinositol synthesis in *Trypanosoma brucei*. *The Journal of Biological Chemistry* **287:** 13313-23

Gosline SJC, Nascimento M, McCall LI, Zilberstein D, Thomas DY, et al. (2011) Intracellular eukaryotic parasites have a distinct unfolded protein response. *PLoS ONE* **6:** e19118

Gott JM, and Emeson RB (2000) Functions and mechanisms of RNA editing. *Annual Review Genetics* **34:** 499-531

Gourbal B, Sonuc N, Bhattacharjee H, Legare D, Sundar S, Ouellette M, et al. (2004) Drug uptake and modulation of drug resistance in *Leishmania* by an aquaglyceroporin. *The Journal of Biological Chemistry* **279:** 31010-31017

Gourley DG, Schuttelkopf AW, Leonard GA, Luba J, Hardy LW, Beverley SM, et al. (2001) Pteridine reductase mechanism correlates pterin metabolism with drug resistance in trypanosomatid parasites. *Nature Structural Biology* **8:** 521-525

Gouzy A, Larrouy-Maumus G, Bottai D, Levillain F, Dumas A, Wallach JB, et al. (2014) *Mycobacterium tuberculosis* exploits asparagine to assimilate nitrogen and resists stress during infection. *PLoS Pathogens* **10:** e1003928

Gowri VS, Ghosh I, Sharma A, Madhubala R (2012) Unusual domain architecture of aminoacyl tRNA synthetases and their paralogs from *Leishmania major*. *BMC genomics* **13:** 621

Gradoni L (2015) Canine Leishmania vaccines: still a long way to go. *Veterinary Parasitology* **208:** 94-100

Graf FE, Baker N, Munday JC, de Koning HP, Horn D, Maser P (2015) Chimerization at the AQP2-AQP3 locus is the genetic basis of melarsoprol-pentamidine cross-resistance in

clinical *Trypanosoma brucei gambiense* isolates. *International Journal of Parasitology Drugs and Drug Resistance* **5(2):** 65-68

Gramiccia M (2003) The identification and variability of the parasites causing leishmaniasis in HIV-positive patients in Italy. *Annual Tropical Medical Parasitology* **97:** 65-73

Gramiccia M, Gradoni L (2005) The current status of zoonotic leishmaniases and approaches to disease control. *International Journal of Parasitology* **35:** 1169-1180

Griffin JE, Gawronski JD, Dejesus MA, Ioerger TR., Akerley BJ, Sassetti CM (2011) High-resolution phenotypic profiling defines genes essential for mycobacterial growth and cholesterol catabolism. *PLoS Pathogens* **7:** e1002251

Grondin K, Roy G, Ouellette M (1996) Formation of extrachromosomal circular amplicons with direct or inverted duplications in drug-resistant *Leishmania tarentolae. Molecular Cell Biology* **16:** 3587-3595

Gualdrón-López M, Michels PAM, Quiñones W, Cáceres AJ, Avilán L, Concepción JL (2013) Drug Targets in Trypanosomal and Leishmanial Pentose Phosphate Pathway. In *Trypanosomatid Diseases: Molecular Routes to Drug Discovery*, Jäger T KO, Flohé L (ed), pp 297-313. Wiley-VCH Verlag GmbH & Co. KGaA, Weinheim, Germany

Guerra JA, Prestes SR, Silveira H, Coelho LI, Gama P, Moura A, et al. (2011) Mucosal Leishmaniasis caused by *Leishmania* (*Viannia*) *braziliensis* and *Leishmania* (*Viannia*) *guynensis* in the Brazilian Amazon. *PLoS Neglected Tropical Diseases* **5:** e980

Gupta S, Igoillo-Esteve M, Michels PA, Cordeiro AT (2011) Glucose-6-phosphate dehydrogenase of trypanosomatids: characterization, target validation, and drug discovery. *Molecular Biology International* **2011:** 135701

Gutiérrez V, Seabra AB, Reguera RM, Khandare J, Caldéron M (2015) New approaches from nanomedecine for treating leishmaniasis. *Chemical Society Reviews* **45(1):** 152-168

Haanstra JR, van Tuijl A, Kessler P, Reijnders W, Michels PAM, Westerhoff HV et al. (2008) Compartmentation prevents a lethal turbo-explosion of glycolysis in trypanosomes.

Proceedings of the National Academy of Sciences of the United States of America **105 (46):** 17718-17723

Hannaert V, Bringaud F, Opperdoes FR, Michels PA (2003) Evolution of energy metabolism and its compartmentation in Kinetoplastida. *Kinetoplastid biology and disease* **2:** 11

Hart DT, Coombs GH (1982) *Leishmania mexicana*: energy metabolism of amastigotes and promastigotes. *Experimental Parasitology* **54:** 397-409

Hartley MA, Ronet C, Zangger H, Beverley SM and Fasel N (2012) *Leishmania* RNA virus: when the host pays the toll. *Frontiers in Cell Infection and Microbiology* **2**: 99

Hasne MP, Ullman B (2005) Identification and characterization of a polyamine permease from the protozoan parasite *Leishmania major*. *The Journal of Biological Chemistry* **280:** 1518815194

Hassell AM, An G, Bledsoe RK, Bynum JM, Carter HL, Deng SJ, et al (2007) Crystallization of protein-ligand complexes. *Acta crystallographica Section D, Biological crystallography* **63:** 72-79

Heby, O, Persson, L., Rentala, M (2007) Targeting the polyamine biosynthetic enzymes: a promising approach to therapy of African sleeping sickness, Chagas' disease, and leishmaniasis. *Amino Acids* **33:** 359-366

Heise N, Opperdoes FR (1999) Purification, localisation and characterisation of glucose-6-phosphate dehydrogenase of *Trypanosoma brucei*. *Molecular and biochemical parasitology* **99:** 21-32

Helfert S, Estevez AM, Bakker B, Michels P, Clayton C (2001) Roles of triosephosphate isomerase and aerobic metabolism in *Trypanosoma brucei*. *The Biochemical journal* **357:** 117-125

Herwaldt BL (1999) Leishmaniasis. *Lancet* **354:** 1191-1199

Hofreuter D, Novik V, Galan JE (2008) Metabolic diversity in *Campylobacter jejuni* enhances specific tissue colonization. *Cell Host Microbe* **4:** 425-433

Horiguchi M, Koyanagi S, Okamoto A, Suzuki SO, Matsunaga M, and Ohdo S (2012) Stress regulated transcription factor ATF4 promotes neoplastic transformation by suppressing expression of the INK4a/ARF cell senescence factors. *Cancer Research* **72:** 395-401

Hsu PD, Lander ES, Zhang F (2014) Development and applications of CRISPR-Cas9 for genome engineering. *Cell* **157:** 1262-1278

Hübel A, Brandau S, Dresel A, Clos J (1995) A member of the ClpB family of stress proteins is expressed during heat shock in *Leishmania* spp. *Molecular Biochemical Parasitology* **70(1-2):** 107-118

Huck JH, Verhoeven NM, Struys EA, Salomons GS, Jakobs C, van der Knaap MS (2004) Ribose-5-phosphate deficiency: new inborn error in the pentose phosphate pathway associated with a slow progressive leukoencephalopathy. *American Journal of Human Genetics* **74:** 745-751

Humbert R, Simoni RD (1980) Genetic and biomedical studies demonstrating a second gene coding for asparagine synthetase in *Escherichia coli*. *Journal of Bacteriology* **142:** 212-220

Ivens AC, Peacock CS, Worthey EA, Murphy L, Aggarwal G, Berriman M, et al. (2005) The genome of the kinetoplastid parasite*, Leishmania major*. *Science* **309:** 436-442

Jackson AP (2007) Origins of amino acid transporter loci in trypanosomatid parasites. *BMC Evolutionary Biology* **7:** 26

Jacobs RT, Nare B, Phillips MA (2011) State of the Art in African Trypanosome Drug Discovery. *Current Tropical Medicinal Chemistry* **11(10):** 1255-1274

Jamdhade MD, Pawar H, Chavan S, Sathe G, Umasankar PK, Mahale KN (2015) Comprehensive proteomic analysis of glycosomes from *Leishmania donovani*. *Journal of Integrative Biology* **19(3):** 157-169

Janzen CJ, van Deursen F, Shi H, Cross GAM, Matthews KR, Ullu E (2006) Expression site silencing and life cycle progression appear normal in Argonaute1-deficient *Trypanosoma brucei*. *Molecular Biochemical Parasitology* **14:** 102-107

Jaramillo M, Gomez MA, Larsson O, Shio MT, Topisirovic I, Contreras, I et al. (2011) *Leishmania* repression of host translation through mTOR cleavage is required for parasite survival and infection. Cell Host Microbe **9:** 331-341

Jha TK (1983) Evaluation of diamidine compound (pentamidine isethionate) in the treatment resistant cases of kala-azar occurring in North Bihar, India. *Transactions of the Royal Society of Tropical Medicine and Hygiene* **77:** 167-170

Jhingran A, Chawla B, Saxena S, Barrett MP, Madhubala R (2009) Paromomycin: uptake and resistance in *Leishmania donovani*. *Molecular and Biochemical Parasitology* **164:** 111-117

Jiang Y, Roberts SC, Jardim A, Carter NS, Shih S, Ariyanayagam M, et al. (1999) Ornithine decarboxylase gene deletion mutants of *Leishmania donovani*. *The Journal of Biological Chemistry* **274:** 3781-3788

Jones SM, Urch JE, Brun R, Harwood JL, Berry C, Gilbert IH (2004) Analogues of thiolactomycin as potential anti-malarial and anti-trypanosomal agents. *Bioorganic & Medicinal Chemistry* **12:** 683-92

Jones SM, Urch JE, Kaiser M, Brun R, Harwood JL, Berry C, et al. (2005) Analogues of thiolactomycin as potential antimalarial agents. *Journal of Medicinal Chemistry* **48:** 5932-5941

Kabashima T, Kawaguchi T, Wadzinski BE, Uyeda K (2003) Xylulose 5-phosphate mediates glucose-induced lipogenesis by xylulose 5-phosphate-activated protein phosphatase in rat liver. *Proceedings of the National Academy of Sciences of the United States of America* **100:** 5107-5112

Kalidas S, Cestari I, Monnerat S, Li Q, Regmi S, Hasle N, et al. (2014) Genetic validation of aminoacyl-tRNA synthetases as drug targets in *Trypanosoma brucei*. *Eukaryotic cell* **13:** 504-516.

Kandpal M, Tekwani BL (1997) Polyamine transport systems of *Leishmania donovani* promastigotes. *Life Sciences* **60:** 1793-1801

Kaneshiro ES, Jayasimhulu K, Lester RL (1986) Characterization of inositol lipids from *Leishmania donovani* promastigotes: identification of an inositol sphingophospholipid. *Journal of Lipid Research* **27:** 1294-1303

Kang S, Hong HS (2008) RNA interference in infectious tropical diseases. *Korean Journal of Parasitology* **46(1):** 1-15

Karplus TM, Jeronimo SMB, Chang H, Helms BK, Burns TL, et al. (2002) Association between the tumor necrosis factor locus and the clinical outcome of *Leishmania chagasi* infection. *Infection and Immunity* **70:** 6919-6925

Kaur PK, Dinesh N, Soumya N, Babu NK, Singh S (2012) Identification and characterization of a novel ribose-5-phosphate isomerase B from *Leishmania donovani*. *Biochemical and Biophysical Research Communications* **421:** 51-56

Kaye P, Scott P (2011) Leishmaniasis: complexity at the host-pathogen interface. *Nature Reviews Microbiology* **9:** 604-615

Kedzierski L (2010) Leishmaniasis vaccine: where are we today? *Journal of Global Infectious Diseases* **2:** 177-185

Keller TH, Shi P-Y, Wang Q-Y (2011) Anti-infectives: can cellular screening deliver? *Current Opinion on Chemical Biology* **15:** 529-533

Kerkhoven EJ, Achcar F, Alibu VP, Burchmore RJ, Gilberts IH, Trybilo M et al. (2013) Handling Uncertainty in Dynamic Models: The Pentose Phosphate Pathway in *Trypanosoma brucei*. *PLoS Computational Biology* **9(12):** e1003371

Khow O, Suntrarachun S (2012) Strategies for production of active eukaryotic proteins in bacterial expression system. *Asian Pacific journal of tropical biomedicine* **2:** 159-162

Kim H, Li Z, Boothroyd C, Cross GAM (2013) Strategies to construct null and conditional null *Trypanosoma brucei* mutants using Cre-recombinase and loxP. *Molecular Biochemical Parasitology* **191(1):** 16-19

Kolev NG, Tschudi C, Ullu E (2011) RNA interference in protozoan parasites: achievements and challenges. *Eukaryotic Cell* **10(9):** 1156-1163

Kraeva N, Ishemgulova A, Lukes J, Yurchenko V (2014) Tetracycline-inducible gene expression system in *Leishmania mexicana*. *Molecular Biochemical Parasitology* **198(1):** 11-13

Krauth-Siegel RL, Comini MA (2008) Redox control in trypanosomatids, parasitic protozoa with trypanothione-based thiol metabolism. *Biochimica et Biophysica Acta* **1780:** 1236-1248

Krieger S, Schwarz W, Ariyanayagam MR, Fairlamb AH, Krauth-Siegel RL, Clayton C (2000) Trypanosomes lacking trypanothione reductase are avirulent and show increased sensitivity to oxidative stress. *Molecular Microbiology* **35:** 542-552

Kullas AL, McClelland M, Yang HJ, Tam JW, Torres A, Porwollik S, et al. (2012) L-asparaginase II produced by *Salmonella typhimurium* inhibits T cell responses and mediates virulence. *Cell Host Microbe* **12:** 791-798

Kulshrestha A, Sharma V, Singh R, Salotra P (2014) Comparative transcript expression analysis of miltefosine-sensitive and miltefosine-resistant *Leishmania donovani*. *Parasitology Research* **113:** 1171-1184

Kurup SP, Tarleton RL (2014) The *Trypanosoma cruzi* flagellum is discarded via asymmetric cell division following invasion and provides early targets for protective $CD8^+$ T cells. *Cell Host and Microbe* **16(4):** 439-449

LaFon SW, Nelson DJ, Berens RL, Marr JJ (1985) Inosine analogs. Their metabolism in mouse L cells and in *Leishmania donovani. The Journal of Biological Chemistry* **260:** 9660-9665

Lahav T, Sivam D, Volpin H, Ronen M, Tsigankov P, Green A, et al. (2011) Multiple levels of gene regulation mediate differentiation of the intracellular pathogen *Leishmania*. *FASEB Journal* **25:** 515-525

Lametschwandtner G, Brocard C, Fransen M, Van Veldhoven P, Berger J, Hartig A (1998) The difference in recognition of terminal tripeptides as peroxisomal targeting signal 1

between yeast and human is due to different affinities of their receptor Pex5p to the cognate signal and to residues adjacent to it. *The Journal of Biological Chemistry* **273:** 33635-33643

Lamontagne J, Papadopoulou B (1999) Developmental regulation of spliced leader RNA gene in *Leishmania donovani* amastigotes is mediated by specific polyadenylation. *The Journal of Biological Chemistry* **274:** 6602-6609

Lander N, Li ZH, Niyogi S, Docampo R (2015) CRISPRCas9-Induced Disruption of Paraflagellar Rod Protein 1 and 2 Genes in *Trypanosoma cruzi* Reveals Their Role in Flagellar Attachment. *mBio* **6(4):** e01012-15

Landfear SM and Ignatushchenko M (2001) The flagellum and flagellar pocket of trypanosomatids. Molecular and Biochemical Parasitology **115(1):** 1-17

Larsen TM, Boehlein SK, Schuster SM, Richards NG, Thoden JB, Holden HM, et al. (1999) Three-dimensional structure of *Escherichia coli* asparagine synthetase B: a short journey from substrate to product. *Biochemistry* **38:** 16146-16157

Laskay T, Diefenbach A, Rollinghoff M, Solbach W (1995) Early parasite containment is decisive for resistance to *Leishmania major* infection. *European Journal of Immunology* **25:** 2220-2227

Leduc D, Gallaud J, Stingl K, de Reuse H (2010) Coupled amino acid deamidase-transport systems essential for *Helicobacter pylori* colonization. *Infection and Immunity* **78:** 2782-2792

Lee SH, Stephens JL, Englund PT (2007) A fatty-acid synthesis mechanism specialized for parasitism. *Nature reviews Microbiology* **5:** 287-297

Lee SH, Stephens JL, Paul KS, Englund PT (2006) Fatty acid synthesis by elongases in trypanosomes *Cell* **126:** 691-699

Legare D, Richard D, Mukhopadhyay R, Stierhof YD, Rosen BP, Haimeur A, et al. (2001) The *Leishmania* ATP-binding cassette protein PGPA is an intracellular metal-thiol transporter ATPase. *The Journal of Biological Chemistry* **276:** 26301-26307

Leifso K, Cohen-Freue G, Dogra N, Murray A, McMaster WR (2007) Genomic and proteomic expression analysis of *Leishmania* promastigote and amastigote life stages: the *Leishmania* genome is constitutively expressed. *Molecular Biochemical Parasitology* **152:** 35-46

Lewis MD, Francisco AF, Taylor MC, Kelly JM (2015) A new experimental model for assessing drug efficacy against *Trypanosoma cruzi* infection based on highly sensitive *in vivo* imaging. *Journal of Biomolecular Screening* **20(1):** 36-43

Li F, Hua SB, Wang CC, Gottesdiener KM (1998) *Trypanosoma brucei brucei*: characterization of an ODC null bloodstream form mutant and the action of alpha-difluoromethylornithine. *Experimental parasitology* **88:** 255-257

Liu Z, Cao J, Gao X, Ma Q, Ren J, Xue Y (2011) GPS-CCD: A novel computational program for prediction of calpain cleavage sites. *PLoS One* **6(4):** e19001

Lodge R, Descoteaux A (2006) Phagocytosis of *Leishmania donovani* amastigotes is Rac1 dependent and occurs in the absence of NADPH oxidase activation. European Journal of Immunology **36:** 2735-2744

Lodge R, Diallo TO, Descoteaux A (2006) *Leishmania donovani* lipophosphoglycan blocks NADPH oxidase assembly at the phagosome membrane. *Cellular Microbiology* **8(12):** 1922-1931

Loiseau PM, Cojean S, Schrevel J (2011) Sitamaquine as a putative antileishmanial drug candidate: from the mechanism of action to the risk of drug resistance. *Parasite* **18:** 115-119

Lopez-Martin C, Perez-Victoria JM, Carvalho L, Castanys S, Gamarro F (2008) Sitamaquine sensitivity in *Leishmania* species is not mediated by drug accumulation in acidocalcisomes. *Antimicrobial Agents and Chemotherapy* **52:** 4030-4036

Lopez-Velez R, Videla S, Marquez M, Boix V, Jimenez-Mejias ME, Gorgolas M, et al. (2004) Amphotericin B lipid complex versus no treatment in the secondary prophylaxis of visceral leishmaniasis in HIV-infected patients. *Journal of Antimicrobial Chemotherapy* **53:** 540-543

Lorenz MV, Bender JA, Fink JR (2004) Transcriptional response to *Candida albicans* upon internalization by macrophages. *Eukaryotic Cell* **3(5):** 1076-1087

Loureiro I, Faria J, Clayton C, Macedo-Ribeiro S, Santarém N, Roy N et al. (2015) Ribose-5-phosphate isomerase B knockdown compromises *Trypanosoma brucei* bloodstream form infectivity. *PLoS Neglected Tropical Diseases* **9(1):** e3430

Loureiro I, Faria J, Clayton C, Ribeiro SM, Roy N, Santarém N, et al. (2013) Knockdown of Asparagine Synthetase A Renders *Trypanosoma brucei* Auxotrophic to Asparagine. *PLoS Neglected Tropical Diseases* **7:** e2578

Lukes J, Guilbride DL, Votypka J, Zikova A, Benne R and Englund PT (2002) Kinetoplast DNA network: evolution of an improbable structure. *Eukaryotic Cell* **1**(**4):** 495-502

Luo H, Gilinger G, Mukherjee D, Bellofatto V (1999) Transcription initiation at the TATA-less spliced leader RNA gene promoter requires at least two DNA-binding proteins and a tripartite architecture that includes an initiator element. *The Journal of Biological Chemistry* **274:** 31947-31954

Lye LF, Owens K, Shi H, Murta SMF, Vieira AC, Turco SJ, et al. (2010) Retention and loss of RNA interference pathways in trypanosomatis protozoans. *PLoS Pathogens* **6(10):** e1001161

Maciel BLL, Lacerda HG, Queiroz JW, Galvao J, Pontes NN, et al. (2008) Association of nutritional status with the response to infection with *Leishmania chagasi*. *American Journal of Tropical Medicine Hygiene* **79:** 591-598

Mackey ZB, Baca AM, Mallari JP, Apsel B, Shelat A, Hansell EJ, et al. (2006) Discovery of trypanocidal compounds by whole cell HTS of *Trypanosoma brucei*. *Chemical Biology & Drug and Design* **67:** 355-363

Maia C, Seblova V, Sadlova J, Votypka J, Volf P (2011) Experimental transmission of *Leishmania infantum* by two major vectors: a comparison between a viscerotropic and a dermotropic strain. *PLoS Neglected Tropical Diseases* **5:** e1181

Majumder S, Dey R, Bhattacharjee S, Rub A, Gupta G, Bhattacharrya Majumdar S et al. (2012) *Leishmania*-induced biphasic ceramide generation in macrophages is crucial for uptake and survival of the parasite. *Journal of Infectious Diseases* **205(10):** 1607-1616

Maltezou HC (2010) Drug resistance in visceral leishmaniasis. *Journal of Biomedicine and Biotechnology* **617521**

Manhas R, Tripathi P, Khan S, Lakshmi BS, Lal SK., Gowri VS, et al. (2014) Identification of functional characterization of a novel bacterial type asparagine synthetase A: a tRNA synthetase paralog from *Leishmania donovani. Journal of Biological Chemistry* **289:** 12096-12108

Marr AK, MacIsaac JL, Jiang R, Airo AM, Kobor MS, McMaster WR (2014) *Leishmania donovani* infection causes distinct epigenetic DNA methylation changes in host macrophages. *PLoS Pathogens* **10:** e1004419

Martinez-Calvillo S, Vizuet-de-Rueda JC, Florencio-Mártinez LE, Manning-Cela RG, Figueroa-Angulo EE (2010) Gene expression in trypanosomatid parasites. *Journal of Biomedicine and Biotechnology* **2010:** 1-15

Martinez-Calvillo S, Yan S, Nguyen D, Fox M, Stuart K, Myler PJ (2003) Transcription of *Leishmania major* Friedlin chromosome 1 initiates in both directions within a single region. *Molecular Cell* **11:** 1291-1299

Martin KL, Smith TK (2006) Phosphatidylinositol synthesis is essential in bloodstream form *Trypanosoma brucei*. *The Biochemical journal* **396:** 287-295

Masterson WJ, Raper J, Doering TL, Hart GW, Englund PT (1990) Fatty acid remodeling: a novel reaction sequence in the biosynthesis of trypanosome glycosyl phosphatidylinositol membrane anchors. *Cell* **62:** 73-80

Mathur RK, Awasthi A, Wadhone P, Ramanmurthy B, Saha B (2004) Reciprocal CD40 signals through p38MAPK and ERK-1/2 induce counteracting immune responses. Nature Medicine **10:** 540-544

Maugeri DA, Cazzulo JJ, Burchmore RJ, Barrett MP, Ogbunude PO (2003) Pentose phosphate pathway metabolism in *Leishmania mexicana*. *FASEB Journal* **130(2):** 117-125

Maurya R, Singh RK, Kumar B, Salotra P, Rai M, Sundar S (2005) Evaluation of PCR for diagnosis of Indian kala-azar and assessment of cure. *Journal of Clinical Microbiology* **43:** 3038-3041

Mbongo N, Loiseau PM, Billion MA, Robert-Gero M (1998) Mechanism of amphotericin B resistance in *Leishmania donovani* promastigotes. *Antimicrobial Agents and Chemotherapy* **42:** 352-357

McCall LI, Matlashewski G (2010) Localization and induction of the A2 virulence factor in *Leishmania*: evidence that A2 is a stress response protein. *Molecular Microbiology* **77:** 518-530

McCall LI, Matlashewski G (2012) Involvement of the *Leishmania donovani* virulence factor A2 in protection against heat and oxidative stress. *Experimental Parasitology* **132:** 109-115

McCall LI, Zhang WW, Matlashewski G (2013) Determinants of the development of Visceral Leismaniasis disease. *PLoS Pathogens* **9(1):** e1003053

McConville MJ, de Souza D, Saunders E, Likic VA, Naderer T (2007) Living in the phagolysosome: metabolism of *Leishmania* amastigotes. *TRENDS in Parasitology* **23(8):** 368-375

McConville MJ, Saunders EC, Kloehn J, Dagley MJ (2015) *Leishmania* carbon metabolism in the macrophage phagolysosome – feast or famine? *F1000Research* **4:** 938

McLatchie AP, Burrell-Saward H, Myburgh E, Lewis MD, Ward TH, Mottram JC, et al. (2013) Highly sensitive *in vivo* imaging of *Trypanosoma brucei* expressing “red-shifted” luciferase. *PLoS Neglected Tropical Diseases* **21(7):** e2571

McMahon-Pratt D, Alexander J (2004) Does the *Leishmania major* paradigm of pathogenesis and protection hold for New World cutaneous leishmaniases or the visceral disease? *Immunology Reviews* **201:** 206-24

McNicoll F, Drummelsmith J, Muller M, Madore E, Boilard N, Ouellette M, et al. (2006) A combined proteomic and transcriptomic approach to the study of stage differentiation in *Leishmania infantum*. *Proteomics* **6:** 3567-3581

Mehrotra S, Fakiola M, Oommen J, Jamieson SE, Mishra A, et al. (2011) Genetic and functional evaluation of the role of CXCR1 and CXCR2 in susceptibility to visceral leishmaniasis in north-east India. BMC Medical Genetics **12:** 162

Mehrotra S, Fakiola M, Mishra A, Sudarshan M, Tiwary P, et al. (2012) Genetic and functional evaluation of the role of DLL1 in susceptibility to visceral leishmaniasis in India. *Infectious Genetics Evolution* **12:** 1195-1201

Mehta SR, Huang R, Yang M, Zhang XQ, Kolli B, Chang KP et al. (2008) Real-time *in vivo* green fluorescent protein imaging of a murine leishmaniasis model as a new tool for *Leishmania* vaccine and drug discovery. *Clinical Vaccine Immunology* **15(12):** 1764-1770

Melby PC, Yang YZ, Cheng J, Zhao WG (1998) Regional differences in the cellular immune response to experimental cutaneous or visceral infection with *Leishmania donovani*. *Infection and Immunity* **66:** 18-27

Merchant SS, Prochnik SE, Vallon O, Harris EH, Karpowicz SJ, et al. (2007) The *Chlamydomonas* genome reveals the evolution of key animal and plant functions. *Science* **318:** 245-250

Merritt C, Stuart K (2013) Identification of essential and non-essential protein kinases by a fusion PCR method for efficient production of transgenic *Trypanosoma brucei. Molecular Biochemical Parasitology* **190(1):** 44-49

Michalska K, Jaskolski M (2006) Structural aspects of L-asparaginases, their friends and relations. *Acta biochimica Polonica* **53:** 627-640

Michell RH (2008) Inositol derivatives: evolution and functions. *Nature Reviews Molecular Cell Biology* **9:** 151-161

Michels PAM, Bringaud F, Herman M, Hannaert V (2006) Metabolic functions of glycosomes in trypanosomatids. *Biochimica et Biophysica Acta (BBA) - Mol Cell Res* **1763 (12):** 1463-1477

Millington OR, Myburgh E, Mottram JC, Alexander J (2010) Imaging of the host/parasite interplay in cutaneous leishmaniasis. *Experimental Parasitology* **126(3):** 310-317

Mina JG, Pan SY, Wansadhipathi NK, Bruce CR, Shams-Eldin H, Schwarz RT, et al. (2009) The *Trypanosoma brucei* sphingolipid synthase, an essential enzyme and drug target. *Molecular and biochemical parasitology* **168:** 16-23

Min B, Pelaschier JT, Graham DE, Tumbula-Hansen D, Soll D (2002) Transfer RNA-dependent amino acid biosynthesis: an essential route to asparagine formation. *Proceedings of the National Academy of Sciences of the United States of America* **99:** 2678-2683

Mobley DL, Dill KA (2009) Binding of small-molecule ligands to proteins: "what you see" is not always "what you get" *Structure* **17:** 489-498

Modabber F, Buffet PA, Torreele E, Milon G, Croft SL (2007) Consultative meeting to develop a strategy for treatment of cutaneous leishmaniasis. Institute Pasteur, Paris. 13-15 June, 2006. Kinetoplastid Biol Dis 6, 3

Mohamed HS, Ibrahim ME, Miller EN, Peacock CS, Khalil EAG, et al. (2003) Genetic susceptibility to visceral leishmaniasis in The Sudan: linkage and association with IL4 and IFNGR1. *Genes and Immunity* **4:** 351-355

Moore KJ, Matlashewski G (1994) Intracellular infection by *Leishmania donovani* inhibits macrophage apoptosis. *Journal of Immunology* **152(6):** 2930-2937

Moore LL, Santrich C, LeBowitz JH (1996) Stage-specific expression of the *Leishmania mexicana* paraflagellar rod protein PFR-2. *Molecular and Biochemical Parasitology* **80:** 125-135

Momeni AZ, Reiszadae MR, Aminjavaheri M (2002) Treatment of cutaneous leishmaniasis with a combination of allopurinol and low-dose meglumine antimoniate. *International Journal of Dermatology* **41:** 441-443

Mony B, MacGregor P, Ivens A, Rojas F, Cowton A, Young J, et al. (2014) Genome-wide dissection of the quorum sensing signalling pathway in *Trypanosoma brucei*. *Nature* **505:** 681-685

Moon S, Siqueira-Neto JL, Moraes CB, Yang G, Kang M, Freitas-Junior LH, et al. (2014) An image-based algorithm for precise and accurate high throughput assessment of drug activity against the human parasite *Trypanosoma cruzi. PLoS Neglected Tropical Diseases* **9(2):** e87188

Moraes MCS, Jesus TCL, Hashimoto NN, Dey M, Schwartz KJ, Alves VS, et al. (2007) Novel Membrane-Bound eIF2 Kinase in the Flagellar Pocket of *Trypanosoma brucei*. *Eukaryotic Cell* **6:** 1979-1991

Morales MA, Watanabe R, Laurent C, Lenormand P, Rousselle JC, Namane A, et al. (2008) Phosphoproteomic analysis of *Leishmania donovani* pro- and amastigote stages. *Proteomics* **8:** 350-363

Moreira D, Rodrigues V, Abengozar M, Rivas L, Rial E, Laforge M, et al. (2015) *Leishmania infantum* modulates host macrophage mitochondrial metabolism by hijacking the SIRT1-AMPK axis. *PLoS Pathogens* **11(3):** e1004684

Moreno SNJ, Docampo R (2009) The role of acidocalcisomes in parasitic protists. *Journal of Eukaryotic Microbiology* **56(3):** 208-213

Mottram JC, McCready BP, Brown KG and Grant KM (1996) Gene disruptions indicate an essential function for the LmmCRK1 cdc2-related kinase of *Leishmania mexicana*. *Molecular Microbiology* **22:** 573-583

Mpamhanga CP, Spinks D, Tulloch LB, Shanks EJ, Robinson DA, Collie IT, et al. (2009) One scaffold, three binding modes: novel and selective pteridine reductase 1 inhibitors derived from fragment hits discovered by virtual screening. *Journal of medicinal chemistry* **52:** 4454-4465

Mukherjee A, Langston LD, Ouellette M (2011) Intrachromosomal tandem duplication and repeat expansion during attempts to inactivate the subtelomeric essential gene *GSH1* in *Leishmania*. *Nucleic Acid Research* **39(17):** 7499-7511

Mukherjee A, Roy G, Guimond C and Ouellette M (2009) The gamma-glutamylcysteine synthetase gene of *Leishmania* is essential and involved in response to oxidants. *Molecular Microbiology* **74:** 914–927

Mukhopadhyay R, Kapoor P, Madhubala R (1996) Characterization of alpha-difluoromethylornithine resistant *Leishmania donovani* and its susceptibility to other inhibitors of the polyamine biosynthetic pathway. *Pharmacological Research* **34:** 43-46

Muller I, Hailu A, Choi B-S, Abebe T, Fuentes JM, et al. (2008) Age-related alteration of arginase activity impacts on severity of leishmaniasis. *PLoS Neglected Tropical Diseases* **2:** e235

Muller M, Padmanabhan PK, Papadopoulou B (2010a) Selective inactivation of SIDER2 retroposon-mediated mRNA decay contributes to stage- and species-specific gene expression in *Leishmania. Molecular Microbiology* **77:** 471-491

Muller M, Padmanabhan PK, Rochette A, Mukherjee D, Smith M, Dumas C, et al. (2010b) Rapid decay of unstable *Leishmania* mRNAs bearing a conserved retroposon signature 3'-UTR motif is initiated by a site-specific endonucleolytic cleavage without prior deadenylation. *Nucleic Acids Research* **38:** 5867-5883

Munday JC, Eze AA, Baker N, Glover L, Clucas C, Aguinaga-André D, et al. (2014) *Trypanosoma brucei* aquaglyceroporin 2 is a high-affinity transporter for pentamidine and melaminophenyl arsenic drugs and the main genetic determinant of resistance to these drugs. *Journal of Antimicrobial Therapy* **69:** 651-663

Muñoz-Elías EJ, McKinney JD (2005) *Mycobacterium tuberculosis* isocitrate lyases 1 and 2jointly required for *in vivo* growth and virulence. *Nature Medicine* **11(6):** 638-644

Murray HW (2005) Prevention of relapse after chemotherapy in a chronic intracellular infection: mechanisms in experimental visceral leishmaniasis. *Journal of Immunology* **174(8):** 4916-4923

Murray HW, Berman JD, Davies CR, Saravia NG (2005) Advances in leishmaniasis. *Lancet* **366:** 1561-1577

Murta SM, Vickers TJ, Scott DA, Beverley SM (2009) Methylene tetrahydrofolate dehydrogenase/cyclohydrolase and the synthesis of 10-CHO-THF are essential in *Leishmania major*. *Molecular Microbiology* **71:** 1386-1401

Musa AM, Younis B, Fadlalla A, Royce C, Balasegaram M, Wasunna M, et al. (2010) Paromomycin for the treatment of visceral leishmaniasis in Sudan: a randomized, open-label, dose-finding study. *PLoS Neglected Tropical Diseases* **4:** e855

Naderer T, Ellis MA, Sernee MF, de Souza DP, Curtis J, Handman E et al. (2006) Virulence of *Leishmania major* in macrophages and mice requires the gluconeogenic enzyme fructose-1,6-bisphosphatase. *Proceedings of the National Academy of Sciences of the United States of America* **103(14):** 5502-5507

Nagaraj VA, Mukhi D, Sathishkumar V, Subramani PA, Ghosh SK, Pandey RR, et al. (2015) Asparagine requirement in *Plasmodium berghei* as a target to prevent malaria transmission and liver infections. *Nature Communications* **6:** 8775

Nakamura M, Yamada M, Hirota Y, Sugimoto K, Oka A, Takanami M (1981) Nucleotide sequence of the asnA gene coding for asparagine synthetase of *E. coli* K-12. *Nucleic Acids Research* **9:** 4669-4676

Nakatsu T, Kato H, Oda J (1998) Crystal structure of asparagine synthetase reveals a close evolutionary relationship to class II aminoacyl-tRNA synthetase. *Nature Structural Biology* **5:** 15-19

Nare B, Hardy LW, Beverley SM (1997) The Roles of Pteridine Reductase 1 and Dihydrofolate Reductase-Thymidylate Synthase in Pteridine Metabolism in the Protozoan Parasite *Leishmania major*. *The Journal of Biological Chemistry* **272(21):** 13883-13891

Naula CM, Logan FM, Wong PE, Barrett P M, Burchmore RJ (2010) A glucose transporter can mediate ribose uptake. *Journal of Biological Chemistry* **285(39):** 29721-29728

Navarro M, Liu J, Muthui D, Ortiz G, Segovia M, Hamers R (1994) Inverted repeat structure and homologous sequences in the LD1 amplicons of *Leishmania* spp. *Molecular and Biochemical Parasitology* **68:** 69-80

Navin TR, Arana BA, Arana FE, Berman JD, Chajon JF (1992) Placebo-controlled clinical trial of sodium stibogluconate (Pentostam) versus ketoconazole for treating cutaneous leishmaniasis in Guatemala. *Journal of Infectious Diseases* **165:** 528-534

Neklesa TK, Tae HS, Schneekloth AR, Stulberg MJ, Corson TW, Sundberg TB, et al. (2011) Small-molecule hydrophobic tagging-induced degradation of HaloTag fusion proteins. *Nature Chemical Biology* **7:** 538-543

Newsholme EA, Rolleston FS, Taylor K (1967) Inhibition of brain hexokinase by glucose 6-phosphate. *The Biochemical journal* **104:** 47P

Ngô H, Tschudi C, Gull K, Ullu E (1998) Double-stranded RNA induces mRNA degradation in *Trypanosoma brucei*. *Proceedings of the National Academy of Sciences of the United States of America* **95:** 14687-14692

Nourbakhsh F, Uliana SR, Smith DF (1996) Characterisation and expression of a stageregulated gene of *Leishmania major*. *Molecular and Biochemical Parasitology* **76:** 201-213

Nylen S, Gautam S. (2010) Immunological perspectives of leishmaniasis. *Journal of Global and Infectious Diseases* **2(2):** 135-146

O'Connell MR, Oakes BL, Sternberg SH, East-Seletsky A, Kaplan M, Doudna JA (2014) Programmable RNA recognition and cleavage by CRISPR/Cas9. *Nature* **516:** 263-266

Odiwuor S, De Doncker S, Maes I, Dujardin JC, Van der Auwera G (2011) Natural *Leishmania donovani/Leishmania aethiopica* hybrids identified from Ethiopia. *Infection, Genetics and Evolution* **11(8):** 2113-2118

Ogbunude PO, Lamour N, Barrett MP (2007) Molecular cloning, expression and characterization of ribokinase of *Leishmania major*. *Acta Biochimica et Biophysica Sinica* **39(6):** 462-466

Oliveira F, Rowton E, Aslan H, Gomes R, Castrovinci PA, Alvarenga PH, et al. (2015) A sand fly salivary protein vaccine shows efficacy against vector-transmitted cutaneous leishmaniasis in a nonhuman primates. *Scientific Reports* **7(290):** 290ra90

Olivier M, Atayde VD, Isnard A, Hassani K and Shio MT (2012) *Leishmania* virulence factors: focus on the metalloprotease GP63. *Microbes and Infection* **14(15):** 1377-1389

Olivier M, Brownsey RW, Reiner NE (1992) Defective stimulus-response coupling in human monocytes infected with *Leishmania donovani* is associated with altered activation and translocation of protein kinase C. *Proceedings of the National Academy of Sciences of the United States of America* **89:** 7481-7485

Olmo A, Arrebola R, Bernier V, Gonzalez-Pacanowska D, Ruiz-Perez LM (1995) Co-existence of circular and multiple linear amplicons in methotrexate-resistant *Leishmania. Nucleic Acids Research* **23:** 2856-2864

Opperdoes FR, Coombs GH (2007) Metabolism of *Leishmania*: proven and predicted. *Trends in Parasitology* **23:** 149-158

Opperdoes FR, Szikora JP (2006) *In silico* prediction of the glycosomal enzymes of *Leishmania major* and trypanosomes. *Molecular and biochemical parasitology* **147:** 193-206

Ouellette M, Hettema E, Wust D, Fase-Fowler F and Borst P (1991) Direct and inverted DNA repeats associated with P-glycoprotein gene amplification in drug resistant *Leishmania*. *EMBO Journal* **10:** 1009-1016

Owino AV, Masiga KD, Limo KM (2008) RNA interference: a pathway to drug target identification and validation in trypanosome. *African Journal of Biochemistry* **2(3):** 66-73

Paila YD, Saha B, Chattopadhyay A (2010) Amphotericin B inhibits entry of *Leishmania donovani* into primary macrophages. *Biochemical and Biophysical Research Communications* **399:** 429-433

Palmeri A, Gherardini PF, Tsigankov P, Ausiello G, Späth GF, Zilberstein D, et al. (2011) PhosTryp: a phosphorylation site predictor specific for parasitic protozoa of the family trypanosomatidae. *BMC Genomics* **12:** 614

Pan D, Nakatsu T, Kato H (2013) Crystal structure of peroxisomal targeting signal-2 bound to its receptor complex Pex7p–Pex21p. *Nature Structural & Molecular Biology* **20(8):** 987-993

Papadopoulou B, Roy G, Mourad W, Leblanc E, Ouellette M (1994) Changes in folate and pterin metabolism after disruption of the *Leishmania* H locus short chain dehydrogenase gene. *The Journal of Biological Chemistry* **269:** 7310-7315

Paris C, Loiseau PM, Bories C, Breard J (2004) Miltefosine induces apoptosis-like death in *Leishmania donovani* promastigotes. *Antimicrobial Agents and Chemotherapy* **48:** 852-859

Parsons M, Furuya T, Pal S, Kessler P (2001) Biogenesis and function of peroxisomes and glycosomes. *Molecular and Biochemical Parasitology* **115:** 19-28

Parsons M, Worthey EA, Ward PN, Mottram JC (2005) Comparative analysis of the kinomes of three pathogenic trypanosomatids: *Leishmania major, Trypanosoma brucei and Trypanosoma cruzi. BMC Genomics* **6:** 127

Pastakia KB, Dwyer DM (1987) Identification and characterization of a ribose transport system in *Leishmania donovani* promastigotes. *Molecular and Biochemical Parasitology* **26(12):** 175-181

Patrick KL, Shi H, Kolev NG, Ersfeld K, Tschudi C, Ullu E (2009) Distinct and overlapping roles for two Dicer-like proteins in the RNA interference pathways of the ancient eukaryote *Trypanosoma brucei*. *Proceedings of the National Academy of Sciences of the United States of America* **106:** 17933-17938

Peacock CS, Seeger K, Harris D, Murphy L, Ruiz JC, et al. (2007) Comparative genomic analysis of three *Leishmania* species that cause diverse human disease. *Nature Genetics* **39:** 839-847

Pedrosa AL, Cruz AK (2002) The effect of location and direction of an episomal gene on the restoration of a phenotype by functional complementation in *Leishmania*. *Molecular and Biochemical Parasitology* **122:** 141-148

Pellecchia M, Bertini I, Cowburn D, Dalvit C, Giralt E, Jahnke W, et al. (2008) Perspectives on NMR in drug discovery: a technique comes of age. *Nature reviews Drug discovery* **7:** 738-745

Peng D, Kurup SP, Yao PY, Minning TA, Tarleton RL (2014) CRISPR-Cas9-mediated single-gene and gene family disruption in *Trypanosoma cruzi*. *mBIO* **6(1):** e02097-14

Perez-Victoria FJ, Castanys S, Gamarro F (2003) *Leishmania donovani* resistance to miltefosine involves a defective inward translocation of the drug. *Antimicrobial Agents and Chemotherapy* **47:** 2397-2403

Peters NC, Egen JG, Secundino N, Debrabant A, Kimblin N, Kamhawi S, et al. (2008) *In vivo* imaging reveals an essential role for neutrophils in leishmaniasis transmitted by sand flies. Science **321(5891):** 970-974

Petrillo-Peixoto M, Beverley SM (1987) *In vitro* activity of sulfonamides and sulfones against *Leishmania major* promastigotes. *Antimicrobial Agents and Chemotherapy* **31:** 1575-1578

Pham JS, Dawson KL, Jackson KE, Lim EE, Pasaje CF, Turner KE, et al. (2014) Aminoacyl-tRNA synthetases as drug targets in eukaryotic parasites. *International journal for parasitology Drugs and drug resistance* **4:** 1-13

Philip N, Water AP (2015) Conditional Degradation of *Plasmodium* Calcineurin Reveals Functions in Parasite Colonization of both Host and Vector. *Cell Host & Microbe* **18:** 122-131

Pillai S, Rajagopal C, Kapoor M, Kumar G, Gupta A, Surolia N (2003) Functional characterization of beta-ketoacyl-ACP reductase (FabG) from *Plasmodium falciparum*. *Biochemical and Biophysical Research Communications* **303:** 387-92

Pinheiro RO, Nunes MP, Pinheiro CS, D'Avilla H, Bozza BT, Takiya CM, et al. (2009) Induction of autophagy correlates with increased parasite load of *Leishmania amazonensis* in BALB/c but not C57BL/6 macrophages. *Microbes and Infection* **11(2):** 181-190

Pink R, Hudson A, Mouriès M-A, Bendig M (2005) Opportunities and challenges in antiparasitic drug discovery. *Nature Reviews Drug Discovery* **4:** 727-740

Pinto WJ, Wells GW, Lester RL (1992) Characterization of enzymatic synthesis of sphingolipid longchain bases in *Saccharomyces cerevisiae*: mutant strains exhibiting long-chain-base auxotrophy are deficient in serine palmitoyltransferase activity. *Journal of Bacteriology* **174:** 2575-2581

Podinovskaia M, Descoteaux A (2015) *Leishmania* and the macrophage: a multifaceted interaction. *Future Microbiology* **10(1):** 111-129

Polando R, Dixit UG, Carter CR, Jones B, Whitcomb JP, Ballhorn W, et al. (2013) The roles of complement receptor 3 and Fcgamma receptors during *Leishmania* phagosome maturation. *Journal of Leukocytes Biology* **93(6):** 921–932

Ponte-Sucre A, Diaz E, Padrón-Nieves M (2013) Drug resistance in *Leishmania* parasites: consequences, molecular mechanisms, and possible treatments. Wien ; New York, Springer-Verlag

Poulin R, Lu L, Ackermann B, Bey P, Pegg AE (1992) Mechanism of the irreversible inactivation of mouse ornithine decarboxylase by alpha-difluoromethylornithine. Characterization of sequences at the inhibitor and coenzyme binding sites. *The Journal of Biological Chemistry* **267:** 150-158

Pourshafie M, Morand S, Virion A, Rakotomanga M, Dupuy C, Loiseau PM (2004) Cloning of S-adenosyl-L-methionine:C-24-Delta-sterol-methyltransferase (ERG6) from *Leishmania*

donovani and characterization of mRNAs in wild-type and amphotericin B-Resistant promastigotes. *Antimicrobial Agents and Chemotherapy* **48:** 2409-2414

Prada CF, Alvarez-Velilla R, Balaña-Fouce R, Prieto C, Calvo-Álvarez E, Escudero-Martínez JM, et al. (2013) Gimatecan and other camptothecin derivatives poison *Leishmania* DNA-topoisomerase IB leading to a strong leishmanicidal effect. *Biochemical Pharmacol*ogy **85:** 1433-1440

Preubert C, Rossbach O, Hung LH, Li D, Bindereif A (2014) Genome-wide RNA-binding analysis of the trypanosome U1 snRNP proteins U1C and U1-70K reveals cis/trans-spliceosomal network. *Nucleic Acids Research* **42(10):** 6603-6615

Price HP, Menon MR, Panethymitaki C, Goulding D, McKean PG, Smith DF (2003) Myristoyl-CoA:protein N-myristoyltransferase, an essential enzyme and potential drug target in kinetoplastid parasites. *The Journal of biological chemistry* **278:** 7206-7214

Proudfoot L, Nikolaev AV, Feng GJ, Wei WQ, Ferguson MA, Brimacombe JS, et al. (1996) Regulation of the expression of nitric oxide synthase and leishmanicidal activity by glycoconjugates of *Leishmania* lipophosphoglycan in murine macrophages. . *Proceedings of the National Academy of Sciences of the United States of America* **93(20):** 10984-10989

Pulido, SA, Muñoz, DL, Restrepo, AM, Mesa, CV, Alzate, JF, Vélez, ID et al. (2012) Improvement of the green fluorescent protein reporter system in *Leishmania* spp. for the *in vitro* and *in vivo* screening of antileishmanial drugs. *Acta Tropica* **122(1):** 36-45

Qian G, Liu C, Wu G, Yin F, Zhao Y, Zhou Y, et al. (2013) AsnB, regulated by diffusible signal factor and global regulator Clp, is involved in aspartate metabolism, resistance to oxidative stress and virulence in *Xanthomonas oryzae pv. oryzicola*. *Molecular plant pathology* **14:** 145-157

Rakotomanga M, Blanc S, Gaudin K, Chaminade P, Loiseau PM (2007) Miltefosine affects lipid metabolism in *Leishmania donovani* promastigotes. *Antimicrobial Agents and Chemotherapy* **51:** 1425-30

Ramakrishnana S, Serricchiob M, Striepena B, Butikoferb P (2013) Lipid Synthesis in Protozoan Parasites: a Comparison between Kinetoplastids and Apicomplexans. *Progress on Lipid Research* **52(4):** 488-512

Ramesh V, Kumar J, Kumar D, Salotra P (2010) A retrospective study of intravenous sodium stibogluconate alone and in combinations with allopurinol, rifampicin, and an immunomodulator in the treatment of Indian post-kala-azar dermal leishmaniasis. *Indian Journal of Dermatology, Venereology and Leprology* **76:** 138-144

Ramesh V, Singh R, Salotra P (2007) Post-kala-azar dermal leishmaniasis – an appraisal. *Tropical Medicine International Health* **12:** 848-851

Ramos F, Wiame JM (1980) Two asparagine synthetases in *Saccharomyces cerevisiae*. *European Journal of Biochemistry* **108:** 373-377

Ramos H, Valdivieso E, Gamargo M, Dagger F, Cohen BE (1996) Amphotericin B kills unicellular leishmanias by forming aqueous pores permeable to small cations and anions. *Journal of Membrane Biology* **152:** 65-75

Rashid JR, Wasunna KM, Gachihi GS, Nyakundi PM, Mbugua J, Kirigi G (1994) The efficacy and safety of ketoconazole in visceral leishmaniasis. *East Africa Medical Journal* **71:** 392-395

Ravel C, Cortes S, Pratlong F, Morio F, Dedet JP, Campino L (2006) First report of genetic hybrids between two very divergent *Leishmania* species: *Leishmania infantum* and *Leishmania major*. *International Journal of Parasitology* **36:** 1383-1388

Raymond F, Boisvert S, Roy G, Ritt JF, Legare, D, Isnard A, et al. (2011) Genome sequencing of the lizard parasite *Leishmania tarentolae* reveals loss of genes associated to the intracellular stage of human pathogenic species. *Nucleic Acids Research* **40(3):** 1131-1147

Reguera RM, Calvo-Álvarez E, Alvarez-Velilla R, Balaña-Fource R (2014) Target-based vs phenotypic screenings in *Leishmania* drug discovery: a marriage of convenience or a dialogue of the deaf? *International Journal of Parasitology: Drugs and Drug Resistance* **4(3):** 355-357

Reithinger R, Dujardin JC (2007) Molecular diagnosis of leishmaniasis: current status and future applications. *Journal of Clinical Microbiology* **45:** 21-25

Reitzer LJ, Magasanik B (1982) Asparagine synthetases of *Klebsiella aerogenes*: properties and regulation of synthesis. *Journal of Bacteriology* **151:** 1299-1313

Ren H, Liu J (2006) AsnB is involved in natural resistance of *Mycobacterium smegmatis* to multiple drugs. *Antimicrobial Agents and Chemotherapy* **50:** 250-255

Requena JM (2011) Lights and shadows on gene organization and regulation of gene expression in *Leishmania. Frontiers in Bioscience* **17:** 2069-2085

Robello C, Navarro P, Castanys S, Gamarro F (1997) A pteridine reductase gene ptr1 contiguous to a P-glycoprotein confers resistance to antifolates in *Trypanosoma cruzi. Molecular and biochemical parasitology* **90:** 525-535

Robertson JG (2005) Mechanistic basis of enzyme-targeted drugs. *Biochemistry* **44:** 5561-5571

Roberts SC, Jiang Y, Gasteier J, Frydman B, Marton LJ, Heby O, et al. (2007) *Leishmania donovani* polyamine biosynthetic enzyme overproducers as tools to investigate the mode of action of cytotoxic polyamine analogs. *Antimicrobial Agents and Chemotherapy* **51:** 438-445

Roberts SC, Jiang Y, Jardim A, Carter NS, Heby O, Ullman B (2001) Genetic analysis of spermidine synthase from *Leishmania donovani. Molecular and Biochemical Parasitology* **115:** 217–226

Roberts SC, Scott J, Gasteier JE, Jiang Y, Brooks B, Jardim A, et al. (2002) S-adenosylmethionine decarboxylase from *Leishmania donovani*. Molecular, genetic, and biochemical characterization of null mutants and overproducers. *The Journal of Biological Chemistry* **277:** 5902-5909

Roberts SC, Tancer MJ, Polinsky MR, Gibson KM, Heby O, Ullman B (2004) Arginase plays a pivotal role in polyamine precursor metabolism in *Leishmania*. Characterization of gene deletion mutants. *The Journal of Biological Chemistry* **279:** 23668-23678

Robinette D, Neamati N, Tomer KB, Borchers CH (2006) Photoaffinity labeling combined with mass spectrometric approaches as a tool for structural proteomics. *Expert review of proteomics* **3:** 399-408

Rochette A, Raymond F, Corbeil J, Ouellette M, Papadopoulou B (2009) Whole-genome comparative RNA expression profiling of axenic and intracellular amastigote forms of *Leishmania infantum*. *Molecular and Biochemical Parasitology* **165(1):** 32-47

Rodríguez-Contreras D, Landfear SM (2006) Metabolic changes in glucose transporter-deficient *Leishmania mexicana* and parasite virulence. *The Journal of Biological Chemistry* **281(29):** 20068-20076

Rodriguez-Gonzalez I, Marin C, Longoni SS, Mateo H, Alunda JM, Minaya G, et al. (2007) Identification of New World *Leishmania* species from Peru by biochemical techniques and multiplex PCR assay. *FEMS Microbiology Letters* **267:** 9-16

Rodriguez NE, Gaur Dixit U, Allen LA, Wilson ME (2011) Stage-specific pathways of *Leishmania infantum chagasi* entry and phagosome maturation in macrophages. *PLoS ONE* **6(4):** e19000

Rogers M, Kropf P, Choi BS, Dillon R, Podinovskaia M, Bates P, et al. (2009) Proteophosophoglycans regurgitated by *Leishmania*-infected sand flies target the L-arginine metabolism of host macrophages to promote parasite survival. *PLoS Pathogens* **5(8):** e1000555

Rogers MB, Downing T, Smith BA, Imamura H, Sanders M, Svobodova M, et al. (2014) Genomic confirmation of hybridisation and recent inbreeding in a vector-isolated *Leishmania* population. *PLoS Genetics* **10(1):** e1009042

Rogers MB, Hilley JD, Dickens NJ, Wilkes J, Bates PA, Depledge DP, et al. (2011) Chromosome and gene copy number variation allow major structural change between species and strains of *Leishmania*. *Genome Research* **21:** 2129-2142

Rogers ME, Corware K, Muller I, Bates PA (2010) *Leishmania infantum* proteophosphoglycans regurgitated by the bite of its natural sand fly vector, *Lutzomyia*

longipalpis, promote parasite establishment in mouse skin and skin-distant tissues. *Microbes and Infection* **12(11):** 875-879

Rogers ME, Hajmova M, Joshi MB, Sadlova J, Dwyer DM, Volf P, *et al.* (2008) *Leishmania* chitinase facilitates colonization of sand fly vectors and enhances transmission to mice. *Cell Microbiology* **10(6):** 1363-1372

Rogers ME, Ilg T, Nikolaev AV, Ferguson MA and Bates PA (2004) Transmission of cutaneous leishmaniasis by sand flies is enhanced by regurgitation of fPPG. *Nature* **430(6998):** 463-467

Rohousová I, Subrahmanyam S, Volfová V, Mu J, Volf P, et al. (2012) Salivary gland transcriptomes and proteomes of *Phlebotomus tobbi* and *Phlebotomus sergenti*, vectors of leishmaniasis. *PLoS Neglected Tropical Diseases* **6:** e1660

Romano A, Inbar E, Debrabant A, Charmoy M, Lawyer P, Ribeiro-Gomes F, et al. (2014) Cross-species genetic exchange between cutaneous and visceral strains of *Leishmania* in the sand fly vector. *Proceedings of the National Academy of Sciences of the United States of America* **47:** 16808-16813

Ronet C, Beverley SM and Fasel N (2011) Muco-cutaneous leishmaniasis in the New World: the ultimate subversion. *Virulence* **2(6):** 547-552

Roos AK, Burgos E, Ericsson DJ, Salmon L, Mowbray SL (2005) Competitive inhibitors of *Mycobacterium tuberculosis* ribose-5-phosphate isomerase B reveal new information about the reaction mechanism. *The Journal of Biological Chemistry* **280:** 6416-6422

Rosenzweig D, Smith D, Opperdoes F, Stern S, Olafson RW, Zilberstein D (2008) Retooling *Leishmania* metabolism: from sand fly gut to human macrophage. *FASEB Journal* **22:** 590-602

Rotureau B, Morales MA, Bastin P, Spath GF (2009) The flagellum-mitogen-activated protein kinase connection in trypanosomatids: a key sensory role in parasite signalling and development? *Cellular Microbiology* **11(5):** 710-718

Roy H, Becker HD, Reinbolt J, Kern D (2003) When contemporary aminoacyl-tRNA synthetases invent their cognate amino acid metabolism. *Proceedings of the National Academy of Sciences of the United States of America* **100:** 9837-9842

Roy S, Kumar GA, Jafurulla M, Mandal C, Chattopadhyay A (2014) Integrity of the Actin Cytoskeleton of Host Macrophages is Essential for *Leishmania donovani* Infection. *Biochimica et Biophysica Acta* **1838(8):** 2011-2018

Ruda GF, Wong PE, Alibu VP, Norval S, Read KD, Barrett MP, et al. (2010) Aryl phosphoramidates of 5-phospho erythronohydroxamic acid, a new class of potent trypanocidal compounds. *Journal of Medicinal Chemistry* **53:** 6071-6078

Sacks D, Kamhawi S (2001) Molecular aspects of parasite-vector and vector-host interactions in Leishmaniasis. *Annual Reviews Microbiology* **55:** 453-83

Sacks D, Noben-Trauth N (2002) The immunology of susceptibility and resistance to *Leishmania major* in mice. *Nature Reviews Immunology* 2: 849-858

Sacks DL, Pimenta PF, McConville MJ, Schneider P and Turco SJ (1995) Stage-specific binding of *Leishmania donovani* to the sand fly vector midgut is regulated by conformational changes in the abundant surface lipophosphoglycan. *Journal of Experimental Medicine* **181(2):** 685-697

Sadeghi S, Seyed N, Etemadzadeh MH, Abediankenari S, Fafati S, Taheri T (2015) *In vitro* infectivity assessment by drug susceptibility comparison of recombinant *Leishmania major* expressing enhanced green fluorescent protein or EGFP-Luciferase fused genes with wild-type parasite. *Korean Journal of Parasitology* **53(4):** 385-394

Sadlova J, Yeo M, Seblova V, Lewis MD, Mauricio I, Volf P, et al. (2011) Visualisation of *Leishmania donovani* fluorescent hybrids during early stage development in the sand fly vector. *PLoS One* **6:** e19851

Santarém N, Tomas A, Ouaissi A, Tavares J, Ferreira N, Manso A, et al. (2005) Antibodies against a *Leishmania infantum* peroxiredoxin as a possible marker for diagnosis of visceral leishmaniasis and for monitoring the efficacy of treatment. *Immunology Letters* **101:** 18-23

Sarkar A, Ghosh S, Pakrashi S, Roy D, Sen S, et al. (2012) *Leishmania* strains causing self-healing cutaneous leishmaniasis have greater susceptibility towards oxidative stress. *Free Radicals Research* **46:** 665-673

Sassetti CM, Boyd DH, Rubin EJ (2003) Genes required for mycobacterial growth defined by high density mutagenesis. *Molecular Microbiology* **48:** 77-84

Saunders EC, DE Souza DP, Naderer T, Sernee MF, Ralton JE, et al. (2010) Central carbon metabolism of *Leishmania* parasites. *Parasitology* **137:** 1303-1313

Saunders EC, Ng WW, Chamber JM, Ng M, Naderer T, et al. (2011) Isoptopomer profiling of *Leishmania mexicana* promastigotes reveals important roles for succinate fermentation and aspartate uptake in TCA cycle anaplerosis, glutamate synthesis and growth. *The Journal of Biological Chemistry* **286:** 27706-27717

Saunders EC, Ng WW, Kloehn J, Chambers JN, Ng M, McConville MJ (2014) Induction of a stringent metabolic response in intracellular stages of *Leishmania mexicana* leads to increased dependence on mitochondrial metabolism. *PLoS Pathogens* **10(1):** e1003888

Scahill MD, Pastar I, Croos GAM (2008) CRE recombinase-based positive-negative selection systems for genetic manipulation in *Trypanosoma brucei*. *Molecular Biochemical Parasitology* **157(1):** 73-82

Schwarz F, Aebi M (2011) Mechanisms and principles of N-linked protein glycosylation. *Current opinion in structural biology* **21:** 576-582

Scianimanico S, Desrosiers M, Dermine JF, Méresse S, Descoteaux A, Desjardins M (1999) Impaired recruitment of the small GTPase rab7 correlates with the inhibition of phagosome maturation by *Leishmania donovani* promastigotes. Cellular Microbiology **1:** 19-32

Scofield MA, Lewis W, Schuster SM (1990) Nucleotide sequence of *Escherichia coli* asnB and deduced amino acid sequence of asparagine synthetase B. *The Journal Biological Chemistry* **265:** 12895-12902

Scotti C, Sommi P, Pasquetto MV, Cappelletti D, Stivala S, Mignosi P, et al. (2010) Cell cycle inhibition by *Helicobacter pylori* L-asparaginase. *PLoS One* **5:** e13892

Secundino NF, Eger-Mangrich I, Braga EM, Santoro MM, Pimenta PF (2005) *Lutzomyia longipalpis* peritrophic matrix: formation, structure, and chemical composition. *Journal of Medicinal Entomology* **42(6):** 928-938

Secundino N, Kimblin N, Peters NC, Lawyer P, Capul AA, Beverley SM, et al. (2010) Proteophosphoglycan confers resistance of *Leishmania major* to midgut digestive enzymes induced by blood feeding in vector sand flies. *Cellular Microbiology* **12(7):** 906-918

Segovia M (1994) *Leishmania* gene amplification: a mechanism of drug resistance. *Annual Tropical Medical Parasitology* **88:** 123-130

Sen S, Roy K, Mukherjee S, Mukhopadhyay R, Roy S (2011) Restoration of IFNγR subunit assembly, IFNγ signaling and parasite clearance in *Leishmania donovani* infected macrophages: role of membrane cholesterol. PLoS Pathogens **7:** e1002229

Shakya N, Sane SA, Vishwakarma P, Bajpai P, Gupta S (2011) Improved treatment of visceral leishmaniasis (kala-azar) by using combination of ketoconazole, miltefosine with an immunomodulator-Picroliv. *Acta Tropica* **119:** 188-193

Shalem O, Sanjana NE, Hartenian E, Shi X, Scott DA, Mikkelsen TS, et al. (2014) Genomescale CRISPR-Cas9 knockout screening in human cells. *Science* **343:** 84–87

Sharlow ER, Lyda TA, Dodson HC, Mustata G, Morris MT, Leimgruber SS, et al. (2010) A target-based high throughput screen yields *Trypanosoma brucei* hexokinase small molecule inhibitors with antiparasitic activity. *PLoS neglected tropical diseases* **4:** e659

Sharma P, Gurumurthy S, Duncan R, Nakhasi HL, Salotra P (2010) Comparative *in vivo* expression of amastigote up regulated *Leishmania* genes in three different forms of Leishmaniasis. *Parasitology International* **59:** 262-264

Sheng C, Ji H, Miao Z, Che X, Yao J, Wang W, et al. (2009) Homology modeling and molecular dynamics simulation of N-myristoyltransferase from protozoan parasites: active site characterization and insights into rational inhibitor design. *Journal of computer-aided molecular design* **23:** 375-389

Shibayama K, Takeuchi H, Wachino J, Mori S, Arakawa Y (2011) Biochemical and pathophysiological characterization of *Helicobacter pylori* asparaginase. *Microbiology and Immunology* **55:** 408-417

Shi H, Djikeng A, Tschudi C, Ullu E (2004) Argonaute protein in the early divergent eukaryote *Trypanosoma brucei*: control of small interfering RNA accumulation and retroposon transcript abundance. *Molecular Cellular Biology* **24:** 420-427

Shi H, Tschudi C and Ullu E (2006) An unusual Dicer-like1 protein fuels the RNA interference pathway in *Trypanosoma brucei*. *RNA* **12:** 2063-2072

Sidik SM, Hackett CG, Tran F, Westwood NJ, Lourido S (2014) Efficient genome engineering of *Toxoplasma gondii* using CRISPR/Cas9. *PLoS one* **9(6):** e100450

Sidoli C, Molteni A, Bellanti B, Redaelli L, Iuzzolino L, Rubino M, et al (2006) Biochemical assay development for drug discovery: a sequential optimization from protein expression to enzymatic activity. *Microbial Cell Factories* **5:** 1-2

Sienkiewicz N, Jaroslawski S, Wyllie S, Fairlamb AH (2008) Chemical and genetic validation of dihydrofolate reductase-thymidylate synthase as a drug target in African trypanosomes. *Molecular microbiology* **69:** 520-533

Sienkiewicz N, Ong HB, Fairlamb AH (2010) *Trypanosoma brucei* pteridine reductase 1 is essential for survival *in vitro* and for virulence in mice. *Molecular microbiology* **77:** 658-671

Singh S, Mukherjee A, Khomutov AR, Persson L, Heby O, Chatterjee M, et al. (2007) Antileishmanial effect of 3-aminooxy-1-aminopropane is due to polyamine depletion. *Antimicrobial Agents and Chemotherapy* **51:** 528-534

Singh, J, Srivastava, A, Jha, P, Sinha, KK, Kundu, B (2015) L-Asparaginase as a new molecular target against leishmaniasis: insights into the mechanism of action and structure-based inhibitor design. *Molecular BioSystems* **11:** 1887-1896

Siqueira-Neto JL, Moon S, Jang J, Yang G, Lee C, Moon HK, et al. (2012) An image-based high-content screening assay for compounds targeting intracellular *Leishmania donovani* amastigotes in human macrophages. *PLoS Neglected Tropical Diseases* **6(6):** e1671

Smith TK, Crossman A, Borissow CN, Paterson MJ, Dix A, Brimacombe JS, et al. (2001) Specificity of GlcNAc-PI de-N-acetylase of GPI biosynthesis and synthesis of parasite-specific suicide substrate inhibitors. *The EMBO journal* **20:** 3322-3332

Sollelis L, Ghorbal M, McPherson CR, Martins RM, Kuk N, Crobu L, et al. (2015) First efficient CRISPR-Cas9-mediated genome editing in *Leishmania* parasites. *Cellular Microbiology* **17(10):** 1405-1412

Sommer JM, Cheng Q-L, Keller G-A, Wang CC (1992) *In vivo* import of firefly luciferase into the glycosomes of *Trypanosoma brucei* and mutational analysis of the C-terminal targeting signal. *Molecular Biology of the Cell* **3:** 749-59

Sorensen KI, Hove-Jensen B (1996) Ribose catabolism of *Escherichia coli*: characterization of RpiB gene encoding ribose-5-phosphate isomerase Band of the RpiR gene, which is involved in the regulation of RpiB expression. *Journal of Bacteriology* **178:** 1003-1011

Sousa AF, Gomes-Alves AG, Benítez D, Comini MA, Flohé L, Jaeger T, et al. (2014) Genetic and chemical analyses reveal that trypanothione synthetase but not glutathionylspermidine synthetase is essential for *Leishmania infantum. Free Radicals Biological Medicine* **73:** 229-238

Souza AE, Waugh S, Coombs GH, Mottram JC (1992) Characterization of a multi-copy gene for a major stage-specific cysteine proteinase of *Leishmania mexicana. FEBS Letters* **311:** 124-127

Spaeth GF, Garraway LA, Turco SJ, Beverley SM (2003) The role(s) of lipophosphoglycan (LPG) in the establishment of *Leishmania major* infections in mammalian hosts. *Proceedings of the National Academy of Sciences of the United States of America* **100(16):** 9536-9541

Spinks D, Shanks EJ, Cleghorn LA, McElroy S, Jones D, James D, et al. (2009) Investigation of trypanothione reductase as a drug target in *Trypanosoma brucei*. *ChemMedChem* **4:** 2060-2069

Stams WA, den Boer ML, Holleman A, Appel IM, Beverloo HB, van Wering ER, et al. (2005) Asparagine synthetase expression is linked with L-asparaginase resistance in TEL-AML1-

negative but not TEL-AML1-positive pediatric acute lymphoblastic leukemia. *Blood* **105:** 4223-4225

Stephens JL, Lee SH, Paul KS, Englund PT (2007) Mitochondrial fatty acid synthesis in *Trypanosoma brucei.* *The Journal of Biological Chemistry* **282:** 4427-4436

Sterkers Y, Lachaud L, Crobu L, Bastien P, Pages M (2011) FISH analysis reveals aneuploidy and continual generation of chromosomal mosaicism in *Leishmania major.* *Cellular Microbiology* **13:** 274-283

Stern AL, Burgos E, Salmon L, Cazzulo JJ (2007) Ribose-5-phosphate isomerase type B from *Trypanosoma cruzi*: kinetic properties and site directed mutagenesis reveal information about the reaction mechanism. *Biochemical Journal* **401:** 279-285

Stern AL, Naworyta A, Cazzulo JJ, Mowbray SL (2011) Structures of type B ribose-5-phosphate isomerase from *Trypanosoma cruzi* shed light on the determinants of sugar specificity in the structural family. *FEBS Journal* **278:** 793-808

Stevens JR, Noyes HA, Schofield CJ and Gibson W (2001) The molecular evolution of Trypanosomatidae. *Advanced Parasitology* **48**: 1-56

Stryer L (1999) Biochemistry, 4th edition, Freeman, New York, 559-565.

Sturm NR, Yu MC, Campbell DA (1999) Transcription termination and 3'-End processing of the spliced leader RNA in kinetoplastids. *Molecular Cell Biology* **19:** 1595-1604

Sudhandiran G, Shaha C (2003) Antimonial-induced increase in intracellular Ca2+ through nonselective cation channels in the host and the parasite is responsible for apoptosis of intracellular *Leishmania donovani* amastigotes. *The Journal of Biological Chemistry* **278:** 25120-25132

Sugiyama A, Kato H, Nishioka T, and Oda J (1992) Overexpression and purification of asparagine synthetase from *Escherichia coli*. *Bioscience, Biotechnology and Biochemistry* **56:** 376-379

Sulahian A, Garin YJF, Pratlong F, Dedet JP, Derouin F (1997) Experimental pathogenicity of viscerotropic and dermotropic isolates of *Leishmania infantum* from immunocompromised and immunocompetent patients in a murine model. *FEMS Immunol Med Microbiol* **17:** 131-138

Sundar S, Sahu M, Mehta H, Gupta A, Kohli U, Rai M, et al. (2002) Non-invasive management of Indian visceral leishmaniasis: clinical application of diagnosis by K39 antigen strip testing at a kala-azar referral unit. *Clinical Infectious Diseases* **35:** 581-586

Sutterwala SS, Hsu FF, Sevova ES, Schwartz KJ, Zhang K, Key P, et al. (2008) Developmentally regulated sphingolipid synthesis in African trypanosomes. *Molecular Microbiology* **70:** 281-96

Sykes ML, Avery VM (2009a) A luciferase based viability assay for ATP detection in 384-well format for high throughput whole cell screening of *Trypanosoma brucei brucei* bloodstream form strain 427. *Parasites and Vectors* **2:** 54

Sykes ML, Avery VM (2009b) Development of an Alamar Blue™ viability assay in 384-well format for high throughput whole cell screening of *Trypanosoma brucei brucei* bloodstream form strain 427. *American Journal of Tropical Medicine and Hygiene* **81:** 665-674

Szoor B, Haanstra JR, Gualdrón-López M, Michels PAM (2014) Evolution, dynamics and specialized functions of glycosomes in metabolism and development of trypanosomatids. *Current Opinion in Microbiology* **22:** 79-87

Tappe D, Muller A, Stich A, (2010) Resolution of cutaneous old world and new world leishmaniasis after oral miltefosine treatment. *American Journal of Tropical Medicine and Hygiene* **82:** 1-3

Taylor PR, Martinez-Pomares L, Stacey M, Lin HH, Brown GD, et al. (2005) Macrophage receptors and immune recognition. *Annual Reviews Immunology* **23:** 901-944

Teixeira SM, Paiva RMC, Kangussu-Marcolino MM, DaRocha WD (2012) Trypanosomatid comparative genomics: contributions to the study of parasite biology and different parasitic diseases. *Genetics and Molecular Biology* **35(1):** 1-17

Terstappen GC, Schlupen C, Raggiaschi R, Gaviraghi G (2007) Target deconvolution strategies in drug discovery. *Nature Reviews Drug Discovery* **6:** 891-903

Thakur CP, Sinha GP, Sharma V, Pandey AK, Sinha PK, Barat D (1993) Efficacy of amphotericin B in multi-drug resistant kala-azar in children in first decade of life. *Indian Journal of Pediatry* **60:** 29-36

Titus RG, Gueiros-Filho FJ, de Freitas LA, Beverley SM (1995) Development of a safe live *Leishmania* vaccine line by gene replacement. *Proceedings of the National Academy of Sciences of the United States of America* **92:** 10267-10271

Torrie LS, Wyllie S, Spinks D, Oza SL, Thompson S, Harrison JR, et al. (2009) Chemical validation of trypanothione synthetase: a potential drug target for human trypanosomiasis. *The Journal of Biological Chemistry* **284:** 36137-36145

Tovar J, Cunningham ML, Smith AC, Croft SL, Fairlamb AH (1998) Downregulation of *Leishmania donovani* trypanothione reductase by heterologous expression of a trans-dominant mutant homologue: effect on parasite intracellular survival. *Proceedings of the National Academy of Sciences of the United States of America* **95(9):** 5311-5316

Trinh MA, Klann E (2013) Translational control by eIF2a kinases in long-lasting synaptic plasticity and long-term memory. *Neurobiology of Learning and Memory* **105:** 93-99

Tulloch LB, Martini VP, Iulek J, Huggan JK, Lee JH, Gibson CL, et al. (2010) Structure-based design of pteridine reductase inhibitors targeting African sleeping sickness and the leishmaniases. *Journal of Medicinal Chemistry* **53:** 221-229

Turco SJ, Descoteaux A (1992) The lipophosphoglycan of *Leishmania* parasites. *Annual Reviews Microbiology* **46:** 65-94

Turco SJ, Spaeth GF, Beverley SM (2001) Is lipophosphoglycan a virulence factor? A surprising diversity between *Leishmania* species. *Trends in Parasitology* **17(5):** 223-226

Ubeda JM, Legare D, Raymond F, Ouameur AA, Boisvert S, Rigault P, et al. (2008) Modulation of gene expression in drug resistant *Leishmania* is associated with gene amplification, gene deletion and chromosome aneuploidy. *Genome Biology* **9:** R115

Ubeda UM, Raymond F, Mukherjee A, Plourde M, Gingras H, Roy G, et al. (2014) Genome-wide stochastic adaptive DNA amplification at direct and inverted DNA repeats in parasite *Leishmania*. *PLoS Biology* **12(5):** e1001868

Ubuka T, and Meister A (1971) Studies on the utilization of asparagine by mouse leukemia cells. *Journal of National Cancer Institute* **46:** 291-298

Ueno N, Wilson ME (2012) Receptor-mediated phagocytosis of *Leishmania*: implications for intracellular survival. *Trends in Parasitology* **28(8):** 335–344

Van der Ploeg LHT (1990) Antigenic variation in African trypanosomes: genetic recombination and transcriptional control of VSG genes. In: Hames BD, Glover DM, editors. Gene Rearrangement. Oxford: IRL Press

Van Griensven J and Diro E (2012) Visceral leishmaniasis. *Infectious Disease Clinics of North America* **26(2):** 309-322

Vanlerberghe V, Diap G, Guerin PJ, Meheus F, Gerstl S, Van der Stuyft P, et al. (2007) Drug policy for visceral leishmaniasis: a cost-effectiveness analysis. *Tropical Medicine International Health* **12:** 274-283

Van Zandbergen G, Bollinger A, Wenzel A, Kamhawi S, Voll R, Klinger M, et al. (2006) *Leishmania* disease development depends on the presence of apoptotic promastigotes in the virulent inoculum. *Proceedings of the National Academy of Sciences of the United States of America* **103(37):** 13837-13842

Van Zandbergen GG, Hermann NN, Laufs HH, Solbach W, Laskay T (2002) *Leishmania* promastigotes release a granulocyte chemotactic factor and induce interleukin-8 release but inhibit gamma interferon-inducible protein 10 production by neutrophil granulocytes. Infection and Immunity **70:** 4177-4184

Van Zandbergen G, Klinger M, Mueller A, Dannenberg S, Gebert A, Solbacj W, et al. (2004) Cutting edge: neutrophil granulocyte serves as a vector for *Leishmania* entry into macrophages. *Journal of Immunology* **173(11):** 6521-6525

Veitch NJ, Maugeri DA, Cazzulo JJ, Lindqvist Y, Barrett MP (2004) Transketolase from *Leishmania mexicana* has a dual subcellular localisation. *Biochemical Journal* **382:** 759-767

Vickers TJ, Beverley SM (2011) Folate metabolic pathways in *Leishmania. Essays Biochemistry* **51:** 63-80

Vince JE, Tull D, Landfear S, McConville MJ (2011) Lysosomal degradation of *Leishmania* hexose and inositol transporters is regulated in a stage-, nutrient- and ubiquitin-dependent manner. *International Journal of Parasitology* **41(7):** 791-800

Vinet AF, Fukuda M, Turco SJ, Descoteaux A (2009) The *Leishmania donovani* lipophosphoglycan excludes the vesicular proton-ATPase from phagosomes by impairing the recruitment of synaptotagmin V. PLoS Pathogens **5:** e1000628

Vinhas V, Andrade BB, Paes F, Bomura A, Clarencio J, Miranda JC, et al. (2007) Human anti-saliva immune response following experimental exposure to the visceral leishmaniasis vector, *Lutzomyia longipalpis. European Journal of Immunology* **37:** 3111-3121

Volf P and Myskova J (2007) Sand flies and *Leishmania*: specific versus permissive vectors. *Trends in Parasitology* **23(3):** 91-92

Walker DM, Oghumu S, Gupta G, McGwire BS, Drew ME, Satoskar AR (2014) Mechanisms of cellular invasion by intracellular parasites. *Cellular Molecular Life Science* **71(7):** 1245-1263

Wang Q, Melzer IM, Kruse M, Sander-Juelch C, and Wiese M (2005) LmxMPK4, a mitogen-activated protein (MAP) kinase homologue essential for promastigotes and amastigotes of *Leishmania mexicana*. *Kinetoplastid Biology and Disease* **4:** 6

Wang T, Wei JJ, Sabatini DM, Lander ES (2014) Genetic screens in human cells using the CRISPR-Cas9 system. *Science* **343:** 80-84

Warburg A, Saraiva E, Lanzaro GC, Titus RG, Neva F (1994) Saliva of *Lutzomyia longipalpis* sibling species differs in its composition and capacity to enhance leishmaniasis. *Philos Trans R Soc Lond B Biol Sci* **345:** 223-230

Wassef MK, Fioretti TB, Dwyer DM (1985) Lipid analyses of isolated surface membranes of *Leishmania donovani* promastigotes. *Lipids* **20:** 108-115

Wenzel A, van Zandbergen G (2009) Lipoxin A4 receptor dependent *Leishmania* infection. Autoimmunity **42:** 331-333

Wheeler RJ, Gluenz E, Gull K (2011) The cell cycle of *Leishmania*: morphogenetic events and their implications for parasite biology. *Molecular Microbiology* **79(3):** 647-662

Wichroski MJ, Ward GE (2003) Biosynthesis of glycosylphosphatidylinositol is essential to the survival of the protozoan parasite *Toxoplasma gondii. Eukaryotic Cell* **2:** 1132-1136

Wiese, M. (1998) A mitogen-activated protein (MAP) kinase homologue of *Leishmania mexicana* is essential for parasite survival in the infected host. *EMBO Journal* **17:** 2619–2628

Willert EK, Phillips MA (2008) Regulated expression of an essential allosteric activator of polyamine biosynthesis in African trypanosomes. *PLoS pathogens* **4:** e1000183

Williams RAM, Westrop GD, Coombs GH (2009) Two pathways for cysteine biosynthesis in *Leishmania major*. *Biochemical Journal* **420:** 451-462

Williams RD, Wang E, Merrill AH Jr (1984) Enzymology of long-chain base synthesis by liver: characterization of serine palmitoyltransferase in rat liver microsomes. *Archives of Biochemistry and Biophysics* **228:** 282-291

Wilson ZN, Gilroy CA, Boitz JM, Ullman B, Yates PA (2012) Genetic Dissection of Pyrimidine Biosynthesis and Salvage in *Leishmania donovani. The Journal of Biological Chemistry* ***287(16):*** *12759-12770*

Wincker P, Ravel C, Blaineau C, Pages M, Jauffret Y, Dedet JP, et al. (1996) The *Leishmania* genome comprises 36 chromosomes conserved across widely divergent human pathogenic species. *Nucleic Acids Research* **24:** 1688-1694

Wise DR, DeBerardinis RJ, Mancuso A, Sayed N, Zhang XY, Pfeiffer HK, et al. (2008) Myc regulates a transcriptional program that stimulates mitochondrial glutaminolysis and leads

to glutamine addiction. *Proceedings of the National Academy of Sciences of the United States of America* **105:** 18782-18787

Wise DR, Thompson CB (2010) Glutamine addiction: a new therapeutic target in cancer. *Trends in Biochemical Science* **35:** 427-433

Woodward, R., and Gull, K. (1990) "Timing of nuclear and kinetoplast DNA replication and early morphological events in the cell cycle of *Trypanosoma brucei*." *J Cell Sci* **95:** 49–57.

Wu Y, El Fakhry Y, Sereno D, Tamar S, Papadopoulou B (2000) A new developmentally regulated gene family in *Leishmania* amastigotes encoding a homolog of amastin surface proteins. *Molecular and Biochemical Parasitology* **110:** 345-357

Wyllie S, Oza SL, Patterson S, Spinks D, Thompson S, Fairlamb AH (2009) Dissecting the essentiality of the bifunctional trypanothione synthetase-amidase in *Trypanosoma brucei* using chemical and genetic methods. *Molecular microbiology* **74(3):** 529-40

Xiao Y, McCloskey DE, Phillips MA (2009) RNA interference-mediated silencing of ornithine decarboxylase and spermidine synthase genes in *Trypanosoma brucei* provides insight into regulation of polyamine biosynthesis. *Eukaryotic cell* **8:** 747-755

Yang H, He X, Zheng Y, Feng W, Xia X, Yu X, Lin Z (2014) Down-regulation of asparagine synthetase induces cell cycle arrest and inhibits cell proliferation of breast cancer. *Chemical biology & drug design* **84:** 578-584

Ye J, Kumanova M, Hart LS, Sloane K, Zhang H, De Panis DN, et al. (2010) The GCN2-ATF4 pathway is critical for tumour cell survival and proliferation in response to nutrient deprivation. *The EMBO Journal* **29:** 2082-2096

Young SA, Smith TK (2010) The essential neutral sphingomyelinase is involved in the trafficking of the variant surface glycoprotein in the bloodstream form of *Trypanosoma brucei*. *Molecular microbiology* **76:** 1461-1482

Zangger H, Ronet C, Desponds C, Kuhlmann FM, Robinson J, Hartley MA, et al. (2013) Detection of *Leishmania* RNA virus in *Leishmania* parasites. *PLoS Neglected Tropical Diseases* **7(1):** e2006

Zeiner GM, Sturm NR, Campbell DA (2003) The *Leishmania tarentolae* spliced leader contains determinants for association with polysomes. *The Journal of Biological Chemistry* **278:** 38269-38275

Zhang C, Xiao B, Jiang Y, Zhao Y, Li Z, Gao H, et al. (2014a) Efficient editing of Malaria parasite genome using CRISPR/Cas9 system. *mBio* **5(4):** e01414-14

Zhang J, Fan J, Venneti S, Cross JR, Takagi T, Bhinder B, et al. (2014b) Asparagine plays a critical role in regulating cellular adaption to glutamine depletion. *Molecular Cell* **56:** 205-218

Zhang Q, Siegel TN, Martins RM, Wang F, Cao J, Gao Q, et al. (2014c) Exonuclease-mediated degradation of nascent RNA silences genes linked to severe malaria. *Nature* **513:** 431-435

Zhang WW, Charest H, Ghedin E, Matlashewski G (1996) Identification and overexpression of the A2 amastigote-specific protein in *Leishmania donovani. Molecular and Biochemical Parasitology* **78:** 79-90

Zhang WW, Matlashewski G (2001) Characterization of the A2-A2rel gene cluster in *Leishmania donovani*: involvement of A2 in visceralization during infection. *Molecular Microbiology* **39:** 935-948

Zhang WW, Matlashewski G (2010) Screening *Leishmania donovani*-specific genes required for visceral infection. *Molecular Microbiology* **77:** 505-517

Zhang WW, Matlashewski G (2015) CRISPR-Cas9-mediatedm genome editing in *Leishmania donovani. mBIO* **6(4):** e00861-15

Zhang WW, Mendez S, Ghosh A, Myler P, Ivens A, et al. (2003) Comparison of the A2 gene locus in *Leishmania donovani* and *Leishmania major* and its control over cutaneous infection. *The Journal of Biological Chemistry* **278:** 35508-35515

Zheng L, T'Kind R, Decuypere S, von Freyend SJ, Coombs GH, Watson DG (2010) Profiling of lipids in *Leishmania donovani* using hydrophilic interaction chromatography in combination with Fourier transform mass spectrometry. *Rapid Communications Mass Spectrometry* **24:** 2074-2082

Zheng S, Haselkorn R (1996) A glutamate/glutamine/aspartate/asparagine transport operon in *Rhodobacter capsulatus*. *Molecular microbiology* **20:** 1001-1011

Zufferey R, Mamoun CB (2002) Choline transport in *Leishmania major* promastigotes and its inhibition by choline and phosphocholine analogs. *Molecular and Biochemical Parasitology* **125:** 127-134